frontiers | Research Topics

Remediation and health risks of heavy metal contaminated soils

Edited by
Qi Liao, Mariusz Gusiatin and Weichun Yang

Published in
Frontiers in Environmental Science

ISSN 1664-8714
ISBN 978-2-8325-5528-6
DOI 10.3389/978-2-8325-5528-6

About Frontiers

Frontiers is more than just an open access publisher of scholarly articles: it is a pioneering approach to the world of academia, radically improving the way scholarly research is managed. The grand vision of Frontiers is a world where all people have an equal opportunity to seek, share and generate knowledge. Frontiers provides immediate and permanent online open access to all its publications, but this alone is not enough to realize our grand goals.

Frontiers journal series

The Frontiers journal series is a multi-tier and interdisciplinary set of open-access, online journals, promising a paradigm shift from the current review, selection and dissemination processes in academic publishing. All Frontiers journals are driven by researchers for researchers; therefore, they constitute a service to the scholarly community. At the same time, the *Frontiers journal series* operates on a revolutionary invention, the tiered publishing system, initially addressing specific communities of scholars, and gradually climbing up to broader public understanding, thus serving the interests of the lay society, too.

Dedication to quality

Each Frontiers article is a landmark of the highest quality, thanks to genuinely collaborative interactions between authors and review editors, who include some of the world's best academicians. Research must be certified by peers before entering a stream of knowledge that may eventually reach the public - and shape society; therefore, Frontiers only applies the most rigorous and unbiased reviews. Frontiers revolutionizes research publishing by freely delivering the most outstanding research, evaluated with no bias from both the academic and social point of view. By applying the most advanced information technologies, Frontiers is catapulting scholarly publishing into a new generation.

What are Frontiers Research Topics?

Frontiers Research Topics are very popular trademarks of the *Frontiers journals series*: they are collections of at least ten articles, all centered on a particular subject. With their unique mix of varied contributions from Original Research to Review Articles, Frontiers Research Topics unify the most influential researchers, the latest key findings and historical advances in a hot research area.

Find out more on how to host your own Frontiers Research Topic or contribute to one as an author by contacting the Frontiers editorial office: frontiersin.org/about/contact

Remediation and health risks of heavy metal contaminated soils

Topic editors

Qi Liao — Central South University, China

Mariusz Gusiatin — University of Warmia and Mazury in Olsztyn, Poland

Weichun Yang — Central South University, China

Citation

Liao, Q., Gusiatin, M., Yang, W., eds. (2024). *Remediation and health risks of heavy metal contaminated soils*. Lausanne: Frontiers Media SA.

doi: 10.3389/978-2-8325-5528-6

Table of contents

frontiers | Frontiers in Environmental Science

TYPE Editorial
PUBLISHED 09 October 2024
DOI 10.3389/fenvs.2024.1501443

OPEN ACCESS

EDITED AND REVIEWED BY
Oladele Ogunseitan,
University of California, Irvine, United States

*CORRESPONDENCE
Qi Liao,
liaoqi@csu.edu.cn
Mariusz Z. Gusiatin,
mariusz.gusiatin@uwm.edu.pl

RECEIVED 25 September 2024
ACCEPTED 01 October 2024
PUBLISHED 09 October 2024

CITATION
Yang W, Liao Q and Gusiatin MZ (2024) Editorial: Remediation and health risks of heavy metal contaminated soils.
Front. Environ. Sci. 12:1501443.
doi: 10.3389/fenvs.2024.1501443

Editorial: Remediation and health risks of heavy metal contaminated soils

Weichun Yang[1], Qi Liao[1]* and Mariusz Z. Gusiatin[2]*

[1]Department of Environmental Engineering, School of Metallurgy and Environment, Central South University, Changsha, Hunan, China, [2]Chinese National Engineering Research Center for Control and Treatment of Heavy Metal Pollution, School of Metallurgy and Environment, Central South University, Changsha, Hunan, China

KEYWORDS

heavy metals, migration and transformation, toxicological effect, health risks, remediation

Editorial on the Research Topic
Remediation and health risks of heavy metal contaminated soils

Introduction

Soil contamination by heavy metals is a major problem for the environment and public health. Metals such as cadmium, lead and metalloids such as arsenic accumulate in the soil as a result of various activities, especially industrial activities and agricultural practices. Once in the soil, these metals can enter the food chain and pose toxic risks to human health. Mitigating these risks requires effective remediation strategies, including physical, chemical and biological methods. Key techniques include phytoremediation (use of plants to absorb pollutants), bioremediation (use of microorganisms to biotransform heavy metals into nontoxic forms) and immobilization (chemical modification of metals to reduce their mobility) (Liu et al., 2018; Rajendran et al., 2022). The success of these methods depends on the type of metal, the extent of contamination, soil properties and environmental factors. Both the remediation of contaminated soils and the associated health risks are crucial for protecting public health and promoting sustainable land use (Panqing et al., 2023).

This Research Topic includes 13 articles dealing with strategies and challenges related to soil contamination with heavy metals. Areas of focus include contamination in agriculture and food systems, risk assessment, innovative remediation techniques and advanced bioremediation methods. These articles examine the impact of agricultural and soil management practices on the uptake of metals by plants and explore the wider implications for public health. Innovative remediation techniques such as zero-valent iron at the nanoscale and bioremediation methods are highlighted, as well as risk assessments of environmental and health impacts. In addition, spatial analysis methods are discussed as tools to identify contamination patterns, with a focus on sustainable practices that mitigate health risks in agriculture. This Research Topic emphasizes the need for an integrated approach involving science, technology and policy to effectively manage the complexity of soil contamination.

Overview of contributions

The mechanisms that drive the migration and accumulation of heavy metals provide important insights into how these pollutants move through and persist in different environmental systems. Fan et al. investigate how chloride ions influence the movement and transformation of cadmium in soil-rice systems, revealing the interactions between agricultural chemicals and heavy metal behavior. Similarly, Farrow et al. investigate the uptake of arsenic and other trace elements in rice and show how soil composition, plant varieties and water management influence metal uptake.

In addition to investigating the mechanisms of heavy metal migration, several studies focus on assessing the risks that these metals pose to both ecosystems and human health. By using comprehensive risk assessment tools, these studies provide valuable insights into the extent of contamination and its potential impacts. Wang et al. conduct an ecological risk assessment of heavy metals in Bosten Lake sediments and identify the sources and severity of contamination. Mohanty et al. focus on the health risks associated with dietary exposure to heavy metals, especially in regions affected by chronic kidney disease. Tang et al. emphasize the importance of geographic and topographic factors in the assessment and remediation of soil contamination, especially in areas with varying terrain. Mohamed et al. use geospatial assessments and microbial strategies to manage contamination in arid regions.

Heavy metal contamination is not only a result of industrial and agricultural activities but can also arise from military operations. Sites used for military training and operations, such as firing ranges, often experience significant soil contamination due to the use of heavy metals in munitions. Addressing contamination in these areas requires specialized remediation strategies. Zhu et al. evaluate contamination in abandoned firing ranges, comparing the efficacy of various remediation techniques and their environmental impact.

Several studies in this Research Topic focus on novel remediation methods that improve both the efficiency and safety of removing heavy metals from contaminated soils. These advances offer promising solutions to mitigate the environmental and health risks posed by metal contamination. Pan et al. describe a synergistic approach using nanoscale zero-valent iron in combination with *Penicillium oxalicum* SL2 for chromium remediation. Kim and Park present the simultaneous removal of arsenic and lead using iron phosphate and analyze the complex interactions between remediation agents and contaminants. Biochar, a material known for its ability to stabilize heavy metals, plays an important role in several studies. Yang et al. develop biochar modified with iron and manganese to immobilize several heavy metals in soils. Naveed et al. investigate how the combination of biochar with polyacrylamide in wastewater irrigation can promote plant growth while reducing metal pollution. This approach not only reduces the environmental and health risks associated with the accumulation of metals in soils, but also increases agricultural productivity through the safe use of wastewater for irrigation.

To improve the effectiveness of remediation measures, integrated bioremediation strategies combining different biological techniques have been proposed. These approaches offer environmentally friendly solutions for dealing with metal-contaminated soils. Pérez-Vázquez et al. are investigating the combined use of bioaugmentation and phytoremediation in landfills, while Garbisu and Alkorta are researching improved phytoremediation methods aimed at reducing the spread of antibiotic resistance in soils contaminated with heavy metals.

Conclusion

Each paper in this Research Topic offers valuable insights into the detection, analysis, and remediation of heavy metal contamination in various environments. The studies emphasize the importance of innovative methods and strategies for addressing these persistent environmental and public health issues. The findings highlight the complex interactions between heavy metals and environmental factors, including agricultural chemicals, bioremediation agents, and topographic Research Topic. These interactions significantly affect the mobility, bioavailability, and ecological impact of heavy metals, underscoring the need for precise and effective remediation strategies. Ongoing research is essential to developing innovative, effective, and sustainable solutions for heavy metal-contaminated sites, with the ultimate goal of protecting both human health and the environment.

Author contributions

WY: Writing–review and editing. QL: Writing–review and editing. MG: Writing–original draft, Writing–review and editing.

Funding

The author(s) declare that no financial support was received for the research, authorship, and/or publication of this article.

Acknowledgments

We thank all the authors and reviewers who contributed to this Research Topic. We thank Frontiers for inviting us to serve as guest editors of this Research Topic, and we thank the editors of Frontiers for their kind cooperation and dedication.

Conflict of interest

The authors declare that the research was conducted in the absence of any commercial or financial relationships that could be construed as a potential conflict of interest.

Publisher's note

References

Liu, L., Li, W., Song, W., and Guo, M. (2018). Remediation techniques for heavy metal-contaminated soils: principles and applicability. *Sci. Total Environ.* 633, 206–219. doi:10.1016/j.scitotenv.2018.03.161

Panqing, Y., Abliz, A., Xiaoli, S., and Aisaiduli, H. (2023). Human health-risk assessment of heavy metal–contaminated soil based on Monte Carlo simulation. *Sci. Rep.* 13 (1), 7033. doi:10.1038/s41598-023-33986-3

Rajendran, S., Priya, T. A. K., Khoo, K. S., Hoang, T. K., Ng, H. S., Munawaroh, H. S. H., et al. (2022). A critical review on various remediation approaches for heavy metal contaminants removal from contaminated soils. *Chemosphere* 287, 132369. doi:10.1016/j.chemosphere.2021.132369

frontiers | Frontiers in Environmental Science

TYPE Original Research
PUBLISHED 23 October 2023
DOI 10.3389/fenvs.2023.1281341

OPEN ACCESS

EDITED BY
Mezbaul Bahar,
The University of Newcastle, Australia

REVIEWED BY
Ying-heng Fei,
Guangzhou University, China
Qingqing Huang,
Chinese Academy of Agricultural Sciences, China

*CORRESPONDENCE
Mengying Si,
simysmile@csu.edu.cn

RECEIVED 22 August 2023
ACCEPTED 12 October 2023
PUBLISHED 23 October 2023

CITATION
Yang Z, Zeng G, Liu L, He F, Arinzechi C, Liao Q, Yang W and Si M (2023), Simultaneous immobilization of lead, cadmium and arsenic in soil by iron-manganese modified biochar. *Front. Environ. Sci.* 11:1281341. doi: 10.3389/fenvs.2023.1281341

Simultaneous immobilization of lead, cadmium and arsenic in soil by iron-manganese modified biochar

Zhihui Yang[1,2], Gai Zeng[1], Lin Liu[1], Fangshu He[1], Chukwuma Arinzechi[1], Qi Liao[1,2], Weichun Yang[1,2] and Mengying Si[1,2]*

[1]Department of Environmental Engineering, School of Metallurgy and Environment, Central South University, Changsha, China, [2]Chinese National Engineering Research Center for Control and Treatment of Heavy Metal Pollution, Changsha, China

Cationic lead/cadmium and anionic arsenic exhibit opposite geochemical behaviors in soils, which makes the synchronous remediation of As, Cd, and Pb challenging. In this study, we developed an iron-manganese modified biochar (BC-Fe-Mn) that prepared from straw with iron (Fe) and manganese (Mn) loading at a pyrolysis temperature of 550 °C. After BC-Fe-Mn immobilization for 90 days, the simultaneous immobilization efficiency of Pb, Cd, and As reached 57%, 51%, and 35%, respectively. Speciation distributions shows that As transformed from specific bound state into weakly low crystallinity iron bound state. Cd transformed from carbonate fraction into Fe-Mn oxide bound fraction, and Pb transformed from carbonate fraction into residual state. During the procedure, simultaneous immobilization mechanisms might involve heavy metal morphological transformation, precipitation/co-precipitation, and surface complexation. Cd and Pb absorbed onto BC-Fe-Mn. Then the increased free iron oxides (Fe_d) reacted with the dissolved As to form iron-arsenic precipitation. The results show that BC-Fe-Mn is a promising material for the simultaneous immobilization of Pb, Cd, and As in multi-metal contaminated soil.

KEYWORDS

biochar, lead, cadmium, arsenic, immobilization

Highlights

- BC-Fe-Mn has been prepared to immobilize Pb, Cd, and As.
- Simultaneous immobilization efficiency of Pb, Cd, and As reached 57%, 51%, and 35%, respectively.
- Cd and Pb absorbed onto BC-Fe-Mn and the increased free iron oxides reacted with the As to form Fe-As precipitation.

1 Introduction

As a vital resource for human survival, soil plays a crucial role in the process of human progress and development. Due to human activities such as non-ferrous metal mining and industrial waste disposal, the content of heavy metals continuously accumulates in soil and

exceed the safety threshold. As reported, more than 13,300 ha in China are polluted by cadmium, with 18.6% considered moderately or lightly polluted, and 7.1% heavily polluted (GAO et al., 2016). According to the 2014 Soil Pollution Survey Report of China, lead (Pb), cadmium (Cd), and arsenic (As) pollution made up 70% of the excess ratio of heavy metal pollution in China. It pose a serious threat to human health through the bioaccumulation and food chain (TóTH et al., 2016). Therefore, an effective technique for simultaneous reducing the toxicity of the Pb, Cd and As in soil was urgently necessary.

Immobilization is advocated due to its easy-operate and high-efficiency properties (IGALAVITHANA et al., 2019). However, the pollution control of Pb, Cd, and As in soil is mainly concentrated on single heavy metals or two at most. There are few studies on the simultaneous stabilization of Pb, Cd, and As. In fact, cationic lead/cadmium and anionic arsenic exhibit opposite chemical behaviors in soil. For example, an increase in soil pH can increase the desorption of As on the soil surface due to the increasing the electronegativity of arsenate and soil particles. Pb and Cd are usually positively charged. When the pH is raised, Pb and Cd can be effectively immobilized (YANG X. et al., 2018). Therefore, their opposite chemical behavior poses a significant challenge for simultaneous immobilization of Pb, Cd, and As in soil.

Biochar (BC) is widely used in remediation of heavy metal contaminated soil (LYU et al., 2018). As compared with other materials, BC is a readily stable carbon-rich material with available porous, high specific surface area. It can increase the cation exchange capacity (CEC) and reduce the availability of heavy metals in soil through precipitation and surface immobilization (LI et al., 2019; TU et al., 2020; LV et al., 2021). Furthermore, an appreciable amount of oxygen-containing groups are contained on the surface, which show high efficiency adsorption of heavy metal cations (CHEN et al., 2021). However, due to the negatively charged surfaces of BC, its ability to remove arsenic anion pollution is clearly limited. For example, Yang's study showed that BC has high stabilization efficiency for Pb, but the immobilization efficiency of arsenic is low (YANG X. et al., 2018). Therefore, it is necessary to modify BC for simultaneous immobilization of Pb, Cd, and As in soil.

Iron/manganese material is characterized by its high reactivity, specific surface area, and surface charge. Fe/Mn-based materials possess strong affinity for As through the formation of surface complexes or precipitates and have been widely used for As immobilization. It can promote the changes of the self-generated structure and surface properties of iron oxides to increase the adsorption capacity of heavy metals in soil (TACK et al., 2006). However, simple iron-manganese compounds exhibit limited adaptability to the soil environment and may even catalyze the activation of other heavy metals in the soil. The products of biochar combined with iron (or manganese) can overcome their shortcomings and give full play to the advantages of BC and iron (or manganese).

Recent reports showed that fabrication the Fe/Mn onto biochars seems a promising strategy to improve the efficiency of simultaneous immobilization of As with Cd and Pb. It has been reported biochar with zero-valent iron (BC-ZVI) has a good removal effect on As by reducing As(V) to As(III) and conformal substitution of As(III) and Fe(III) in the newly formed FeOOH (BAKSHI et al., 2018). The hydroxyl groups on iron oxides can effectively adsorb As and form precipitates (FU et al., 2017). As can also undergo coordination reactions on the surface of manganese oxides to form As-MnO_2 complexes (VILLALOBOS et al., 2014). After modified with the iron and/or manganese, the number of functional groups on the surface of BC, such as carboxyl, hydroxyl, and phenolic hydroxyl, can be significantly increased, which can form oxygen-containing complexes with heavy metal ions via stabilization absorption configurations (O'REILLY and HOCHELLA, 2003; SONG et al., 2014; LI et al., 2017). Moreover, studies have shown that iron-manganese composites have an excellent ability to remove lead from solution due to the interaction between active functional carboxyl groups and hydroxyl groups on the surface (REN et al., 2012; HU et al., 2017). Manganese-iron binary oxide-biochar composite (FMBC) with good adsorption of Cd and copper (Cu) was prepared via impregnation/sintering method (ZHOU et al., 2018). Therefore, the combination of BC and iron-manganese materials possess great potential to overcome their respective shortcomings for the simultaneous immobilization of Pb, Cd, and As in soil.

This research hopes to develop an iron-manganese modified BC material to simultaneous immobilized the Pb, Cd, and As in multi-metal contaminated soil. The transformation process of Pb, Cd, and As in soil were studied by analyzing the speciation distribution of heavy metals and the properties of iron-manganese particles in soil. This study will provide a reliable strategy for the remediation of multi-metal contaminated soil.

2 Materials and methods

2.1 Soil pretreatment and characterization

Contaminated soil samples were collected from an abandoned factory in Changde, China. The samples were air-dried and crushed at room temperature, and thoroughly mixed after removing stones and plant rhizomes. The mixed soil was passed through a 20–100 mesh screen, and then digested using a mixture of HNO_3-HCl-HF to determine the total concentration of Pb, Cd, and As using K. Kameda's method (KAMEDA et al., 2017). The extraction of soil free iron oxide (Fe_d) was conducted using the dithionite-citric acid-bicarbonate procedure, whereas the extraction of soil amorphous iron oxide (Fe_o) was carried out using a solution of 0.2 mol L^{-1} ammonium oxalate. The concentration of crystalline iron oxide (Fe_c) was determined by subtracting the Fe_o content from the total Fe_d content. (CUI et al., 2020). All digested and extracted samples were measured by inductively coupled plasma optical emission spectrometry (ICP-OES, TCP-5100-VDV). The As in soil were extracted by sodium bicarbonate and measured by atomic fluorescence spectrometer (HGF-V2). Cation exchange capacity (CEC) was determined using the 1 mol L^{-1} NH_4Ac method (SONG et al., 2017). The properties of soil samples are exhibited in Table 1.

2.2 Preparation of modified BC and characterization

The preparation of BC and modified BC are as follows: the rice straw (obtained from Changsha city, China) was soaked in an

TABLE 1 Heavy metal content in soil.

Properties	Value
Soil pH	6.55
CEC (cmol/kg)	5.28
Total Pb (mg kg^{-1})	1800
Total Cd (mg kg^{-1})	69
Total As (mg kg^{-1})	650
DTPA-extractable Pb (mg kg^{-1})	1,200
DTPA-extractable Cd (mg kg^{-1})	61
$NaHCO_3$-extractable As (mg kg^{-1})	80

appropriate amount of deionized water and stirred for 2 h followed by drying in a constant temperature oven at 105 °C for 24 h and ground into powder. The powder was then sifted via a 40-mesh griddle. 10 g of rice straw powder was then pyrolyzed at a rate of 5 °C·min^{-1}–550 °C for 2 h in a controlled atmosphere furnace under N_2 atmosphere. As-prepared solid was washed quickly with ethanol and deionized water for 3–4 times, and finally dried in a drying oven under N_2 atmosphere to obtain BC.

10 g of rice straw powder was soaked in 175 ml of 0.02 mol L^{-1} $MnCl_2$, $FeCl_3$, or $MnCl_2$ + $FeCl_3$ solution, the preparation scheme are shown in the Fig. S1, respectively, under magnetic stirring for 2 h. Then the solid samples were prepared under identical conditions to obtain BC-Mn, BC-Fe, and BC-Fe-Mn, respectively.

2.3 Simultaneous immobilization of lead, cadmium, and arsenic in soil: batch tests

The performance of the materials on the simultaneous immobilization of Pb, Cd, and As in soil were investigated through batch tests in 150 ml sealed plastic bottles, which contained 50 g of Pb, Cd, and As composite contaminated soil. Four different agents, i.e., BC, BC-Mn, BC-Fe, and BC-Fe-Mn were added to the soil system, respectively, with a dosage of 5 wt%. Water was added to the batch systems to maintain the water content at 80 wt%. Soil samples were withdrawn at different time points. Soil samples were naturally air-dried and crushed for further analyses. All experiments were performed at room temperature of 25 °C and carried out in triplicate.

2.4 Sample analysis

To investigate the effectiveness stabilization efficiency of heavy metals, the contents of $NaHCO_3$-extractable As and DTPA-extractable Pb and Cd in soil samples were assessed using the method described by Liang (YANG et al., 2018b) and McLaren (MCLAREN et al., 1998). The efficiency of the as-prepared materials in heavy metals immobilization (η) was calculated using Eq. 1:

$$\eta = \frac{C_0\text{-}C_t}{C_0} * 100\%$$

C_0 represents the initial leaching concentration of metals in soils; C_e refers to the leaching concentration of metals in soils after 90 days passivation.

The speciation distributions of Pb and Cd were assessed using a five-step sequential extraction method (SEP) (TESSIER et al., 1979); while, the speciation of arsenic was extracted according to the method of (WENZEL et al., 2001). These methods classify Pb and Cd in soil into five fractions namely; exchangeable fraction, carbonate bound fraction, Fe-Mn oxide bound fraction, organic bound fraction, and residual fraction, and classify As into five fractions: non-specific bound arsenic, specific bound arsenic, amorphous or low crystallinity iron bound arsenic, crystalline iron or aluminum oxide bound arsenic and arsenic residue.

2.5 Separation of magnetic particles in soil

10 g of the soil after immobilization was added into a 500 ml beaker, which contained 200 ml of deionized water. Then the suspension was placed on magnetic stirring apparatus at the stirring speed of 200 rpm for 2 h. After sealed in a self-sealing bag, the strong magnet was placed along the outside wall of the beaker to collect the magnetic materials. The collected materials were washed with deionized water for several times and dried at 40 °C.

2.6 Method of analysis

Soil pH was measured at a solid-water ratio of 1:2.5 using a pH meter. The BC and modified BC were characterized by scanning electron microscope (SEM, JSM-IT300LA, Japan), which was equipped with an energy dispersive spectrometer (EDS. JED-2300, Japan). X-ray photoelectron spectroscopy (XPS, Thermo Scientific K-Alpha, United States) was employed to characterize the element composition and valence states of the materials before and after reaction. The composition and crystalline structure of the materials were analyzed via an X-ray diffractometer (XRD, Rigaku D/max-2500, Japan). Fourier-transformed infrared (FTIR, Perkin Elmer, United States) were employed to detect the functional groups on the surface of the biochar.

3 Results and discussion

3.1 Fe and Mn modification of BC

Figure 1(a~d) displays the SEM and SEM-EDS images with element mapping of the modified BC. The BC had a tough structure with a rough and compact surface. In contrast, the modified BC possessed a porous structure. In order to explore the iron and manganese modification on the surface of BC, the SEM-coupled

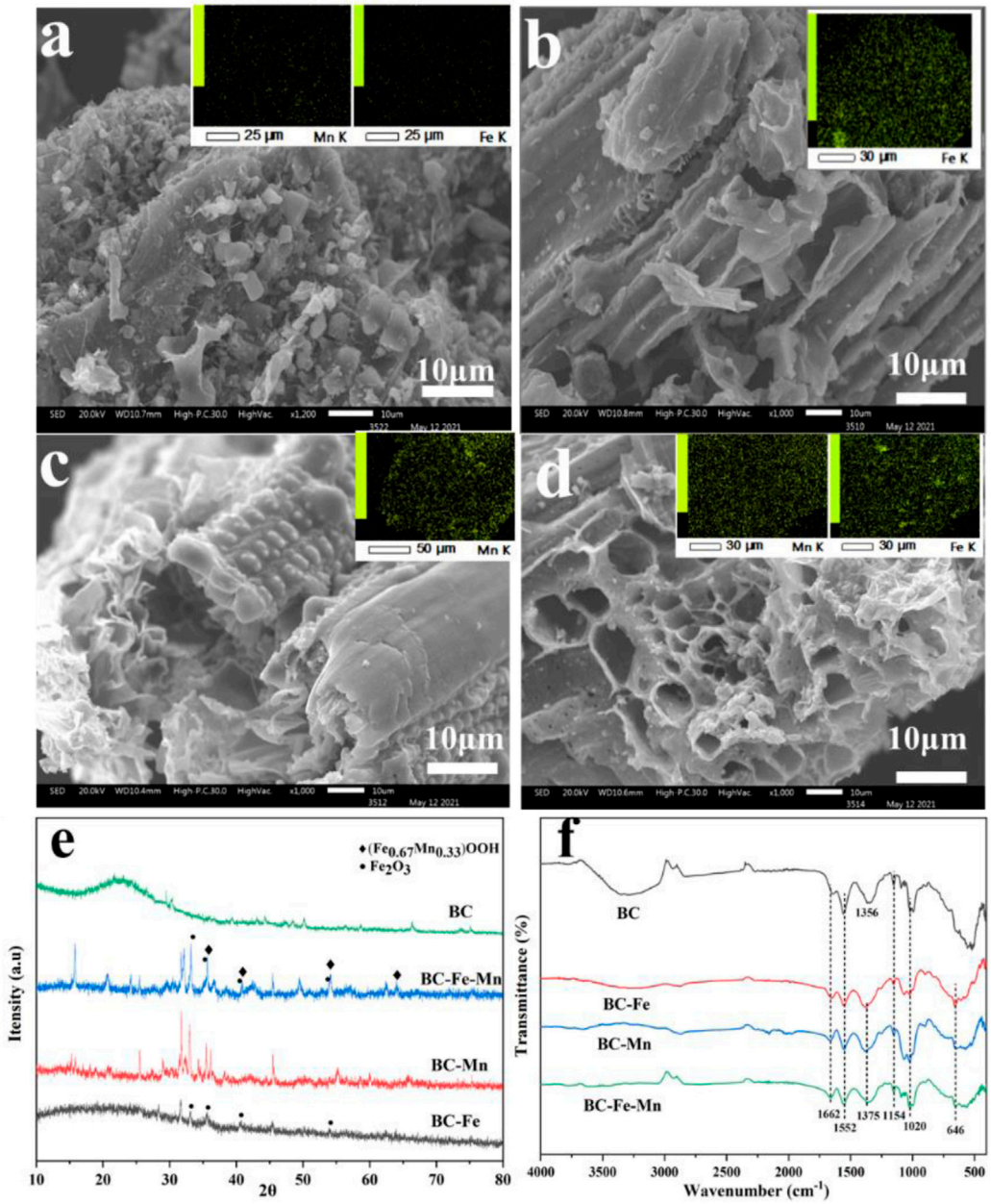

FIGURE 1
(A–D) SEM-EDS of BC **(A)**, BC-Fe **(B)**, BC-Mn **(C)**, and BC-Fe-Mn **(D)**; XRD **(E)** and FTIR **(F)** of different materials.

elemental mapping images of modified BC was analyzed. As shown in Figure 1A, almost no Fe and Mn existed on the surface of BC. However, after modification, Fe and Mn were evenly distributed on the surface of the materials. The properties of the BC-based materials prepared under various modified conditions are shown in Table 2. The content of C, H, O, and N atoms in BC decreased significantly. The C content of iron or/and manganese modified BC decreased by 12.7%–19.2% along with the introduction of metal elements. The C elements of BC participates in the reduction of metal elements and is consumed at high temperature during modification process (HOCH et al., 2008). Moreover, reduction of hydrogen and oxygen content generally involves dehydration and decarboxylation. As reported by Glaser et al., a BC with a low H/C ratio (<60%) and a low O/C ratio (<40%) has good stability and can be used as a soil conditioner (SCHIMMELPFENNIG and GLASER, 2012). Hence, the modified BC prepared in this study has the potential to improve the remediation.

The XRD pattern of the modified BC is shown in Figure 1E. There were no sharp absorption peaks of manganese after Mn modification. It indicated that manganese oxide might exist on BC in the form of amorphous phase. Conversely, after Fe modification, the diffraction peaks at 33.12°, 35.60°, 40.82°, and 54.00° in XRD patterns were associated with Fe_2O_3 (PDF#89–0,597). During high temperature calcination, $FeCl_3$ was converted into FeOOH and loaded on the BC as Fe_2O_3. When the $MnCl_2$ was introduced into the calcination, certian Mn might

TABLE 2 The basic properties of BC derived from the different modified conditions.

Sample	Elemental analysis					
	C (wt%)	H (wt%)	O (wt%)	N (wt%)	H/c (%)	O/C (%)
BC	54.24	2.43	13.36	1.27	4.48	24.63
BC-Fe	41.5	1.69	13.32	1.11	4.07	32.10
BC-Mn	35.49	1.99	13.95	0.96	5.61	39.31
BC-Fe-Mn	35.03	1.63	9.17	0.96	4.65	26.18

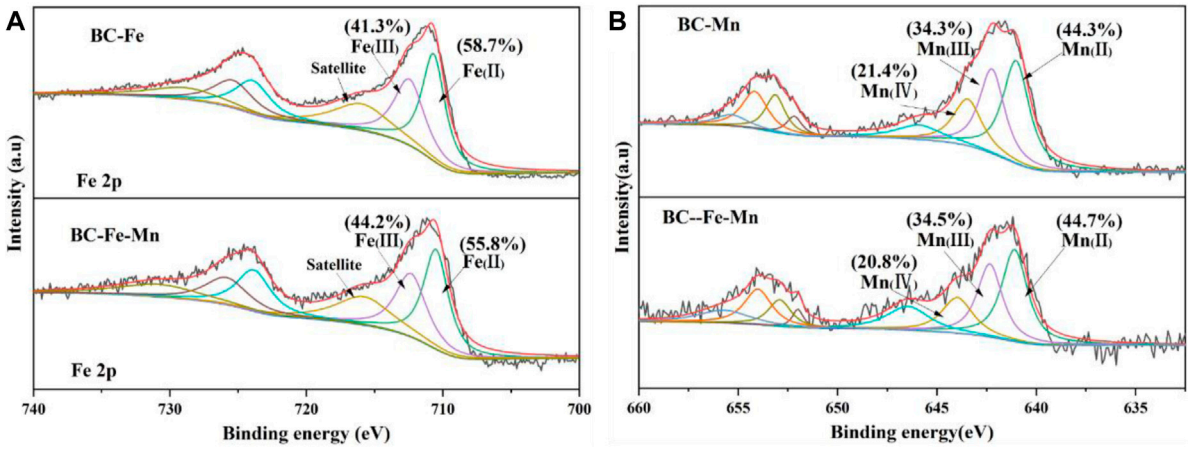

FIGURE 2
XPS spectra of the different types of BC. Fe2p XPS spectra of BC-Fe and BC-Fe-Mn **(A)**; Mn2p XPS spectra of BC-Mn and BC-Fe-Mn **(B)**.

replace Fe in FeOOH to form $(Fe_{0.67}Mn_{0.33})OOH$ during the transformation of FeOOH to Fe_2O_3 with the increase of calcination temperature (LI et al., 2022a). Accordingly, the application of Fe and Mn modification resulted in the appearance of two obvious peaks. The diffraction peaks at 35.67°, 40.99°, 54.23°, and 64.18° corresponded to $(Fe_{0.67}Mn_{0.33})OOH$ diffraction (PDF-#14–0,557), and the peaks at 33.12°, 35.60°, 40.82°, and 54.00° corresponded to the diffraction of Fe_2O_3 (PDF-#89–0,597). As shown in Figure 1F, FTIR was used to analyze the properties of the functional groups in BC. The absorption peak at 1,552 cm^{-1} corresponds to the stretching vibration of C-N, while peak at 1,662 cm^{-1} corresponds to the C-O vibration (LI et al., 2022b). The absorption peak at 1,356 cm^{-1} is attributed to the -COO vibration on the BC. It significantly shifts to 1,375 cm^{-1} in the modified BC, which might indicate that the introduction of iron or/and manganese during the modification (ZHANG et al., 2019a; TAN et al., 2022). The absorption peak at 646 cm^{-1} belongs to the absorption peak of Fe-O, which comes from the Fe-O vibration in Fe_2O_3 (LI et al., 2022a). These functional group structures suggest that the addition of iron results in the formation of new functional groups, whereas, the modified BC still retains its organic structures.

XPS analysis of the modified materials was carried out as Figure 2. Fe 2p and Mn 2p peaks were detected on the surface of BC after modification. The Fe 2p XPS spectra (Figure 2A) showed that the peaks at 712.5 eV and 710.8 eV were attributed to Fe(III) compounds and Fe(II) compounds, respectively (ZHU et al., 2020). While the peaks at 643.5, 641.8, and 640.8 eV (Figure 2B) were attributed to Mn(IV), Mn(III), and Mn(II) (TAN et al., 2022). On the surface of BC-Fe, Fe(III) accounted for 41.3% of the total surface atomic number of Fe. While on the surface of BC-Fe-Mn, the content of Fe(III) increased to 44.2%. At the same time, the proportion of Mn(IV) (20.8%) on the surface of BC-Fe-Mn was lower than that of BC-Mn (21.4%). It might be that certain Fe(II) was oxidized by the Mn(IV) to form Fe(III) as the introduction of iron and manganese during the calcination.

3.2 Simultaneous immobilization of Pb-Cd-As contaminated soil

Figure 3 shows the immobilization efficiency of Pb, Cd, and As by the BC as a function of time. After 90 days of remediation, only 6.5% and 20% of Pb and Cd were immobilized by BC, respectively. It proved that a great deal of Pb and Cd in soil could not be adsorbed onto BC. Moreover, the content of As in soil increased with the remediation. One of the possible reasons was that the addition of BC increased the pH value of the soil from 6.55 to 7.23, increasing the negative charge sites for the adsorption of metal cation. In contract, the competitive adsorption of BC with anionic arsenate resulted in the increase of available As in soil. Despite Fe modification, the

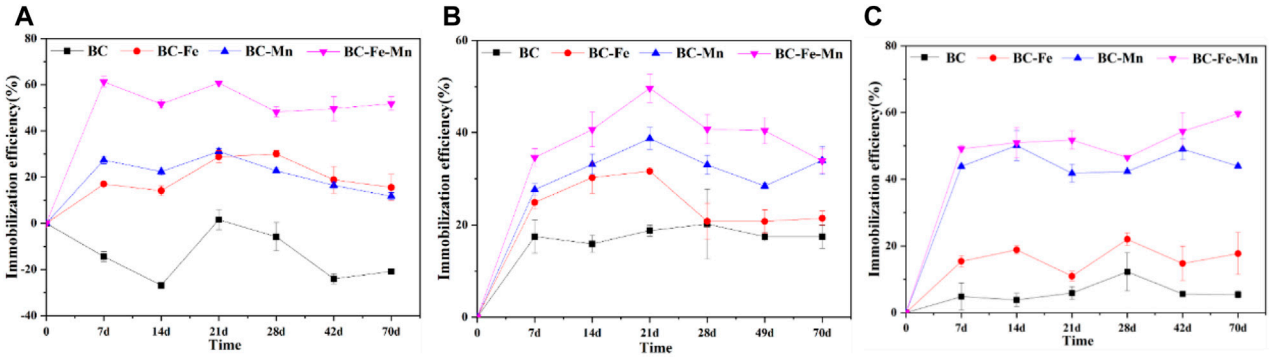

FIGURE 3
The immobilization efficiency of the various modified BC for As **(A)**, Cd **(B)**, and Pb **(C)** in soil with 5% addition of material as a function of time and material.

immobilization efficiency of As, Cd, and Pb remained low (15.5%, 21.5%, and 17.7%, respectively). The similar results were also observed by Wang et al. (WANG et al., 2020). As for the BC-Mn, the immobilization efficiency of As, Cd, and Pb increased at the initial stage (21 days) and then leveled out. The maximum immobilization efficiency of As, Cd, and Pb reached 31.1%, 38.8%, and 50.1%, respectively. During the BC-Fe-Mn remediation, the immobilization efficiencies increased with the reaction time. After 90 days, the immobilization efficiencies on Pb, Cd, and As reached 57%, 51% and 35%, respectively. Moreover, the water-soluble Pb and As were almost removed within 14 days, and more than 99% of the water-soluble Cd could be stabilized after 49 days (Fig. S2). The materials can be ranked based on their efficiency in the following order: BC-Fe-Mn > BC-Mn > BC-Fe > BC (Pb and Cd) and BC-Fe-Mn > BC-Fe > BC-Mn > BC (As). Therefore, BC-Fe-Mn exhibited the best immobilization efficiency for lead, cadmium and arsenic in soil.

3.3 Changes of soil properties

The pH of soil plays an important role in immobilization of heavy metals in soil. The application of BC resulted in a significant increase in the pH of soil (from 6.55 to 7.23, Table 3). During the pyrolysis process of the biomass, the base cations (primarily K, Ca, Na, Mg) were converted into oxides, hydroxides, and carbonates (HOUBEN et al., 2013). These alkaline substances dissolve and compete with As for the adsorption sites, resulting in As activation in soil. When the modified BC were employed in the soil remediation, the leaching of iron or manganese would cause the acidification of soil (TAO et al., 2019). Herein, the soil pH exhibited varying degrees of decrease after the application of modified BC (ranging from 6.55 to 5.66). Cd and Pb would be activated and released due to the acidification (MICHáLEKOVá-RICHV et al., 2016). The decreased pH also caused a decrease of negative charge in variable charge soil, thereby decreasing adsorption of cationic metals. Therefore, the slight change in the BC-Fe-Mn system will benefit the simultaneous immobilization of Pb, Cd, and As. The cation exchange capacity (CEC) is a dynamic component that affects the

TABLE 3 The basic properties of soil after the reaction was completed.

Material	CK	BC	BC-Fe	BC-Mn	BC-Fe-Mn
pH	6.55	7.23	5.66	5.71	6.07
CEC (cmol/kg $^{-1}$)	5.28	5.87	3.59	4.12	3.37

stability of soil. Upon completion of the reaction, CEC in soil changed significantly. In acidic soils, the disproportionate replacement of cations by H^+ results in a decrease in negative charge, which leads to a reduction in CEC (SHARMA et al., 2015). Thus, the reduction of CEC in soil may be the result of immobilization of the heavy metals during remediation (SONG et al., 2017).

3.4 Speciation distributions of Pb, Cd, and As

The relationship between the morphological transitions of BC-Fe-Mn and the immobilization efficiency of heavy metals in soil was studied. As shown in Figure 4, there was no non-specifically fraction of As in soil. With the extension of time, the content of specifically-sorbed As decreased by 10%. The amorphous iron bound As increased 9%. This may be due to the formation of stable iron arsenate compounds between As and Fe (SHAN and TONG, 2013). As for the Cd, the carbonate bound (CB) fraction showed a significant decrease from 19% to 8%. The content of Fe-Mn oxide bound (OM) fraction and residual fraction (RS) increased by 4% and 7%, respectively. Therefore, the environmentally sensitive fraction of Cd transformed into a more stable state. Meanwhile, the CB fraction of Pb decreased, and the RS and OM fraction increased. Pb generally exchanges with the Mg^{2+} and Ca^{2+} on the surface of BC to form stable complexes (LI et al., 2018; BANDARA et al., 2019). It interacts with–COO–, –O–and C–π on BC to generate organically bound fraction (SUN et al., 2021; T et al., 2015). Based on speciation analysis, it can be seen that Pb, Cd, and As can be converted to a more stable state under the effect of BC-Fe-Mn. And the amorphous iron bound (or OX fraction) and RS fraction are the main forms of Cd and As conversion, while OM fraction and RS fraction are the main forms of lead conversion.

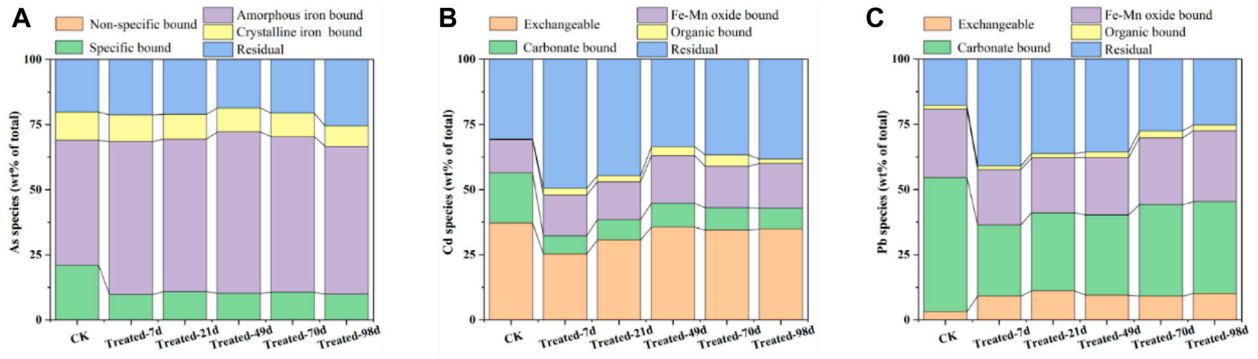

FIGURE 4
The SEP morphological changes of arsenic **(A)**, cadmium **(B)** and lead **(C)** in soil after BC-Fe-Mn modification.

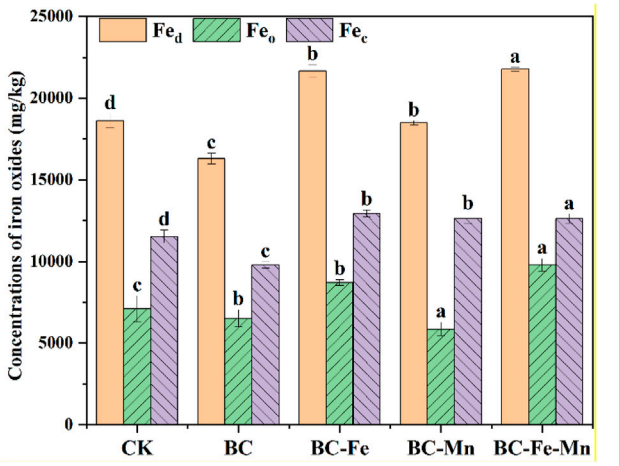

FIGURE 5
Soil iron oxide fractions after reaction. Fe_d, free iron oxides; Fe_o, amorphous iron oxides; and Fe_c, crystal iron oxides. Means (n = 3) followed by different letters above the columns indicate significant difference at $P < 0.05$.

3.5 Changes in iron oxide fractions

In soil, iron oxide is the main carrier of positive and negative charge and has a high affinity for heavy metals such as As, Cd, and Pb (GUO et al., 2021). Compared to CK, BC reduced the content of Fe_d, Fe_o, and Fe_c (Figure 5), indicating that the activity of iron oxide in soil was inhibited after BC application. This may be a potential explanation for the ineffective As immobilization following BC application. The content of Fe_d remained unchanged after the BC-Mn application, whereas the amount of Fe_o decreased and the amount of Fe_c increased. It suggested that additional manganese can promote transformation of iron into crystalline phase (LUO et al., 2018), leading to the aging of iron oxide in soil. When BC-Fe and BC-Fe-Mn were introduced into soil, it could be supplied as a iron source to convert into the unstable and poorly crystalline iron oxide (ferrihydrite) in soil via the hydrolysis of Fe^{2+} and Fe^{3+} (CUDENNEC and LECERF, 2006). Consequently, the Fe_d content increased from 18,622 mg kg^{-1} to 21,700 and 22,100 mg kg^{-1}, and the activity of iron in soil was enhanced. Compared with CK, the content of Fe_o in BC-Fe and BC-Fe-Mn system showed a substantial increase. It increased by 1700 mg kg^{-1} and 2,700 mg kg^{-1} after BC-Fe and BC-Fe-Mn application, respectively. It proved that manganese may enhance iron activation, when iron and manganese were coexist on BC (GASPARATO and S, 2012; ZHENG et al., 2020). As well known, Fe_d and Fe_o are effective Fe oxide components that facilitate the adsorption of metals by soil aggregates. Herein, the increase of Fe_d and Fe_o after BC-Fe-Mn application could improve the simultaneous immobilization.

3.6 Simultaneous immobilization mechanism in soil

BC-Fe-Mn significantly influence the form of iron oxides in soil and promotes the transformation of heavy metals into iron-manganese fractions. In order to further explore the immobilization mechanism of Pb, Cd, and As, the iron-containing magnetic particles (MPs) in soil were isolated and analyzed through XRD, XPS and SEM. MPs separated from soil after BC reaction presented as agglomeration state (Supplementary Figure S3). The MP extracted from the natural soil exhibited a granular structure, while the MP extracted from BC-based materials treated soil had a scale-like surface. The XRD patterns (Supplementary Figure S4) showed the MPs were mainly consisted of iron-manganese composite carboxyl oxide ($Fe_{0.67}Mn_{0.33}$)OOH (PDF-#14–0,557) and Fe_2O_3 (PDF-#33–0,664). This ($Fe_{0.67}Mn_{0.33}$)OOH molecule possessed abundant oxygen vacancies and -OH, which exhibited a strong affinity towards heavy metals (LI et al., 2022a).

Surface element results were shown in the Supplementary Table S1. The concentration of As and Cd on the surface of MP were significantly higher than that of soil. It suggested that the MP is one of the reaction sites of simultaneous immobilization in soil. After the BC-Fe-Mn application, the content of As on MP increased by 90.4% as compared with the CK. It might be due to that the released Fe reacted with the adsorbed As to form the iron-arsenic precipitation during the immobilization (SHAN and TONG, 2013). The XPS spectra of MP were shown in Figure 7. The peaks at 712.5 eV was attributed to Fe(III) $2p_{3/2}$. The peak at

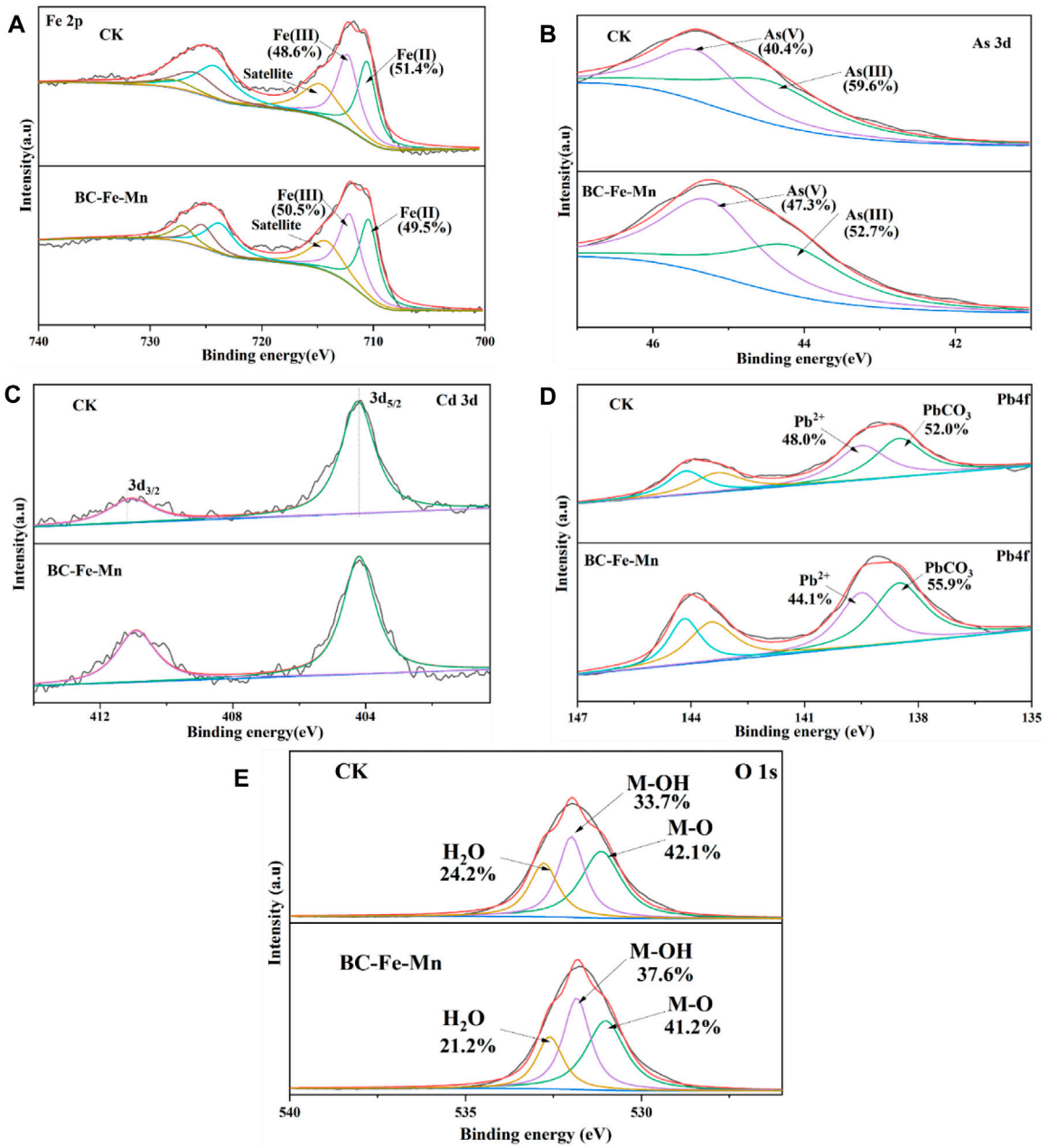

FIGURE 6
XPS spectrum of MP isolated from CK and BC-Fe-Mn treated soil. Fe 2p XPS spectra of CK and BC-Fe-Mn **(A)**; As 3d XPS spectra of CK and BC-Fe-Mn **(B)**; Cd 3d XPS spectra of CK and BC-Fe-Mn **(C)**; Pb 4f XPS spectra of CK and BC-Fe-Mn **(D)**; O 1s XPS spectra of CK and BC-Fe-Mn **(E)**.

710.2 eV was associated with the $2p_{3/2}$ orbitals from Fe(II) (ZHU et al., 2020). On the surface of MP separated from CK, the Fe species consisted of 51.4% Fe(II) and 48.6% Fe(III). While on the surface of MP isolated from BC-Fe-Mn reaction, the content of Fe(III) increased to 50.5%, and the content of Fe(II) decreased to 49.5%. This is probably due to the oxidative effect of Mn in BC-Fe-Mn, which could convert certain Fe(II) into Fe(III) (SUN et al., 2018). It is also possible that the iron oxide (iron hydride) generated by the hydrolysis of free ferric iron in the material adsorbed on the MP, increasing the content of Fe^{3+} (CUDENNEC and LECERF, 2006). Meanwhile, Figure 6B shown the peaks at 44.2 and 44.5 eV belonged to the signals of As(III) and As(V), respectively. The content of As(V) on the surface of MP from BC-Fe-Mn (47.3%) is higher than that from CK (40.4%), revealing the reduction of Mn(IV) → Mn(III) → Mn(II) might lead to effective As(III) oxidation to As(V).

Thus, the BC-Fe-Mn promoted the oxidation of As(III) during the remediation. The peaks at 411.6 eV and 404.8 eV were assigned to the $3d_{3/2}$ and $3d_{5/2}$ orbitals from Cd (Figure 6C), respectively (LIANG et al., 2017). It indicated that Cd was immobilized in the form of $Cd(OH)_2$ and Cd-Fe hydroxide (WANG et al., 2021a). Moreover, the peaks at 138.8 eV and 139.9 eV represented $PbCO_3$/PbO and Pb^{2+}, respectively (ZHANG et al., 2019b). The increased content of $PbCO_3$ (from 52.0% to 55.9%) showed that BC-Fe-Mn

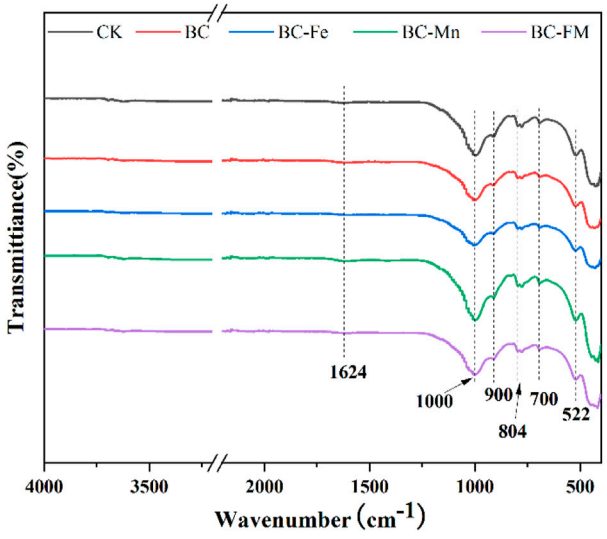

FIGURE 7
FTIR spectra of MP samples of BC-Fe-Mn, BC-Mn, BC-Fe, BC, and CK for 90 d.

induced the Pb immobilization in soil. The fitted O 1s spectrum (Figure 6E) presented three peaks at 530.8, 532.1 and 533.2 eV, characteristic of lattice oxygen (O^{2-}), hydroxyl (-OH), and adsorbed water (H_2O), respectively. Following remediation under BC-Fe-Mn, a reduction in O^{2-} moiety was observed from 42.1% to 41.2%. It suggested that the heavy metals gradually replaced the hydroxyl groups during sorption.

The FTIR spectra of the MPs are shown in Figure 7. The absorption peak at 522 cm^{-1} corresponds to the Mn-O vibration of MnO_6 octahedron (HOU et al., 2017), and the absorption peak near 1,624 cm^{-1} is the band of the O-H bending vibration band. The absorption peak around 890 cm^{-1} is associated with Fe-OH. The band at 900 cm^{-1} is assigned to -OH in goethite (XIAO et al., 2017). The peaks observed at 1,000 cm^{-1} and 700 cm^{-1} belongs to the Fe-OH and Mn-OH (XIAO et al., 2020) deformation vibration of iron-manganese oxides (XIONG et al., 2017; TAN et al., 2022). In general, the vacancies of manganese and iron oxides lead to the double-coordinated unsaturation, which tend to form O- and adsorb protons to form stable -OH to achieve charge balance. Thus, Mn-O and Fe-O can bond with heavy metals. Heavy metal cations in soils compete with protons to occupy the adsorption sites on iron-manganese oxides due to their strong charge interaction (LIN et al., 2020; JIN et al., 2022). Therefore, Mn-O and Fe-O are important functional groups for Cd immobilization. After immobilization, the peaks of Fe/Mn-OH appeared at higher wavenumbers, which may be attributed the decrease in the bond strength of Fe/Mn-O due to the solid electron donating effect of Cd in Fe/Mn-O-Cd (PENG et al., 2015; WANG et al., 2021b). The absorption peak at 816 cm^{-1} corresponded to As-OH or As-O-Fe stretching vibration. (HAN et al., 2016). Probably indicating the participation of As on MPs through the formation of an internal spherical bidentate binuclear complex adsorption (LIN et al., 2020). Furthermore, the formation of Fe-O-As(V) complex is also responsible for the adsorption of As(V) to Fe-O due to the strong binding ability of arsenic and iron (SHAN and TONG, 2013). It further proved that As also adsorbed on the surface of iron and manganese oxides.

Fe_2O_3 and $(Fe_{0.67}Mn_{0.33})OOH$ played an important role in the immobilization of heavy metals in soil. When the BC-Fe-Mn was introduced, Cd and Pb were absorbed and combined with OH, C-π, -COO functional groups on BC-Fe-Mn. As(III) firstly adsorbed on the surface of BC-Fe-Mn. The more electro-positive standard redox potential of the Fe(III)/Fe(II) couple (+0.771 V), the Mn(III)/Mn(II) couple (+1.51 V), and the Mn(IV)/Mn(II) couple (+1.23 V) than that of As(V)/As(III) (+0.56 V) enables the oxidation of As(III) by Mn(IV) and Mn(III), as described by Eq. 1–Eq. 3:

$$2Fe^{3+} + HAsO_2 + 2H_2O \rightarrow Fe^{2+} + H_3AsO_4 + 4H^+ \quad (1)$$

$$2MnO_4^- + 5HAsO_2 + 6H^+ + 2H_2O \rightarrow 2Mn^{2+} + 5H_3AsO_4 \quad (2)$$

$$MnO_2 + HAsO_2 + 2H^+ \rightarrow Mn^{2+} + H_3AsO_4 \quad (3)$$

$$2Fe^{2+} + MnO_2 + 4H^+ \rightarrow 2Fe^{3+} + Mn^{2+} + 2H_2O \quad (4)$$

$$5Fe^{2+} + MnO_4^- + 8H^+ \rightarrow 5Fe^{3+} + Mn^{2+} + 4H_2O \quad (5)$$

Moreover, the standard redox potential of the MnO_2/Mn^{2+} and MnO_4^-/Mn^{2+} is also more electro-positive than that of Fe^{3+}/Fe^{2+}, thus Mn oxides are capable of oxidizing Fe^{2+} to Fe^{3+} as described by Eq. (4-5). Then, the reduction of Mn(IV) → Mn(III) → Mn(II) leads to effective As(III) oxidation to As(V). Meanwhile, Fe/Mn in BC-Fe-Mn hydrolyzed to generate protons, thereby reducing the pH of the soil. The decrease in pH activated iron oxides in soil, leading to an increase in free iron oxides. The free iron oxide then reacted with dissolved As, resulting in iron-arsenic precipitation and an increase in As immobilization in soil. After treatment with BC-Fe-Mn, As and Cd transformed to the Fe-Mn oxide bound fraction, while Pb transformed to the residual fraction in soil.

4 Conclusion

In this study, iron and manganese were employed to modified the BC. The obtained BC-Fe-Mn could reduce the content of available As, Cd, and Pb by 35%, 51%, and 57% in soil. It also promoted the heavy metals to transform from the available state into relative stable state. Moreover, simultaneous immobilization mechanisms have been detected. It might involve heavy metal morphological transformation, precipitation/co-precipitation, and surface complexation. During the procedure, Cd and Pb absorbed and combined with OH, C-π, -COO functional groups on BC-Fe-Mn. BC-Fe-Mn promoted the increase of free iron oxides, which reacted with the dissolved As to form iron-arsenic precipitation. This work provides a promising remediation strategy for simultaneous immobilization of Pb, Cd, and As in soil and promote the insight of simultaneous immobilization mechanisms.

Data availability statement

The original contributions presented in the study are included in the article/Supplementary Material, further inquiries can be directed to the corresponding author.

Author contributions

ZY: Project administration, Supervision, Writing–original draft. GZ: Formal Analysis, Investigation, Methodology, Visualization, Writing–original draft. LL: Methodology, Writing–review and editing. FH: Formal Analysis, Writing–review and editing. CA: Writing–review and editing. QL: Writing–review and editing. WY: Writing–review and editing. MS: Conceptualization, Investigation, Methodology, Writing–review and editing.

Funding

The author(s) declare financial support was received for the research, authorship, and/or publication of this article. This work was financially supported by National Natural Science Foundation of China (U20A20267) and Major Program Natural Science Foundation of Hunan Province of China (2021JC0001).

Conflict of interest

The authors declare that the research was conducted in the absence of any commercial or financial relationships that could be construed as a potential conflict of interest.

Publisher's note

All claims expressed in this article are solely those of the authors and do not necessarily represent those of their affiliated organizations, or those of the publisher, the editors and the reviewers. Any product that may be evaluated in this article, or claim that may be made by its manufacturer, is not guaranteed or endorsed by the publisher.

Supplementary material

The Supplementary Material for this article can be found online at: https://www.frontiersin.org/articles/10.3389/fenvs.2023.1281341/full#supplementary-material

References

Bakshi, S., Banik, C., Rathke, S. J., and Laird, D. A. (2018). Arsenic sorption on zero-valent iron-biochar complexes. *Water Res.* 137, 153–163. doi:10.1016/j.watres.2018.03.021

Bandara, T., Franks, A., Xu, J., Bolan, N., Wang, H., and Tang, C. (2019). Chemical and biological immobilization mechanisms of potentially toxic elements in biochar-amended soils. *Crit. Rev. Environ. Sci. Technol.* 50 (9), 903–978. doi:10.1080/10643389.2019.1642832

Chen, D., Liu, W., Wang, Y., and Lu, P. (2021). Effect of biochar aging on the adsorption and stabilization of Pb in soil. *J. Soils Sediments* 22 (1), 56–66. doi:10.1007/s11368-021-03059-x

Cudennec, Y., and Lecerf, A. (2006). The transformation of ferrihydrite into goethite or hematite, revisited. *J. solid state Chem.* 179 (3), 716–722. doi:10.1016/j.jssc.2005.11.030

Cui, H., Zhang, X., Wu, Q., Zhang, S., Xu, L., Zhou, J., et al. (2020). Hematite enhances the immobilization of copper, cadmium and phosphorus in soil amended with hydroxyapatite under flooded conditions. *Sci. Total Environ.* 708, 134590. doi:10.1016/j.scitotenv.2019.134590

Fu, D., He, Z., Su, S., Xu, B., Liu, Y., and Zhao, Y. (2017). Fabrication of α-FeOOH decorated graphene oxide-carbon nanotubes aerogel and its application in adsorption of arsenic species. *J. Colloid Interface Sci.* 505, 105–114. doi:10.1016/j.jcis.2017.05.091

Gao, Z., Fu, W., Zhang, M., Zhao, K., Tunney, H., and Guan, Y. (2016). Potentially hazardous metals contamination in soil-rice system and it's spatial variation in Shengzhou City, China. *J. Geochem. Explor.* 167, 62–69. doi:10.1016/j.gexplo.2016.05.006

Gasparatos, D. (2012). Sequestration of heavy metals from soil with Fe–Mn concretions and nodules. *Environ. Chem. Lett.* 11 (1), 1–9. doi:10.1007/s10311-012-0386-y

Guo, Y., Li, X., Liang, L., Lin, Z., Su, X., and Zhang, W. (2021). Immobilization of cadmium in contaminated soils using sulfidated nanoscale zero-valent iron: effectiveness and remediation mechanism. *J. Hazard. Mater.* 420, 126605. doi:10.1016/j.jhazmat.2021.126605

Han, X., Song, J., Li, Y.-L., Jia, S. Y., Wang, W. H., Huang, F. G., et al. (2016). As(III) removal and speciation of Fe (Oxyhydr)oxides during simultaneous oxidation of As(III) and Fe(II). *Chemosphere* 147, 337–344. doi:10.1016/j.chemosphere.2015.12.128

Hoch, L. B., Mack, E. J., Hydutsky, B. W., Hershman, J. M., Skluzacek, J. M., and Mallouk, T. E. (2008). Carbothermal synthesis of carbon-supported nanoscale zero-valent iron particles for the remediation of hexavalent chromium. *Environ. Sci. Technol.* 42 (7), 2600–2605. doi:10.1021/es702589u

Hou, J., Luo, J., Song, S., Li, Y., and Li, Q. (2017). The remarkable effect of the coexisting arsenite and arsenate species ratios on arsenic removal by manganese oxide. *Chem. Eng. J.* 315, 159–166. doi:10.1016/j.cej.2016.12.115

Houben, D., Evrard, L., and Sonnet, P. (2013). Mobility, bioavailability and pH-dependent leaching of cadmium, zinc and lead in a contaminated soil amended with biochar. *Chemosphere* 92 (11), 1450–1457. doi:10.1016/j.chemosphere.2013.03.055

Hu, Q., Liu, Y., Gu, X., and Zhao, Y. (2017). Adsorption behavior and mechanism of different arsenic species on mesoporous MnFe 2 O 4 magnetic nanoparticles. *Chemosphere* 181, 328–336. doi:10.1016/j.chemosphere.2017.04.049

Igalavithana, A. D., Kwon, E. E., Vithanage, M., Rinklebe, J., Moon, D. H., Meers, E., et al. (2019). Soil lead immobilization by biochars in short-term laboratory incubation studies. *Environ. Int.* 127, 190–198. doi:10.1016/j.envint.2019.03.031

Jin, C., Li, Z., Huang, M., Ding, X., Zhou, M., Cai, C., et al. (2022). Cadmium immobilization in lake sediment using different crystallographic manganese oxides: performance and mechanism. *J. Environ. Manag.* 313, 114995. doi:10.1016/j.jenvman.2022.114995

Kameda, K., Hashimoto, Y., Wang, S.-L., Hirai, Y., and Miyahara, H. (2017). Simultaneous and continuous stabilization of as and Pb in contaminated solution and soil by a ferrihydrite-gypsum sorbent. *J. Hazard. Mater.* 327, 171–179. doi:10.1016/j.jhazmat.2016.12.039

Li, B., Yang, L., Wang, C.-Q., Zhang, Q. p., Liu, Q. c., Li, Y. d., et al. (2017). Adsorption of Cd(II) from aqueous solutions by rape straw biochar derived from different modification processes. *Chemosphere* 175, 332–340. doi:10.1016/j.chemosphere.2017.02.061

Li, H., Li, Z., Khaliq, M. A., Xie, T., Chen, Y., and Wang, G. (2019). Chlorine weaken the immobilization of Cd in soil-rice systems by biochar. *Chemosphere* 235, 1172–1179. doi:10.1016/j.chemosphere.2019.06.203

Li, H., Xu, H., Zhou, S., Yu, Y., Zhou, Li, H. C., et al. (2018). Distribution and transformation of lead in rice plants grown in contaminated soil amended with biochar and lime. *Ecotoxicol. Environ. Saf.* 165, 589–596. doi:10.1016/j.ecoenv.2018.09.039

Li, M., He, Z., Zhong, H., Sun, W., Hu, L., and Luo, M. (2022a). Fe0.67Mn0.33)OOH riched in oxygen vacancies facilitated the PMS activation of modified EMR for refractory foaming agent removal from mineral processing wastewater. *Chem. Eng. J.* 441, 136024. doi:10.1016/j.cej.2022.136024

Li, Q., Liang, W., Liu, F., Wang, G., Wan, J., Zhang, W., et al. (2022b). Simultaneous immobilization of arsenic, lead and cadmium by magnesium-aluminum modified biochar in mining soil. *J. Environ. Manag.* 310, 114792. doi:10.1016/j.jenvman.2022.114792

Liang, J., Li, X., Yu, Z., Zeng, G., Luo, Y., Jiang, L., et al. (2017). Amorphous MnO2 modified biochar derived from aerobically composted swine manure for adsorption of Pb (II) and Cd (II). *ACS Sustain. Chem. Eng.* 5 (6), 5049–5058. doi:10.1021/acssuschemeng.7b00434

Lin, L., Li, J., Yang, X., Yan, X., Feng, T., Liu, Z., et al. (2020). Simultaneous immobilization of arsenic and cadmium in paddy soil by Fe-Mn binary oxide. *Elem. Sci. Anthropocene* 8 (1). doi:10.1525/elementa.2020.094

Luo, Y., Ding, J., Shen, Y., Tan, W., Qiu, G., and Liu, F. (2018). Symbiosis mechanism of iron and manganese oxides in oxic aqueous systems. *Chem. Geol.* 488, 162–170. doi:10.1016/j.chemgeo.2018.04.030

Lv, G., Yang, T., Chen, Y., Hou, H., Liu, X., Li, J., et al. (2021). Biochar-based fertilizer enhanced Cd immobilization and soil quality in soil-rice system. *Ecol. Eng.* 171, 106396. doi:10.1016/j.ecoleng.2021.106396

Lyu, H., Zhao, H., Tang, J., Gong, Y., Huang, Y., Wu, Q., et al. (2018). Immobilization of hexavalent chromium in contaminated soils using biochar supported nanoscale iron sulfide composite. *Chemosphere* 194, 360–369. doi:10.1016/j.chemosphere.2017.11.182

Mclaren, R. G., Naidu, R., Smith, J., and Tiller, K. G. (1998). *Fractionation and distribution of arsenic in soils contaminated by cattle dip*. Hoboken, New Jersey, U.S.A: Wiley Online Library.

MichálLEKOVá-Richveisová, B., FrišťáK, V., PipíŠKA, M., Ďuriška, L., Moreno-Jimenez, E., and Soja, G. (2016). Iron-impregnated biochars as effective phosphate sorption materials. *Environ. Sci. Pollut. Res.* 24 (1), 463–475. doi:10.1007/s11356-016-7820-9

O'Reilly, S. E., and Hochella, M. F. (2003). Lead sorption efficiencies of natural and synthetic Mn and Fe-oxides. *Geochimica Cosmochimica Acta* 67 (23), 4471–4487. doi:10.1016/s0016-7037(03)00413-7

Peng, L., Zeng, Q., Tie, B., Lei, M., Yang, J., Luo, S., et al. (2015). Manganese Dioxide nanosheet suspension: a novel absorbent for Cadmium(II) contamination in waterbody. *J. Colloid Interface Sci.* 456, 108–115. doi:10.1016/j.jcis.2015.06.017

Ren, Y., Li, N., Feng, J., Luan, T., Wen, Q., Li, Z., et al. (2012). Adsorption of Pb(II) and Cu(II) from aqueous solution on magnetic porous ferrospinel MnFe2O4. *J. Colloid Interface Sci.* 367 (1), 415–421. doi:10.1016/j.jcis.2011.10.022

Schimmelpfennig, S., and Glaser, B. (2012). One step forward toward characterization: some important material properties to distinguish biochars. *J. Environ. Qual.* 41 (4), 1001–1013. doi:10.2134/jeq2011.0146

Shan, C., and Tong, M. (2013). Efficient removal of trace arsenite through oxidation and adsorption by magnetic nanoparticles modified with Fe–Mn binary oxide. *Water Res.* 47 (10), 3411–3421. doi:10.1016/j.watres.2013.03.035

Sharma, A., Weindorf, D. C., Wang, D., and Chakraborty, S. (2015). Characterizing soils via portable X-ray fluorescence spectrometer: 4. Cation exchange capacity (CEC). *Geoderma* 239-240, 130–134. doi:10.1016/j.geoderma.2014.10.001

Song, B., Zeng, G., Gong, J., Liang, J., Xu, P., Liu, Z., et al. (2017). Evaluation methods for assessing effectiveness of *in situ* remediation of soil and sediment contaminated with organic pollutants and heavy metals. *Environ. Int.* 105, 43–55. doi:10.1016/j.envint.2017.05.001

Song, Z., Lian, F., Yu, Z., Zhu, L., Xing, B., and Qiu, W. (2014). Synthesis and characterization of a novel MnOx-loaded biochar and its adsorption properties for Cu2+ in aqueous solution. *Chem. Eng. J.* 242, 36–42. doi:10.1016/j.cej.2013.12.061

Sun, Q., Cui, P.-X., Fan, T.-T., Wu, S., Zhu, M., Alves, M. E., et al. (2018). Effects of Fe(II) on Cd(II) immobilization by Mn(III)-rich δ-MnO2. *Chem. Eng. J.* 353, 167–175. doi:10.1016/j.cej.2018.07.120

Sun, T., Xu, Y., Sun, Y., Wang, L., Liang, X., and Jia, H. (2021). Crayfish shell biochar for the mitigation of Pb contaminated water and soil: characteristics, mechanisms, and applications. *Environ. Pollut.* 271, 116308. doi:10.1016/j.envpol.2020.116308

Tan, X., Liu, Y., Zeng, G., Wang, X., Hu, X., Gu, Y., et al. (2015). Application of biochar for the removal of pollutants from aqueous solutions. *Chemosphere* 125, 70–85. doi:10.1016/j.chemosphere.2014.12.058

Tack, F. M. G., Van Ranst, E., Lievens, C., and Vandenberghe, R. (2006). Soil solution Cd, Cu and Zn concentrations as affected by short-time drying or wetting: the role of hydrous oxides of Fe and Mn. *Geoderma* 137 (1-2), 83–89. doi:10.1016/j.geoderma.2006.07.003

Tan, W.-T., Zhou, H., Tang, S.-F., Zeng, P., Gu, J. F., and Liao, B. H. (2022). Enhancing Cd(II) adsorption on rice straw biochar by modification of iron and manganese oxides. *Environ. Pollut.* 300, 118899. doi:10.1016/j.envpol.2022.118899

Tao, H.-Y., Ge, H., Shi, J., Liu, X., Guo, W., Zhang, M., et al. (2019). The characteristics of oestrone mobility in water and soil by the addition of Ca-biochar and Fe–Mn-biochar derived from Litchi chinensis Sonn. *Environ. Geochem. Health* 42 (6), 1601–1615. doi:10.1007/s10653-019-00477-2

Tessier, A., Campbell, P. G., and Bisson, M. (1979). Sequential extraction procedure for the speciation of particulate trace metals. *Anal. Chem.* 51 (7), 844–851. doi:10.1021/ac50043a017

TóTH, G., Hermann, T., Da Silva, M. R., and Montanarella, L. (2016). Heavy metals in agricultural soils of the European Union with implications for food safety. *Environ. Int.* 88, 299–309. doi:10.1016/j.envint.2015.12.017

Tu, C., Wei, J., Guan, F., Liu, Y., Sun, Y., and Luo, Y. (2020). Biochar and bacteria inoculated biochar enhanced Cd and Cu immobilization and enzymatic activity in a polluted soil. *Environ. Int.* 137, 105576. doi:10.1016/j.envint.2020.105576

Villalobos, M., Escobar-Quiroz, I. N., and Salazar-Camacho, C. (2014). The influence of particle size and structure on the sorption and oxidation behavior of birnessite: I. Adsorption of As(V) and oxidation of As(III). *Geochimica Cosmochimica Acta* 125, 564–581. doi:10.1016/j.gca.2013.10.029

Wang, M., Hu, C., Xu, J., Jing, X., Rahim, H. U., and Cai, X. (2021a). Facile combinations of thiosulfate and zerovalent iron synergically immobilize cadmium in soils through mild extraction and facilitated immobilization. *J. Hazard. Mater.* 407, 124806. doi:10.1016/j.jhazmat.2020.124806

Wang, W., Lu, T., Liu, L., Yang, X., Sun, X., Qiu, G., et al. (2021b). Zeolite-supported manganese oxides decrease the Cd uptake of wheat plants in Cd-contaminated weakly alkaline arable soils. *J. Hazard. Mater.* 419, 126464. doi:10.1016/j.jhazmat.2021.126464

Wang, Y.-M., Wang, S.-W., Wang, C.-Q., Zhang, Z. y., Zhang, J. q., Meng, M., et al. (2020). Simultaneous immobilization of soil Cd(II) and as(V) by Fe-modified biochar. *Int. J. Environ. Res. Public Health* 17 (3), 827. doi:10.3390/ijerph17030827

Wenzel, W. W., Kirchbaumer, N., Prohaska, T., Stingeder, G., Lombi, E., and Adriano, D. C. (2001). Arsenic fractionation in soils using an improved sequential extraction procedure. *Anal. Chim. acta* 436 (2), 309–323. doi:10.1016/s0003-2670(01)00924-2

Xiao, J., Hu, R., Chen, G., and Xing, B. (2020). Facile synthesis of multifunctional bone biochar composites decorated with Fe/Mn oxide micro-nanoparticles: physicochemical properties, heavy metals sorption behavior and mechanism. *J. Hazard. Mater.* 399, 123067. doi:10.1016/j.jhazmat.2020.123067

Xiao, W., Jones, A. M., Collins, R. N., Bligh, M. W., and Waite, T. D. (2017). Use of fourier transform infrared spectroscopy to examine the Fe(II)-Catalyzed transformation of ferrihydrite. *Talanta* 175, 30–37. doi:10.1016/j.talanta.2017.07.018

Xiong, Y., Tong, Q., Shan, W., Xing, Z., Wang, Y., Wen, S., et al. (2017). Arsenic transformation and adsorption by iron hydroxide/manganese dioxide doped straw activated carbon. *Appl. Surf. Sci.* 416, 618–627. doi:10.1016/j.apsusc.2017.04.145

Yang, X., Igalavithana, A. D., Oh, S.-E., Nam, H., Zhang, M., Wang, C. H., et al. (2018a). Characterization of bioenergy biochar and its utilization for metal/metalloid immobilization in contaminated soil. *Sci. Total Environ.* 640-641, 704–713. doi:10.1016/j.scitotenv.2018.05.298

Yang, Z., Liang, L., Yang, W., Shi, W., Tong, Y., Chai, L., et al. (2018b). Simultaneous immobilization of cadmium and lead in contaminated soils by hybrid bio-nanocomposites of fungal hyphae and nano-hydroxyapatites. *Environ. Sci. Pollut. Res.* 25 (12), 11970–11980. doi:10.1007/s11356-018-1492-6

Zhang, J., Shao, J., Jin, Q., Li, Z., Zhang, X., Chen, Y., et al. (2019b). Sludge-based biochar activation to enhance Pb(II) adsorption. *Fuel* 252, 101–108. doi:10.1016/j.fuel.2019.04.096

Zhang, L., Guo, J., Huang, X., Wang, W., Sun, P., Li, Y., et al. (2019a). Functionalized biochar-supported magnetic MnFe2O4 nanocomposite for the removal of Pb(ii) and Cd(ii). *RSC Adv.* 9 (1), 365–376. doi:10.1039/c8ra09061k

Zheng, Q., Hou, J., Hartley, W., Ren, L., Wang, M., Tu, S., et al. (2020). As(III) adsorption on Fe-Mn binary oxides: are Fe and Mn oxides synergistic or antagonistic for arsenic removal? *Chem. Eng. J.* 389, 124470. doi:10.1016/j.cej.2020.124470

Zhou, Q., Lin, L., Qiu, W., Song, Z., and Liao, B. (2018). Supplementation with ferromanganese oxide–impregnated biochar composite reduces cadmium uptake by indica rice (Oryza sativa L.). *J. Clean. Prod.* 184, 1052–1059. doi:10.1016/j.jclepro.2018.02.248

Zhu, S., Qu, T., Irshad, M. K., and Shang, J. (2020). Simultaneous removal of Cd(II) and As(III) from co-contaminated aqueous solution by α-FeOOH modified biochar. *Biochar* 2 (1), 81–92. doi:10.1007/s42773-020-00040-8

frontiers | Frontiers in Environmental Science

TYPE Original Research
PUBLISHED 26 October 2023
DOI 10.3389/fenvs.2023.1248373

OPEN ACCESS

EDITED BY
Weichun Yang,
Central South University, China

REVIEWED BY
Jajati Mandal,
University of Salford, United Kingdom
Tarit Roychowdhury,
Jadavpur University, India

*CORRESPONDENCE
Shraddha Mohanty,
shraddha.mohanty001@gmail.com

RECEIVED 27 June 2023
ACCEPTED 13 October 2023
PUBLISHED 26 October 2023

CITATION
Mohanty S, Nayak RK, Jena B, Padhan K, Mohapatra KK, Sahoo SK, Dash PK, Das J, Behera SK, Sahu A, Nayak JK, Padhan S and Datta D (2023), Heavy metal contamination in rice, pulses, and vegetables from CKDu-endemic areas in Cuttack district, India: a health risk assessment.
Front. Environ. Sci. 11:1248373.
doi: 10.3389/fenvs.2023.1248373

Heavy metal contamination in rice, pulses, and vegetables from CKDu-endemic areas in Cuttack district, India: a health risk assessment

Shraddha Mohanty[1]*, Rabindra Kumar Nayak[1], Bandita Jena[1], Kshitipati Padhan[1], Kiran Kumar Mohapatra[1], Sanjib Kumar Sahoo[1], Prava Kiran Dash[1], Jyotirmayee Das[1], Sujit Kumar Behera[2], Anukiran Sahu[2], Jitendra Kumar Nayak[3], Sudipta Padhan[4] and Diptanu Datta[5]

[1]Department of Soil Science and Agricultural Chemistry, Odisha University of Agriculture and Technology, Bhubaneswar, Odisha, India, [2]Department of Nematology, Odisha University of Agriculture and Technology, Bhubaneswar, Odisha, India, [3]Department of Agronomy, Odisha University of Agriculture and Technology, Bhubaneswar, Odisha, India, [4]Department of Plant Protection, College of Horticulture, Birsa Agricultural University, Ranchi, India, [5]Department of Plant Pathology, Institute of Agricultural Sciences, Siksha "O" Anusandhan (Deemed to be University), Bhubaneswar, Odisha, India

Introduction: Chronic kidney disease of unknown aetiology (CKDu) is an emerging public health concern in India. The present study was carried out to investigate the concentrations of potentially toxic heavy metals (Cd, Pb, Ni, Cr, Hg, and As) in locally grown food crops (rice, pulses, and vegetables) in CKDu prevalent areas of Cuttack district, India.

Methods: Exposure risks from food crops were analysed, including estimated daily intake, hazard quotient, hazard index, and carcinogenic risk.

Result: The overall heavy metal concentrations in the crop samples were in the following order: Pb>Ni>Cd>Cr>As>Hg. The mean concentration of heavy metals in different crops were as follows, ranked from highest to lowest: spinach, rice, okra, mustard, potato, carrot, tomato, green gram, black gram. A statistical multivariate analysis revealed that the primary sources of Cd, Pb, Ni, Cr, Hg, and As in crop samples were both natural and human activities. For lead, target hazard quotient (THQ) values in rice were greater than 1, indicating significant noncarcinogenic health risks to both adults and children.

Discussion: While the majority of the crop samples had Pb levels below the permissible level (10^{-5}), the target carcinogenic risk of Cd was higher than the USEPA threshold value (10^{-4}), showing a cancer risk to adults and children. This study concluded that long-term intake of locally grown food crops may produce a significant health risk to the local inhabitants, and that of regular heavy metal monitoring is strongly recommended in this region.

KEYWORDS

rice, leafy vegetables, CKDu, noncarcinogenic risk, hazard index, carcinogenic risk

1 Introduction

The contamination of soil and crops (grains, fruits, and vegetables) with hazardous metals, viz., cadmium (Cd), lead (Pb), chromium (Cr), nickel (Ni), copper (Cu), and zinc (Zn), is detrimental to the environment owing to their persistent and non-biodegradable nature and is primarily caused by natural and anthropogenic processes (Radwan and Salama, 2006; Shah et al., 2010; Muhammad et al., 2011; Sekomo et al., 2011). Heavy metals are taken up by crops together with other necessary soil nutrients, and the buildup of these metals is typically greater in crops cultivated in polluted soils than in those grown in uncontaminated soils (Jan et al., 2010; Yang et al., 2011; Ratul et al., 2018). Weathering of metal-bearing minerals and volcanic eruptions are natural or geological sources of heavy metals in the environment. Nevertheless, the use of wastewater for irrigation purposes has been found to have a significant effect on the buildup of both inorganic and organic contaminants within the soil (Arora et al., 2008; Rehman et al., 2019). Consequently, these contaminants can be taken up by plants that are subjected to irrigation with such wastewater (Singh et al., 2004; Rashid et al., 2022). Undoubtedly, the utilisation of wastewater for irrigation has resulted in a reduction in the demand on freshwater resources. Heavy metals deposited in food crops have been shown to reach the human body by inhalation and consumption (Mamat et al., 2014; Abuduwaili et al., 2015). These metals, once inside the body, interfere with enzymes, slowing or stopping essential physiological processes. Over time, they can lead to serious health issues, including anaemia, kidney failure, and brain damage (Pappas et al., 2006; Mitra et al., 2022). For example, the consumption of food contaminated with Cd has been linked to both acute and chronic health effects, including kidney damage, poor bone development, hypertension, and even cancer (Raknuzzaman et al., 2016).

Chronic kidney disease of unknown aetiology (CKDu) is a kidney disease that progresses very slowly and is almost asymptomatic until severe and cannot be attributed to diabetes, hypertension, or any other known causes (Gooneratne et al., 2008; Jayasumana et al., 2013). In Cuttack district, India, the disease was identified for the first time in the early 2000s. The male population of the area is more susceptible to the disease compared to the women by a ratio of 3:2. However, young men under the age of 50 who participated in agricultural activities had a higher prevalence of the disease (Varma, 2015; Senapati et al., 2018; ICMR, 2020; Mohanty et al., 2020). Almost every household in the area has been diagnosed with the sickness. The cause of CKDu being endemic to a particular region is still unclear, and many researchers are striving to uncover it as thousands of people suffer from this illness. There are 697.5 million people with chronic kidney disease worldwide, with 115.1 million of them being Indian (Cockwell and lori-Ann, 2020). The key histological characteristics of CKDu are interstitial fibrosis, interstitial mononuclear cell infiltration, and tubular atrophy. These histological changes suggest a role for nephrotoxins in the origins of CKDu (Nanayakkara et al., 2012).

At high exposure levels (more than prescribed limit set by FAO/WHO, 2019; Table 2), cadmium (Cd), lead (Pb), and mercury (Hg) are regarded as nephrotoxins (Ekong et al., 2006; Johri et al., 2010; Soderland et al., 2010; Evans and Elinder, 2011). Metals progressively accumulate in the body through chronic low-level exposure, especially in industrialising countries. Pb, Hg, and Cd are found in air, food, petrol, polluted crops, and seafood (Jarup, 2003; Soderland et al., 2010). Phosphate fertilisers are the main source of heavy metal contamination in soil, as the phosphate minerals contain Cd as a natural impurity. Cd accumulation in plants beyond its permissible limit (0.05 mg/kg) can inhibit nutrient assimilation,

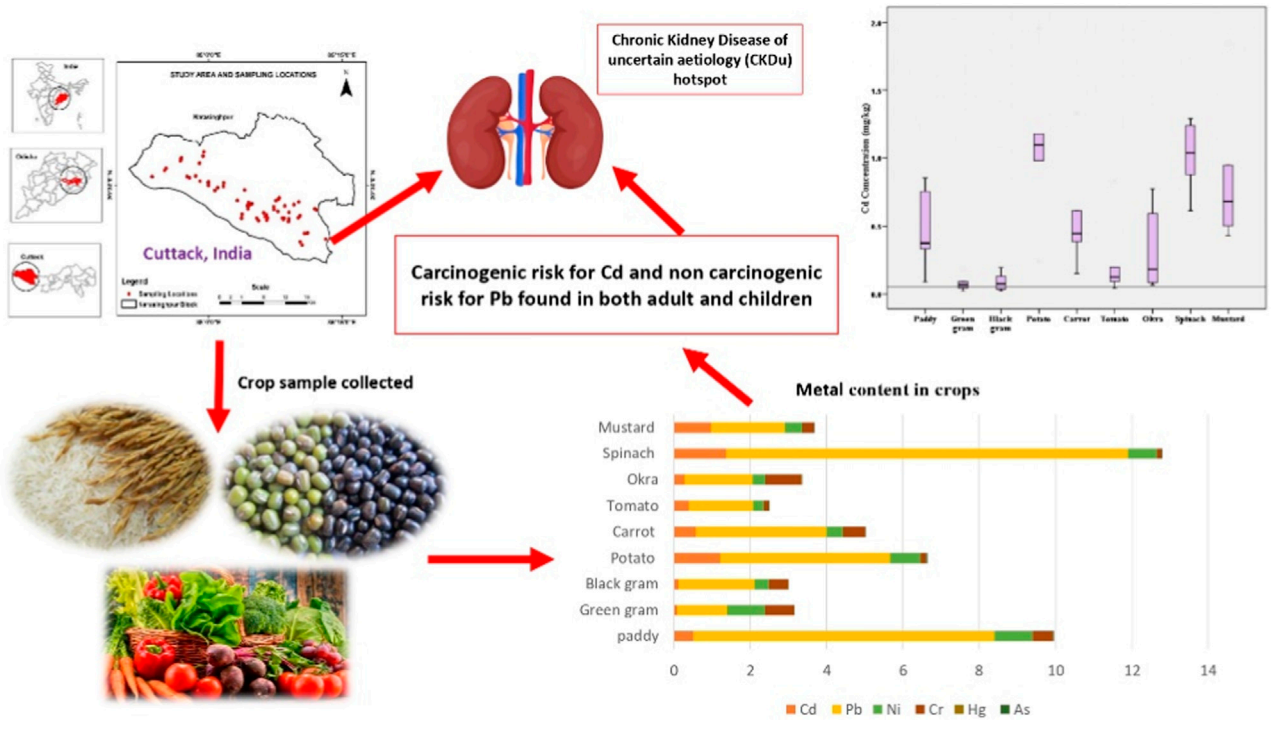

GRAPHICAL ABSTRACT

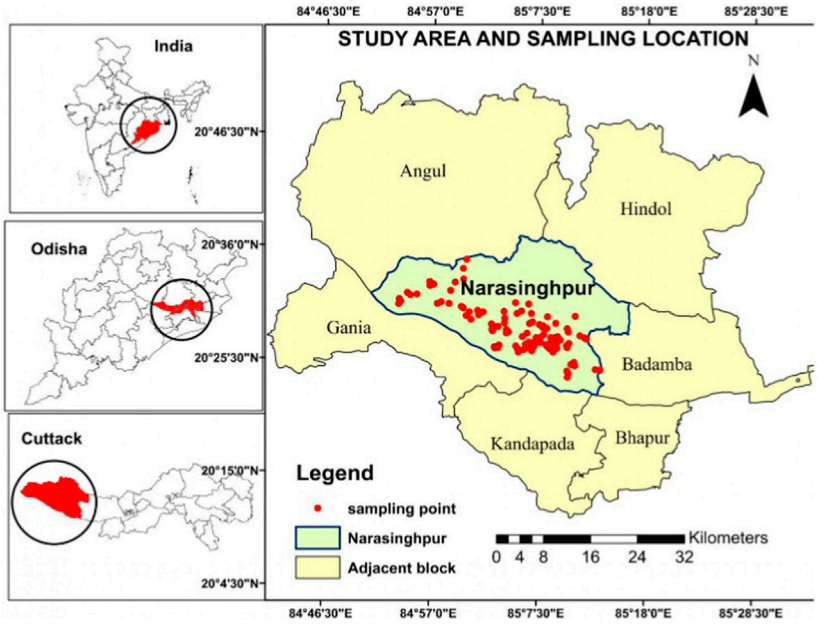

FIGURE 1
Sampling location in Cuttack district, Odisha.

carbohydrate metabolism, photosynthesis, and enzymatic activities, which in turn reduce yield (Nazar et al., 2012; Bakhshayesh et al., 2014). Cd deposits irreversibly in the human lungs, liver, and kidneys (Sobukola et al., 2010). It can trigger organ oxidative stress, inflammation, and lipid peroxidation (Prozialeck et al., 2006; Johri et al., 2010). Chronic low Cd exposure can damage renal proximal tubules and lower the glomerular filtration rate (GFR) in animal models (Thijssen et al., 2007). Also it may worsen diabetic kidney disease in humans and animals (Edwards and Prozialeck, 2009). Kidneys and liver produce a specialised protein called metallothionein, which protects the cells from Cd by binding tightly to it. Cancers of the prostate, kidneys, and ovaries have been linked to chronic Cd exposure (Nazar et al., 2012). Lead (Pb) is a hazardous metal that can enter the body via air, food, and water and cannot be eliminated by washing contaminated fruits and vegetables (Abbas et al., 2010). It is added to fuel as an anti-knocking agent; therefore, it is possible that this is another source of the high Pb levels seen in some leafy crops (Zamor et al., 2012). Pb poisoning causes mitochondrial enlargement in renal tubular cells and reduces energy generation (Evans and Elinder, 2011). Occupational exposure to mercury vapour may trigger albuminuria and acute membranous nephropathy (Li et al., 2010). The interrelation between chronic kidney disease (CKDu) and exposure to environmental toxins has been investigated primarily in western nations, with few data available for Asian countries.

No efforts have been made to detect heavy metals in the edible parts of locally grown crops that are consumed frequently by the inhabitants of the study area. Thus, this study examined the risk of six harmful heavy metals (Cd, Pb, Ni, Cr, Hg, and As) in CKDu affected areas of Cuttack district, Odisha. The quantities of heavy metals in rice, pulse, and vegetable crops were measured, and the health risk to nearby populations was estimated based on potential carcinogenic and noncarcinogenic risk factors.

2 Materials and methods

2.1 Study area

This study region in Cuttack, India, extended from 21°24′29″N to 81°40′19″E in latitude and longitude. The study area encompasses 3,432 km^2. The majority of the area falls under Narasinghpur block. The Narsinghpur block consisted of 157 villages and 98,000 residents. The average altitude was between 50 and 100 m, and the maximum was 337 m. In the highlands, red soils were found, whereas around the Mahanadi River, younger alluvial soil can be found. Potash and lime are present, but nitrogen, phosphorus, and humus are absent from these recent alluvial soils. The area under study comprises granitic rocks along with khondalite and charnokite minerals, which cover a nearly equal area in hard rock terrain (CGWB, 2013). The details of the sampling site are given in Figure 1.

2.2 Crop sampling

Nine crops, i.e., one cereal (rice), two pulses (green gram and black gram), and six vegetables belonging to three different groups of vegetable crops: root, fruit, and leafy vegetables (potato, carrot, tomato, okra, and spinach), were selected for the study, as these crops were mostly consumed and frequently grown in the study area according to our socioeconomic survey. The description of the examined crops is shown in Table 1. Samples from each site were collected in triplicate. A total of 118 crop samples were collected between January and March 2022. These samples were collected from the fields and taken to the laboratory for further analysis in polythene bags with proper tags. Each sample was washed with double-distilled water to eliminate grime and grease from the surface of the crop samples. Then the samples were cut into small

TABLE 1 Details of crops under study.

Sl.No.	Plant species	Family	English name	Part used	No. of samples
1	*Oryza sativa* L.	Poaceae	Rice	Grain	29
2	*Vigna radiata* L.	Fabaceae	Moong	Seed	20
3	*Vigna mungo* L.	Fabaceae	Urad	Seed	12
4	*Solanum tuberosum* L.	Solanaceae	Potato	Tubers	11
5	*Daucus carota* L.	Apiaceae	Carrot	Underground stem	5
6	*Solanum lycopersicum* L.	Solanaceae	Tomato	Fruit	11
7	*Abelmoschus esculentus* L.	Malvaceae	Okra	Fruit	8
8	*Spinacia oleracea* L.	Amaranthaceae	Spinach	Leaf	10
9	*Brassica juncea* L.	Brassicaceae	Mustard	Leaf	12

pieces with a stainless steel knife and air-dried for a week to reduce their moisture content. After air drying, samples were stored for 7 days in an oven at 65°C. The moisture content of samples was also determined by using the gravimetric method. After dehydrating the plant samples in an oven, they were grounded to a fine powder using a wooden mortar and pestle. Finally, the samples were stored at room temperature in airtight containers for further analysis (Sharma et al., 2009; Bhatia et al., 2015).

2.3 Heavy metal analysis

Plant samples were weighed precisely at 0.5 g and pre-digested overnight in 5 ml of nitric acid (HNO_3) before being digested with 5 ml of diacid (NHO_3+$HClO_4$) mixture on a heated plate under a hood until a clear solution was obtained. The recovery of Cd, Pb, Ni, Cr, Hg, As were 96%, 95%, 97%, 95%, 94%, 97%, respectively after digestion. The volume of the digested sample solution was increased to 50 ml with double-distilled water. Inductively coupled plasma optical emission spectroscopy (ICP-OES) (Model Avio 200) was utilised to determine the concentration of heavy metals (Cd, Pb, Ni, Cr, Hg, and As) in the digested and filtered samples by using a standard solution of each metal. Standard solutions were prepared for each element under study. The blank solution, which lacked the crop sample material, was made to calibrate the initial reading and minimise metal contamination in crop samples. The value of metals in unknown sample solutions (ppm) was multiplied by the dilution factor to determine the actual metal concentration in dried plant samples. Metal analysis of plant samples was conducted in accordance with standard procedures and methodology (Singh et al., 1999).

2.4 Quality check

The examination of specimens were conducted for the purposes of ensuring and maintaining quality control. Throughout the analytical procedures, the chemicals and reagents utilised were of analytical-grade quality. Double distilled water (DDW) was utilised in the preparation of the necessary reagents, standards, and analytical samples for processing and dilution purposes. Calibration curves were generated for each heavy metal under investigation. The analysis of blanks was conducted with regular frequency in order to maintain the analytical quality. To prevent any potential contamination in the equipment, procedural cleaning was performed at regular intervals using DDW during the whole analysis. The instrumental detection limit (IDL) values were found to be lower than both the method detection limit (MDL) and method quantification limit (MQL) values, indicating the high sensitivity of the inductively coupled plasma optical emission spectroscopy instrument for estimating heavy metals. Samples prepared for metal analysis included procedural blanks, replicate analyses, standard solutions and certified reference material (CRM) of white cabbage (BCR-679, European Commission Joint Research Centre, Institute for Reference Materials and Measurements). The certified values for Cd, Pb, Ni, Cr, Hg, and As are 1.66 ± 0.07, 37.21 ± 0.12, 27.0 ± 0.8, 11.23 ± 0.2, 6.17 ± 1.4, 3.21 ± 0.5 mg/kg, respectively. The values obtained for different metals viz., Cd, Pb, Cr, Ni, As, Hg were 94%, 92%, 88%, 86%, 84%, 89% of the certified value, respectively.

2.5 Health risk assessment

2.5.1 Estimated daily intakes (EDIs)

Estimated daily intakes (EDIs) of heavy metals (Cd, Pb, Ni, Cr, Hg, and As) (mg/day) were determined by multiplying the average concentration of heavy metals in crops by the weight of these foods consumed by a person. They are computed according to the following formula:

$$EDI = \frac{C_m \times C_f \times F_{IR} \times E_f \times D_e}{W_b \times T_{av}} \times 10^{-3}$$

Where, C_m represents crop metal concentration (mg/kg), C_f represents the conversion factor of crops into dry weight (0.085) (Arora et al., 2008), F_{IR} represents the average food consumption rate that was determined through a questionnaire survey in the study area (total of 378 individuals from the Narasinghpur block were surveyed), and then the data were used to compute the average food consumption rate shown in Table 5, E_f represents the exposure frequency (365 days), D_e represents the exposure duration

(70 years), T_{av} represents the average time of exposure (365 days × 70) and W_b represents the average body weight of an individual (70 kg for adults and 15 kg for children) (WHO, 1985; USEPA, 2010).

2.5.2 Target hazard quotient (THQ)

The United States Environmental Protection Agency's (USEPA) risk-based concentration table (USEPA, 2010) was used as the basis for the calculation of non-carcinogenic risks. Using the THQ, which is the ratio of single metal exposure over a given time to a reference dose (Df) for that metal over the same time period, the noncarcinogenic risk of ingesting metals through food crops were evaluated. The THQ can be estimated with the following equation:

$$THQ = \frac{EDI}{D_f}$$

Where, EDI is the estimated daily intake and D_f is the reference dose for metals. D_f for Cd, Pb, Ni, Cr, Hg, and As is 0.001, 0.0035, 0.02, 0.003, 0.0003, and 0.0003 mg/kg/day, respectively (USEPA, 2006). THQ values more than one indicates harmful noncarcinogenic effect on human health. However, THQ value less than one considered to be safe for consumption (Antoine et al., 2017).

2.5.3 Hazard index (HI)

The hazard index (HI) was developed to quantify the potential noncarcinogenic impacts of multiple heavy metals, and it is based on the risk assessment standards established by the USEPA. (1999). It is the sum of the hazard quotients (USEPA, 2010). The following equation is used to calculate the hazard index:

$$HI = \sum THQ$$
$$= THQ_{Cd} + THQ_{Pb} + THQ_{Ni} + THQ_{Cr} + THQ_{Hg} + THQ_{AS}$$

If HI is greater than one, then exposure to multiple elements has a negative impact on human health. The extent of the negative effect is considered to be proportional to the total of multiple metal exposures (Proshad et al., 2020).

2.5.4 Carcinogenic risk

The equation described in USEPA risk-based concentration (USEPA, 2006) can be used to estimate the target carcinogenic hazards associated with metals like Cd and Pb, which have been shown to cause cancer in humans. It can be calculated using the following formula:

$$CR = EDI \times CFS_O$$
$$TCR = \sum CR$$

Here, CR represents the carcinogenic risk, EDI represents the estimated daily intake, and CS_o represents the carcinogenic slope factor for metals (ATSDR, 2010; Feed, 2013; Wei et al., 2020). Cd and Pb have oral cancer slope factors (CPSo) of 0.38 and 0.0085 mg kg^{-1} day^{-1}, respectively. TCR values below 10^{-6} correspond to low cancer-causing risks; between 10^{-5} and 10^{-4} correspond to moderate cancer-causing risks; and between 10^{-3} and 10^{-1} correspond to high cancer-causing risks (Demirezen and Aksoy, 2006; Liu et al., 2006; USEPA, 2015).

2.6 Statistical analysis

IBM SPSS 22.0 software was used to perform statistical analysis of the data. Standard deviations and mean concentrations of metals in rice, pulses, and vegetables were calculated. The potential source of metals in food samples can be interpreted through a multivariate analysis using principal components. KMO values for this particular study is found to be 0.839 indicating the sampling is adequate for conducting factor analysis (Dodge, 2008). In the principal component analysis (PCA), eigen values were extracted to determine the principal components (PC). A dendrogram was constructed using Ward's method to categorize crops into different groups. From the cluster analysis, similarities and differences between samples with respect to metal content were identified. The rest of the calculations were done in Microsoft Excel 2013.

3 Results and discussion

3.1 Total heavy metal concentration in crops

The total concentration of Cd, Pb, Ni, Cr, Hg, and As in rice, pulses, and vegetables (mg/kg) was assessed, and their values were presented in Table 2 and Figure 2. The overall heavy metal concentrations in the samples were as follows: Pb>Ni>Cd>Cr>As>Hg. Among crop species, the average concentration of metals was as follows: spinach > rice > okra > mustard > potato > carrot > tomato > green gram > black gram. When comparing the metal concentration in crop samples with the permitted limit given by FAO/WHO (2019), it was found that the metal concentration in 89.91%, 100%, 0%, 0%, 10.08%, and 2.52% of samples, respectively, was above the permissible limit for Cd, Pb, Ni, Cr, Hg, and As (Table 2; Figure 2). Heavy metal concentrations were observed to vary significantly between samples due to environmental factors such as temperature, rainfall, crop growth stage, and metal accumulation and absorption capacities (Liu et al., 2006; Pandey and Pandey, 2009; Saha and Zaman, 2013; Garg et al., 2014). Phyto-accumulation of heavy metals, for instance, was shown to be greater in cassava tubers than in leaves (Harrison et al., 2018).

The average concentration of Pb (mg/kg) in the crop sample followed the decreasing order of spinach (10.51), paddy (7.88), potato (4.45), carrot (3.41), black gram (1.99), mustard (1.93), okra (1.78), tomato (1.68), and green gram (1.31) (Table 2). It was observed that the lead concentration in all samples was higher than the standard value (0.1 mg/kg) (FAO/WHO, 2019), suggesting excessive lead contamination in food crops grown in the study area and potential health risks to consumers. It was clear that spinach, paddy, potato, carrot, black gram, mustard, okra, tomato, and green gram contain 105, 79, 44.5, 34, 20, 19, 18, 17, and 13 times more concentrations of Pb than the MAC (Table 2). Cd and Pb accumulate in the renal cortex and bone, respectively. Metals have decades-long biological half-lives. Due to these long half-lives (Cd > 30 years), sustained, low-level exposure might produce excess accumulation in organs, especially in the kidney, which can disrupt the physiological function of the organ (Sharma et al., 2007; Navas-Acien et al., 2009).

TABLE 2 Metal concentration (mg/kg) in crop samples.

Common name	Scientific name	Cd	Pb	Ni	Cr	Hg	As
		(mg/kg)					
paddy (n=29)	*Oryza sativa* L.	0.52±0.43	7.88±5.86	1.00±0.47	0.54±0.14	0.005±0.012	0.019±0.027
Green gram (n=20)	*Vigna radiata* L.	0.09±0.06	1.31±0.87	0.99±0.46	0.77±0.11	ND	0.013±0.015
Black gram (n=12)	*Vigna mungo* L.	0.12±0.11	1.99±0.94	0.38±0.31	0.51±0.18	0.001±0.004	0.008±0.006
Potato (n=11)	*Solanum tuberosum* L.	1.22±0.95	4.45±2.37	0.80±0.39	0.15±0.05	0.004±0.006	0.037±0.054
Carrot (n=5)	*Daucus carota* L.	0.58±0.45	3.41±1.21	0.43±0.28	0.60±0.13	ND	0.009±0.006
Tomato (n=11)	*Solanum lycopersicum* L.	0.39±0.34	1.68±1.12	0.29±0.18	0.13±0.18	0.002±0.006	0.020±0.022
Okra (n=8)	*Abelmoschus esculentus* L.	0.27±0.26	1.78±1.08	0.34±0.19	0.94±0.09	0.019±0.028	0.016±0.014
Spinach (n=10)	*Spinacia oleracea* L.	1.37±0.73	10.51±5.98	0.76±0.32	0.12±0.09	0.002±0.005	0.013±0.012
Mustard (n=12)	*Brassica juncea* L.	0.97±0.49	1.93±1.15	0.46±0.17	0.30±0.35	ND	0.013±0.015
Permissible limit FAO/WHO, (2019)		0.05	0.10	10	2.3	0.01	0.10
Percent Sample exceeding permissible limit		89.91	100.00	0.00	0.00	10.08	2.52

The average Ni concentration in crops varied from 0.29 (tomato) to 1 mg/kg (rice) (Table 2). In crop samples, the concentration of Ni was as follows: rice > green gram > potato > spinach > mustard > carrot > black gram > okra > tomato. The concentration of nickel in all samples was less than the standard amount (10 mg/kg) (JECFA, 2003; FAO/WHO, 2019; WHO, 2011), showing that nickel did not contaminate the food samples (Figure 2).

Cadmium is a hazardous heavy metal present in very low concentrations in the environment. Air and water are known to be the primary sources of Cd exposure (FSANZ, 2003). The average Cd content varied from 0.09 (green gram) to 1.37 (spinach) mg/kg. In crop samples, the average Cd concentration (mg/kg) was as follows: spinach (1.37), potato (1.22), mustard (0.94), carrot (0.58), paddy (0.52), tomato (0.39), okra (0.27), black gram (0.12), green gram (0.09). In accordance with the maximum allowable concentration (MAC), the cadmium concentration in 89.91% of samples was higher than the standard value (0.05 mg/kg) (FAO/WHO, 2019). It was found that spinach, potato, mustard, carrot, paddy, tomato, okra, black gram, and green gram contain Cd concentrations that are 27, 24, 19, 12, 10, 8, 5, 2.5, and 2 times more than the maximum allowable concentration (MAC) (Table 2).

The average Cr concentration varied from 0.12 (spinach) to 0.94 mg/kg (okra) (Table 2). In crop samples, the average Cr content were as follows: okra > green gram > carrot > paddy > black gram > mustard > potato > tomato > spinach. Chromium concentrations in all samples were less than the standard value (2.3 mg/kg) (FAO/WHO, 2019), showing no chromium contamination of food samples (Figure 2).

The mean As concentration (mg/kg) in crop samples was in descending order as follows: potato (0.037), tomato (0.020), paddy (0.019), okra (0.016), green gram, mustard, okra (0.013), and black gram (0.008). According to Table 2, the arsenic concentration of 2.52 percent of the samples were higher than the standard value (0.1 mg/kg) given by FAO/WHO. (2019), which may pose a health risk to consumers. Rapid transfer of As from soil to plant, irrational use of As rich fertilizers and pesticides, and use of contaminated groundwater for irrigation may contribute to the presence of arsenic in crops (Alam et al., 2003; Renner, 2004; Neumann et al., 2010; Bhuiyan et al., 2011; Roberts et al., 2011; Polizzotto et al., 2013).

The average Hg concentration varied from 0 (green gram, carrot, and mustard) to 0.019 mg/kg (okra) (Table 2). Average Hg concentrations in crop samples were as follows: okra > paddy > potato > tomato > spinach > black gram > green gram > carrot > mustard. According to MAC, the Hg concentration in 10% of samples was higher than the standard value (0.01 mg/kg) given by FAO/WHO (2019), indicating a low level of mercury contamination in food samples (Figure 2).

Long-term consumption of food crops contaminated with heavy metals may pose numerous health risks to humans. Therefore, routine monitoring is essential to avoid excess accumulation of these metals in the food chain (Sharma et al., 2009; Kananke et al., 2014; Noor et al., 2022). According to Yana et al. (2012), heavy metals in leafy vegetables come from both soil and smelting waste gases, while those in fruits and roots come from soil and may vary by season (Tani and Barrington, 2005). Chronic exposure to Cd, Pb, As, and Hg causes renal tubular alterations, especially in the proximal convoluted tubule, and, in rare cases, acute renal failure that leads to chronic kidney disease (Gunawardana et al., 2006; Ferraro et al., 2010; Rango et al., 2015; Asraf et al., 2021). Lead is linked to terminal stages, although more research is needed (Ekong et al., 2006; Garcia and Arceo, 2018). In CKDu affected areas of Sri Lanka, Ni, Cd, Cr, and Pb contamination levels in vegetables exceeded FAO/WHO standards for human consumption (Bandara et al., 2010; Kananke et al., 2014; Kananke et al., 2016). In sensitive individuals with hypertension or diabetes, consumption of foods with high Cd may synergistically develop and progress CKD (Kim et al., 2015). The main irrigation source in the study area is the Mahanadi River, which flows adjacent to it and contains contaminated water and detritus. In Mahanadi sediments, Pb and Cd enrichment factors were higher, indicating contamination from many external sources (Nayak et al., 2002; Swain et al., 2021; Samal et al., 2022).

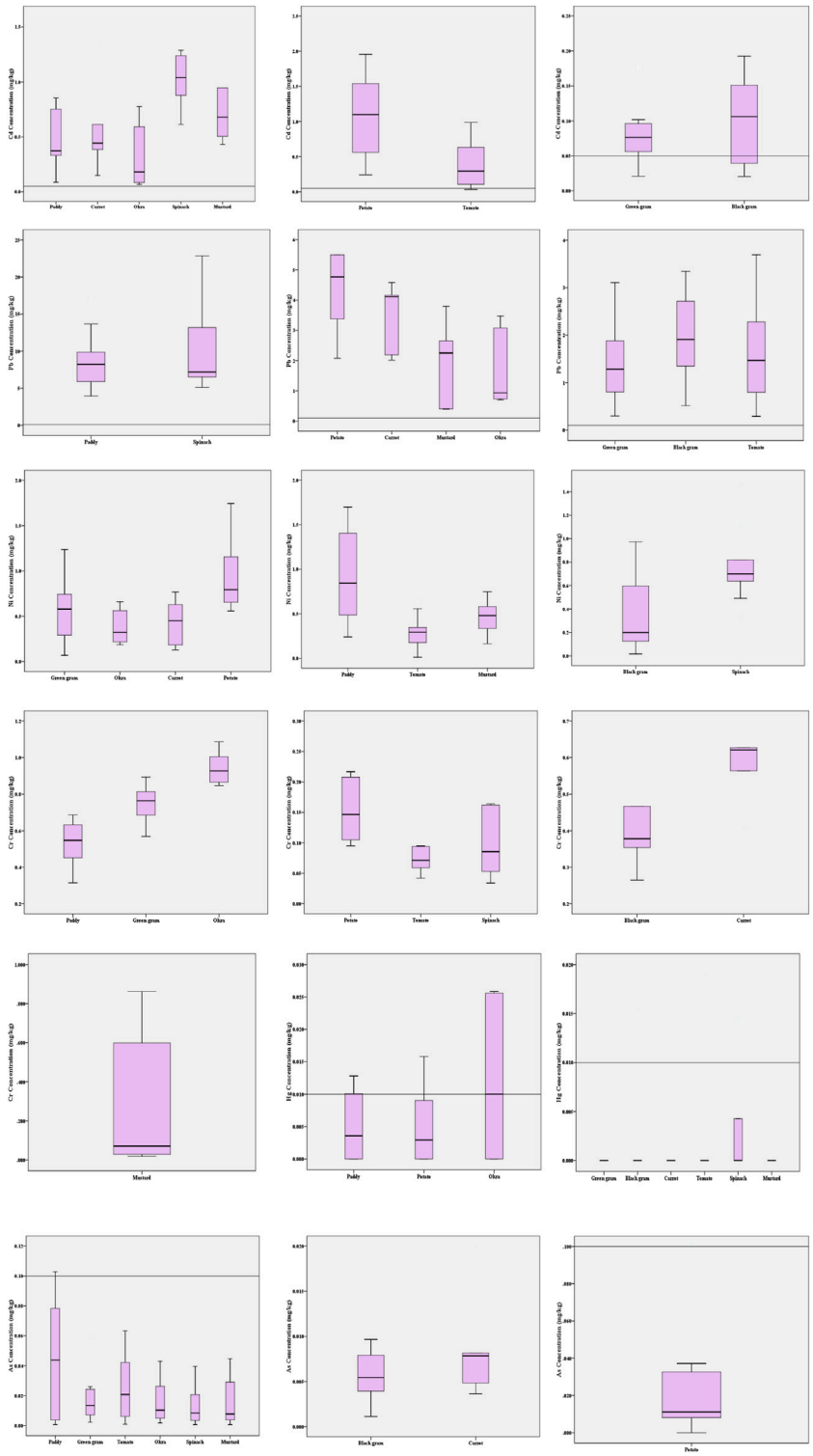

FIGURE 2
Heavy metals distribution in crop samples (n = 118) collected from CKDu hotspot of Cuttack district, India.

3.2 Correlation coefficient matrix of heavy metals

To determine the relationships between the metals in food samples, statistical analyses were conducted. From the intermetallic interaction in a particulate medium, the source and migration routes of the metals can be predicted (Raknuzzaman et al., 2016; Muhammad et al., 2021). The correlation coefficient matrix of heavy metals in food samples taken from CKDu-endemic regions in the Cuttack district is

TABLE 3 Pearson correlation coefficient of heavy metals in crop samples.

	Cd	Pb	Ni	Cr	Hg	As
Cd	1					
Pb	.277**	1				
Ni	.229*	.280**	1			
Cr	−.363**	−0.175	0.178	1		
Hg	−0.024	0.066	−0.061	.202*	1	
As	0.097	0.166	0.088	−0.111	0.07	1

**Correlation is significant at the 0.01 level (2-tailed).
*Correlation is significant at the 0.05 level (2-tailed).

presented in Table 3. Cd showed significant positive correlations with Pb and Ni (r = 0.277**, r = 0.229**), while significant negative correlations were seen between Cd and Cr (r = −363**). Pb and Cr both showed positive correlations with Ni and Hg, respectively, that were statistically significant (r = 0.280** and r = 0.202*, respectively). According to Abbasi et al. (2013) and Mohammed et al. (2003), the combinations exhibited a strong positive association, showing that the traits were related and may have derived from the same sources. Other connections between the components of the meal sample were not significant.

3.3 Analysis of the source of heavy metals in crops

Principal component analysis (PCA) was performed to determine the possible sources of heavy metals in the food crop collected from the study area (Franco-Uria et al., 2009; Kikuchi et al., 2009; Manea et al., 2020). Table 4 and Figure 3 display the results of PCA. Three principal components were found, and together they accounted for 67.01% of the variations in food crops. The variances explained by the first three PCs for crop samples were 28.40%, 21.11%, and 17.48%, respectively. PC1 has a strong correlation with Cd and Pb, PC2 has a strong correlation with Ni and Cr, and PC3 has a strong correlation with Hg and As. Cd had accumulated in the analyzed crops as a result of the widespread use of phosphate (P) fertilizers in agricultural soils (Mortvedt, 1996; Nziguheba and Smoulders, 2008; Hove et al., 2020); hence, Pb, which was significantly related to Cd in PC1, may also be significantly influenced by irrational use of fertilizers and agrochemicals (Huang et al., 2007; Atafar et al., 2010; Iqbal et al., 2021). Decades of intensive cultivation in the agricultural region and long-term application of fertilizer may be a significant source of heavy metal accumulation in crops. The Mahanadi River, which borders the affected area, contains additional evidence of industrial and anthropogenic contamination in its water and sediments (Behera et al., 2013; Raj et al., 2013; Swain et al., 2021). In conclusion, PC1 and PC3 can be inferred as anthropogenic components, which are more significantly influenced by human actions (fertilizer application) than other components. A significant association between Cr and Ni in PC2 indicated their origin from lithogenic sources as they have been detected in the parent materials of rural soils across the globe, with minimal temporal and spatial variation (Facchinelli et al., 2001; Salonen and Korkka-Niemi, 2007; Spurgeon et al., 2008; Wu et al., 2010; Kladsomboon et al., 2020). Thus, metals in PC1, PC2, and PC3 may derived from a variety of natural and anthropogenic sources, including industrial effluents, agricultural activities, and the granitic bedrock underlying the research region. Also from the dendrogram constructed using Ward's method, several cluster configurations were identified and food samples belonging to the same cluster shared similar characteristics with respect to their metal contamination level (Figure 4). Within a distance of five on the dendrogram scale, the main clusters of various food items developed, including potatoes, tomatoes, rice, spinach, carrots, mustard, black gram, okra, and green gram.

3.4 Health risk assessment

The USEPA has developed several indices (both non-carcinogenic and carcinogenic) to predict the potential health risk posed by long-term exposure to hazardous metals (Ali et al., 2019).

3.4.1 Estimated daily intake (EDI)

The most prevalent route of trace metal exposure for humans is through food (WHO, 1985; Kumar et al., 2019; Saraswat et al., 2023); however, inhalation and skin contact are also possible (ATSDR, 2010). Rice, pulses, and vegetables may make up a significant share of the Indian population's total diet, and EDI is a significant method for assessing the health hazards associated with heavy metals through the consumption of these food items (Alam et al., 2003; Alsafran et al., 2021). Its calculation is based on the total metal concentration in food and their consumption rate in adults and children; the results are presented in Table 5. If the ratio of EDI to Df is less than Df, the health risk is minimal; if it is between 1 and 5 times the Df, there is a low health risk; five to ten times the Df, there is a moderate health risk; more than ten times the Df, there is a high health risk (Ali et al., 2019; Saxena et al., 2019). Based on the EDI/Df ratio, we determined that the metal content in pulses is between 5 and 10 times higher, posing a moderate health risk, while the metal content in rice and vegetables is greater than 10 times higher, posing a high health risk for consuming these crops grown in this region. Based on these results, we concluded that Cd, Pb, and Ni posed the greatest threat to the health of adults and children living in endemic regions of CKDu in the Cuttack district of India.

3.4.2 Target hazard quotient (THQ)

THQ is linked to a noncarcinogenic health risk, and its value less than 1 is considered as permissible (Rattan et al., 2005). If THQ levels exceed a certain threshold, it will pose a health risk (USEPA, 1989; Bounar et al., 2020). The calculated THQ value was presented in Table 6. In this investigation, for Pb, THQ values in rice were greater than 1. Therefore, their THQ levels may pose a noncarcinogenic risk to the population in this region. From these values, we determined that for Cd and Pb, the THQ values of spinach and mustard were higher than those of other vegetables and pulses under study (Gupta et al., 2019), whereas no such pattern was observed for other elements.

TABLE 4 Total variance explained and component matrices for the heavy metals in crops collected from Cuttack district, India.

Component	Initial eigenvalues			Extraction sums of squared loadings			Rotation sums of squared loadings		
	Total	% Of variance	Cumulative %	Total	% Of variance	Cumulative %	Total	% Of variance	Cumulative %
1	1.70	28.40	28.40	1.70	28.40	28.40	1.50	24.97	24.97
2	1.27	21.11	49.51	1.27	21.11	49.51	1.40	23.34	48.31
3	1.05	17.49	67.01	1.05	17.49	67.01	1.12	18.69	67.01
4	0.88	14.66	81.66						
5	0.69	11.43	93.09						
6	0.42	6.91	100.00						
	Component Matrix			Rotated Component Matrix			Component Transformation Matrix		
Element	PC1	PC2	PC3	PC1	PC2	PC3	PC1	PC2	PC3
Cd	0.75	−0.12	−0.05	−0.63	0.43	0.05	−0.74	0.64	0.20
Pb	0.69	0.29	0.05	−0.33	0.59	0.31	0.65	0.60	0.46
Ni	0.44	0.60	−0.54	0.16	0.90	−0.10	−0.18	−0.47	0.87
Cr	−0.54	0.70	−0.20	0.89	0.17	0.04			
Hg	−0.11	0.53	0.67	0.31	−0.07	0.80			
As	0.40	0.18	0.52	−0.27	0.12	0.61			

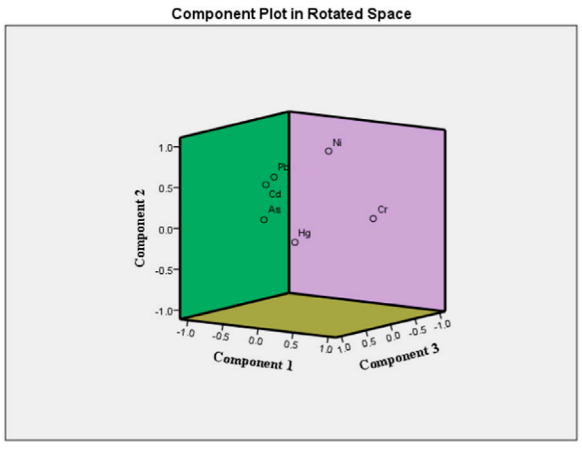

FIGURE 3
Principal component analysis (PCA) of heavy metals in food samples (*n* = 118) collected from different agricultural fields of Cuttack district, Odisha.

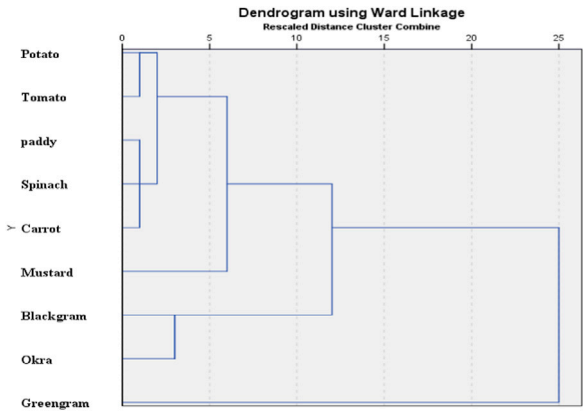

FIGURE 4
Cluster analysis of crop samples (*n* = 118) collected from Cuttack district, India.

3.4.3 Hazard index (HI)

HI provides a measure of the cumulative impact of harmful metals on human health through consumption of contaminated food crops (Filimon et al., 2021), and the data in Table 6 demonstrated that HI values for rice were higher than the allowed limit. Hence, consumption of rice grown in the study area may be associated with noncancerogenic health risks. The hazard index for adults and children was as follows: rice>spinach>potato>carrot>tomato>okra>mustard>green gram>black gram. In this study, only a limited number of food crops were evaluated to estimate the noncarcinogenic health risk. So, the results only considered a minor portion of the actual threat to the people in the study area.

3.4.4 Target carcinogenic risk (TCR)

Toxic metals are thought to have potential adverse effects on human health, and research suggests that exposure to certain carcinogenic metals, especially over extended periods of time, can raise the risk of developing cancer. TCR is an estimate of the expected malignancy. Then, it also indicates the possibility of cancer-causing hazards developing within an individual. TCR for

TABLE 5 Consumption rate (g/person/day), estimated daily intake (EDI) and total estimated daily intake (EDI) (mg/kg bw/day) of heavy metals from rice, pulse and vegetables for adult and children.

Food stuff	Consumption rate (g/person/day)		Cd		Pb		Ni		Cr		Hg		As		TEDI	
	Adult	Children	Adult	Children	Adult	Children	Adult	Children	Adult	Children	Adult	Children	Adult	Children	Adult	Children
Rice	400	160	0.00025	0.000467	0.003826	0.007143	0.004862	0.009075	0.00026	0.000485	2.38E-06	4.44E-06	9.21E-06	1.72E-05	0.0092	0.0172
Green gram	45	18	4.84E-06	9.03E-06	7.14E-05	0.000133	0.00054	0.001009	4.18E-05	7.8E-05	0	0	7.05E-07	1.32E-06	0.0007	0.0012
Black gram	35	14	5.07E-06	9.47E-06	8.45E-05	0.000158	0.000372	0.000695	2.17E-05	4.06E-05	5.48E-08	1.02E-07	3.5E-07	6.53E-07	0.0005	0.0009
Potato	59	23	5.86E-05	0.000107	0.000319	0.00058	0.000786	0.001429	2.48E-05	4.51E-05	2.84E-07	5.16E-07	2.64E-06	4.8E-06	0.0012	0.0022
Carrot	43	17	3.05E-05	5.63E-05	0.000178	0.000329	0.000643	0.001186	3.11E-05	5.74E-05	0	0	4.63E-07	8.54E-07	0.0009	0.0016
Tomato	53	21	2.53E-05	4.67E-05	0.000108	0.0002	0.000699	0.001292	8.19E-06	1.51E-05	1.32E-07	2.43E-07	1.3E-06	2.41E-06	0.0008	0.0016
Okra	51	20	1.7E-05	3.11E-05	0.00011	0.000202	0.000394	0.000721	5.83E-05	0.000107	1.19E-06	2.17E-06	9.91E-07	1.81E-06	0.0006	0.0011
Spinach	38	15	6.34E-05	0.000117	0.000393	0.000724	0.00063	0.00116	5.48E-06	1.01E-05	8.74E-08	1.61E-07	6.11E-07	1.13E-06	0.0011	0.0020
Mustard	30	12	3.55E-05	6.63E-05	7.02E-05	0.000131	0.000169	0.000315	1.11E-05	2.07E-05	0	0	4.71E-07	8.79E-07	0.0003	0.0005

10.3389/fenvs.2023.1248373

TABLE 6 Target hazard quotient (THQ) (noncarcinogenic risk), hazard index (HI) and total target hazard quotient (TTHQ) of heavy metals from rice, pulses and vegetables for adult and children.

	Cd		Pb		Ni		Cr		Hg		As		TTHQ (adult)	TTHQ (children)
	Adult	Children	Adult	Children	Adult	Children	Adult	Children	Adult	Children	Adult	Children		
Rice	0.250	0.467	1.093	2.041	0.243	0.454	0.087	0.162	0.008	0.015	0.031	0.057	1.712	3.196
Green gram	0.005	0.009	0.020	0.038	0.027	0.050	0.014	0.026	0.000	0.000	0.002	0.004	0.069	0.128
Black gram	0.005	0.009	0.024	0.045	0.019	0.035	0.007	0.014	0.000	0.000	0.001	0.002	0.056	0.105
Potato	0.059	0.107	0.091	0.166	0.039	0.071	0.008	0.015	0.001	0.002	0.009	0.016	0.207	0.377
Carrot	0.031	0.056	0.051	0.094	0.032	0.059	0.010	0.019	0.000	0.000	0.002	0.003	0.125	0.231
Tomato	0.025	0.047	0.031	0.057	0.035	0.065	0.003	0.005	0.000	0.001	0.004	0.008	0.099	0.182
Okra	0.017	0.031	0.032	0.058	0.020	0.036	0.019	0.036	0.004	0.007	0.003	0.006	0.095	0.174
Spinach	0.063	0.117	0.112	0.207	0.031	0.058	0.002	0.003	0	0.001	0.002	0.004	0.211	0.389
Mustard	0.036	0.066	0.020	0.037	0.008	0.016	0.004	0.007	0	0.000	0.002	0.003	0.069	0.129
HI	0.491	0.910	1.474	2.742	0.455	0.844	0.154	0.286	0.014	0.025	0.056	0.103	2.644	4.912

10.3389/fenvs.2023.1248373

TABLE 7 Carcinogenic risks of Cd and Pb due to consumption rice, pulse and vegetables for adult and children.

Crop sample	Cd	Cd	Pb	Pb
	Adult	Children	Adult	Children
Rice	9.52E-05	1.78E-04	3.25E-05	6.07E-05
Green gram	1.84E-06	3.43E-06	6.07E-07	1.13E-06
Black gram	1.93E-06	3.6E-06	7.18E-07	1.34E-06
Potato	2.23E-05	4.05E-05	2.71E-06	4.93E-06
Carrot	1.16E-05	2.14E-05	1.51E-06	2.79E-06
Tomato	9.6E-06	1.78E-05	9.18E-07	1.7E-06
Okra	6.46E-06	1.18E-05	9.39E-07	1.72E-06
Spinach	2.41E-05	4.44E-05	3.34E-06	6.15E-06
Mustard	1.35E-05	2.52E-05	5.97E-07	1.11E-06
Total	1.86E-04	3.46E-04	4.39E-05	8.16E-05

Cd and Pb via consumption of contaminated food crops, as estimated by EDI and CPSo values, is displayed in Table 7. If TCR values are between 10^{-6} and 10^{-5}, they are associated with low cancer risks; if they are between 10^{-5} and 10^{-4}, they are associated with moderate risks; and if they are between 10^{-3} and 10^{-1}, they are associated with high risks (Ali et al., 2019). The TCR values for Cd in the crop samples were 1.86E-04 and 3.46E-04 for adults and children, respectively (Table 7). Similarly, for Pb, it was 4.39E-05 for adults and 8.16E-05 for children. The cumulative carcinogenic risk of Cd from the foods was greater than 10^{-4}, indicating cancer risk to both adults and children in the study area. In the current study, however, the TCR of Pb is between 10^{-5} and 10^{-4}, posing a moderate cancer risk (USEPA, 1989; USEPA, 2015; Fonge et al., 2021). Due to the high cadmium content of some local foods, residents of the endemic area may consume more cadmium than is healthy on a daily basis. This can have serious consequences for the kidneys, especially in the young, the elderly, and those with underlying medical conditions. A cross-sectional investigation suggested cadmium as a risk factor for CKDu in Sri Lanka due to its greater urinary excretion and dose-effect connection with CKDu stages. When exposed to nephrotoxins, selenium deficiency and genetic vulnerability may predispose to CKDu (Jayatilake et al., 2013; Gupta et al., 2021). Therefore, the potential carcinogenic hazards posed by food consumption to residents of the CKDu endemic area must not be ignored. Thus, the present research demonstrates unequivocally that the Cuttack populace's consumption of these foods poses a cancer risk.

4 Conclusion

The current study examined the heavy metal concentration of commonly consumed and locally grown food crops in CKDu-endemic areas of Cuttack district, India. It was found that the levels of Cd, Pb, Hg, and As in rice, pulses, and vegetables exceeded the WHO and FAO permissible levels. Metal concentrations in food samples were as follows: Pb>Ni>Cd>Cr>As>Hg. A multivariate study revealed that Cd, Pb, Ni, Cr, Hg, and As in dietary samples were primarily caused by both natural and anthropogenic activities. EDI for Cd and Pb was increased in both adults and children. THQ for Pb was over the permissible limit, putting consumers at high risk for non-cancerogenic risks associated with Pb. Based on the calculated hazard index for adults and children, it was evident that consuming rice was not safe. While the risk of Pb from the majority of meals was below the permitted level of 10^{-5}, the total carcinogenic risk of Cd was greater than 10^{-4}, indicating a cancer risk to both adults and children in the study area. Longitudinal studies are needed to assess the links between heavy metals like Cd and Pb and kidney impairment due to their extensive prevalence in the environment and the lack of treatment strategies to reduce their effects. Thus, chronic impacts might be determined and environmental monitoring increased to lower chemical concentrations. We recommend combining governmental and private sector efforts with research centres to further study into the disease's causes and remedies.

Data availability statement

The original contributions presented in the study are included in the article/Supplementary Material, further inquiries can be directed to the corresponding author.

Author contributions

SM and RN: Conceptualization, Methodology, Software; SM and KM: Data curation, Writing–TableOriginal draft preparation. SM, KP, and BJ: Visualization, Investigation. RN and BJ: Supervision: SM, KKM, and SS: Software, Validation: PD, JD, AS, SB, JN, and SP: Writing–Reviewing and Editing. All authors contributed to the article and approved the submitted version.

Acknowledgments

Author SM has received financial support from University Grant Commission (UGC), New Delhi, India in form of Junior Research Fellowship (JRF) during her PhD tenure to conduct this research work.

Conflict of interest

The authors declare that the research was conducted in the absence of any commercial or financial relationships that could be construed as a potential conflict of interest.

Publisher's note

References

Abbas, M., Parveen, Z., Iqbal, M., Riazuddin, S., Ahmed, M., Bhutto, R., et al. (2010). Monitoring of toxic metals (cadmium, lead, arsenic and mercury) in vegetables of sindh, Pakistan. *Kathmandu Univ. J. Sci. Eng. Technol.* 6 (II), 60–65. doi:10.3126/kuset.v6i2.4013

Abbasi, A. M., Iqbal, J., Khan, M. A., and Shah, M. H. (2013). Health risk assessment and multivariate apportionment of trace metals in wild leafy vegetables from Lesser Himalayas, Pakistan. *Pak. Ecotox. Environ. Saf.* 92, 237–244. doi:10.1016/j.ecoenv.2013.02.011

Abuduwailil, J., Zhaoyong, Z., and Fengqing, J. (2015). Evaluation of the pollution and human health risks posed by heavy metals in the atmospheric dust in Ebinur Basin in Northwest China. *Environ. Sci. Pollut. Res.* 1–14, 14018–14031. doi:10.1007/s11356-015-4625-1

Alam, M. G. M., Snow, T., and Tanaka, A. (2003). Arsenic and heavy metal contamination of vegetables grown in Samta village, Bangladesh. *Sci. Total. Environ.* 308, 83–96. doi:10.1016/s0048-9697(02)00651-4

Ali, H., Khan, E., and Ilahi, I. (2019) Environmental Chemistry and Ecotoxicology of Hazardous Heavy Metals: Environmental Persistence, Toxicity, and Bioaccumulation. *Journal of Chemistry*.

Alsafran, M., Usman, K., Rizwan, M., Ahmed, T., and Al Jabri, H. (2021). The carcinogenic and non-carcinogenic health risks of metal(oid)s bioaccumulation in leafy vegetables: a consumption advisory. *Front. Environ. Sci.* 9, 742269. doi:10.3389/fenvs.2021.742269

Antoine, J. M. R., Fung, L. A. H., and Grant, C. N. (2017). Assessment of the potential health risks associated with the aluminium, arsenic, cadmium and lead content in selected fruits and vegetables grown in Jamaica. *Toxicol. Rep.* 4, 181–187. doi:10.1016/j.toxrep.2017.03.006

Arora, M., Kiran, B., Rani, S., Rani, A., Kaur, B., and Mittal, N. (2008). Heavy metal accumulation in vegetables irrigated with water from different sources. *Food. Chem.* 111, 811–815. doi:10.1016/j.foodchem.2008.04.049

Ashraf, I., Ahmad, F., Sharif, A., Altaf, A. R., and Teng, H. (2021). Heavy metals assessment in water, soil, vegetables and their associated health risks via consumption of vegetables, district kasur, Pakistan. *SN Appl. Sci.* 3, 552. doi:10.1007/s42452-021-04547-y

Atafar, Z., Mesdaghinia, A., Nouri, J., Homaee, M., Yunesian, M., Ahmadimoghaddam, M., et al. (2010). Effect of fertilizer application on soil heavy metal concentration. *Environ. Monit. Assess.* 160 (1), 83–89. doi:10.1007/s10661-008-0659-x

ATSDR (Agency for toxic substance and disease registry) (2010). *Public health assessment and health consultation*. Washington, Quicy: CENEX supply and marketing. Avaliable At: https://www.atsdr.cdc.gov.

Bakhshayesh, B. E., Delkash, M., and Scholz, M. (2014). Response of vegetables to cadmium-enriched soil. *Water* 6, 1246–1256. doi:10.3390/w6051246

Bandara, J. M., Wijewardena, H. V., Liyanege, J., Upul, M. A., and Bandara, J. M. (2010). Chronic renal failure in Sri Lanka caused by elevated dietary cadmium: trojan horse of the green revolution. *Toxicol. Lett.* 198 (1), 33–39. doi:10.1016/j.toxlet.2010.04.016

Behera, B. C., Mishra, R. R., Patra, J. K., Sarangi, K., Dutta, S. K., and Thatoi, H. N. (2013). Impact of heavy metals on bacterial communities from mangrove soils of the Mahanadi Delta (India). *Chem. Ecol.* 29, 604–619. doi:10.1080/02757540.2013.810719

Bhatia, A., Singh, S., and Kumar, A. (2015). Heavy metal contamination of soil, irrigation water and vegetables in peri-urban agricultural areas and markets of Delhi. *Water Environ. Res.* 87 (11), 2027–2034. doi:10.2175/106143015x14362865226833

Bhuiyan, M. A. H., Suruvi, N. I., Dampare, S. B., Islam, M. A., Quraishi, S. B., Ganyaglo, S., et al. (2011). Investigation of the possible sources of heavy metal contamination in lagoon and canal water in the tannery industrial area in Dhaka, Bangladesh. *Environ. Monit. Assess.* 175 (1), 633–649. doi:10.1007/s10661-010-1557-6

Bounar, A., Boukaka, K., and Leghouchi, E. (2020). Determination of heavy metals in tomatoes cultivated under green houses and human health risk assessment. *Qas* 12 (1), 76–86. doi:10.15586/qas2019.639

CGWB (2013). *Groundwater information booklet of Cuttack district, Odisha*. Bhubaneswar, India: Central Ground Water Board, South eastern region.

Cockwell, P., and Lori-Ann, F. (2020). The global burden of chronic kidney disease. *Lancet* 395 (10225), 662–664. doi:10.1016/S0140-6736(19)32977-0

Demirezen, D., and Aksoy, A. (2006). Heavy metal levels in vegetables in Turkey are within safe limits for Cu, Zn, Ni and exceeded for Cd and Pb. *J. Food Qual.* 29 (3), 252–265. doi:10.1111/j.1745-4557.2006.00072.x

Dodge, Y. (2008). *The concise encyclopedia of statistics*. New York: Springer.

Edwards, J. R., and Prozialeck, W. C. (2009). Cadmium, diabetes and chronic kidney disease. *Toxicol. Appl. Pharmacol.* 238, 289–293. doi:10.1016/j.taap.2009.03.007

Ekong, E. B., Jaar, B. G., and Weaver, V. M. (2006). Lead-related nephrotoxicity: a review of the epidemiologic evidence. *Kidney. Int.* 70, 2074–2084. doi:10.1038/sj.ki.5001809

Evans, M., and Elinder, C. G. (2011). Chronic renal failure from lead: myth or evidence-based fact? Kidney. *Int* 79, 272–279. doi:10.1038/ki.2010.394

Facchinelli, A., Sacchi, E., and Mallen, L. (2001). Multivariate statistical and GIS-based approach to identify heavy metal sources in soils. *Environ. Pollut.* 114 (3), 313–324. doi:10.1016/s0269-7491(00)00243-8

FAO/WHO (Food and Agriculture Organization/World Health Organization) (2019). General standard for contaminants and toxins in food and feed. Codex alimentarius commission. Available at: http://www.fao.org/fao-who-codexalimentarius/sh-proxy/en/?lnk=1&url=%253A%252F%252Fworkspace.fao.org%252Fsites%252Fcodex%252FStandards%252FCXS%2B193-1995%252FCXS_193e.pdf.

Feed, F. (2013). *Maximum limit of heavy metals*. Iran: Iranian National Standard, Institute of Standard and Industrial Research of Iran.

Ferraro, P. M., Costanzi, S., Naticchia, A., Sturniolo, A., and Gambaro, G. (2010). Low-level exposure to cadmium increases the risk of chronic kidney disease: analysis of the NHANES 1999–2006. *BMC Public Health* 10, 304. doi:10.1186/1471-2458-10-304

Filimon, M. N., Caraba, I. V., Popescu, R., Dumitrescu, G., Verdes, D., Petculescu Ciochina, L., et al. (2021). Potential ecological and human health risks of heavy metals in soils in selected copper mining areas-A case study: the bor area. *Ijerph* 18 (4), 1516. doi:10.3390/ijerph18041516

Fonge, B. A., Larissa, M. T., Egbe, A. M., Afanga, Y. A., Frum, N. G., and Ngole-Jeme, V. M. (2021). An assessment of heavy metal exposure risk associated with consumption of cabbage and carrot grown in a tropical savannah region. *Int. J. Environ. Health Sustain.* 7 (1), 1–19. doi:10.1080/27658511.2021.1909860

Franco-Uria, A., Lopez-Mateo, C., Roca, E., and Fernández-Marcos, M. L. (2009). Source identification of heavy metals in pasture land by multivariate analysis in NW Spain. *J. Hazard. Mater.* 1651, 1008–1015. doi:10.1016/j.jhazmat.2008.10.118

FSANZ (2003). *The 20th Australian Total Diet Survey: a total dietsurvey of pesticide residues and contaminants*. Canberra, Australia: Food Standards Australia New Zealand.

Garcia, J. D. D., and Arceo, E. (2018). Renal damage associated with heavy metals: review work. *Rev. Colomb. Nefrol.* 5 (1), 43–53. doi:10.22265/acnef.5.2.254

Garg, V. K., Yadav, P., Mor, S., Singh, B., and Pulhani, V. (2014). Heavy metals bioconcentration from soil to vegetables and assessment of health risk caused by their ingestion. *Biol. Trace Elem. Res.* 157, 256–265. doi:10.1007/s12011-014-9892-z

Gooneratne, I. K., Ranaweera, A. K., Liyanarachchi, N. P., Gunawardane, N., and Lanerolle, R. D. (2008). Epidemiology of chronic kidney disease in a Sri Lankan population. *Int. J. Diabetes Dev. Ctries.* 28, 60–64. doi:10.4103/0973-3930.43101

Gunawardana, C. G., Martínez, R. E., Xiao, W., and Templeton, D. M. (2006). Cadmium inhibits both intrinsic and extrinsic apoptotic pathways in renal mesangial cells. *Am. J. Physiol. Ren. Physiol.* 290, 1074–1082. doi:10.1152/ajprenal.00067.2005

Gupta, N., Yadav, K. K., Kumar, V., Cabral-Pinto, M. M. S., Alam, M., Kumar, S., et al. (2021). Appraisal of contamination of heavy metals and health risk in agricultural soil of jhansi city, India. *Environ. Toxicol. Pharmacol.* 88, 103740. doi:10.1016/j.etap.2021.103740

Gupta, N., Yadav, K. K., Kumar, V., Kumar, S., Chadd, R. P., and Kumar, A. (2019). Trace elements in soil-vegetables interface: translocation, bioaccumulation, toxicity and amelioration - a review. *Sci. Total Environ.* 651, 2927–2942. doi:10.1016/j.scitotenv.2018.10.047

Harrison, U. E., Osu, S. R., and Ekanem, J. O. (2018). Heavy metals accumulation in leaves and tubers of cassava (<i>Manihot esculenta</i> Crantz) grown in crude oil contaminated soil at Ikot Ada Udo, Nigeria. *J. Appl. Sci. Environ. Manag.* 22 (6), 845–851. doi:10.4314/jasem.v22i6.1

Hove, G., Rathaha, T., and Mugiya, P. (2020). The impact of human activities on the environment, case of mhondongori in zvishavane, Zimbabwe. *J. Geosci. Environ. Prot.* 8, 330–349. doi:10.4236/gep.2020.810021

Huang, S., Liao, Q., Hua, M., Wu, X., Bi, K., Yan, C., et al. (2007). Survey of heavy metal pollution and assessment of agricultural soil in Yangzhong district, Jiangsu Province, China. *Chemosphere* 67 (11), 2148–2155. doi:10.1016/j.chemosphere.2006.12.043

ICMR (2020). *Annual report (2019-2020)*. New Delhi: Division of Publication and Information on behalf of the Secretary DHR & DG, ICMR, 147–148. Avaliable At: https://main.icmr.nic.in/sites/default/files/annualrepoorts/ICMRAREnglish201920.

Iqbal, J., Su, C., Rashid, A., Yang, N., Baloch, M. Y. J., Talpur, S. A., et al. (2021). Hydrogeochemical assessment of groundwater and suitability analysis for domestic and agricultural utility in southern Punjab, Pakistan. *Pak. Water.* 13, 3589. doi:10.3390/w13243589

Jan, F. A., Ishaq, M., Khan, S., Ihsanullah, I., Ahmad, I., and Shakirullah, M. (2010). A comparative study of human health risks via consumption of food crops grown on wastewater irrigated soil (Peshawar) and relatively clean water irrigated soil (lower Dir). *J. Hazard. Mater.* 179, 612–621. doi:10.1016/j.jhazmat.2010.03.047

Jarup, L. (2003). Hazards of heavy metal contamination. *Br. Med. Bull.* 68, 167–182. doi:10.1093/bmb/ldg032

Jayasumana, M. A. C. S., Paranagama, P. A., Amarasinghe, M. D., Wijewardane, K. M. R. C., Dahanayake, K. S., Fonseka, S. I., et al. (2013). Possible link of chronic arsenic toxicity with chronic kidney disease of unknown etiology in Sri Lanka. *J. Nat. Sci. Res.* 3 (1), 64–73.

Jayatilake, N., Mendis, S., Maheepala, P., and Mehta, R. (2013). Chronic kidney disease of uncertain aetiology: prevalence and causative factors in a developing country. *BMC Nephrol.* 14 (1), 180–189. doi:10.1186/1471-2369-14-180

JECFA (2003). *Food additives and food contaminants*. Rome: FAO procedural guidelines for the Joint FAO/WHO Expert Committee on Food Additives. Available at: http://apps.who.int/food-additives-contaminants-jecfadatabase/chemical.aspx?chemID=1376

Johri, N., Jacquillet, G., and Unwin, R. (2010). Heavy metal poisoning: the effects of cadmium on the kidney. *Biometals* 23, 783–792. doi:10.1007/s10534-010-9328-y

Kananke, T., Wansapala, J., and Gunaratne, A. (2016). Detection of Ni, Cd, and Cu in green leafy vegetables collected from different cultivation areas in and around Colombo District, Sri Lanka. *Env. Moni. Assess.* 188 (3), 187–212. doi:10.1007/s10661-016-5195-5

Kananke, T., Wansapala, J., and Gunaratne, A. (2014). Heavy metal contamination in green leafy vegetables collected from selected market sites of piliyandala area, colombo district, Sri Lanka. *Am. J. Food Sci. Technol.* 2 (5), 139–144. doi:10.12691/ajfst-2-5-1

Kikuchi, T., Furuichi, T., Hai, H. T., and Tanaka, S. (2009). Assessment of heavy metal pollution in river water of Hanoi, Vietnam using multivariate analyses. *Bull. Environ. Contam. Toxicol.* 83, 575–582. doi:10.1007/s00128-009-9815-4

Kim, N. H., Hyun, Y. Y., Lee, K. B., Chang, Y., Ryu, S., Oh, K. H., et al. (2015). Environmental heavy metal exposure and chronic kidney disease in the general population. *J. Korean Med. Sci.* 30 (3), 272–277. doi:10.3346/jkms.2015.30.3.272

Kladsomboon, S., Jaiyen, C., Choprathumma, C., Tusai, T., and Apilux, A. (2020). Heavy metals contamination in soil, surface water, crops, and resident blood in uthai district, phra nakhon Si ayutthaya, Thailand. *Environ. Geochem. Health* 42, 545–561. doi:10.1007/s10653-019-00388-2

Kumar, S., Prasad, S., Yadav, K. K., Shrivastava, M., Gupta, N., Nagar, S., et al. (2019). Hazardous heavy metals contamination of vegetables and food chain: role of sustainable remediation approaches - a review. *Environ. Res.* 179, 108792. doi:10.1016/j.envres.2019.108792

Li, S. J., Zhang, S. H., Chen, H. P., Zeng, C. H., Zheng, C. X., Li, L. S., et al. (2010). Mercury-induced membranous nephropathy: clinical and pathological features. *Clin. J. Am. Soc. Nephrol.* 5, 439–444. doi:10.2215/cjn.07571009

Liu, C. W., Liang, C. P., Huang, F. M., and Hsueh, Y. M. (2006). Assessing the human health risks from exposure of inorganic arsenic through oyster (*Crassostrea gigas*) consumption in Taiwan. *Sci. Total. Environ.* 361 (1–3), 57–66. doi:10.1016/j.scitotenv.2005.06.005

Mamat, Z., Yimit, H., Ji, R. Z. A., and Eziz, M. (2014). Source identification and hazardous risk delineation of heavy metal contamination in Yanqi basin, northwest China. *Sci. Total. Environ.* 493, 1098–1111. doi:10.1016/j.scitotenv.2014.03.087

Manea, D. N., Ienciu, A. A., Stef, R., Smuleac, I. L., Gergen, I. I., and Nica, D. V. (2020). Health risk assessment of dietary heavy metals intake from fruits and vegetables grown in selected old mining areas—a case study: the Banat area of Southern Carpathians. *Int. J. Environ. Res. Public Health* 17, 5172. doi:10.3390/ijerph17145172

Mitra, S., Chakraborty, A. J., Tareq, A. M., Emran, T. B., Nainu, F. Y., Khusro, A., et al. (2022). Impact of heavy metals on the environment and human health: novel therapeutic insights to counter the toxicity. *J. King Saud Univ. Sci.* 34 (3), 101865. doi:10.1016/j.jksus.2022.101865

Mohamed, A. E., Rashed, M. N., and Mofty, A. (2003). Assessment of essential and toxic elements in some kinds of vegetables. *Ecotoxicol. Environ. Saf.* 55, 251–260. doi:10.1016/s0147-6513(03)00026-5

Mohanty, N. K., Sahoo, K. C., Pati, S., Sahu, A. K., and Mohanty, R. (2020). Prevalence of chronic kidney disease in Cuttack district of Odisha, India. *Int. J. Env. Res. Public Health.* 17, 456. doi:10.3390/ijerph17020456

Mortvedt, J. (1996). Heavy metal contaminants in inorganic and organic fertilizers. *Nutr. Cycl. Agroecosyst.* 43 (1), 55–61. doi:10.1007/bf00747683

Muhammad, M., Habib, I. Y., Hamza, I., Mikail, T. A., Yunusa, A., Muhammad, I. A., et al. (2021). Heavy metals contamination of agricultural land and their impact on food safety. *Ejnfs* 13 (1), 104–111. doi:10.9734/ejnfs/2021/v13i130354

Muhammad, S., Shah, M. T., and Khan, S. (2011). Health risk assessment of heavy metals and their source apportionment in drinking water of Kohistan region, northern Pakistan. *Microchem. J.* 98, 334–343. doi:10.1016/j.microc.2011.03.003

Nanayakkara, S., Komiya, T., Ratnatunga, N., Senevirathna, S. T., Harada, K. H., Hitomi, T., et al. (2012). Tubulointerstitial damage as the major pathological lesion in endemic chronic kidney disease among farmers in North Central Province of Sri Lanka. *Environ. Health. Prev. Med.* 17, 213–221. doi:10.1007/s12199-011-0243-9

Navas-Acien, A., Tellez-Plaza, M., Guallar, E., Muntner, P., Silbergeld, E., Jaar, B., et al. (2009). Blood cadmium and lead and chronic kidney disease in US adults: a joint analysis. *Am. J. Epidemiol.* 170, 1156–1164. doi:10.1093/aje/kwp248

Nayak, B. B., Das, J., Panda, U. C., and Acharya, B. C. (2002). "Industrial effluents and municipal sewage contamination of Mahanadi estuarine water, Orissa," in *Proceedings, published allied* (New Delhi, India: Allied Publishers Pvt. Ltd), 77–86.

Nazar, R., Iqbal, N., Masood, A., Iqbal, M., Khan, R., Syeed, S., et al. (2012). Cadmium toxicity in plants and role of mineral nutrients in its alleviation. *Am. J. Plant Sci.* 3, 1476–1489. doi:10.4236/ajps.2012.310178

Neumann, R. B., Ashfaque, K., Badruzzaman, A. B. M., Ashraf Ali, M., Shoemaker, J. K., and Harvey, C. F. (2010). Anthropogenic influences on groundwater arsenic concentrations in Bangladesh. *Nat. Geosci.* 3, 46–52. doi:10.1038/ngeo685

Noor, S., Rashid, A., Javed, A., Khattak, J. A., and Farooqi, A. (2022). Hydrogeological properties, sources provenance, and health risk exposure of fluoride in the groundwater of Batkhela, Pakistan. *Environ. Technol. Innovation* 25, 102239. doi:10.1016/j.eti.2021.102239

Nziguheba, G., and Smolders, E. (2008). Inputs of trace elements in agricultural soils via phosphate fertilizers in European countries. *Sci. Total Environ.* 390 (1), 53–57. doi:10.1016/j.scitotenv.2007.09.031

Pandey, J., and Pandey, U. (2009). Accumulation of heavy metals in dietary vegetables and cultivated soil horizon in organic farming system in relation to atmospheric deposition in a seasonally dry tropical region of India. *Environ. Monit. Assess.* 148, 61–74. doi:10.1007/s10661-007-0139-8

Pappas, R., Polzin, G., Zhang, L., Watson, C., Paschal, D., and Ashley, D. (2006). Cadmium, lead, and thallium in mainstream tobacco smoke particulate. *Food Chem. Toxicol.* 44, 714–723. doi:10.1016/j.fct.2005.10.004

Polizzotto, M. L., Lineberger, E. M., Matteson, A. R., Neumann, R. B., Badruzzaman, A. B. M., and Ashraf Ali, M. (2013). Arsenic transport in irrigation water across rice-field soils in Bangladesh. *Environ. Pollut.* 179, 210–217. doi:10.1016/j.envpol.2013.04.025

Proshad, R., Islam, M. S., Tusher, T. R., Zhang, D., Khadka, S., Gao, J., et al. (2020). Appraisal of heavy metal toxicity in surface water with human health risk by a novel approach: a study on an urban river in vicinity to industrial areas of Bangladesh. *Toxin Rev.* 40, 803–819. doi:10.1080/15569543.2020.1780615

Prozialeck, W. C., Edwards, J. R., and Woods, J. M. (2006). The vascular endothelium as a target of cadmium toxicity. *Life Sci.* 79, 1493–1506. doi:10.1016/j.lfs.2006.05.007

Radwan, M. A., and Salama, A. K. (2006). Market basket survey for some heavy metals in Egyptian fruits and vegetables. *Food Chem. Toxicol.* 44 (8), 1273–1278. doi:10.1016/j.fct.2006.02.004

Raj, S., Jee, P. K., and Panda, C. R. (2013). Textural and heavy metal distribution in sediments of Mahanadi estuary, East coast of India. *Indian J. geo-mar. Sci.* 42, 370–374.

Raknuzzaman, M., Ahmed, M. K., Islam, M. S., Habibullah-Al-Mamun, M., Tokumura, M., Sekine, M., et al. (2016). Assessment of trace metals in surface water and sediment collected from polluted coastal areas of Bangladesh. *J. Wat. Environ. Technol.* 14, 247–259. doi:10.2965/jwet.15-038

Rango, T., Jeuland, M., Manthrithilake, H., and McCornick, P. (2015). Nephrotoxic contaminants in drinking water and urine, and chronic kidney disease in rural Sri Lanka. *Sci. Total Environ.* 518-519, 574–585. doi:10.1016/j.scitotenv.2015.02.097

Rashid, A., Ayub, M., Khan, S., Ullah, Z., Ali, L., Gao, X., et al. (2022). Hydrogeochemical assessment of carcinogenic and non-carcinogenic health risks of potentially toxic elements in aquifers of the Hindukush ranges, Pakistan: insights from groundwater pollution indexing, GIS-based, and multivariate statistical approaches. *Environ. Sci. Pollut. Res.* 29, 75744–75768. doi:10.1007/s11356-022-21172-3

Rattan, R. K., Datta, S. P., Chhonkar, P. K., Suribabu, K., and Singh, A. K. (2005). Long-term impact of irrigation with waste water effluents on heavy metal content in soils, crops and groundwater—a case study. *Agric. Ecosyst. Environ.* 109, 310–322. doi:10.1016/j.agee.2005.02.025

Ratul, A. K., Hassan, M., and Uddin, M. K. (2018). Potential health risk of heavy metals accumulation in vegetables irrigated with polluted river water. *Int. Food Res. J.* 25 (1), 329–338.

Rehman, K., Bukhari, S. M., Andleeb, S., Mahmood, A., Erinle, K. O., Naeem, M. M., et al. (2019). Ecological risk assessment of heavy metals in vegetables irrigated with groundwater and wastewater: the particular case of Sahiwal district in Pakistan. *Agric. Water Manag.* 226, 105816. doi:10.1016/j.agwat.2019.105816

Renner, R. (2004). Arsenic and lead leach out of popular fertilizer. *Environ. Sci. Technol.* 38, 382–383A. doi:10.1021/es040642c

Roberts, L. C., Hug, S. J., Voegelin, A., Dittmar, J., Kretzschmar, R., Wehrli, B., et al. (2011). Arsenic dynamics in pore water of an intermittently irrigated paddy field in Bangladesh. *Environ. Sci. Tech.* 45, 971–976. doi:10.1021/es102882q

Saha, N., and Zaman, M. R. (2013). Evaluation of possible health risks of heavy metals by consumption of food stuffs available in the central market of Rajshahi City, Bangladesh. *Environ. Monit. Assess.* 185, 3867–3878. doi:10.1007/s10661-012-2835-2

Salonen, V. P., and Korkka-Niemi, K. (2007). Influence of parent sediments on the concentration of heavy metals in urban and suburban soils in Turku, Finland. *Appl. Geochem.* 22 (5), 906–918. doi:10.1016/j.apgeochem.2007.02.003

Samal, P., Singarasubramanian, S. R., Manoj, M. C., Srivastava, J., Dsouza, N., Balakrishna, K., et al. (2022). Heavy metal contamination assessment and its associated human health risk evaluation in the Mahanadi River sediments, India. *Int. J. Environ. Sci. Technol.* 20, 10673–10694. doi:10.1007/s13762-022-04630-w

Saraswat, A., Ram, S., Raza, M. B., Islam, S., Sharma, S., Omeka, M. E., et al. (2023). Potentially toxic metals contamination, health risk, and source

apportionment in the agricultural soils around industrial areas, Firozabad, Uttar Pradesh, India: a multivariate statistical approach. *Environ. Monit. Assess.* 195, 863. doi:10.1007/s10661-023-11476-3

Saxena, G., Purchase, D., Mulla, S. I., Saratale, G. D., and Bharagava, R. N. (2019). Phytoremediation of heavy metal-contaminated sites: eco-environmental concerns, field studies, sustainability issues, and future prospects. *Rev. Environ. Contam. Toxicol.* 249, 71–131. doi:10.1007/398_2019_24

Sekomo, C. B., Nkurang, E., Rousseau, D. P., and Lens, P. N. (2011). Fate of heavy metals in an urban natural wetland: the Nyabugogo Swamp (Rwanda). *Water Air Soil Pollut.* 214, 321–333. doi:10.1007/s11270-010-0426-9

Senapati, N. N., Lenka, D., Behera, S., Mahapatra, A., and Kar, C. (2018). An epidemiologic review of chronic kidney disease of unknown etiology (CKDu). *Int. J. Sci. Res.* 7 (1), 608–609.

Shah, M. T., Shaheen, B., and Khan, S. (2010). Pedo and biogeochemical studies of mafic and ultramfic rocks in the Mingora and Kabal areas, Swat, Pakistan. *Environ. Earth Sci.* 60, 1091–1102. doi:10.1007/s12665-009-0253-8

Sharma, R. K., Agrawal, M., and Marshall, F. M. (2007). Heavy metal contamination of soil and vegetables in suburban areas of Varanasi, India. *Ecotoxicol. Environ. Saf.* 66, 258–266. doi:10.1016/j.ecoenv.2005.11.007

Sharma, R. K., Agrawal, M., and Marshall, F. M. (2009). Heavy metals in vegetables collected from production and market sites of a tropical urban area of India. *Food chemi. Toxicol.* 47 (3), 583–591. doi:10.1016/j.fct.2008.12.016

Singh, D., Chhonkar, P. K., and Pandey, R. N. (1999). *Soil plant water analysis: a methods manual*. New Delhi: IARI.

Singh, K. P., Mohan, D., Sinha, S., and Dalwani, R. (2004). Impact assessment of treated/untreated wastewater toxicants discharged by sewage treatment plants on health, agricultural, and environmental quality in the wastewater disposal area. *Chemosphere* 55, 227–255. doi:10.1016/j.chemosphere.2003.10.050

Sobukola, O. P., Adeniran, O. M., Odedairo, A. A., and Kajihausa, O. E. (2010). Heavy metal levels of some fruits and leafy vegetables from selected markets in Lagos, Nigeria. *Afr. J. Food Sci.* 4 (2), 389–393.

Soderland, P., Lovekar, S., Weiner, D. E., Brooks, D. R., and Kaufman, J. S. (2010). Chronic kidney disease associated with environmental toxins and exposures. *Adv. Chronic Kidney Dis.* 17, 254–264. doi:10.1053/j.ackd.2010.03.011

Spurgeon, D. J., Rowland, P., Ainsworth, G., Rothery, P., Long, S., and Black, H. I. J. (2008). Geographical and pedological drivers of distribution and risks to soil fauna of seven metals (Cd, Cu, Cr, Ni, 728 J Soils Sediments (2013) 13:720–729 Pb, V and Zn) in British soils. *Environ. Pollut.* 153 (2), 273–283. doi:10.1016/j.envpol.2007.08.027

Swain, S., Pattanayak, A. A., Sahu, B. K., Satapathy, D. R., and Panda, C. R. (2021). Time-series monitoring and ecological risk assessment of heavy metal pollution in Mahanadi estuary, east coast of India. *Regional Stud. Mar. Sci.* 47, 101923–104855. doi:10.1016/j.rsma.2021.101923

Tani, F. H., and Barrington, S. (2005). Zinc and copper uptake by plants under two transpiration ratios Part I. Wheat (*Triticum aestivum* L.). *Environ. Pollut.* 138, 548–558. doi:10.1016/j.envpol.2004.06.004

Thijssen, S., Maringwa, J., Faes, C., Lambrichts, I., and VanKerkhove, E. (2007). Chronic exposure of mice to environmentally relevant, low doses of cadmium leads to early renal damage, not predicted by blood or urine cadmium levels. *Toxicol* 229, 145–156. doi:10.1016/j.tox.2006.10.011

USEPA (2015). *Regional Screening level (RSL) for chemical contaminant at superfound sites*. Cincinnati, Ohio: U.S. Environmental Protection Agency, 176. Available at: http://www.epa.gov/reg3hwmd/risk/human/index.htm.

USEPA (2010). Risk based concentration table. Available at: http://www.epa.gov/reg3hwmd/risk/human/index.htm.

USEPA (1999). "Screening level ecological risks assessment protocol for hazardous waste combustion facilities," in *Appendix E: toxicity reference values* (Cincinnati, Ohio: United States Environmental Protection Agency). Available at: https://archive.epa.gov/epawaste/hazard/tsd/td/web/pdf/appx-e.pdf

USEPA (US Environmental Protection Agency) (1989). *Risk assessment guidance for superfund, human health evaluation manual (Part A)*. Washington, DC, USA: EPA.

USEPA (2006). *USEPA Region III risk-based concentration table: technical background information*. Washington: Unites States Environmental Protection Agency.

Varma, P. P. (2015). Prevalence of chronic kidney disease in India: where are we heading? *Indian J. Nephrol.* 25 (3), 133–135.

Wei, R., Wang, X., Tang, W., Yang, Y., Gao, Y., Zhong, H., et al. (2020). Bioaccumulations and potential human health risks assessment of heavy metals in ppk-expressing transgenic rice. *Sci. Total Environ.* 710, 136496. doi:10.1016/j.scitotenv.2020.136496

WHO (2011). *Guidelines for drinking water quality*. 4th edn. Geneva, Switzerland: WHO Press.

WHO (1985). *Guidelines for the study of dietary intakes of chemical contaminants WHO offset publication*. Geneva: World Health Organization, 1–100.

Wu, S., Xia, X., Lin, C., Chen, X., and Zhou, C. (2010). Levels of arsenic and heavy metals in the rural soils of Beijing and their changes over the last two decades (1985–2008). *J. Hazard Mater.* 179 (1), 860–868. doi:10.1016/j.jhazmat.2010.03.084

Yana, C., Kelin, L., and Jian, Z. (2012). Analysis of heavy metal pollution in soil-vegetables at mining area in Hunan. *Chin. Agric. Sci. Bull.* 28, 226–232.

Yang, Q. W., Xu, Y., Liu, S. J., He, J. F., and Long, F. Y. (2011). Concentration and potential health risk of heavy metals in market vegetables in Chongqing, China. *Ecotoxicol. Environ. Saf.* 74, 1664–1669. doi:10.1016/j.ecoenv.2011.05.006

Zamor, P. W., Jesu, J. D., Sia, G., Ragragio, E., Su, M. L. S., and Villanueva, S. (2012). Assessing lead concentrations in leafy vegetables in selected private markets in metro manila, Philippines. *J. Appl. Tech. Environ. Sanit.* 2 (3), 175–178.

frontiers | Frontiers in Environmental Science

TYPE Perspective
PUBLISHED 02 February 2024
DOI 10.3389/fenvs.2024.1307631

OPEN ACCESS

EDITED BY
Qi Liao,
Central South University, China

REVIEWED BY
Agnieszka Klimkowicz-Pawlas,
Institute of Soil Science and Plant Cultivation, Poland

*CORRESPONDENCE
Itziar Alkorta,
itzi.alkorta@ehu.eus

RECEIVED 04 October 2023
ACCEPTED 23 January 2024
PUBLISHED 02 February 2024

CITATION
Garbisu C and Alkorta I (2024), Enhanced phytoremediation of metal contaminated soils aimed at decreasing the risk of antibiotic resistance dissemination.
Front. Environ. Sci. 12:1307631.
doi: 10.3389/fenvs.2024.1307631

Enhanced phytoremediation of metal contaminated soils aimed at decreasing the risk of antibiotic resistance dissemination

Carlos Garbisu[1] and Itziar Alkorta[2]*

[1]Department of Conservation of Natural Resources, NEIKER–Basque Institute for Agricultural Research and Development, Basque Research and Technology Alliance (BRTA), Derio, Spain, [2]Department of Biochemistry and Molecular Biology, University of the Basque Country (UPV/EHU), Bilbao, Spain

The enhanced phytoremediation of metal contaminated soils holds great promise for the recovery of soil health and functionality, while providing a range of co-benefits, from an environmental and human health perspective, derived from the revegetation of the degraded sites and the concomitant delivery of ecosystem services. Due to diverse evolutionary co-selection mechanisms between metal resistance and antibiotic resistance in bacteria, metal contaminated soils are considered potential reservoirs of antibiotic resistant bacteria (ARB) which can contribute to the existing antibiotic resistance crisis. During the enhanced phytoremediation of metal contaminated soils, the application of organic wastes (e.g., manure, slurry, sewage sludge) as soil amendments can aggravate the risk of antibiotic resistance spread, because they often contain ARB which harbor antibiotic resistance genes (ARGs) that can then be propagated among soil bacterial populations through horizontal gene transfer (HGT). Due to the magnitude and criticality of the antibiotic resistance crisis, as well as the higher risk of spread and dispersal of ARB and ARGs (they make copies of themselves) compared to metals, it is proposed here to aim enhanced phytoremediation strategies towards decreasing the soil resistome (and, hence, the risk of its potential link with the human resistome), while reducing total and/or bioavailable metal concentrations and restoring soil health and the delivery of ecosystem services. To this purpose, a decalogue of practices is tentatively suggested. Finally, a proper management of plant and soil microbial compositions is a most crucial aspect, together with the selection of the right organic wastes and phytoremediation practices.

KEYWORDS

antibiotics, antimicrobials, bioremediation, metal pollution, resistome, soil

1 Introduction

Metal phytoremediation strategies have important drawbacks that are hindering their commercial use (Wang and Delavar, 2023). Phytoextraction can reduce total metal concentrations, but it requires unacceptably long times to decrease such concentrations below regulatory limits (Tang, 2023). The main limitation of phytostabilisation is that it does not reduce total metal concentrations in soil, as it is based on the use of excluders that reduce metal bioavailability, but not total concentrations. Besides, phytoremediation is limited to the surface area and depth occupied by the roots and can increase the risk of metal accumulation up the trophic chain (El Rasafi et al., 2023). In an attempt to overcome these

limitations, several enhanced phytoremediation strategies have been proposed. Thus, inorganic and organic amendments are used to assist the revegetation of metal contaminated soils (Moreira et al., 2021). Compared to inorganic amendments, organic amendments have certain advantages: high accessibility, low costs, reuse of wastes, increase of soil organic matter, supply of nutrients, improvement of soil structure, enhancement of microbial activity (which can then help control soilborne pathogens) (Janvier et al., 2007; Núñez-Zofío et al., 2011), *etc.* Another strategy, microbial-assisted phytoremediation, is based on the inoculation of plant growth-promoting bacteria (PGPB) (Waseem et al., 2024) and/or fungi (Ahmad et al., 2024), often as consortia, to facilitate plant growth and performance under the harsh conditions that characterize contaminated soils (Alkorta et al., 2017; Alkorta and Garbisu, 2021). The presence of fungi can promote bacterial distribution as they are known to use fungal hyphae to disperse in the soil under unsaturated conditions (Kohlmeier et al., 2005). Likewise, the combination of amendments, plants (phytoremediation), microorganisms (bioremediation), and earthworms (vermiremediation) is also promising for soil remediation (Lacalle et al., 2020). Interestingly, the phytoremediation field has recently shifted towards phytomanagement (Moreira et al., 2021), a concept focused on the use of plants to generate products and ecosystem services while remediating a contaminated soil.

Metal contaminated sites can conceal other risks different from those associated to metal toxicity. Relevantly, metal contaminated soils can be reservoirs of antibiotic resistant bacteria (ARB) and antibiotic resistance genes (ARGs) (Cai et al., 2023; Song et al., 2024). Due to the criticality of the antibiotic resistance crisis and the higher risk of spread and dispersal of ARB and ARGs, compared to metals, it is proposed here to aim enhanced phytoremediation strategies towards decreasing the soil resistome, while reducing metal concentrations and restoring soil health. This antibiotic resistance-centered approach to metal phytoremediation could promote its commercial use and interest for soil managers. Several papers can be found in the literature on i) the biological remediation of antibiotic contaminated soils, e.g., removal of antibiotics via bioremediation or microbial-assisted phytoremediation; or 2) the presence of ARB and ARGs in metal contaminated soils due to co-selection mechanisms. But, to our knowledge, the abovementioned proposal is a novel proposal.

2 Metal contamination and antibiotic resistance

In order to attract attention to a field of knowledge, it is convenient to point out its links with human health and/or wellbeing. Metals can be toxic to humans and, as such, they have always attracted our attention from a human health perspective (Tian et al., 2023). But, although metal toxicity by itself is more than enough reason to take the remediation of metal contaminated sites very seriously, to this risk, we must add the fact that these sites have been linked to one of the greatest threats to public health: the emergence and dissemination of ARB harboring ARGs (Edet et al., 2023).

Given the criticality of the antibiotic resistance crisis, the links between the soil resistome and the human resistome is currently a topic of much interest (Liao et al., 2022). The selective pressure that the presence of antibiotics may exert on ARB proliferation in soil is of particular concern, as soil contains a number of bacterial genera of clinical relevance (Serwecińska, 2020). Much interest exists on the relationship between the use of organic amendments of animal (manure, slurry) and/or urban (sewage sludge) origin as fertilizers and the soil resistome (Jauregi et al., 2021a; Jauregi et al., 2021b; Jauregi et al., 2023). Manure is acknowledged as a reservoir of ARB and ARGs (Zhu et al., 2013), which can be disseminated in the environment through horizontal gene transfer (HGT) among bacteria mediated by mobile genetic elements (MGEs) (Heuer et al., 2011; Urra et al., 2019). Once in the soil, the ARB initially present in the manure can die or survive and then inhabit the abiotic and/or biotic component of the soil matrix. The presence of antibiotics and their transformation products in the amendments can alter the composition of soil microbial communities with consequences for the soil resistome and mobilome (Gillings, 2013; Nesme and Simonet, 2015).

The link between metal contamination and AR is based on the fact that metal contamination can lead to the spread of AR through co-selection mechanisms, such as *co-resistance* (several resistance systems in the same genetic element), *cross-resistance* (one resistance system confers resistance to both a metal and an antibiotic), and *co-regulation* (when resistance to antibiotics and metals are controlled by a single regulatory gene) (Baker-Austin et al., 2006; Wales and Davies, 2015; Ohore et al., 2019). Due to the AR crisis and the degree of metal contamination in many environmental matrices, much attention is being paid to the study of the role of metal contamination as selective agent in the proliferation of environmental antibiotic resistance (Jauregi et al., 2021b). For instance, ARGs can be found in metal contaminated mines (Garbisu et al., 2018). Importantly, owing to the long residence times of metals in soil, they represent a recalcitrant selection pressure on ARB.

3 Enhanced phytoremediation aimed at reducing antibiotic resistance

Many metal contaminated sites are not being remediated for economic and/or technical reasons. In an attempt to find ways to encourage the remediation of metal contaminated soils, here it is proposed to direct enhanced phytoremediation strategies to reduce the risk of the environmental resistome present in metal contaminated soils. This novel proposal is based on three facts: 1) soil is one of our most important resources, and as such we must do our best to restore its functionality when degraded; ii) the link between the soil resistome and the human resistome is a threat to the effectiveness of antibiotics in medicinal practice and we must do over best to disrupt such link; and iii) there is a higher risk of spread and dispersal of ARB and ARGs (they make copies of themselves), compared to metals. It is crucial to design enhanced phytoremediation practices taking into consideration the possibility to reduce the risk of antibiotic resistance in the metal contaminated site under remediation, as well as its propagation to other environmental matrices, while decreasing total and/or bioavailable metal concentrations, restoring soil functioning, and providing ecosystem services.

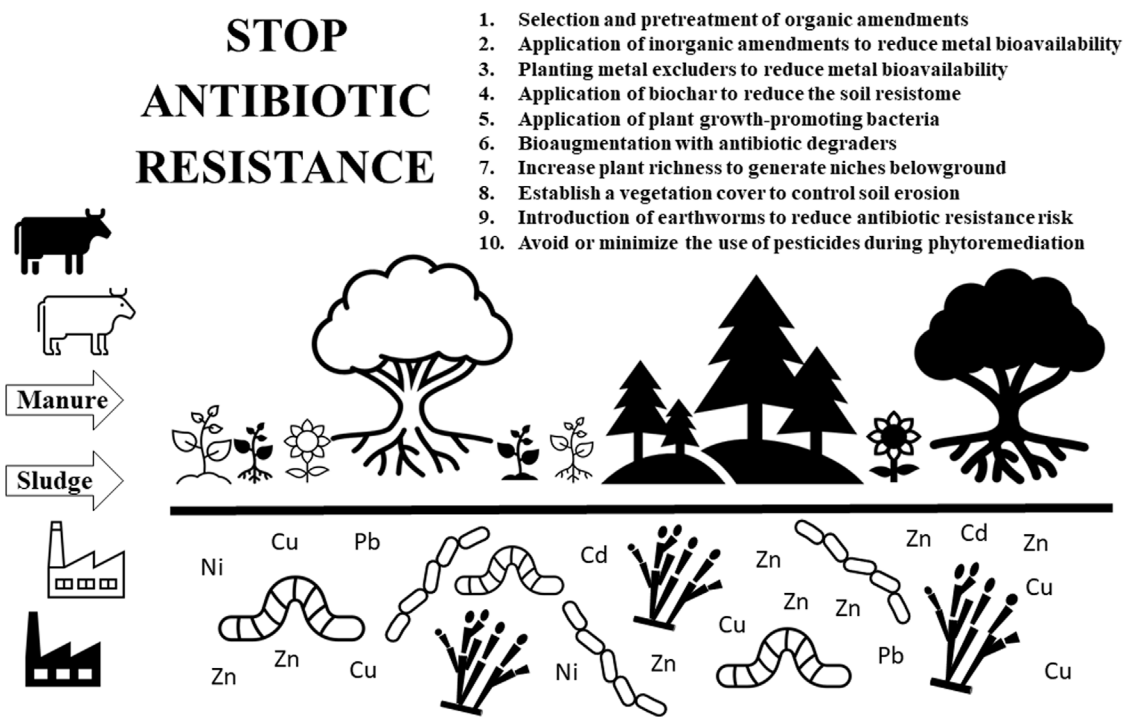

FIGURE 1
Tentative decalogue of practices that must be taken into account during the enhanced phytoremediation of metal contaminated soil in order to minimize the risk of antibiotic resistance.

The following is a brief description of practices, in the form of a tentative decalogue (Figure 1), that must be taken into consideration during the implementation of enhanced phytoremediation strategies in order to minimize the antibiotic resistance risk, while addressing the risks associated with the presence of metals.

(1) *Selection and pretreatment of organic amendments:* it is desirable to select those amendments that have a lower content of metals and antibiotics (as well as of ARB, ARGs, and MGEs). Although, in most cases, a thorough analysis of the composition of the amendments is not available (especially regarding the content of antibiotics, not to mention the abundance of ARB, ARGs, or MGEs), from the origin of the amendments (urban *versus* animal origin, manure from one livestock species *versus* another, manure from an ecological *versus* an industrial farm, *etc.*), it is possible to estimate which ones represent a lower risk. However, the most important factor is probably the type of pretreatment applied to the amendment prior to its use: storage, composting, anaerobic digestion, *etc.* It is crucial to opt for amendments that have been properly treated for hygienisation purposes or composted. Manure pretreatment, by means of composting or anaerobic digestion, can reduce the burden of ARB and ARGs, as well as destroy antibiotic residues (Tran et al., 2021; Wang et al., 2021). Although neither composting nor storage completely eliminate the risk of antibiotic resistance, composting is normally more effective (Zalewska et al., 2023). A thermal hydrolysis pre-treatment combined with anaerobic digestion has been reported to reduce the abundance of ARGs and MGEs in sewage sludge (Sun et al., 2019). The use of exogenous additives, such as nanomaterials, during manure composting has been shown to reduce the ARG abundances (Jiang et al., 2023). Jiang et al. (2023) reported the effectiveness of the addition of SiO_2 nanoparticles during manure composting to decrease the propagation of ARGs. Nnorom et al. (2023) reviewed the use of carbon- and iron-based conductive materials (biochar, activated carbon, zerovalent iron) as additives to mitigate the proliferation of ARGs during the anaerobic digestion of sludge and manure, and concluded that they can decrease ARG abundances in the digestate by easing selective pressure, changing microbial community structure, and diminishing HGT.

(2) *Application of inorganic amendments to reduce metal bioavailability:* another strategy to minimize the risk of co-selection between metal and antibiotic resistance is to decrease the levels of bioavailable metals in soil. A well-known strategy is the application of lime to increase soil pH and, hence, reduce bioavailable concentrations. Many other amendments (iron oxides, phosphates, ashes, *etc.*) have been used for chemical stabilization in metal contaminated soils (Kumpiene et al., 2019). When dealing with metal phytoremediation, one must decide whether to mobilize or immobilize the metals (Bolan et al., 2014), since mobilizing agents (chelating agents, desorbing agents) enhance plant metal uptake but at the same time increase the risk of metal leaching, while immobilizing agents

(precipitating agents, sorbent materials) reduce both metal transfer to the food chain and leaching but require monitoring and management to guarantee the long-term stability of the immobilized metals.

(3) *Planting metal excluders to reduce metal bioavailability:* phytostabilisation with excluders is focused on the reduction of bioavailable concentrations, so that metal toxicity and mobility are decreased (Moreira et al., 2021). The level of bacterial exposure to metals is decreased and, concomitantly, the selection pressure to become tolerant to those metals, minimizing the appearance of antibiotic resistance via co-selection.

(4) *Application of biochar to reduce the soil resistome:* apart from the use of biochar aimed at modifying soil properties, including bioavailable concentrations (Moreira et al., 2021), much research has been done on the effect of biochar on the soil resistome (Cheng et al., 2021). Biochar has been reported to reduce the accumulation of ARGs in soil and their transfer to crops, among other reasons, due to the biochar´s ability to decrease, through sorption, the mobility and bioavailability of antibiotics and metals, as well as to its effect on microbial community composition derived from the induced changes on soil physicochemical properties (Ye et al., 2016; Duan et al., 2017; Chen et al., 2018; He et al., 2019; Cheng et al., 2021). Field aging can modify the biochar's effect on the resistome of manured soil (Cheng et al., 2021). Finally, the addition of biochar during composting can accelerate antibiotics removal and reduce the accumulation of ARGs (Tong et al., 2022).

(5) *Application of plant growth-promoting bacteria:* the application of PGPB is becoming common practice during the phytoremediation of contaminated soils (Moreira et al., 2021). The application to soil of ecologically competitive PGPB could, theoretically speaking, outcompete the ARB present in the soil via, for instance, competition for resources and space. Antibiotic resistant bacteria introduced via the application of amendments can be viewed as invasive species and, as such, the possibility of their control by means of the introduction of highly competitive equivalents comes out as a potentially suitable strategy to reduce the risk of their dissemination. Biodiversity, and in particular soil biodiversity, can control invasive species (Bach et al., 2020). The generation of soil niches for potential microbial competitors of ARB derived from aboveground plant richness also emerges as a possibility for the control of ARB. It is important to emphasize that only antibiotic-susceptible PGPB must be used because PGPB often harbor ARGs (Mahdi et al., 2021).

(6) *Bioaugmentation with antibiotic degraders:* apart from the risk of the introduction of antibiotics to soil via organic amendments, many soil microbial species (particularly, actinobacteria and fungi) naturally produce antibiotics for competition purposes or as signalling molecules that facilitate intra- or interspecies interactions (Romero et al., 2011). Microorganisms have produced antibiotics for millions of years and, then, ARGs are often isolated from pristine environments, not subjected to antibiotic residues derived from human usage (Bhullar et al., 2012). In metal contaminated soils subjected to enhanced phytoremediation, this natural resistome must be added to the metal-derived resistome and the manured-associated resistome. The presence of natural or exogenous antibiotics in the soil causes a selective pressure on exposed bacteria to become resistant. The possibility of antibiotic bioremediation via bioaugmentation with microbial antibiotic degraders (Hong et al., 2020) can be a suitable option to decrease the risk of antibiotic resistance dissemination in soils under remediation. Apart from bacterial degraders, fungal-based remediation (mycoremediation) shows great potential for the removal of antibiotics (Čvančarová et al., 2015; Olicón-Hernández et al., 2017; Jalali et al., 2023). Interestingly, fungal hyphae serve as vectors for bacteria to travel across the soil, the so-called hyphal highways along which bacteria can swim in the water film that coats the hyphae or, alternatively, travel passively by settling at the tip of the growing hyphae (Guennoc et al., 2018).

(7) *Increase plant richness to generate niches belowground:* when ARB enter the soil during the application of manure, they can be regarded as invasive species whose success will rely on abiotic and biotic factors, such as, for instance, their ecological fitness, ecological valence under those conditions, dispersal ability, capacity for acclimation and adaptation, *etc.* Chen et al. (2019), in a study on the possibility of using microbial diversity against ARB invasion, reported that soil microbial diversity was negatively correlated with ARG abundance and concluded that a high soil microbial diversity works as a barrier against antibiotic resistance dissemination. Plant richness has been linked to belowground microbial diversity, probably due to the generation of niches derived from diverse litter types and root exudates (Wardle et al., 2004). In principle, the implementation of high plant richness aboveground (different species of grasses, shrubs, trees, and at different stages of growth and development) should increase the number of niches belowground and, concomitantly, a high diversity of microorganisms that could limit the growth of ARB or outcompete them. Besides, the promotion of biodiversity under phytoremediation has been reported to have many benefits (Garbisu et al., 2020).

(8) *Establish a vegetation cover to control soil erosion:* to avoid the dispersal of soil ARB to other environmental compartments (e.g., air, water), it is critical to establish a permanent full vegetation cover to minimize the risk of such dispersal through erosion. On the other hand, erosion has been reported to reduce soil microbial diversity (Qiu et al., 2021).

(9) *Introduction of earthworms to reduce antibiotic resistance risk:* although still a controversial issue, there are quite a few studies that have found a decrease in soil ARG abundances in the presence of earthworms. Li et al. (2022) found that earthworms can reduce the dissemination potential of ARGs by changing bacterial co-occurrence patterns in soil. Zhu et al. (2021) observed that the presence of earthworms decreased the abundance of ARGs in soils, suggesting that

vermiremediation could be a suitable method to reduce risks associated to the presence of ARGs in soils. During vermicomposting of sewage sludge, earthworms have shown to decrease ARG abundance (Huang et al., 2020).

(10) *Avoid or minimize the use of pesticides during phytoremediation:* during phytoremediation, pesticides are often used to control weeds in the early stages of site management (Kidd et al., 2015). But herbicide use has been shown to be positively correlated with antibiotic resistance (Kurenbach et al., 2018; Xu et al., 2019), among other reasons, possibly due to changes in herbicide-mediated gene expression, leading to activation of bacterial ARGs (Staub et al., 2012). Liao et al. (2021) reported that the application of glyphosate, glufosinate, and dicamba increased the abundance of ARGs and MGEs in soil, without changes in the abundance or diversity of bacterial communities. Moreover, herbicide exposure increased conjugation frequency of multidrug resistance plasmids, thus promoting ARG spread among bacterial populations (Liao et al., 2021).

4 Conclusion

Metal contaminated soils can be a reservoir of ARB and ARGs. The application of organic amendments during enhanced phytoremediation, as well as the inoculation of PGPB, can aggravate this problem. Here, it is proposed to aim enhanced phytoremediation strategies towards decreasing the soil resistome, while reducing total and/or bioavailable metal concentrations and restoring soil health and the delivery of ecosystem services. To this purpose, a decalogue of practices has been tentatively suggested. Nonetheless, it must be emphasized that the soil is a highly complex, heterogeneous, and dynamic ecosystem, whose functioning is still greatly unknown, and then one must be extremely cautious when proposing specific soil practices or measures as, quite often, they do not have the expected outcome or even show the opposite effect. In consequence, it is crucial to first test the suitability of the ten practices proposed here under the specific edaphoclimatic and contamination conditions of the site of interest. The ultimate goal of this perspective article has been to bring attention to the antibiotic resistance problem in metal contaminated soils subjected to enhanced phytoremediation. Importantly, this antibiotic resistance-centered approach to soil metal phytoremediation could promote its commercial use and interest for soil managers.

Data availability statement

The raw data supporting the conclusion of this article will be made available by the authors, without undue reservation.

Author contributions

CG: Conceptualization, Writing–original draft, Writing–review and editing. IA: Conceptualization, Writing–original draft, Writing–review and editing.

Funding

The author(s) declare financial support was received for the research, authorship, and/or publication of this article. This work was supported by MCIN/AEI/10.13039/501100011033 (PID 2020-116495RB-I00), Basque Government (IT1578-22), and Euskampus–JRL Environmental Antibiotic Resistance.

Acknowledgments

The authors wish to thank support from Euskampus–JRL Environmental Antibiotic Resistance.

Conflict of interest

The authors declare that the research was conducted in the absence of any commercial or financial relationships that could be construed as a potential conflict of interest.

Publisher's note

References

Ahmad, J., Marsidi, N., Abdullah, S. R. S., Hasan, H. A., Othman, A. R., Ismail, N. I., et al. (2024). Integrating phytoremediation and mycoremediation with biosurfactant-producing fungi for hydrocarbon removal and the potential production of secondary resources. *Chemosphere* 349, 140881. doi:10.1016/j.chemosphere.2023.140881

Alkorta, I., Epelde, L., and Garbisu, C. (2017). Environmental parameters altered by climate change affect the activity of soil microorganisms involved in bioremediation. *FEMS Microbiol. Lett.* 364, fnx200. doi:10.1093/femsle/fnx200

Alkorta, I., and Garbisu, C. (2021). Reflections and insights on the evolution of the biological remediation of contaminated soils. *Front. Environ. Sci.* 9, 734628. doi:10.3389/fenvs.2021.734628

Bach, E. M., Ramirez, K. S., Fraser, T. D., and Wall, D. H. (2020). Soil biodiversity integrates solutions for a sustainable future. *Sustainability* 12, 2662. doi:10.3390/su12072662

Baker-Austin, C., Wright, M. S., Stepanauskas, R., and McArthur, J. V. (2006). Co-selection of antibiotic and metal resistance. *Trends Microbiol.* 14, 176–182. doi:10.1016/J.TIM.2006.02.006

Bhullar, K., Waglechner, N., Pawlowski, A., Koteva, K., Banks, E. D., Johnston, M. D., et al. (2012). Antibiotic resistance is prevalent in an isolated cave microbiome. *PLoS ONE* 7 (4), e34953. doi:10.1371/journal.pone.0034953

Bolan, N., Kunhikrishnan, A., Thangarajan, R., Kumpiene, J., Park, J., Makino, T., et al. (2014). Remediation of heavy metal(loid)s contaminated soils – to mobilize or to immobilize? *J. Hazard. Mater.* 266, 141–166. doi:10.1016/j.jhazmat.2013.12.018

Cai, P., Chen, Q., Du, W., Yang, S., Li, J., Cai, H., et al. (2023). Deciphering the dynamics of metal and antibiotic resistome profiles under different metal(loid) contamination levels. *J. Hazard. Mater.* 455, 131567. doi:10.1016/j.jhazmat.2023.131567

Chen, Q.-L., An, X.-L., Zheng, B.-X., Gillings, M., Peñuelas, J., Cui, L., et al. (2019). Loss of soil microbial diversity exacerbates spread of antibiotic resistance. *Soil Ecol. Lett.* 1, 3–13. doi:10.1007/s42832-019-0011-0

Chen, Q.-L., Fan, X.-T., Zhu, D., An, X.-L., Su, J.-Q., and Cui, L. (2018). Effect of biochar amendment on the alleviation of antibiotic resistance in soil and phyllosphere of *Brassica chinensis* L. *Soil Biol. biochem.* 119, 74–82. doi:10.1016/j.soilbio.2018.01.015

Cheng, J.-H., Tang, X.-Y., Su, J.-Q., and Liu, C. (2021). Field aging alters biochar's effect on antibiotic resistome in manured soil. *Environ. Pollut.* 288, 117719. doi:10.1016/j.envpol.2021.117719

Čvančarová, M., Moeder, M., Filipová, A., and Cajthaml, T. (2015). Biotransformation of fluoroquinolone antibiotics by ligninolytic fungi–metabolites, enzymes, and residual antibacterial activity. *Chemosphere* 136, 311–320. doi:10.1016/j.chemosphere.2014.12.012

Duan, M., Li, H., Gu, J., Tuo, X., Sun, W., Qian, X., et al. (2017). Effects of biochar on reducing the abundance of oxytetracycline, antibiotic resistance genes, and human pathogenic bacteria in soil and lettuce. *Environ. Pollut.* 224, 787–795. doi:10.1016/j.envpol.2017.01.021

Edet, U. O., Bassey, I. U., and Joseph, A. P. (2023). Heavy metal co-resistance with antibiotics amongst bacteria isolates from an open dumpsite soil. *Heliyon* 9, e13457. doi:10.1016/j.heliyon.2023.e13457

El Rasafi, T., Haouas, A., Tallou, A., Chakouri, M., Aallam, Y., El Moukhtari, A., et al. (2023). Recent progress on emerging technologies for trace elements-contaminated soil remediation. *Chemosphere* 341, 140121. doi:10.1016/j.chemosphere.2023.140121

Garbisu, C., Alkorta, I., Kidd, P., Epelde, L., and Mench, M. (2020). Keep and promote biodiversity at polluted sites under phytomanagement. *Environ. Sci. Pollut. Res.* 27, 44820–44834. doi:10.1007/s11356-020-10854-5

Garbisu, C., Garaiyurrebaso, O., Lanzén, A., Álvarez-Rodríguez, I., Arana, L., Blanco, F., et al. (2018). Mobile genetic elements and antibiotic resistance in mine soil amended with organic wastes. *Sci. Total Environ.* 621, 725–733. doi:10.1016/j.scitotenv.2017.11.221

Gillings, M. R. (2013). Evolutionary consequences of antibiotic use for the resistome, mobilome and microbial pangenome. *Front. Microbiol.* 4, 4. doi:10.3389/fmicb.2013.00004

Guennoc, C. M., Rose, C., Labbé, J., and Deveau, A. (2018). Bacterial biofilm formation on the hyphae of ectomycorrhizal fungi: a widespread ability under controls? *FEMS Microbiol. Ecol.* 94, fiy093. doi:10.1093/femsec/fiy093

He, Y., Liu, C., Tang, X., Xian, Q., Zhang, J., and Guan, Z. L. (2019). Biochar impacts on sorption-desorption of oxytetracycline and florfenicol in an alkaline farmland soil as affected by field ageing. *Sci. Total Environ.* 671, 928–936. doi:10.1016/j.scitotenv.2019.03.414

Heuer, H., Schmitt, H., and Smalla, K. (2011). Antibiotic resistance gene spread due to manure application on agricultural fields. *Curr. Opin. Microbiol.* 14, 236–243. doi:10.1016/j.mib.2011.04.009

Hong, X., Zhao, Y., Zhuang, R., Liu, J., Guo, G., Chen, J., et al. (2020). Bioremediation of tetracycline antibiotics-contaminated soil by bioaugmentation. *RSC Adv.* 10, 33086–33102. doi:10.1039/d0ra04705h

Huang, K., Xia, H., Zhang, Y., Li, J., Cui, G., Li, F., et al. (2020). Elimination of antibiotic resistance genes and human pathogenic bacteria by earthworms during vermicomposting of dewatered sludge by metagenomic analysis. *Bioresour. Technol.* 297, 122451. doi:10.1016/j.biortech.2019.122451

Jalali, F. M., Chahkandi, B., Gheibi, M., Eftekhari, M., Behzadian, K., and Campos, L. C. (2023). Developing a smart and clean technology for bioremediation of antibiotic contamination in arable lands. *Sustain. Chem. Pharm.* 33, 101127. doi:10.1016/j.scp.2023.101127

Janvier, C., Villeneuve, F., Alabouvette, C., Edel-Hermann, V., Mateille, T., and Steinberg, C. (2007). Soil health through soil disease suppression: which strategy from descriptors to indicators? *Soil Biol. biochem.* 39, 1–23. doi:10.1016/j.soilbio.2006.07.001

Jauregi, L., Epelde, L., Alkorta, I., and Garbisu, C. (2021a). Antibiotic resistance in agricultural soil and crops associated to the application of cow manure-derived amendments from conventional and organic livestock farms. *Front. Vet. Sci.* 8, 633858. doi:10.3389/fvets.2021.633858

Jauregi, L., Epelde, L., Alkorta, I., and Garbisu, C. (2021b). Agricultural soils amended with thermally-dried anaerobically-digested sewage sludge showed increased risk of antibiotic resistance dissemination. *Front. Microbiol.* 12, 666854. doi:10.3389/fmicb.2021.666854

Jauregi, L., Epelde, L., Artamendi, M., Blanco, F., and Garbisu, C. (2023). Induced development of oxytetracycline tolerance in bacterial communities from soil amended with well-aged cow manure. *Ecotoxicology* 32, 418–428. doi:10.1007/s10646-023-02650-x

Jiang, H., Zhang, L., Wang, X., Gu, J., Song, Z., Wei, S., et al. (2023). Reductions in abundances of intracellular and extracellular antibiotic resistance genes by SiO2 nanoparticles during composting driven by mobile genetic elements. *J. Environ. Manage.* 341, 118071. doi:10.1016/j.jenvman.2023.118071

Kidd, P., Mench, M., Alvarez-Lopez, V., Bert, V., Dimitriou, I., Friesl-Hanl, W., et al. (2015). Agronomic practices for improving gentle remediation of trace element-contaminated soils. *Int. J. Phytorem.* 17, 1005–1037. doi:10.1080/15226514.2014.1003788

Kohlmeier, S., Smits, T. H. M., Ford, R. M., Keel, C., Harms, H., and Wick, L. Y. (2005). Taking the fungal highway: mobilization of pollutant-degrading bacteria by fungi. *Environ. Sci. Technol.* 39 (12), 4640–4646. doi:10.1021/es047979z

Kumpiene, J., Antelo, J., Brännvall, E., Carabante, I., Ek, K., Komárek, M., et al. (2019). *In situ* chemical stabilization of trace element-contaminated soil - field demonstrations and barriers to transition from laboratory to the field - a review. *Appl. Geochem.* 100, 335–351. doi:10.1016/j.apgeochem.2018.12.003

Kurenbach, B., Hill, A. M., Godsoe, W., van Hamelsveld, S., and Heinemann, J. A. (2018). Agrichemicals and antibiotics in combination increase antibiotic resistance evolution. *PeerJ* 6, e5801. doi:10.7717/peerj.5801

Lacalle, R. G., Aparicio, J. D., Artetxe, U., Urionabarrenetxea, E., Polti, M. A., Soto, M., et al. (2020). Gentle remediation options for soil with mixed chromium (VI) and lindane pollution: biostimulation, bioaugmentation, phytoremediation and vermiremediation. *Heliyon* 6, e04550. doi:10.1016/j.heliyon.2020.e04550

Li, H., Luo, Q.-P., Pu, Q., Yang, X.-R., An, X.-L., Zhu, D., et al. (2022). Earthworms reduce the dissemination potential of antibiotic resistance genes by changing bacterial co-occurrence patterns in soil. *J. Hazard. Mat.* 426, 128127. doi:10.1016/j.jhazmat.2021.128127

Liao, H., Li, H., Duan, C.-S., Zhou, X.-Y., An, X.-L., Zhu, Y.-G., et al. (2022). Metagenomic and viromic analysis reveal the anthropogenic impacts on the plasmid and phage borne transferable resistome in soil. *Environ. Int.* 170, 107595. doi:10.1016/j.envint.2022.107595

Liao, H., Li, X., Yang, Q., Bai, Y., Cui, P., Wen, C., et al. (2021). Herbicide selection promotes antibiotic resistance in soil microbiomes. *Mol. Biol. Evol.* 38, 2337–2350. doi:10.1093/molbev/msab029

Mahdi, I., Fahsi, N., Hijri, M., and Sobeh, M. (2022). Antibiotic resistance in plant growth promoting bacteria: a comprehensive review and future perspectives to mitigate potential gene invasion risks. *Front. Microbiol.* 13, 999988. doi:10.3389/fmicb.2022.999988

Moreira, H., Pereira, S. I. A., Mench, M., Garbisu, C., Kidd, P., and Castro, P. M. L. (2021). Phytomanagement of metal(loid)-contaminated soils: options, efficiency and value. *Front. Environ. Sci.* 9, 661423. doi:10.3389/fenvs.2021.661423

Nesme, J., and Simonet, P. (2015). The soil resistome: a critical review on antibiotic resistance origins, ecology and dissemination potential in telluric bacteria. *Environ. Microbiol.* 17, 913–930. doi:10.1111/1462-2920.12631

Nnorom, M.-A., Saroj, D., Avery, L., Hough, R., and Guo, B. (2023). A review of the impact of conductive materials on antibiotic resistance genes during the anaerobic digestion of sewage sludge and animal manure. *J. Hazard. Mat.* 446, 130628. doi:10.1016/j.jhazmat.2022.130628

Núñez-Zofío, M., Larregla, S., and Carlos Garbisu, C. (2011). Application of organic amendments followed by soil plastic mulching reduces the incidence of *Phytophthora capsici* in pepper crops under temperate climate. *Crop Prot.* 30, 1563–1572. doi:10.1016/j.cropro.2011.08.020

Ohore, O. E., Addo, F. G., Zhang, S., Han, N., and Anim-Larbi, K. (2019). Distribution and relationship between antimicrobial resistance genes and heavy metals in surface sediments of Taihu Lake, China. *J. Environ. Sci.* 77, 323–335. doi:10.1016/j.jes.2018.09.004

Olicón-Hernández, D. R., González-López, J., and Aranda, E. (2017). Overview on the biochemical potential of filamentous fungi to degrade pharmaceutical compounds. *Front. Microbiol.* 8, 1792. doi:10.3389/fmicb.2017.01792

Qiu, L., Zhang, Q., Zhu, H., Reich, P. B., Banerjee, S., van der Heijden, M. G. A., et al. (2021). Erosion reduces soil microbial diversity, network complexity and multifunctionality. *ISME J.* 15, 2474–2489. doi:10.1038/s41396-021-00913-1

Romero, D., Traxler, M. F., López, D., and Kolter, R. (2011). Antibiotics as signal molecules. *Chem. Rev.* 111, 5492–5505. doi:10.1021/cr2000509

Serwecińska, L. (2020). Antimicrobials and antibiotic-resistant bacteria: a risk to the environment and to public health. *Water* 12, 3313. doi:10.3390/w12123313

Song, J., Chen, Y., Mi, H., Xu, R., Zhang, W., Wang, C., et al. (2024). Prevalence of antibiotic and metal resistance genes in phytoremediated cadmium and zinc contaminated soil assisted by chitosan and *Trichoderma harzianum*. *Environ. Int.* 183, 108394. doi:10.1016/j.envint.2023.108394

Staub, J. M., Brand, L., Tran, M., Kong, Y., and Rogers, S. G. (2012). Bacterial glyphosate resistance conferred by overexpression of an *E. coli* membrane efflux transporter. *J. Ind. Microbiol. Biotechnol.* 39, 641–647. doi:10.1007/s10295-011-1057-x

Sun, C., Li, W., Chen, Z., Qin, W., and Wen, X. (2019). Responses of antibiotics, antibiotic resistance genes, and mobile genetic elements in sewage sludge to thermal hydrolysis pre-treatment and various anaerobic digestion conditions. *Environ. Int.* 133, 105156. doi:10.1016/j.envint.2019.105156

Tang, K. H. D. (2023). Phytoremediation: where do we go from here? *Biocatal. Agric. Biotechnol.* 50, 102721. doi:10.1016/j.bcab.2023.102721

Tian, W., Zhang, M., Zong, D., Li, W., Li, X., Wang, Z., et al. (2023). Are high-risk heavy metal(loid)s contaminated vegetables detrimental to human health? A study of incorporating bioaccessibility and toxicity into accurate health risk assessment. *Sci. Total Environ.* 897, 165514. doi:10.1016/j.scitotenv.2023.165514

Tong, Z., Liu, F., Tian, Y., Zhang, J., Liu, H., Duan, J., et al. (2022). Effect of biochar on antibiotics and antibiotic resistance genes variations during co-composting of pig manure and corn straw. *Front. Bioeng. Biotechnol.* 10, 960476. doi:10.3389/fbioe.2022.960476

Tran, T. T., Scott, A., Tien, Y.-C., Murray, R., Boerlin, P., Pearl, D. L., et al. (2021). On-farm anaerobic digestion of dairy manure reduces the abundance of antibiotic resistance-associated gene targets and the potential for plasmid transfer. *Appl. Environ. Microbiol.* 87, 20. e0298020. doi:10.1128/AEM.02980-20

Urra, J., Alkorta, I., Lanzén, A., Mijangos, I., and Garbisu, C. (2019). The application of fresh and composted horse and chicken manure affects soil quality, microbial composition and antibiotic resistance. *Appl. Soil Ecol.* 135, 73–84. doi:10.1016/j.apsoil.2018.11.005

Wales, A. D., and Davies, R. H. (2015). Co-selection of resistance to antibiotics, biocides and heavy metals, and its relevance to foodborne pathogens. *Antibiotics* 4, 567–604. doi:10.3390/antibiotics4040567

Wang, J., and Delavar, M. A. (2023). Techno-economic analysis of phytoremediation: a strategic rethinking. *Sci. Total Environ.* 902, 165949. doi:10.1016/j.scitotenv.2023.165949

Wang, Y., Pandey, P. K., Kuppu, S., Pereira, R., Aly, S., and Zhang, R. (2021). Degradation of antibiotic resistance genes and mobile gene elements in dairy manure anerobic digestion. *PLoS ONE* 16, e0254836. doi:10.1371/journal.pone.0254836

Wardle, D. A., Bardgett, R. D., Klironomos, J. N., Setälä, H., Van Der Putten, W. H., and Wall, D. H. (2004). Ecological linkages between aboveground and belowground biota. *Science* 304, 1629–1633. doi:10.1126/science.1094875

Waseem, M., Khilji, S. A., Tariq, S., Jamal, A., Alomrani, S. O., and Javed, T. (2024). Phytoremediation of heavy metals from industrially contaminated soil using sunflower (*Helianthus annus* L.) by inoculation of two indigenous bacteria. *Plant Stress* 11, 100297. doi:10.1016/j.stress.2023.100297

Xu, X., Zarecki, R., Medina, S., Ofaim, S., Liu, X., Chen, C., et al. (2019). Modeling microbial communities from atrazine contaminated soils promotes the development of biostimulation solutions. *ISME J.* 13, 494–508. doi:10.1038/s41396-018-0288-5

Ye, M., Sun, M., Feng, Y., Wan, J., Xie, S., Tian, D., et al. (2016). Effect of biochar amendment on the control of soil sulfonamides, antibiotic-resistant bacteria, and gene enrichment in lettuce tissues. *J. Hazard. Mater.* 309, 219–227. doi:10.1016/j.jhazmat.2015.10.074

Zalewska, M., Błażejewska, A., Czapko, A., and Popowska, M. (2023). Pig manure treatment strategies for mitigating the spread of antibiotic resistance. *Sci. Rep.* 13, 11999. doi:10.1038/s41598-023-39204-4

Zhu, D., Delgado-Baquerizo, M., Su, J. Q., Ding, J., Li, H., Gillings, M. R., et al. (2021). Deciphering potential roles of earthworms in mitigation of antibiotic resistance in the soils from diverse ecosystems. *Environ. Sci. Technol.* 55, 7445–7455. doi:10.1021/acs.est.1c00811

Zhu, Y. G., Johnson, T. A., Su, J. Q., Qiao, M., Guo, G. X., Stedtfeld, R. D., et al. (2013). Diverse and abundant antibiotic resistance genes in Chinese swine farms. *Proc. Natl. Acad. Sci. U. S. A.* 110, 3435–3440. doi:10.1073/pnas.1222743110

frontiers | Frontiers in Environmental Science

TYPE Review
PUBLISHED 12 March 2024
DOI 10.3389/fenvs.2024.1352603

OPEN ACCESS

EDITED BY
Qi Liao,
Central South University, China

REVIEWED BY
John Yang,
Lincoln University, United States
Quanqing Zhang,
University of California, Riverside, United States

*CORRESPONDENCE
Fenghe Wang,
wangfenghe@njust.edu.cn

†These authors have contributed equally to this work and share first authorship

RECEIVED 08 December 2023
ACCEPTED 19 February 2024
PUBLISHED 12 March 2024

CITATION
Zhu Y, Che R, Tu B, Miao J, Lu X, Li J, Zhu Y and Wang F (2024), Contamination and remediation of contaminated firing ranges—an overview. *Front. Environ. Sci.* 12:1352603. doi: 10.3389/fenvs.2024.1352603

Contamination and remediation of contaminated firing ranges—an overview

Yining Zhu[1,2,3,4†], Ruijie Che[2,3,4†], Biyang Tu[2,3,4], Jiahe Miao[2,3,4], Xinya Lu[2,3,4], Jining Li[2,3,4], Yongbing Zhu[1] and Fenghe Wang[1,2,3*]

[1]State Key Laboratory of NBC Protection for Civilian, Beijing, China, [2]School of Environment, Nanjing Normal University, Nanjing, Jiangsu, China, [3]School of Chemistry and Chemical Engineering, Nanjing University of Science and Technology, Nanjing, Jiangsu, China, [4]Jiangsu Province Engineering Research Center of Environmental Risk Prevention and Emergency Response Technology, Nanjing, Jiangsu, China

Land and groundwater resources are fundamental pillars of sustainable human development. The negligent abandonment of ammunition and its fragments during range activities can result in severe contamination of range sites, thereby posing a significant risk to both the ecological environment and human health. Nevertheless, numerous uncertainties persist regarding the comprehension of range contaminated sites. In this study, the literature on the range of contaminated sites decommissioned after 2000 was systematically examined to consolidate basic information related to these sites, such as contaminant types, contamination status, and remediation measures. Considerable attention is devoted to investigating the advancement of diverse techniques, such as phytoremediation, chemical leaching, and solidification/stabilization, to remediate polluted areas within decommissioned firing ranges. Among the various types of remediation means, physical remediation and chemical remediation have higher remediation efficiency, but generally have higher costs and are prone to secondary pollution. Bioremediation is low cost and environmentally friendly, but has a long restoration cycle. The choice of remediation method should be based on actual needs. Additionally, this study puts forth prospective avenues for future research. Ultimately, this endeavor aims to attract the interest of scholars toward the remediation of contaminated sites within firing ranges, thereby making a valuable contribution to both human wellbeing and sustainable progress.

KEYWORDS

shooting range, heavy metal, polycyclic aromatic hydrocarbon (PAH), pollution, remediation

1 Introduction

The maintenance of operational readiness for troops necessitates military training involving live ammunition, which inevitably leads to soil and groundwater contamination in the surrounding areas. Due to the dispersion of training ranges across diverse soil types, the interaction of contaminants from range activities and their impact on specific receptors pose challenges in terms of prediction. The utilization of metallic lead is prevalent in the production of bullets and lead projectiles due to its exceptional attributes of high density, corrosion resistance, and ductility Dinake et al. (2019). The primary components of ammunition utilized for range training are a Pb-Sb core, which constitutes

approximately 95% of the bullet, and a Cu-Zn casing, accounting for approximately 5% of the bullet. The core is primarily composed of Pb (>90%), Pb-Sb alloy (<5%), As (<0.5%), and Ni (<0.5%), whereas the casing is composed of a Cu-Zn (90%/10%) alloy (Dermatas et al., 2006a). Currently, firing ranges are located all over the world, including Asia, Europe, Africa and the Americas (Cao et al., 2003; Sorvari et al., 2006; Mathee et al., 2017; Khan et al., 2021). According to reports, approximately 100,000 outdoor and military firing ranges worldwide are utilized for shooting activities, resulting in an annual release of up to 72,600 tons of Pb from munitions onto the soils of these diverse national ranges (Rodríguez-Seijo et al., 2017). Furthermore, copper (Cu) is employed as a constituent in jacketed bullets alongside lead (Pb), antimony (Sb) serves as a hardening agent for lead, nickel (Ni) or zinc (Zn) are utilized as alloys in the copper jacketed bullets, arsenic (As) coexists within lead and is a constituent of lead shotgun shells, chromium (Cr) acts as an alloy material for certain bullet types, and clay targets contain a range of 3,000 to 40,000 mg of polycyclic aromatic hydrocarbons (PAHs) per kilogram (ITRC, 2003; Laporte-Saumure et al., 2011). The release of heavy metals and organic contaminants from firing ranges due to munitions weathering can result in their deposition in range soils and subsequent diffusion into the surrounding environment via pore space, surface or groundwater. Consequently, the detection of contamination of varying magnitudes has been observed in nearly all range environments. Pb, one of the priority metal contaminants in firing ranges, has been found in concentrations up to tens of thousands of mg/kg in contaminated ranges around the world, with the highest levels on berm (Hardison Jr et al., 2004; Mendes et al., 2023). Clay fragments piled up in the range contain large amounts of coal tar and petroleum asphalt, which can contain as much as 3,000–40,000 mg/kg of PAHs (Wolf et al., 2020). Some studies have shown that heavy metal concentrations in shooting range soils worldwide are much higher than background concentrations in agricultural soils, with Pb concentrations tens or even hundreds of times higher (Sanderson et al., 2018).

The bioavailability and bioaccessibility of pollutants at the target range determine the toxicity level of the pollutants, and higher bioavailability indicates higher levels of soil toxicity, which, to a certain extent, will lead to a decrease in the growth rate and level of plant growth, a decrease in the abundance of microbial communities, and an impediment to the cycling of soil nutrients, *etc.* (Fayiga and Saha, 2016a; Sanderson et al., 2018). Due to their inherent inertness in typical soil, groundwater, and surface water conditions, the persistence of contaminants in range sites can be prolonged in the absence of remediation efforts. Range pollution also has potential impacts on the natural environment and human health. For example, large quantities of metal fragments released into the environment as a result of shooting activities can be partially transformed into metal secondary minerals, thereby increasing the potential for the transport of heavy metals in the environment and expanding the scope of heavy pollution (Dermatas et al., 2006b). Inorganic heavy metals and organic pollutants, *etc.*, in the range may pollute groundwater and nearby surface water through migration, *etc.*, affecting the health of aquatic ecosystems (Mendes et al., 2023). In addition, direct exposure of humans to the environment around shooting ranges, inhalation of dust, or ingestion of heavy metals such as Pb, Zn, Ni, As and other (loid) heavy metals through the food chain can lead to a certain degree to cardiovascular disease, anemia, kidney damage and even cancer, *etc.* (Urrutia-Goyes et al., 2017; Kazery et al., 2021; Ni et al., 2023a). In contrast, only a small amount of Pb contamination ingested by adults through the various exposure routes enters their bloodstream, while the amount of lead that enters a child's bloodstream can be much higher. Pollutants of all kinds (especially the heavy metal Pb) are particularly dangerous to infants and young children, and can cause irreversible damage to their developing brains and nervous systems (Fayiga and Saha, 2016b). Consequently, the remediation of contaminated range sites and the mitigation of hazards posed to surrounding soils and waters resulting from range activities hold paramount importance in enhancing the environmental quality and public health of such sites.

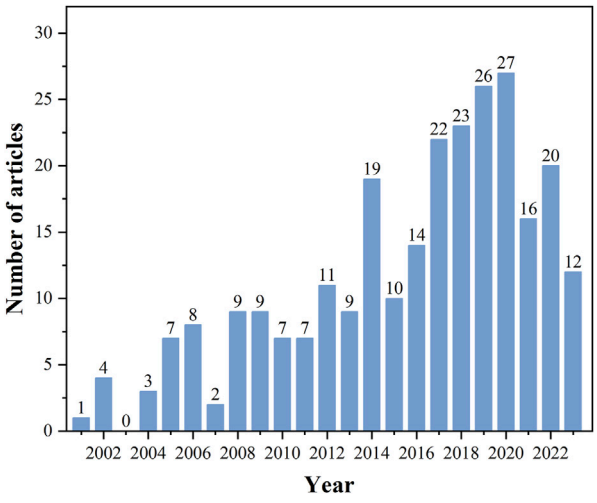

FIGURE 1
WOS database literature publications in the field related to remediation of contaminated sites at target ranges, 2001–2023.

Based on our current understanding, a comprehensive assessment of the contamination levels and remediation efforts at range sites is lacking. In this study, we aim to provide a concise overview of the significant research developments over the past decades, followed by an examination of the present contamination status across various countries. Furthermore, we will emphasize the remediation strategies employed and the associated challenges encountered in this context. In addition, we emphasize gaps in future research with a view to harvesting better ways of managing pollution at range sites.

2 Bibliometric analysis of abandoned ranges

The detrimental impact of pollution stemming from military activities extends to both the environment and human health (Gómez-Sagasti et al., 2021). Of particular concern on a global scale is the escalating issue of heavy metal contamination in soils resulting from conventional shooting practices. Neglected ranges, lacking any form of remediation, pose a significant threat to environmental pollution (Sanderson et al., 2018; Reigosa-Alonso et al., 2021). The disintegration and deterioration of ammunition contribute to heightened levels of

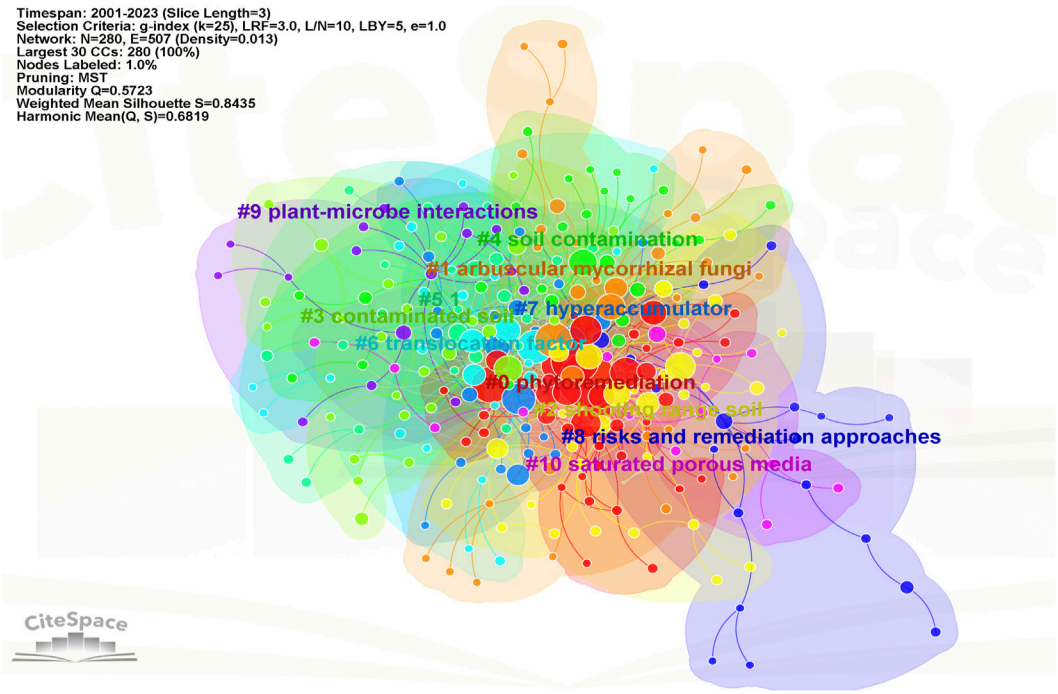

FIGURE 2
Keyword clustering of literature related to remediation of contaminated sites at the range, 2001–2023.

toxic metals within the soil, with the degree of contamination intensifying as the range ages (Fayiga and Saha, 2016a). In spite of the benefits offered by these metals in the production of ammunition, the presence of heavy metals, such as lead, can result in detrimental effects on the human nervous system, kidneys, and other bodily functions by interfering with the proper functioning of biological enzymes (Dinake and Kelebemang, 2019). Current research on the remediation of contamination at the range site focuses on soil flora characterization, hyper-enriched plants, health risks, and the uptake and transformation of pollutants (Lewińska et al., 2019; Wolf et al., 2020; Luo et al., 2023).

Figure 1 illustrates the quantity of publications pertaining to pollution remediation of target range sites from 2001 to the present. Since the onset of the 21st century, scholarly investigations in this domain have experienced a gradual upsurge, reaching their pinnacle during the period of 2017–2020, with an average annual publication count of 24.5. Subsequently, the number of publications in this field exhibited a decline. The 266 relevant literatures screened in the WOS database were used as the data source and imported into the bibliometric analysis software Citespace to draw the keyword clustering map with keywords as the emergence (Figure 2). There are 280 keyword nodes (N), and 507 connecting lines (E) in the keyword clustering map. Among them, the top five keywords with the highest frequency were heavy metals, remediation, lead, phytoremediation, and accumulation, and the five keywords with the highest centrality, i.e., the strongest connections to the rest of the keywords, were plants, shooting range soils, growth, phytoremediation and accumulation (Supplementary Table S3). The remaining research statistics in related fields are described in detail in the Supplementary Material.

3 Contaminants in contaminated sites at firing ranges

The issue of soil contamination at firing ranges has garnered growing scholarly interest in recent years, primarily due to the substantial accumulation of pollutants resulting from shooting activities and the extensive global distribution of these ranges. Statistical data reveals that the U.S. Department of Defense is responsible for supervising over 3,000 military ranges dedicated to light weapons, alongside approximately 9,000 non-military outdoor ranges. According to the National Shooting Sports Foundation, it is estimated that there are approximately 10,000 firing ranges in the United States (Fayiga and Saha, 2016a). In comparison, Finland possesses around 2,000 firing ranges, which accounts for 10% of the overall number of contaminated sites. The range soils in these locations contain various contaminants such as lead (Pb), antimony (Sb), copper (Cu), selenium (As), zinc (Zn), nickel (Ni), chromium (Cr), and polycyclic aromatic hydrocarbons (PAHs). These contaminants primarily originate from warheads and warhead fragments, cartridges and cartridge fragments, targets, and various additives.

3.1 Heavy metals and metalloids

After being discharged, bullets make contact with the soil and undergo weathering, resulting in their fragmentation and pulverization. This process leads to the accumulation of substantial amounts of heavy metals in the soil, with firing ranges being recognized as a potential origin of soil contamination by diverse heavy metals (Sanderson et al., 2018).

Lead constitutes the predominant element in lead bullets, comprising 93.1% of their overall mass (Laporte-Saumure et al., 2011). Lead bullets have been extensively employed worldwide over recent decades, establishing lead as the primary material utilized in bullet production (Pain et al., 2019). Consequently, firing ranges emerge as the second most significant source of lead (Pb) contamination in the environment, following the battery industry. Furthermore, copper (Cu) finds application in jacketed bullets, antimony (Sb) serves as a hardening agent for lead, nickel (Ni) or zinc (Zn) are employed as alloys in copper jacketed bullets, arsenic (As) coexists with lead in shotgun shells, and chromium (Cr) acts as an alloy in certain bullet varieties (ITRC, 2003; Laporte-Saumure et al., 2011). Despite constituting a minor proportion of a bullet's overall mass, the persistent utilization of firing ranges is anticipated to lead to the gradual buildup of these metallic elements, particularly copper (Cu) and antimony (Sb), within range soils. The prevalence of heavy metal contamination in shooting range soils has garnered significant attention, with reports of such contamination emerging from diverse regions across the globe.

According to data published by the American Lead Industry Almanac, the utilization of lead in ammunition manufacturing amounted to 85,300 and 79,300 tons in 2014 and 2015, respectively. This accounted for 6% of the overall lead consumption mix in the United States, ranking second highest after the usage of lead-acid batteries (Guberman, 2017). The findings of a survey conducted by Bannon et al. (2009) on firing ranges in eight states in the U.S. revealed that the concentration of total Pb in topsoil ranged from 4,549 to 24,484 mg/kg, significantly surpassing the limit established by the USEPA, which is set at 400 mg/kg. Furthermore, the soil is also subjected to environmental risks due to elevated levels of Sb (ranging from 7 to 91 mg/kg), Cu (ranging from 223 to 2,936 mg/kg), Ni (ranging from 3 to 247 mg/kg), Zn (ranging from 102 to 284 mg/kg), Mn (ranging from 83 to 930 mg/kg), and As (ranging from 2.8 to 27.9 mg/kg).

In Korea, there exists a considerable number of active small arms firing ranges, totaling 1,400 (MOE, 2005). However, there is a dearth of information regarding the impact of heavy metals found in lead bullets on the soil within military firing ranges (Moon et al., 2013). Lee and Park, (2008) conducted a comparative analysis of heavy metal concentrations at the Maehyang-ri shooting range and other firing ranges in Korea. Their investigation revealed the predominant heavy metal contaminants at the Maehyang-ri shooting range. Notably, the copper concentration in the study area was found to be 23 times higher than the average soil concentration in Korea (114.4 ± 5.7 mg/kg), while the lead concentration exceeded the soil contamination standard (362.3 ± 20.5 mg/kg) by 1.2 times. In their study, (Moon et al., 2013), conducted an analysis of the geochemical properties of soils contaminated with heavy metals at a military shooting range in South Korea. The findings revealed significant contamination of Pb in the range soils, with evidence indicating varying degrees of anthropogenic Pb sources. Specifically, the surface (0–10 cm), subsurface (10–30 cm), and deep (30–50 cm) soils exhibited concentrations of Pb ranging from 5,127 to 28,040 mg/kg, 4,147–24,043 mg/kg, and 185–19,763 mg/kg, respectively. Additionally, trace amounts of Cu, Ni, Cd, and Zn were also detected.

According to Okkenhaug et al. (2018), Switzerland possesses a total of 2,000 firing ranges, which collectively contribute to the deposition of approximately 400–500 tons of lead bullets annually. In a study conducted by Knechtenhofer et al. (2003) in Losone, Ticino, Switzerland, the soil of these firing ranges was examined, revealing the presence of various heavy metals such as Pb (ranging from 22 to 12,533 mg/kg), Sb (ranging from 0.3 to 676 mg/kg), Cu (ranging from 9.8 to 148.9 mg/kg), Ni (ranging from 43.9 to 64 mg/kg), Zn (ranging from 57.4 to 87 mg/kg), and Mn (ranging from 180 to 550 mg/kg). In their study, Česynaitė et al. (2023) investigated a military range located in Alytus, Lithuania. Their findings revealed the presence of Pb concentrations reaching up to 54,600 ± 5,300 mg/kg in soils situated 45 m away from the firing line. Similarly, Česynaitė et al. (2021) conducted their own analysis on soils within the same area, at distances ranging from −5–45 m from the firing line. Their results indicated the presence of Pb concentrations ranging from 217 to 53,023 mg/kg, as well as varying concentrations of Sb, Cu, Ni, Zn, and Mn, with values reaching up to 59,978 mg/kg, respectively. The concentrations of antimony (Sb), copper (Cu), nickel (Ni), zinc (Zn), and manganese (Mn) were observed to range from 0 to 599.78, 6.1 to 24, 3.7 to 11.5, 1.7 to 2.7, and 170–215 mg/kg, respectively.

In their study, Wang et al. (2022) examined the attributes of heavy metal pollution in the uppermost layer of soil within a military training field for heavy weapons in Tibet, China. Additionally, the researchers assessed the potential ecological hazards associated with heavy metal contamination in the uppermost layer of soil within an artillery range situated at the aforementioned military training field. The findings indicate that the concentration of heavy metal elements, specifically As (ranging from 25.2 to 122 mg/kg) and Cu (ranging from 20.6 to 116 mg/kg), in the soil of the firing range exceeded the background levels observed in the surrounding regional soil. This disparity can be attributed to the dissimilar composition of gunpowder and metal materials used in heavy weapons compared to light weapons. The extensive use of copper-coated steel cartridges and arsenic-containing gunpowder during artillery landing and bombing operations has resulted in the contamination of heavy metal elements, namely As and Cu.

In Norway, there exists an estimated count of 3,000 firing ranges, encompassing both civilian and military facilities. Among these, 1,700 are currently operational. Furthermore, the production of bullets necessitates the annual consumption of approximately 700 tons of lead (Pb) and copper (Cu) (Okkenhaug et al., 2018). Consequently, the utilization of these bullets engenders an environmental hazard, impacting not only the soil within the ranges but also the surrounding aquatic ecosystem. The study conducted by Mariussen et al. (2017) examined the environmental conditions of mires and revealed relatively low concentrations of Pb (13 mg/kg), Sb (0.83 mg/kg), Cu (5.2 mg/kg), and Zn (1.1 mg/kg) in the soil. However, elevated concentrations of Pb (2,500 μg/L), Sb (150 μg/L), Cu (900 μg/L), and Zn (1,600 μg/L) were detected in the Subsurface soil water. These high concentrations of heavy metals in the Subsurface soil water are consistent with the findings of Okkenhaug et al. (2018), which also indicate heavy metal pollution in the groundwater and downstream surface water surrounding the range. Bullets used on firing ranges contain mainly Pb, Cu, Zn and Sb, while lead-free bullets contain steel (Johnsen and Aaneby, 2019).

Table 1 presents a comprehensive compilation of reports pertaining to the overall environmental heavy metal content

TABLE 1 Total contents of heavy metals in shooting ranges from different countries.

Country	Sample position	Pollutants and concentrations (mg/kg in soil and μg/L in water)								References
		Pb	Sb	Cu	Ni	Cr	Zn	Mn	As	
Norway	Top soil	13	0.83	5.2	—	—	1.1	—	—	Mariussen et al. (2017)
	Discharge water	180	65	42	—	—	63	—	—	Mariussen et al. (2017)
	Subsurface soil water	2,500	150	900	—	—	1,600	—	—	Mariussen et al. (2017)
	Groundwater	22 ± 5	11 ± 2	16 ± 6	—	—	—	—	—	Okkenhaug et al. (2018)
	Downstream surface water	6.9 ± 1	7.4 ± 0.1	24 ± 0.0	—	—	—	—	—	Okkenhaug et al. (2018)
Botswana	Field soil	—	—	67.4 ~ 1,569	—	—	—	25.9 ~ 953.8	—	Dinake et al. (2018)
	Field soil	—	38 ~ 283	—	—	—	—	—	—	Dinake et al. (2022)
	Field soil	685 ~ 20,882	—	—	—	—	—	—	—	Kelebemang et al. (2017)
Lithuania	5–30 m from the firing line	390 ± 90	<1.5	—	5.5 ± 1.6	—	—	—	—	Česynaitė et al. (2023)
	45 m from the firing line	54,600 ± 5,300	530 ± 50	—	7.9 ± 0.5	—	—	—	—	Česynaitė et al. (2023)
	Field soil	217 ~ 53,023	0 ~ 599.78	6.1 ~ 24	3.7 ~ 11.5	—	1.7 ~ 2.7	170 ~ 215	—	Česynaitė et al. (2021)
	Field soil	6,758 ~ 8,272	—	—	—	—	—	—	—	Sujetoviene and Cesynaite (2020)
Cyprus	Field soil	78 ~ 7,265	—	—	—	—	—	—	—	Christou et al. (2022)
South Korea	Surface field soil	5,127 ~ 28,040	—	273 ~ 1,073	7 ~ 27	n.d. ~ 267	—	—	—	Moon et al. (2021)
	Field soil (5–15 cm)	4,147 ~ 24,043	—	183 ~ 927	7 ~ 13	n.d. ~ 170	—	—	—	Moon et al. (2021)
	Field soil (15–30 cm)	185 ~ 19,763	—	9–623	2 ~ 13	0 ~ 63	—	—	—	Moon et al. (2021)
	Field soil	362.3 ± 20.5		114.4 ± 5.7						Lee and Park (2008)
Australia	Field soil	399 ~ 10,403	6.57 ~ 252	28.7 ~ 1,250	1.35 ~ 8.8	—	5.63 ~ 153	—	3.08 ~ 15.8	Sanderson et al. (2012)
Spain	Field soil	55 ~ 6,309		19 ~ 98	11 ~ 33	40 ~ 79	34 ~ 264	—	—	Rodríguez-Seijo et al. (2016a)
Switzerland	Field soil	22 ~ 12,533	<0.3 ~ 676	9.8 ~ 148.9	43.9 ~ 64	—	57.4 ~ 87	180 ~ 550	—	Knechtenhofer et al. (2003)
Finnish	Shotgun field soil	350 ~ 1,300	n.d. ~ 1,200	20 ~ 59	4 ~ 15	—	21 ~ 90	—	n.d. ~ 200	Sorvari (2007)
	Rifle field soil	9,600 ~ 19,800	22 ~ 330	320 ~ 970	8.5 ~ 16	—	52 ~ 76	—	n.d	Sorvari (2007)
America	Field soil	4,549 ~ 24,484	7 ~ 91	223 ~ 2,936	3 ~ 247	—	102 ~ 284	83 ~ 930	2.8 ~ 27.9	Bannon et al. (2009)
Canada	Field soil	14,400 ~ 27,100	150 ~ 570	1830 ~ 7,720	—	—	260 ~ 1,080	—	—	Laporte-Saumure et al. (2011)
	Field soil	3,368 ± 170	73 ± 5	245 ± 11	—	—	177 ± 2	—	—	Lafond et al. (2014)
China	Field soil	37.2 ~ 66.9	—	20.6 ~ 116	18.8 ~ 28.8	29.1 ~ 56.4	71.1 ~ 142	497 ~ 696	25.2 ~ 122	Wang et al. (2022a)

n.d. = not detected,/ = not determined.

TABLE 2 Total contents of various pollutants in shooting ranges.

Pollutants	Molecular formula	Country	Sample position	Concentrations (mg/kg in soil, μg/L in water)	References
PAHs	—	Spain	Soil	38 ~ 360	Rodríguez-Seijo et al. (2017)
		America	Soil	373	Wolf et al. (2020)
		America	Soil	2,431	
		America	Soil	1,324	Frakes et al. (2007)
Nitroglycerine	$C_3H_5N_3O_9$	America	Soil	<0.02 ~ 69.64	Clausen et al. (2011)
2,4-Dinitrotoluene	$C_7H_6N_2O_4$	America	Soil	<0.014 ~ 1.51	Clausen et al. (2011)
		America	Soil	205.69 ± 54.44	He et al. (2007)
		Canada	Soil	0 ~ 247.4	Jugnia et al. (2018)
2,6-Dinitrotoluene	$C_7H_6N_2O_4$	America	Soil	<0.18	Clausen et al. (2011)
		America	Soil	34.84 ± 8.09	He et al. (2007)
TNT	$C_7H_5N_3O_6$	Canada	Soil	<0.25 ~ 0.49	Robidoux et al. (2004)
2-ADNT	$C_7H_7N_3O_4$	Canada	Soil	<0.25 ~ 1.06	Robidoux et al. (2004)
4-ADNT	$C_7H_7N_3O_4$	Canada	Soil	0.25 ~ 6.68	Robidoux et al. (2004)
HMX	$C_4H_8N_8O_8$	Canada	Soil	14 ~ 696	Robidoux et al. (2004)
RDX	$C_3H_6N_6O_6$	Canada	Soil	<0.25 ~ 2.8	Robidoux et al. (2004)
		Canada	Groundwater	3.52 ~ 196.7	Jugnia et al. (2019)
		Canada	Soil	0 ~ 0.4	Jugnia et al. (2018)

found in firing ranges across various countries. The concentrations of copper and lead in the soils of these firing ranges exhibit significant variability, which can be attributed to factors such as range utilization, soil properties, and geographical location.

3.2 Organic substance

In contrast to the extensive attention given to the public health implications associated with heavy metals like Pb and Sb in shooting range soils, there exists a notable dearth of research conducted by scholars on the topic of organic matter in these soils. The concentrations of various organic contaminants at contaminated sites are provided in Table 2 for reference.

Clay targets were composed of coal tar pitch or petroleum (30–32 wt%), clay or limestone (67–70 wt%), and fluorescent paint. Each kilogram of clay targets contains 3,000 ~ 40,000 mg of PAHs. Significant PAHs contamination was generated at the outdoor range due to the accumulation of clay target debris. Rodríguez-Seijo et al. (2017) investigated soil from an abandoned shooting range in Monforte de Lemos, NW Spain. PAHs detected included acenaphthylene (6.0 ~ 56 mg/kg), acenaphthene + fluorene (0.58 ~ 5.4 mg/kg), phenanthrene, anthracene (0.25 ~ 2.4 mg/kg), fluoranthene (5.5 ~ 30 mg/kg), pyrene (3.5 ~ 28 mg/kg), Benzo [a] anthracene (2.8 ~ 29 mg/kg), Chrysene (2.7 ~ 27 mg/kg), Benzo[b] fluoranthene (6.8 ~ 70 mg/kg), Benzo[k]fluoranthene (1.9 ~ 19 mg/kg), benzo [a]pyrene (3 ~ 35 mg/kg), Dibenzo[a,h] anthracene (2.1 ~ 26 mg/kg) and Indeno[1,2,3-c,d]pyrene + benzo[g,h,i]perylene (1.8 ~ 23 mg/kg). The total concentration of polycyclic aromatic hydrocarbons (PAHs) in the soil ranged from 38 to 360 mg/kg, significantly surpassing the background value for natural Spanish soils (0.61 mg/kg). Based on chemical and ecotoxicological data, the soils in this particular area pose a high risk. In a study conducted in California and Florida, United States, researchers investigated outdoor range soils and found total PAH concentrations of 2,431 and 1,324 mg/kg, respectively (Frakes et al., 2007). Wolf et al. (2020) demonstrated that decommissioned firing ranges in California, USA, had a total PAH concentration of 373 mg/kg, with high molecular weight PAHs accounting for 84% of the total.

Nitroglycerine (NG), 2,4-dinitrotoluene (2,4-DNT) and 2,6-Dinitrotoluene (2,6-DNT) are commonly used as energetics, stabilizing agents, or filler compounds in small arms ammunition. They are therefore deposited in the soil during military training. In their study, Clausen et al. (2011) examined the presence of NG, 2,4-DNT, and 2,6-DNT in soils at Camp Edwards, United States. The concentrations of these contaminants were found to be below 0.02 ~ 69.64, below 0.014 ~ 1.51, and below 0.18 mg/kg, respectively. Through their analysis of NG, 2,4-DNT, and the fate of 2,6-DNT, the authors established the existence of a potential threat to the groundwater at Camp Edwards, Massachusetts Military Reservation.

The release of chemical constituents and degradation intermediates from munitions occurs both during the manufacturing process and as a result of explosions in military activities. Examples of such compounds include RDX (1,3,5-trinitro-1,3,5-triazine), TNT (2,4,6-trinitrotoluene), HMX

TABLE 3 Comparison of several major remediation technologies for contaminated sites at shooting ranges.

Restoration type	Restoration techniques	Principle	Applicability	Restoration efficiency	Advantages	Disadvantages	References
Physical remediation	Soil replacement	Replacement of contaminated soil with clean uncontaminated soil	Suitable for surface soil remediation of small contaminated sites	Removal of soil contaminants can be achieved in a relatively short period of time	Efficient remediation of small areas of heavily contaminated topsoil in a short period of time	High cost; need to consider reprocessing of raw contaminated soil; not applicable to large-scale site contaminated soil remediation	Douay et al. (2008), Jiang et al. (2021)
	Mechanical screening	Sieving of soil into particles of different sizes to remove contaminants	Suitable for soil remediation of small contaminated sites	Shorter repair cycles	Low cost; environmentally friendly	Does not completely remove contaminants; not widely applicable	Zhang et al. (2020), Chang et al. (2022)
	Electrokinetic remediation	Utilizes the electrodynamic effect to drive contaminants from the soil to be removed with the fluid medium	Suitable for soil remediation of low permeability contaminated sites	Rapid removal of soil contaminants	Low cost; easy operation; not limited by soil permeability	Low removal efficiency for non-migratory pollutants; may cause changes in soil pH, temperature	Ouhadi et al. (2010), Saini et al. (2021)
Chemical remediation	Solidification/ Stabilization	Immobilizes the contaminant in the medium and keeps it in a more stable state	Suitable for soil remediation of heavy metal and highly polluted sites	Removal of soil contaminants can be achieved in a relatively short period of time	Low cost; easy operation; better treatment results	Cannot remove contaminants; long-term monitoring is required after repair	Scanferla et al. (2009), Kim et al. (2023)
	Chemical leaching	A solution containing a flushing aid is injected into the soil to clean and elute the contaminants therein	Suitable for soil remediation of highly permeable and contaminated sites	Removal of soil contaminants can be achieved in a relatively short period of time	Efficient and rapid; suitable for large-scale remediation of heavily contaminated soils	High cost; potential for secondary pollution problems; leads to reduced soil fertility	Xu et al. (2021), Uwayezu et al. (2024)
	Electrodialysis remediation	Porewater in the soil moves under the force of an applied electric field, carrying away pollutants	Suitable for soil remediation of low permeability contaminated sites	Faster repair time	Low cost; easy operation; not limited by soil permeability	Low removal efficiency for water-insoluble pollutants; may cause changes in soil physical and chemical properties	Ottosen et al. (2005), Pedersen et al. (2018), Skibsted et al. (2018)
Biological remediation	Phytoremediation	Effective soil remediation by utilizing the purification function of plants themselves	Suitable for surface soil remediation of small contaminated sites	The restoration cycle is long	Low cost; environmentally friendly; less destructive to soil structure	Time-consuming; low biomass; poor deep soil remediation; there are limitations to the scope of adaptation	Khan et al. (2021a), Mankė et al. (2024)
	Microbial remediation	Microorganisms degrade and metabolize pollutants as energy sources, among other things	Suitable for remediation of specific types of contaminated site soils	Longer restoration time	Strong enrichment capacity; good restoration effect; environmentally friendly	Complex screening and incubation, not suitable for treating high concentrations of pollutants	Kim et al. (2010), Rodríguez-Seijo et al. (2016b)

(1,3,5,7-tetranitro-1,3,5,7-tetrazacyclooctane), among others. These substances, even at low concentrations, have the potential to endanger the ecosystem. Robidoux et al. (2004) conducted an assessment of the toxicity levels of RDX, TNT, and HMX in soil samples obtained from a military contaminated site located in Western Canada. The concentrations of these substances were measured to be less than 0.25–2.8 mg/kg for RDX, less than 0.25–0.49 mg/kg for TNT, and 14–696 mg/kg for HMX. Additionally, the study also determined the presence of two metabolites of TNT, namely, 2-amino-4,6-dinitrotoluene (2-ADNT) and 4-amino-2,6-dinitrotoluene (4-ADNT), with concentrations ranging from less than 0.25–1.06 mg/kg for 2-ADNT and less than 0.25–6.68 mg/kg for 4-ADNT. The findings of Jugnia et al. (2019, 2018) revealed that soil from contaminated sites in Eastern Ontario, Canada, may potentially endanger soil organisms, as indicated by toxicity evaluations conducted on microorganisms, earthworms, and plants. The concentration of RDX, a military-related contaminant, was determined to range

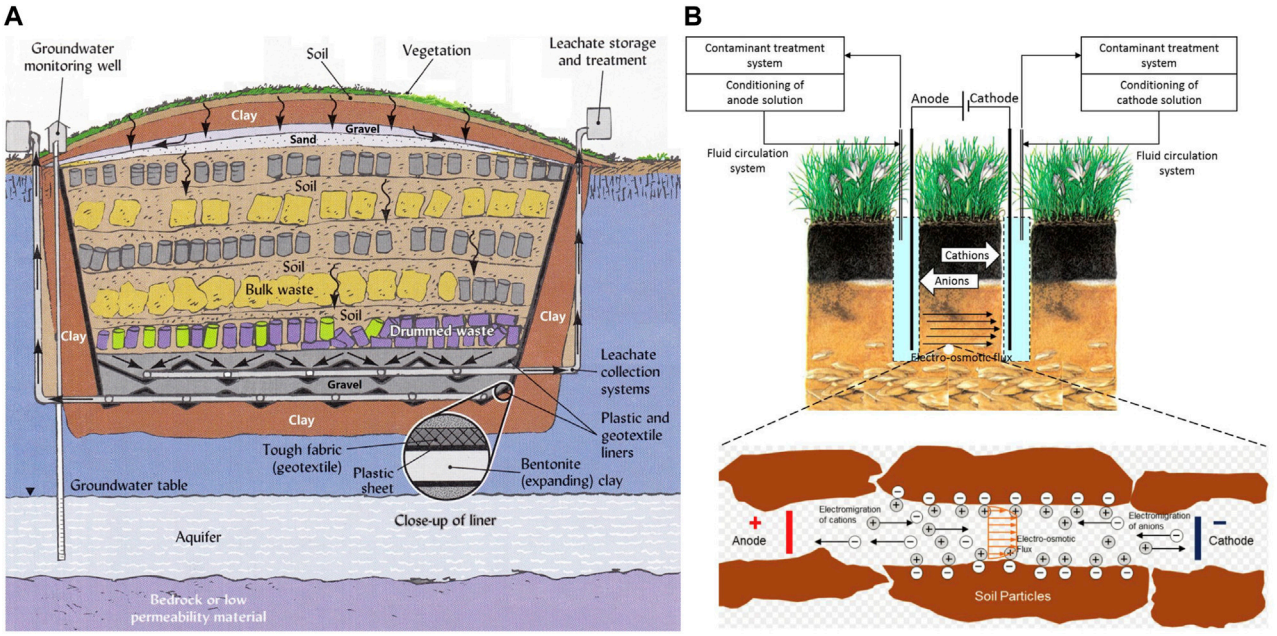

FIGURE 3
Physical restoration techniques. **(A)** Schematic cross-section of the soil filling process. This figure has been reprinted from Liu et al. (2018), with permission of the publisher. **(B)** Removal of ionic contaminants from soil by electrokinetic remediation techniques and its main mechanisms. This figure has been reprinted from Cameselle et al. (2013), with permission of the publisher.

from 0 to 0.4 mg/kg in soil and 3.52 ~ 196.7 μg/L in groundwater at the aforementioned site.

4 Contaminated site remediation technologies for decommissioned firing ranges

Currently, contaminated soils at range sites are remediated mainly by physical remediation, chemical remediation, and bioremediation (Table 3). Among them, physical remediation includes soil replacement, mechanical screening, electric remediation and vitrification. Physical remediation technology has a shorter remediation cycle and is suitable for short-term pollution remediation. Chemical remediation is mainly represented by curing/stabilization, chemical drenching and electrodialysis remediation, which can realize efficient remediation of highly polluted sites (Befkadu and Chen, 2018; Ni et al., 2023b). Bioremediation has become more popular in recent years, mainly including phytoremediation and microbial remediation, which is low-cost and a kind of environmentally friendly *in-situ* remediation technology with a broader development prospect (Xu et al., 2019; Raimondo et al., 2020).

4.1 Physical restoration techniques

Common physical remediation techniques employed for contaminated soils at firing ranges encompass soil replacement, mechanical screening, electrokinetic remediation and vitrification (Figure 3).

4.1.1 Soil replacement

The conventional approach of directly excavating and transporting contaminated soil to a landfill is merely a customary method (Sorvari et al., 2006). Nevertheless, given the remote nature of range locations and their limited asset worth, the utilization of such mass transportation proves to be economically unviable and unsuitable for the remediation of contaminated soils originating from firing ranges (Allen, 2001).

4.1.2 Mechanical screening

Mechanical screening can be effective in removing large particle size contaminants such as bullets and their fragments. In their study, Yin et al. (2010) employed three effective management practices to address the detrimental environmental effects of lead bullets in range soils. These practices included the substitution of soil berm with sand berm, the application of lime to the sand berm, and the removal of lead bullets from berm soils through mechanical sieving. The replacement of soil berm with sand berm resulted in a reduction of the total soil Pb content from 277 to 57 mg/kg after a period of 11 months. The substitution of a soil berm with a liming sand berm resulted in a decrease in the overall concentration of lead (Pb) in the soil, reducing it from a range of 497–777 mg/kg to a range of 302–362 mg/kg after a period of 15 months. Despite the elimination of the initial source of soil Pb through mechanical sieving, the sieving process itself introduced metallic Pb into the soil particles smaller than 2 mm, leading to an increase in the total soil Pb content from 4,694 to 11,479 mg/kg. Thangavadivel et al. (2018) employed a heavy particle concentrator and orbital screening technique to eliminate lead particles. Subsequently, they subjected the treated soil to high-performance concrete as a secondary treatment. This combined approach successfully achieved a 91%

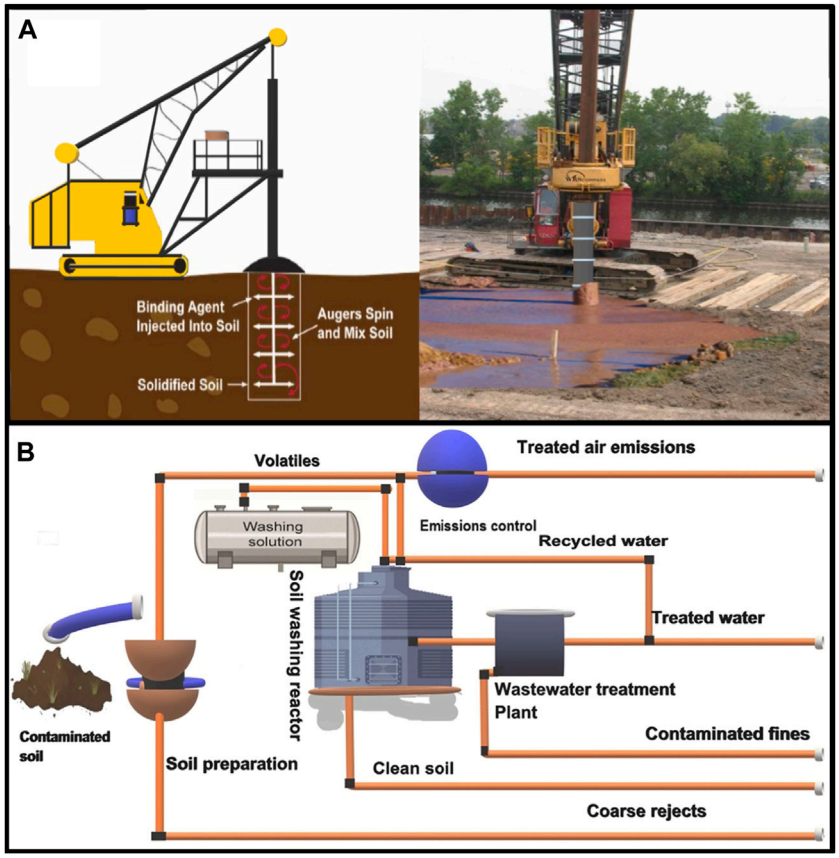

FIGURE 4
Examples of chemical remediation techniques. **(A)** Chemical immobilization technique; **(B)** Schematic diagram of the chemical leaching process. This figure has been reprinted from Khan et al. (2021), with permission of the publisher.

removal of total lead content. Moreover, the resulting lead concentration in the treated soil fell below the threshold set by the Australian National Environmental Protection Measure Health Investigation Level for Soil Contaminant.

4.1.3 Electrokinetic remediation

Electrokinetic remediation is a class of *in situ* physical remediation technology, mainly by applying a small electric current between the anode and cathode in the contaminated soil to achieve the removal of pollution (Saini et al., 2021). Cai et al. (2022) found that both continuous power supply and intermittent power failure can effectively remove Cd contamination from soil through a comparative experiment of soil electrokinetic remediation, in which the efficiency of remediation with intermittent power failure is higher. In addition to effective remediation of inorganically contaminated soils, electrokinetic remediation technology can be used in combination with surfactants, nanoparticles and oxides for effective removal of soil organic matter (Cameselle and Gouveia, 2018).

4.1.4 Vitrification

In-situ vitrification technology converts heavily contaminated soils into inert and non-migratory vitrified briquettes, reducing the spread and dispersion of soil contamination (Shu et al., 2020). The technology can effectively control the contamination of soil with many heavy metals, including radionuclides (Buelt and Farnsworth, 1991; Yasunari et al., 2011). However, the soil vitrification treatments were relatively long and the soil immobilization was not homogeneous (Chen et al., 2019).

4.2 Chemical remediation technology

There are very extensive studies on chemical remediation techniques for remediating contaminated soils at the range, including solidification/stabilization, chemical leaching, electrodialysis, and others.

4.2.1 Solidification/stabilization

The process of solidifying/stabilization involves the incorporation of solidifying/stabilizing agents into the treated soil, resulting in the transformation of toxic heavy metals present in the soil into insoluble forms that exhibit reduced mobility and toxicity (Figure 4A). This process effectively hinders the leaching of heavy metals, thereby rendering it environmentally sustainable. Additionally, the treated soil can be reused, further enhancing the overall efficacy of this technology. Furthermore, the versatility of this approach allows for its application in various scenarios (Mulligan et al., 2001; Guo et al., 2006). Notably, in certain

instances, this technology has demonstrated the capability to diminish soil lead concentrations to levels that comply with the maximum contamination limits established by both the U.S. Environmental Protection Agency (USEPA) and the World Health Organization (WHO) (Dinake and Kelebemang, 2019). Stabilization techniques can also be used in conjunction with other remediation tools to achieve higher removal results. Remediation of co-contaminated soil by extraction/degradation of organic contaminants and stabilization of Pb, Islam and Park, (2017) investigated the effect of hydrothermal treatment under subcritical conditions on the immobilization of lead in contaminated soil from a target range. The process resulted in a substantial conversion of the bioavailable portion of lead into a comparatively stable fraction, leading to a reduction in the bioavailable fraction from 41.33% to 14.66%. The application of high-temperature treatment appears to be effective in reducing the bioavailability and ecotoxicity of soils contaminated with Pb. Furthermore, the remediation of the affected range soils resulted in a shift from a high risk of pollution and ecological risk to a medium risk (Islam and Park, 2017). Commonly used solidification/stabilization materials include phosphorus-containing materials (poultry wastes, waste cattle bones, and gypsum wastes) (Cao et al., 2009), lime-containing materials (lime, eggshells, oyster shells, and mussel shells) (Cui et al., 2023), biochar materials (Shen et al., 2016), and iron-based materials (iron salts, nanoFe) (Azizi et al., 2017).

Phosphate-stabilized remediation has been implemented as a means of regulating the movement and accessibility of heavy metals within range soils, owing to its capacity to stabilize lead-phosphate deposits across a broad pH spectrum. The substances employed for phosphate stabilization encompass hydroxyapatite, phosphate rock, and phosphates (Ogawa et al., 2015; Han et al., 2022; Mi et al., 2023). The findings of the investigation conducted by Fayiga and Saha, (2016a) demonstrated a substantial decrease in Pb levels, from 800 mg/L to below 1 mg/L, subsequent to the application of phosphate rock and phosphoric acid in range soil. In their study, Sanderson et al. (2015) employed phosphate amendments for the remediation of polluted soils in a firing range. The application of phosphate resulted in a notable reduction of lead bioavailability in the soil, with a decrease of 55%. Furthermore, the leaching rate and weathering degree of lead bullets exhibited a significant decline, reaching up to 98%, following the application of phosphate onto the bullet surfaces. In their study, Ogawa et al. (2015) employed a combined application of hydroxyphosphate lime and ferrihydric compounds, resulting in the inhibition of 99.9% of water-soluble Pb and 95.5% of water-soluble Sb. These inhibitory effects were found to be superior to those observed when hydroxyphosphate lime or ferrihydric compounds were applied individually. Similarly, Yan et al. (2016) utilized alkali residues obtained during phosphorus adsorption to immobilize lead in soil within a limited area in Jiangsu, China. Phosphorus-loaded alkali slag and calcined phosphorus-loaded alkali slag exhibited conversion rates of over 60% and 90% for soil Pb into residual fractions, respectively. Conversely, raw alkali slag and calcined alkali slag without phosphorus only achieved conversion rates of 14% and 35% for soil Pb into residual fractions, respectively. It is important to acknowledge that the remediation of phosphate in range soils necessitates careful consideration of the potential eutrophication risk stemming from elevated phosphorus application rates.

Lime-based materials have proven effective in serving as remediation agents for contaminated soils at the range due to their ability to adsorb heavy metals and/or form insoluble minerals in the soil (Li et al., 2019; Sun et al., 2023). In a study conducted by Levonmäki and Hartikainen, (2007), the remediation efficiencies of two lime-based agents with varying reactivities, namely, calcium carbonate and blast furnace slag, were compared in relation to Pb remediation in range soils. After a 21-day reaction period, it was found that calcium carbonate exhibited greater mobility in reducing Pb compared to blast furnace slag. In their study, Conesa et al. (2010) effectively employed the application of $Ca(OH)_2$ and humic acid amendment to extract metallic antimony from various soil samples in Switzerland. Ahmad et al. (2012), on the other hand, utilized eggshell waste as a means to immobilize Pb in a military firing soil in South Korea. Their findings revealed that the inclusion of 5% eggshells and calcinated eggshells resulted in a significant reduction of the TCLP-Pb content in the soil by 68.8%. Moreover, the Pb content and performance achieved with these additions were comparable to those achieved with pure $CaCO_3$ and CaO, respectively. Therefore, these modifiers have the potential to be used as lead fixatives as alternatives to calcium carbonate and calcium oxide.

In recent years, there has been a growing interest in the utilization of natural or waste materials for the immobilization of trace metals, primarily due to their cost-effectiveness. One such material, biochar (BC), has been recognized as an effective adsorbent for the immobilization of trace metals (Zou et al., 2023). In a study conducted by Ahmad et al. (2012), highly contaminated military range soil in South Korea was treated using mussel shells, bovine bone, and biochar. The findings revealed that the bioavailability of lead in the soil treated with mussel shells, cow bones, and biochar was reduced by 92.5%, 84.8%, and 48.5%, respectively. In their study, Ahmad et al. (2016) conducted an investigation utilizing soybean straw and pine needle derived biochar to assess the immobilization of Pb and Cu in range soils. The results demonstrated that the soybean straw based biochar exhibited a higher efficacy in immobilizing Pb (88%) and Cu (87%) compared to the pine needle based biochar. In their study, Rajapaksha et al. (2015) examined the impact of various soil amendments, including trichocarp ragweed biomass and its derived biochar at different temperatures (300°C and 700°C), natural iron oxides (NRE), alumina trihydrate, and silver nanoparticles, on the immobilization of heavy metals in the soils of the designated site following 1 year of soil cultivation. The findings revealed that all of these soil amendments resulted in a reduction in the concentration of extractable Pb and Cu in the soil. Notably, the biochar produced at 300°C exhibited the highest efficacy in immobilizing the heavy metals. In their study, Vithanage et al. (2017) examined the impact of carbon nanotubes and biochar derived from soybean straw on the bio-efficacy of Pb, Cu, and Sb in range soils. The researchers discovered that biochar produced from soybean straw effectively immobilized bioeffective Pb and Cu in the range soils, resulting in reductions of 17.6% and 16.2% respectively. This immobilization was achieved at a lower cost. However, neither modifier proved effective in immobilizing Sb. In a separate study, Silvani et al. (2019) developed a waste wood biochar and a wood shrub iron enriched design biochar for the remediation of low TOC range soils. The findings indicate that the inclusion of 20% BC

resulted in a 61% reduction in Pb leaching and a 12% reduction in Sb leaching, while the addition of Fe-BC led to a 99% decrease in Pb leaching and a 40% decrease in Sb leaching. These results demonstrate the efficacy of modified biomass waste in remediating contaminated soils within the desired range.

It is worth noting that iron-based materials, including iron hydrate and acicular ferrite, are commonly employed as amendments in contaminated soils within the range. These iron-based adsorbents function by immobilizing heavy metals through the process of adsorption (Zhao et al., 2023). The weathering and corrosion of zero-valent iron (Fe^0) occurs when exposed to air and moisture, resulting in the formation of different iron (hydrogen) oxides. These oxides create additional adsorption and binding sites for heavy metals in the soil (Wang et al., 2022). Okkenhaug et al. (2016) successfully employed iron-based adsorbents to immobilize Pb and Sb, achieving immobilization rates of 89%–90% for Sb and 89%–99% for Pb in heavy metal-contaminated soil at the Norway Range. Tandy et al. (2017) conducted a study to assess the impact of two red mud amendments (ViroSoilTM 1 and 2) and two reductant treatments (zero-valent iron and ferrous sulfate) on the leaching of metal (loid) from the soil in the Switzerland range. The purpose of their research was to investigate the effects of these treatments. The findings of the study demonstrated that the utilization of ferrous sulfate resulted in the reduction of SbV to SbIII, effectively preventing Sb leaching. However, it was observed that the acidifying effect of ferrous sulfate, along with the reducing and dissolving impact of manganese oxides, had a detrimental influence on Pb leaching. Moreover, the combination of red mud amendment and ferrous sulfate exhibited comparable efficacy to FeSO4 alone in immobilizing Sb and reducing Pb leaching. In a separate study conducted by Mariussen et al. (2017), ferric hydroxide powder and zero-valent iron powder were mixed in range soils to assess their overall effectiveness as stabilizers for contaminated soils in the range. The concentration of Pb, Cu and Zn in soil leachate was reduced by 79%–99% when these two additives were mixed into acidic soil. In their study, Barker et al. (2023) performed soil column experiments to investigate the impact of two remediation treatments, namely, ferric chloride/calcium carbonate and nano-zero-valent iron (nZVI), on the immobilization of Pb and Sb in range soils. The results revealed that the incorporation of nZVI had minimal effect on the immobilization of Pb and Sb in the soils. On the other hand, the amendments of $FeCl_2$ and $CaCO_3$ led to a reduction of over 80% in the concentrations of Sb in the soil pore-water. In their study, Khan et al. (2023) conducted the preparation of biochar derived from pine-one waste, followed by the enrichment of biochar with Fe and Al salts to create engineered biochar. The results indicated that all three biochars effectively immobilized Sb (V) within the soil range. Notably, the Fe biochar exhibited superior immobilization capacity compared to the other two biochars, attributed to the heightened affinity of Sb (V) towards the Fe-binding functional groups present on its surface.

4.2.2 Chemical leaching

Chemical leaching, which involves the use of acids, bases, and chelating agents, is a commonly employed and effective method for treating heavy metals in range soils due to its rapid remediation capabilities and cost-effectiveness (Figure 4B and Figure 5). In the study conducted by Lafond et al. (2012), it was found that the application of 1 M sulfuric acid and 4 M sodium hydroxide effectively eliminated 75% of the Pb in the contaminated soil from a Canadian range, as well as Cu, Sb, and Zn. Lafond et al. (2013) employed chemical leaching techniques to eliminate heavy metal contaminants from a small Canadian military range. Through their investigation, they determined that the combination of sulfuric acid leaching and the introduction of sodium chloride proved to be the most efficient approach. Furthermore, when implemented alongside a continuous leaching process, this method achieved a removal rate of 96% for Cu, 99% for Pb, 84% for Sb, and 86% for Zn in Canadian military small ranges. Subsequently, a counter-current leaching process was employed, resulting in the removal of 93.2% ± 3.5%, 91.5% ± 5.7%, 82.2% ± 10.9%, and 30.0% ± 11.4% of Cu, Pb, Sb, and Zn, respectively, from the targeted range soils (Lafond et al., 2014).

Although ethylenediaminetetraacetic acid (EDTA) is a commonly used chelating agent, its toxicity and persistent presence in the environment make it unsuitable for long-term application (Wu et al., 2015). In their study, Ni et al. (2023a) investigated the substitution of [S,S]-ethylenediamine succinic acid, N,N-dicarboxymethyl glutamic acid, and 3-hydroxy-2,2-iminodisuccinic acid for EDTA in the Japanese Imari Range soil to facilitate cleaning and chemical immobilization. The authors found a positive correlation between the soil washing parameters and the Pb removal effect of the chelating agents. Furthermore, the application of $FeCl_3$ and CaO as post-treatment significantly reduced the soluble Pb content in the soil that underwent chelator washing. This remediation strategy, which combines chemical leaching with curing/stabilization, can be a practical treatment method for extracting large amounts of lead from soil and inhibiting residual lead leaching. Etim, (2017) employed acetic acid in conjunction with varying concentrations of potassium chloride and the electrochemical reduction method to address soil remediation in Nigeria. Notably, the utilization of a 5% acetic acid and 5% KCL wash solution yielded the most favorable outcomes, with lead removal rates ranging from 74.9% to 86.9%. This particular solution exhibits potential as a viable alternative to potent acids and chelating agents. Moreover, subsequent treatment of the leachate containing Pb through the utilization of Al-Al and Al-Fe bipolar electrodes resulted in removal rates of 93.7% and 94.5% respectively.

The presence of high concentrations of strong acids in heavy metal-contaminated range soil, which is intended for reuse, poses a significant risk to soil microorganisms and can adversely affect the soil's physicochemical properties. Additionally, chelating agents are not a viable option for treating range soil due to their costly nature and drawbacks, including limited treatment efficacy and the requirement for subsequent treatment.

4.2.3 Electrodialysis remediation technology

Electrodialysis remediation technology offers a solution by effectively extracting heavy metals from the soil, resulting in a final concentration below the established effects levels (Figure 6). In their study, Pedersen et al. (2019) employed multivariate analysis to concurrently evaluate the impacts of soil properties and experimental variables on the electrodialysis process for the elimination of Cu and Pb from soils at three designated locations. To represent *in situ* and *ex situ* remediation

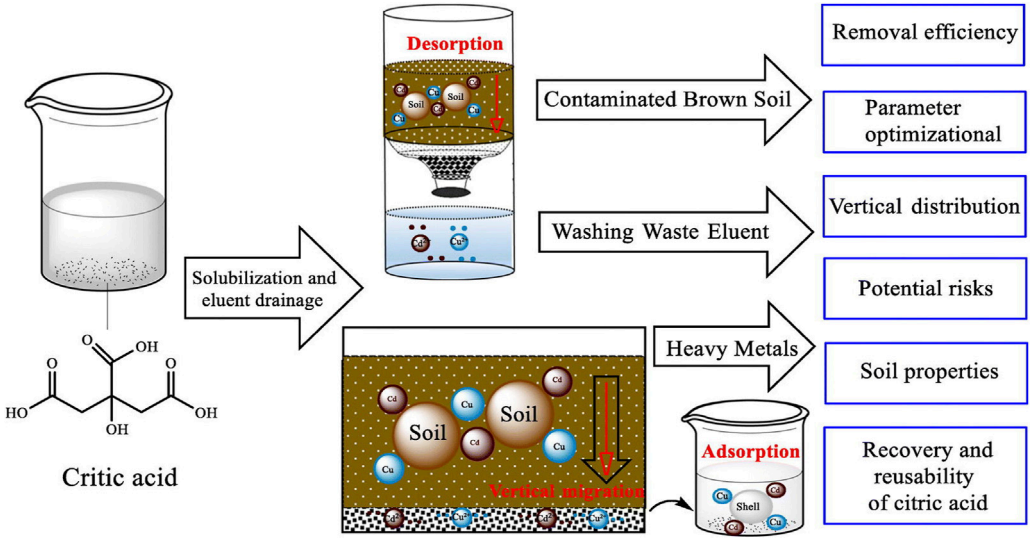

FIGURE 5
Removal of Cd and Cu from contaminated soil by combined solubilization and leachate drainage systems. This figure has been reprinted from Yang et al. (2022), with permission of the publisher.

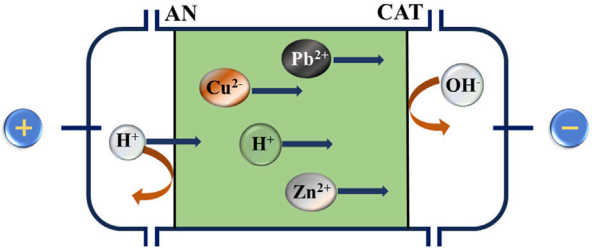

FIGURE 6
Schematic diagram of soil electrodialysis remediation technology. Where AN denotes an anion exchange membrane and CAT denotes a cation exchange membrane.

conditions, laboratory-scale fixed and agitated units were utilized. The agitation unit exhibited higher removal rates of Cu and Pb (ranging from 9% to 81%) compared to the fixed unit (ranging from 0% to 41%) within the identical experimental setting. The findings of the multivariate analysis (MVA) indicate that the impact of soil type on the effectiveness of remediation is contingent upon the specific metal being targeted and varies across different fixation and agitation configurations. Enhancing the removal of copper through adjustments to the experimental setup is more feasible in the agitation setup, which can be achieved by augmenting the current density. On the other hand, optimizing the removal of lead can be accomplished by prolonging the treatment duration and, in the agitation setup, by also increasing the current density.

4.3 Bioremediation

Bioremediation is currently a popular remediation technology for site contamination remediation (Figure 7). This remediation method utilizes a biodegradation process to remove contaminants from the environment, thereby minimizing environmental risks (Seagren, 2024). For various types of inorganic metals and organic pollutants such as polycyclic aromatic hydrocarbons (PAHs) in the contaminated soil of the target range, common bioremediation methods include phytoremediation and microbial remediation techniques (Ni et al., 2023a; Ansari et al., 2023).

4.3.1 Phytoremediation

Certain plant species possess the capacity to assimilate and endure deleterious heavy metals present in the soil within a given area. These plants can be employed to hyperaccumulate the aforementioned heavy metals, thereby facilitating the utilization and regulation of soil contaminated with heavy metals in the above-mentioned area (Figure 8). Consequently, this procedure curtails the movement and percolation of heavy metals in the soil by immobilizing and stabilizing them, thereby diminishing their interaction with organisms, a phenomenon known as phytoremediation. Hyperaccumulating plants can transfer toxic heavy metals that they have absorbed to the above-ground parts of the plant, such as shoots and leaves, at concentrations significantly higher (ranging from 100 to 1,000 times) than those observed in non-hyperaccumulating plants. Additionally, it is noteworthy that the absorption of these high concentrations of heavy metals does not elicit any toxic effects on the plant (Singh et al., 2016). The ability of plants to accumulate metals is regulated by their growth rate and their capability to translocate metals to aboveground tissues. *In situ* phytoremediation can manifest in various forms, including phytoextraction, root filtration, phytostabilization, and phytovolatilization. However, two main forms of phytoextraction and phytostabilization have been used in the contaminated soil of the range.

Phytoextraction is the process of utilizing specific plant species to extract contaminants from the soil, thereby reducing the overall concentration of soil pollutants (Suresh and Ravishankar, 2004).

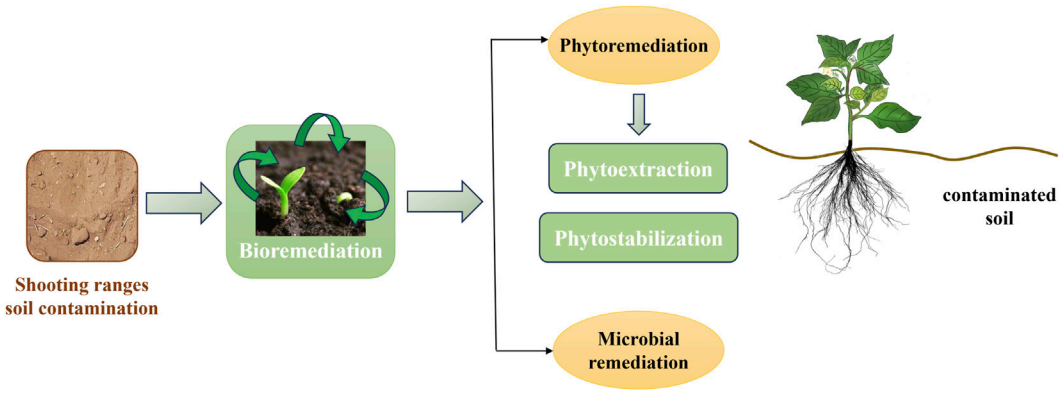

FIGURE 7
Soil bioremediation techniques for heavy metal and organic pollution.

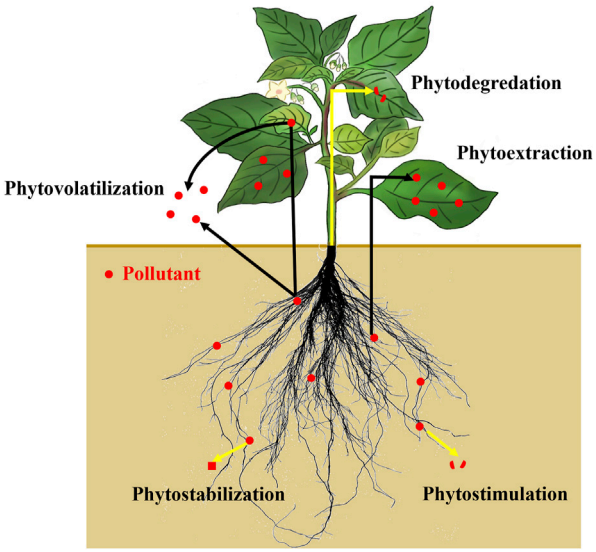

FIGURE 8
Phytoremediation mechanism diagram. Main pathways of Phytoremediation includes phytodegradation, phytovolatilization, phytoextraction, phytostabilization and phytostimulation.

Perennial herbaceous plants, due to their rapid growth, substantial biomass, extensive root systems, and moderate tolerance to pollutants, are generally considered suitable candidates for remediating heavy metal contamination (Yang et al., 2005). Numerous plant species, including various brassicas, clover (Pennisetum), trillium (Panikum), willow, and tobacco, have been extensively studied for their phytoextraction capabilities to different metals (Grispen et al., 2006; Abdel-Sabour and Al-Salama, 2007; Neugschwandtner et al., 2008; Purakayastha et al., 2008). Significant advancements have been achieved in the utilization of this technique for the improvement and restoration of range soil. In their research, Koelmel and Amarasiriwardena, (2012) employed laser ablation-inductively coupled plasma mass spectrometry (LA-ICP-MS) to investigate the spatial distribution of Cu, Pb, Sb, and Zn within the rhizomes of herbaceous ferns in range soils. The findings of their study indicated that the inner amyloplast cortex adjacent to the cortex exhibited elevated concentrations of Pb, Cu, and Zn within the rhizome tissue. In the outer amyloplast cortex, Pb was found to be concentrated, while Cu and Zn were evenly distributed in the cortex on both sides at the control site. This finding provides a basis for the effective implementation of phytoextraction techniques in the remediation of soils containing Pb and Sb. According to a study conducted by Tariq and Ashraf, (2016), which compared the uptake of Pb by oilseed rape, sunflower, pea, and maize in soils with high Pb concentrations (1,331 mg/kg), peas demonstrated the ability to uptake up to 96.23% of Pb and exhibited the highest Bioaccumulation Coefficient (BCF), indicating its hyper-enrichment properties. (Khan et al., 2021). examined the efficacy of phytoremediation in addressing soil contamination caused by firing ranges in Pakistan. Through conducting room temperature experiments, the researchers discovered that both dogbane and annual herb quinoa demonstrated the capacity to absorb Pb from the soil via their root systems and subsequently transport it above ground. Moreover, these plants exhibited resilience even when exposed to higher doses, thus qualifying them as Pb hyperaccumulating plants. However, it is worth noting that quinoa displayed necrotic/greening toxic effects. Consequently, dogbane emerges as a more effective candidate for remediating Pb in shooting range soils. In their study, Conesa et al. (2011) conducted potting experiments to investigate the uptake of three Swiss plants in Pb-contaminated range soils. The results indicated that common wheat exhibited a higher absorption of Pb in its root system (~200 mg/kg) compared to perennial ryegrass (130 mg/kg) and longleaf plantain (110 mg/kg). Furthermore, the bioconcentration factors (BCFs) for all three plants were found to be less than 1, suggesting that the utilization of these plants in phytoremediation practices for range soil contamination can effectively mitigate the risk of lead transfer to the food chain. Hockmann et al. (2018) examined the uptake of Sb, Pb, Cu, and Zn by four commonly found forage grasses, namely, perennial ryegrass, white clover, longleaf plantain, and bluntleaf sourmilfoil. The investigation took place in the field, specifically on abandoned and aerobic range soils, and involved both flooded and drained conditions. The findings revealed significant variations in the uptake of Pb, Cu, and Zn among the different species, with Pb and Zn

exhibiting the most pronounced impact on metal uptake. Interestingly, the levels of lead and zinc in blunt-leaved Rhodiola rosea were found to be 2–4 times higher under drained conditions compared to flooded conditions.

Phytostabilization encompasses the utilization of plants, fertilizers, and soil amendments to sequester and immobilize micronutrient-contaminated soils, thereby diminishing their bioavailability (Nsanganwimana et al., 2015). Notably, certain biofuel crops, namely, manzanita and willowherb, have exhibited promising capabilities for plant stabilization in Eastern Europe and the United States of America (Andrejić et al., 2019). Additionally, grass species offer advantages as phytostabilizing plants due to their tendency to accumulate fewer metals in their above-ground tissues compared to other species. Wilde et al. (2005) observed a noteworthy increase in Pb concentration within the root system of vetiver, while the leaves showed minimal enrichment. This accumulation of Pb in the root system highlights the potential of vetiver for phytostabilization, as it can effectively control Pb levels in the soil and subsequently reduce the risk of contaminant diffusion. Furthermore, the study showcased the significant potential of utilizing vetiver in conjunction with diverse amendments for the treatment of lead-contaminated range soils. Andrés Rodríguez-Seijo et al. (2016a) discovered that filamentous shearwaters have the potential to serve as an effective plant stabilizer for lead in the soils examined, as well as in soils with comparable attributes. The findings revealed that the roots of the grass exhibited high concentrations of Pb (1,107 mg/kg), while the branches displayed lower concentrations.

The incorporation of amendments in the phytoremediation process of range soils can effectively enhance the plant's ability to remediate such soils. Liu et al. (2013) observed a noteworthy rise in the quantity of exchangeable Sb in range soils after biochar treatment, but a decrease in accumulation in corn plants. Hashimoto et al. (2008) discovered that incorporating amendments, specifically poultry waste, into *Panicum maximum* Jacq. plants effectively stabilized high levels of Pb (19,600 ± 730 mg/kg) in the soil within a designated target range. This approach not only mitigated the cumulative dissolution of Pb in leachate and the concentration of Pb in water within the soil profile but also minimized the potential risk of Pb contamination in the target area. The findings of Alasmary et al. (2021) demonstrated that the incorporation of manzanita along with organic and inorganic phosphorus amendments yielded favorable outcomes in terms of stabilizing Pb in range soils, while concurrently mitigating potential environmental hazards and enhancing soil health.

4.3.2 Microbial remediation

Furthermore, alongside plants, the utilization of certain microorganisms can also be considered for range restoration purposes. Studies have shown that in response to environmental stresses at contaminated sites, microbial communities in soil adopt different strategies to cope with such environmental changes (Liu et al., 2023). Jugnia et al. (2019) observed that microorganisms effectively reduced RDX levels in groundwater in the range to below 0.1 µg/L. Notably, *Geobacter*, *Clostridium*, *Klebsiella* and *Bacteriodales* exhibited predominant activity as active organisms, and the introduction of waste glycerol further augmented the biodegradation of RDX. The utilization of waste glycerol in range soils demonstrated comparable enhancement of RDX biodegradation, while exhibiting limited impact on the biodegradation of 2,4-DNT (Jugnia et al., 2018). According to Lee and Kim, (2010), the utilization of a microbial-mediated leaching process known as bioleaching has been suggested as a means to eliminate heavy metals from soils and sediments. Among the microorganisms commonly employed in this process, Thiobacillus thiophilus sulfoxidans stands out as a prominent choice due to its capacity to support growth through the oxidation of reduced sulfide and utilization of carbon dioxide as an energy source for cellular metabolism. The acidophilic oxidizing Thiobacillus thiophilus was employed by the researchers to augment the biological activity in the bioleaching process. Additionally, they integrated acid-enhanced and EDTA-enhanced electrokinetic techniques, which demonstrated a notable removal of lead (92.7%) compared to non-biological methods. Moreover, plant roots contribute nutrients to root microorganisms, facilitating a synergistic plant and microbial remediation approach that exhibits exceptional efficacy (Sas-Nowosielska et al., 2008). Wolf et al. (2020) conducted a study utilizing integrated bioremediation techniques to address the presence of polycyclic aromatic hydrocarbons (PAHs) in soils contaminated by outdoor ranges. The researchers evaluated the effectiveness of various remediation approaches, including phytoremediation, bioaugmentation with *Mycobacterium* wambachii PYR-1, and the use of surfactant modifiers, either individually or in combination. The investigation revealed that the dissipation of PAHs, particularly in the inter-root region, notably in dogbane plants, was accompanied by alterations in enzyme activities and enhancements in lettuce seed germination. Repeated applications of *Mycobacterium avium* subspecies PYR-1 resulted in a significant enhancement in the dissipation of high molecular weight PAHs when compared to the control group without inoculation. Conversely, the application efficacy of rhamnolipid biosurfactant or Brij-35 was found to be limited, necessitating further investigations to determine the optimal concentration of surfactant and the interval for repeat application.

Bioremediation offers an advantage over alternative soil remediation techniques due to its minimal disruption to the ecosystem (Tangahu et al., 2011), and its ability to preserve soil structure throughout the remediation process. Significantly, bioremediation is characterized by minimal chemical usage, cost-effectiveness, and environmental friendliness (Sanderson et al., 2018). Moreover, bioremediation encompasses additional advantageous processes, including the capacity of plants to mitigate heavy metal accumulation in the soil through root system immobilization, thereby reducing soil erosion and weathering-induced dust emissions, as well as mitigating the adverse effects of rainwater runoff on soil quality.

5 Prospects

This paper highlights the research gaps and technical challenges that are crucial for the advancement of efficient remediation technologies in addressing range sites. Current research on

pollution remediation technologies for range sites still has certain deficiencies. For example, most of the current research only stays at the level of theoretical and laboratory validation of pollution control, and the feasibility of practical operation is not fully considered. Meanwhile, experimental validation generally selects only a small sample, limiting the generalizability of the results. In addition, most of the current studies do not pay enough attention to the correlation between environmental factors such as temperature and precipitation at the range site and factors such as anthropogenic activities and site contamination, which also makes the research perspective more one-sided. The following aspects can be considered in the future to optimize the current research on contamination-free management of range sites.

(1) It emphasizes the predominant presence of Pb as the primary pollutant in firing ranges and the limited focus of researchers on remediating this pollutant. However, it is important to recognize that the associated contaminants, such as Sb, Cu, Zn, Ni, As, PAHs, and RDX, which are introduced through the weathering of munitions and clay targets, may possess equal or greater ecotoxicity. This is because these pollutants have a higher proportion of bioavailable metals than Pb or are highly bioconcentrated. Simultaneously, the researchers' remediation measures were exclusively aimed at addressing soil contamination within the range area. However, it has been reported that elevated levels of contamination have also been detected in the surrounding groundwater and surface water (Okkenhaug et al., 2018; Jugnia et al., 2019). Furthermore, it is noteworthy that mercury (Hg) compounds were historically utilized as primers for rifle and pistol ammunition (Stauffer et al., 2017). Despite the discontinuation of mercury-containing munitions in the 1960s, the resulting pollution cannot be disregarded. Regrettably, limited research has been conducted in this area, and the natural recovery processes tend to be sluggish. Hence, it is imperative to direct attention towards the comprehensive contamination level of the range site, prioritizing the overall efficacy of site remediation rather than solely pursuing high removal efficiency of individual matrices and contaminants.

(2) Emerging bioremediation technologies are being developed to offer economically feasible and environmentally sustainable solutions for the decontamination of firing range sites, capable of effectively addressing large-scale contamination. However, there is a lack of comprehensive understanding regarding the precise mechanisms of remediation. Therefore, it is imperative to integrate spectroscopic, imaging, genomics, metabolomics, and proteomics techniques to elucidate the fate of pollutants during the remediation process. This will enable a thorough comprehension of the purification mechanisms associated with each remediation measure employed at contaminated sites.

(3) It is important to note that while various remediation measures can mitigate the risks posed by elevated levels of contaminants in soils and decrease the ecotoxicity of metals and organics, their effectiveness may vary depending on the receptors and contaminants present at specific study sites. Even though these measures generally led to a decrease in exchangeable metals or the removal of contaminants from the site, the bioavailability of co-contaminants in the treated soils remained relatively elevated. To achieve equilibrium in the immobilization of various contaminants across diverse soil properties, it is imperative to use suitable models for contaminant removal that are tailored to the specific site, soil characteristics, contaminant quantity and composition, as well as the binding mechanisms of contaminants in the soil. In addition to the reduction of metals in the exchangeable state in the soil, due attention should also be given to the possibility of re-activation of stabilized metal fractions. Additionally, a comprehensive approach that combines existing remediation technologies should be considered to enhance the efficacy of remediation, while also taking into account cost-effectiveness. For phytoremediation techniques, the rational post-treatment of metal-accumulating plants is also a current and urgent consideration. Subsequently, pilot-scale treatability studies are conducted to evaluate the ecological risk posed by toxic contaminants and establish safety thresholds for environmental elements, thereby customizing the implementation of remediation strategies to individual sites.

(4) The majority of previous research about the remediation of range contamination has predominantly concentrated on the examination of contaminated area samples within controlled laboratory settings. Consequently, there exists a scarcity of information regarding the practical implementation of these remediation strategies for the treatment of contaminated soil and groundwater in their natural environment. Hence, it is imperative to devise *in situ* remediation technologies that possess distinct advantages, including reduced expenses, expedited remediation duration, and minimal adverse impact on the surrounding ecosystem.

(5) The utilization of artificial intelligence can enhance the comprehension of range site contamination and pollution, facilitating improved management of contaminated sites.

6 Conclusion

The issue of site contamination resulting from range activities has garnered heightened attention in recent years. Currently, worldwide range pollution is still a persistent environmental problem that needs to be solved. A number of studies have shown that range pollution is widespread and that the organic and inorganic pollutants produced have serious adverse effects on the surrounding soil and groundwater environment, and even on human beings in the vicinity. Starting from the current status of range contamination, this review systematically describes several major types of contamination remediation technologies and draws the following conclusions:

(1) Traditional military shooting methods result in a large number of toxic heavy metals and organic pollutants remaining in the shooting range soil environment, and the degree of contamination increases with the aging of the soil.

(2) Through bibliometric statistics, it was found that current research on the remediation of shooting range contamination is centered on several aspects, such as soil flora characteristics, human health risks, and pollution uptake and transformation.
(3) This review article systematically discusses measures taken to address contamination at firing ranges, with a specific emphasis on the effectiveness of bioremediation, physicoremediation, and chemoremediation in addressing a wide range of inorganic and organic pollutants found in water and soil. A substantial body of academic literature suggests that these remediation techniques hold significant promise for on-site remediation of contaminants in both soil and groundwater at contaminated sites.
(4) The review further identified several crucial areas for research and highlighted gaps in existing knowledge, which can serve as a valuable guide for the future implementation of these promising remediation strategies.

Further investigation in this field is anticipated to enhance our comprehension of the destiny, transportation, and remediation of contaminants at range sites, as well as improve our ability to assess and mitigate the risks associated with range site contamination. Moreover, it will enable us to effectively respond to the resultant contamination, thereby safeguarding the ecological security of range sites and human health, which holds immense importance.

Author contributions

YiZ: Conceptualization, Data curation, Formal Analysis, Methodology, Writing–original draft. RC: Data curation, Methodology, Writing–original draft. BT: Investigation, Methodology, Writing–original draft. JM: Investigation, Methodology, Writing–original draft. XL: Investigation, Writing–original draft. JL: Writing–review and editing. YoZ: Data curation, Funding acquisition, Writing–review and editing. FW: Funding acquisition, Supervision, Visualization, Writing–review and editing.

Funding

The author(s) declare that financial support was received for the research, authorship, and/or publication of this article. This work was financially supported by the State Key Laboratory of NBC Protection for Civilian (SKLNBC 2021-18), the Major Project of College Natural Science Foundation of Jiangsu Province (21KJA610005), and the special fund from the Key Laboratory for Soft Chemistry and Functional Materials of Ministry of Education (Project No. 2021–01).

Acknowledgments

All the authors are grateful to the reviewers and editors.

Conflict of interest

The authors declare that the research was conducted in the absence of any commercial or financial relationships that could be construed as a potential conflict of interest.

Publisher's note

Supplementary material

The Supplementary Material for this article can be found online at: https://www.frontiersin.org/articles/10.3389/fenvs.2024.1352603/full#supplementary-material

References

Abdel-Sabour, M. F., and Al-Salama, Y. J. (2007). Zinc and cobalt phytoextraction by different plant species. *Remediation* 18, 109–119. doi:10.1002/rem.20155

Ahmad, M., Hashimoto, Y., Moon, D. H., Lee, S. S., and Ok, Y. S. (2012). Immobilization of lead in a Korean military shooting range soil using eggshell waste: an integrated mechanistic approach. *J. Hazard. Mater.* 209 (210), 392–401. doi:10.1016/j.jhazmat.2012.01.047

Ahmad, M., Ok, Y. S., Rajapaksha, A. U., Lim, J. E., Kim, B.-Y., Ahn, J.-H., et al. (2016). Lead and copper immobilization in a shooting range soil using soybean stover- and pine needle-derived biochars: chemical, microbial and spectroscopic assessments. *J. Hazard. Mater.* 301, 179–186. doi:10.1016/j.jhazmat.2015.08.029

Alasmary, Z., Hettiarachchi, G. M., Roozeboom, K. L., Davis, L. C., Erickson, L. E., Pidlisnyuk, V., et al. (2021). Phytostabilization of a contaminated military site using Miscanthus and soil amendments. *J. Environ. Qual.* 50, 1220–1232. doi:10.1002/jeq2.20268

Allen, A. (2001). Containment landfills: the myth of sustainability. *Eng. Geol.* 60, 3–19. doi:10.1016/S0013-7952(00)00084-3

Andrejic, G., Šinžar-Sekulić, J., Prica, M., Dželetović, Ž., and Rakić, T. (2019). Phytoremediation potential and physiological response of Miscanthus × giganteus cultivated on fertilized and non-fertilized flotation tailings. *Environ. Sci. Pollut. Res.* 26, 34658–34669. doi:10.1007/s11356-019-06543-7

Ansari, F., Momina, A., and Rafatullah, M. (2023). Review on bioremediation technologies of polycyclic aromatic hydrocarbons (PAHs) from soil: mechanisms and future perspective. *Int. Biodeterior. Biodegrad.* 179, 105582. doi:10.1016/j.ibiod.2023.105582

Azizi, S., Mahdavi Shahri, M., and Mohamad, R. (2017). Green synthesis of zinc oxide nanoparticles for enhanced adsorption of lead ions from aqueous solutions: equilibrium, kinetic and thermodynamic studies. *Molecules* 22, 831. doi:10.3390/molecules22060831

Bannon, D. I., Drexler, J. W., Fent, G. M., Casteel, S. W., Hunter, P. J., Brattin, W. J., et al. (2009). Evaluation of small arms range soils for metal contamination and lead bioavailability. *Environ. Sci. Technol.* 43, 9071–9076. doi:10.1021/es901834h

Barker, A. J., Douglas, T. A., Spaleta, K. J., and Trainor, T. P. (2023). Attenuation of Pb and Sb in shooting range soils by Fe amendments. *Chemosphere* 318, 137899. doi:10.1016/j.chemosphere.2023.137899

Befkadu, A. A., and Chen, Q. (2018). Surfactant-enhanced soil washing for removal of petroleum hydrocarbons from contaminated soils: a review. *Pedosphere* 28, 383–410. doi:10.1016/S1002-0160(18)60027-X

Buelt, J. L., and Farnsworth, R. K. (1991). *In situ* vitrification of soils containing various metals. *Nucl. Technol.* 96, 178–184. doi:10.13182/NT91-A34603

Cai, Z., Sun, Y., Deng, Y., Zheng, X., Sun, S., Sinkkonen, A., et al. (2022). Enhanced electrokinetic remediation of cadmium (Cd)-Contaminated soil with interval power breaking. *Int. J. Environ. Res.* 16, 31. doi:10.1007/s41742-022-00409-6

Cameselle, C., and Gouveia, S. (2018). Electrokinetic remediation for the removal of organic contaminants in soils. *Curr. Opin. Electrochem.* 11, 41–47. doi:10.1016/j.coelec.2018.07.005

Cameselle, C., Gouveia, S., Akretche, D. E., Belhadj, B., Cameselle, C., Gouveia, S., et al. (2013). Advances in electrokinetic remediation for the removal of organic contaminants in soils. *Org. Pollut. - Monit. Risk Treat. (IntechOpen)*. doi:10.5772/54334

Cao, X., Ma, L. Q., Chen, M., Hardison, D. W., and Harris, W. G. (2003). Lead transformation and distribution in the soils of shooting ranges in Florida, USA. *Sci. Total Environ.* 307, 179–189. doi:10.1016/S0048-9697(02)00543-0

Cao, X., Wahbi, A., Ma, L., Li, B., and Yang, Y. (2009). Immobilization of Zn, Cu, and Pb in contaminated soils using phosphate rock and phosphoric acid. *J. Hazard. Mater.* 164, 555–564. doi:10.1016/j.jhazmat.2008.08.034

Česynaitė, J., Praspaliauskas, M., Pedišius, N., and Sujetovienė, G. (2021). Biological assessment of contaminated shooting range soil using earthworm biomarkers. *Ecotoxicology* 30, 2024–2035. doi:10.1007/s10646-021-02463-w

Česynaitė, J., Praspaliauskas, M., and Sujetovienė, G. (2023). Bioaccumulation of trace metal(loid)s and toxic response of Lactuca sativa grown in shooting range soil. *Toxicol. Environ. Chem.* 105, 28–41. doi:10.1080/02772248.2023.2199996

Chang, J.-H., Wang, Y.-L., Dong, C.-D., and Shen, S.-Y. (2022). The particle-size sieving technique to remediate Pb- and Cu-contaminated agricultural soil. *Environ. Geotech.* 9, 124–132. doi:10.1680/jenge.19.00162

Chen, S., Shu, X., Tang, H., Mao, X., Xu, C., and Lu, X. (2019). Microwave vitrification of uranium-contaminated soil for nuclear test site and chemical stability. *Ceram. Int.* 45, 13334–13339. doi:10.1016/j.ceramint.2019.04.026

Christou, A., Hadjisterkotis, E., Dalias, P., Demetriou, E., Christofidou, M., Kozakou, S., et al. (2022). Lead contamination of soils, sediments, and vegetation in a shooting range and adjacent terrestrial and aquatic ecosystems: a holistic approach for evaluating potential risks. *Chemosphere* 292, 133424. doi:10.1016/j.chemosphere.2021.133424

Clausen, J. L., Scott, C., and Osgerby, I. (2011). Fate of nitroglycerin and dinitrotoluene in soil at small arms training ranges. *Soil Sediment Contam. An Int. J.* 20, 649–671. doi:10.1080/15320383.2011.594108

Conesa, H. M., Wieser, M., Gasser, M., Hockmann, K., Evangelou, M. W. H., Studer, B., et al. (2010). Effects of three amendments on extractability and fractionation of Pb, Cu, Ni and Sb in two shooting range soils. *J. Hazard. Mater.* 181, 845–850. doi:10.1016/j.jhazmat.2010.05.090

Conesa, H. M., Wieser, M., Studer, B., and Schulin, R. (2011). Effects of vegetation and fertilizer on metal and Sb plant uptake in a calcareous shooting range soil. *Ecol. Eng.* 37, 654–658. doi:10.1016/j.ecoleng.2010.11.001

Cui, W., Li, X., Duan, W., Xie, M., and Dong, X. (2023). Heavy metal stabilization remediation in polluted soils with stabilizing materials: a review. *Environ. Geochem Health* 45, 4127–4163. doi:10.1007/s10653-023-01522-x

Dermatas, D., Cao, X., Tsaneva, V., Shen, G., and Grubb, D. G. (2006a). Fate and behavior of metal(loid) contaminants in an organic matter-rich shooting range soil: implications for remediation. *Water Air Soil Pollut. Focus* 6, 143–155. doi:10.1007/s11267-005-9003-4

Dermatas, D., Menounou, N., Dadachov, M., Dutko, P., Shen, G., Xu, X., et al. (2006b). Lead leachability in firing range soils. *Environ. Eng. Sci.* 23, 88–101. doi:10.1089/ees.2006.23.88

Dinake, P., and Kelebemang, R. (2019). Critical assessment of mechanistic pathways for chemical remediation techniques applied to Pb impacted soils at shooting ranges – a review. *Environ. Pollut. Bioavailab.* 31, 282–305. doi:10.1080/26395940.2019.1676170

Dinake, P., Kelebemang, R., and Sehube, N. (2019). A comprehensive approach to speciation of lead and its contamination of firing range soils: a review. *Soil Sediment Contam. An Int. J.* 28, 431–459. doi:10.1080/15320383.2019.1597831

Dinake, P., Maphane, O., Sebogisi, K., and Kamwi, O. (2018). Pollution status of shooting range soils from Cd, Cu, Mn, Ni and Zn found in ammunition. *Cogent Environ. Sci.* 4, 1528701. doi:10.1080/23311843.2018.1528701

Dinake, P., Mokgosi, S. M., Kelebemang, R., Kereeditse, T. T., and Motswetla, O. (2022). Pollution assessment of antimony in shooting range soils. *South Afr. J. Chem.* 76, 72–78. doi:10.17159/0379-4350/2022/v76a11

Douay, F., Roussel, H., Pruvot, C., Loriette, A., and Fourrier, H. (2008). Assessment of a remediation technique using the replacement of contaminated soils in kitchen gardens nearby a former lead smelter in Northern France. *Sci. Total Environ.* 401, 29–38. doi:10.1016/j.scitotenv.2008.03.025

Etim, E. U. (2017). Lead removal from contaminated shooting range soil using acetic acid potassium chloride washing solutions and electrochemical reduction. *J. Health Pollut.* 7, 22–31. doi:10.5696/2156-9614-7-13.22

Fayiga, A. O., and Saha, U. K. (2016a). Soil pollution at outdoor shooting ranges: health effects, bioavailability and best management practices. *Environ. Pollut.* 216, 135–145. doi:10.1016/j.envpol.2016.05.062

Fayiga, A. O., and Saha, U. K. (2016b). Soil pollution at outdoor shooting ranges: health effects, bioavailability and best management practices. *Environ. Pollut.* 216, 135–145. doi:10.1016/j.envpol.2016.05.062

Frakes, R. A., Boughner, E. A., Boggs, J. F., Tutton, J., and Bargar, T. A. (2007). Delineation of the nature and extent of contamination at the former NAS key west skeet club on great white heron national wildlife refuge. *Fish Wildl. Serv.* Available at: https://ecos.fws.gov/ServCat/DownloadFile/21637?Reference=23118.

Gómez-Sagasti, M. T., Anza, M., Hidalgo, J., Artetxe, U., Garbisu, C., and Becerril, J. M. (2021). Recent trends in sustainable remediation of Pb-contaminated shooting range soils: rethinking waste management within a circular economy. *Processes* 9, 572. doi:10.3390/pr9040572

Grispen, V. M. J., Nelissen, H. J. M., and Verkleij, J. A. C. (2006). Phytoextraction with Brassica napus L.: a tool for sustainable management of heavy metal contaminated soils. *Environ. Pollut.* 144, 77–83. doi:10.1016/j.envpol.2006.01.007

Guberman (2017). Lead statistics and information | U.S. Geological survey. Available at: https://www.usgs.gov/centers/national-minerals-information-center/lead-statistics-and-information (Accessed October 25, 2023).

Guo, G., Zhou, Q., and Ma, L. Q. (2006). Availability and assessment of fixing additives for the *in situ* remediation of heavy metal contaminated soils: a review. *Environ. Monit. Assess.* 116, 513–528. doi:10.1007/s10661-006-7668-4

Han, L.-J., Li, J.-S., Xue, Q., Guo, M.-Z., Wang, P., and Poon, C. S. (2022). Enzymatically induced phosphate precipitation (EIPP) for stabilization/solidification (S/S) treatment of heavy metal tailings. *Constr. Build. Mater.* 314, 125577. doi:10.1016/j.conbuildmat.2021.125577

Hardison, D. W., Jr, Ma, L. Q., Luongo, T., and Harris, W. G. (2004). Lead contamination in shooting range soils from abrasion of lead bullets and subsequent weathering. *Sci. Total Environ.* 328, 175–183. doi:10.1016/j.scitotenv.2003.12.013

Hashimoto, Y., Matsufuru, H., and Sato, T. (2008). Attenuation of lead leachability in shooting range soils using poultry waste amendments in combination with indigenous plant species. *Chemosphere* 73, 643–649. doi:10.1016/j.chemosphere.2008.07.033

He, Y., Joseph, B. H., and Sung, S. H. (2007). Biodegradation of 2,4- and 2,6-dinitrotoluene in a pilot-scale system for soil contaminated with explosive compounds. *Environ. Sci.* 28, 613–616. doi:10.3321/j.issn:0250-3301.2007.03.030

Hockmann, K., Tandy, S., Studer, B., Evangelou, M. W. H., and Schulin, R. (2018). Plant uptake and availability of antimony, lead, copper and zinc in oxic and reduced shooting range soil. *Environ. Pollut.* 238, 255–262. doi:10.1016/j.envpol.2018.03.014

Islam, M. N., and Park, J.-H. (2017). Immobilization and reduction of bioavailability of lead in shooting range soil through hydrothermal treatment. *J. Environ. Manag.* 191, 172–178. doi:10.1016/j.jenvman.2017.01.017

ITRC (2003). *Characterization and remediation of soils at closed small arms firing ranges*. Interstate Technology and Regulatory Council. Available at: https://itrcweb.org/home.

Jiang, S., Duan, L., Dai, G., and Shu, Y. (2021). Immobilization of heavy metal(loid)s in acid paddy soil by soil replacement-biochar amendment technology under normal wet condition. *Environ. Sci. Pollut. Res.* 28, 68886–68896. doi:10.1007/s11356-021-14757-x

Johnsen, I. V., and Aaneby, J. (2019). Soil intake in ruminants grazing on heavy-metal contaminated shooting ranges. *Sci. Total Environ.* 687, 41–49. doi:10.1016/j.scitotenv.2019.06.086

Jugnia, L.-B., Manno, D., Dodard, S., Greer, C. W., and Hendry, M. (2019). Manipulating redox conditions to enhance *in situ* bioremediation of RDX in groundwater at a contaminated site. *Sci. Total Environ.* 676, 368–377. doi:10.1016/j.scitotenv.2019.04.045

Jugnia, L. B., Manno, D., Drouin, K., and Hendry, M. (2018). *In situ* pilot test for bioremediation of energetic compound-contaminated soil at a former military demolition range site. *Environ. Sci. Pollut. Res.* 25, 19436–19445. doi:10.1007/s11356-018-2115-y

Kazery, J. A., Proctor, G., Larson, S. L., Ballard, J. H., Knotek-Smith, H. M., Zhang, Q., et al. (2021). Distribution and fractionation of uranium in weapon tested range soils. *ACS Earth Space Chem.* 5, 356–364. doi:10.1021/acsearthspacechem.0c00326

Kelebemang, R., Dinake, P., Sehube, N., Daniel, B., Totolo, O., and Laetsang, M. (2017). Speciation and mobility of lead in shooting range soils. *Chem. Speciat. Bioavailab.* 29, 143–152. doi:10.1080/09542299.2017.1349552

Khan, A. Z., Khan, S., Muhammad, S., Baig, S. A., Khan, A., Nasir, M. J., et al. (2021a). Lead contamination in shooting range soils and its phytoremediation in Pakistan: a greenhouse experiment. *Arab. J. Geosci.* 14, 4. doi:10.1007/s12517-020-06301-x

Khan, B. A., Ahmad, M., Iqbal, S., Ullah, F., Bolan, N., Solaiman, Z. M., et al. (2023). Adsorption and immobilization performance of pine-cone pristine and engineered biochars for antimony in aqueous solution and military shooting range soil: an integrated novel approach. *Environ. Pollut.* 317, 120723. doi:10.1016/j.envpol.2022.120723

Khan, S., Naushad, Mu., Lima, E. C., Zhang, S., Shaheen, S. M., and Rinklebe, J. (2021b). Global soil pollution by toxic elements: current status and future perspectives on the risk assessment and remediation strategies – a review. *J. Hazard. Mater.* 417, 126039. doi:10.1016/j.jhazmat.2021.126039

Kim, S., Baek, K., and Lee, I. (2010). Phytoremediation and microbial community structure of soil from a metal-contaminated military shooting range: comparisons of

field and pot experiments. *J. Environ. Sci. Health, Part A* 45, 389–394. doi:10.1080/10934520903467832

Kim, S., Choi, J., and Jeong, S.-W. (2023). Changes in the health of metal-contaminated soil before and after stabilization and solidification. *Environ. Pollut.* 331, 121929. doi:10.1016/j.envpol.2023.121929

Knechtenhofer, L. A., Xifra, I. O., Scheinost, A. C., Flühler, H., and Kretzschmar, R. (2003). Fate of heavy metals in a strongly acidic shooting-range soil: small-scale metal distribution and its relation to preferential water flow. *J. Plant Nutr. Soil Sci.* 166, 84–92. doi:10.1002/jpln.200390017

Koelmel, J., and Amarasiriwardena, D. (2012). Imaging of metal bioaccumulation in Hay-scented fern (Dennstaedtia punctilobula) rhizomes growing on contaminated soils by laser ablation ICP-MS. *Environ. Pollut.* 168, 62–70. doi:10.1016/j.envpol.2012.03.035

Lafond, S., Blais, J.-F., Martel, R., and Mercier, G. (2012). Chemical leaching of antimony and other metals from small arms shooting range soil. *Water Air Soil Pollut.* 224, 1371. doi:10.1007/s11270-012-1371-6

Lafond, S., Blais, J.-F., Mercier, G., and Martel, R. (2013). Counter-current acid leaching process for the removal of Cu, Pb, Sb and Zn from shooting range soil. *Environ. Technol.* 34, 2377–2387. doi:10.1080/09593330.2013.770560

Lafond, S., Blais, J.-F., Mercier, G., and Martel, R. (2014). A counter-current acid leaching process for the remediation of contaminated soils from a small-arms shooting range. *Soil Sediment Contam. An Int. J.* 23, 194–210. doi:10.1080/15320383.2014.808171

Laporte-Saumure, M., Martel, R., and Mercier, G. (2011). Characterization and metal availability of copper, lead, antimony and zinc contamination at four Canadian small arms firing ranges. *Environ. Technol.* 32, 767–781. doi:10.1080/09593330.2010.512298

Lee, J.-H., and Park, K.-S. (2008). Heavy metal distribution in soils from the maehyang-ri Inland shooting range area. *J. Korean Soc. Water Environ.* 24, 407–414.

Lee, K.-Y., and Kim, K.-W. (2010). Heavy metal removal from shooting range soil by hybrid electrokinetics with bacteria and enhancing agents. *Environ. Sci. Technol.* 44, 9482–9487. doi:10.1021/es102615a

Levonmäki, M., and Hartikainen, H. (2007). Efficiency of liming in controlling the mobility of lead in shooting range soils as assessed by different experimental approaches. *Sci. Total Environ.* 388, 1–7. doi:10.1016/j.scitotenv.2007.07.055

Lewińska, K., Karczewska, A., Siepak, M., Szopka, K., Gałka, B., and Iqbal, M. (2019). Effects of waterlogging on the solubility of antimony and arsenic in variously treated shooting range soils. *Appl. Geochem.* 105, 7–16. doi:10.1016/j.apgeochem.2019.04.005

Li, W., Ni, P., and Yi, Y. (2019). Comparison of reactive magnesia, quick lime, and ordinary Portland cement for stabilization/solidification of heavy metal-contaminated soils. *Sci. Total Environ.* 671, 741–753. doi:10.1016/j.scitotenv.2019.03.270

Liu, L., Li, W., Song, W., and Guo, M. (2018). Remediation techniques for heavy metal-contaminated soils: principles and applicability. *Sci. Total Environ.* 633, 206–219. doi:10.1016/j.scitotenv.2018.03.161

Liu, S., Shi, Y., Sun, M., Huang, D., Shu, W., and Ye, M. (2023). The community assembly for understanding the viral-assisted response of bacterial community to Cr-contamination in soils. *J. Hazard. Mater.* 441, 129975. doi:10.1016/j.jhazmat.2022.129975

Liu, Z., Chen, L., Zhang, Z., Li, Y., Dong, Y., and Sun, Y. (2013). Synthesis of multi-walled carbon nanotube–hydroxyapatite composites and its application in the sorption of Co(II) from aqueous solutions. *J. Mol. Liq.* 179, 46–53. doi:10.1016/j.molliq.2012.12.011

Luo, J., Li, Y., Cao, H., Zhu, Y., Liu, X., Li, H., et al. (2023). Variations of microbiota in three types of typical military contaminated sites: diversities, structures, influence factors, and co-occurrence patterns. *J. Hazard. Mater.* 443, 130290. doi:10.1016/j.jhazmat.2022.130290

Mankė, J., Praspaliauskas, M., Pedišius, N., and Sujetovienė, G. (2024). Evaluation of phytoremediation efficiency of shooting range soil using the bioaccumulation potential and sensitivity of different plant species. *Ecol. Eng.* 198, 107134. doi:10.1016/j.ecoleng.2023.107134

Mariussen, E., Johnsen, I. V., and Strømseng, A. E. (2017). Distribution and mobility of lead (Pb), copper (Cu), zinc (Zn), and antimony (Sb) from ammunition residues on shooting ranges for small arms located on mires. *Environ. Sci. Pollut. Res.* 24, 10182–10196. doi:10.1007/s11356-017-8647-8

Mathee, A., de Jager, P., Naidoo, S., and Naicker, N. (2017). Exposure to lead in South African shooting ranges. *Environ. Res.* 153, 93–98. doi:10.1016/j.envres.2016.11.021

Mendes, G. P., Soares, L. C., Viegas, R. M. A., Chiavone-Filho, O., and do Nascimento, C. A. O. (2023). Lead (Pb) in shooting range soil: a systematic literature review of contaminant behavior, risk assessment, and remediation options. *Water Air Soil Pollut.* 235, 1. doi:10.1007/s11270-023-06783-x

Mi, R., Zhang, Z., Ji, W., Liu, S., Kai, M. F., lin, K., et al. (2023). Solidification/stabilisation behaviours of Zn2+ in magnesium potassium phosphate cement: experiments and density functional theory study. *Environ. Res.* 231, 116247. doi:10.1016/j.envres.2023.116247

MOE (2005). *The development of hybrid electrokinetic remediation technique using solar energy on shooting range soils contaminated by heavy metals, Gwachun, Kyunggi Republic of Korea*. Korea: MOE: Gwachun, 40–63.

Moon, D. H., Cheong, K. H., Khim, J., Wazne, M., Hyun, S., Park, J.-H., et al. (2013). Stabilization of Pb2+ and Cu2+ contaminated firing range soil using calcined oyster shells and waste cow bones. *Chemosphere* 91, 1349–1354. doi:10.1016/j.chemosphere.2013.02.007

Moon, I., Kim, H., Jeong, S., Choi, H., Park, J., and Lee, I. (2021). Chemical properties of heavy metal-contaminated soils from a Korean military shooting range: evaluation of Pb sources using Pb Isotope ratios. *Appl. Sci.* 11, 7099. doi:10.3390/app11157099

Mulligan, C. N., Yong, R. N., and Gibbs, B. F. (2001). An evaluation of technologies for the heavy metal remediation of dredged sediments. *J. Hazard. Mater.* 85, 145–163. doi:10.1016/S0304-3894(01)00226-6

Neugschwandtner, R. W., Tlustoš, P., Komárek, M., and Száková, J. (2008). Phytoextraction of Pb and Cd from a contaminated agricultural soil using different EDTA application regimes: laboratory versus field scale measures of efficiency. *Geoderma* 144, 446–454. doi:10.1016/j.geoderma.2007.11.021

Ni, S., Rahman, S., Kasai, S., Yoshioka, S., Wong, K. H., Mashio, A. S., et al. (2023a). Remediation of lead-contaminated shooting range soil: biodegradable chelator-assisted washing and subsequent post-treatment using FeCl3 and CaO. *Environ. Technol. Innovation* 31, 103172. doi:10.1016/j.eti.2023.103172

Ni, S., Rahman, S., Kasai, S., Yoshioka, S., Wong, K. H., Mashio, A. S., et al. (2023b). Remediation of lead-contaminated shooting range soil: biodegradable chelator-assisted washing and subsequent post-treatment using FeCl3 and CaO. *Environ. Technol. Innovation* 31, 103172. doi:10.1016/j.eti.2023.103172

Nsanganwimana, F., Pourrut, B., Waterlot, C., Louvel, B., Bidar, G., Labidi, S., et al. (2015). Metal accumulation and shoot yield of Miscanthus×giganteus growing in contaminated agricultural soils: insights into agronomic practices. *Agric. Ecosyst. Environ.* 213, 61–71. doi:10.1016/j.agee.2015.07.023

Ogawa, S., Katoh, M., and Sato, T. (2015). Simultaneous lead and antimony immobilization in shooting range soil by a combined application of hydroxyapatite and ferrihydrite. *Environ. Technol.* 36, 2647–2656. doi:10.1080/09593330.2015.1042071

Okkenhaug, G., Grasshorn Gebhardt, K.-A., Amstaetter, K., Lassen Bue, H., Herzel, H., Mariussen, E., et al. (2016). Antimony (Sb) and lead (Pb) in contaminated shooting range soils: Sb and Pb mobility and immobilization by iron based sorbents, a field study. *J. Hazard. Mater.* 307, 336–343. doi:10.1016/j.jhazmat.2016.01.005

Okkenhaug, G., Smebye, A. B., Pabst, T., Amundsen, C. E., Sævarsson, H., and Breedveld, G. D. (2018). Shooting range contamination: mobility and transport of lead (Pb), copper (Cu) and antimony (Sb) in contaminated peatland. *J. Soils Sediments* 18, 3310–3323. doi:10.1007/s11368-017-1739-8

Ottosen, L. M., Pedersen, A. J., Ribeiro, A. B., and Hansen, H. K. (2005). Case study on the strategy and application of enhancement solutions to improve remediation of soils contaminated with Cu, Pb and Zn by means of electrodialysis. *Eng. Geol.* 77, 317–329. doi:10.1016/j.enggeo.2004.07.021

Ouhadi, V. R., Yong, R. N., Shariatmadari, N., Saeidijam, S., Goodarzi, A. R., and Safari-Zanjani, M. (2010). Impact of carbonate on the efficiency of heavy metal removal from kaolinite soil by the electrokinetic soil remediation method. *J. Hazard. Mater.* 173, 87–94. doi:10.1016/j.jhazmat.2009.08.052

Pain, D. J., Mateo, R., and Green, R. E. (2019). Effects of lead from ammunition on birds and other wildlife: a review and update. *Ambio* 48, 935–953. doi:10.1007/s13280-019-01159-0

Pedersen, K. B., Jensen, P. E., Ottosen, L. M., and Barlindhaug, J. (2018). Influence of electrode placement for mobilising and removing metals during electrodialytic remediation of metals from shooting range soil. *Chemosphere* 210, 683–691. doi:10.1016/j.chemosphere.2018.07.063

Pedersen, K. B., Jensen, P. E., Ottosen, L. M., and Barlindhaug, J. (2019). Applying multivariate analysis for optimising the electrodialytic removal of Cu and Pb from shooting range soils. *J. Hazard. Mater.* 368, 869–876. doi:10.1016/j.jhazmat.2018.10.014

Purakayastha, T. J., Viswanath, T., Bhadraray, S., Chhonkar, P. K., Adhikari, P. P., and Suribabu, K. (2008). Phytoextraction of zinc, copper, nickel and lead from a contaminated soil by different species of Brassica. *Int. J. Phytoremediation* 10, 61–72. doi:10.1080/15226510701827077

Raimondo, E. E., Saez, J. M., Aparicio, J. D., Fuentes, M. S., and Benimeli, C. S. (2020). Coupling of bioaugmentation and biostimulation to improve lindane removal from different soil types. *Chemosphere* 238, 124512. doi:10.1016/j.chemosphere.2019.124512

Rajapaksha, A. U., Ahmad, M., Vithanage, M., Kim, K.-R., Chang, J. Y., Lee, S. S., et al. (2015). The role of biochar, natural iron oxides, and nanomaterials as soil amendments for immobilizing metals in shooting range soil. *Environ. Geochem Health* 37, 931–942. doi:10.1007/s10653-015-9694-z

Reigosa-Alonso, A., Lorenzo Dacunha, R., Arenas-Lago, D., Vega, F. A., and Rodríguez-Seijo, A. (2021). Soils from abandoned shooting range facilities as contamination source of potentially toxic elements: distribution among soil geochemical fractions. *Environ. Geochem Health* 43, 4283–4297. doi:10.1007/s10653-021-00900-7

Robidoux, P. Y., Gong, P., Sarrazin, M., Bardai, G., Paquet, L., Hawari, J., et al. (2004). Toxicity assessment of contaminated soils from an antitank firing range. *Ecotoxicol. Environ. Saf.* 58, 300–313. doi:10.1016/j.ecoenv.2003.11.004

Rodríguez-Seijo, A., Alfaya, M. C., Andrade, M. L., and Vega, F. A. (2016a). Copper, chromium, nickel, lead and zinc levels and pollution degree in firing range soils. *Land Degrad. Dev.* 27, 1721–1730. doi:10.1002/ldr.2497

Rodríguez-Seijo, A., Cachada, A., Gavina, A., Duarte, A. C., Vega, F. A., Andrade, M. L., et al. (2017). Lead and PAHs contamination of an old shooting range: a case study with a holistic approach. *Sci. Total Environ.* 575, 367–377. doi:10.1016/j.scitotenv.2016.10.018

Rodríguez-Seijo, A., Lago-Vila, M., Andrade, M. L., and Vega, F. A. (2016b). Pb pollution in soils from a trap shooting range and the phytoremediation ability of Agrostis capillaris L. *Environ. Sci. Pollut. Res.* 23, 1312–1323. doi:10.1007/s11356-015-5340-7

Saini, A., Bekele, D. N., Chadalavada, S., Fang, C., and Naidu, R. (2021). Electrokinetic remediation of petroleum hydrocarbon contaminated soil (I). *Environ. Technol. Innovation* 23, 101585. doi:10.1016/j.eti.2021.101585

Sanderson, P., Naidu, R., Bolan, N., Bowman, M., and Mclure, S. (2012). Effect of soil type on distribution and bioaccessibility of metal contaminants in shooting range soils. *Sci. Total Environ.* 438, 452–462. doi:10.1016/j.scitotenv.2012.08.014

Sanderson, P., Naidu, R., Bolan, N., Lim, J. E., and Ok, Y. S. (2015). Chemical stabilisation of lead in shooting range soils with phosphate and magnesium oxide: synchrotron investigation. *J. Hazard. Mater.* 299, 395–403. doi:10.1016/j.jhazmat.2015.06.056

Sanderson, P., Qi, F., Seshadri, B., Wijayawardena, A., and Naidu, R. (2018). Contamination, fate and management of metals in shooting range soils—a review. *Curr. Pollut. Rep.* 4, 175–187. doi:10.1007/s40726-018-0089-5

Sas-Nowosielska, A., Galimska-Stypa, R., Kucharski, R., Zielonka, U., Małkowski, E., and Gray, L. (2008). Remediation aspect of microbial changes of plant rhizosphere in mercury contaminated soil. *Environ. Monit. Assess.* 137, 101–109. doi:10.1007/s10661-007-9732-0

Scanferla, P., Ferrari, G., Pellay, R., Volpi Ghirardini, A., Zanetto, G., and Libralato, G. (2009). An innovative stabilization/solidification treatment for contaminated soil remediation: demonstration project results. *J. Soils Sediments.* 9, 229–236. doi:10.1007/s11368-009-0067-z

Seagren, E. A. (2024). "Bioremediation," in *Encyclopedia of Toxicology*. Editor P. Wexler Fourth Edition (Oxford: Academic Press), 145–159. doi:10.1016/B978-0-12-824315-2.00413-9

Shen, Z., Som, A. M., Wang, F., Jin, F., McMillan, O., and Al-Tabbaa, A. (2016). Long-term impact of biochar on the immobilisation of nickel (II) and zinc (II) and the revegetation of a contaminated site. *Sci. Total Environ.* 542, 771–776. doi:10.1016/j.scitotenv.2015.10.057

Shu, X., Li, Y., Huang, W., Chen, S., Xu, C., Zhang, S., et al. (2020). Rapid vitrification of uranium-contaminated soil: effect and mechanism. *Environ. Pollut.* 263, 114539. doi:10.1016/j.envpol.2020.114539

Silvani, L., Cornelissen, G., Botnen Smebye, A., Zhang, Y., Okkenhaug, G., Zimmerman, A. R., et al. (2019). Can biochar and designer biochar be used to remediate per- and polyfluorinated alkyl substances (PFAS) and lead and antimony contaminated soils? *Sci. Total Environ.* 694, 133693. doi:10.1016/j.scitotenv.2019.133693

Singh, S., Parihar, P., Singh, R., Singh, V. P., and Prasad, S. M. (2016). Heavy metal tolerance in plants: role of transcriptomics, proteomics, metabolomics, and ionomics. *Front. Plant Sci.* 6, 1143. doi:10.3389/fpls.2015.01143

Skibsted, G., Ottosen, L. M., Elektorowicz, M., and Jensen, P. E. (2018). Effect of long-term electrodialytic soil remediation on Pb removal and soil weathering. *J. Hazard. Mater.* 358, 459–466. doi:10.1016/j.jhazmat.2018.05.033

Sorvari, J. (2007). Environmental risks at Finnish shooting ranges—a case study. *Hum. Ecol. Risk Assess. An Int. J.* 13, 1111–1146. doi:10.1080/10807030701506124

Sorvari, J., Antikainen, R., and Pyy, O. (2006). Environmental contamination at Finnish shooting ranges—the scope of the problem and management options. *Sci. Total Environ.* 366, 21–31. doi:10.1016/j.scitotenv.2005.12.019

Stauffer, M., Pignolet, A., and Corcho Alvarado, J. A. (2017). Persistent mercury contamination in shooting range soils: the legacy from former primers. *Bull. Environ. Contam. Toxicol.* 98, 14–21. doi:10.1007/s00128-016-1976-3

Sujetoviene, G., and Cesynaite, J. (2020). Changes in physicochemical properties and contamination with lead in outdoor shooting range soils. *Environ. Eng. Manag. J.* 19, 1025–1031. doi:10.30638/eemj.2020.097

Sun, Z., Chen, W.-B., Zhao, R.-D., Shen, P., Yin, J.-H., and Chen, Y. (2023). Effect of seawater on solidification/stabilisation treatment of marine soft soil slurry by lime-activated ISSA and GGBS. *Eng. Geol.* 323, 107216. doi:10.1016/j.enggeo.2023.107216

Suresh, B., and Ravishankar, G. A. (2004). Phytoremediation—a novel and promising approach for environmental clean-up. *Crit. Rev. Biotechnol.* 24, 97–124. doi:10.1080/07388550490493627

Tandy, S., Meier, N., and Schulin, R. (2017). Use of soil amendments to immobilize antimony and lead in moderately contaminated shooting range soils. *J. Hazard. Mater.* 324, 617–625. doi:10.1016/j.jhazmat.2016.11.034

Tangahu, B. V., Sheikh Abdullah, S. R., Basri, H., Idris, M., Anuar, N., and Mukhlisin, M. (2011). A review on heavy metals (as, Pb, and Hg) uptake by plants through phytoremediation. *Int. J. Chem. Eng.* 2011, 9391611–e939231. doi:10.1155/2011/939161

Tariq, S. R., and Ashraf, A. (2016). Comparative evaluation of phytoremediation of metal contaminated soil of firing range by four different plant species. *Arabian J. Chem.* 9, 806–814. doi:10.1016/j.arabjc.2013.09.024

Thangavadivel, K., Ranganathan, S., Sanderson, P., Chadalavada, S., Naidu, R., and Bowman, M. (2018). Case study of testing heavy-particle concentrator-aided remediation of lead-contaminated rifle shooting range soil. *Remediat. J.* 28, 67–74. doi:10.1002/rem.21561

Urrutia-Goyes, R., Mahlknecht, J., Argyraki, A., and Ornelas-Soto, N. (2017). Trace element soil contamination at a former shooting range in Athens, Greece. *Geoderma Reg.* 10, 191–199. doi:10.1016/j.geodrs.2017.08.002

Uwayezu, J. N., Ren, Z., Sonnenschein, S., Leiviskä, T., Lejon, T., van Hees, P., et al. (2024). Combination of separation and degradation methods after PFAS soil washing. *Sci. Total Environ.* 907, 168137. doi:10.1016/j.scitotenv.2023.168137

Vithanage, M., Herath, I., Almaroai, Y. A., Rajapaksha, A. U., Huang, L., Sung, J.-K., et al. (2017). Effects of carbon nanotube and biochar on bioavailability of Pb, Cu and Sb in multi-metal contaminated soil. *Environ. Geochem Health* 39, 1409–1420. doi:10.1007/s10653-017-9941-6

Wang, L., Li, H., Li, A., and Deng, J. (2022a). Study on characteristics and ecological risks of heavy metal pollution in soil of projectile range in military training ground - a case of a training ground in Tibet. *Environ. Chem.*, 2646–2654. doi:10.7524/j.issn.0254-6108.2022012705

Wang, P., Shen, F., Li, R., Guo, D., Liang, W., Liu, T., et al. (2022b). Remediation of Cd and Zn contaminated soil by zero valent iron (Fe0): a field trial. *Environ. Technol. Innovation* 28, 102603. doi:10.1016/j.eti.2022.102603

Wilde, E. W., Brigmon, R. L., Dunn, D. L., Heitkamp, M. A., and Dagnan, D. C. (2005). Phytoextraction of lead from firing range soil by Vetiver grass. *Chemosphere* 61, 1451–1457. doi:10.1016/j.chemosphere.2005.04.059

Wolf, D. C., Cryder, Z., Khoury, R., Carlan, C., and Gan, J. (2020). Bioremediation of PAH-contaminated shooting range soil using integrated approaches. *Sci. Total Environ.* 726, 138440. doi:10.1016/j.scitotenv.2020.138440

Wu, Q., Cui, Y., Li, Q., and Sun, J. (2015). Effective removal of heavy metals from industrial sludge with the aid of a biodegradable chelating ligand GLDA. *J. Hazard. Mater.* 283, 748–754. doi:10.1016/j.jhazmat.2014.10.027

Xu, D.-M., Fu, R.-B., Wang, J.-X., Shi, Y.-X., and Guo, X.-P. (2021). Chemical stabilization remediation for heavy metals in contaminated soils on the latest decade: available stabilizing materials and associated evaluation methods-A critical review. *J. Clean. Prod.* 321, 128730. doi:10.1016/j.jclepro.2021.128730

Xu, L., Xing, X., Liang, J., Peng, J., and Zhou, J. (2019). *In situ* phytoremediation of copper and cadmium in a co-contaminated soil and its biological and physical effects. *RSC Adv.* 9, 993–1003. doi:10.1039/C8RA07645F

Yan, Y., Qi, F., Seshadri, B., Xu, Y., Hou, J., Ok, Y. S., et al. (2016). Utilization of phosphorus loaded alkaline residue to immobilize lead in a shooting range soil. *Chemosphere* 162, 315–323. doi:10.1016/j.chemosphere.2016.07.068

Yang, S., Li, Y., Si, S., Liu, G., Yun, H., Tu, C., et al. (2022). Feasibility of a combined solubilization and eluent drainage system to remove Cd and Cu from agricultural soil. *Sci. Total Environ.* 807, 150733. doi:10.1016/j.scitotenv.2021.150733

Yang, X., Feng, Y., He, Z., and Stoffella, P. J. (2005). Molecular mechanisms of heavy metal hyperaccumulation and phytoremediation. *J. Trace Elem. Med. Biol.* 18, 339–353. doi:10.1016/j.jtemb.2005.02.007

Yasunari, T. J., Stohl, A., Hayano, R. S., Burkhart, J. F., Eckhardt, S., and Yasunari, T. (2011). Cesium-137 deposition and contamination of Japanese soils due to the Fukushima nuclear accident. *Proc. Natl. Acad. Sci.* 108, 19530–19534. doi:10.1073/pnas.1112058108

Yin, X., Saha, U. K., and Ma, L. Q. (2010). Effectiveness of best management practices in reducing Pb-bullet weathering in a shooting range in Florida. *J. Hazard. Mater.* 179, 895–900. doi:10.1016/j.jhazmat.2010.03.089

Zhang, J., Wang, L., Wang, M., Xiao, Y., and Han, Y. (2020). Mechanochemical remediation of petroleum hydrocarbons contaminated soil and its effects on soil properties. *Chem. Industry Eng. Prog.* 39, 4726–4733. doi:10.16085/j.issn.1000-6613.2020-0246

Zhao, X., Sang, L., Song, H., Liang, W., Gong, K., Peng, C., et al. (2023). Stabilization of Ni by rhamnolipid modified nano zero-valent iron in soil: effect of simulated acid rain and microbial response. *Chemosphere* 341, 140008. doi:10.1016/j.chemosphere.2023.140008

Zou, Z., Qin, Y., Zhang, T., and Tan, K. (2023). Enhancing road performance of lead-contaminated soil through biochar-cement solidification: an experimental study. *J. Environ. Manag.* 348, 119315. doi:10.1016/j.jenvman.2023.119315

frontiers | Frontiers in Environmental Science

TYPE Original Research
PUBLISHED 10 April 2024
DOI 10.3389/fenvs.2024.1291917

OPEN ACCESS

EDITED BY
Qi Liao,
Central South University, China

REVIEWED BY
Mohammadhassan Salehi,
Shahrekord University, Iran
Sandhya Patidar,
Heriot-Watt University, United Kingdom

*CORRESPONDENCE
Donghui Zhang,
zhangdonghui@alu.cdut.edu.cn

RECEIVED 10 September 2023
ACCEPTED 26 March 2024
PUBLISHED 10 April 2024

CITATION
Tang Y, Zhang D, Xu H, Dai L, Xu Q, Zhang Z and Jing X (2024), The role of topography feedbacks in enrichment of heavy metal elements in terrace type region.
Front. Environ. Sci. 12:1291917.
doi: 10.3389/fenvs.2024.1291917

The role of topography feedbacks in enrichment of heavy metal elements in terrace type region

Yuanyuan Tang[1,2], Donghui Zhang[3]*, Honggen Xu[1], Liangliang Dai[1], Qingyang Xu[1], Zhijie Zhang[4] and Xiaodong Jing[5]

[1]Changsha General Survey of Natural Resources Center, Changsha, China, [2]China University of Geosciences, Beijing, China, [3]Institute of Remote Sensing Satellite, China Academy of Space Technology, Beijing, China, [4]School of Geography, Development & Environment, University of Arizona, Tucson, AZ, United States, [5]Geomatics Engineering Department, Sichuan College of Architectural Technology, Deyang, China

Minerals, metallurgy, and other production activities will cause a large number of heavy metal elements to leak into the natural environment. A large number of heavy metal elements have been found in the farmland soil, where the adsorption of plants enhances the enrichment. Here, we have selected a region with three terraces to conduct a whole-area soil sample collection and satellite hyperspectral data processing study to explore the role of terrain in this enrichment process. Five spectral transformation methods and four feature enhancement algorithms were designed, and the content extraction model was established to quantitatively retrieve eight heavy metal elements. The results indicates that the three terraces are the source state, transition state, and stable state of heavy metals respectively with the decrease of elevation; The correlation coefficient of various heavy metal elements exceeds 0.92, and the enrichment pattern is consistent although slope and aspect have no significant correlation with the enrichment of heavy metal elements; Local Cd exceeds 30.00%, Hg exceeds 10 times, and As exceeds 48.30% according to the indicator provisions of Chinese national standard (GB 15618-2018). Such knowledge extends our understanding of the abundance, migration, and enrichment of heavy metals from the perspective of topography, which is crucial for pollution assessment and soil remediation.

KEYWORDS

heavy metals in soil, hyperspectral remote sensing, landform, terraces, element enrichment

1 Introduction

Heavy metal elements caused by mineral exploitation in mountainous areas flow from high altitude regions to low altitude regions and accumulate in densely populated valley plains (Shin et al., 2020; Cai et al., 2022). Unfortunately, this transportation process will pollute all farmland soil (Zhou et al., 2021). The enrichment of heavy metal elements,

Abbreviations: OHS, Orbita Hyper Spectral; FLAASH, Fast Line-of-sight Atmospheric Analysis of Spectral Hypercubes; DEM, Digital Elevation Model; PLSR, Partial Least Squares Regression; NMI, Normalized Mutual Information; MI, Mutual Information; MIC, Maximal Information Coefficient; Pearson, Pearson Correlation Coefficient; STD, Standard Deviation; TB, Terabyte; STS, Source state, Transition state, and Stable state; UAV, Unmanned Aerial Vehicle.

through the adsorption of biological roots, is finally partially absorbed by the human body, leading to public health problems (Banerjee et al., 2017; Agyeman et al., 2022; Wang et al., 2022). The traditional monitoring method is to carry out soil sampling (Guo et al., 2021), laboratory testing (Hou et al., 2019), and interpolation analysis technology on a yearly basis (Cai et al., 2022). The difficulty lies in the huge cost and timeliness cannot meet the public demand (Liu et al., 2017; Chen et al., 2022).

The combination of spectroscopy and chemometrics can be used as a practical, fast, low-cost and quantitative method (Liu et al., 2021). The general process of traditional soil heavy metal hyperspectral monitoring includes collecting representative soil samples to ensure sample quantity and quality, performing pretreatments such as drying, grinding, and sieving to obtain samples suitable for acquiring hyperspectral remote sensing data (Mezned et al., 2022). Obtaining the soil sample's reflectance spectral data using a hyperspectral remote sensing instrument. Preprocessing the acquired spectral data, including atmospheric correction, radiometric correction, and comparison of ground object similarity (Harmel et al., 2012; Agyeman et al., 2022). Extracting the characteristic wavelength bands of soil heavy metal elements from the processed spectral data. Establishing the relationship between characteristic wavelength bands and soil heavy metal element content to obtain a quantitative inversion model (Ben-Dor et al., 2006; Tong et al., 2010). Performing hyperspectral inversion of soil heavy metal element content. Using the established quantitative inversion model, converting spectral data into spatial distribution maps of soil heavy metal element content (Ben Dor et al., 2022; Cai et al., 2022). A series of new discoveries have been made in soil zinc and nickel concentration distribution (Guo et al., 2021), heavy metal cations (Shin et al., 2020), soil Cr and Ni concentrations (Han L et al., 2022), soil mercury pollution (Han et al., 2021), clay minerals (Zhou et al., 2021), and toxic minerals (Dkhala et al., 2020). Heavy metals in soil generally belong to trace level, and it is difficult to find characteristic bands (Li et al., 2021; Zhang B. et al., 2022; Cai et al., 2022). Although several spectrum segments of heavy metals have been obtained, their universality is difficult to be recognized (Guo et al., 2021). A large number of spectral preprocessing methods have been used to improve the amount of spectral information and the accuracy of the model (Chen et al., 2019; Bian et al., 2021; Zhang B. et al., 2022).

The content of soil heavy metals usually decreases with the increase of terrain elevation, especially in areas with large differences in elevation such as mountainous regions, because heavy metals in the soil usually deposit to low-altitude areas with the flow of water and other substances (Saidi et al., 2022). Hydrological conditions also have some influence on the transport and accumulation of soil heavy metals, such as extreme weather events like heavy rains which can lead to an increase in soil heavy metal content (Mendes et al., 2022; Zhao et al., 2022). Excessive use of mining, smelting, and chemical fertilizers releases toxic pollutants such as Zn, Pb, or Cd into the soil, thus poisoning the soil and further harming the growth of crops (Xue et al., 2020; Li B. et al., 2022). Snow melting, frozen soil melting, and rainfall can transport soil matter to low-lying areas (Ou et al., 2021). In addition, the effect of terrain makes it very difficult for traditional sampling methods to determine the source and transportation route of pollutants (Guo et al., 2021; Ou et al., 2021). Heavy metals are exported from pollution sources, transported by water systems from streams near mountains, and absorbed and enriched by the land through which they pass, forming a complete transmission chain (Banerjee et al., 2017). Different crops will absorb different types of heavy metals, and the roots and straws further form new enrichment forms (Xue et al., 2020; Li Y. et al., 2022). The content of soil heavy metals varies in different geological environments, for example, the content of soil heavy metals is usually higher in geological environments such as igneous rocks and metamorphic rocks than in sedimentary rocks (Brossard et al., 2016; Wan et al., 2021). Overall, the content of soil heavy metals is closely related to factors such as terrain, hydrological conditions, and geological background, and a comprehensive consideration of these factors is needed to accurately assess the pollution status of soil heavy metals.

The application of hyperspectral remote sensing technology in the extraction of heavy metals from soil is a highly researched area, however, there are still some limitations and shortcomings in practical applications. Firstly, although hyperspectral remote sensing technology can capture more spectral information of objects, the information obtained in the extraction of soil heavy metals may not necessarily reflect the true content of heavy metals in the soil. Therefore, it is necessary to process and analyze the spectral data obtained by hyperspectral remote sensing technology to obtain more accurate information on heavy metal content. Secondly, the widely used methods of hyperspectral remote sensing technology in the field of soil heavy metal extraction all have certain limitations. For example, these methods require a large amount of sample data for training and are susceptible to the influence of data noise, leading to inaccurate identification results. Finally, despite the rapid and non-destructive detection advantages of hyperspectral remote sensing technology, there are still some difficulties in practical applications. For example, the cost of spectrometers is relatively high, the operation is complex, and requires professional personnel for operation and analysis.

Although hyperspectral remote sensing technology has tremendous potential in the field of soil heavy metal extraction, there are still limitations and shortcomings in practical applications. The next step in research needs to further improve the analysis methods of hyperspectral remote sensing technology and combine them with other methods to enhance the accuracy and reliability of soil heavy metal extraction. At the same time, it is necessary to reduce instrument costs, improve data processing efficiency, and enable hyperspectral remote sensing technology to be widely applied in the monitoring of soil heavy metal pollution and environmental assessment, providing a scientific basis for the management of soil pollution.

To understand the relationship between soil heavy metals and terraces, here, we collected soil samples from a county and hyperspectral satellite data for a day with good weather conditions. Eight typical heavy metal elements were quantitatively extracted through data preprocessing, algorithm implementation, precision evaluation, mapping, and analysis (Liu et al., 2017; Han L et al., 2022; Mezned et al., 2022). The strength of heavy metal content along the three terraces and the distribution patterns of heavy metal content in soil along the topography were studied by introducing slope, aspect, and pH data (Chen et al., 2019; Agyeman et al., 2022; Cai et al., 2022; Giniyatullin et al., 2022). The types of heavy metals exceeding the standard in the study area are obtained under the provisions of the Chinese national standard GB 15618-2018. The above knowledge broadens the understanding of

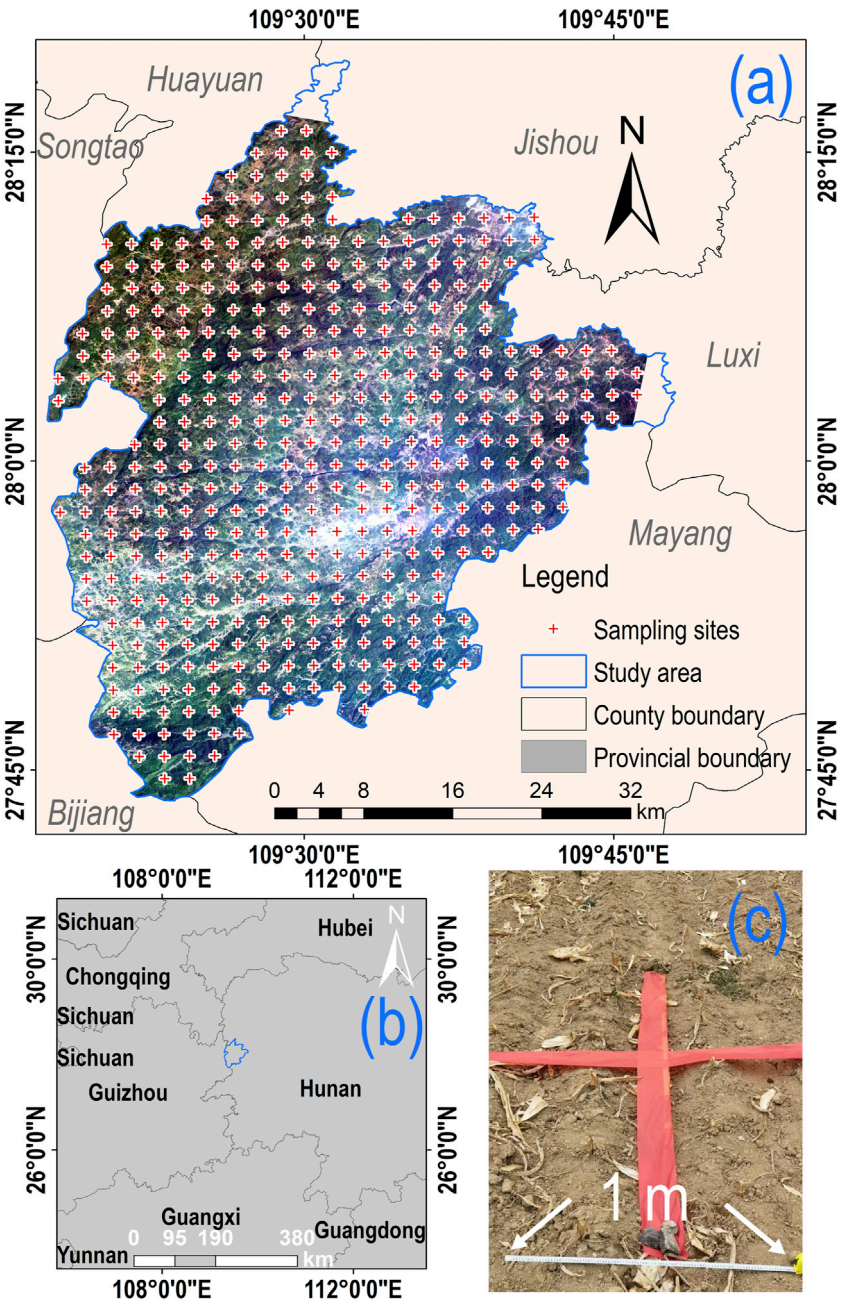

FIGURE 1
The distribution of the study area and sampling points. **(A)** The geographical distribution of the research area and sampling points; **(B)** Geographic site of the study area; **(C)** Synchronously determine GPS coordinates when collecting soil samples. Then take the soil within a 1 m range and send it to the laboratory for analysis and analysis.

heavy metal transport and enrichment, and is essential for the assessment and soil remediation.

2 Materials and methods

2.1 The study area

Fenghuang County, Xiangxi Tujia and Miao Autonomous Prefecture, Hunan Province is selected as the study area (109°18′E~109°48′E, 27°44′N~28°19′N) (Figure 1). The study area has undulating terrain, with main landforms including mountains, valleys, and hills. The area is crisscrossed by mountain ranges, with major peaks such as Jietian Peak and Wuling Peak. Multiple rivers flow through the area, including the Tuo River and Simeng River. Additionally, Fenghuang County also has some relatively gentle hilly areas. The soil types are diverse, with mountain soils mainly composed of weathered rocks forming yellow-brown soil, rich in minerals and organic matter, suitable for vegetation growth. Sandy soils are mainly

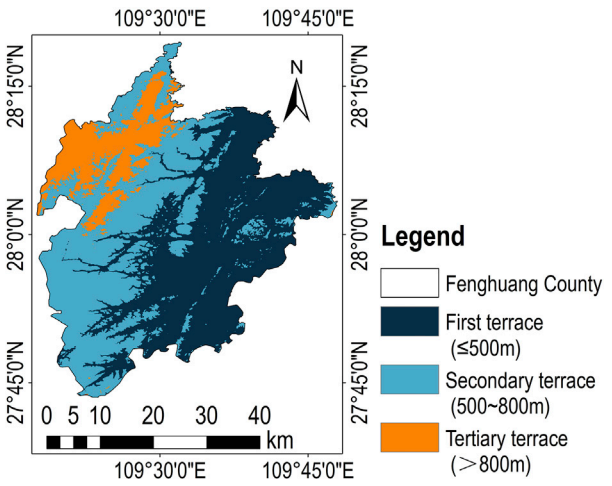

FIGURE 2
The study is divided into three terraces, which are valley hilly zone, middle and low mountain zone, and middle mountain zone from east to west.

distributed in the valley areas, with a higher content of sand particles and good drainage. Huang soils are widely distributed, with thick soil layers and high fertility, suitable for cultivation and agricultural development (Xue et al., 2020). The total area is about 1,760 km^2, and the terrain is divided into three terraces (Agyeman et al., 2022). The eastern part is a valley and hilly area with an altitude of less than 500 m, the middle part is a middle and low mountain area with an altitude of 500–800 m, and the western part is a middle mountain area with an altitude of more than 800 m (Figure 2). There has been a tradition of mineral mining since ancient times, with phosphate ore, manganese ore, vanadium ore, iron ore, and coal mining as the main mining. The waste liquid generated in the process of mineral development flows into the soil through physical and chemical processes due to the special tertiary terrace, resulting in potential heavy metal pollution risk (Lu et al., 2019; Chen et al., 2022).

Soil samples were collected at equidistant intervals of 2 km in the study area. And a total of 421 soil samples were obtained within a period of 1 month. Soil samples from the depth of 0–10 cm on the ground surface is collected at each point according to the longitude and latitude (Han B et al., 2022). They are sealed into polyethylene bags after removing plant roots, leaves, and stones with a mesh of 0.01 m. Send the collected soil samples to the Wuhan Mineral Resources Supervision and Testing Center of the Ministry of Land and Resources of China for physical and chemical analysis (Ben Dor et al., 2022). The contents of eight heavy metals such as cadmium, mercury, arsenic, lead, chromium, copper, nickel, and zinc were obtained. Among them, Cd, Pb, Cu, and Zn are measured by inductively coupled plasma mass spectrometry; Hg and As are determined by hydride generation-atomic fluorescence spectrometry; Cr is determined by X-ray fluorescence spectrometry; Ni was determined by inductively coupled plasma atomic emission spectrometry. A total of 421 samples were collected and divided into a modeling set and a validation set in a 7:3 ratio (Xue et al., 2020; Zhang B. et al., 2022; Mezned et al., 2022) (Table 1).

2.2 Hyperspectral data acquisition and processing

OHS is the only commercial hyperspectral satellite in China that has completed the launch and networking. The spatial resolution is 10m, and the imaging range is 150 km × 2,500 km. The spectral resolution in the wavelength range of 400 nm–1,000 nm is 2.5 nm. This satellite data contains 32 spectral bands with a spatial resolution of 10 m [36]. Each group of satellite data contains a metadata file that records information such as payload, center point longitude and latitude, data acquisition time, satellite observation angle, solar altitude angle, etc., for subsequent data preprocessing (Zhang B. et al., 2022; Bouzidi et al., 2022). Data in 13 September 2022 were used in the study.

The process of data processing is divided into four steps: radiation correction, atmospheric correction, orthophoto

TABLE 1 Eight heavy metal content values were obtained for each soil sample, including the minimum, maximum, mean, and standard deviation values (Figure 1A).

Serial number	Value	Class	Heavy metal element							
			Cd	Hg	As	Pb	Cr	Cu	Ni	Zn
1	Minimum	Modeling set	0.16	0.05	1.61	18.80	47.10	18.80	18.80	55.50
		Validation Set	0.11	0.04	1.63	20.50	52.70	18.70	20.10	55.60
2	Maximum	Modeling set	2.55	83.9	58.40	264.00	159.00	143.00	75.70	582.00
		Validation Set	2.65	1.68	42.00	79.40	178.00	75.30	59.10	188.00
3	Average	Modeling set	0.51	0.74	16.60	46.50	77.50	34.80	37.80	113.00
		Validation Set	0.37	0.21	10.90	32.80	69.90	28.90	31.80	85.30
4	Standard deviation	Modeling set	0.30	4.56	8.72	24.90	14.20	10.50	7.67	47.50
		Validation Set	0.27	0.25	7.21	10.30	14.60	7.19	7.19	22.40

Note: The unit is mg kg^{-1}.
Each soil sample is taken from 1 m × A 1 m plot (Figure 1C). The sample weight is 1 kg, which can meet the basic requirements for heavy metal element analysis and validation.

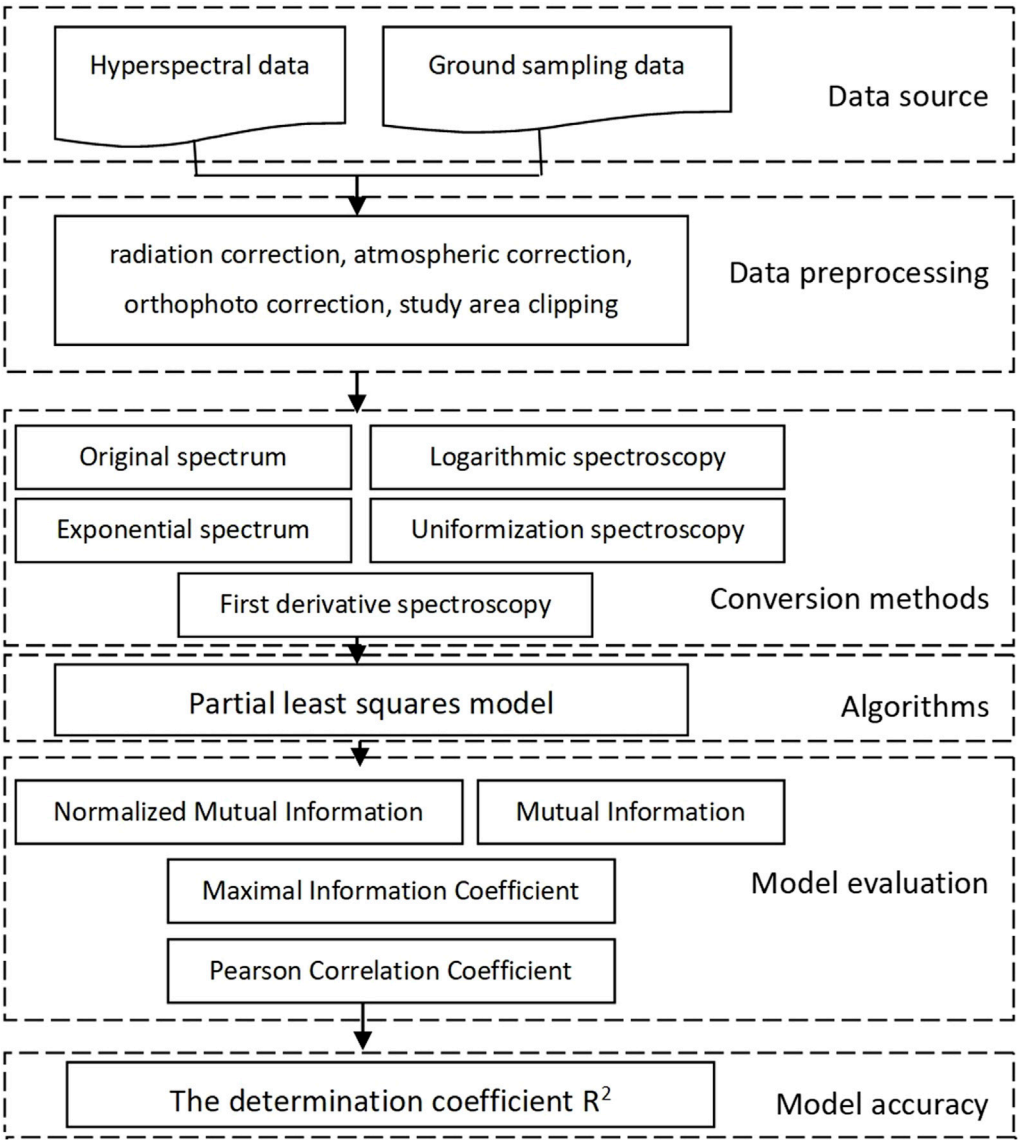

FIGURE 3
Algorithm flowchart from data acquisition to model selection.

TABLE 2 The spectral transformation method selected in the study.

Serial number	Transformation method	Process formulas
1	Original spectrum	$X_i = R_i$
2	Logarithm	$X_i = \mathrm{Ln}\ (R_i)$
3	Exponential	$X_i = e^{R_i}$
4	Homogenization	$X_i = (R_i - R_{min})/(R_{max} - R_{min})$
5	First-order differential	$X_i = R_i'$

Note: X_i is the processed spectral reflectivity; R_i is the spectral reflectivity; i is the band variable; R_{min} is the minimum reflectivity; R_{max} is the maximum reflectivity; and C_i is the envelope curve value.

Spectral transformation can provide better data understanding, information extraction, and data processing effects in spectral analysis and remote sensing applications, helping to reveal information on surface features, environmental changes, and target recognition.

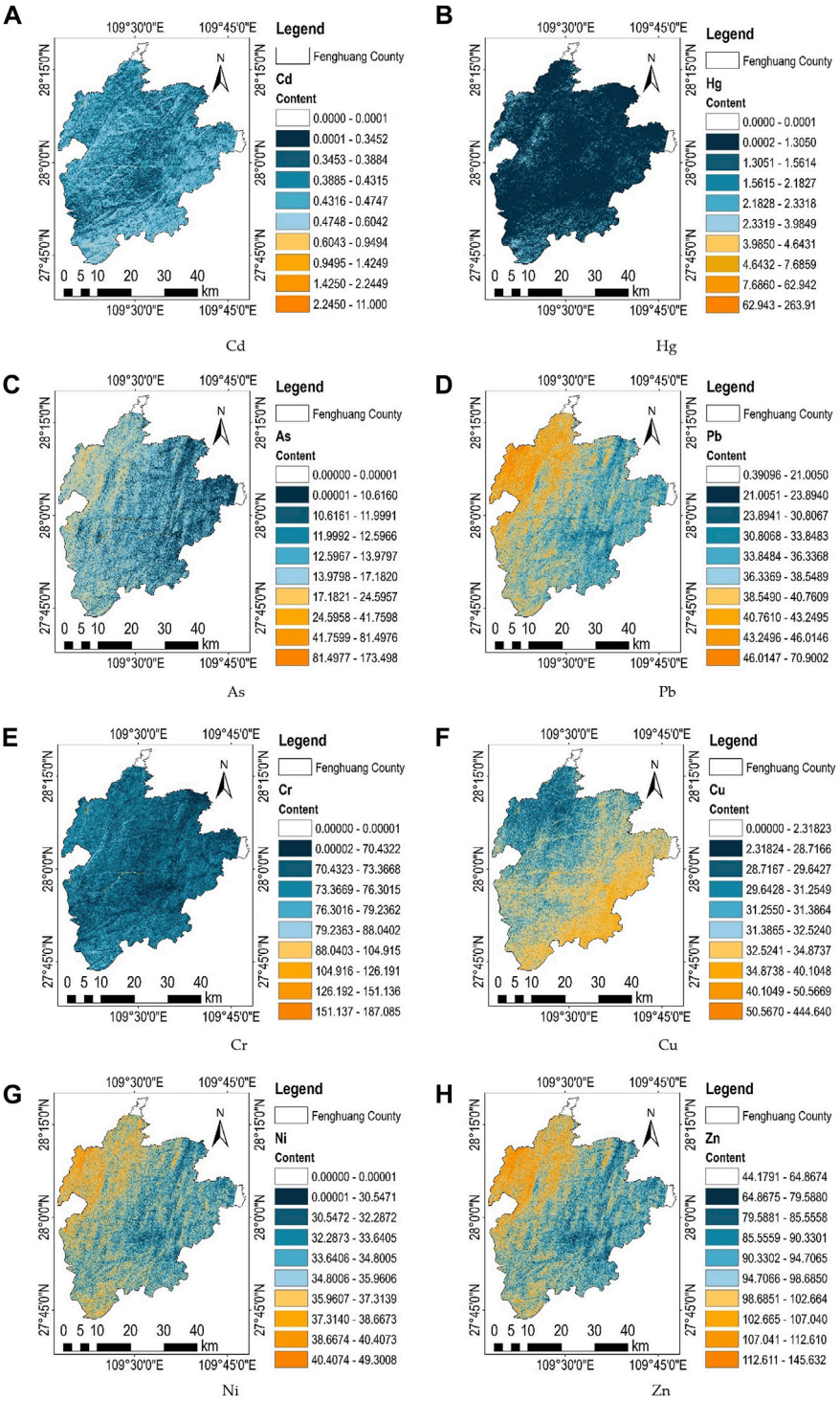

FIGURE 4
Mapping results of 9 soil components calculated from hyperspectral data. **(A)** The distribution of Cd is generally lower than 0.50 mg/kg, showing scattered distribution in the valley; **(B)** The distribution of Hg is lower than 1.50 mg/kg as a whole, and it is star-shaped in the study area; **(C)** The average value of As is 7.23 mg/kg, which is characterized by north-south distribution and significant high in individual regions; **(D)** The average value of Pb is 28.68 mg/kg, and there is a significant correlation between its distribution and terraces; **(E)** The content of Cr is lower than 80 mg/kg in most areas, but it is significantly higher in the valley; **(F)** The average content of Cu is 16.98 mg/kg, and its distribution is also closely related to terrace; **(G)** The average content of Ni is 18.38 mg/kg, and there is also a certain correlation between distribution and terraces; **(H)** The average content of Zn is 75.92 mg/kg, and the content of the first terrace is significantly higher.

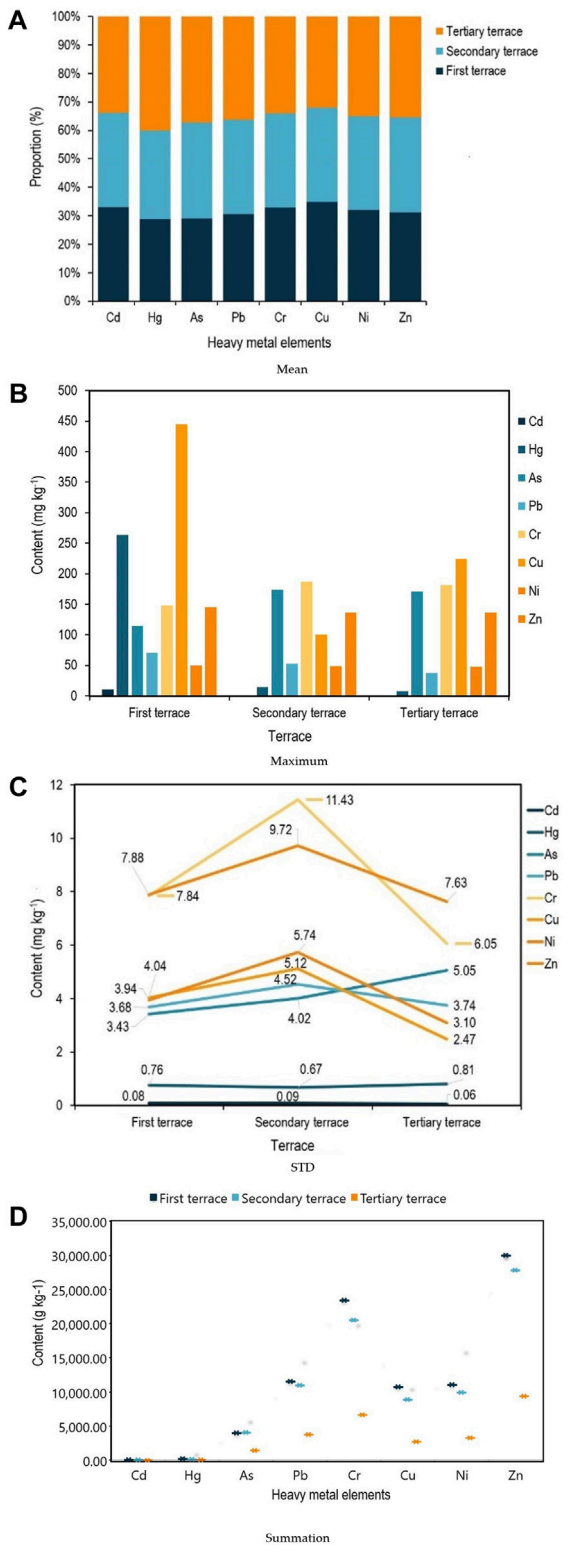

FIGURE 5
Statistical results of heavy metals in different terraces. **(A)** The highest Cu content is distributed outside the first terrace, while the average content of the other seven heavy metal elements is highest in the third terrace; **(B)** The maximum values of As and Cr appear in the second terrace, while the maximum values of the other six heavy metals appear in the first terrace at higher altitudes; **(C)** The maximum STD values of Hg and As appear in the third terrace, while the maximum STD values of the other six heavy metals appear in the second terrace at higher altitudes; **(D)** The total content of As element is the highest in the second terrace, while the other seven elements have the highest content in the first terrace at higher altitudes.

(*Continued*)

FIGURE 5 (Continued)

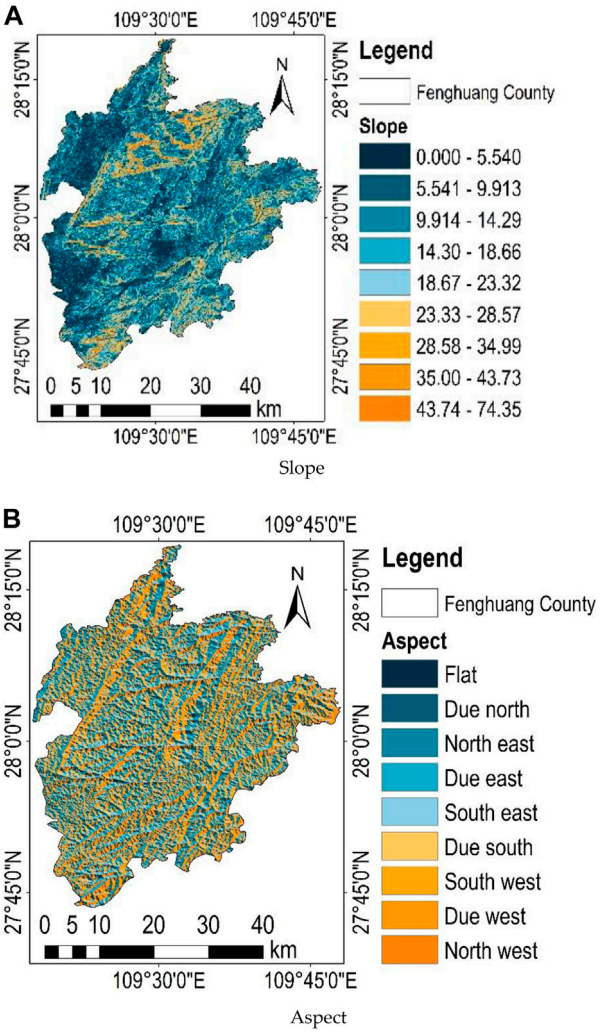

FIGURE 6
Response of heavy metals to topography. **(A)** Larger slope mainly occurs in the valley area due to the cutting effect of water system; the slope fluctuates violently; **(B)** The study area presents a south-north and east-west intersection trend, and southward and westward directions become the main existence mode of slope direction.

correction, and study area clipping (Meng et al., 2021). Firstly, radiation correction. By using pre collected sensor response functions for calibration, the radiation distortion caused by the characteristics of the sensor itself is removed (Wang et al., 2022). Secondly, by utilizing the FLAASH algorithm and using an atmospheric transport model, the impact of the atmosphere on the image is estimated and corrected, and this impact is removed (Agyeman et al., 2022). Thirdly, use elevation data to generate a digital surface model, and then register satellite images with DSM to achieve ortho-correction. This method can consider the height

TABLE 3 Response relationship between heavy metals, slope, and aspect.

	Slope	Aspect	Cd	Hg	As	Pb	Cr	Cu	Ni	Zn
Slope	/	0.05	0.05	0.07	−0.02	−0.01	0.00	0.00	0.00	0.01
Aspect	0.05	/	0.01	−0.05	−0.01	−0.02	0.00	0.00	0.00	0.00
Cd	0.05	0.01	/	0.68	0.92	0.95	0.98	0.98	0.98	0.97
Hg	0.07	−0.05	0.68	/	0.63	0.64	0.63	0.62	0.63	0.65
As	−0.02	−0.01	0.92	0.63	/	0.94	0.95	0.92	0.94	0.94
Pb	−0.01	−0.02	0.95	0.64	0.94	/	0.96	0.94	0.97	0.99
Cr	0.00	0.00	0.98	0.63	0.95	0.96	/	0.99	1.00	0.97
Cu	0.00	0.00	0.98	0.62	0.92	0.94	0.99	/	0.99	0.95
Ni	0.00	0.00	0.98	0.63	0.94	0.97	1.00	0.99	/	0.98
Zn	0.01	0.00	0.97	0.65	0.94	0.99	0.97	0.95	0.98	/

There is no significant correlation between slope and aspect, which is determined by geological conditions. Moreover, there is no statistical correlation between slope and aspect with all heavy metal elements. The correlation coefficient of other seven heavy metals is greater than 0.90 in addition to Hg. The special physical properties of Hg lead to this phenomenon, and the general correlation coefficient is about 0.62.

TABLE 4 National standards issued by China in 2018 (GB 15618–2018), Soil environment quality–Risk control standard for soil contamination of agricultural land.

Serial number	Contaminants	Heavy metal element			
		pH≤5.5	5.5<pH≤6.5	6.5<pH≤7.5	pH>7.5
1	Cd	0.30	0.30	0.30	0.60
2	Hg	0.50	0.50	0.60	1.00
3	As	30.00	30.00	25.00	20.00
4	Pb	70.00	90.00	120.00	170.00
5	Cr	150.00	150.00	200.00	250.00
6	Cu	50.00	50.00	100.00	100.00
7	Ni	60.00	70.00	100.00	190.00
8	Zn	200.00	200.00	250.00	300.00

Note: The unit is mg kg^{-1}.
The national standard divides paddy field and dry land. The paper adopts a strict risk screening value since most of the study area belongs to paddy and dry rotation land.

difference of ground objects and improve the spatial positioning accuracy of the image (Agyeman et al., 2022). Fourthly, Fourthly, use vector boundaries and spatial analysis algorithms to crop the image into parts that intersect or are included within the boundaries (Wang et al., 2018). Finally, the reflectance data of satellite remote sensing images in the study area were obtained (Meng et al., 2021).

2.3 Algorithms

A set of algorithm processes was designed to better establish the relationship between spectrum and content. Firstly, the spectral data underwent five types of transformations to highlight the spectral characteristics. Secondly, the data was divided into a modeling set and a validation set, and the content of the modeling set was used to establish a partial least squares model with the spectral values. Thirdly, the modeling results were evaluated using the calculated values of NMI, MI, MIC, and Pearson, and the relatively optimal model was selected. Fourthly, the optimal model was applied to the validation dataset, and the predicted values were evaluated against the laboratory values using the indicators R^2 to determine the effectiveness of the model (Figure 3).

Five spectral data transformation methods were selected, including original spectrum, logarithmic spectrum, exponential spectrum, homogenization spectrum, and first derivative spectrum (Xue et al., 2020; Tan et al., 2021; Li B. et al., 2022). The original spectrum is not processed, and the pixel spectrum is directly taken for modeling; Logarithmic spectrum is a discrete way to make the spectrum close to normal distribution (Xu et al., 2022); Exponential spectrum can improve the value of low reflectivity and restrain the value of high reflectivity; The homogenization spectrum can remove the systematic error generated in the preprocessing process; The first derivative spectrum can amplify the mutation

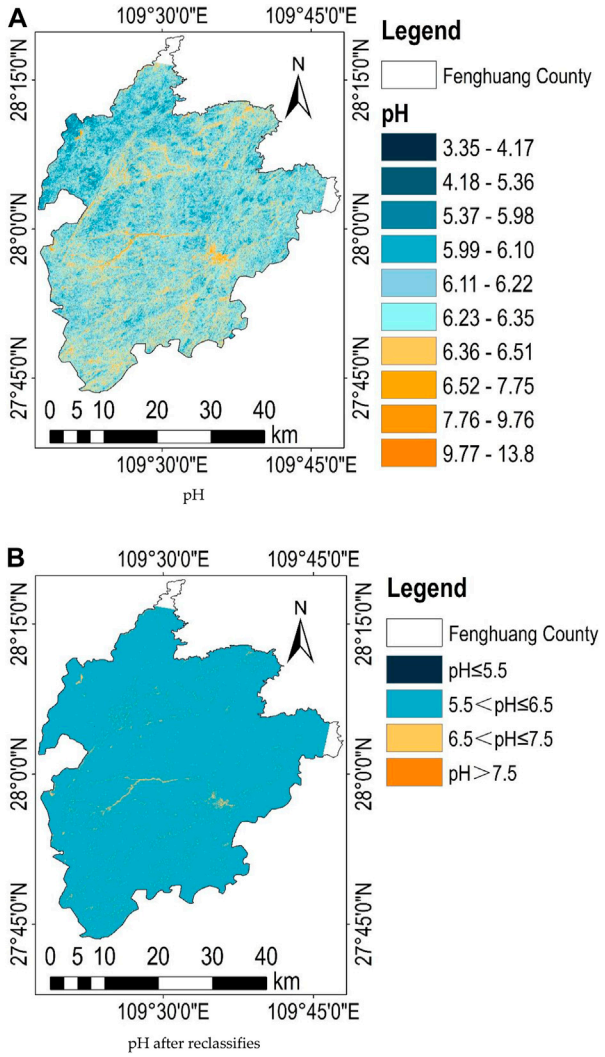

FIGURE 7
Distribution and grade of pH value. **(A)** The soil is weakly acidic as a whole; **(B)** The pH value of more than 98% of the area is the second category, between 5.5 and 6.5.

position of reflectivity and help to find the characteristic band (Table 2).

The purpose of selecting different spectral data conversion methods is to extract or emphasize information from different aspects of spectral data, to better adapt to subsequent data analysis and modeling needs.

(1) Original spectrum: Without any processing, model directly using pixel spectra. This method can preserve the characteristics of the original data and is suitable for data analysis that does not require additional processing in certain situations.
(2) Logarithmic spectroscopy: Performing logarithmic transformation on a spectrum to make it closer to a normal distribution can aid in the application of certain statistical methods, such as linear regression.
(3) Exponential spectrum: can increase the value of low reflectivity and suppress the value of high reflectivity. This method can adjust the dynamic range of spectral data, making some details more prominent in visualization and analysis.
(4) Uniformization spectroscopy: This method can remove systematic errors generated during preprocessing, making spectral data more accurate and reliable.
(5) First derivative spectroscopy: By calculating the first derivative of the spectrum, the position of abrupt changes in reflectance can be magnified, which helps to identify characteristic bands or edge positions. This method can extract local variation information from spectral data, which is helpful for the detection and analysis of specific features.

PLSR is selected as the modeling algorithm (Li B. et al., 2022; Mezned et al., 2022; Wang et al., 2022). PLSR (Partial Least Squares Regression) is a commonly used multivariate statistical modeling algorithm that has the following advantages in spectral processing.

(1) Solving the problem of multicollinearity: In spectral data, there is correlation and overlap between different bands, which may lead to the problem of multicollinearity in traditional linear regression methods. PLSR can effectively solve multicollinearity problems and improve the stability and accuracy of modeling by transforming predictive and response variables into new composite variables.
(2) Performs well in small sample situations: Spectral data typically has high dimensionality and relatively small sample sizes, which can make traditional regression methods difficult to obtain reliable results. PLSR uses multiple principal components to represent the variability

TABLE 5 Results of heavy metal elements exceeding the standard in the national standard (GB 15618-2018).

Serial number	Class	Mean content of heavy metal element							
		Cd	Hg	As	Pb	Cr	Cu	Ni	Zn
1	pH≤5.5	0.29	8.53	0.66	57.50	3.49	20.68	44.11	129.53
2	5.5≤pH≤6.5	0.43	0.82	13.76	37.66	72.78	32.31	35.01	95.83
3	6.5≤pH≤7.5	0.52	0.73	15.95	35.26	76.17	35.10	35.92	96.41
4	pH>7.5	1.09	11.27	29.66	15.37	42.20	29.69	29.13	83.31

Note: The unit is mg kg^{-1}.
The content of Cd, Hg, and As exceeds the standard value, which has potential risks to the local ecological environment.

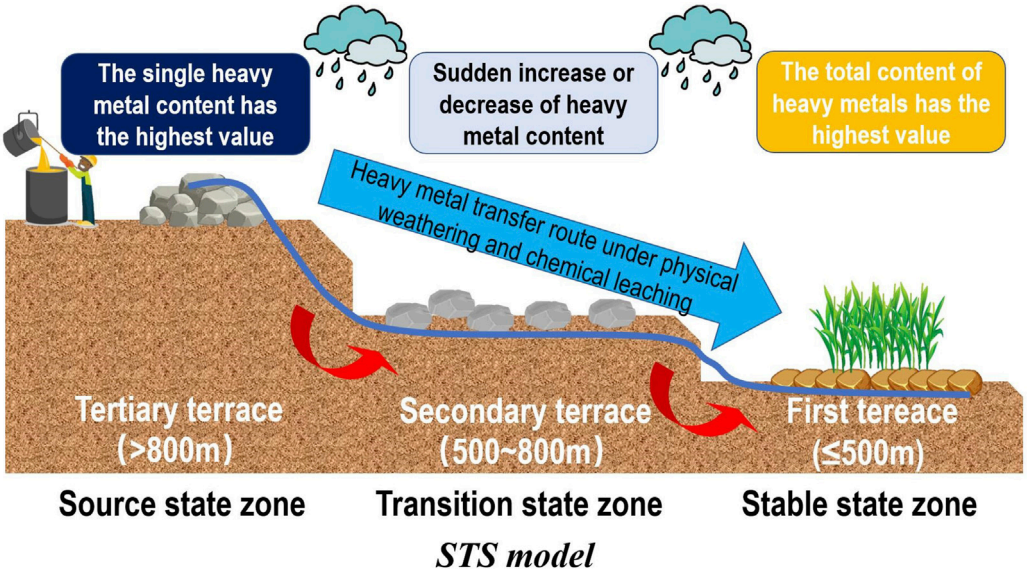

FIGURE 8
The transport patterns of heavy metals in terraced areas. Heavy metals migrate from high-altitude terraces to low-altitude terraces, forming STS models, namely source state, transition state, and stable state.

of the original spectral data, which can better fit the data in small sample situations and reduce the risk of overfitting.

(3) Considering the characteristics of spectral data: PLSR is based on the principle of principal component analysis, which selects principal components to explain the variability of spectral data to the greatest extent possible. This enables PLSR to capture key features in spectral data and effectively utilize these features for modeling and prediction.

(4) Strong interpretability: PLSR can generate weight coefficients to explain the contribution of different bands to response variables in spectral data. This makes the PLSR model highly interpretable, helping researchers understand the relationship between spectral data and response variables, and further analyze and interpret them.

This method is used to find the basic relationship between reflectivity X and heavy metal content Y, and characterizes reflectivity into four correlation coefficients such as NMI, MI, MIC and Pearson.

NMI is a measure of the similarity of two reflectivity, with a range of [0,1]. The higher the value is, the more similar the two clustering results are (Huang et al., 2022). The formula is,

$$NMI(Y,C) = \frac{2 \times I(Y;C)}{H(Y) + H(C)}$$

Where, Y is the true category of data; C is the clustering result; $H(Y)$ and $H(C)$ are the cross entropy, $H(X) = -\sum_{i=1}^{|X|} P(i)\log P(i)$, where the log is based on 2; $I(Y;C)$ is the mutual information and $I(Y;C) = H(Y) - H(Y|C)$.

MI is an information quantity, which is the uncertainty of a random variable reduced by knowing another random variable (Wang et al., 2022). If two variables X and Y are limited, and their respective marginal probability densities and joint probability densities are $p(x)$, $p(y)$, and $p(x, y)$, then the mutual information $I(X;Y)$ between them can be defined as,

$$I(X;Y) = \sum_x \sum_y p(x,y)\log\frac{p(x,y)}{p(x)p(y)}$$

Where, the minimum value of $I(X;Y)$ is 0, which means that there is no overlapping information between the two variables, that is, completely independent or mutually independent; On the contrary, the larger the value of $I(X;Y)$, the higher the degree of interdependence between the two variables, indicating that there is more common information shared between the two variables.

The MIC coefficient can evaluate different types of association relationships efficiently to find a wide range of relationship types, with a value range of [0,1], and has good robustness (Zhou et al., 2022). The formula is,

$$MIC(X;Y) = \max_{|X||Y|<B(n)} \frac{I(X;Y)}{\log_2(min(|X|,|Y|))}$$

Where, the range of $MIC(X;Y)$ values is [0,1], $B(n)$ is the upper limit value of the grid interval $n_X \times n_Y$, and n_X and n_Y are the number of samples for X and Y, respectively.

Pearson coefficient is used to measure the linear correlation degree between two variables X and Y, and its value is between −1 and 1 (Giniyatullin et al., 2022). The formula is,

$$r = \frac{\sum(x_i - \bar{x})(y_i - \bar{y})}{\sqrt{\sum(x_i - \bar{x})^2 \sum(y_i - \bar{y})^2}}$$

Where, $\bar{x}$, $\bar{y}$ is the mean of X and Y variable samples respectively, where $X=(x_1,x_2,\ldots,x_n)$ and $Y=(y_1,y_2,\ldots,y_n)$ is the sample dataset for X and Y, n is the number of samples, and r is the calculated Pearson correlation between the two variables.

The determination coefficient R^2 are commonly used evaluation indicators in hyperspectral quantitative remote sensing to evaluate

the fitting degree and prediction accuracy of models. The coefficient R^2 is used to measure the explanatory power of the model to the observed data, that is, the proportion of variance that the model can explain the dependent variable. The value range of R^2 is between 0 and 1, and the closer it is to 1, the better the model fits and can explain more variance; On the contrary, the closer to 0, the worse the fitting effect of the model and the inability to explain variance. By comparing the R^2 values of different models, it can be determined which model is more suitable for fitting the data (Liu et al., 2021; Zhang D. et al., 2022).

3 Results

3.1 The strength of heavy metal content along the three terraces

The distribution of eight heavy metals presents different laws according to the calculation results (Wang et al., 2018; Poppiel et al., 2020; Zhang D. et al., 2022). The distribution of Cd, Hg, and Cr contents has no significant relationship with terrace; The distribution of As, Pb, Ni, and Zn contents is positively correlated with altitude; The content of Cu is negatively correlated with the altitude (Figure 4).

Heavy metal elements are mainly distributed on the third terrace, which is consistent with the actual situation of mining (Figure 5A). The content of Cu is the only highest mean value distributed on the first terrace. It is speculated that human production and living activities lead to this phenomenon since there is no copper deposit in the area (Taghizadeh-Mehrjardi et al., 2021). The maximum content of heavy metals in each terrace mostly occurs in the first terrace, and only As and Cr do not follow this rule (Shin et al., 2020). The maximum pollution value still appears in the first terrace with high population density although there is a positive correlation between elevation and distribution (Figure 5B). The second terrace is in the transition zone connecting the other two terraces, and most of the content mutations occur in this area (Figure 5C). The first terrace is significantly higher than the other two terraces, even several times by calculate the total content of all heavy metals (Figure 5D). Heavy metals are enriched in this terrace with the rain, weathering, and erosion, as well as the impact of human production activities (Wang et al., 2018; Han L et al., 2022).

3.2 Distribution patterns of heavy metal content in soil along the topography

Slope and aspect are the most important indicators of terrain (Agyeman et al., 2022; Cai et al., 2022). The slope of the study area is between 0°–75° (Figure 6A), and the slope direction is mainly south and west (Figure 6B). There is no significant correlation between the two. The former is denudation under river cutting and weathering, and the latter is fault zone and mineralization caused by geological activities (Jiji, 2021; Giniyatullin et al., 2022).

The correlation coefficient is only 0.05, which verifies that they are independent from each other from a mathematical point of view (Table 3). The aspect and slope have negligible correlation with Cd, Hg, As, and Pb, but have no correlation with the other four elements. It reveals that elevation is the only determining factor, independent of slope and aspect (Demattê et al., 2015; Chen et al., 2022). The correlation coefficient between Hg and other seven heavy metal elements is between 0.62–0.68. However, the correlation coefficient between the other seven heavy metal elements exceeded 0.92, especially the correlation coefficient of Cr, Cu, and Ni reached 0.98. The effects of mining, transportation, rehabilitation, and soil erosion have resulted in the enrichment of these heavy metal elements in the same places (Chen et al., 2022; Giniyatullin et al., 2022) (Figure 6C). This also explains that part of the local farmland will be fallow, because the crops planted often exceed the standard of heavy metals and fail to meet the requirements of safe food (Xue et al., 2020; Chen et al., 2023).

3.3 Assessment of heavy metal pollution in soil

The soil risk assessment was conducted according to the national standard, Soil environment quality—Risk control standard for soil contamination of agricultural land (GB 15618-2018) issued by China in 2018 (Table 4). Measure the pH value of the collected soil samples (Dkhala et al., 2020; Mezned et al., 2022) (Figure 7A). The pH is divided into four categories, and the area proportions of the four levels are 0.01%, 98.35%, 1.64%, and 0.00% respectively (Figure 7B).

Cd is the most serious heavy metal in the soil and the average content is 0.43 mg kg^{-1}, 0.52 mg kg^{-1}, and 1.09 mg kg^{-1} respectively, when the pH exceeds 5.50 which is 30.23%, 42.31%, and 63.30% higher than the national standard (Bian et al., 2021). The average content of Hg element in the two grades of pH ≤ 5.50 and pH > 7.50 is 8.53 mg kg^{-1} and 11.27 mg kg^{-1}, which are 16.06 times and 10.27 times higher than the national standard respectively. As element exceeded the standard in the range of pH > 7.50, and the average content was 29.66 mg kg^{-1}, which is 48.30% higher than the 20.00 mg kg^{-1} required by the national standard. The other five heavy metal elements are below the requirements of the national standard, and are significantly lower than the threshold. There is no risk of heavy metal pollution (Giniyatullin et al., 2022) (Table 5).

4 Discussion

In recent years, with the strengthening of China's efforts to control air pollution and water pollution, these two environmental factors have initially met the requirements of healthy life [12,16]. In contrast, the seriousness of soil problems still exists, and there are not many reliable technical means (Xue et al., 2020; Ou et al., 2021). There is water, air bubbles, microorganisms, organic matter, minerals, and other substances in the soil (Han et al., 2021; Ou et al., 2021; Wang et al., 2021; Zhou et al., 2021). In terms of mechanism, speculation is based on the interaction principle between matter and electromagnetic radiation, while in terms of statistics, prediction models are established using a large amount of hyperspectral data and data analysis methods. This comprehensive application can improve the accuracy and reliability of heavy metal content, and play an important role in environmental protection, agricultural management, and other fields (Meng et al., 2021; Han B et al., 2022). The difficulty of the problem is that heavy metal

elements in soil exist in trace or even micro amount forms (Lu et al., 2019). Current research shows that it is extremely difficult to determine the characteristic bands of each heavy metal element (Xue et al., 2020; Zhou et al., 2021; Zhang D. et al., 2022; Lin et al., 2022). This is easy to understand, because the content of heavy metal elements has a characteristic position in the spectrum, and this farmland can even extract minerals.

There are two ways to solve this problem. Firstly, the content of heavy metals can be extracted indirectly by determining the content relationship between heavy metals and other components with characteristic bands in the soil (Huang et al., 2022). There is a close relationship between heavy metal elements and soil moisture (Liu et al., 2017). The study indicates that the stability of soil aggregate water is gradually enhanced with the increase of Al, Fe, and Mn oxide content (Shin et al., 2020); There is a close relationship between Fe and Mn oxides (Zhou et al., 2021); Fe and Mn oxides will co-precipitate and oxidate with heavy metal pollutants arsenic, thus reducing the degree of heavy metal pollution (Zhou et al., 2021); Al can inhibit the decomposition of soil organic matter through adsorption and inhibition of microbial activity (Taghizadeh-Mehrjardi et al., 2021). Therefore, the content of heavy metals can be deduced by extracting the content of soil water, oxide, and organic matter (Lu et al., 2019; Wang et al., 2021; Zhou et al., 2021). Secondly, the heavy metal content and hyperspectral data are trained and learned on a large scale through machine learning algorithm, and the information is extracted from the statistical sense (Zhang B. et al., 2022; Giniyatullin et al., 2022; Lin et al., 2022). A series of breakthroughs have been made in relevant research although this method cannot answer the physical and chemical mechanism of heavy metal elements from the mechanism (Shin et al., 2020; Li Y. et al., 2022). From the results, the spectral principle is inversely inferred, and the closed-loop of the research is realized.

Our research combines the advantages and disadvantages of the above two methods. The PLSR model with stable information extraction is selected for TB level modeling and accuracy verification (Hou et al., 2019; Dkhala et al., 2020; Mezned et al., 2022). There are three discussion points extended. Firstly, the content of heavy metal elements in different terraces has three forms, that are generation, transition, and stability. Obviously, mineral occurrences in mountainous areas have become the source of heavy metals, known as the source state due to the impact of human production and living activities (Banerjee et al., 2017). Most heavy metal elements converge in the third terrace with the joint action of weather, climate, and water and soil, forming a potential risk area of soil heavy metal elements, called stable state (Shin et al., 2020). The secondary terrace becomes the pathway of heavy metal elements and forms the place where heavy metal elements are transported in the soil, which is called the transition state (Banerjee et al., 2017). This theory can be named STS model. Therefore, the strategy should obviously be to control the source state, block the transition state, and repair the stable state in order to control heavy metal pollution (Lin et al., 2022).

Additionally, the distribution pattern of heavy metal elements should be closely related to topography since terrain is an important factor in heavy metal transport (Han L et al., 2022). Terrain will lead to changes in water flow, sunshine, wind direction, and other environmental factors, which will lead to differences in the content of heavy metals (Liu et al., 2017; Bian et al., 2021). Thirdly, the prediction and early warning of local heavy metal exceeding the standard can give a comprehensive assessment conclusion of the environment based on the results of hyperspectral extraction of heavy metal elements (Shin et al., 2020; Tan et al., 2021). It can not only guide scientific pollution quality and soil remediation, but also identify potential risk sources and guide the government in carrying out relevant work (Chen et al., 2012; Bian et al., 2021; Wang et al., 2021).

It is an effective means to solve the problem of rapid extraction of regional soil heavy metal information whether the spectrometer is equipped on satellite (Bian et al., 2021), aircraft (Wang et al., 2022), UAV (Chen et al., 2022), or handheld (Hou et al., 2019). The low efficiency and uncontrollable factors of traditional sampling analysis urgently require the intervention of new technologies (Banerjee et al., 2017; Guo et al., 2021). Future research on hyperspectral technology in the field of heavy metal content should focus on improving the universality of models, breaking through regional and temporal limitations, and achieving true practicality. By improving data collection and processing, model development and optimization, model generalization and transfer learning, as well as practical application and validation, research can promote the widespread application of hyperspectral technology in this field and bring greater value to environmental protection and agricultural management (Guo et al., 2021; Taghizadeh-Mehrjardi et al., 2021).

Our research has identified the transport patterns of heavy metals in terraced areas. The abundance of heavy metals in soil is limited by terraces; Topography feedbacks affects both the abundance and spatial distribution of heavy metal content; And heavy metals migrate from high-altitude terraces to low-altitude terraces, forming STS models, namely source state, transition state, and stable state are the highlights of this paper (Figure 8).

5 Conclusion

To our best knowledge, the present study quantifies the relationship between different geological terraces and the transport and enrichment of heavy metal elements in soil for the first time (Shi et al., 2018). In general, our findings have improved our understanding of the migration and accumulation of heavy metals in the process of mineral development and residents' life from the perspectives of topography, environment, chemistry, etc. (Lu et al., 2019; Wang et al., 2020; Agyeman et al., 2022). Although the slope and aspect are not enough to dominate the spatial distribution of heavy metal elements, different elevations determine the enrichment of heavy metal elements (Ou et al., 2021; Taghizadeh-Mehrjardi et al., 2021). We have accurately assessed the excess of heavy metals in the study area with reference to relevant national standards in order to assess the extent of this enrichment (Chen et al., 2012). The above conclusions were reached, and the time factor was not fully considered as only one period of data is available (Liu et al., 2021; Li B. et al., 2022). Further research is needed to assess

whether the accumulation of heavy metals in the soil changes in time and how to affect the soil ecosystem function of the terrace.

Data availability statement

The original contributions presented in the study are included in the article/supplementary material, further inquiries can be directed to the corresponding author.

Author contributions

YT: Conceptualization, Data curation, Formal Analysis, Investigation, Methodology, Software, Writing–original draft, Writing–review and editing. DZ: Conceptualization, Data curation, Formal Analysis, Funding acquisition, Investigation, Methodology, Project administration, Validation, Writing–original draft, Writing–review and editing. HX: Conceptualization, Data curation, Formal Analysis, Funding acquisition, Investigation, Methodology, Project administration, Validation, Writing–original draft, Writing–review and editing. LD: Formal Analysis, Investigation, Resources, Software, Validation, Writing–review and editing. QX: Methodology, Resources, Software, Writing–review and editing. ZZ: Methodology, Resources, Software, Writing–review and editing. XJ: Data curation, Formal Analysis, Investigation, Supervision, Writing–review and editing.

Funding

The author(s) declare financial support was received for the research, authorship, and/or publication of this article. This research was funded by the Survey of Land Quality in Western Hunan of China Geological Survey Geochemical (No. ZD20220214), the Science and Technology Innovation Fund of Command Center of Integrated Natural Resources Survey Center (No. KC20220013), the Comprehensive investigation on ecological restoration in the Huaihua Shaoyang area of southwestern Hunan (No. DD20230480), the Sichuan College of Architectural Technology Innovation Team (No. SCJYKYCXTD 2023), and the National Key Research and Development Program of China (No. 2022YFB3902000, No. 2022YFB3902001).

Acknowledgments

We would like to thank the editors and reviewers for their valuable opinions and suggestions that improved this research.

Conflict of interest

The authors declare that the research was conducted in the absence of any commercial or financial relationships that could be construed as a potential conflict of interest.

Publisher's note

References

Agyeman, P. C., Khosravi, V., Michael Kebonye, N., John, K., Borůvka, L., and Vašát, R. (2022). Using spectral indices and terrain attribute datasets and their combination in the prediction of cadmium content in agricultural soil. *Comput. Electron. Agric.* 198, 107077. doi:10.1016/j.compag.2022.107077

Banerjee, B. P., Raval, S., Zhai, H., and Cullen, P. J. (2017). Health condition assessment for vegetation exposed to heavy metal pollution through airborne hyperspectral data. *Environ. Monit. Assess.* 189, 604. doi:10.1007/s10661-017-6333-4

Ben Dor, E., Francos, N., Ogen, Y., and Banin, A. (2022). Aggregate size distribution of arid and semiarid laboratory soils (<2 mm) as predicted by VIS-NIR-SWIR spectroscopy. *Geoderma* 416, 115819. doi:10.1016/j.geoderma.2022.115819

Ben-Dor, E., Levin, N., Singer, A., Karnieli, A., Braun, O., and Kidron, G. J. (2006). Quantitative mapping of the soil rubification process on sand dunes using an airborne hyperspectral sensor. *Geoderma* 131, 1–21. doi:10.1016/j.geoderma.2005.02.011

Bian, Z., Sun, L., Tian, K., Liu, B., Zhang, X., Mao, Z., et al. (2021). Estimation of heavy metals in tailings and soils using hyperspectral technology: a case study in a tin-polymetallic mining area. *Bull. Environ. Contam. Toxicol.* 107, 1022–1031. doi:10.1007/s00128-021-03311-7

Bouzidi, W., Mezned, N., and Abdeljaoued, S. (2022). Mineralogical mapping using EO-1 Hyperion data for iron mine identification. *J. Appl. Rem. Sens.* 16. doi:10.1117/1.JRS.16.024514

Brossard, M., Marion, R., and Carrére, V. (2016). Deconvolution of SWIR reflectance spectra for automatic mineral identification in hyperspectral imaging. *Remote Sens. Lett.* 7, 581–590. doi:10.1080/2150704X.2016.1168946

Cai, Z., Lei, S., Zhao, Y., Gong, C., Wang, W., and Du, C. (2022). Spatial distribution and migration characteristics of heavy metals in grassland open-pit coal mine dump soil interface. *IJERPH* 19, 4441. doi:10.3390/ijerph19084441

Chen, H. W., Chen, C.-Y., Nguyen, K. L. P., Chen, B.-J., and Tsai, C.-H. (2022). Hyperspectral sensing of heavy metals in soil by integrating AI and UAV technology. *Environ. Monit. Assess.* 194, 518. doi:10.1007/s10661-022-10125-5

Chen, X., Lee, H., and Lee, M. (2019). Feasibility of using hyperspectral remote sensing for environmental heavy metal monitoring. *Int. Arch. Photogramm. Remote Sens. Spat. Inf. Sci.* XLII-3/W7, 1–4. doi:10.5194/isprs-archives-XLII-3-W7-1-2019

Chen, X., Yang, Y., Zhang, D., Li, X., Gao, Y., Zhang, L., et al. (2023). Response mechanism of leaf area index and main nutrient content in mangrove supported by hyperspectral data. *Forests* 14, 754. doi:10.3390/f14040754

Chen, Y., Liu, Y., Liu, Y., Lin, A., Kong, X., Liu, D., et al. (2012). Mapping of Cu and Pb contaminations in soil using combined geochemistry, topography, and remote sensing: a case study in the le'an river floodplain, China. *IJERPH* 9, 1874–1886. doi:10.3390/ijerph9051874

Demattê, J. A. M., Alves, M. R., Gallo, B. C., Fongaro, C. T., Souza, A. B. e., Romero, D. J., et al. (2015). Hyperspectral remote sensing as an alternative to estimate soil attributes. *Rev. CIÊNCIA AGRONÔMICA* 46. doi:10.5935/1806-6690.20150001

Dkhala, B., Mezned, N., Gomez, C., and Abdeljaouad, S. (2020). Hyperspectral field spectroscopy and SENTINEL-2 Multispectral data for minerals with high pollution potential content estimation and mapping. *Sci. Total Environ.* 740, 140160. doi:10.1016/j.scitotenv.2020.140160

Giniyatullin, K. G., Sahabiev, I. A., Smirnova, E. V., Urazmetov, I. A., Okunev, R. V., and Gordeeva, K. A. (2022). Digital mapping of indicators that determine the sorption properties of soils in relation to pollutants, according to remote sensing data of the Earth using machine learning. *Georesursy* 24, 84–92. doi:10.18599/grs.2022.1.8

Guo, F., Xu, Z., Ma, H., Liu, X., Tang, S., Yang, Z., et al. (2021). Estimating chromium concentration in arable soil based on the optimal principal components by hyperspectral data. *Ecol. Indic.* 133, 108400. doi:10.1016/j.ecolind.2021.108400

Han, A., Lu, X., Qing, S., Bao, Y., Bao, Y., Ma, Q., et al. (2021). Rapid determination of low heavy metal concentrations in grassland soils around mining using vis–NIR spectroscopy: a case study of inner Mongolia, China. *Sensors* 21, 3220. doi:10.3390/s21093220

Han, B., Yun, Y., Cui, Q., Peng, J., and Wang, L. (2022). Retrieval of heavy metal content in soil using GF-5 satellite images based on GA-XGBoost model. *Laser optoelectron. Prog.* 59, 1230001. doi:10.3788/LOP202259.1230001

Han L, L., Chang, S., Chen, R., Liu, Z., Zhao, Y., Li, R., et al. (2022). Monitoring soil mercury content based on hyperspectral data and machine learning methods. *J. Appl. Rem. Sens.* 16. doi:10.1117/1.JRS.16.024518

Harmel, T., Gilerson, A., Tonizzo, A., Chowdhary, J., Weidemann, A., Arnone, R., et al. (2012). Polarization impacts on the water-leaving radiance retrieval from above-water radiometric measurements. *Appl. Opt.* 51, 8324–8340. doi:10.1364/AO.51.008324

Hou, L., Li, X., and Li, F. (2019). Hyperspectral-based inversion of heavy metal content in the soil of coal mining areas. *J. Environ. Qual.* 48, 57–63. doi:10.2134/jeq2018.04.0130

Huang, J., Zhang, Q., and Guo, Y. (2022). "Effect of remote sensing image pixel decomposition on the spectral response of soil heavy metals," in *International conference on cognitive based information processing and applications (CIPA 2021) lecture notes on data engineering and communications technologies*. Editors B. J. Jansen, H. Liang, and J. Ye (Singapore: Springer Singapore), 182–193. doi:10.1007/978-981-16-5854-9_23

Jiji, G. W. (2021). A study on the analysis of heavy metal concentration using spectral mixture modelling approach and regression in Tirupur, India. *Earth Sci. Inf.* 14, 2077–2086. doi:10.1007/s12145-021-00678-3

Li, B., Li, C., Dong, C., Li, P., Ma, J., and Ye, D. (2022a). Mechanism of lead pollution detection in soil using terahertz spectrum. *Int. J. Environ. Sci. Technol.* 19, 7243–7250. doi:10.1007/s13762-021-03588-5

Li, N., Dong, X., Gan, F., and Zou, Z. (2021). "Extraction of soil mineral information based on hyperspectral image," in *Aopc 2021: optical spectroscopy and imaging*. Editors H. Zhao, J. Liu, L. Xu, and Y. Wang (Beijing, China: SPIE). doi:10.1117/12.2601998

Li, Y., Yang, K., Wu, B., Wang, S., Hou, Z., and Ding, X. (2022b). Identification of soil heavy metal pollution by constructing 2D plane using hyperspectral index. *Spectrochimica Acta Part A Mol. Biomol. Spectrosc.* 278, 121318. doi:10.1016/j.saa.2022.121318

Lin, N., Jiang, R., Li, G., Yang, Q., Li, D., and Yang, X. (2022). Estimating the heavy metal contents in farmland soil from hyperspectral images based on Stacked AdaBoost ensemble learning. *Ecol. Indic.* 143, 109330. doi:10.1016/j.ecolind.2022.109330

Liu, K., Zhao, D., Fang, J., Zhang, X., Zhang, Q., and Li, X. (2017). Estimation of heavy-metal contamination in soil using remote sensing spectroscopy and a statistical approach. *J. Indian Soc. Remote Sens.* 45, 805–813. doi:10.1007/s12524-016-0648-4

Liu, W., Yu, Q., Niu, T., Yang, L., and Liu, H. (2021). Inversion of soil heavy metal content based on spectral characteristics of peach trees. *Forests* 12, 1208. doi:10.3390/f12091208

Lu, Q., Wang, S., Bai, X., Liu, F., Wang, M., Wang, J., et al. (2019). Rapid inversion of heavy metal concentration in karst grain producing areas based on hyperspectral bands associated with soil components. *Microchem. J.* 148, 404–411. doi:10.1016/j.microc.2019.05.031

Mendes, W. de S., Demattê, J. A. M., Minasny, B., Silvero, N. E. Q., Bonfatti, B. R., Safanelli, J. L., et al. (2022). Free iron oxide content in tropical soils predicted by integrative digital mapping. *Soil Tillage Res.* 219, 105346. doi:10.1016/j.still.2022.105346

Meng, X., Bao, Y., Ye, Q., Liu, H., Zhang, X., Tang, H., et al. (2021). Soil organic matter prediction model with satellite hyperspectral image based on optimized denoising method. *Remote Sens.* 13, 2273. doi:10.3390/rs13122273

Mezned, N., Alayet, F., Dkhala, B., and Abdeljaouad, S. (2022). Field hyperspectral data and OLI8 multispectral imagery for heavy metal content prediction and mapping around an abandoned Pb–Zn mining site in northern Tunisia. *Heliyon* 8, e09712. doi:10.1016/j.heliyon.2022.e09712

Ou, D., Tan, K., Lai, J., Jia, X., Wang, X., Chen, Y., et al. (2021). Semi-supervised DNN regression on airborne hyperspectral imagery for improved spatial soil properties prediction. *Geoderma* 385, 114875. doi:10.1016/j.geoderma.2020.114875

Poppiel, R. R., Lacerda, M. P. C., Rizzo, R., Safanelli, J. L., Bonfatti, B. R., Silvero, N. E. Q., et al. (2020). Soil color and mineralogy mapping using proximal and remote sensing in midwest Brazil. *Remote Sens.* 12, 1197. doi:10.3390/rs12071197

Saidi, S., Ayoubi, S., Shirvani, M., Azizi, K., and Zeraatpisheh, M. (2022). Comparison of different machine learning methods for predicting cation exchange capacity using environmental and remote sensing data. *Sensors* 22, 6890. doi:10.3390/s22186890

Shi, T., Guo, L., Chen, Y., Wang, W., Shi, Z., Li, Q., et al. (2018). Proximal and remote sensing techniques for mapping of soil contamination with heavy metals. *Appl. Spectrosc. Rev.* 53, 783–805. doi:10.1080/05704928.2018.1442346

Shin, H., Yu, J., Wang, L., Jeong, Y., and Kim, J. (2020). Spectral interference of heavy metal contamination on spectral signals of moisture content for heavy metal contaminated soils. *IEEE Trans. Geosci. Remote Sens.* 58, 2266–2275. doi:10.1109/TGRS.2019.2946297

Taghizadeh-Mehrjardi, R., Fathizad, H., Ali Hakimzadeh Ardakani, M., Sodaiezadeh, H., Kerry, R., Heung, B., et al. (2021). Spatio-temporal analysis of heavy metals in arid soils at the catchment scale using digital soil assessment and a random forest model. *Remote Sens.* 13, 1698. doi:10.3390/rs13091698

Tan, K., Ma, W., Chen, L., Wang, H., Du, Q., Du, P., et al. (2021). Estimating the distribution trend of soil heavy metals in mining area from HyMap airborne hyperspectral imagery based on ensemble learning. *J. Hazard. Mater.* 401, 123288. doi:10.1016/j.jhazmat.2020.123288

Tong, X., Xie, H., Qiu, Y., Zhang, H., Song, L., Zhang, Y., et al. (2010). Quantitative monitoring of inland water using remote sensing of the upper reaches of the Huangpu River, China. *Int. J. Remote Sens.* 31, 2471–2492. doi:10.1080/01431160902994440

Wan, Y., Fan, Y., and Jin, M. (2021). Application of hyperspectral remote sensing for supplementary investigation of polymetallic deposits in Huaniushan ore region, northwestern China. *Sci. Rep.* 11, 440. doi:10.1038/s41598-020-79864-0

Wang, F., Gao, J., and Zha, Y. (2018). Hyperspectral sensing of heavy metals in soil and vegetation: feasibility and challenges. *ISPRS J. Photogrammetry Remote Sens.* 136, 73–84. doi:10.1016/j.isprsjprs.2017.12.003

Wang, S., Zhang, C., Zhan, Y., Zhang, Y., Lou, T., and Xue, F. (2020). Evaluation of ecological risk of heavy metals in watershed soils in the Daxia River Basin. *AIP Adv.* 10, 055109. doi:10.1063/5.0004869

Wang, X., Gong, C., Ji, T., Hu, Y., and Li, L. (2021). Inland water quality parameters retrieval based on the VIP-SPCA by hyperspectral remote sensing. *J. Appl. Remote Sens.* 15, 042609. doi:10.1117/1.JRS.15.042609

Wang, Y., Zhang, X., Sun, W., Wang, J., Ding, S., and Liu, S. (2022). Effects of hyperspectral data with different spectral resolutions on the estimation of soil heavy metal content: from ground-based and airborne data to satellite-simulated data. *Sci. Total Environ.* 838, 156129. doi:10.1016/j.scitotenv.2022.156129

Xu, S., Zhao, Y., Wang, M., and Shi, X. (2022). A comparison of machine learning algorithms for mapping soil iron parameters indicative of pedogenic processes by hyperspectral imaging of intact soil profiles. *Eur. J Soil Sci.* 73. doi:10.1111/ejss.13204

Xue, Y., Zou, B., Wen, Y., Tu, Y., and Xiong, L. (2020). Hyperspectral inversion of chromium content in soil using support vector machine combined with lab and field spectra. *Sustainability* 12, 4441. doi:10.3390/su12114441

Zhang, B., Guo, B., Zou, B., Wei, W., Lei, Y., and Li, T. (2022a). Retrieving soil heavy metals concentrations based on GaoFen-5 hyperspectral satellite image at an opencast coal mine, Inner Mongolia, China. *Environ. Pollut.* 300, 118981. doi:10.1016/j.envpol.2022.118981

Zhang, D., Zhang, L., Sun, X., Gao, Y., Lan, Z., Wang, Y., et al. (2022b). A new method for calculating water quality parameters by integrating space-ground hyperspectral data and spectral-*in situ* assay data. *Remote Sens.* 14, 3652. doi:10.3390/rs14153652

Zhang, D., Zhu, Z., Zhang, L., Sun, X., Zhang, Z., Zhang, W., et al. (2023). Response of industrial warm drainage to tide revealed by airborne and sea surface observations. *Remote Sens.* 15, 205. doi:10.3390/rs15010205

Zhao, H., Gan, S., Yuan, X., Hu, L., Wang, J., and Liu, S. (2022). Application of a fractional order differential to the hyperspectral inversion of soil iron oxide. *Agriculture* 12, 1163. doi:10.3390/agriculture12081163

Zhou, M., Zou, B., Tu, Y., Feng, H., He, C., Ma, X., et al. (2022). Spectral response feature bands extracted from near standard soil samples for estimating soil Pb in a mining area. *Geocarto Int.* 37, 13248–13267. doi:10.1080/10106049.2022.2076921

Zhou, W., Yang, H., Xie, L., Li, H., Huang, L., Zhao, Y., et al. (2021). Hyperspectral inversion of soil heavy metals in Three-River Source Region based on random forest model. *CATENA* 202, 105222. doi:10.1016/j.catena.2021.105222

frontiers | Frontiers in Environmental Science

TYPE Original Research
PUBLISHED 16 April 2024
DOI 10.3389/fenvs.2024.1381409

OPEN ACCESS

EDITED BY
Khandaker Rayhan Mahbub,
Primary Industries and Resources South Australia, Australia

REVIEWED BY
Richard K. Omole,
Obafemi Awolowo University, Nigeria
Edwin Hualpa Cutipa,
National University of San Marcos, Peru

*CORRESPONDENCE
Elsayed Said Mohamed,
salama55@mail.ru

RECEIVED 05 February 2024
ACCEPTED 02 April 2024
PUBLISHED 16 April 2024

CITATION
Mohamed ES, Jalhoum MEM, Hendawy E, El-Adly AM, Nawar S, Rebouh NY, Saleh A and Shokr MS (2024), Geospatial evaluation and bio-remediation of heavy metal-contaminated soils in arid zones.
Front. Environ. Sci. 12:1381409.
doi: 10.3389/fenvs.2024.1381409

Geospatial evaluation and bio-remediation of heavy metal-contaminated soils in arid zones

Elsayed Said Mohamed[1,2]*, Mohamed E. M. Jalhoum[1], Ehab Hendawy[1], Ahmed M. El-Adly[3], Said Nawar[4], Nazih Y. Rebouh[2], Ahmed Saleh[1] and Mohamed. S. Shokr[5]

[1]National Authority for Remote Sensing and Space Sciences, Cairo, Egypt, [2]Department of Environmental Management, Institute of Environmental Engineering (RUDN University), Moscow, Russia, [3]Botany and Microbiology Department, Faculty of Science, Al-Azhar University, Assiut, Egypt, [4]Soil and Water Department, Faculty of Agriculture, Suez Canal University, Ismailia, Egypt, [5]Soil and Water Department, Faculty of Agriculture, Tanta University, Tanta, Egypt

Introduction: Soil pollution directly impacts food quality and the lives of both humans and animals. The concentration of heavy metals in Egypt's drain-side soils is rising, which is detrimental to the quality of the soil and crops. The key to reducing the detrimental effects on the ecosystem is having accurate maps of the spatial distribution of heavy metals and the subsequent use of environmentally sustainable remediation approaches. The objective of this work is to assess soil contamination utilizing spatial mapping of heavy metals, determine contamination levels using Principal Component Analysis (PCA), and calculate both the contamination severity and the potential for bioremediation in the soils surrounding the main drain of Bahr El-Baqar. Furthermore, evaluating the capacity of microorganisms (bacteria, fungi, and "Actinomycetes) to degrade heavy elements in the soil.

Methodology: 146 soil sample locations were randomly selected near the Bahr El-Baqar drain to examine the degree of soil pollution Ordinary Kriging (OK), method was used to map and analyze the spatial distribution of soil contamination by seven heavy metals (Cr, Fe, Zn, Cd, Pb, As, and Ni). Modified contamination degree (mCd) and PCA were used to assess the research area's soil pollution levels. The process involved isolating, identifying, and classifying the microorganisms present in the soil of the study area. The study findings showed that variography suggested the Stable model effectively matched pH, SOM, and Cd values. Furthermore, the exponential model proved suitable for predicting Fe, Pb and Ni, while the spherical model was appropriate for Ni, Cr, and Zn.

Results: The study revealed three levels of contamination, with an extremely high degree (EHDC) affecting approximately 97.49% of the area. The EHDC exhibited average concentrations of heavy metals: 79.23 ± 17.81 for Cr, 20,014.08 ± 4545.91 for Fe, 201.31 ± 112.97 for Zn, 1.33 ± 1.37 for Cd, 40.96 ± 26.36 for Pb, 211.47 ± 13.96 for As, and 46.15 ± 9.72 for Ni. Isolation and identification of microorganisms showed a significant influence on the breakdown of both organic and inorganic pollutants in the environment. The study demonstrated exceptionally high removal efficiency for As and Cr, with a removal efficiency reached 100%, achieved by *Rhizopus oryzae*, *Pseudomonas aeruginosa*, and *Bacillus thuringiensis*.

Conclusion: This study has designated management zones for soil contamination by mapping soil pollutants, geo-identified them, and found potential microorganisms that could significantly reduce soil pollution levels.

KEYWORDS

wastewater, GIS, PCA, novel bioremediation, Nile Delta

1 Introduction

Soil plays a crucial role in supporting life on our planet. Approximately 95% of the world's food supply is generated from soil, which also offers additional benefits such as biomass production, safeguarding natural resources, and conserving biodiversity (Ferrira et al., 2022). The processes of soil degradation, because of industrial and agricultural activities, along with increasing urbanization, lead to a decline in soil functions and ecosystem services (Dubey et al., 2020; Hendawy et al., 2019). The heavy metals, such as Zn, Fe, Cu, Mo, and Mn, play essential roles in trace amounts for plants, animals, and microbes. However, an excessive concentration of heavy metals beyond the necessary minimum levels can be considered toxic and harmful to life, even though some are not required by plants. For instance, mercury (Hg), cadmium (Cd), and lead (Pb) are heavy metals that are not essential for living organisms. Therefore, the presence of these heavy metals can disrupt the life cycles of organisms (Alsabhan et al., 2022). Recent research indicates that toxic metal contamination is a significant issue that affects both rural and urban areas, having detrimental effects on ecosystem and environmental sustainability (El-Behairt et al., 2022). Soil contamination is a major global problem that endangers both human health and ecological health (Singh and Singh, 2020). Over the past two decades, Egypt's soils have been subjected to rising levels of soil contamination, which has reduced soil productivity and quality (Abdelrahman et al., 2019; Baroudy et al., 2020). Potentially toxic metals (PTMs) are harmful pollutants because they can cause death, and bio-accumulation, and are not easily degradable (Kumar et al., 2022). Pollution has an adverse effect on plants and soils, which makes it extremely dangerous for food security. This immediately eliminates the beneficial bacteria in the soil, lowers the amount of organic matter in the soil, makes the soil unusable for agriculture, and causes an imbalance in soil nutrients impacts plant growth and the way plants interact with microorganisms, which in turn impacts the soil's quality and crop yield (Ayilara et al., 2023). Inhibiting enzyme activity, competing with necessary cations, and creating oxidative stress are only a few of the ways that an excess of PTMs stresses the soil biota (Nowicka, 2022). Consequently, the entire life cycle of the plant, From the initial stage of seed germination to reaching maturity, the process is negatively impacted, resulting in decreased crop yields and compromised quality (Yang et al., 2021). Numerous food, feed, and forage plants, often referred to as hyperaccumulators, exhibit strong resistance to metal stress and can absorb excessive potentially toxic metals (PTMs), subsequently transporting them to their above-ground parts (Chen et al., 2022; Abuzaid et al., 2019). The main source of soil pollutants is anthropogenic activity. According to (Peña, 2022; Gautam et al., 2023), Both organic and inorganic contaminants can move to the soil components through various pathways, such as the application of fertilizers and pesticides, inadequate wastewater disposal, the usage of plastics, as well as the combustion of fossil fuels. Remediation is very difficult and expensive after these pollutants have gotten into the soil matrix. Additionally, through the food chain, they can offer serious health hazards. Analyzing the spatial distribution of PTM concentration is the first step in improving soil pollution assessment (Hammam et al., 2022). This approach identifies contaminated regions and is a crucial step in risk management (Wang et al., 2021). This has prompted the utilization of Geographic Information Systems (GIS) for the spatial distribution of potentially toxic metals (PTMs) in numerous soils all over the world (Zhen et al., 2019; Ahmed and Pandey, 2020; Gozukara, 2021). Kriging is a potent geo-statistical technique during the examination of soil property spatial distribution and the integration of data into raster maps through spatial interpolation. To determine the spatial structure of soil variables, variograms and related metrics (nugget, sill, and range) are essentially used (Shi and Wang, 2020; Abuzaid et al., 2022). This technique's fundamental application, ordinary kriging (OK), offers an accurate and optimal forecast (Golden et al., 2019). By using a variety of variograms, OK replicates spatial variability and provides a range of map outputs while reducing the variation of prediction errors (Dad and Shafiq, 2021). Numerous studies have been done so far to address the issue of soil contamination by creating workable risk assessment and remediation techniques. To solve this issue, researchers have investigated both biological and non-biological strategies. Various methods, including physical, chemical, and biological approaches, are available According to (Liu et al., 2018), physical approaches include physically removing, washing, encapsulating, and electro-kinetically extracting contaminants from soil. To immobilize and lower the bioavailability of contaminants, chemical techniques such as soil precipitation and solidification are used (Jiang et al., 2023). To eliminate or change pollutants into less hazardous species, biological techniques use plants and microorganisms. Because they may reduce pollutants without creating secondary contaminants and are more cost-effective than physical measures, biological solutions are regarded as the most promising of these strategies (Gustave et al., 2021). Bioaugmentation is a well-established method for remediating heavy metal contamination in the environment. It involves introducing native and external microorganisms capable of with-standing and mitigating the toxic effects of heavy metals (Hassan et al., 2019; Purwanti et al., 2020). Micro-organisms native to the contaminated soil are isolated and then re-introduced into the same contaminated soil (Purwanti et al., 2020). Fungi have emerged as a highly effective option for remedying heavy metal contamination due to their substantial biomass and adsorption capabilities. Additionally, they produce various extracellular metabolites, such as proteins and enzymes, and their biomass can serve as a valuable natural

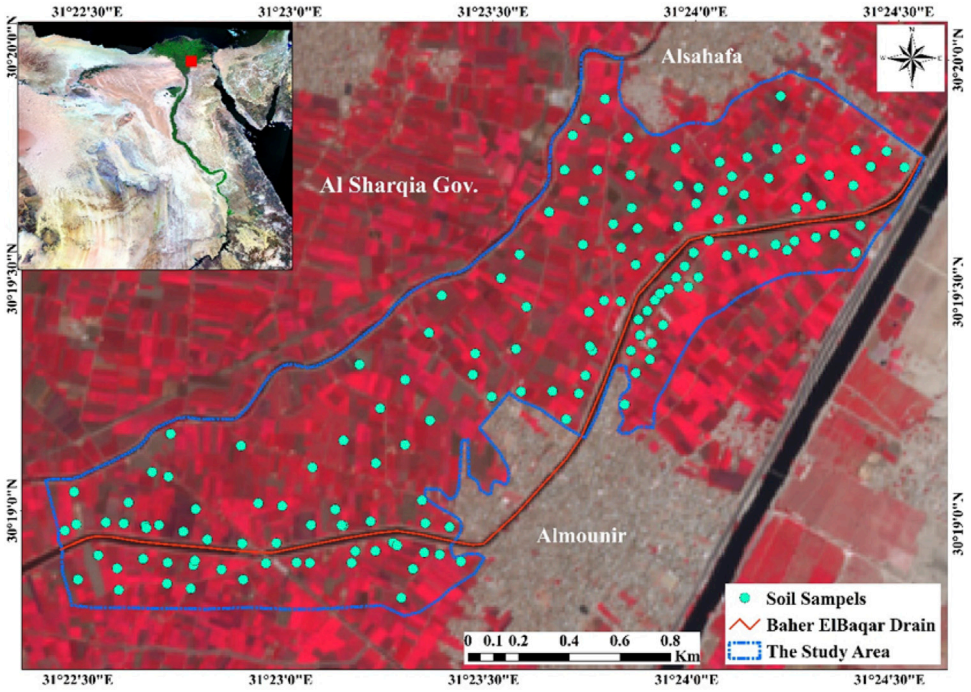

FIGURE 1
Location map of the study area.

resource for treating industrial effluents (Dell'Anno et al., 2022). Fungi contribute to the cleanup of heavy metal-contaminated environments through both metabolically active mechanisms like biomineralization, biotransformation, bioprecipitation, and bioaccumulation, as well as metabolically passive mechanisms such as biosorption (Goutam et al., 2021; Mohamadhasani and Rahimi, 2022). Abu-Elsaoud et al. (2017) observed that inoculation with an indigenous mycorrhizal fungus (Funneliformis geosporum) enhances soil quality and increases wheat yields, even in the presence of high concentrations of Zn, by reducing zinc accumulation in wheat plants. On the other hand, exogenous microorganisms are collected from locations external to the contaminated areas and introduced into the targeted contaminated area (Huang and Ye, 2020). Various processes used for remediating heavy metals with the help of microbes include biosorption, bioaccumulation, bio-chelation, bio-digestion, biomineralization, and biotransformation as described by (Girma, 2015). The selection of microorganisms depends on two main criteria: their ability to degrade the targeted pollutants and their capacity to endure and flourish in various environments. Microorganisms such as bacteria, fungi, yeast, actinomycetes, and algae exhibit resilience and adaptability across a wide range of conditions, allowing them to effectively eliminate heavy metals from polluted areas. This capability primarily arises from the composition of microbial cell walls, which consist of polysaccharides, lipids, and proteins. These components play a crucial role in binding metal ions through carboxylate, hydroxyl, amino, and phosphate groups, leading to the creation of non-toxic complex compounds according to (Girma, 2015; Huang and Ye, 2020; Nwaehiri et al., 2020; Purwanti et al., 2020). According to (Chabukdhara et al., 2017), *Candida spherica* has been identified as a producer of biosurfactants that exhibit high removal efficiencies, with removal rates of 95%, 90%, and 79% for iron (Fe), zinc (Zn), and lead (Pb), respectively. Furthermore, it has been discovered that C (Luna et al., 2016). Vulgaris biomass serves as an exceptionally effective biosorbent for the removal of cadmium (Cd^{2+}), copper (Cu^{2+}), and lead (Pb^{2+}) from a mixed solution containing 50 mg dm^{-3} of each metal ion. The removal efficiencies for these metals are notably high, reaching 95.5%, 97.7%, and 99.4%, respectively (Goher et al., 2016).

This research aims to generate a spatial distribution of soil heavy metals and determine contamination levels, in the soils surrounding Bahr El-Baqar drain. Additionally, discover novel enzymatic biodegrading agents produced by various microorganisms, which have the potential to extract heavy metals from the soil.

2 Materials and methods

2.1 Description of the research location

The investigated area is located south Al-shrkia Governorate adjacent Bahr El-Baqar's drain. The drain collects the wastewater from Sharqia Governorate's Belbeis and Qalubiya minor drains. El-Baqar's main drain. Figure 1, showed latitudes 30° 18′47.05″ N to 30° 20′0.64″ N, and longitudes 31° 22′25.03″ E to 31° 24′35.84″ E. The area covers 294.67 ha. Two primary sources of irrigation are employed: water from the Bahr al-Baqar drain and groundwater. As for the soil in this region, it is primarily characterized by clay to sandy texture. The crop patterns in the region varied between wheat and clover, as well as

tomatoes, strawberries, and peas. Sentinel-2A satellite data from October 2022 included a high-resolution image used to show the location of the study area.

2.2 Collecting of samples and lab analysis

Several 146 soil sample locations were randomly selected near the Bahr El-Baqar drain (Figure 1) to examine the degree of soil pollution. GPS has been used to keep track of each location's coordinates. This involved grinding the samples, air-drying them, and sieving them through a 2 mm. Subsequently, the samples were subjected to analysis for electrical conductivity (EC) in soil paste extracts, pH levels, and soil organic matter (SOM). To assess the concentrations of Cr, Fe, Zn, Cd, Pb, As, and Ni, the samples, the entire quantities of these metals were extracted according to the guidelines provided by the United States Environmental Protection Agency (USEPA). This extraction process, known as Method 3052, entails acid digestion with microwave assistance, utilizing concentrated HNO3, HF, and HCl. The metal concentrations were determined using Inductively Coupled Plasma Optical Emission Spectroscopy (Thermo ICP-MS type iCAP-RQ), and each measurement was conducted three times.

2.3 Statistical analysis

The application of PCA aids in the identification of pollution sources. The statistical software package SPSS 28.0 is utilized to determine the existence of variance explained by each significant component and the number of significant factors by extracting their eigenvalues from the correlation matrix. Before conducting Principal Component Analysis (PCA), the Kaiser-Meyer-Olkin (KMO) test was employed to assess the sample's suitability for each variable (Kaiser, 1960). The resulting z-scores were subjected to Pearson's correlation to investigate metal correlations in soils. The Kaiser-Meyer-Olkin measure of sample adequacy, Bartlett's test of sphericity, Varimax rotation, and principal component (PC) approach were used in the factor analysis of the correlation matrix to find possible metal sources. Absolute loading values greater than 0.75 were considered highly significant, values between 0.75 and 0.5 indicated a moderate association, and values falling in the range of 0.49 to 0.30 suggested a weak association with the principal component and the PCs with eigenvalues >1.0 were the only ones taken into consideration (Fan et al., 2019).

2.4 Kriging interpolation for studied variables

Utilizing the Kriging interpolation method, geostatistical studies were completed in ArcGIS 10.4 (36). The following semi-variogram models were employed with ordinary kriging (OK) (Eq. 1):

$$\gamma(h)\frac{1}{2N(H)}\sum_{\alpha=1}^{N(h)}[Z(X_\alpha+h)]^2 \quad (1)$$

Where, (h) (h) represents the semivariance at a specified lag distance "h," "N(h)" signifies the count of sample pairs at that particular lag distance, "Z (X_α)" denotes the value at a specific sample site, and "Z (X_α+h)" signifies the value at a sample site located at a distance "h" from the original location.

To establish spatial variation parameters, including the nugget (C0), partial sill (C), sill (C0 + C), and range (a), experimental semi-variograms are fitted using various models through the least square method. The nugget, which characterizes short-range variability, corresponds to the semi-variogram at a lag distance of zero. The sill, indicative of the overall sample variability, is the point at which the model flattens out. Range refers to the lag distance at which the sill is encountered (Goenster-Jordan et al., 2018). To evaluate the accuracy and effectiveness of OK models, the study utilized the cross-validation technique, considering predictive errors such as mean error (ME), root mean square error (RMSE), mean standardized error (MSE), root mean square standardized error (RMSSE), and average standard error (ASE). Model selection was determined based on the following criteria: the lowest ME and MSE (approaching zero), identical RMSE and ASE values, and an RMSSE value close to one, indicating the most suitable model (Mallik et al., 2020; Sebei et al., 2020). These errors' mathematical expressions are as follows (Eqs 2–4):

$$\mathrm{MSE}=\frac{1}{n}\sum_{i=1}^{n}[x_i-y_i] \quad (2)$$

$$\mathrm{RMSE}=\sqrt{\frac{1}{n}\sum_{i=1}^{n}[x_i-y_i]^2} \quad (3)$$

$$\mathrm{RMSE}=\sqrt{\frac{1}{n}\sum_{i=1}^{n}[x_i-y_i]^2\Big/\sigma M(yi)} \quad (4)$$

In this context, "n" signifies the count of predicted values within a cluster of nearby soil samples, while "x_i" and "y_ denote the actual and predicted values, respectively. Additionally, "σM" stands for the standardized error of the predicted values.

2.5 Contamination factor (CF) and the modified degree of contamination (mCd)

According to (Håkanson, 1980), the contamination factor (CF) serves as a measure to express the degree of contamination. This CF ratio is computed by dividing the concentration of each metal in the sediment by its corresponding background value. To assess the overall contamination of various heavy metals in each soil sample, a modified degree of contamination (mCd) was employed, as developed by (Abrahim and Parker, 2008; Cheng et al., 2015). The calculation of mCd involves the use of the following formulas (Eq. 5):

$$mCd=\sum\frac{CF}{n} \quad (5)$$

n is number of studied elements.

The terms used to categorize the mCd are as follows:

mCd <1.5: Indicates negligible to very minimal contamination.

1.5 ≤ mCd <2: Implies a low level of contamination.

2 ≤ mCd <4: Signifies a moderate level of contamination.

4 ≤ mCd <8: Represents a substantial degree of contamination.

TABLE 1 Statistics of studies variables and recommended values of heavy metal concentrations for 146 samples.

Variable	Minimum	Maximum	Mean	Stander deviation	Average upper earth crust, after wedepohl (1995) mg kg^{-1}
Cr (mg kg^{-1})	28.6	146.6	77.3	18.55	35
Fe (mg kg^{-1})	6468.17	38526.67	19565.15	4751.74	30890
Zn (mg kg^{-1})	51.31	931.22	191.56	112.23	52
Cd (mg kg^{-1})	0.24	25.46	1.48	2.52	0.1
Pb (mg kg^{-1})	11.47	203.87	40.80	29.26	17
AS (mg kg^{-1})	164.93	267.54	208.78	15.84	2
Ni (mg kg^{-1})	21.29	82.14	45.39	10.04	18.6
PH	6.20	8.41	7.69	0.36	
O.M (%)	0.21	0.88	0.45	0.13	
EC (dS m^{-1})	0.14	8.05	1.33	2.32	

8 ≤ mCd <16: Reflects an exceptionally high degree of contamination.

16 ≤ mCd <32: Points to an extraordinarily high degree of contamination.

mCd ≥32: Corresponds to an extremely high level of contamination.

2.6 Isolation and grouping of microorganisms

2.6.1 Isolation

To extract microorganisms from soil samples, we initiated the process by combining precisely 10 g of soil with 90 mL of deionized water. For isolating bacteria, actinomycetes and fungi from effluent samples, we diluted 10 mL of the effluent with 90 mL of deionized water. Next, the mixture underwent vigorous shaking using an automated orbital shaker (Searchtech Nig Ltd.) at 180 rpm for 3 h. Subsequently, the resulting suspension underwent ten-fold serial dilution. Subsequently, we aseptically dispensed 0.1 mL aliquots from each of these dilutions (10^{-2}, 10^{-3}, 10^{-4}, or 10^{-5}) onto nutrient agar, starch nitrate agar and potato dextrose agar plates (for bacteria, actinomycetes and fungi, respectively) using the spread plate technique. These plates were incubated at 38°C for 24 h (for bacteria) and incubated at 28°C for 3–7 days (for actinomycetes and fungi) in an incubator. After the incubation period, the colonies that developed were sub-cultured to obtain pure samples for subsequent identification and grouping.

2.6.2 Grouping

Bacterial and actinomyctes isolates underwent meticulous identification through the assessment of their biochemical, physiological, and morphological traits, including detailed examination of colony morphology and the use of staining techniques. Following Bargey's manual, this comprehensive approach facilitated precise characterization of bacterial species and actinomycetes. In contrast, fungal isolates were primarily identified using morphological methods, which involved observations of colony and microscopic morphology. Through careful scrutiny of these characteristics, fungal species were accurately distinguished and classified.

2.7 Microbial bioremediation of soil heavy metal

The evaluation of microbial remediation of heavy metals in soil employed a precise microbial culture technique. Initially, a targeted microorganism was introduced into heavily polluted soil. Subsequently, the soil underwent incubation under controlled conditions: 38°C for 48 h to facilitate bacterial activity and 28°C for 96 h to support fungal and actinomycetes growth. Following the incubation period, the concentration of remaining heavy metals was quantified using a spectrophotometer and compared against pre-injection levels. To ascertain the concentration of unabsorbed metal ions and gauge the effectiveness of microbial restoration, an atomic absorption spectrophotometer was employed. This methodological approach allowed for a thorough assessment of how microbial activity influenced the remediation of heavy metal contamination in soil, shedding light on the efficacy of bacterial and fungal processes in metal ion absorption and retention.

2.8 The percentage of heavy metal bioremediation

The determination of heavy metal loss percentage and bioaccumulation factor adhered to the methodology outlined by Akhtar et al. (2013). Calculating the reduction in heavy metal content involved subtracting the initial concentration of heavy metals (measured at 0 h) from the final concentration (measured after 96 h). To assess the impact of microorganisms on heavy metal reduction, the amount of metal lost in a medium

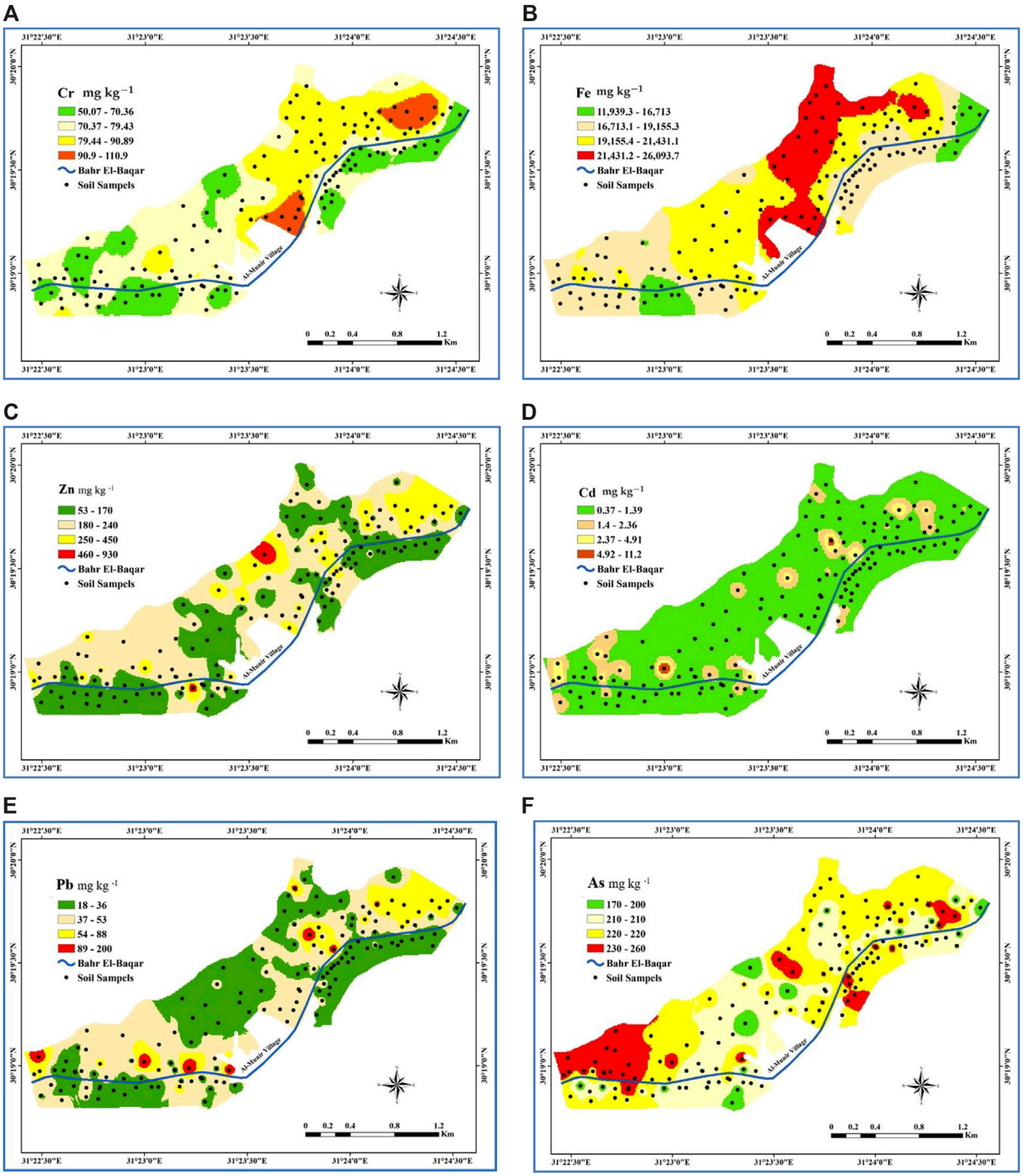

FIGURE 2
(Continued).

with microorganisms was compared to that in a medium lacking microorganisms. The bioaccumulation factor was calculated as the ratio of heavy metal content within the microorganism to the heavy metal content in the medium after 96 h. This comprehensive analysis provided insight into the efficacy of microbial activity in mitigating heavy metal contamination and elucidated the role of microorganisms in metal accumulation processes.

3 Results and discussion

3.1 Soil characteristics and heavy metals

Wastewater from urban areas, agricultural fields, and industrial facilities flows into the Bahr El-Baqar drain, resulting in soil contamination since this irrigation water source is low in the area. The total volume of drainage water in the Bahr El-Baqar

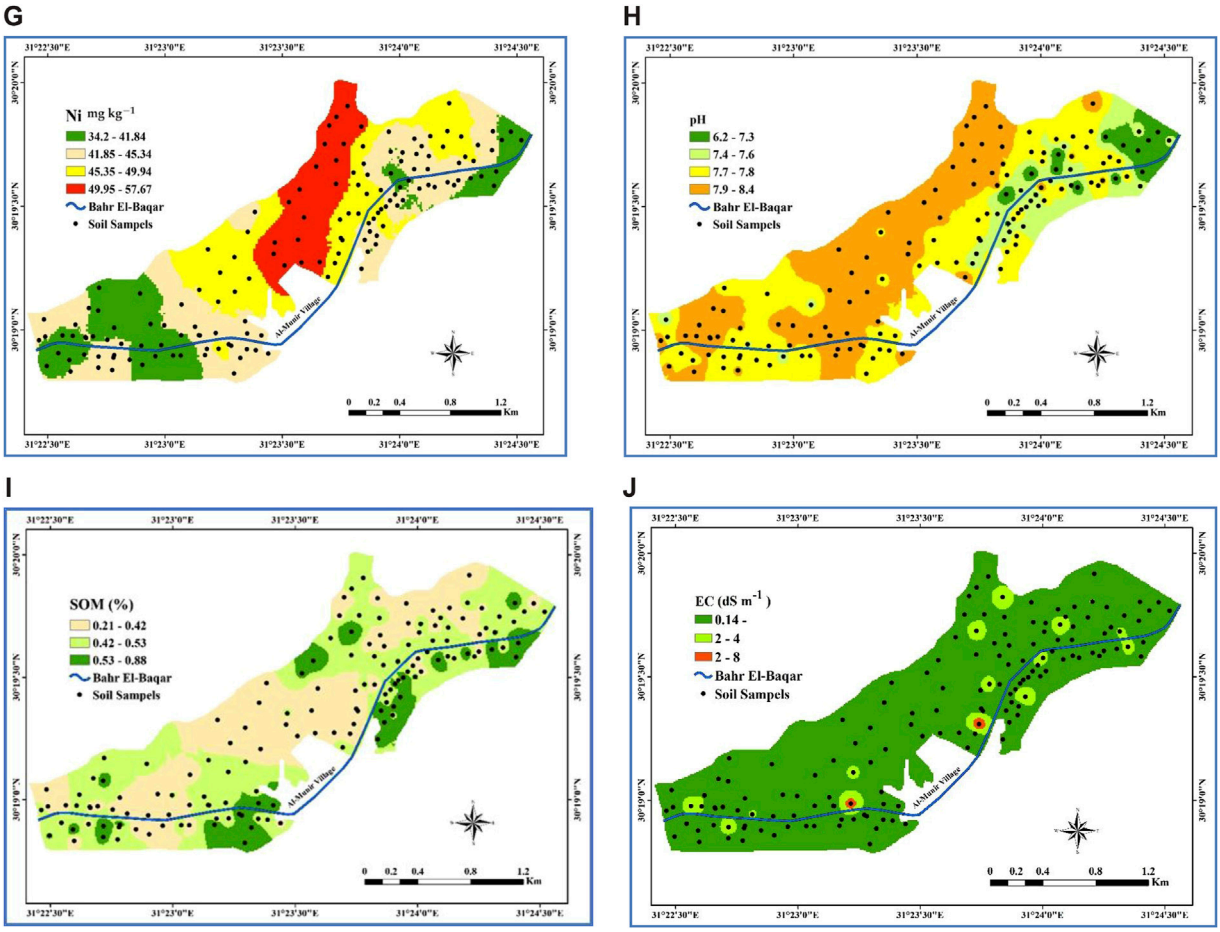

FIGURE 2
(Continued). Ordinary kriging maps of soil properties and heavy metals total concentrations; **(A)** is spatial distribution of Cr (mg kg^{-1}), **(B)** is spatial distribution of Fe (mg kg^{-1}), **(C)** is spatial distribution of Zn (mg kg^{-1}), **(D)** is spatial distribution of Cd (mg kg^{-1}), **(E)** is spatial distribution of Pb (mg kg^{-1}), **(F)** is spatial distribution of As (mg kg^{-1}), **(G)** is spatial distribution of Ni (mg kg^{-1}), **(H)** is spatial distribution of pH, **(I)** is spatial distribution of SOM (%), and **(J)** is spatial distribution of EC (dS m^{-1}).

drain is mixed by 40%, industrial sources contribute 2%, and agricultural sources contribute 58%, according to data from (Saad, 1997; El-Bady, 2014; Nawar et al., 2023). In total, the wastewater discharged into the Bahr El-Baqar drain amounts to 2,049,030 m^3 day^{-1} (El-Bady, 2014). Table 1 provides descriptive analysis data for the soil heavy metals: Cr, Fe, Zn, Cd, Pb, As, and Ni that were studied. The total content of chromium varied from 28.61 to 146.45, with an average of 77.29 ± 18.55 mg kg^{-1}. The average content of iron was 19565.15 ± 4751.74 mg kg^{-1}, varying from 6468.17 to 38526.67. The average total zinc concentration was 191.56 ± 112.231 mg kg^{-1}, with a range varying from 51.31 to 931.22. The average total cadmium content is 1.48 ± 2.52 mg kg^{-1}. Pb, As, and Ni total concentrations were 11.47–203.87, 164.933–267.544, and 21.296–82.143 mg kg^{-1}, respectively. Except for Fe, all means of the heavy metals under study were greater than background values (Wedepohl, 1995) (Table 1). All environmental media contain chromium, which is an element Referring to elements and minerals inherently occurring in the Earth's crust. Although human activity releases significantly bigger amounts of chromium Releasing it into the atmosphere, the flow of continental dust. Is the main natural source (Mohamed et al., 2023). The research area's typical Fe content is lower than that of the upper earth crust on average (Wedepohl, 1995) (Table 1). Although humans and plants both need zinc, excessive amounts of the metal can be dangerous (Swartjes, 2011). Hence, it is vital to regulate the correct quantity in agricultural soils. It could cause problems with the immune system and digestive tract, among other immediate and detrimental effects. Furthermore, high zinc levels might hinder the absorption of copper, resulting in symptoms of copper deficiency (Swartjes, 2011).

The widespread use of herbicides, phosphate fertilizers, and sewage sludge has been linked to soil contamination with cadmium (Cd), as discussed in (Khan et al., 2021). Considering that a substantial portion of this cadmium enters the human body via food sources that accumulate it from the soil, it becomes crucial to establish soil protection measures to preserve or enhance the existing conditions. This may include measures like restricting the use of phosphorus fertilizers with high cadmium content to prevent further contamination. While ingestion of dust and soil can also result in Pb exposure, the food chain is the main cause of exposure (Abuzaid et al., 2019). Even at relatively low lead levels, lead (Pb) can cause damage to the brain and nervous system, particularly in youngsters. As a result, a comprehensive

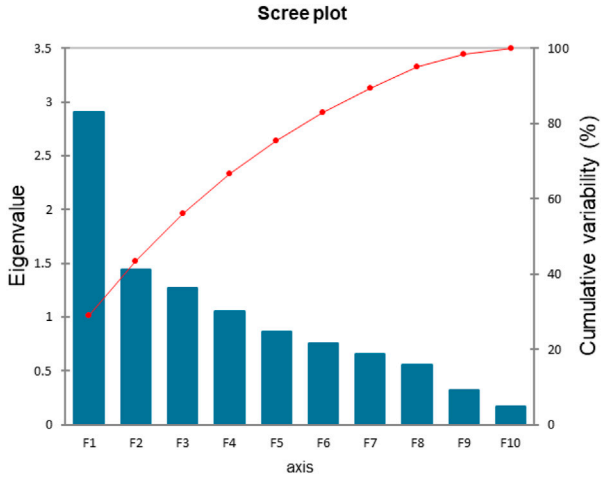

FIGURE 3
Scree plot for eigenvalue and cumulative variability (%) of PCAs.

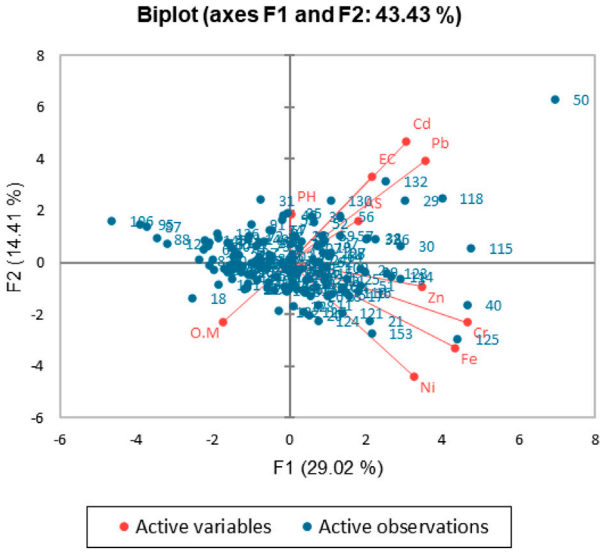

FIGURE 4
Biplot of Principal component.

assessment of the risk posed by lead in topsoil is required. Clayey soils are expected to contain higher concentrations of arsenic, which is generally believed to have a geological origin. But there's a lot of anthropogenic arsenic pollution because there are more man-made than natural sources of arsenic released into the environment (ATSDR, 2000). In addition, the primary sources of soil nickel (Ni) contamination stem from industries involved in metal plating, fossil fuel utilization, nickel mining, and electroplating. Besides, these human-induced origins, phosphate-based agricultural fertilizers, atmospheric deposition, inorganic fertilizers, sewage sludge, and various waste materials are used as soil amendments, adding to the potential sources of soil contamination (Wuana and Okieimen, 2011; Mcgrath, 1995; Parth et al., 2011; Senesi et al., 1999; Luo et al., 2009). On the other hand, soil pH plays a crucial role in influencing nutrient availability to plant roots, biological activity under varying soil conditions, and the activity of enzymes (Nicholson et al., 2003; Neina, 2019). The pH contents varied between 6.20 and 8.40. The EC values across the study area exhibited significant variability, with an average of 1.33 ± 2.32 dS m^{-1}, ranging from 0.14 to 8.05 dS m^{-1}. The elevated EC levels observed in certain parts of the study region could be attributed to the high salinity of the groundwater. Arid regions, in particular, are known for typical phenomena such as soil salinization and alteration (Stavi et al., 2021). The long-term process of land salinization and sodification jeopardizes both agricultural crop productivity and environmental sustainability (Singh, 2015; Ivushkin et al., 2019; Jamil et al., 2021; Shrivastava and Kumar 2021).

3.2 Mapping and variography analysis

The variography as represented in Supplementary Table S1 showed that, pH, SOM, and Cd values were all fitted by the Stable model. Six properties were properly mapped by both the exponential and spherical models: Cr, Zn, and As for the spherical, and Fe, Pb, and Ni for the exponential. The nugget-to-sill ratio was employed to evaluate the spatial relationships. Dependency (SDC). If this ratio is less than 0.25, between 0.25 and 0.75, or more than 0.75, the SDC is considered strong, moderate, or weak (Cambardella et al., 1994). The nugget-to-sill ratio of all the models' parameters ranged from 0 to 0.70. Furthermore, all models exhibited a substantial spatial dependence (SDC) ranging from moderate to strong predictions, according to the data. In Figure 2, it is evident that the northern regions of the study area displayed the most elevated levels of heavy metal concentrations. According to the geographical distribution maps of those metals that were analyzed. These sites are near urban areas, where various forms of pollution affect drainage systems and irrigation channels (Mohamed et al., 2023). For every parameter that was chosen, the MSE values were nearly equal to zero, but the RMSSE values were nearly equal to one. Nevertheless, ASE levels were low in every model that was produced.

3.3 Interpretation of PCA

There is positive correlation between studied metals. A shared origin could be suggested by the metals' extremely positive connection (Nazzal et al., 2015). SOM had a negative association with each of the variables, regardless of the strength of the connection. The overall concentrations of Cr, Fe, Cd, and Pb showed strong positive relationships with soil EC. Soil pH had a negative connection with every element (except from Fe and Cd), regardless of the strength of the correlation (Supplementary Table S2).

The soil sample was considered suitable based on a KMO value of 0.59. which was more than 0.5 (Said et al., 2020; Shokr et al., 2022). With 146 observations and 10 variables, a PCA may be produced. Due to their eigenvalues being greater than 1, the first three Principal Components (PCs) were employed by Kaiser's (Kaiser, 1960) technique, whereas the remaining PCs were disregarded (Supplementary Table S3; Figure 3). According to the findings, 56.45% of the variance can be explained by the first three

10.3389/fenvs.2024.1381409

TABLE 2 Quantitative analysis of clusters.

Variable		N	Mean	Std. Deviation	Std. Error	Minimum	Maximum
Cr	I	79	87.45 a	15.86962	1.78547	56.44	146.45
	II	63	63.29 b	11.11115	1.39987	28.62	86.47
	III	4	97.19 a	13.15226	6.57613	84.92	112.55
Fe	I	79	22174.33 a	4064.30978	457.27058	14030.57	38526.68
	II	63	16038.63 b	2866.46467	361.14060	6468.17	21237.00
	III	4	23576.46 a	5489.71786	2744.85893	17958.21	30332.33
Zn	I	79	233.50 a	130.64351	14.69854	95.14	931.22
	II	63	136.68 b	50.24626	6.33043	51.32	263.94
	III	4	227.78 a	39.19313	19.59657	188.20	266.26
Cd	I	79	1.70 b	2.95116	.33203	.24	25.47
	II	63	.816 b	.49260	.06206	.24	2.85
	III	4	7.7483 a	3.60290	1.80145	2.67	11.06
Pb	I	79	45.15 b	25.82091	2.90508	17.43	154.02
	II	63	28.34 b	9.70198	1.22233	11.47	66.99
	III	4	151.24 a	45.76228	22.88114	100.40	203.87
As	I	79	212.00 a	13.89635	1.56346	180.48	247.34
	II	63	205.09 a	17.71148	2.23144	164.93	267.54
	III	4	203.31- a	5.92183	2.96091	198.09	209.62
Ni	I	79	49.69 a	10.17595	1.14488	32.67	82.14
	II	63	39.55 b	6.31078	.79508	21.30	53.55
	III	4	52.30 a	9.53346	4.76673	44.13	65.34
pH	I	79	7.71 a	.32307	.03635	6.74	8.41
	II	63	7.6 a	.41393	.05215	6.20	8.23
	III	4	7.72 a	.23424	.11712	7.40	7.90
OM	I	79	.43 a	.11465	.01290	.21	.78
	II	63	.49 a	.15231	.01919	.29	.88
	III	4	.40 a	.05164	.02582	.34	.46
EC	I	79	1.36 a	2.36858	.26649	.14	8.05
	II	63	1.18 a	2.18988	.27590	.18	7.98
	III	4	3.10 a	3.41476	1.70738	.48	7.80

PCs. The first PC1, responsible for 29.02% of the overall variance, demonstrates more pronounced positive correlations with Cr, Fe, Zn, Pb, As, and Ni, as indicated by the factor loadings. In contrast, the second PC2, which accounts for 14.41% of the total variance, is notably linked with pH and EC. Additionally, the PC3, correlated with SOM, contributes to 12.74% of the overall variance. The PCA displays the PC scores of the samples and the variable loadings.

Figure 4 showed, the principal component analysis biplot of F1 (29.02%) and F2 (14.41%), rescaling the loadings plot and score plot to present them together on a single plot. The variables are depicted as arrows in the biplot arrows in the biplot, and the cosine of the angle formed by the arrows between each pair of variables determines the correlation between them. The correlation between variables is stronger when the angle between each pair of arrows is narrower (Smith et al., 2002). A variable like SOM, though, was correlated negatively with other variables and was connected to them at a nearly 180° angle (Suárez et al., 2016).

3.4 Cluster analysis

When compared to other clusters, the observations in this cluster are similar to one another (Jain and Dubes, 1988; Penkova, 2017). In this study, Agglomerative Hierarchical

TABLE 3 Classes of contamination entire investigated area.

Classes	Cr (mg kg^{-1})	Fe (mg kg^{-1})	Zn (mg kg^{-1})	Cd (mg kg^{-1})	Pb (mg kg^{-1})	As (mg kg^{-1})	Ni (mg kg^{-1})	Area (hectare)	%
VHDC	89.18 ± 2.14	24489.07 ± 1448.61	301.89 ± 50.38	18.26 ± 10.19	162.94 ± 12.62	215.03 ± 23.95	55.73 ± 3.38	6.05	2.05
EHDC	79.23 ± 17.81	20014.08 ± 4545.91	201.31 ± 112.97	1.33 ± 1.37	40.96 ± 26.36	211.47 ± 13.96	46.15 ± 9.72	287.4	97.49
UHDC	59.07 ± 15.98	15047.86 ± 4192.95	93.04 ± 23.87	0.57 ± 0.27	23.23 ± 6.74	184.93 ± 9.83	37.51 ± 9.64	1.35	0.46

Note: VHDC, stands for a very high degree of contamination, EHDC, represents an extremely high degree of contamination, and UHDC, corresponds to an ultra-high degree of contamination. Positive values indicate significant differences between pairs of means.

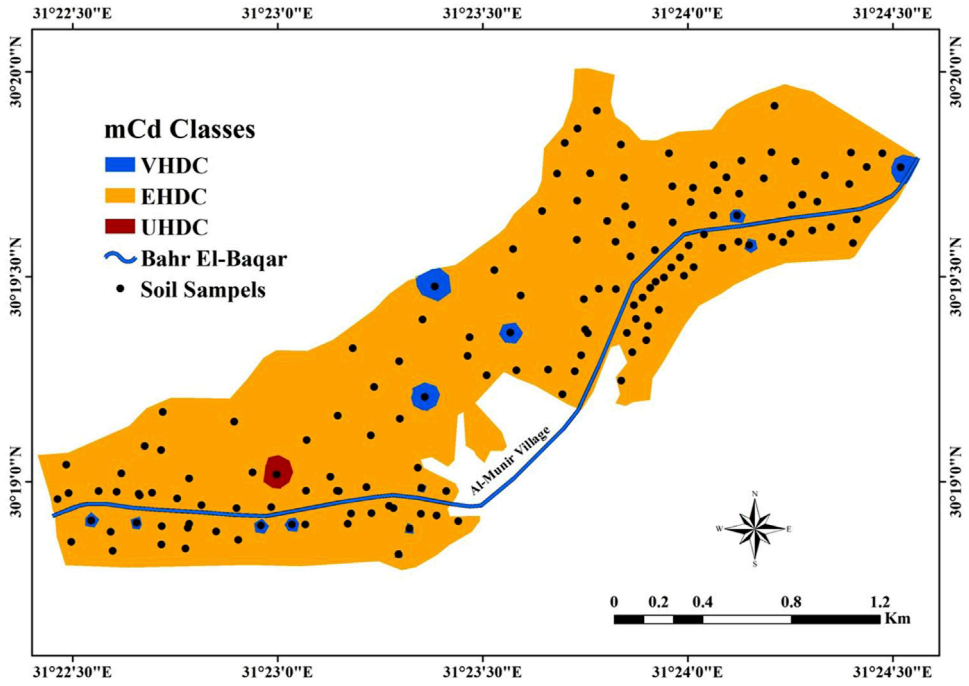

FIGURE 5
Spatial distribution of mCd.

Clustering (AHC) was employed to categorize the data into three distinct clusters (Supplementary Figure S1). The dendrogram shown in Supplementary Figure S1 illustrates the distinctions among the three clusters., with each cluster possessing unique attributes. According to descriptive data presented in Table 2, there are 79 observations in the first cluster, 63 in the second, and 4 in the third. Except for As, the acquired data demonstrated significant differences on all heavy metals between the three clusters. However, there were no appreciable variations in pH, EC, or SOM between the three clusters. Data from soil types affected by heavy metals in El-Minia Governorate, Egypt, were successfully subjected to clustering analysis (Hammam et al., 2022).

3.5 Modified degree of contamination (mCd)

Table 3 and Figure 5 illustrate, there were three classifications of pollution in the research region. Most of the investigated region (97.49%) was EHDC, with average concentrations of heavy metals to this degree being 79.23 ± 17.81, 20014.08 ± 4545.91, 201.31 ± 112.97, 1.33 ± 1.37, 40.96 ± 26.36, 211.47 ± 13.96, and46.15 ± 9.72 for Cr, Fe, Zn, Cd, Pb, As, and Ni, respectively. Numerous forms of pollution are brought about by human activity in this field of study, including contamination from irrigation water sources and agricultural management (Mohmed et al., 2023). Moreover, the extremely high degree only occupies 0.46 percent of the whole area.

3.6 Isolation and identification of bacteria

The results showed that a total of 13 bacterial isolates were successfully obtained from contaminated soil samples as follows: 4 isolates from the soil irrigated with fresh water, 3 from soil irrigated with sewage water, 4 from soil irrigated with artesian water, and 2 from the sediment in-depth sewage (refer to Supplementary Table S4). These isolated bacteria were categorized into nine phenotypes based on their characteristics, such as colony shape, Gram stain, spore formation, presence of

TABLE 4 Determination of the highest heavy metal removal efficiency (%) related to the most potent microorganism.

Heavy metal	High removal efficiency (%)of heavy metal	Microbial species
Cd	93	*Rhizopus oryzae*
As	100	*Rhizopus oryzae, Pseudomonas aeurginosa*
Zn	84	*Actioplanes* sp.
Pb	72	*Aspergillus fumigatus*
Cr	100	*Rhizopus oryzae, Bacillus thuringeinsis*
Ni	56	*Aspergillus versicolor*
Fe	90	*Streptomyces* sp.

capsules, oxygen requirements, and motility. Besides their morphological, biochemical, and physiological traits. The results showed a nine bacterial species were identified as: Enterobacter *cloacae, Bacillus cereus, Bacillus thuringeinsis, Pseudomonas aeurginosa, Pseudomonas veronii, Klebsiella pneumonia, E. coli, Staphylococcus aureaus, Staphylococcus saprophyticus*.

3.7 Isolation and identification of fungi

The findings indicated that a total of 7 fungal isolates were successfully acquired from the contaminated soil samples. These isolates were distributed as follows: 3 isolates from soil irrigated with fresh water, 2 isolates from soil irrigated with sewage water, and 2 isolates from soil irrigated with artesian water (refer to Supplementary Table S4). Based on their morphological and cultural characteristics, the isolated fungi were categorized into three fungal species: Aspergillus fumigatus, Aspergillus versicolor, and Rhizopus oryzae (as shown in Supplementary Figure S2). The results obtained regarding the impact of fungi on soil pollutants align with prior research, confirming a negative correlation between cadmium and the abundance of both bacteria and fungi. Conversely, a positive correlation was observed between fungi and zinc. The influence of soil properties on fungal diversity was also evident. Therefore, it can be concluded that significant variations exist in the soil characteristics within this region. (Alsabhan et al., 2022; Sahu et al., 2023).

3.8 Isolation and identification of actinomycetes

The results of actinomycete isolates revealed that a total of 9 isolates were successfully collected from the contaminated soil. These isolates were distributed as follows: 5 isolates from soil irrigated with sewage water, 1 isolate from soil irrigated with artesian water, and 3 isolates from sediments in deep sewage (refer to Supplementary Table S4). These isolates were categorized into four phenotypes based on characteristics such as colony shape, Gram stain, spore formation, presence of capsules, oxygen requirements, and motility. Additionally, the morphological, biochemical, and physiological characteristics as follow: *Streptomyces* sp., *Actioplanes* sp., *Sporichthya* sp. *And Actinomyces sp*. The findings indicated that *Actioplanes sp*. Is efficacious in reducing the levels of various heavy metals, including Cr, Zn, Fe, As, Cd, and Ni. Moreover, incorporating actinomycetes into the system enhances the complexity of the microbial network structure and strengthens the stability of the microecology around the plant's roots. Additionally, the combined application of soil amendments and actinomycetes can promote plant growth (Hamid et al., 2021; Xu et al., 2023).

3.9 Microbial remediation of heavy metals

Many studies confirm that biological methods are effective in treating pollution. They have demonstrated that microorganisms, including bacteria, fungi, and algae, can remediate environments contaminated with heavy metals (Neboht et al., 2013; Kim et al., 2015). Among all microorganisms isolated in our study, *Rhizopus oryzae and Actioplanes sp*. showed highest removal for 5 different heavy metal, followed by *Enterobacter cloacae* and *P. veronii* showed removal for 4 different heavy metal, while *E. coli*, *Staphylococcus aureaus* and *Actinomyces sp*. Do not have any effect on one of heavy metal bioremediation as illustrated in Supplementary Table S4. Conversely, numerous microbial species, such as bacteria and fungi found in *Bacillus*, *Pseudomonas*, *Streptomyces*, Aspergillus, and Penicillium, possess substantial removal capabilities (Tastan et al., 2010; Dasola et al., 2014; Wierzba- 2015). *Escherichia coli* K-12 exhibits the broadest capacity for absorbing various metal ions, with its outer membrane capable of absorbing over 30 different types of metal ions (Dermont et al., 2008). Rhizopus can uptake heavy metal ions such as Zn, Cu, Cd, and Pb, among others. This finding is consistent with (Abd-Alla et al., 2012) *Thiobacillus* can assimilate heavy metal ions, along with inorganic ions like sulfur (S), resulting in the formation of a precipitate when combined with metal ions, which can be subsequently separated from the soil (Leusch et al., 1995).

3.9.1 Percentage of heavy metal bioremediation

As presented in Table 4, the highest removal efficiency for heavy metals, such as and Cr, reaching 100%, was achieved by *R. oryzae*, *Pseudomonas aeruginosa*, and *Bacillus* thuringiensis. On the other hand, the lowest removal efficiency, 56%, was observed for the heavy metal Ni, and this was recorded for Aspergillus versicolor. These results demonstrate the remarkable efficacy of Rhizopus oryzae, *P. aeruginosa*, and *Bacillus* thuringiensis in removing heavy metals, particularly As and Cr, while highlighting the need for further investigation and optimization when dealing with Ni removal by Aspergillus versicolor (Luna et al., 2016).

4 Conclusion

This study proved that variography Analysis models are a useful tool for forecasting the heavy metals' spatial distribution maps in the investigated area. Additionally, the fusion of AHC and PCA produced unique classification of the study region into three zones, each with distinct characteristics from one another in terms of heavy metal content and pattern. In addition, we looked at the potential of actinomycetes, fungi, and bacteria as microorganisms to lessen the consequences of different types of soil pollution. To carry out the process, the microorganisms found in the core of the study soil had to be isolated, identified, and classified. The study area was divided into three pollutant categories. The majority of the examined region (97.49%) was extremely high degree of contamination (EHDC). It raises a serious concern for the local ecosystems, every pollution level was higher than the threshold of its average concentration in the surface crust of the earth except for Fe. The separation and identification of microorganisms (fungi, bacteria, and actinomycetes) has been found to have a major impact on the decomposition of environmental contaminants, both organic and inorganic. The soil in the study area contained four phenotypes of actinomycetes, three fungal species, and nine bacterial species, according to the findings. Additionally, the investigation showed that *R. oryzae*, *P. aeruginosa*, and *Bacillus thuringiensis* were able to attain 100% removal efficiency for As and Cr, which is an extraordinarily high level of removal efficiency. In conclusion, defining management zones for soil contamination through the process of mapping soil pollutants, geographical identification, and then identifying the kinds of microorganisms capable of lowering soil pollution levels is a crucial and efficient aspect of precise management.

Data availability statement

The original contributions presented in the study are included in the article/Supplementary Material, further inquiries can be directed to the corresponding authors.

Author contributions

EM: Conceptualization, Methodology, Supervision, Visualization, Writing–original draft, Writing–review and editing. MJ: Data curation, Methodology, Software, Writing–original draft, Writing–review and editing. EH: Writing–original draft, Writing–review and editing. AE-A: Writing–original draft, Writing–review and editing. SN: Conceptualization, Writing–original draft, Writing–review and editing. NR: Resources, Validation, Writing–original draft, Writing–review and editing. AS: Writing–original draft, Writing–review and editing. MS: Writing–original draft, Writing–review and editing.

Funding

The author(s) declare that financial support was received for the research, authorship, and/or publication of this article. This paper was supported by the RUDN University Strategic Academic Leadership Program.

Acknowledgments

The authors would like to thank the National Authority for Remote Sensing and Space Science (NARSS) for funding the field survey laboratory analysis and remote sensing work.

Conflict of interest

The authors declare that the research was conducted in the absence of any commercial or financial relationships that could be construed as a potential conflict of interest.

Publisher's note

Author disclaimer

Supplementary material

The Supplementary Material for this article can be found online at: https://www.frontiersin.org/articles/10.3389/fenvs.2024.1381409/full#supplementary-material

References

Abd-Alla, M. H., Morsy, F. M., El-Enany, A. W. E., and Ohyama, T. (2012). Isolation and characterization of a heavy-metal-resistant isolate of Rhizobium leguminosarum bv. viciae potentially applicable for biosorption of Cd2+ and Co2+. *Int. Biodeter. Biodegr.* 67, 48–55. doi:10.1016/j.ibiod.2011.10.008

Abdelrahman, M. A. E., Shalaby, A., and Mohamed, E. S. (2019). Comparison of two soil quality indices using two methods based on geographic information system. *J. Remote Sens. Space Sci.* 22, 127–136. doi:10.1016/j.ejrs.2018.03.001

Abrahim, G., and Parker, R. (2008). Assessment of heavy metal enrichment factors and the degree of contamination in marine sediments from Tamaki Estuary, Auckland, New Zealand. *Environ. Monit. Assess.* 136, 227–238. doi:10.1007/s10661-007-9678-2

Abu-Elsaoud, A. M., Nafady, N. A., and Abdel-Azeem, A. M. (2017). Arbuscular mycorrhizal strategy for zinc mycoremediation and diminished translocation to shoots and grains in wheat. *Plos One* 12 (11), e0188220–e0188221. doi:10.1371/journal.pone.0188220

Abuzaid, A. S., Bassouny, M., Jahin, H., and Abdelhafez, A. (2019). Stabilization of lead and copper in a contaminated Typic Torripsament soil using humic substances. *Clean. Soil Air Water* 47, 1800309. doi:10.1002/clen.201800309

Abuzaid, A. S., Mazrou, Y. S. A., El Baroudy, A. A., Ding, Z., and Shokr, M. S. (2022). Multi-indicator and geospatial based approaches for assessing variation of land quality in arid agroecosystems. *Sustainability* 14, 5840. doi:10.3390/su14105840

Ahmad, N., and Pandey, P. (2020). Spatio-temporal distribution, ecological risk assessment, and multivariate analysis of heavy metals in bathing district, Punjab, India. *Water Air Soil Pollut.* 231, 431. doi:10.1007/s11270-020-04767-9

Akhtar, M. S., Chali, B., and Azam, T. (2013). Bioremediation of arsenic and lead by plants and microbes from contaminated soil. *Res. Plant Sci.* 1 (3), 68–73. doi:10.12691/plant-1-3-4

Alsabhan, A. H., Perveen, K., and Alwadi, A. S. (2022). Heavy metal content and microbial population in the soil of Riyadh Region, Saudi Arabia. *J. King Saud University-Science* 34 (1), 101671. doi:10.1016/j.jksus.2021.101671

ATSDR (United States Agency for Toxic Substances and Disease Registry) (2000). *Toxicological profile for arsenic*. Washington, DC, USA: US Department of Health and Human Services, Public Health Service, Agency for Toxic Substances and Disease Registry, 428.

Ayilara, M. S., Adeleke, B. S., Adebajo, M. T., Akinola, S. A., Fayose, C. A., Adeyemi, U. T., et al. (2023). Remediation by enhanced natural attenuation; an environment-friendly remediation approach. *Front. Environ. Sci.* 11, 1182586. doi:10.3389/fenvs.2023.1182586

Baroudy, A. A. E., Ali, A. M., Mohamed, E. S., Moghanm, F. S., Shokr, M. S., Savin, I., et al. (2020). Modeling land suitability for rice crop using remote sensing and soil quality indicators: the case study of the nile delta. *Sustainability* 12, 9653. doi:10.3390/su12229653

Cambardella, C. A., Moorman, T. B., Novak, J. M., Parkin, T. B., Karlen, D. L., Turco, R. F., et al. (1994). Field-scale variability of soil properties in central Iowa soils. *Soil Sci. Soc. Am. J.* 58, 1501–1511. doi:10.2136/sssaj1994.03615995005800050033x

Chabukdhara, M., Gupta, S. K., and Gogoi, M. (2017). "Phytoremediation of heavy metals coupled with generation of bioenergy," in *Algal biofuels*. Editors S. Gupta, A. Malik, and F. Bux (Cham.: Springer), 163–188. doi:10.1007/978-3-319-51010-1_9

Chen, L., Beiyuan, J., Hu, W., Zhang, Z., Duan, C., Cui, Q., et al. (2022). Phytoremediation of potentially toxic elements (PTEs) contaminated soils using alfalfa (Medicago sativa L.): a comprehensive review. *Chemosphere* 293, 133577. doi:10.1016/j.chemosphere.2022.133577

Cheng, Q., Wang, R., Huang, W., Wang, W., and Li, X. (2015). Assessment of heavy metal contamination in the sediments from the yellow river wetland national nature reserve (the sanmenxia section), China. *Environ. Sci. Pollut. Res.* 22, 8586–8593. doi:10.1007/s11356-014-4041-y

Dad, J. M., and Shafiq, M. U. (2021). Spatial variability and delineation of management zones based on soil micronutrient status in apple orchard soils of Kashmir valley, India. *Environ. Monit. Assess.* 193, 797. doi:10.1007/s10661-021-09588-9

Dasola, A. M., Adeyemi, A. L., Tunbosun, L. A., Abidemi, O. O., and Razaq, S. O. (2014). Kinetic and equilibrium studies of the heavy metal remediation potential of Helix pomentia. *Afr. J. Pure Appl. Chem.* 8, 123–133. doi:10.5897/AJPAC2014.0544

Dell'anno, F., Rastelli, E., Buschi, E., Barone, G., Beolchini, F., and Dell'anno, A. (2022). Fungi can be more effective than bacteria for the bioremediation of marine sediments highly contaminated with heavy metals. *Microorganisms* 10 (5), 993. doi:10.3390/microorganisms10050993

Dermont, G., Bergeron, M., Mercier, G., and Richerlaflèche, M. (2008). Soil washing for metal removal: a review of physical/chemical technologies and field applications. *J. Hazard. Mater.* 152, 1–31. doi:10.1016/j.jhazmat.2007.10.043

Dubey, P. K., Singh, A., Raghubanshi, A., and Abhilash, P. (2020). Steering the restoration of degraded agroecosystems during the united nations decade on ecosystem restoration. *J. Environ. Manag.* 280, 111798. doi:10.1016/j.jenvman.2020.111798

El-Bady, M. S. (2014). Spatial distribution of some important heavy metals in the soils south of Manzala Lake in Bahr El-Baqar region, Egypt. *Nova J. Eng. Appl. Sci.* 3, 1–12. doi:10.4236/gep.2015.36017

El Behairy, R. A., El Baroudy, A. A., Ibrahim, M. M., Mohamed, E. S., Rebouh, N. Y., and Shokr, M. S. (2022). Combination of GIS and multivariate analysis to assess the soil heavy metal contamination in some arid zones. *Agronomy* 12, 2871. doi:10.3390/agronomy12112871

Fan, S., Wang, X., Lei, J., Ran, Q., Ren, Y., and Zhou, J. (2019). Spatial distribution and source identification of heavy metals in a typical Pb/Zn smelter in an arid area of northwest China. *Hum. Ecol. Risk Assess.* 25, 1661–1687. doi:10.1080/10807039.2018.1539640

Ferreira, C. S., Seifollahi-Aghmiuni, S., Destouni, G., Ghajarnia, N., and Kalantari, Z. (2022). Soil degradation in the European Mediterranean region: processes, status and consequences. *Sci. Total Environ.* 805, 150106. doi:10.1016/j.scitotenv.2021.150106

Gautam, K., Sharma, P., Dwivedi, S., Singh, A., Gaur, V. K., Varjani, S., et al. (2023). A review on control and abatement of soil pollution by heavy metals: emphasis on artificial intelligence in recovery of contaminated soil. *Environ. Res.* 115592, 115592. doi:10.1016/j.envres.2023.115592

Girma, G. (2015). Microbial bioremediation of some heavy metals in soils. *Egypt. Acad. J. Biol. Sci. G Microbiol.* 6 (1), 147–161. doi:10.21608/eajbsg.2015.16483

Goenster-Jordan, S., Jannoura, R., Jordan, G., Buerkert, A., and Joergensen, R. G. (2018). Spatial variability of soil properties in the floodplain of a river oasis in the Mongolian Altay Mountains. *Geoderma* 330, 99–106. doi:10.1016/j.geoderma.2018.05.028

Goher, M. E., El-Monem, A. M. A., Abdel-Satar, A. M., Ali, M. H., Hussian, A. E. M., and Napiórkowska-Krzebietke, A. (2016). *Biosorption of some toxic metals from aqueous solution using non-living algal cells of Chlorella vulgaris*.

Golden, N., Zhang, C., Potito, A., Gibson, P. J., Bargary, N., and Morrison, L. (2019). Use of ordinary cokriging with magnetic susceptibility for mapping lead concentrations in soils of an urban contaminated site. *J. Soils Sediments* 20, 1357–1370. doi:10.1007/s11368-019-02537-7

Goutam, J., Sharma, J., Singh, R., and Sharma, D. (2021). "Fungal-mediated bioremediation of heavy metal–polluted environment," in *Microbial rejuvenation of polluted environment. Microorganisms for sustainability*. Editors D. G. Panpatte and Y. K. Jhala (Singapore: Springer), 26. doi:10.1007/978-981-15-74559_3

Gozukara, G. (2021). Rapid land use prediction via portable X-ray fluorescence (pXRF) data on the dried lakebed of Avlan Lake in Turkey. *Geoderma Reg.* 28, e00464. doi:10.1016/j.geodrs.2021.e00464

Gozukara, G., Acar, M., Ozlu, E., Dengiz, O., Hartemink, A. E., and Zhang, Y. (2022). A soil quality index using Vis-NIR and pXRF spectra of a soil profile. *Catena* 211, 105954. doi:10.1016/j.catena.2021.105954

Gustave, W., Yuan, Z., Liu, F., and Chen, Z. (2021). Mechanisms and challenges of microbial fuel cells for soil heavy metal (loid) s remediation. *Sci. Total Environ.* 756, 143865. doi:10.1016/j.scitotenv(2020).143865

Håkanson, L. (1980). An ecological risk index for aquatic pollution control: a sedimentological approach. *Water Res.* 14, 975–1001. doi:10.1016/0043-1354(80)90143-8

Hamid, Y., Tang, L., Hussain, B., Usman, M., Liu, L., Ulhassan, Z., et al. (2021). Sepiolite clay: a review of its applications to immobilize toxic metals in contaminated soils and its implications in soil–plant system. *Environ. Technol. Innovation* 23, 101598. doi:10.1016/j.eti.2021.101598

Hammam, A. A., Mohamed, W. S., Sayed, S.E.-E., Kucher, D. E., and Mohamed, E. S. (2022). Assessment of soil contamination using GIS and multi-variate analysis: a case study in el-minia governorate, Egypt. *Agronomy* 12, 1197. doi:10.3390/agronomy12051197

Hassan, A., Pariatamby, A., Ahmed, A., Auta, H. S., and Hamid, F. S. (2019). Enhanced bioremediation of heavy metal contaminated landfill soil using filamentous fungi consortia: a demonstration of bioaugmentation potential. *Water Air Soil Pollut.* 230, 215. doi:10.1007/s11270-019-4227-5

Hendawy, E., Belal, A. A., Mohamed, E. S., Elfadaly, A., Murgante, B., Aldosari, A. A., et al. (2019). The prediction and assessment of the impacts of soil sealing on agricultural land in the North Nile Delta (Egypt) using satellite data and GIS modeling. *Sustainability* 11 (17), 4662. doi:10.3390/su11174662

Huang, H., Ye, L., and Zhou, Z. (2020). Sharing earth with all life. *High-Risk Pollut. Wastewater* 42, 209–210. doi:10.1016/j.pld.2020.08.002

Ivushkin, K., Bartholomeus, H., Bregt, A. K., Pulatov, A., Kempen, B., and De Sousa, L. (2019). Global mapping of soil salinity change. *Remote Sens. Environ.* 231, 111260. doi:10.1016/j.rse.2019.111260

Jain, A. K., and Dubes, R. C. (1988). *Algorithms for clustering data*. Hoboken, NJ: Prentice-Hall, Inc.

Jamil, A., Riaz, S., Ashraf, M., and Foolad, M. R. (2021). Gene expression profiling of plants under salt stress. *Crit. Rev. Plant Sci.* 30, 435–458. doi:10.1080/07352689.2011.605739

Jiang, M., He, L., Niazi, N. K., Wang, H., Gustave, W., Vithanage, M., et al. (2023). Nanobiochar for the remediation of contaminated soil and water: challenges and opportunities. *Biochar* 5 (1), 2. doi:10.1007/s42773-022-00201-x

Kaiser, H. F. (1960). The application of electronic computers to factor analysis. *Educ. Psychol. Meas.* 20, 141–151. doi:10.1177/001316446002000116

Khan, S., Naushad, M., Lima, E. C., Zhang, S., Shaheen, S. M., and Rinklebe, J. (2021). Global soil pollution by toxic elements: current status and future perspectives on the risk assessment and remediation strategies—a review. *J. Hazard. Mater.* 417, 126039. doi:10.1016/j.jhazmat.2021.126039

Kim, I. H., Choi, J. H., Joo, J. O., Kim, Y. K., Choi, J. W., and Oh, B. K. (2015). Development of a microbe-zeolite carrier for the effective elimination of heavy metals from seawater. *J. Microbiol. Biotechnol.* 25 (9), 1542–1546. doi:10.4014/jmb.1504.04067

Kumar, V., Pandita, S., and Setia, R. (2022). A meta-analysis of potential ecological risk evaluation of heavy metals in sediments and soils. *Gondwana Res.* 103, 487–501. doi:10.1016/j.gr.2021.10.028

Leusch, A., Holan, Z. R., and Volesky, B. (1995). Biosorption of heavy metals (Cd, Cu, Ni, Pb, Zn) by chemically-reinforced biomass of marine algae. *J. Chem. Technol. Biotechnol.* 62, 279–288. doi:10.1002/jctb.280620311

Liu, L., Li, W., Song, W., and Guo, M. (2018). Remediation techniques for heavy metal-contaminated soils: principles and applicability. *Sci. Total Environ.* 633, 206–219. doi:10.1016/j.scitotenv.2018.03.161

Luna, J. M., Rufino, R. D., and Sarubbo, L. A. (2016). Biosurfactant from *Candida sphaerica* UCP0995 exhibiting heavy metal remediation properties. *Process Saf. Environ. Prot.* 102, 558–566. doi:10.1016/j.psep.2016.05.010

Luo, L., Ma, Y. B., Zhang, S. Z., Wei, D. P., and Zhu, Y. G. (2009). An inventory of trace element inputs to agricultural soils in China. *J. Environ. Manag.* 90, 2524–2530. doi:10.1016/j.jenvman.2009.01.011

Mallik, S., Mishra, U., and Paul, N. (2020). Groundwater suitability analysis for drinking using GIS-based fuzzy logic. *Ecol. Indic.* 121, 107179. doi:10.1016/j.ecolind.2020.107179

Mcgrath, S. P. (1995). in *Nickel in heavy metals in soils*. Editor B. J. Alloway 2nd ed. (London, UK: Blackie Academic and Professional), 371.

Mohamadhasani, F., and Rahimi, M. (2022). *Growth response and mycoremediation of heavy by fungus Pleurotus sp*. doi:10.1038/s41598-022-24349-5

Mohamed, E. S., Jalhoum, M. E., Belal, A. A., Hendawy, E., Azab, Y. F., Kucher, D. E., et al. (2023). A novel approach for predicting heavy metal contamination based on adaptive neuro-fuzzy inference system and GIS in an arid ecosystem. *Agronomy* 13 (7), 1873. doi:10.3390/agronomy13071873

Nawar, S., Mohamed, E. S., Essam-Eldeen Sayed, S., Mohamed, W. S., Rebouh, N. Y., and Hammam, A. A. (2023). Estimation of key potentially toxic elements in arid agricultural soils using Vis-NIR spectroscopy with variable selection and PLSR algorithms. *Front. Environ. Sci.* 11, 1222871. doi:10.3389/fenvs.2023.1222871

Nazzal, Y., Al-Arifi, N., Jafri, M. K., Kishawy, H. A., A Ghrefat, H., M El-Waheidi, M., et al. (2015). Study the urban soils contamination by heavy metals for selected industrial locations in the Greater Toronto area, Canada, using multivariate statistical analysis. *Geol. Croat.* 68 (2), 147–159. doi:10.4154/gc.2015.10

Neboht, H. A., Ilusanya, O. A., Ezekoye, C. C., and Orji, F. A. (2013). Assessment of IjebuIgbo Abattoir effluent and its impact on the ecology of the receiving soil and river. *J. Environ. Sci. Toxicol. Food Technol.* 7 (5), 61–67. doi:10.9790/2402-0756167

Neina, D. (2019). The role of soil pH in plant nutrition and soil remediation. *Appl. Environ. soil Sci.* 2019, 1–9. doi:10.1155/2019/5794869

Nicholson, F. A., Smith, S. R., Alloway, B. J., Carlton-Smith, C., and Chambers, B. J. (2003). An inventory of heavy metals inputs to agricultural soils in England and Wales. *Sci. Total Environ.* 311, 205–219. doi:10.1016/s0048-9697(03)00139-6

Nowicka, B. (2022). Heavy metal-induced stress in eukaryotic algae mechanisms of heavy metal toxicity and tolerance with particular emphasis on oxidative stress in exposed cells and the role of antioxidant response. *Environ. Sci. Pollut. Res.* 29, 16860–16911. doi:10.1007/s11356-021-18419-w

Nwaehiri, U. L., Akwukwaegbu, P. I., and Nwoke, B. E. B. (2020). Bacterial remediation of heavy metal polluted soil and effluent from paper mill industry. *Environ. Health Toxicol.* 35, 1–10. doi:10.5620/eaht.e2020009

Parth, V., Murthy, N. N., and Saxena, P. R. (2011). Assessment of heavy metal contamination in soil around hazardous waste disposal sites in Hyderabad City (India): natural and anthropogenic implications. *J. Environ. Res. Manag.* 2, 27–34.

Peña, A. (2022). A comprehensive review of recent research concerning the role of low molecular weight organic acids on the fate of organic pollutants in soil. *J. Hazard. Mat.* 434, 128875. doi:10.1016/j.jhazmat.2022.128875

Penkova, T. (2017). Principal component analysis and cluster analysis for evaluating the natural and anthropogenic territory safety. *Procedia Comput. Sci.* 112, 99–108. doi:10.1016/j.procs.2017.08.179

Purwanti, I. F., Kurniawan, S. B., Titah, H. S., and Tangahu, B. V. (2018). Identification of acid and aluminium resistant bacteria isolated from aluminum recycling area. *Int. J. Civ. Eng. Technol.* 9, 945–954.

Purwanti, I. F., Obenu, A., Tangahu, B. V., Kurniawan, S. B., Imron, M. F., and Abdullah, S. R. S. (2020). Bioaugmentation of Vibrio alginolyticus in phytoremediation of aluminium-contaminated soil using Scirpus grossus and Thypa angustifolia. *Heliyon* 6, e05004. doi:10.1016/j.heliyon.2020.e05004

Saad, A. (1997). *Environmental hydrogeologic impacts of ground water withdrawal in the eastern nile delta region with emphasis on ground-water pollution potential*. Cairo, Egypt: Ain Shams University. Ph.D. Thesis.

Sahu, V., Mani, D., Singh, B., Mohasin, M., and Verma, J. (2023). Enrichment of Cd, Cr, Pb and biological detoxification strategies in sewage irrigated soils. *Int. J. Plant and Soil Sci.* 35 (18), 599–609. doi:10.9734/ijpss/2023/v35i183325

Said, M. E. S., Ali, A. M., Borin, M., Abd-Elmabod, S. K., Aldosari, A. A., Khalil, M. M. N., et al. (2020). On the use of multivariate analysis and land evaluation for potential agricultural development of the northwestern coast of Egypt. *Agronomy* 10, 1318. doi:10.3390/agronomy10091318

Sebei, A., Chaabani, A., Abdelmalek-Babbou, C., Helali, M. A., Dhahri, F., and Chaabani, F. (2020). Evaluation of pollution by heavy metals of an abandoned Pb-Zn mine in northern Tunisia using sequential fractionation and geostatistical mapping. *Environ. Sci. Pollut. Res.* 27, 43942–43957. doi:10.1007/s11356-020-10101-x

Senesi, G. S., Baldassarre, G., Senesi, N., and Radina, B. (1999). Trace element inputs into soils by anthropogenic activities and implications for human health. *Chemosphere* 39, 343–377. doi:10.1016/s0045-6535(99)00115-0

Shi, C., and Wang, Y. (2020). Non-parametric machine learning methods for interpolation of spatially varying non-stationary and non-Gaussian geotechnical properties. *Geosci. Front.* 12, 339–350. doi:10.1016/j.gsf.2020.01.011

Shokr, M. S., Abdellatif, M. A., El Behairy, R. A., Abdelhameed, H. H., El Baroudy, A. A., Mohamed, E. S., et al. (2022). Assessment of potential heavy metal contamination hazards based on GIS and multivariate analysis in some mediterranean zones. *Agronomy* 12, 3220. doi:10.3390/agronomy12123220

Shrivastava, P., and Kumar, R. (2021). Soil salinity: a serious environmental issue and plant growth promoting bacteria as one of the tools for its alleviation. *Saudi J. Biol. Sci.* 22, 123–131. doi:10.1016/j.sjbs.2014.12.001

Singh, A. (2015). Soil salinization and waterlogging: a threat to environment and agricultural sustainability. *Ecol. Indic.* 57, 128–130. doi:10.1016/j.ecolind.2015.04.027

Singh, S. P., and Singh, M. K. (2020). "Soil pollution and human health," in *Plant responses to soil pollution*. Editors P. Singh, S. K. Singh, and S. M. Prasad (Singapore: Springer). doi:10.1007/978-981-15-4964-9_13

Smith, A., Cullis, B., and Thompson, R. (2002). "Exploring variety-environment data using random effects AMMI models with adjustments for spatial field trend: Part 1: theory," in *Quantitative genetics, genomics and plant breeding* (Wallingford: CABI).

Stavi, I., Thevs, N., and Priori, S. (2021). Soil salinity and sodicity in drylands: a review of causes, effects, monitoring, and restoration measures. *Front. Environ. Sci.* 330. doi:10.3389/fenvs.2021.712831

Suárez, M. H., Pérez, D. M., Rodríguez-Rodríguez, E. M., Romero, C. D., Borreguero, F. E., and Galindo-Villardón, P. (2016). The compositional HJ-biplot—a new approach to identifying the links among bioactive compounds of tomatoes. *Int. J. Mol. Sci.* 17, 1828. doi:10.3390/ijms17111828

Swartjes, F. A. (2011). "Introduction to contaminated site management," in *Dealing with contaminated sites* (Berlin/Heidelberg, Germany: Springer Science Business Media B.V.).

Tastan, B. E., Ertuğrul, S., and Dönmez, G. (2010). Effective bioremoval of reactive dye and heavy metals by Aspergillus versicolor. *Bioresour. Technol.* 101, 870–876. doi:10.1016/j.biortech.2009.08.099

Wang, N., Guan, Q., Sun, Y., Wang, B., Ma, Y., Shao, W., et al. (2021). Predicting the spatial pollution of soil heavy metals by using the distance determination coefficient method. *Sci. Total. Environ.* 799, 149452. doi:10.1016/j.scitotenv.2021.149452

Wedepohl, K. H. (1995). The composition of the continental crust. *Geochimica Cosmochimica Acta* 59, 1,217–1,239. doi:10.1016/0016-7037(95)00038-2

Wierzba, S. (2015). Biosorption of lead (II), zinc (II) and nickel (II) from industrial wastewater by Stenotrophomonas maltophilia and Bacillus subtilis. *Pol. J. Chem. Technol.* 17, 79–87. doi:10.1515/pjct-2015-0012

Wuana, R. A., and Okieimen, F. E. (2011). Heavy metals in contaminated soils: a review of sources, chemistry, risks and best available strategies for remediation. *Int. Sch. Res. Not.*, 402647. doi:10.5402/2011/402647

Xu, T., Xi, J., Ke, J., Wang, Y., Chen, X., Zhang, Z., et al. (2023). Deciphering soil amendments and actinomycetes for remediation of cadmium (Cd) contaminated farmland. *Ecotoxicol. Environ. Saf.* 249, 114388. doi:10.1016/j.ecoenv.2022.114388

Yang, Z., Yang, F., Liu, J.-L., Wu, H.-T., Yang, H., Shi, Y., et al. (2021). Heavy metal transporters: functional mechanisms, regulation, and application in phytoremediation. *Sci. Total. Environ.* 809, 151099. doi:10.1016/j.scitotenv.2021.151099

Zhen, J., Pei, T., and Xie, S. (2019). Kriging methods with auxiliary nighttime lights data to detect potentially toxic metals concentrations in soil. *Sci. Total. Environ.* 659, 363–371. doi:10.1016/j.scitotenv.2018.12.330

frontiers | Frontiers in Environmental Science

TYPE Original Research
PUBLISHED 18 April 2024
DOI 10.3389/fenvs.2024.1358561

OPEN ACCESS

EDITED BY
Qi Liao,
Central South University, China

REVIEWED BY
Ksenija Jakovljevic,
University of Belgrade, Serbia
Sudipta Rakshit,
Tennessee State University, United States

*CORRESPONDENCE
Jin Hee Park,
pjinh@chungbuk.ac.kr

RECEIVED 20 December 2023
ACCEPTED 11 March 2024
PUBLISHED 18 April 2024

CITATION
Kim HN and Park JH (2024), Simultaneous removal of arsenic and lead by iron phosphate and its potential for immobilization in mixed-contaminated soil.
Front. Environ. Sci. 12:1358561.
doi: 10.3389/fenvs.2024.1358561

Simultaneous removal of arsenic and lead by iron phosphate and its potential for immobilization in mixed-contaminated soil

Han Na Kim and Jin Hee Park*

Department of Environmental and Biological Chemistry, Chungbuk National University, Cheongju, Republic of Korea

Cationic metals such as lead (Pb) and metalloids such as arsenic (As) in contaminated soil can be simultaneously immobilized by iron phosphate because As(V) is stabilized by binding to iron (hydr)oxides and metals precipitate with phosphate. However, phosphate competes with As for sorption sites, which may affect the simultaneous stabilization of Pb and As. Therefore, the purpose of this study was to evaluate the simultaneous stabilization of As and Pb using iron phosphate both in single- and multi-metal solutions and soil. In both single- and multiple-element solutions, Pb was completely removed by iron phosphate. Arsenic immobilization was explained by the Freundlich isotherm. Arsenate [As(V)] removal by iron phosphate decreased with increasing pH, while arsenite [As(III)] removal increased with increasing pH. The extraction of bioavailable As from contaminated soil increased after incubation with iron phosphate, whereas the concentration of bioavailable Pb decreased. The increase in bioavailable As can be attributed to As substitution by phosphate, which was not immobilized by iron. Although both As and Pb can be removed by iron phosphate in aqueous solutions, an iron phosphate mineral with relatively low Ksp should be used to simultaneously immobilize As and Pb in soil.

KEYWORDS

adsorption, precipitation, stabilization, oxyanions, metals

1 Introduction

Place's Agricultural land surrounding abandoned mines is often contaminated with metal(loid)s. Arsenic (As) is one of the elements found in higher concentrations in mine sites, often associated with metals such as cadmium (Cd), copper (Cu), lead (Pb), and zinc (Zn) (Bolan et al., 2014). These pollutants adversely affect plants growing on croplands and migrate into the surrounding waterways and air, thereby increasing environmental pollution problems (Esshaimi et al., 2012). Arsenic is a highly toxic carcinogen, and the consumption of As-contaminated rice may cause liver, kidney, lung, and skin cancer (Yu et al., 2003; Chikkanna et al., 2019).

Metals such as Cd, Cu, Pb, and Zn are some of the elements usually found near mine sites in concentrations that might be toxic to biological systems (Han et al., 2002; Sayadi, 2014). Metals can be absorbed and bioaccumulated in crops and living organisms to high concentrations. This poses significant threats to the overall health of ecosystems and may ultimately lead to the death of organisms (Nagajvoti

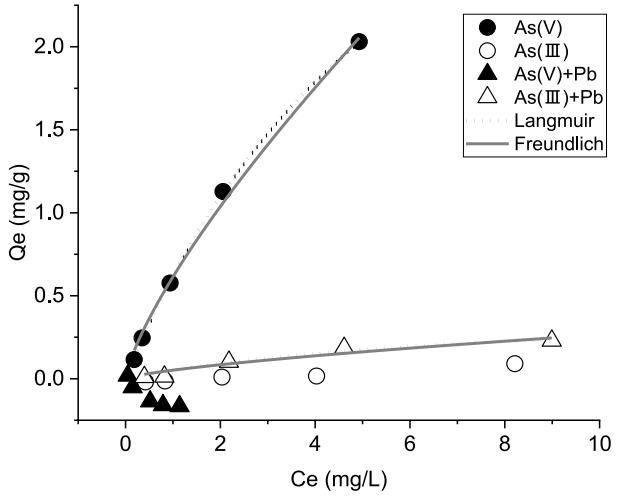

FIGURE 1
Langmuir and Freundlich isotherm models for As adsorption on iron phosphate.

et al., 2010). Soil pollutants such as metals and metalloids often occur with more than one element in increased concentration, and it is necessary to control them simultaneously (Martin, 2012).

However, the physicochemical properties of metals such as Pb and metalloids such as As are very different, so it is difficult to control them simultaneously. Arsenic exists as a neutral form, such as organic water-soluble H_3AsO_3 and $AsO(OH)_3$, or as an oxyanion in the natural environment, so it has different chemical properties from metallic contaminants that normally exist in cationic forms (Stollenwerk, 2003; Cortes-Arriagada and Ortega, 2020). Toxic metal(loid)s such as As, Cd, Cu, Pb, and Zn can be stabilized by changing the pH and redox potential (Sharma et al., 2015). For example, as the pH increases, arsenate adsorption decreases because the iron (Fe) mineral surface has a net negative charge, weakening its binding to minerals and increasing its mobility and toxicity (Raven et al., 1998). In contrast, Pb precipitates as lead hydroxide at a pH higher than 6, reducing mobility and toxicity (Payne and Abdel-Fattah, 2004). Furthermore, lower Eh conditions contribute to the reduction of As(V) to As(III), increasing the toxicity and release of metals bound to Fe/Mn oxides because of the decomposition of Fe/Mn oxides under reducing conditions (Yang et al., 2022). The mobility of metals in soil generally decreases with increasing pH; however, As(V) can be desorbed or mobilized because its mobility increases with increasing pH, causing it to diffuse into the environment (Stollenwerk, 2003; Kim et al., 2011).

Most of As exists as arsenite [As(III)] and arsenate [As(V)] in soil and water environments, and As(III) is more mobile and toxic than As(V) (Moon et al., 2004). Both As(III) and As(V) adsorb to iron (hydr)oxides such as goethite and ferrihydrite, which effectively remove As and lower its toxicity (Smedley and Kinniburgh, 2002; Sundar and Chakravarty, 2010; Park et al., 2016; Zhang et al., 2019). Specifically, the ferric-arsenate [Fe(III)–As(V)] precipitate and its natural mineral form (scorodite, $FeAsO_4{\cdot}2H_2O$) occur in the As-contaminated soil (Zhao et al., 2021). Once As in the soil is co-precipitated with iron (hydr)oxides as ferric-arsenate, the toxicity and mobility of As will be reduced (Aredes et al., 2013).

The stabilization mechanism of metals such as Cd and Pb includes precipitation with phosphates by substituting cations in phosphate compounds (Wang et al., 2001; Bolan et al., 2014). In addition, because phosphate is a nutrient essential for plant growth, treatment with phosphates tends to promote growth in metal-contaminated soils (Cao et al., 2003; Soares and Siqueira, 2008). However, phosphate treatment in contaminated soil adversely affects the stability of As because its chemical properties are similar to those of phosphates, which induces competition for adsorption sites on iron oxides (Hughes, 2002; Theodoratos et al., 2002; Kaur et al., 2011). Therefore, it is difficult to simultaneously control As and metals by phosphate treatment in soil.

Cui et al. (2010) suggested that As and Pb could be immobilized by Fe and phosphate, respectively, and they amended iron as ferrous sulfate and phosphate as calcium magnesium phosphate, phosphate rock, and single super-phosphate. However, because oxyanions such as As and antimony (Sb) in the soil environment are stabilized by iron oxides and metals with divalent cations are stabilized by phosphate (Liang et al., 2014; Sazakli et al., 2015), compounds containing both Fe and phosphate may simultaneously control multiple metals and metalloids. Therefore, the objective of this study was to evaluate the possibility of simultaneous stabilization of As and Pb using iron phosphate. The concomitant removal of As and Pb by iron phosphate was evaluated in solutions with different pH values. In addition, the application of iron phosphate for the remediation of soil contaminated with multiple metals and metalloids was tested.

TABLE 1 Arsenic adsorption isothermal equation parameters.

Species	Langmuir parameters			Freundlich parameters		
	Q_m (mg/g)	b (L/mg)	R^2	K_f (mg/g)	n	R^2
As(V)	5.120	0.135	0.963	1.773	1.153	0.992
As(III)	0.060	0.394	0.147	1.137	0.997	0.475
As(V)+Pb	NA*	NA	NA	NA	NA	NA
As(III) +Pb	37.879	1.467	0.884	4.900	0.874	0.930

*Not available.

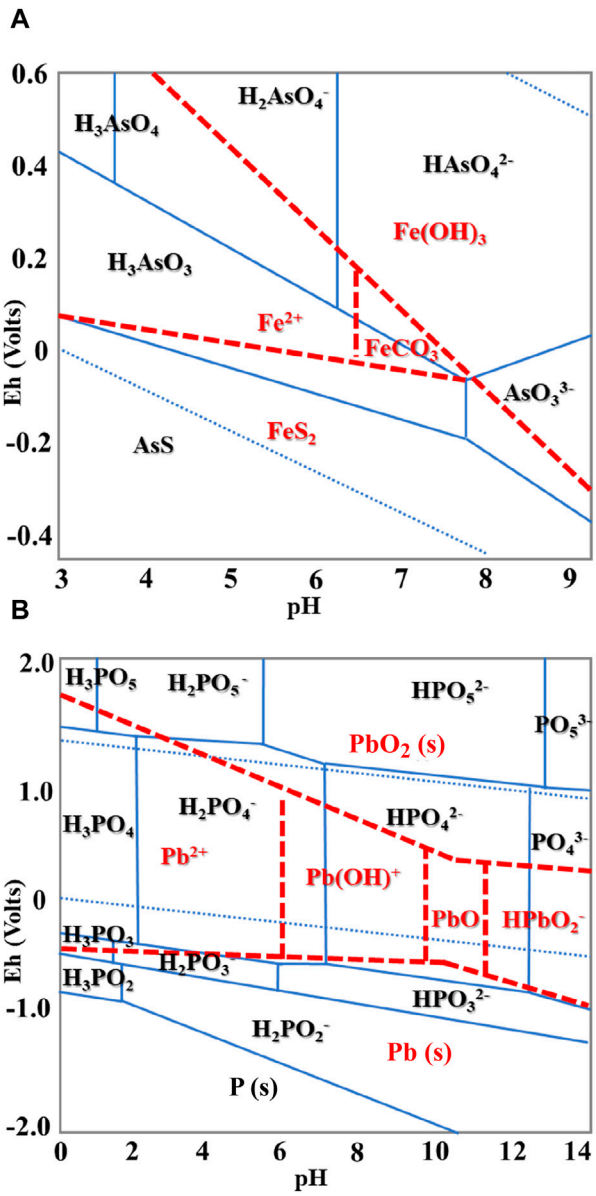

FIGURE 2
Eh–pH diagram of As and Fe **(A)** and Pb and phosphate **(B)**.

2 Materials and methods

2.1 Iron phosphate synthesis

Iron phosphate ($FePO_4$) was prepared by mixing 25 mL of 0.83 M Iron(III) chloride hexahydrate and 25 mL of 0.83 M dibasic anhydrous sodium phosphate in a 50-mL conical tube. After mixing, the solution was left to react for 30 min, and the white precipitate was recovered by centrifugation at 4,000 rpm for 10 min. The precipitate was washed several times with deionized water to remove the remaining ions and then dried in an oven at 60°C.

The mineralogy was confirmed using X-ray diffraction (Rigaku, JP/SmartLab, 9 kW). The surface structure and composition were analyzed using scanning electron microscopy combined with an energy-dispersive X-ray spectroscopy (EDS) (Zeiss Ultra Plus). Specific surface areas were measured using the Brunauer–Emmett–Teller (BET) protocol (Micromeritics, ASAP 2020).

2.2 Metal removal using iron phosphate

Metal removal experiments were conducted in single and mixed solutions of As and Pb. The As(V) stock solution was prepared from sodium arsenate heptahydrate ($Na_2HAsO_4{\cdot}7H_2O$). The As(III) stock solution was prepared from sodium arsenite ($NaAsO_2$). The Pb stock solution was prepared from lead nitrate [$Pb(NO_3)_2$]. The As concentration in the solutions ranged from 0.5 to 10 mg/L, and the concentration for the Pb solutions was 5–100 mg/L. Solutions containing both As and Pb were prepared by mixing stock solutions to adjust the final concentration to be the same as for a single-element solution. To evaluate the pH effect on metal or As immobilization, the solution pH was adjusted using acetate buffer, Tris-HCl buffer, and glycine buffer to achieve pH 5, 7, and 10, respectively.

The experiment was conducted by mixing 0.05 g of iron phosphate and 20 mL of elemental solution in a 50-mL conical tube and shaking it for 24 h at 180 rpm (Kim and Park, 2023). The suspension was filtered using a 0.45 μm syringe filter, and the concentrations of As, Pb, Fe, and P were measured using inductively coupled plasma optical emission spectroscopy (ICP-OES, PerkinElmer, Avio 500).

Through the calculation of the adsorption isotherm, the chemical reactions and properties of the minerals and solutions can be determined (Olsen and Watanabe, 1957). The data on the immobilization of As by iron phosphate were analyzed using the Langmuir and Freundlich isotherm models. The Langmuir (Eq. 1) and Freundlich (Eq. 2) isotherms can be written as follows:

$$q_e = \frac{bQ_mC_e}{1+bC_e} \text{ Langmuir isotherm} \quad (1)$$

$$q_e = K_f C_e^n \text{ Freundlich isotherm} \quad (2)$$

where, q_e (mg/g) is the amount of As adsorbed per gram of iron phosphate, Q_m (mg/g) is the maximum amount of the adsorbed As, and C_e (mg/L) is the equilibrium concentration of As. b (L/mg) is the Langmuir adsorption constant, which is related to the affinity of the binding sites. K_f ((mg/g)(L/mg)$^{1/n}$) is the Freundlich adsorption constant, and n is related to the adsorption intensity.

2.3 Incubation of metal- and arsenic-contaminated soils with iron phosphate

Loamy sand soil contaminated with metal(loid)s such as As, Cd, Cu, Pb, and Zn was collected around an abandoned metal mine, dried at room temperature, and sieved to collect particles <2 mm in size. The pH and EC of the soil were measured after shaking 5 g of soil in 25 mL of deionized water for 30 min. The organic matter in the soil was analyzed using the Walkley–Black method (Walkley and Black, 1934). The total element concentrations were determined by digesting the soil with aqua regia. The chemical properties of the soil are presented in Supplementary Table S1. To immobilize the As, Cd, Cu, Pb, and Zn with iron phosphate, 10 g of mine soil was mixed with different amounts of iron phosphates (5, 10, and 20 g/kg). The water content of the soil was kept at 15% by adding 2 mL of

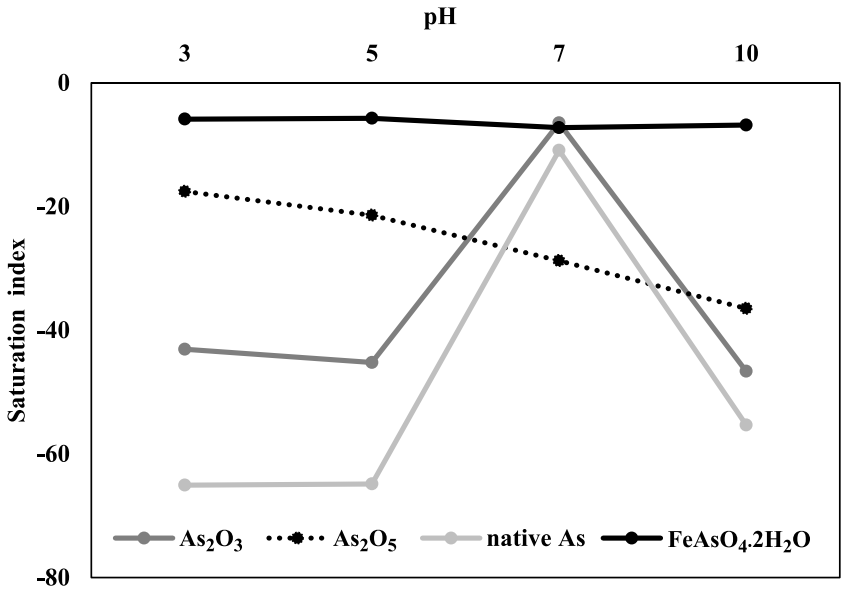

FIGURE 3
Saturation index plot showing the potential precipitation of As as a function of pH.

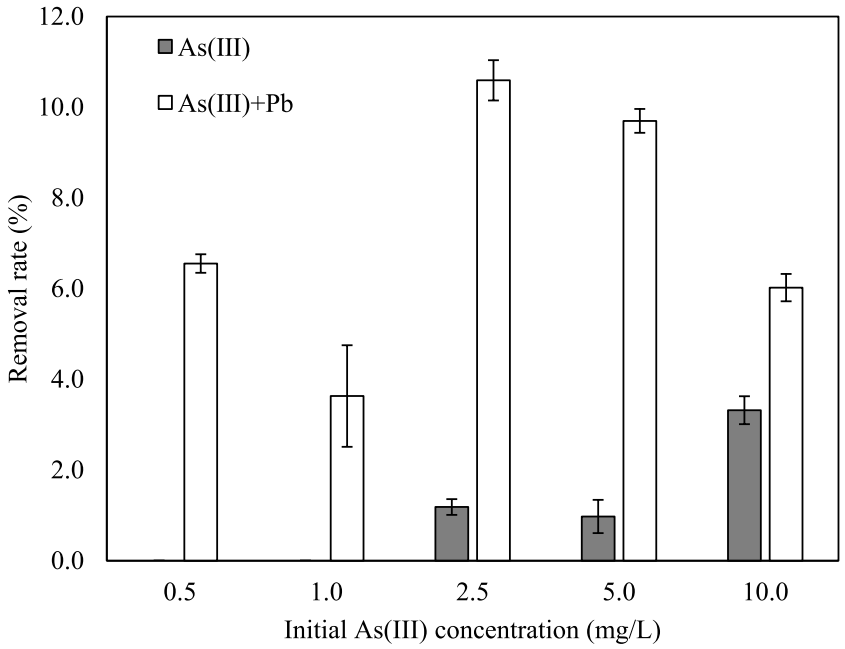

FIGURE 4
Removal rate of As(III) in single As(III) solution and mixed As(III) solution with Pb.

deionized water and then incubating it in an incubator at 25°C for 7 days. To evaluate the immobilization of the target elements in the soil, they were extracted from soil samples in 25 mL of deionized water and 50 mL of 0.05 M $(NH_4)_2SO_4$ for 2 h at 180 rpm in a shaker (Taghizadeh-Toosi et al., 2012). The supernatant was separated by centrifugation at 4,000 rpm for 10 min and then filtered through a 0.45-μm syringe filter. Then, the bioavailable metal and As concentrations were analyzed using ICP-OES.

3 Results and discussion

3.1 Adsorption isotherm

XRD and SEM-EDX analysis showed amorphous iron phosphate with fine particles (Supplementary Figures S1, S2). The BET specific surface area of the iron phosphate was measured and found to be 72.2 ± 0.2 m^2/g due to the small size of the nanoparticles.

TABLE 2 Phosphorus concentration (mg/L) in solution after the removal of As(V), As(III), and Pb by iron phosphate.

Elements in solution	Initial elemental concentration (mg/L)				
	As 0.5, Pb 5	As 1, Pb 10	As 2.5, Pb 25	As 5, Pb 50	As 10, Pb 100
As(V)	6.86 ± 0.02	7.25 ± 0.10	7.50 ± 0.10	8.24 ± 0.04	8.99 ± 0.03
As(III)	7.81 ± 0.26	8.43 ± 0.18	8.45 ± 0.17	8.18 ± 0.07	9.10 ± 0.24
Pb	6.40 ± 0.03	6.11 ± 0.11	5.81 ± 0.09	5.35 ± 0.05	4.59 ± 0.06
As(V)+Pb	6.55 ± 0.04	6.80 ± 0.18	6.56 ± 0.20	6.28 ± 0.12	5.72 ± 0.08
As(III) +Pb	8.02 ± 0.42	8.37 ± 0.65	7.21 ± 0.02	6.21 ± 0.18	5.55 ± 0.15

TABLE 3 Iron and P concentrations after the removal of As(V), As(III), and Pb at different pH values.

Chemical species		pH			
		3	5	7	10
Fe in solution (mg/L)	As(V)	ND	ND	29.27 ± 1.23	14.57 ± 2.39
	As(III)	ND	ND	25.82 ± 1.00	10.41 ± 4.89
	Pb	ND	ND	26.77 ± 0.19	18.42 ± 1.67
	As(V)+Pb	ND	ND	26.64 ± 0.99	0.32 ± 0.11
	As(III) +Pb	ND	ND	21.69 ± 0.99	0.85 ± 0.60
P in solution (mg/L)	As(V)	10.26 ± 0.21	9.06 ± 0.13	42.05 ± 0.63	96.55 ± 2.47
	As(III)	8.33 ± 0.21	7.48 ± 0.13	39.88 ± 0.63	86.15 ± 1.25
	Pb	6.28 ± 0.14	9.78 ± 0.12	39.60 ± 1.94	102.18 ± 0.34
	As(V)+Pb	7.11 ± 0.24	8.24 ± 0.14	41.37 ± 1.25	64.30 ± 3.80
	As(III) +Pb	5.89 ± 0.24	6.87 ± 1.29	35.88 ± 0.97	60.40 ± 1.84

ND: Not detected.

Arsenate was immobilized by iron phosphate, and the immobilization rate ranged from 50.7% to 63.7%, depending on the initial As(V) concentration. As the concentration of As in the initial solution increased, the phosphorus (P) concentration increased in the final solution (Table 2). This suggests that As(V) substitutes for phosphate in iron phosphate (Tawfik and Viola, 2011). Arsenate, as the phosphate analog, induced the release of phosphate because of competition for sorption sites (Lambkin and Alloway, 2003). However, Fe was not released during As(V) immobilization, indicating that As(V) reacted with Fe and was removed from the solution.

The immobilization data were well-fitted to both the Langmuir and Freundlich isotherms. The Freundlich adsorption isotherm better explained As(V) adsorption (R^2 = 0.99) than the Langmuir adsorption isotherm did (R^2 = 0.96) (Figure 1; Table 1). The absence of a plateau in Figure 1 further supports the conclusion that the Freundlich adsorption isotherm is a more suitable model for explaining the adsorption behavior observed in the study. The maximum adsorption amount (Q_m) calculated based on the Langmuir isotherm model was 5.12 mg/g (Table 1). The Langmuir isotherm implies monolayer adsorption, whereas the Freundlich adsorption isotherm shows multilayer adsorption (Priya et al., 2022). A better fit to the Freundlich adsorption isotherm suggests that the adsorbent has a higher adsorption capacity (Zhou et al., 2017). Although the immobilization of As(V) and As(III) by iron phosphate was explained by the Freundlich adsorption isotherm, the surface precipitation of As by iron phosphate cannot be excluded. Ardes et al. (2013) showed that surface precipitation might result from the kinetics of adsorption/desorption, which can be recognized as ternary adsorption. Tiwari and Pandey (2013) also explained that Fe(III) and As(V) were precipitated, followed by the complexation of As with ferrihydrite.

The precipitation reaction requires partial dissolution of Fe from minerals to induce surface precipitate. When iron phosphate reacted with As, dissolved Fe resulted in the formation of various precipitates associated with As(V) (Lenoble et al., 2005). Iron was released in the solution at a pH higher than 7, which indicates the possibility of surface precipitation in alkaline conditions (Table 3). Under the experimental condition (pH 3), As exists as H_3AsO_3 and Fe is in the form of Fe^{2+} according to the Eh–pH diagram of As and Fe, which might contribute to both adsorption and surface precipitation (Figure 2A). However, Fe^{2+} was not detected in the experimental solution, suggesting that As sorption was mainly

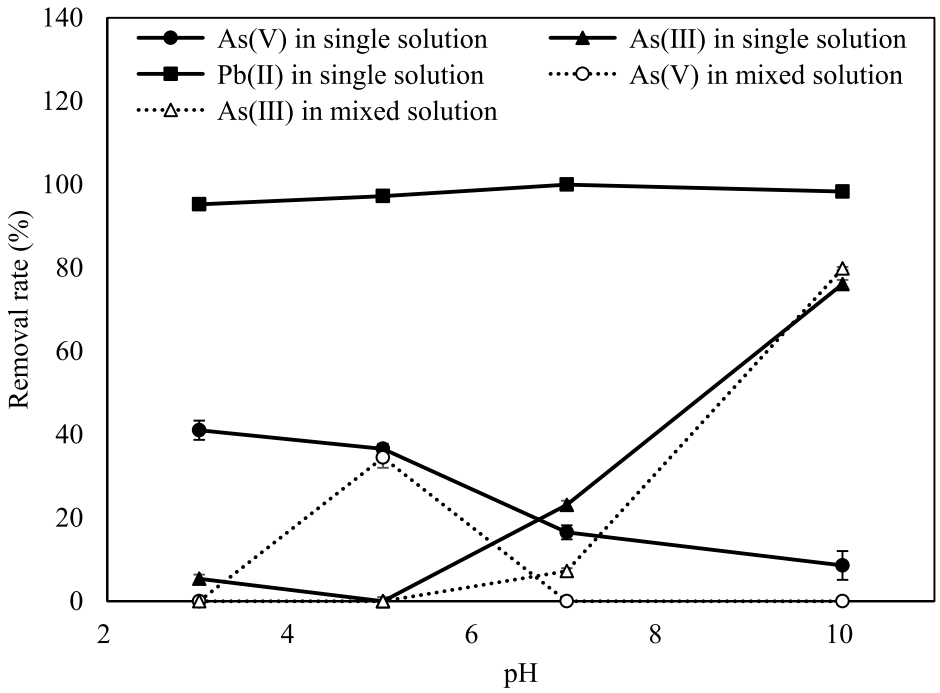

FIGURE 5
Removal rate of As(V), As(III), and Pb in a single solution and As(V) and As(III) when mixed with Pb according to different solution pH values.

attributed by the adsorption process (Aredes et al., 2013). Gallegos-Garcia et al. (2012) also reported that As showed a high affinity for iron (hydr)oxide minerals, and ion exchange adsorption of As on the mineral surface was the As removal mechanism when Fe was not eluted.

To evaluate the possibility of As precipitation with iron phosphate, geochemical modeling using PHREEQC was implemented with the following solution properties: temperature, 25°C; pH, 3, 5, 7, and 10; pe, 4; solution density, 1; As(V), 10 mg/L; sodium (Na), 9.7 mg/L; Fe, 0, 0, 29.3, and 14.6 mg/L; P, 10.3, 9.1, 42.1, and 96.6 mg/L; and strengite ($FePO_4{\cdot}2H_2O$), 2.5 g/L, respectively. The results showed that the saturation index of $FeAsO_4{\cdot}2H_2O$ ranged from −5 to −7 according to pH, indicating that there is a possibility of As precipitation with Fe if the condition changes (Figure 3). At pH 7, the saturation index of As_2O_3 and native As increased, which is related to the release of Fe from iron phosphate, resulting in the possibility of As mineral precipitation (Figure 3).

Arsenite was not immobilized by iron phosphate at the initial low As(III) concentration and was only slightly removed at a higher As(III) concentration (Figure 4). Because As(III) has higher mobility than As(V), it is estimated that the immobilization rate was lower (Oremland and Stolz, 2003). Therefore, it is necessary to oxidize As(III) and adsorb it as As(V) in the real environment.

Lead was not detected in the solution, and the concentration of released P decreased as the Pb concentration increased because of the precipitation of P with Pb (Table 2). Because almost 100% of Pb was removed, an adsorption isotherm model was not applied for Pb removal. According to the Eh–pH diagram of Pb and phosphate, Pb and P exist as Pb^{2+} and $H_2PO_4^-$, respectively, in the experimental condition, precipitation might be the main mechanism of Pb removal in the solution (Figure 2B). The phosphate concentration increased with increasing pH in the solution, showing that there is a possibility of Pb precipitation with phosphate (Table 3). Cao et al. (2003) also reported that Pb removal from the solution by phosphate primarily involves the precipitation of metal phosphate along with some ion exchange processes and surface complexation reactions on the phosphate rock.

In the mixed solution of As(V) and Pb, the initial As(V) and Pb concentrations decreased, indicating that As(V) reacted with Pb and precipitated. When soil is contaminated with both As and Pb and lead arsenate is formed, their bioavailability is reduced compared to when As and Pb are present separately in the soil. Thus, in this case, having both reduces their environmental impact (Gamble et al., 2018; Li et al., 2019).

In the simultaneous removal of As(III) and Pb by iron phosphate, As(III) did not react with Pb. Arsenite removal was higher in the mixed solution than in the single-element solution, and 100% of Pb was removed by iron phosphate (Figure 4). The reason for the higher removal of both As(III) and Pb in the mixed solution can be attributed to the oxidation of As(III) by Fe(III), followed by phosphate substitution and the reaction of Pb with the released phosphate (Lenoble et al., 2005). The Fe released from the reaction of Pb and phosphate might participate in the reaction of Fe with As(III), leading to a higher As(III) removal rate in mixed solution than in single element solution. Arsenite adsorption in the mixed solution was better explained by the Freundlich isotherm than by the Langmuir isotherm (Figure 1).

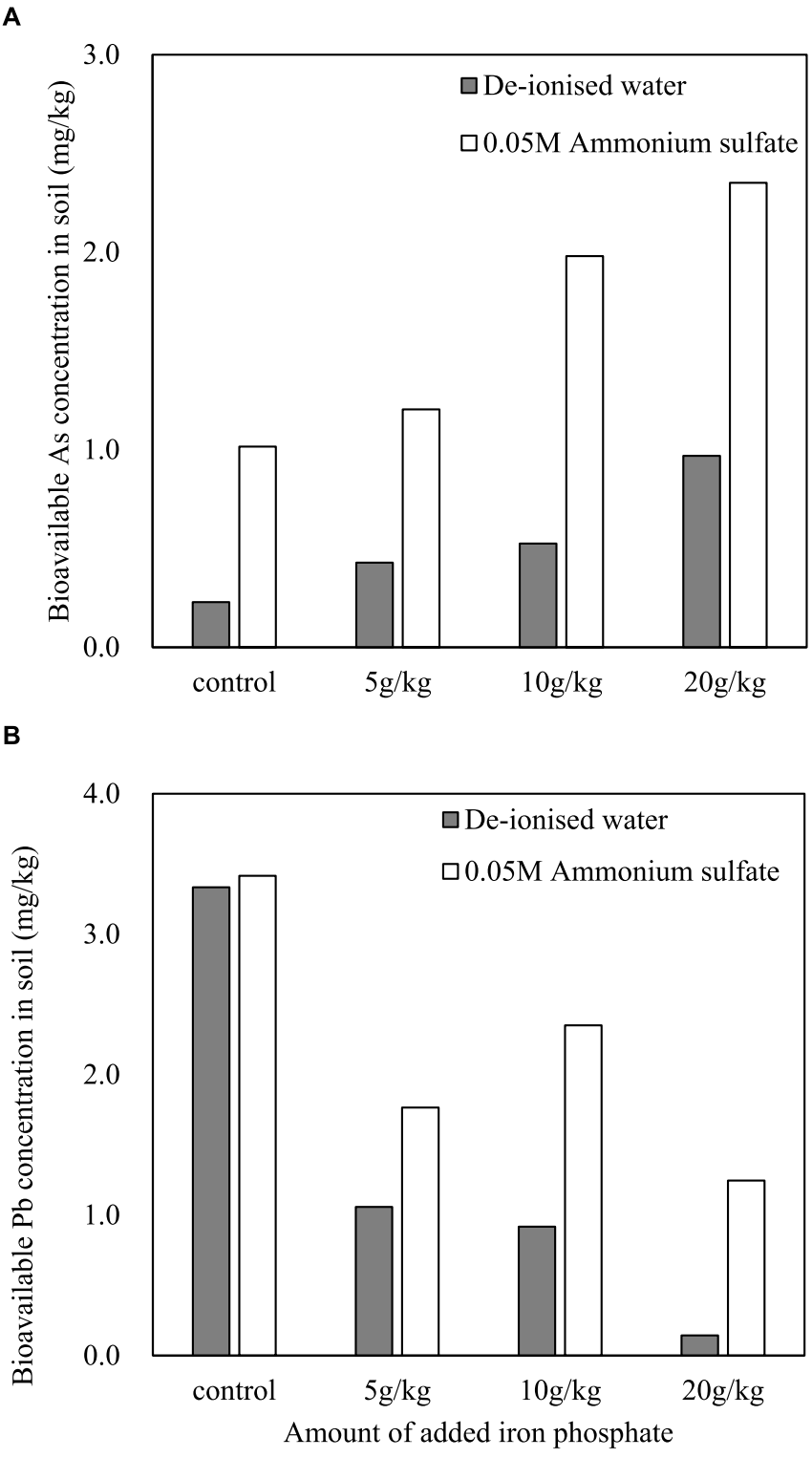

FIGURE 6
Arsenic **(A)** and Pb **(B)** concentrations extracted with de-ionized water and 0.05 M ammonium sulfate from mine soil after incubation with iron phosphate.

3.2 Effect of pH on metal and arsenic removal

As the pH increased, As(V) immobilization decreased, while As(III) immobilization showed the opposite tendency (Figure 5). Decreased As(V) immobilization can be explained by negatively charged As species predominant in the pH range of 2–12 and an increase in negative mineral surface at a higher pH than pH_{ZPC} (Mamindy-Pajany et al., 2011). Arsenic is oxidized at low pH and mainly exists in the form of As(V) in the natural environment (Bissen and Frimmel, 2003; Tabelin et al., 2020). The removal rates of As(V) and As(III) are contradictory because As(V) competes with hydroxide ions, which promotes desorption when the pH increases, thereby increasing mobility (Kim et al., 2019).

The iron concentration was analyzed and found to be the highest at pH 7.8 in the adsorption experiment. This might be because iron is oxidized and precipitated as a hydroxide as the pH increases (Table 3) (Liu et al., 2005). The phosphorus concentration also increased as the pH rose due to an increase in the substitution of As(V) and OH^- for phosphate (Table 3) (Borgnino et al., 2006; Barrow, 2017). The phosphorus concentration in the As(III)-dissolved solution also increased with increasing pH because of the substitution of phosphate by OH^- (Deng et al., 2018). As the pH increased, more phosphate dissolved in the solution, which enhanced the rate of Pb removal (Table 3; Figure 5). However, Pb has a high removal rate (>90%) at all pH levels, so a slight effect of pH on Pb removal was observed (Figure 5). This is mainly because Pb has a high removal rate compared to other elements and less adsorption competition with hydrogen ions (Weng et al., 2011; Kocabaş-Ataklı and Yürüm, 2013).

The pH effect on the simultaneous removal of As and Pb by iron phosphate in a mixed solution was evaluated. However, the initially measured As and Pb concentrations were low in various pH ranges because lead arsenate was formed (Figure 5). The co-precipitation of As(III) and Pb increased with increasing pH, and As(III) further increased in the mixed solution compared to the single As(III) solution (Figure 5). The iron concentration increased to pH 7 and decreased after that, which might react with As(III) (Table 3).

3.3 Contaminated soil incubation experiments

As the amount of added iron phosphate increased, the concentration of extracted As increased (Figure 6A). Free phosphate ions existed in the iron phosphate substituted for As in the soil and thus increased As mobility. Although bioavailable As increased with increasing iron phosphate, the Pb concentration in the extraction decreased with increasing application of iron phosphate (Figure 6B). Because the reactivity of phosphate for immobilization with Pb (and for As substitution) is higher than that of iron for immobilization with As, the extracted As was not immobilized by the released Fe (Figure 4). In addition, the relatively high solubility product of iron phosphate might cause the substitution of arsenate by phosphate because phosphate is a chemical analog of As(V) (Strawn, 2018).

Lenoble et al. (2005) showed that As was removed by iron phosphate in solution by solid dissolution and phosphate/arsenate exchange. However, they did not test As immobilization in soil. In our study, As mobility increased with iron phosphate, even though As was removed by iron phosphate in solution. In addition, a variety of minerals and competing ions in soil might result in different stabilizations of As in the solution and soil. Therefore, the reactivity of phosphate should be considered for the simultaneous immobilization of As and Pb using iron phosphate compounds in soil. With the reduced reactivity of phosphate, the substitution of As by phosphate will be less, and the simultaneous immobilization of both As and metals can be achieved. For example, oxidizing a part of pyrite (FeS_2) and coating the surface of pyrite with phosphoric acid to produce iron phosphate ($FePO_4$) decreased As and some of the metals in soil (Fytas and Evaneglou, 1998). Although the immobilization rate of iron phosphate varies from metal to metal, it is possible to simultaneously adsorb As, Cd, and Pb (Yuan et al., 2017).

4 Conclusion

Both As and Pb showed higher removal in a mixed-element solution than in single-element solutions. In the case of As(III), a small amount was adsorbed with iron phosphate in the single-element solution, but in the mixed solution with Pb, As(III) removal increased. Therefore, a synergistic effect was found when iron phosphate was applied to multiple-element-contaminated water. The removal of As was affected by pH, and the pH effect on the removal revealed a contrast between As(III) and As(V). The treatment of metal(loid)-contaminated soil with iron phosphate decreased the bioavailable Pb concentration but increased the As concentration. This suggests that the competition between As and phosphate interfered with As immobilization in the soil. Therefore, iron phosphate is a potential candidate for the remediation of water contaminated with a mixture of As and metals. However, when treating contaminated soil, it is necessary to control the pH and consider the reactivity of iron phosphate.

Data availability statement

The original contributions presented in the study are included in the article/Supplementary Material; further inquiries can be directed to the corresponding author.

Author contributions

HK: writing–original draft. JP: writing–original draft and writing–review and editing.

Funding

The author(s) declare that financial support was received for the research, authorship, and/or publication of this article. This research was supported by the “Regional Innovation Strategy (RIS)” through the National Research Foundation of Korea (NRF) funded by the Ministry of Education (MOE) (2021RIS-001).

Conflict of interest

The authors declare that the research was conducted in the absence of any commercial or financial relationships that could be construed as a potential conflict of interest.

Publisher's note

All claims expressed in this article are solely those of the authors and do not necessarily represent those of their affiliated organizations, or those of the publisher, the editors, and the reviewers. Any product that may be evaluated in this article, or claim that may be made by its manufacturer, is not guaranteed or endorsed by the publisher.

Supplementary material

The Supplementary Material for this article can be found online at: https://www.frontiersin.org/articles/10.3389/fenvs.2024.1358561/full#supplementary-material

References

Aredes, S., Klein, B., and Pawlik, M. (2013). The removal of arsenic from water using natural iron oxide minerals. *J. Clean. Prod.* 60, 71–76. doi:10.1016/j.jclepro.2012.10.035

Barrow, N. J. (2017). The effects of pH on phosphate uptake from the soil. *Plant soil* 410 (1-2), 401–410. doi:10.1007/s11104-016-3008-9

Bissen, M., and Frimmel, F. H. (2003). Arsenic—a review. Part I: occurrence, toxicity, speciation, mobility. *Acta hydrochimica hydrobiologica* 31 (1), 9–18. doi:10.1002/aheh.200390025

Bolan, N., Kunhikrishnan, A., Thangarajan, R., Kumpiene, J., Park, J., Makino, T., et al. (2014). Remediation of heavy metal (loid) s contaminated soils–to mobilize or to immobilize? *J. Hazard. Mater.* 266, 141–166. doi:10.1016/j.jhazmat.2013.12.018

Borgnino, L., Avena, M., and De Pauli, C. (2006). Surface properties of sediments from two Argentinean reservoirs and the rate of phosphate release. *Water Res.* 40 (14), 2659–2666. doi:10.1016/j.watres.2006.05.007

Cao, X., Ma, L. Q., and Shiralipour, A. (2003). Effects of compost and phosphate amendments on arsenic mobility in soils and arsenic uptake by the hyperaccumulator, Pteris vittata L. *Environ. Pollut.* 126 (2), 157–167. doi:10.1016/s0269-7491(03)00208-2

Chikkanna, A., Mehan, L., Sarath, P. K., and Ghosh, D. (2019). "Arsenic exposures, poisoning, and threat to human health: arsenic affecting human health," in *Environmental exposures and human health challenges* Pennsylvania, PA, USA (IGI Global), 86–105.

Cortes-Arriagada, D., and Ortega, D. E. (2020). Removal of arsenic from water using iron-doped phosphorene nanoadsorbents: a theoretical DFT study with solvent effects. *J. Mol. Liq.* 307, 112958. doi:10.1016/j.molliq.2020.112958

Cui, Y., Du, X., Weng, L., and Van Riemsdijk, W. H. (2010). Assessment of *in situ* immobilization of lead (Pb) and arsenic (As) in contaminated soils with phosphate and iron: solubility and bioaccessibility. *Water, Air, & Soil Pollut.* 213 (1), 95–104. doi:10.1007/s11270-010-0370-8

Deng, Y., Li, Y., Li, X., Sun, Y., Ma, J., Lei, M., et al. (2018). Influence of calcium and phosphate on pH dependency of arsenite and arsenate adsorption to goethite. *Chemosphere* 199, 617–624. doi:10.1016/j.chemosphere.2018.02.018

Esshaimi, M., Ouazzani, N., Avila, M., Perez, G., Valiente, M., and Mandi, L. (2012). Heavy metal contamination of soils and water resources Kettara abandoned mine. *Am. J. Environ. Sci.* 8 (3), 253–261. doi:10.3844/ajessp.2012.253.261

Fytas, K., and Evangelou, B. (1998). Phosphate coating on pyrite to prevent acid mine drainage. *Int. J. Surf. Min. Reclam. Environ.* 12 (3), 101–104. doi:10.1080/09208118908944031

Gallegos-Garcia, M., Ramírez-Muñiz, K., and Song, S. (2012). Arsenic removal from water by adsorption using iron oxide minerals as adsorbents: a review. *Mineral Process. Extr. Metallurgy Rev.* 33 (5), 301–315. doi:10.1080/08827508.2011.584219

Gamble, A. V., Givens, A. K., and Sparks, D. L. (2018). Arsenic speciation and availability in orchard soils historically contaminated with lead arsenate. *J. Environ. Qual.* 47 (1), 121–128. doi:10.2134/jeq2017.07.0264

Han, F. X., Banin, A., Su, Y., Monts, D. L., Plodinec, J. M., Kingery, W. L., et al. (2002). Industrial age anthropogenic inputs of heavy metals into the pedosphere. *Naturwissenschaften* 89 (11), 497–504. doi:10.1007/s00114-002-0373-4

Hughes, M. F. (2002). Arsenic toxicity and potential mechanisms of action. *Toxicol. Lett.* 133 (1), 1–16. doi:10.1016/s0378-4274(02)00084-x

Kaur, S., Kamli, M. R., and Ali, A. (2011). Role of arsenic and its resistance in nature. *Can. J. Microbiol.* 57 (10), 769–774. doi:10.1139/w11-062

Kim, H. C., Lee, J. U., Roh, Y., and Shim, Y. S. (2011). Column experiments on removal of dissolved arsenic using microorganism and nano-sized pd-akaganeite particles. *J. of Korean Society for Geosystem Engineering*. 48. 613-622 .

Kim, H. N., and Park, J. H. (2023). Concurrent sorption of antimony and lead by iron phosphate and its possible application for multi-oxyanion contaminated soil. *Environ. Sci. Pollut. Res.* 30 (9), 22835–22842. doi:10.1007/s11356-022-23800-4

Kim, Y. J., Choi, S. Y., and Kim, Y. H. (2019). Synthesis of iron oxide and adsorption of arsenic on iron oxide. *J. Environ. Sci. Int.* 28 (1), 99–106. doi:10.5322/jesi.2019.28.1.99

Kocabaş-Ataklı, Z. Ö., and Yürüm, Y. (2013). Synthesis and characterization of anatase nanoadsorbent and application in removal of lead, copper and arsenic from water. *Chem. Eng. J.* 225, 625–635. doi:10.1016/j.cej.2013.03.106

Lambkin, D. C., and Alloway, B. J. (2003). Arsenate-induced phosphate release from soils and its effect on plant phosphorus. *Water, Air, Soil Pollut.* 144, 41–56. doi:10.1023/a:1022949015848

Lenoble, V., Laclautre, C., Deluchat, V., Serpaud, B., and Bollinger, J. C. (2005). Arsenic removal by adsorption on iron(III) phosphate. *J. Hazard. Mater.* 123 (1-3), 262–268. doi:10.1016/j.jhazmat.2005.04.005

Li, H. B., Chen, X. Q., Wang, J. Y., Li, M. Y., Zhao, D., Luo, X. S., et al. (2019). Antagonistic interactions between arsenic, lead, and cadmium in the mouse gastrointestinal tract and their influences on metal relative bioavailability in contaminated soils. *Environ. Sci. Technol.* 53 (24), 14264–14272. doi:10.1021/acs.est.9b03656

Liang, Y., Cao, X., Zhao, L., and Arellano, E. (2014). Biochar-and phosphate-induced immobilization of heavy metals in contaminated soil and water: implication on simultaneous remediation of contaminated soil and groundwater. *Environ. Sci. Pollut. Res.* 21 (6), 4665–4674. doi:10.1007/s11356-013-2423-1

Liu, H., Wei, Y., Sun, Y., and Wei, W. (2005). Dependence of the mechanism of phase transformation of Fe (III) hydroxide on pH. *Colloids Surfaces A Physicochem. Eng. Aspects* 252 (2-3), 201–205. doi:10.1016/j.colsurfa.2004.10.105

Mamindy-Pajany, Y., Hurel, C., Marmier, N., and Roméo, M. (2011). Arsenic (V) adsorption from aqueous solution onto goethite, hematite, magnetite and zero-valent iron: effects of pH, concentration and reversibility. *Desalination* 281, 93–99. doi:10.1016/j.desal.2011.07.046

Martin, M. H. (2012). *Biological monitoring of heavy metal pollution: land and air*. Berlin, Germany Springer Science & Business Media.

Moon, D. H., Dermatas, D., and Menounou, N. (2004). Arsenic immobilization by calcium–arsenic precipitates in lime treated soils. *Sci. Total Environ.* 330 (1-3), 171–185. doi:10.1016/j.scitotenv.2004.03.016

Nagajyoti, P. C., Lee, K. D., and Sreekanth, T. V. M. (2010). Heavy metals, occurrence and toxicity for plants: a review. *Environ. Chem. Lett.* 8 (3), 199–216. doi:10.1007/s10311-010-0297-8

Olsen, S. R., and Watanabe, F. S. (1957). A method to determine a phosphorus adsorption maximum of soils as measured by the Langmuir isotherm. *Soil Sci. Soc. Am. J.* 21 (2), 144–149. doi:10.2136/sssaj1957.03615995002100020004x

Oremland, R. S., and Stolz, J. F. (2003). The ecology of arsenic. *Science* 300 (5621), 939–944. doi:10.1126/science.1081903

Park, J. H., Han, Y. S., and Ahn, J. S. (2016). Comparison of arsenic co-precipitation and adsorption by iron minerals and the mechanism of arsenic natural attenuation in a mine stream. *Water Res.* 106, 295–303. doi:10.1016/j.watres.2016.10.006

Payne, K. B., and Abdel-Fattah, T. M. (2004). Adsorption of divalent lead ions by zeolites and activated carbon: effects of pH, temperature, and ionic strength. *J. Environ. Sci. Health, Part A* 39 (9), 2275–2291. doi:10.1081/lesa-200026265

Priya, V. N., Rajkumar, M., Mobika, J., and Sibi, S. L. (2022). Adsorption of as (v) ions from aqueous solution by carboxymethyl cellulose incorporated layered double hydroxide/reduced graphene oxide nanocomposites: isotherm and kinetic studies. *Environmental Technology & Innovation*. 26 102268. doi:10.1016/j.eti.2022.102268

Raven, K. P., Jain, A., and Loeppert, R. H. (1998). Arsenite and arsenate adsorption on ferrihydrite: kinetics, equilibrium, and adsorption envelopes. *Environ. Sci. Technol.* 32 (3), 344–349. doi:10.1021/es970421p

Sayadi, M. H. (2014). Impact of land use on the distribution of toxic metals in surface soils in Birjand city, Iran. *Proc. Int. Acad. Ecol. Environ. Sci.* 4 (1), 18. doi:10.5277/epe180301

Sazakli, E., Zouvelou, S. V., Kalavrouziotis, I., and Leotsinidis, M. (2015). Arsenic and antimony removal from drinking water by adsorption on granular ferric oxide. *Water Sci. Technol.* 71 (4), 622–629. doi:10.2166/wst.2014.460

Schock, M. R., Scheckel, K. G., DeSantis, M., and Gerke, T. L. (2005). Mode of occurrence, treatment, and monitoring significance of tetravalent lead. *Proc. 2005 AWWA WQTC, Quebec City, Quebec*, 1–15.

Sharma, V. K., Filip, J., Zboril, R., and Varma, R. S. (2015). Natural inorganic nanoparticles–formation, fate, and toxicity in the environment. *Chem. Soc. Rev.* 44 (23), 8410–8423. doi:10.1039/c5cs00236b

Smedley, P. L., and Kinniburgh, D. G. (2002). A review of the source, behaviour and distribution of arsenic in natural waters. *Appl. Geochem.* 17 (5), 517–568. doi:10.1016/s0883-2927(02)00018-5

Soares, C. R., and Siqueira, J. O. (2008). Mycorrhiza and phosphate protection of tropical grass species against heavy metal toxicity in multi-contaminated soil. *Biol. Fertil. Soils* 44 (6), 833–841. doi:10.1007/s00374-007-0265-z

Stollenwerk, K. G. (2003). "Geochemical processes controlling transport of arsenic in groundwater: a review of adsorption," in *Arsenic in ground water* Berlin, Germany (Springer), 67–100.

Strawn, D. G. (2018). Review of interactions between phosphorus and arsenic in soils from four case studies. *Geochem. Trans.* 19 (1), 10–13. doi:10.1186/s12932-018-0055-6

Sundar, S., and Chakravarty, J. (2010). Antimony toxicity. *Int. J. Environ. Res. Public Health* 7 (12), 4267–4277. doi:10.3390/ijerph7124267

Tabelin, C. B., Corpuz, R. D., Igarashi, T., Villacorte-Tabelin, M., Alorro, R. D., Yoo, K., et al. (2020). Acid mine drainage formation and arsenic mobility under strongly acidic conditions: importance of soluble phases, iron oxyhydroxides/oxides and nature of oxidation layer on pyrite. *J. Hazard. Mater.* 399, 122844. doi:10.1016/j.jhazmat.2020.122844

Taghizadeh-Toosi, A., Clough, T. J., Sherlock, R. R., and Condron, L. M. (2012). Biochar adsorbed ammonia is bioavailable. *Plant soil* 350 (1), 57–69. doi:10.1007/s11104-011-0870-3

Tawfik, D. S., and Viola, R. E. (2011). Arsenate replacing phosphate: alternative life chemistries and ion promiscuity. *Biochemistry* 50 (7), 1128–1134. doi:10.1021/bi200002a

Theodoratos, P., Papassiopi, N., and Xenidis, A. (2002). Evaluation of monobasic calcium phosphate for the immobilization of heavy metals in contaminated soils from Lavrion. *J. Hazard. Mater.* 94 (2), 135–146. doi:10.1016/s0304-3894(02)00061-4

Tiwari, S. K., and Pandey, V. K. (2013). Removal of arsenic from drinking water by precipitation and adsorption or cementation: an environmental prospective. *Recent Res. Sci. Technol.* 5 (5), 88–91.

Walkley, A., and Black, I. A. (1934). An examination of the Degtjareff method for determining soil organic matter, and a proposed modification of the chromic acid titration method. *Soil Sci.* 37 (1), 29–38. doi:10.1097/00010694-193401000-00003

Wang, Y. M., Chen, T. C., Yeh, K. J., and Shue, M. F. (2001). Stabilization of an elevated heavy metal contaminated site. *J. Hazard. Mater.* 88 (1), 63–74. doi:10.1016/s0304-3894(01)00289-8

Weng, L., Vega, F. A., and Van Riemsdijk, W. H. (2011). Competitive and synergistic effects in pH dependent phosphate adsorption in soils: LCD modeling. *Environ. Sci. Technol.* 45 (19), 8420–8428. doi:10.1021/es201844d

Yang, J., Guo, Z., Jiang, L., Sarkodie, E. K., Li, K., Shi, J., et al. (2022). Cadmium, lead and arsenic contamination in an abandoned nonferrous metal smelting site in southern China: chemical speciation and mobility. *Ecotoxicol. Environ. Saf.* 239, 113617. doi:10.1016/j.ecoenv.2022.113617

Yu, W. H., Harvey, C. M., and Harvey, C. F. (2003). Arsenic in groundwater in Bangladesh: a geostatistical and epidemiological framework for evaluating health effects and potential remedies. *Water Resour. Res.* 39 (6), 1146–1163. doi:10.1029/2002wr001327

Yuan, Y., Chai, L., Yang, Z., and Yang, W. (2017). Simultaneous immobilization of lead, cadmium, and arsenic in combined contaminated soil with iron hydroxyl phosphate. *J. Soils Sediments* 17 (2), 432–439. doi:10.1007/s11368-016-1540-0

Zhang, T., Zeng, X., Zhang, H., Lin, Q., Su, S., Wang, Y., et al. (2019). The effect of the ferrihydrite dissolution/transformation process on mobility of arsenic in soils: investigated by coupling a two-step sequential extraction with the diffusive gradient in the thin films (DGT) technique. *Geoderma* 352, 22–32. doi:10.1016/j.geoderma.2019.05.042

Zhao, Z., Meng, Y., Yuan, Q., Wang, Y., Lin, L., Liu, W., et al. (2021). Microbial mobilization of arsenic from iron-bearing clay mineral through iron, arsenate, and simultaneous iron-arsenate reduction pathways. *Sci. Total Environ.* 763, 144613. doi:10.1016/j.scitotenv.2020.144613

Zhou, L., Yu, Q., Cui, Y., Xie, F., Li, W., Li, Y., et al. (2017). Adsorption properties of activated carbon from reed with a high adsorption capacity. *Ecol. Eng.* 102, 443–450. doi:10.1016/j.ecoleng.2017.02.036

frontiers | Frontiers in Environmental Science

TYPE Original Research
PUBLISHED 07 May 2024
DOI 10.3389/fenvs.2024.1398849

OPEN ACCESS

EDITED BY
Qi Liao,
Central South University, China

REVIEWED BY
Pei Lei,
Nanjing Normal University, China
Yanbin Li,
Ocean University of China, China

*CORRESPONDENCE
Dilinuer Aji,
dilnur@xjnu.edu.cn

RECEIVED 10 March 2024
ACCEPTED 19 April 2024
PUBLISHED 07 May 2024

CITATION
Wang K, Aji D, Li P and Hu C (2024), Characterization of heavy metal contamination in wetland sediments of Bosten lake and evaluation of potential ecological risk, China. *Front. Environ. Sci.* 12:1398849. doi: 10.3389/fenvs.2024.1398849

Characterization of heavy metal contamination in wetland sediments of Bosten lake and evaluation of potential ecological risk, China

Kai Wang[1,2], Dilinuer Aji[1,2]*, Pingping Li[1,2] and Congqiao Hu[1,2]

[1]College of Geographic Science and Tourism, Xinjiang Normal University, Urumqi, China, [2]Key Laboratory of Lake Environment and Resources in Arid Area of Xinjiang, Urumqi, China

In November 2023, twenty-two sediment samples were collected from the Bosten Lake wetland in Xinjiang to determine the concentrations of eight heavy metals: arsenic (As), cadmium (Cd), chromium (Cr), copper (Cu), mercury (Hg), nickel (Ni), lead (Pb), and zinc (Zn). This data was used to assess heavy metal contamination and potential ecological risks in the sediments using the Pollution Load Index (*PLI*) and the Potential Ecological Risk Index (*RI*). Additionally, multivariate statistical analysis and Positive Matrix Factorization (PMF) were employed to elucidate potential sources and their contributions to contamination. The following are the main conclusions: (1) average concentrations of Zn, Cd, Cr, Pb, and Hg in the sediments surpassed Xinjiang soil background levels by factors of 1.01, 3.58, 1.32, 1.94, and 1.53, respectively. (2) Sediments demonstrated severe pollution with Cd, slight pollution with Zn, Cr, Pb, and Hg, while Cu and Ni indicated mild pollution and As showed non-polluted levels. The overall *PLI* average (1.01) suggested slight contamination. (3) The descending order of average single ecological risk values were Cd, Hg, Pb, Cu, Ni, Cr, As, and Zn, with a comprehensive RI averaging at 184.07, signaling a moderate ecological risk. (4) Source apportionment revealed that Zn, Cu, Pb, and Ni were influenced by transportation and household waste emissions, while Cr and As were dictated by natural background levels. Hg predominately originated from fossil fuel combustion and Cd from agricultural activities. (5) Mixed sources accounted for the following percentage contributions to sediment heavy metal content: transportation and domestic waste (30.41%), natural background (25.88%), fossil fuel combustion (22.40%), and agricultural activities (21.31%). With anthropogenic inputs exceeding those of natural origins, it is imperative to prioritize the management of Cd, Hg, and Pb as primary pollutants within the region.

KEYWORDS

wetlands, sediment heavy metals, Xinjiang, pollution assessment, source analysis, ecological risk

1 Introduction

Heavy metals are toxic, environmentally persistent, and bioaccumulative, posing significant threats to both ecosystem integrity and human health via food chain trans-fer (Ouyang et al., 2018; Qiao et al., 2019). Recent anthropogenic discharges, particularly into aquatic ecosystems, have significantly increased the environmental burden of heavy metals (Duan and Tan, 2013; Yuan et al., 2014; Zhang et al., 2007). Within aquatic environments, heavy metals may concentrate in sediments through adsorption, complexation, flocculation, and sedimentation, and can be remobilized into the water column under changing thermal conditions (Wang E. et al., 2023).

Recognized as vital components of the planet's ecosystem, alongside forests and oceans, wetlands are instrumental in preserving biodiversity, sustaining ecological equilibrium, moderating climate, conserving water resources, flood mitigation, drought prevention, soil erosion control, and pollutant filtration (Yong, 2002; Yongze and Xuan., 2001). Lakeshore wet-lands, in particular, embody a crucial intersection between terrestrial and lake ecosystems, distinguished by exceptional productivity and biodiversity. They serve as natural barriers that retain pollutants, stabilize lake shores, and maintain regional biological diversity (Anbumozhi et al., 2005; Chai et al., 2010). The influx of heavy metals from anthropogenic sources into these wetlands poses significant environmental threats and risks (Li F. et al., 2019; Wang et al., 2019). Thus, monitoring heavy metal levels in lakeshore wetland sediments is essential for wetland health assessment, and controlling such pollution is vital for wetland conservation and restoration. Consequently, investigating pollution levels, source attribution, and potential ecological risks in these sediments is crucial for safeguarding and rejuvenating wetland environments.

Heavy metals are introduced to lakes from natural occurrences and human activities, including hydrological processes, erosion, atmospheric deposition, agricultural runoff, and industrial discharge (Merciai et al., 2014; Zhang et al., 2022; Ros et al., 2014). Most heavy metals settle in sediments, with only a minor fraction remaining dissolved in water (Liu and Dilinuer, 2014). Although extensive research covers the pollution characteristics, ecological risks, and origins of heavy metals in various ecological wetlands (Jiao et al., 2014; Ni et al., 2023; Wang X. M. et al., 2023; Kalani et al., 2021; Engin et al., 2015), arid zone wetlands have received less attention due to climatic challenges and habitat fragmentation. This study examines the western wetlands of Bosten Lake, China's largest freshwater lake in an arid region, a critical recharge zone for the Tarim River and an essential water resource for the Bayin'guoleng Mongol Autonomous Prefecture. The lake's ecological health has deteriorated due to industrial and agricultural effluents and overuse, making its wetlands, which lie at the confluence of the lake and human-inhabited areas, paramount for the ecological welfare of the lake, its biodiversity, and the livelihood of the local populace. This research enriches the understanding of heavy metal pollution in the arid wetlands of China by contributing extensive pollution data and environmental analysis, aspiring to offer scientific direction and a theoretical foundation.

2 Materials and methods

2.1 Study area

Bosten Lake (Figure 1), located in Bohu County within the southeast Yanqi Basin of the Xin-jiang Uygur Autonomous Region (441°45′–42°15′N, 86°–87°26′E), is recognized as China's largest inland freshwater lake with significant throughput. Encompassing an area of 7,710.4 km^2, the Bosten Lake basin is composed of the Kaidu River, the Peacock River basin, and extensive wetlands associated with Bosten Lake (Ye et al., 2020). Positioned at the heart of the Eurasian continent, this region experiences a pronounced inland arid cli-mate, characterized by low humidity, infrequent rainfall with an average annual precipitation of 68.2 mm, and high evapotranspiration rates between 1,800 and 2,000 mm annually. As a semi-enclosed lake with limited hydrodynamic activity, Bosten Lake has extended water retention periods and is surrounded by nearly 20,300 ha of reed wetlands, making it one of Xinjiang's two pivotal fishery hubs (Liu et al., 2017). These wetlands not only serve as critical regulators of the ecological balance in the Bosten Lake Basin but also have a direct impact on the sustainable development of the region's socio-economic environment. In recent decades, the escalating pace of economic growth within the area has led to a progressive deterioration in the water quality of the Bosten Lake wetlands.

2.2 Sample collection and processing measurements

Sediments (0–10 cm) were collected from 22 locations within Bosten Lake wetlands in November 2023 using a Peterson grab (ETC200, China). The distribution of the sampling sites is depicted in Figure 1. GPS technology was employed to accurately pinpoint all sampling sites. Subsequently, sediments were stored in clean, air-expelled, sealed polyethylene bags and maintained at low temperatures during transit. Upon arrival at the laboratory, samples underwent freeze-drying, pulverization, and sieving through a 100-mesh nylon mesh. The prepared samples were reserved for subsequent analysis.

For heavy metal determination, the samples were digested using a tetra-acid mixture (HCl-HNO_3-HF-$HClO_4$). Post-digestion, 1 mL of the clear supernatant was di-luted to 10 mL. Concentrations of heavy metals—As, Cu, Zn, Pb, Cd, Ni, and Cr—were quantified using an Agilent 7700X inductively coupled plasma mass spectrometer (ICP-MS). Hg analyses were conducted with a Hydra-C fully automated mercury analyzer (Wang et al., 2004). Prior to experimentation, all laboratory containers were acid washed with 2 mol/L HNO_3 for 24 h and rinsed thoroughly. All reagents employed were of analytical grade. To ensure the accuracy and precision of the measurement data, a standard solution established the calibration standard curve for the instruments (Hydra-C automatic mercury meter and ICP-MS). The resultant correlation coefficients (R) exceeded 0.9992, and relative standard deviations (RSDs) were below 5%, denoting reliable instrument readings. Quality control of the experimental methods was maintained by employing standard material (GBW07314) alongside sediment samples for simultaneous experiments, with recoveries calculated

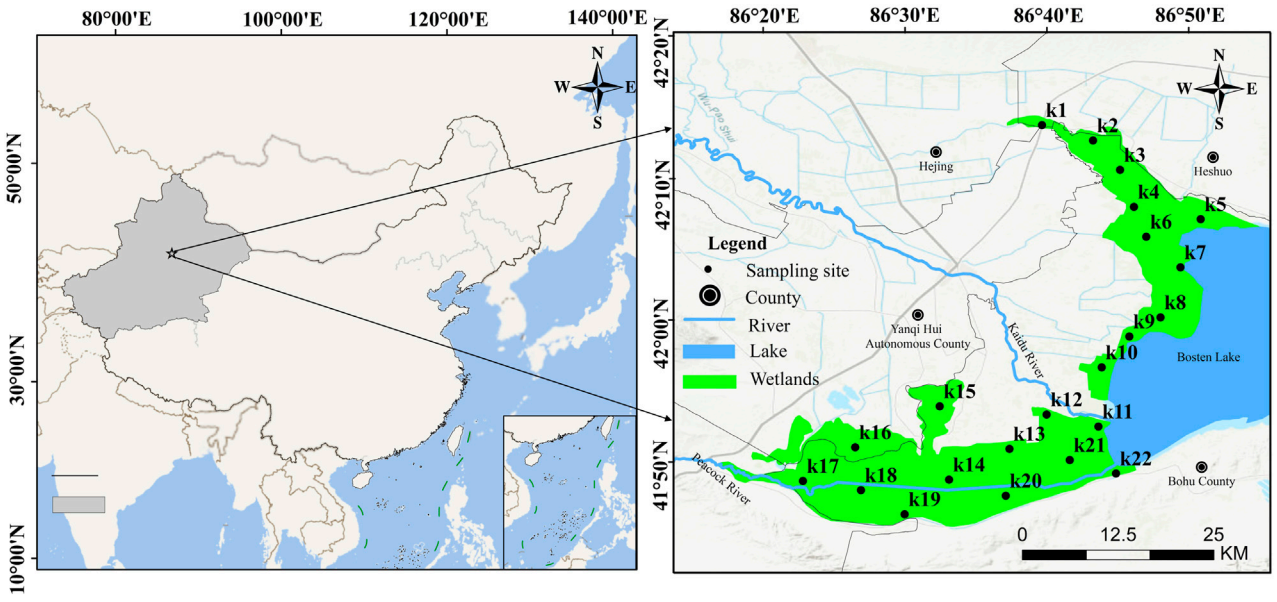

FIGURE 1
Overview of the study area.

TABLE 1 Heavy metal contamination index (CF), pollution load index (PLI) grading criteria.

CF	Level	*PLI*	Level
CF ≤0.7	No pollution	*PLI* ≤1	No pollution
0.7< *CF* ≤1	Mild pollution	1< *PLI* ≤2	Slight pollution
1< *CF* ≤2	Slight pollution	2< *PLI* ≤3	Moderate pollution
2< *CF* ≤3	Moderate pollution	*PLI* ≥3	Severe pollution
CF ≥3	Severe pollution		

by comparing standard material measurements to known values. The recoveries of heavy metals ranged from 90% to 110%, signifying that the errors introduced by heavy metals in sediment sample testing and analysis were negligible.

2.3 Pollution load index method

Pollution load index (pollution load index, PLI) is a pollution evaluation method proposed by Tomlinson et al. in the study related to the grading of heavy metal pollution level, which can express the degree of the contribution of each heavy metal to the pollution as well as the trend of the spatial and temporal changes of the heavy metal (Tomlinson et al., 1980), which is calculated by the formula:

$$CF_i = c_i / c_n \quad (1)$$

$$PLI = \sqrt[n]{CF_1 \times CF_2 \times \cdots CF_n} \quad (2)$$

formula CF_i is the pollution index of heavy metal i; c_i is the test concentration of heavy metal i; c_n is the evaluation standard of heavy metal i. In this study, the background value of Xinjiang soil was used as the evaluation standard. The pollution grading standards of *CF* (NY/T 395-2000) and *PLI* (Li et al., 2015) are shown in Table 1.

2.4 Potential ecological risk index methodology

The Potential Ecological Risk Index method proposed by Hakanson was used to evaluate the potential ecological risk of sediment heavy metals in the study area (Hakanson, 1980). The potential ecological risk index (*RI*)can reflect the pollution level of individual heavy metal elements and also express the joint effect of all heavy metal elements participating in the selection. The formulas for the potential ecological risk index E_j^i for a single heavy metal element and the combined potential ecological risk index RI_j for several heavy metal elements are as follows:

$$RI_j = \sum_{i=1}^{n} E_j^i = \sum_{i=1}^{n} T^i \times C_j^i = \sum_{i=1}^{n} T_i \times \frac{c_j^i}{c_r^i} \quad (3)$$

formula: RI_j is the potential ecological risk index of heavy metals in sample point j; E_j^i is the potential ecological risk index of heavy metal i in sample point j; C_j^i is the pollution index of heavy metal i in sample point j; c_j^i is the measured concentration of heavy metal i in soil in sample point j; and c_r^i is the reference value of heavy metal i (the background value of soil elements in Xinjiang was used as the reference value) (Zheng, 2017); T^i is the toxicity coefficient of heavy metal i, reflecting the response of heavy metals in the aqueous, solid and biological phases, which can comprehensively reflect the toxicity of heavy metals, the pollution level and the sensitivity of pollution (the toxicity coefficients of heavy metals As, Cd, Cr, Cu, Hg, Ni, Pb, and Zn are 10, 30, 2, 5, 40, 5, 5, 5, and 1, respectively). Risk level grading criteria are shown in Table 2.

TABLE 2 Heavy metal ecological hazard factor (E), ecological risk index (RI) grading criteria.

E	RI	Level
$E \leq 40$	$RI \leq 150$	negligible risks
$40 < E \leq 80$	$150 < RI \leq 300$	moderate risks
$80 < E \leq 160$	$300 < RI \leq 600$	significant risks
$160 < E \leq 320$	$600 < RI \leq 1{,}200$	high level of risk
$E > 320$	$RI > 1{,}200$	extremely high level of risk

2.5 Potential ecological risk index methodology

Positive definite matrix factor analysis model (PMF) is a quantitative pollution source factor analysis method based on multivariate statistical techniques (Taghvaee et al., 2018).

$$x_{ij} = \sum_{k=1}^{p} g_{ik} f_{kj} + e_{ij} \tag{4}$$

$$Q = \sum_{i=1}^{n}\sum_{j=1}^{m}\left(\frac{e_{ij}}{u_{ij}}\right)^2 \tag{5}$$

$$u_{ij} = \begin{cases} \frac{5}{6} \times \mathrm{MDI}, x_{ij} \leq \mathrm{MDI} \\ \sqrt{(p \cdot C)^2 + (\mathrm{MDI})^2}, x_{ij} > \mathrm{MDI} \end{cases} \tag{6}$$

Where: x_{ij} is the content of metal j in sample i, g_{ik} is the contribution of pollutant k in sample i, f_{kj} is the eigenvalue of pollutant k to the content of heavy metal j, e_{ij} is the residual matrix, u_{ij} is the uncertainty of metal j in sample i, p is the relative standard deviation, C is the measured concentration of the heavy metal, and MDL is the detection limit.

2.6 Data analysis

Data processing was performed using Microsoft Excel, while the two-dimensional spatial distribution mapping of features was conducted with ArcGIS 10.8. Origin2021 software facilitated the normal distribution testing and correlation analysis of the data. Moreover, EPA PMF5.0 software assisted in pinpointing potential anthropogenic sources of heavy metals in the sediment samples.

3 Results and discussion

3.1 Descriptive statistics of heavy metals in wetlands

Table 3 presents the descriptive statistics for heavy metal concentrations in sediment samples, including the range, mean, median, standard deviation, coefficient of variation (CV), skewness, and kurtosis. On average, the concentrations for Zn, Cr, Pb, Cu, Ni, As, Cd, and Hg were 69.82, 65.00, 37.63, 25.63, 22.14, 1.70, 0.43, and 0.026 mg/kg, respectively. When compared to the background values of soil elements in Xinjiang, the levels of As were lower in all sampled sites. In contrast, the concentrations of Cd and Pb were higher, peaking at 5.5 and 4.1 times above the background values, respectively. Although the median and mean concentrations of Ni and Cu did not surpass the background levels, their maximum concentrations did, reaching 1.5 and 2.3 times higher, respectively. The median and mean levels of Zn, Cr, and Hg exceeded the background values, while their minimum concentrations did not. The exceedance rates for Pb, Cd, and Cr were 100%, 95.46%, and 68.18%, respectively, suggesting that these may be the primary contaminants in the wetland sediments. The CVs for Zn, Pb, and Ni were classified as medium variability at 33.11%, 31.34%, and 30.07%, respectively ($15\% < CV < 35\%$). In comparison, As, Cd, Cr, Cu, and Hg exhibited high variability with CVs of 75.59%, 40.11%, 38.90%, 55.54%, and 57.82%, respectively ($CV > 36\%$). This high variability indicates an uneven spatial distribution and the potential influence of point source pollution. According to skewness, the rank of the eight heavy metals was Pb > Cd > Zn > Hg > As > Ni > Cu > Cr. With all kurtosis values below 3, the data distribution for these metals is broadly platykurtic.

When compared to the average concentrations of heavy metals in sediments from the Zhanjiang Mangrove Wetlands, the Medeca Wetlands, the Setiu Wetland, the Uchalli Wetland,

TABLE 3 Descriptive statistics of heavy metals in sediments.

Elemental	Range (mg/kg)	Mean (mg/kg)	Median	SD	CV (%)	Kurtosis	Skewness	Proportion (%)	Background value (mg/kg)
Zn	34–142	69.82	67.5	23.11	33.11	1.33	3.50	45.46	68.8
As	0.49–5.43	1.70	1.23	1.29	75.59	1.94	3.33	0	11.2
Cd	0.17–0.66	0.43	0.40	0.17	40.11	1.67	4.41	95.46	0.12
Cr	32–117	65.00	57.00	25.28	38.90	0.78	−0.46	68.18	49.3
Cu	7–62	25.63	22.00	14.24	55.54	0.94	0.43	36.36	26.7
Pb	20–79	37.63	37.00	11.79	31.34	2.09	6.85	100.00	19.4
Hg	0.006–0.05	0.026	0.025	0.015	57.82	1.51	3.49	31.82	0.017
Ni	11–40	22.14	21.00	6.66	30.07	0.99	1.36	22.73	26.6

TABLE 4 Comparison of mean values of heavy metals in sediments of Bosten Lake wetland with sediments of other wetlands (mg/kg).

Region	Zn	As	Cd	Cr	Cu	Pb	Hg	Ni	reference
Bosten Lake wetland, China	69.82	1.70	0.43	65.00	25.63	37.63	0.026	22.14	This study
Mangrove Wetlands, China	67.85	9.78	0.04	28.71	25.90	20.64	0.09	96.44	Luo et al. (2019)
Medeca wetlands, China	82.31	21.62	0.14	56.84	15.08	21.23	0.04	21.08	Li et al. (2022)
Setiu wetland, Malaysia	6.22	4.37	0.06	16.16	4.94	5.79	—	4.04	Rasendra et al. (2021)
Uchalli Wetland, Pakistan	0.51	25.34	0.29	0.25	0.09	0.13	—	0.22	Bhatti et al. (2019)
East Kolkata Wetlands, India	28.87	5.79	0.42	7.10	7.12	4.32	0.23	4.53	Kumar et al. (2023)

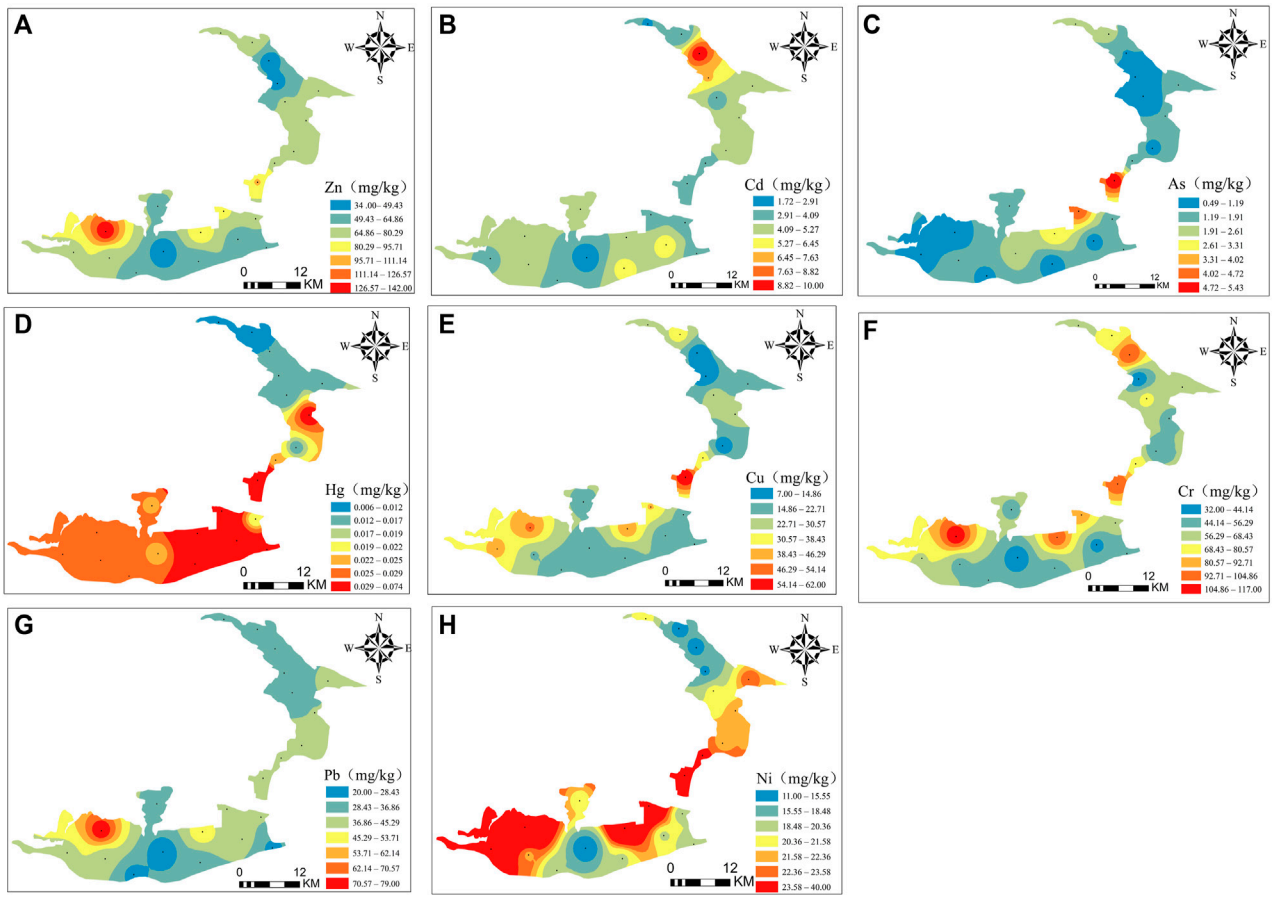

FIGURE 2
Spatial distribution map of heavy metals in wetlands. **(A–H)** represent (Zn, Cd, As, Hg, Cu, Cr, Pb, Ni), respectively.

and the East Kolkata Wetlands, the contents of Ni and Cu in the Bosten Lake wetland sediments were found to be lower than those of the Zhanjiang Mangrove Wetlands but markedly higher than those in the remaining wetlands (Table 4). Moreover, levels of As, Cd, Pb, and Cr were significantly elevated compared with those of all five referenced regions. Zn concentrations were only exceeded by those in the Medeca Wetlands, and Hg levels were only outstripped by measurements from the East Kolkata Wetlands. Overall, the heavy metal concentration in the sediments of Bosten Lake's wetlands is characterized by an intermediate to high level.

3.2 Characteristics of spatial distribution of heavy metal content in wetland sediments

This study utilized inverse distance interpolation to visualize the spatial distribution of eight heavy metals in the wetland sediments of Bosten Lake (Figure 2). The distribution patterns for Hg and Ni were similar, showcasing consistently elevated values in the wetland's southern section and at the Kaidu River inlet, while levels in the north were notably lower. Zn, Cu, and Pb concentrations, with the exception of Cr, were reduced in the northern region; Cd concentration peaks were mainly found in the wet-land's northern extents, whereas As

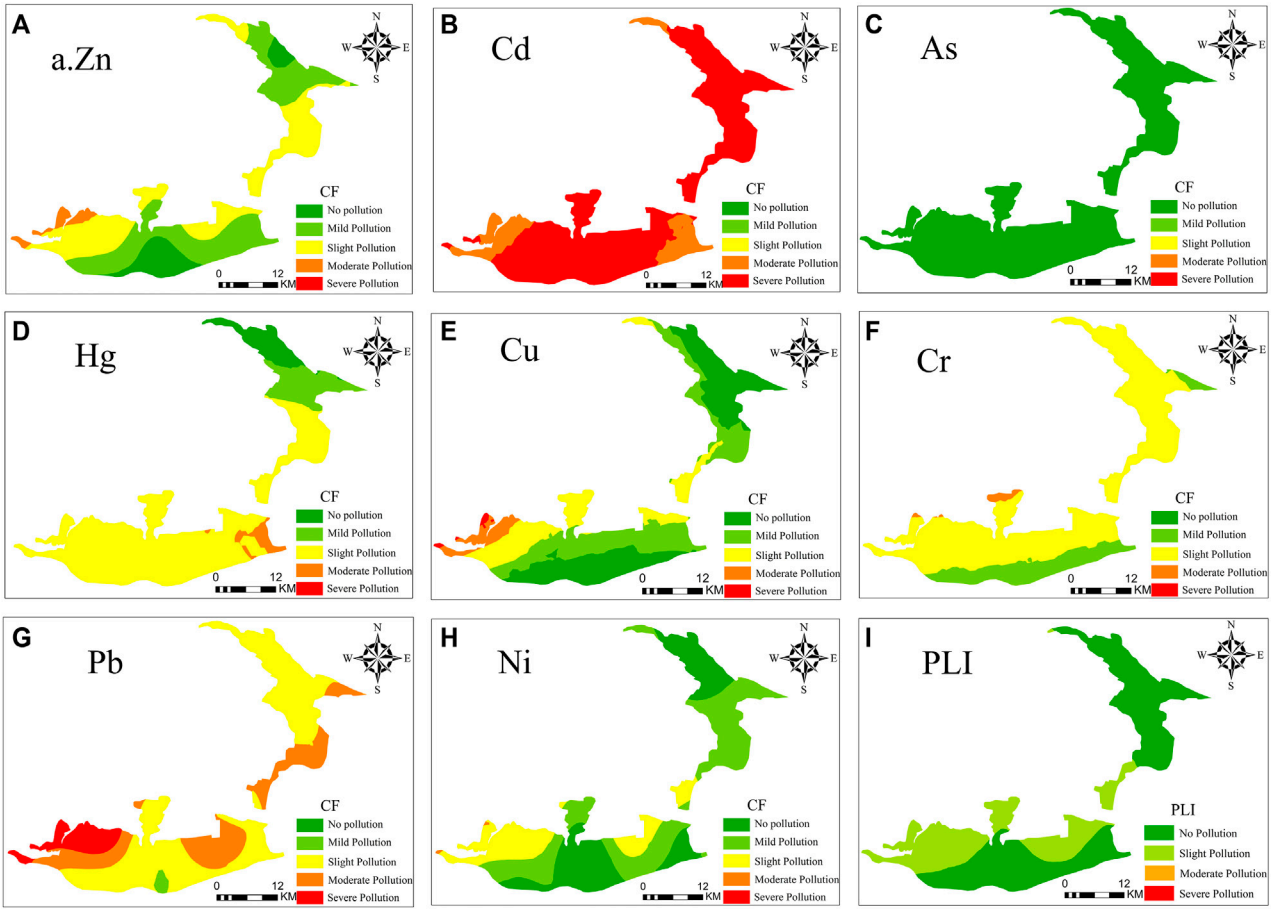

FIGURE 3
Spatial distribution of CF **(A–H)** for (Zn, Cd, As, Hg, Cu, Cr, Pb, and Ni, respectively) and PLI **(I)** in soil heavy metals from wetland sediments in Bosten Lake.

exhibited high concentrations primarily at the Kaidu River inlet. Field observations revealed that the hotspots for heavy metal accumulation are predominantly situated near traffic routes, river inlets, agricultural lands, and the Bosten Lake tourist area. These areas experience significant human activity, and it is likely that pollutants from vehicular traffic and agricultural runoff are con-tributing to the wetland's contamination.

3.3 Spatial variation in heavy metal contamination of sediments

Sediments exhibit natural spatial variability, and thus the heavy metal content from a specific sampling point reflects the environmental conditions of that site alone. The Kriging technique was employed to map the spatial distribution patterns of heavy metal contamination across the sediment. Figure 3 demonstrates these patterns using both the contamination factor (CF) (Figures 3A–H) and pollution load index (PLI) (Figure 3I) for Bosten Lake wetlands. Notably, Figure 3 illustrates that the spatial distribution patterns of the environmental risks, indicated by individual pollution indices for the eight studied heavy metals, vary considerably. Cd is characterized by the highest degree of pollution and the most extensive contaminated area, generally classified as moderate to severe pollution. Pb ranks second in terms of pollution extent and intensity, predominantly displaying regional pollution symptomatic of moderate contamination, except for the southern wetland fringe where a small segment falls within the heavily polluted bracket. Cr and Hg both primarily reflect low levels of pollution, yet their spatial distribution is markedly distinct. Cr decreases in pollution degree from north to south, with light pollution sporadically positioned along the southern border. Conversely, Hg pollution intensifies in the same direction. The pollutants Cu, Ni, and Zn exemplify a parallel arrangement of light pollution, minor pollution, and unpolluted zones–with the majority of the study area experiencing minor to no pollution and light pollution centering around the Kaidu River mouth and the southern periphery of the wetland. As, in contrast, shows no detectable pollution throughout the study area.

The mean pollution index values for each heavy metal in the wetland sediments of Lake Bosten, presented in descending order, are as follows: Cd (3.62), Pb (1.94), Hg (1.55), Cr (1.32), Zn (1.01), Cu (0.96), Ni (0.83), and As (0.15). According to these indices, Cd is classified as severely polluted; Pb, Hg, Cr, and Zn as moderately polluted; Cu and Ni as mildly polluted; and As unpolluted. The analysis of sample point distributions across varying pollution levels (Table 5) reveals that 100% of sampling points for As fall under non-

TABLE 5 Proportion (%) and statistical analysis of the number of sample points with different pollution levels of CF and PLI in the wetlands of Lake Bosten.

Elemental	No pollution	Mild pollution	Slight pollution	Moderate pollution	Severe pollution	Mean
Zn	13.64	40.91	40.91	4.55	0	1.01
As	100	0	0	0	0	0.15
Cr	9.09	22.73	50.00	18.18	0	1.32
Cu	36.36	27.27	31.82	4.55	0	0.96
Pb	0	0	63.64	31.82	4.55	1.94
Hg	9.09	22.73	40.91	22.73	4.55	1.55
Ni	27.27	54.55	18.18	0	0	0.83
Cd	0	0	4.55	31.82	63.64	3.62
PLI	No pollution	Mild pollution	Max	Min	mean	
	68.19	31.81	1.75	0.62	1.01	

pollution. In contrast, the percentages of sampling points with slight, moderate, and severe pollution levels for Cd are 4.55%, 31.82%, and 63.64%, respectively. Most sampling points for Cr, Pb, and Hg show slight pollution at 50.00%, 63.64%, and 87.37%, respectively, with a smaller proportion at 40.91% for Cr. Zn contamination is largely characterized by mild or slight pollution, each accounting for 40.91%. Ni predominantly exhibits mild pollution, representing 54.55% of sampling points, whereas Cu displays regional pollution variation, with non-polluted, slight, mild, and moderate contamination levels constituting 36.36%, 27.27%, 31.82%, and 4.55% of points, respectively.

From the Bosten Lake wetland sediment heavy metal pollution load index (PLI) varied between 0.62 and 1.75, with an average value of 1.01, showing mild pollution. The number of sample points with PLI belonging to no pollution and mild pollution accounted for 68.19% and 31.81% of the total number of sample points, respectively. In terms of spatial distribution (Figure 3I), light pollution was mainly distributed in the river inlet and the southern edge area of the wetland, while the northern part of the wetland was less polluted and dominated by no pollution.

The sediments of Bosten Lake, along with those from various other regions, display the most pronounced heavy metal contamination for Cd, Pb, and Hg. Research conducted by Jane Yuefeng and colleagues (Jian et al., 2023) on the wetlands surrounding the Bohai Sea identified exceptionally high levels of single-factor pollution of Cd and Hg. Similarly, studies by Yang Pan et al. (Yang et al., 2021) on Chaohu Lake revealed that the mean concentrations of Cd and Hg significantly exceeded the soil background levels in Anhui Province, with the risk index for Cd reaching a level indicative of serious pollution, thereby constituting the primary pollutant. Further studies by Zhou Feng et al. (Zhou et al., 2023) on Longyang Lake and Moshui Lake in Wuhan City indicated that Cd was the predominant contributor to heavy metal pollution and ecological risk, with the sediment cumulative index method suggesting a state of moderate pollution in these lakes. These high levels of contamination are attributable to China's status as a major agricultural nation where crop cultivation often occurs near water bodies and the widespread use of conventional fertilizers, which can lead to Cd pollution in the sediments of lakes, rivers, and wetlands.

3.4 Potential ecological risks and regional differences in wetland sediment contamination

The single and comprehensive potential ecological risk indices (E and RI, respectively) for heavy metals in the wetland sediments of Bosten Lake were assessed at each sampling location. In the Xinjiang region, the background values for river sediments are not yet well-established; therefore, this study has opted to employ the available soil background values as a reference. The assessment was conducted according to Hakanson's criteria for potential ecological risk. The average values of the individual potential ecological risk indices for heavy metals in the sediments, arranged in descending order of risk, were as follows (Table 6): Cd (108.53), Hg (61.93), Pb (9.70), Cu (4.80), Ni (4.16), Cr (2.64), As (1.52), and Zn (1.01). Ecological risk levels for Zn, As, Cr, Pb, Ni, and Cu were negligible across all sampling sites. However, Cd exhibited a predominantly significant risks level, with 68.18% of the sampling points falling into this category. The risk index for Hg varied regionally, with negligible, moderate, significant, and high risk levels represented by 36.36%, 40.91%, 18.18%, and 4.55% of the total sampling points, respectively. Consequently, Cd and Hg represent the primary ecological risk concerns for heavy metals in the wetland sediments of Bosten Lake.

The average value of the integrated potential ecological risk index (RI) for heavy metal pollution in the wetland sediments of the Bosten Lake Basin was 184.07, signifying a moderate ecological risk. The variation ranged from 99.23 to 288.16. Respectively, 22.73% of the sample points faced a slight risk, while 77.27% faced a moderate risk. According to Hakanson's evaluation criteria, the predominant potential ecological risk within the study area was moderate, with no incidents of high or severe ecological risk detected. The spatial distribution pattern of RI, illustrated in Figure 4, reveals that RI is unevenly dispersed, with negligible risks identified along the edge of the northern wetland and moderate risks prevalent in all other regions. A comparison of the spatial distribution patterns of Cd and Hg contents shows a correlation between the areas at moderate RI risk and the areas with elevated levels of Cd and Hg. This indicates

TABLE 6 Proportion (%) and statistical analysis of the number of sample points of different risk levels in the wetland sediments of Lake Bosten in relation to the total number of sam-ple points.

E	Negligible risks	Moderate risks	Significant risks	High level of risk	Mean
Zn	100	0	0	0	1.01
As	100	0	0	0	1.52
Cr	100	0	0	0	2.64
Cd	0	22.73	68.18	9.09	108.53
Pb	100	0	0	0	9.70
Hg	36.36	40.91	18.18	4.55	61.93
Ni	100	0	0	0	4.16
Cu	100	0	0	0	4.80
RI	negligible risks	moderate risks	Max	Min	mean
	22.73	77.27	288.16	99.23	184.07

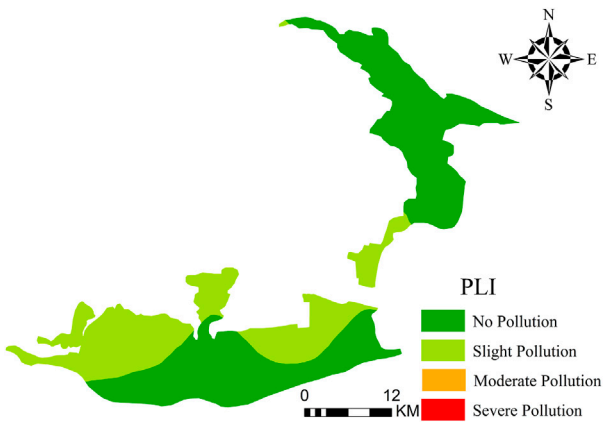

FIGURE 4
Potential ecological risk distribution of sediment heavy metal synthesis in Lake Bosten wetland.

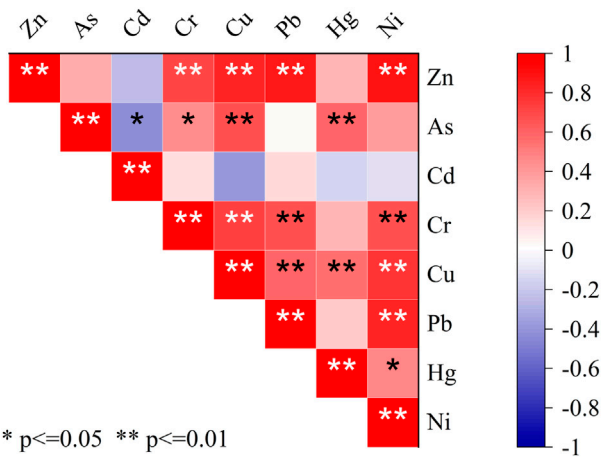

FIGURE 5
Sediment heavy metal correlation heat map.

that Cd and Hg are the principal contributors to the moderate risk level. Due to its higher toxicity coefficient, Cd poses a greater ecological hazard and has a larger impact on ecological risks.

3.5 Analysis of the sources of heavy metal pollution in wetland sediments of Bosten Lake

3.5.1 Correlation analysis of heavy metal elements in sediments

Correlation analysis and principal component analysis can be used to identify the sources of heavy metals in sediments. The results of correlation analysis among heavy metals showed that (Figure 5), sediment Ni in the study area showed highly significant positive correlation with Cr, Cu, Pb ($p < 0.01$), and significant positive correlation with Hg ($p < 0.05$); Hg showed highly significant positive correlation with As, Cu; Cu showed highly significant positive correlation with Zn, As, and Cr; Pb showed highly significant positive correlation with Cr, Cu, and Zn, and significant positive correlation with Zn; Cd showed significant negative correlation with As; and Cd showed significant negative correlation with As. Pb was positively correlated with Cr, Cu and Zn, Cr was positively correlated with Zn, Cr was positively correlated with Zn, and As was positively correlated with As; Cd was negatively correlated with As. The strong correlation between the heavy metal elements suggests that these elements may have com-mon anthropogenic and natural sources of pollution.

3.5.2 Principal component analysis (PCA) of heavy metal elements in sediments

Principal component analysis (PCA) was conducted to elucidate the sources of heavy metal pollution in the study area, thereby extending the insights gained from correlation analysis (Han et al., 2022). The Kaiser-Meyer-Olkin (KMO) statistic and Bartlett's test of sphericity were employed to verify the suitability of PCA for the heavy metal distribution data across eight sediment samples. With a KMO value of 0.706 and a sphericity test yielding a significance level of zero, the results confirmed that the heavy metal elements were

TABLE 7 Principal component analysis of heavy metals in sediments.

Elemental	PC1	PC2	PC3	PC4
Zn	0.935	0.236	−0.211	0.058
As	0.044	0.771	−0.351	0.468
Cd	−0.024	−0.096	0.985	−0.063
Cr	0.644	0.697	0.248	0.021
Cu	0.661	0.55	−0.311	0.309
Pb	0.964	0.011	0.179	0.037
Hg	0.182	0.203	−0.047	0.952
Ni	0.885	0.187	−0.07	0.319
eigenvalue	3.475	1.525	1.335	1.331
variance contribution/%	43.433	19.062	16.691	16.641
Cumulative contribution/%	43.433	62.496	79.187	95.828

interrelated rather than independent, meeting the necessary prerequisites for PCA. Subsequent PCA with varimax rotation on the dataset identified four principal components with eigenvalues of 3.475, 1.525, 1.335, and 1.331, cumulatively accounting for 95.828% of the variance in data; these findings substantively under-score the sources of heavy metal pollution in the region, detailed in Table 7.

The contribution of the first component (PC1) was 43.433%, in which four elements, Zn, Cu, Pb and Ni, had high loading values, indicating that the five heavy metal elements in the wetland sediments for Lake Bosten had similar sources. Against the results of descriptive statistics (Table 1), the mean values of Zn, Cu, and Ni were close to or slightly larger than the background values for Xinjiang soils, and the correlation between these elements was also strong (Figure 5), with a consistent pattern of contamination distribution (Figure 3). It has been shown that the main sources of Cu, Ni, and Zn are industrial activities, agriculture, and domestic garbage discharge, etc. (Wang et al., 2022), and the settlements around the wetland were distributed in the edge of the wetland in a point-like manner, and at the same time, with the development of the tourism industry, the tourists have little awareness of environmental protection, and the frequent discharge of domestic sewage affects the concentration of the heavy metals to a certain degree, and at the same time, Pb was identified as the transportation source, and the wetland sampling process found that transportation routes surrounded the edge of the wetland. During the wetland sampling process, it was found that the major transportation routes surrounded the edge of the wetland. Since the 1970s, the use of leaded gasoline has been restricted globally, but it is still an important source of lead pollution (Del Rio-Salas et al., 2012; Zhu et al., 2001), while some local villagers still keep the leaded gasoline vehicles as a means of agricultural transportation, which suggests that PC1 is a mixed source of transportation and domestic waste emissions.

The contribution of the second component (PC2) was 19.062%, in which As and Cr had high positive loadings, and the loadings of As were significantly higher than those of Cr. The study showed that Cr and As were significantly correlated with soil-forming matrices, soil-forming processes and geological activities (Zhang et al., 2022; Li W. D. et al., 2019), and the correlation between Cr and As was significant, and the contents of As in all the sample sites were much smaller than the background values of Xinjiang soils. Some studies have shown that As is significantly correlated with natural soil-forming matrices or soil-forming processes, but natural leaching causes the whole As content in the surface soil to be continuously exported, which results in the topsoil As content being lower than the background value (Zhao et al., 2022; Chen et al., 2022), suggesting that PC2 is a natural background source, in addition to which the mean value of Cr is slightly greater than the background value of Xinjiang soils, and it also occupies a larger proportion in PC1, suggesting that in addition to the No. 1 matrices source, Cr is also affected by the transportation and domestic waste emission sources, which is also similar to the results of Maimaiti Tursun's study in the cultivated area of Bosten Lake (Maimaitituerxun et al., 2017).

With a 16.345% contribution to variance, PC3 includes solely Cd with notably high positive loading, indicative of a distinctive and singular pollution profile. Cd's significant negative correlation with As and a concentration notably exceeding the regional background for soils point towards its isolated behavior. Research denotes Cd as a signature element of agricultural activities, where the prolonged misuse of agricultural inputs, such as fertilizers, culminates in Cd accumulation, harmonized with mechanical wear from agricultural machinery contributing to Cd-laden soil deposition (Zhang et al., 2018; Hu et al., 2022). The prevalence of farmland cultivating chili peppers around the study zone, alongside the rising scale and intensity of agricultural practices, affirms agricultural input as a principal factor for Cd enrichment in sediment, categorizing PC3 predominantly as an agricultural activities source.

Finally, the fourth principal component (PC4), also contributing 16.345% to the variance, revealed a significant positive loading exclusively for Hg. Hg enrichment correlates with coal combustion and non-ferrous metal smelting as primary pollution sources (Wang et al., 2021) Considering the Xinjiang locale, characterized by a temperate continental climate and coal-dependent heating practices among residents, atmospheric deposition and surface runoff are the main pathways for Hg-laden particles and gases to reach and accumulate in sediments, identifying PC4 as indicative of fossil fuel combustion.

3.5.3 Positive Matrix Factorization (PMF) model

The origins of Zn, As, Cd, Cr, Cu, Pb, Hg, and Ni pollution were investigated by employing the Positive Matrix Factorization (PMF) model. After numerous iterations, the optimal number of factors was determined to be four, as shown in Figure 6A. PMF revealed four pollution sources for the heavy metals under scrutiny. Zn, Cu, Pb, and Ni predominantly originated from mixed sources of transportation and domestic waste emissions, with contribution rates to Factor 1 of 51.50%, 50.70%, 41.5%, and 40.30%, respectively. Hg was primarily attributed to fossil fuel combustion, contributing 71.4% to Factor 3. Cd was linked to agricultural activities, with a 71.8% contribution to Factor 4. As and Cr largely emanated from natural sources, with As contributing 80.60% to Factor 2 and Cr showing significant contributions of 40.20% and 31.70% to Factors 1 and 2, respectively. This aligns with PCA findings, corroborating the presence of mixed traffic and

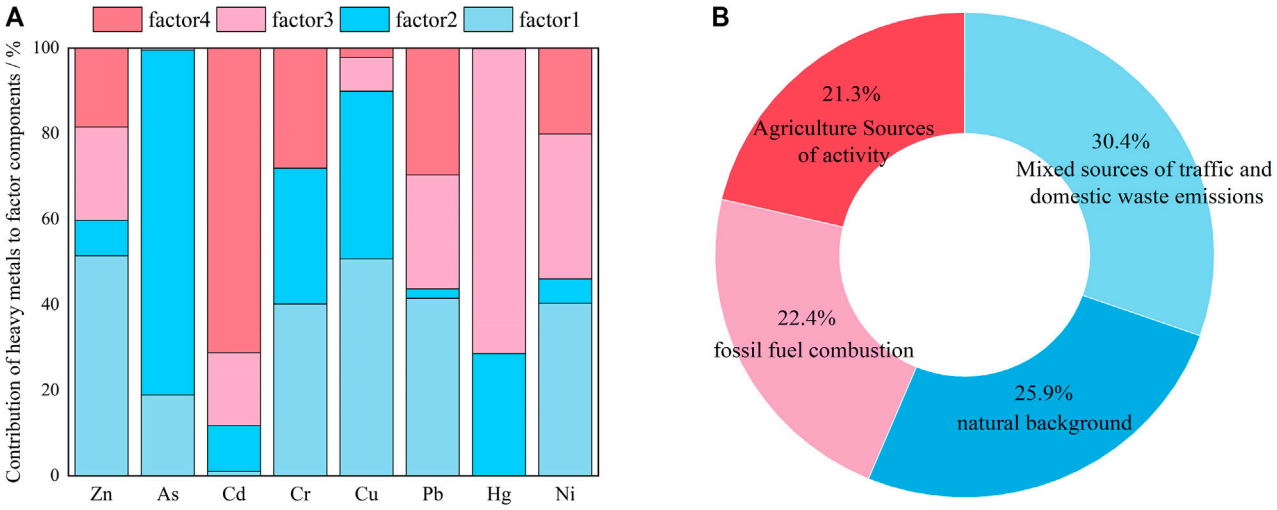

FIGURE 6
Sediment heavy metal PMF analysis pollution source composition spectrum **(A)** and its component contribution **(B)**.

domestic waste emissions in addition to natural sources for Cr. Consequently, Factor 2 is likely a natural source.

Considering the overall contribution to heavy metal pollution in sediments across the study area (Figure 6B), mixed transportation and domestic waste discharges, natural sources, fossil fuel combustion, and agricultural activities accounted for 30.41%, 25.88%, 22.40%, and 21.31% of the pollution, respectively. This implies that anthropo-genic sources in the Lake Bosten Wetland sediments have a more substantial impact than natural sources.

4 Conclusion

The average values of Zn, Cd, Cr, Pb and Hg in the sediments of Lake Bosten are higher than the background values of soil elements in Xinjiang, and As, Cu and Ni are lower than the background values of soil.

The spatial distribution pattern of environmental risks reflected by the CF values of eight heavy metals in the wetland sediments of Bosten Lake is different, and the order of the average CF values of each heavy metal element is as follows: Cd > Pb > Hg > Cr > Zn > Cu > Ni > As, Cd belongs to the heavy pollution and contamination, Pb, Hg, Cr, and Zn are mildly contaminated, Cu and Ni are mildly contaminated, and As is not contaminated. Cd, Pb, Hg are polluted areas and high degree of pollution and Hg are polluted area and high degree of pollution, which to some extent increased the degree and scope of heavy metal pollution in wet-land sediments in the study area. The mean value of heavy metal PLI in farmland soil in the study area showed mild pollution.

The mean values of the potential ecological risk indices of each heavy metal in the wetland sediments of Lake Bosten were in the following order: Cd > Hg > Pb > Cu > Ni > Cr > As > Zn. The mean value of the RI in the study area showed moderate ecological risk.

The homology of Zn, Cu, Pb and Ni in the wetland sediments of Bosten Lake is significant, mainly originating from the mixed sources of transportation and domestic garbage discharge; As and Cr are mainly influenced by the natural parent material; Hg mainly originates from fossil combustion; and Cd mainly originates from agricultural activities.

The sources of heavy metal pollution in the sediments of Bosten Lake wetland can be categorized into four types, i.e., mixed sources of traffic and domestic waste discharge, natural parent sources, fossil combustion, and sources of agricultural activities, which contributed 30.41%, 25.88%, 22.40%, and 21.31% to the enrichment of soil heavy metals, with anthropogenic sources contributing more than the natural sources, respectively.

Agricultural activities should be carried out scientifically, the management of discharges from recreational spots should be strengthened, and coal combustion and traffic emissions should be rationalized, so as to ensure the safe use of the wetlands of Lake Bosten and consolidate the ecological environment barrier of the Lake Bosten wetlands.

Data availability statement

The original contributions presented in the study are included in the article/Supplementary material, further inquiries can be directed to the corresponding author.

Author contributions

KW: Writing–original draft, Conceptualization, Data curation, Investigation, Methodology, Project administration, Resources, Software, Validation, Visualization, Writing–review and editing. DA: Funding acquisition, Writing–review and editing. PL: Investigation, Writing–review and editing. CH: Supervision, Writing–review and editing.

Funding

The author(s) declare that financial support was received for the research, authorship, and/or publication of this article. This project was funded by the National Natural Science Foundation Program (42361006).

Acknowledgments

We thank the reviewers for their constructive comments and suggestions that have helped to improve the original manuscript. Thanks are also due to the editorial staff.

Conflict of interest

The authors declare that the research was conducted in the absence of any commercial or financial relationships that could be construed as a potential conflict of interest.

Publisher's note

References

Anbumozhi, V., Radhakrishnan, J., and Yamaji, E. (2005). Impact of riparian buffer zones on water quality and associated management considerations. *Ecol. Eng.* 24 (5), 517–523. doi:10.1016/j.ecoleng.2004.01.007

Bhatti, S. G., Tabinda, A. B., Yasin, F., Mehmood, A., Salman, M., Yasar, A., et al. (2019). Ecological risk assessment of metals in sediments and selective plants of Uchalli Wetland Complex (UWC)-a Ramsar site. *Environ. Sci. Pollut. Res. Int.* 26 (19), 19136–19152. doi:10.1007/s11356-019-04711-3

Chai, P. H., Dai, Y. R., Liang, W., Chen, S. P., and Wu, Z. B. (2010). Progress of ecological restoration research in the lakeshore zone. *Chin. Acad. Eng. Sci.* 12 (06), 32–35.

Chen, M., Peng, Y. X., Huang, Y. X., and Zhang, R. D. (2022). Spatial distribution characteristics and source analysis of soil heavy metals in watersheds of typical lead-zinc mining areas in Yangshuo, China. *Environ. Sci.* 43 (10), 4545–4555. doi:10.13227/j.hjkx.202201127

Del Rio-Salas, R., Ruiz, J., De la O-Villanueva, M., Valencia-Moreno, M., Moreno-Rodríguez, V., Gómez-Alvarez, A., et al. (2012). Tracing geogenic and anthropogenic sources in urban dusts: insights from lead isotopes. *Atmos. Environ.* 60, 202–210. doi:10.1016/j.atmosenv.2012.06.061

Duan, J., and Tan, J. (2013). Atmospheric heavy metals and Arsenic in China: situation, sources and control policies. *Atmos. Environ.* 74, 93–101. doi:10.1016/j.atmosenv.2013.03.031

Engin, M. S., Uyanik, A., and Kutbay, H. G. (2015). Accumulation of heavy metals in water, sediments and wetland plants of kizilirmak delta (samsun, Turkey). *Int. J. Phytoremediation* 17, 66–75. doi:10.1080/15226514.2013.828019

Hakanson, L. (1980). An ecological risk index for aquatic pollution control. A sedimentological approach. *Water Res.* 14 (8), 975–1001. doi:10.1016/0043-1354(80)90143-8

Han, C. L., Luo, B. S., Chang, C. Y., Deng, Y. R. ., Xiong, J., and Wang, J. (2022). Analysis of the causes of heavy metal pollution in regional agricultural soils based on multiple methods. *J. Ecol. Rural Environ.* 38 (02), 176–183. doi:10.19741/j.issn.1673-4831.2021.0178

Hu, J., Zhao, X. Y., Wang, T. T., Gou, K. X., and Wang, C. L. (2022). Characterization, evaluation and source analysis of heavy metal distribution in soil of fen river riparian zone in taiyuan city, China. *Environ. Sci.* 43 (05), 2500–2509. doi:10.13227/j.hjkx.202107258

Jian, Y. F., Yue, F. J., Zhu, Z. Z., Liu, X. L., and Zhang, Y. L. (2023). Analysis of spatial and temporal changes and sources of heavy metals in coastal wetlands around the Bohai Sea. *China Environ. Sci.* 43 (11), 6025–6038. doi:10.19674/j.cnki.issn1000-6923.20230808.002

Jiao, W., Wei, O., Hao, F., Wang, F., and Liu, B. (2014). Long-term cultivation impact on the heavy metal behavior in a reclaimed wetland, Northeast China. *J. Soils Sediments* 14, 567–576. doi:10.1007/s11368-013-0812-1

Kalani, N., Riazi, B., Karbassi, A., and Moattar, F. (2021). Measurement and ecological risk assessment of heavy metals accumulated in sediment and water collected from Gomishan international wetland, Iran. *Water Sci. Technol. a J. Int. Assoc. Water Pollut. Res.* 84 (6), 1498–1508. doi:10.2166/wst.2021.317

Kumar, N., Chandan, N. K., Bhushan, S., Singh, D. K., and Kumar, S. (2023). Health risk assessment and metal contamination in fish, water and soil sediments in the East Kolkata Wetlands, India, Ramsar site. *Sci. Rep.* 13 (1), 1546. doi:10.1038/s41598-023-28801-y

Li, F., Liu, Y. N., Guo, D. F., Qi, X. T., Zang, S. Y., and Ni, H. W. (2019a). Spatial distribution of heavy metals and potential ecological risks in songjiang wetland, harbin, China. *Environ. Sci. Res.* 32 (11). doi:10.13198/j.issn.1001-6929.2019.01.10

Li, W., Zhang, N., Xiong, J., Gao, H. T., Sun, J., Zhang, Q. Y., et al. (2022). Characterization of soil heavy metal distribution and evaluation of pollution in Medica wetlands. *Appl. Chem.* 51 (12), 3514–3518+3523. doi:10.16581/j.cnki.issn1671-3206.20221031.012

Li, W. D., Cui, Y. X., Zeng, C. C., Zhu, Y. Q., Peng, Y., Wang, K., et al. (2019b). Pollution characteristics and source analysis of heavy metals in farmland soils in the taige canal valley. *Environ. Sci.* 40 (11), 5073–5081. doi:10.13227/j.hjkx.201903252

Li, Y. M., Ma, J. H., Liu, D. X., Sun, Y. L., and Chen, Y. F. (2015). Evaluation of heavy metal pollution and potential ecological risks in kaifeng urban soil. *Environ. Sci.* 36 (03), 1037–1044. doi:10.13227/j.hjkx.2015.03.037

Liu, H. F., Liu, W., Liu, Y. Y., Liu, C., and Shen, Y. X. (2017). Distribution characteristics of Cu, Ni and Pb in the wetland of Bosten Lake and its ecological risk. *Arid. Zone Stud.* 34 (02), 390–394. doi:10.13866/j.azr.2017.02.21

Liu, X., and Dilinuer, A. J. (2021). Removal effects of surface flow artificial wetland on heavy metal ions in water body on the west bank of Bosten Lake. *Wetl. Sci.* 2014 (91), 220–231. doi:10.13248/j.cnki.wetlandsci.01.014

Luo, S. Y., Xing, W. L., Liang, W. L., Deng, Z. Y., Liu, X. L., and Quan, X. W. (2019). Speciation, ecological risk assessment and source analysis of heavy metals in the surface sediments of mangrove wetland in Zhanjiang Bay. *Ecol. Environ. Sci.* 28 (2), 348–358. doi:10.16258/j.cnki.1674-5906.2019.02.017

Maimaitituerxun, A., Ajiguli, M., Ainiwaer, M., and Ma, G. F. (2017). Evaluation of heavy metal pollution and potential ecological risk of oasis farmland soil in Bosten Lake Basin. *Geogr. J.* 72 (09), 1680–1694. doi:10.11821/dlxb201709012

Merciai, R., Guasch, H., Kumar, A., Sabater, S., and García-Berthou, E. (2014). Trace metal concentration and fish size: variation among fish species in a Mediterranean river. *Ecotoxicol. Environ. Saf.* 107, 154–161. doi:10.1016/j.ecoenv.2014.05.006

Ni, X., Zhao, G., Ye, S., Li, G., Yuan, H., He, L., et al. (2023). Spatial distribution and sources of heavy metals in the sediment and soils of the Yancheng coastal ecosystem and associated ecological risks. *Environ. Sci. Pollut. Res.* 30 (7), 18843–18860. doi:10.1007/s11356-022-23295-z

NY/T 395-2000 (2024) *Technical specification for farmland soil environmental quality monitoring.*

Ouyang, W., Wang, Y., Lin, C., He, M., Hao, F., Liu, H., et al. (2018). Heavy metal loss from agricultural watershed to aquatic system: a scientometrics review. *Sci. Total Environ.* 637–638, 208–220. doi:10.1016/j.scitotenv.2018.04.434

Qiao, P., Lei, M., Yang, S., Yang, J., Zhou, X., Dong, N., et al. (2019). Development of a model to simulate soil heavy metals lateral migration quantity based on SWAT in Huanjiang watershed, China. *J. Environ. Sci.* 77, 115–129. doi:10.1016/j.jes.2018.06.020

Rasendra, T., Md, H. R., Baharim, N. B., and Carnicelli, S. (2021). Source identification and ecological risk assessment of heavy metal pollution in sediments of Setiu wetland, Malaysia. *Environ. Forensics* 23, 241–254. doi:10.1080/15275922.2021.1892871

Ros, À., Colomer, J., Serra, T., Pujol, D., Soler, M., and Casamitjana, X. (2014). Experimental observations on sediment resuspension within submerged model canopies under oscillatory flow. *Cont. Shelf Res.* 91, 220–231. doi:10.1016/J.CSR.2014.10.004

Taghvaee, S., Sowlat, M. H., Mousavi, A., Hassanvand, M. S., Yunesian, M., Naddafi, K., et al. (2018). Source apportionment of ambient PM2.5 in two locations in central Tehran using the Positive Matrix Factorization (PMF) model. *Sci. total Environ.* 628-629, 672–686. doi:10.1016/j.scitotenv.2018.02.096

Tomlinson, D. L., Wilson, J. G., Harris, C., and Jeffrey, D. W. (1980). Problems in the assessment of heavy-metal levels in estuaries and the formation of a pollution index. *Helgoländer Meeresunters.* 33, 566–575. doi:10.1007/bf02414780

Wang, C. Y., Li, Y. C., Yu, C. G., and Wang, D. P. (2021) Characterization of soil heavy metal distribution and source analysis in northeastern Huludao, China. *China Environ. Sci.*, 41(11): 5227–5236. doi:10.19674/j.cnki.issn1000-6923.20210608.007

Wang, E., Zhang, K., Chang, S., Zhang, M., and Fu, Q. (2023a). Spatiotemporal distribution and pollution risk assessment of heavy metals in sediments of main water supply reservoirs in central zhuhai city. *Huan jing ke xue= Huanjing kexue* 44 (1), 189–197. doi:10.13227/j.hjkx.202204006

Wang, H., Wang, C. X., Wang, Z. J., and Cao, Z. (2004). Fractionation of heavy metals in surface sediments of taihu lake, East China. *Environ. Geochem. Health* 26, 303–309. doi:10.1023/b:egah.0000039594.19432.80

Wang, J., Ge, J., Yang, X., Cheng, D., Yuan, C., Liu, Z., et al. (2022). Distribution and ecological risk assessment of heavy metals in sediments of Dajiuhu Lake Wetland in Shennongjia, China. *Environ. Sci. Pollut. Res.* 30, 25999–26011. doi:10.1007/s11356-022-23952-3

Wang, X. M., Shen, J., Fan, T. Y., Chu, Z. X., Dong, Z. B., Dong, P., et al. (2023b). Characteristics of heavy metal distribution and health risk evaluation of Wuhu inland river water environment. *J. Yangtze River Acad. Sci.* 12-291-9. doi:10.11988/ckyyb.20230602

Wang, Z. J., Liu, S. J., Zheng, J., and Li, Y. F. (2019). Soil heavy metal pollution and its ecological risk evaluation in Caohai Basin. *J. Ecol. Environ.* 28 (12). doi:10.16258/j.cnki.1674-5906.2019.12.017

Yang, P., Yang, C. H., Ma, X. Y., and Yin, H. Bl. (2021). Characteristics of sediment pollution and dredging decision in the estuary of Nanfang River, Chaohu Lake. *Environ. Sci.* 42 (02), 712–722. doi:10.13227/j.hjkx.202005320

Ye, Z., Yang, Y., Zhou, H., and Guo, B. (2020). Ecological water rights of the Bosten Lake wetlands in Xinjiang, China. *Wetlands* 40, 2597–2607. doi:10.1007/s13157-020-01379-1

Yong, Y. (2002). Main characteristics, progress and prospect of international wetland science research. *Prog. Geogr.* (2), 111–120.

Yongze, Z., and Xuan, W. (2001). A review of ecological restoration studies on natural wetland. *Acta Ecol. Sin.* 21 (2), 309–314.

Yuan, H., Liu, E., Shen, J., Zhou, H., Geng, Q. F., and An, S. (2014). Characteristics and origins of heavy metals in sediments from Ximen Co Lake during summer monsoon season, a deep lake on the eastern Tibetan Plateau. *J. Geochem. Explor.* 136, 76–83. doi:10.1016/j.gexplo.2013.10.008

Zhang, M. Y., Cui, L. J., and Sheng, L. X. (2007). Pollution and ecological risk assessment of heavy metals in the Hengshuihu Wetland. *Wetl. Sci.* 5 (4), 362–369. doi:10.13248/j.cnki.wetlandsci.2007.04.012

Zhang, S., Ye, H., Zhang, A., Ma, Y., Liu, Q., Shu, Q., et al. (2022). Pollution characteristics, sources, and health risk assessment of heavy metals in the surface soil of lushan scenic area, jiangxi Province, China. *Front. Environ. Sci.* 10. doi:10.3389/fenvs.2022.891092

Zhang, Z., Lu, Y., Li, H., Tu, Y., Liu, B., and Yang, Z. (2018). Assessment of heavy metal contamination, distribution and source identification in the sediments from the Zijiang River, China. *Sci. total Environ.* 645, 235–243. doi:10.1016/j.scitotenv.2018.07.026

Zhao, X. L., Li, X., Lu, X. B., Wang, T. ., Zhang, S. L., Guo, X. C., et al. (2022). Characterization of heavy metal contamination in surface sediments of Dongjiang Lake and evaluation of potential ecological risk. *Environ. Sci.* 43 (06), 3048–3057. doi:10.13227/j.hjkx.202109123

Zheng, G. G. (2017) *Theory and practice of research on heavy metal pollution of agricultural soil.* Beijing: China Environmental Science Publishing House.

Zhou, F., Li, P., Wen, M. Z., Xin, X. L., Liu, L., Zhang, Y., et al. (2023). Ecological risk assessment of heavy metals in sediments of Longyang Lake and Moshui Lake, wuhan, China. *China Environ. Sci.* 43 (10), 5433–5443. doi:10.19674/j.cnki.issn1000-6923.2023.0179

Zhu, B., Chen, Y., and Peng, J. (2001). Lead isotope geochemistry of the urban environment in the Pearl River Delta. *Appl. Geochem* 16, 409–417. doi:10.1016/s0883-2927(00)00047-0

frontiers | Frontiers in Environmental Science

TYPE Original Research
PUBLISHED 08 May 2024
DOI 10.3389/fenvs.2024.1370820

OPEN ACCESS

EDITED BY
Qi Liao,
Central South University, China

REVIEWED BY
Agnieszka Klimkowicz-Pawlas,
Institute of Soil Science and Plant Cultivation, Poland
Antonio Calisi,
Università del Piemonte Orientale, Italy

*CORRESPONDENCE
M. Soto,
manu.soto@ehu.eus

RECEIVED 15 January 2024
ACCEPTED 18 March 2024
PUBLISHED 08 May 2024

CITATION
Pérez-Vázquez A, Urionabarrenetxea E, Artetxe U, Rutkoski CF, Gomez-Sagasti MT, Garcia-Velasco N, Zaldibar B, Anza M, Epelde L, Garbisu C, Becerril JM and Soto M (2024), Integrative assessment of *in situ* combined bioremediation strategies applied to remediate soils spilled with sewage sludges. *Front. Environ. Sci.* 12:1370820. doi: 10.3389/fenvs.2024.1370820

Integrative assessment of *in situ* combined bioremediation strategies applied to remediate soils spilled with sewage sludges

A. Pérez-Vázquez[1], E. Urionabarrenetxea[1], U. Artetxe[2], C. F. Rutkoski[1], M. T. Gomez-Sagasti[2], N. Garcia-Velasco[1], B. Zaldibar[1], M. Anza[3], L. Epelde[3], C. Garbisu[3], J. M. Becerril[2] and M. Soto[1]*

[1]Cell Biology in Environmental Toxicology (CBET) Research Group (Plentziako Itsas Estazioa-Universidad del País Vasco/Euskal Herriko Unibertsitatea), Plentzia, Spain, [2]NEIKER-Basque Institute for Agricultural Research and Development, Derio, Spain, [3]Ecofisko Research Group, Department of Plant Biology and Ecology (Universidad del País Vasco/Euskal Herriko Unibertsitatea), Leioa, Spain

Landfills and waste disposal sites in the Basque Country are summarized in the inventory of soils that either currently support or have supported potentially polluting activities or facilities (Law 4/2015). Notably, "Landfill 17," located in Gernika-Lumo, has been receiving, for decades, sewage sludges from the local wastewater treatment plant (WWTP) as agricultural amendment. In order to decontaminate and recover soil functionality, a combination of bioremediation (which involved bioagumentation and phyto- and vermitechnologies) and complementary bioremediation strategy (i.e., promotion and maintenance of the native vegetation) was implemented *in situ*. Physicochemical and ecotoxicological characterization were achieved. Furthermore, an ecotoxicological assessment of the soils upon flora and fauna was carried out through the application of different bioassays and biomarkers. Additionally, an integrative biomarker response (IBR/n) index was calculated to provide a holistic view of the soil general status. Critical pollutants [Cd, Cr, Ni, Pb, benzo(a)pyrene, and dieldrin] were observed in most of the treated sites. Microbial parameters did not present remarkable differences among sites. However, plant indicators pointed the non-treated site (MN8) as the unhealthiest. This was also observed in earthworms' immune system, where cytotoxicity appears when exposed to non-treated soils. In conclusion, this field study showed that the combination of bioaugmentation, phytoremediation with native species, and vermiremediation is highly useful in eliminating mixed contamination, improving soil health, and ultimately restoring ecosystem functionality and biodiversity.

KEYWORDS

biomarkers, integrative biomarker response, landfill, mixed contamination, phytoremediation

Abbreviations: WWTP, wastewater treatment plant; CTA, catalase; AChE, acetylcholinesterase; GST, glutathione S-transferase; GSH, glutathione; CbE, carboxylesterase; MDA, malondialdehyde; BR, basal respiration; IBR/n, integrated biological response index; PI, pollution index; calcein-AM, calcein–acetoxymethyl.

1 Introduction

The intensification of human activities and rapid industrialization stands as a primary cause of environmental pollution and degradation (Antoci et al., 2018) mainly due to faulty spillages, landfills, and industrial waste disposals, threatening human and ecosystem health. Soil pollution has emerged as a major environmental concern due to its relevance supporting essential services for the society (Míguez et al., 2020). Thus, the degradation and loss of ecosystems pose a great threat to human safety and health, leading to scarcity of productive lands. In order to mitigate the ecological and human health risks linked with soil pollution, the recognition of the resulting ecological and human health hazards requires management and remediation techniques, with the last one relying on physicochemical and, where feasible, biological remediation technologies (Jan et al., 2015). Nowadays, physicochemical techniques are widely used, although they can lead to problems such as soil erosion or fertility and functionality loss, thus breaking ecosystem balance and inducing negative and irreversible effects upon biodiversity (Jan et al., 2015; Morillo and Villaverde, 2017). As a sustainable alternative, several biological remediation (bioremediation) methods, such as those based on microbes (e.g., bioaugmentation), plants (e.g., phytoremediation), and earthworms (vermiremediation), have been demonstrated to be cost-effective tools, despite the drawback of being more time-consuming processes to mitigate. Bioaugmentation, phytoremediation, and vermiremediation have recently been applied in soils concomitantly polluted with organic and inorganic compounds (hereafter co-polluted) due to their high removal efficiencies (Lacalle et al., 2018; Lacalle et al., 2020; Aparicio et al., 2021), which are even higher when combined (Lacalle et al., 2020; Aparicio et al., 2021; Urionabarrenetxea et al., 2021).

In 2012, 16.5% of the total surface of the Basque Country (Spain) was considered potentially contaminated, while 2.7%–6.5% was considered already contaminated (Basque Government, 2023). Thus, the Basque Country, 2023 Government developed an inventory of soils that support or have supported potentially polluting activities or facilities (Law 4/2015) that has been updated in 2022 (Basque Government, 2023). This inventory includes "Landfill 17," located in Gernika-Lumo (Basque Country, Spain), where sewage sludges—from the local wastewater treatment plant (WWTP)—were diffusely scattered for decades as amendment with agricultural purposes. Here, several quantitative risk analyses were carried out by the University of the Basque Country (UPV/EHU) highlighting the worst case scenarios (MN1, MN2, MN3, MN4, MN5, MN7, and MN8) with threatening pollutants [cadmium, lead, nickel, chromium benzo(a)pyrene, and dieldrin] (Urionabarrenetxea et al., 2021). Based on the gathered data, the local administration prohibited the use of these soils with agricultural purposes, suggesting the application of remediation techniques. Thus, Urionabarrenetxea et al. (2021) conducted a field trial in "Landfill 17" to ascertain the best bioremediation technologies (bioaugmentation and phyto- and vermiremediation) or their combination for contaminant reduction. As a result of the mentioned study, the combination of the three technologies was selected as the most efficient method and applied at large scale in the whole "Landfill 17" by using *Burkholderia xenovorans* LB400 and *Penibacillus* sp. bacterial strains for the bioaugmentation; alfalfa (*Medicago sativa*) for phytoremediation; and *Eisenia fetida* earthworms for vermiremediation.

Subsequently, quantitative risk analysis showed the efficiency, in terms of risk reduction, of the large-scale application of the triple bioremediation technique. However, and after considering the nature of the contamination, the local administration kept banning the use of lands with agricultural purposes and recommended keeping remediating the area in the following years. Therefore, in April 2021, a complementary bioremediation strategy based on the promotion and maintenance of the native vegetation was carried out at "Landfill 17." The main objective of the study was twofold: to continue stabilizing and removing soil contaminants and, simultaneously, restore and recover ecosystem health and biodiversity, all through the establishment of native herbaceous and woody species, such as *Salix* sp. or *Alnus* sp.

To assess the effectiveness of a bioremediation process, it is necessary to evaluate the ecosystem's health status through biological indicators spanning different trophic levels (Pankhurst et al., 1997; Garbisu et al., 2007), in order to assess aboveground and belowground biota status. Microbial parameters measured in soil microbial communities (e.g., soil respiration, microbial carbon biomass, and functional diversity) along with plant production and diversity are essential for comprehensively assessing soil health and recovery, due to their direct linkage with ecosystem processes and their high sensitivity (Pankhurst et al., 1997; Gómez-Sagasti et al., 2012, 2021).

Furthermore, toxicity assays are useful tools to evaluate and monitor the presence of soil contamination and its effects (Aparicio et al., 2019; Urionabarrenetxea et al., 2021, 2022). These assays rely on the use of sentinel/model organisms to evaluate toxicity. To assess soil phytotoxicity, one of the most used assays is the root elongation test. The US-EPA (1982) guideline recommends the use of *Cucumis sativus* L. as the sentinel species, among others, due to its sensitivity and quick response (Visioli et al., 2014; Franco et al., 2017; Lacalle et al., 2018). Similarly, *Eisenia fetida* earthworm has been widely used as an indicator of soil health and toxicity (Irizar et al., 2015b) in standard tests (OECD, 1984) and field works (Aparicio et al., 2021; Urionabarrenetxea et al., 2021) to evaluate the toxic effects of single or mixtures of pollutants. Earthworms can take up chemicals via the dermis—from leachates or porewater and via the digestive tract—by soil ingestion (Rodriguez-Campos et al., 2014).

Biomarkers are measurements at the tissue, cellular, biochemical, and molecular levels that have been raised as a tool to detect changes at lower organization levels, providing early signs of alterations at the population, community, or ecosystem levels (Cajaraville et al., 1993). Recently, the use of multi-biomarker approaches has gained significance in evaluating the health status of co-polluted soils from a holistic point of view (Htwe et al., 2022). For instance, oxidative stress can not only be assessed by measuring glutathione-S-transferase (GST), carboxylesterase (CbE), and catalase (CAT) activities but also by measuring carbonyl protein and malondialdehyde (MDA) content. GST is a phase II biotransformation enzyme that helps detoxify pollutants by conjugating xenobiotics with GSH and making them get more easily excreted (Hellou et al., 2012). CbE is an esterase that belongs to a superfamily of enzymes that hydrolyze carboxylic

ester bonds and is another enzyme that aids in the excretion of xenobiotics (Wang et al., 2018). CAT, on the other hand, consists of an antioxidant enzyme, responsible for the degradation of H_2O_2, preventing the formation and accumulation of reactive oxygen species (ROS) that can damage cells (Asensio et al., 2013). Carbonyl protein is a marker of protein oxidative damage in earthworms under stress (Vasylkiv et al., 2010), and MDA is a product of lipid membrane peroxidation that is formed upon oxidative stress through the production of reactive oxygen species; it can reflect the level of biological damage, being an indicator of the cellular membrane status (Pirinccioglu et al., 2010).

At the cellular level, immune cells of earthworms named coelomocytes have been widely studied in the last decades as the target system to assess contaminated sites, as they have demonstrated the capacity to predict alterations caused by contamination (Plytycz and Morgan, 2011a; Kwak et al., 2014; Irizar et al., 2015a; García-Velasco et al., 2019; Urionabarrenetxea et al., 2022). *E. fetida* coelomocytes are divided into two main subpopulations: amoebocytes and eleocytes. Amoebocytes accomplish phagocytosis of foreign particles, while eleocytes contribute to homeostasis in earthworms (Plytycz et al., 2009; Plytycz et al., 2010). Similarly, when organisms are exposed to environmental pollution, reactive oxygen species (ROS) are produced, leading to oxidative damage in proteins, nucleic acids, lipids, and other macromolecules (Hellou et al., 2012).

To achieve a holistic perspective of the health status of an ecosystem (Beliaeff and Burgeot, 2002; Broeg and Lehtonen, 2006), the integrative biomarker response (IBR/n) index is a great tool that integrates biomarkers and biological indicators at different biological levels and provides a reliable picture of the health status of a population or community.

As noted, field-scale bioremediation studies are required with a comprehensive risk assessment that includes physical, chemical, and biological, as well as ecotoxicological indicators. The present field study addresses this gap in knowledge and aims to 1) characterize soil's potential toxicity and soil health status of the co-polluted "Landfill 17" and 2) assess the recovery of soil health and biodiversity in one and a half years after the implementation of the complementary remediation strategy, not only through physical–chemical indicators but also through biological and ecotoxicological indicators representative of the soil biota (microbial, plants, and worms).

2 Material and methods

2.1 Phase I: sampling site

In October 2022, a year-and-a-half after the establishment of the complementary bioremediation strategy, the soil and vegetation samples were collected from the six sampling sites previously selected by the administration for pollution and remediation monitoring at "Landfill 17," located in Gernika-Lumo (Basque Country, Spain). These sites were denoted as MN1, MN2, MN3, MN4, MN5, and MN7. Each of them had a size of 2 m × 2 m. As we have indicated above, MN8 was considered to be the control (non-treated) site.

Three biological replicates were uniformly distributed in each site, using quadrats of 50 cm × 50 cm size each. First, the vegetation cover of each quadrat was manually collected to estimate plant biomass and plant biodiversity and to determine phytoextraction. Subsequently, sets of soil samples were manually collected in each quadrat to a depth of 0.2 m for the analysis of physical–chemical and biological properties and ecotoxicological assays.

2.2 Phase II: chemical and ecotoxicological assessment

2.2.1 Organisms for ecotoxicological analysis

For the ecotoxicological assays, cucumber (*Cucumis sativus* L.) seeds and *Eisenia fetida* earthworms were used. Cucumber *C. sativus* seeds were obtained from a commercial provider (Semillas Batlle) and maintained at constant temperature (4°C) and dark conditions, under humidity not exceeding 10%. Among the stocked seeds, only those without abnormalities and similar size were chosen. Meanwhile, *E. fetida* earthworms were purchased from the commercial supplier Lombrinatur (Almeria, Spain), and specimens were maintained under constant and controlled conditions (19°C and 60% relative humidity until the experiment). Stocked earthworms were weekly fed with antibiotic-free horse manure. For the assay, clitellated organisms between 300 and 600 mg were employed (OECD, 1984).

2.2.2 Soil processing and analysis

Once in the terrarium, the soil samples were sieved (2 mm) and kept in the cold chamber to be used for organic matter content determination and chemical and ecotoxicological characterization. Additionally, the water holding capacity (WHC) of each biological replicate was estimated based on the dry and humidity weights of the soils in order to achieve OECD (1984) ideal conditions for the standardized test.

In soil samples, the organic matter was quantified with weight loss on ignition at 550°C; a complete chemical characterization was also carried out encompassing the analysis of up to 84 compounds. For this chemical characterization, 200 g of each soil sample was used. Heavy metals (As, Cd, Cr, Cu, Hg, Mo, Ni, Pb, and Zn) were analyzed through ICP-MS (Inductively coupled plasma mass spectrometry). Meanwhile, the majority of phenols, hydrocarbons, and aromatic and halogenated compounds were analyzed by using GC-MS (Gas chromatography/Mass spectrometry). A part of the hydrocarbons were analyzed using GS-FID (Gas Chromatography With Flame Ionization Detection).

This study focused on Cd, Cr, Ni, Pb, benzo(a)pyrene, and dieldrin, as they are classified as critical pollutants by the local government. The pollution index (PI) was calculated according to Hakanson (1980), so the obtained data were normalized for each pollutant according to the reference values in the legislation (VIE-B values classified as "other uses") established by the Basque Country norm (Law 4/2015). The following equation was used: $PI = C/Cn$, where C corresponds to soil concentration and Cn corresponds to threshold value from the Basque norm. Then, the sum of all individual pollution indexes was obtained for each site.

At the same time, soil leachates were prepared as indicated by the Spanish legislation BOE, 2002 A-1697 (BOE núm. 25), following the German standard DIN 38414-S4 (Deutsches Institut fur Normung, 1984 480/id) (Urionabarrenetxea et al., 2022). Thus,

10 grams of dry soil were mixed with 100 mL of distilled water and stirred for 24 h to afterwards be filtered through a 0.45-μm pore PVDF filter. Ni, Cr, Cd, and Pb were quantified through GC-FID by external analysis in SGIker general services of UPV/EHU, Leioa, and the leachates were stored at 4°C until use.

2.2.3 Biological indicators

2.2.3.1 Microbial communities

In order to assess microbial communities, parameters related with their activities and functional richness were measured in three soil biological replicates per sample. Basal respiration (mg C kg^{-1} h^{-1}) was determined following ISO 16072 (2002), measuring CO_2 evolution. According to Epelde et al. (2008), the average well color development (AWCD), number of utilized substrates (NUS), and Shannon's diversity index ($H' = -\Sigma pi \log_2 pi$) were determined from Biolog EcoPlates™.

2.2.3.2 Plant diversity and biomass

Plants from each quadrat were harvested and taxonomically identified at the genus level and, if possible, at the species level in order to determine the diversity of each site. Plant diversity was calculated using the Shannon Index [$H' = -\Sigma(pi\ log2\ pi)$, where *pi* is the proportional dry weight of the *i* species]. Once in the laboratory, shoots of woody and herbaceous plants were separated by species, dried at 80°C for 48 h, and weighted to determine the production of plant biomass.

2.2.4 Metal extraction in plants

Metal extraction in plants was determined in dried shoots, although for *Salix atrocinerea*, only the leaves were analyzed. Following the US-EPA Method 3051A (2007) protocol with modifications, the plant samples were oven dried at 80°C for 48 h to be milled afterward. A representative and homogeneous analytical sample of each biological replicate weighing approximately 0.25 g was subjected to acid digestion. Once the digestion process was completed, the samples were cooled and diluted with ultrapure water until a maximum concentration of HNO_3 <1%. All samples were externally analyzed by AGRUPAlab (reference UNE-EN ISO/IEC 17025:2017), where Cd, Cr, and Ni were quantified through ICP-MS using all inner standards, following the QA/QC criteria established by the ENAC (Spanish National Accreditation Body).

2.2.5 Ecotoxicological bioassays with plants

2.2.5.1 Root elongation test with *Cucumis sativus* L. seeds

To assess soil phytotoxicity, the root elongation bioassay with cucumber (*C. sativus*) was carried out following the EPA 850.4230 modified protocol (Lacalle et al., 2018).Briefly, the seeds were pre-germinated under controlled conditions (photoperiod 14/10 h day/night, temperature 25/18°C day/night, and photosynthetic photon flux density of 100 μmol photon m^{-2} s^{-1}). Concurrently, 10 g of soil from each biological replicate of each site was sieved (2 mm) and dried in an incubator for 7 days at room temperature (25°C) to prevent microbial community damage. Dried soils were placed in Petri dishes with 10 mL of deionized water. Finally, a black filter paper (Filter-Lab® 1457) was placed on top of each Petri dish with moistened soil.

After 72 h, seven pre-germinated seeds were positioned in the dishes with the soils and sealed with Parafilm® to be incubated in a Sanyo germination chamber for another 72 h under the same conditions above. Images of the seedlings were taken at the beginning and after the incubation to be processed utilizing Fiji-ImageJ software (Schindelin et al., 2012). Root elongation was calculated using the formula $R = R_{T72h} - R_{T0}$, with a common scale for all.

2.2.6 Bioassays with earthworms

2.2.6.1 Filter paper test

In order to evaluate potential toxicity through dermal exposure, the OECD "filter paper test" guideline (OECD, 1984) was followed, with mortality and weight loss being the main endpoints. A total of 10 technical replicates per treatment were prepared in vials containing 1 mL of elutriate and one specimen. The experiment was carried out under constant temperature (19°C) and dark conditions. Earthworms were weighted at the beginning and after 72 h; mortality was recorded after this period.

2.2.6.2 Artificial soil test

Soil test with *E. fetida* (OECD, 1984) was performed to consider a more realistic scenario where the digestive path could also be relevant for the toxicity assessment. In this case, three biological replicates per group were used, and OECD soils were used as the negative control (labeled as "Control"). All soil samples were moistened with deionized water up to 40% of their WHC, as previously estimated (Section 2.2.2). In each glass container, 750 g of soil and 10 specimens were placed. After 14 days (under 19°C and constant light conditions), mortality and weight loss were measured.

The composition of OECD artificial soil was (dry weight): 70% of industrial sand, 20% kaolin clay, and 10% sphagnum peat. A pH of 6.0 ± 0.5 was achieved by adding 0.1% of powdered calcium carbonate ($CaCO_3$).

2.2.7 Earthworm chemical analysis

After soil testing, five earthworms per biological replicate were separated for chemical analysis. After depurating their gut contents in a filter paper for 24 h, the earthworms were preserved at −80°C and subjected to lyophilization. An external chemical analysis through ICP-MS was carried out by SGiker General Services at EHU/UPV (Leioa) after a previous microwave digestion. The metal species Cd, Cr, Ni, and Pb were detected using all inner standards following the QA/QC criteria established by the ENAC (Spanish Agency for Accreditation).

2.2.8 Coelomocyte extrusion and cell counting

Four earthworms per treatment were reacquired after 14 days of exposure and gently massaged to remove soil particles retained in their digestive tracts. Coelomocyte extrusion was done by immersing them into extrusion fluid (1 mL, PBS with 0.02% EDTA/earthworm) and subjecting them to electrical stimulation (9 V) (Irizar et al., 2014a). This allows the release of coelomic fluid and coelomocytes from the dorsal pores (Irizar et al., 2014a).

The obtained solution was transferred into falcon tubes and centrifuged. The supernatant was then removed, and the pellet was resuspended with PBS solution. Afterward, the cells were counted in a hemocytometer (Neubauer chamber), and the final concentration was adjusted to 1.106 cells mL^{-1} in all treatments. Regarding the viability assay, solutions were placed in 96-well microplates and incubated to let coelomocytes stabilize and then centrifuged to complete cell adhesion to the bottom.

2.2.9 Calcein–acetoxymethyl viability assay

Coelomocyte viability was assessed by the calcein–acetoxymethyl (calcein-AM) assay according to García-Velasco et al. (2019). This is a fluorometric method that provides a simple, rapid, and accurate response of cytoxicity by dyeing with calcein-AM. Dye enters viable cells where it is converted by intracellular esterases to calcein that provides an intense signal when (with an intact plasma membrane) is retained by cells. Firstly, the supernatant was discarded from the plates and the cells were incubated with 2.5 µM calcein-AM (100 µL per well, six replicates).

In parallel, three wells per experimental group were filled with 100 µL of PBS instead of calcein-AM to measure basal fluorescence of the cells. A cleaning step was carried out by removing the supernatant and replacing it with PBS twice. Excitation was performed at 490 ± 20 nm, and emission was measured at 520 ± 20 nm in a Flex fluorometer for the plates.

2.2.10 Biochemical markers

2.2.10.1 Sample preparation and homogenization

Two earthworms per biological replicate were taken from the soil test containers after 14 days of exposure, frozen directly in liquid nitrogen, and kept at −80°C for further analyses. A total of 200 mg of the post-clitellar section of the earthworm was dissected according to Irizar et al. (2014b) and homogenized using homogenization buffer (50 mM Tris-sucrose, pH 7.4, 1:2 w/v) in a Precellys 24-Dual at 4°C. The suspension was centrifuged, and the supernatant was collected and divided in aliquots, which were preserved at −80°C and used to analyze the activity of the enzymes: glutathione-S-transferase (GST), carboxylesterase (CbE), catalase (CAT), and acetylcholinesterase (AChE) and the levels of malondialdehyde (MDA), carbonyl proteins, and total protein quantification. All analyses were performed in 96-well flat-bottom microplates, measuring each biological replicate in duplicate using a BioTek Eon microplate spectrophotometer at 20°C.

2.2.10.2 Enzyme activity

Oxidative stress in *E. fetida* was assessed measuring the levels of 1) detoxification enzymes, reflected by glutathione S-transferase (GST) and carboxylesterase (CbE); 2) effects upon the antioxidant defense system, by analyzing catalase activity (CAT). Additionally, to evaluate general stress and effects of pollution in the nervous system, acetylcholinesterase (AChE) was measured (Tiwari et al., 2016).

Thus, GST activity was determined according to Keen et al. (1976), measuring the formation of the CDNB-GSH conjugate at 340 nm in 28 µL of the sample for 2 min. CAT activity was analyzed according to Aebi (1984), where H_2O_2 consumption by CAT in 3 µL of the sample for 1 min was measured at 240 nm. CbE and AChE enzyme activities were analyzed separately according to Ellman et al. (1961), using a 5,5-dithiobis-2-nitrobenzoic acid (DTNB) solution. For CbE, the reaction started when 10 µL phenylthioacetate was added to a mixture of 5 µL of the sample with DTNB. Similarly, for AChE, acetylthioacetate iodine was used as the substrate in a 10-µL sample. The absorbance at 412 nm was followed for 2 min.

For protein quantification, 10 µL of the sample was analyzed through the Bradford method (Bradford, 1976), utilizing 200 µL of the Bradford reagent. Quantification was performed measuring absorbance at 595 nm, and concentrations were obtained through a calibration curve developed with bovine serum albumin as the standard, whose concentrations ranged from 0 to 3.5 mg mL^{-1}. Enzyme activities were expressed as U mg^{-1} protein or mU mg^{-1} protein, U corresponds to the enzyme units. It is important to note that enzyme activity has been represented as percentage with respect to the control.

2.2.10.3 Lipid peroxidation

Lipid peroxidation was assessed by quantifying carbonyl protein and MDA. Carbonylated proteins were quantified by adapting the method from Parvez and Raisuddin (2005), measuring 2,4-dinitrophenylhydrazine protein derivate at 370 nm. Protein carbonyl levels were expressed as percentage with respect to the control and calculated using the quantified protein content and the corresponding extinction coefficient (ε_{370} = 0.022 mM^{-1} cm^{-1}). MDA was determined following Almeida et al. (2005) by measuring spectrophotometrically the thiobarbituric acid derivate of malonaldehyde at 535 nm. The MDA levels were expressed as percentage with respect to the control and calculated based on a tetramethoxypropane standard curve with concentration values within 0 and 1.5 µmol mL^{-1}.

2.2.11 Statistical analysis

Data analyses were performed using the RStudio software (version 4.2.2) and graphs using Excel. Test for outliers was carried out using the Grubbs test and removed if detected according to the reported criteria (Meshalkin et al., 2023). Data normality and homoscedasticity were checked using the Shapiro–Wilk and Levene's tests, respectively. Parametric data were studied with one-way ANOVA coupled with Tukey for pairwise comparisons and Dunnett's test, to study differences between sites (MN1–MN7) with the non-treated site (MN8) and negative controls. Non-parametric data were studied using the Kruskal–Wallis test, followed by Dunn's test. The confidence at the 95% level was considered.

2.3 Phase III: integrative tool

2.3.1 Integrative biomarker response (IBR/n)

To integrate the different biomarker responses from "Landfill 17" soils at different biological and ecological levels, biomarkers from the biochemical to the community levels—acetylcholinesterase (AChE), glutathione S-transferase (GST), calcein content (CAL), plant biomass (PB), and basal respiration (BR)—were selected to provide a holistic and simplified view of the general state of the soil (Beliaeff and Burgeoot, 2002; Marigómez et al., 2013).

The IBR was calculated using a multivariate method, according to the following procedure: 1) calculation of the mean and standard deviation for each sample; 2) standardization of the data for each sample $xi' = (xi - x)/s$, where x is the standardized value of the biomarker, xi represents the biomarker value of each sample, x is the mean value, and s is the standard deviation of the biomarkers calculated from all compared samples; 3) addition of the standardized value calculated for each sample to the absolute standardized value of the minimum value in the data set: $yi = xi'$

TABLE 1 Basque Country norm thresholds of the critical compounds [cadmium, chromium, nickel, lead, benzo(a) pyrene, and dieldrin] and their measured concentrations in all the selected soils from "Landfill 17" in 2021 and its respective pollution index (PI).

	VIE-B (other uses)	MN1	MN2	MN3	MN4	MN7	MN8
Cd (mg kg^{-1})	5	**6**	**9**	**6**	**18**	**7**	**9**
Cr (mg kg^{-1})	200	89	120	92	**210**	170	**520**
Ni (mg kg^{-1})	110	42	52	44	78	77	**210**
Pb (mg kg^{-1})	120	52	59	68	120	65	92
B(a)P (mg kg^{-1})	0.02	**0.06**	**0.04**	**0.06**	**0.1**	**0.07**	**0.21**
Dieldrin (μg kg^{-1})	10	3	10	4.5	9	4.7	5
PI		0.96	1.06	1.01	2.04	1.24	3.01

Marked in bold are concentrations above the Basque Country norm.

TABLE 2 Basque Country norm thresholds of the critical compounds [cadmium, chromium, nickel, lead, benzo(a) pyrene, and dieldrin], their measured concentrations, the respective pollution index of each soil, and the organic matter (OM) content in "Landfill 17" soils collected in October 2022.

	VIE-B (other uses)	MN1	MN2	MN3	MN4	MN7	MN8
Cd (mg kg^{-1})	5	**5.25 ± 0.42**	**6.67 ± 0.91**	**12.07 ± 2.11**	**5.75 ± 2.35**	4.74 ± 0.12	**6.03 ± 0.33**
Cr (mg kg^{-1})	200	84.27 ± 11.26	87.33 ± 11.39	152.00 ± 12.98	77.93 ± 27.76	129.33 ± 6.42	**371.67 ± 41.50**
Ni (mg kg^{-1})	110	34.77 ± 4.94	35.26 ± 3.34	52.43 ± 3.71	38.00 ± 8.98	55.47 ± 3.02	**154.00 ± 19.03**
Pb (mg kg^{-1})	120	50.50 ± 5.34	51.30 ± 6.07	85.13 ± 6.65	59.43 ± 23.05	55.27 ± 1.77	72.83 ± 7.68
B(a)P (mg kg^{-1})	0.02	**0.03 ± 0.00**	0.02 ± 0.00	**0.04 ± 0.00**	**0.05 ± 0.01**	**0.05 ± 0.02**	**0.05 ± 0.00**
Dieldrin (μg kg^{-1})	10	<LOD	<LOD	<LOD	<LOD	<LOD	<LOD
PI		0.77	0.76	1.23	0.84	0.98	1.45
OM % (p/p)		7.51 ± 0.39	7.75 ± 0.63	11.97 ± 1.30	9.81 ± 2.77	8.40 ± 0.53	8.06 ± 3.08

Values represented as mean ± standard deviation (n = 3). Marked in bold are the average concentrations above the Basque Country Norm.

+ $|xmin'|$; 4) making of the start plot and calculation of the triangular areas as $Ai = (yi \times yi + 1 \times sin\alpha)/2$, where yi and "yi + 1" are the standardized values of each biomarker and the next biomarker in the start plot, respectively, and "α" is the angle (in radians) formed by the two consecutive axes; and 5) calculation of the IBR index, IBR = ΣAi·IBR value is directly dependent on the number of biomarkers used, so the obtained values of IBR must be divided by the number of biomarkers used (IBR/n), according to Broeg and Lehtonen (2006).

3 Results

3.1 Soil processing and analysis

At the end of the remediation strategy, in October 2022, the concentrations of all the critical pollutants [Cd, Cr, Ni, Pb, and B(a)P] were reduced compared with levels in 2021 (Table 1) in all the soils, except in MN3, where the metal concentrations were higher (Table 2). Cd and B(a)P still were above the reference values established by the Basque Country norm (Law 4/2015) in all sites. Despite this, MN8 soils (non-treated) remain the most polluted site, with values of Cd, Ni, and B(a)P above the reference values.

In 2022, soils from "Landfill 17" showed a higher presence of heavy metals than dieldrin and B(a)P, which were considerably below the overall (Table 2). In fact, dieldrin was under the limit of detection in all the sampling points (Table 2). Regarding heavy metals, Cr displayed the highest average concentrations with values ranging from 77.93 mg·kg^{-1} (MN4) to 371.67 mg·kg^{-1} (MN8, non-treated). MN8 also presented high levels of Ni, achieving a value of 154.00 mg·kg^{-1}. Meanwhile, MN3 soils (historically the most polluted) showed the highest concentrations for Cd and Pb, 12.07 and 85.13 mg·kg^{-1}, respectively. As overall, the highest pollution indexes were obtained for MN3 and MN8 points. According to the reference values, Cd concentrations trespassed the thresholds in all the soils except for MN7. Furthermore, MN8 showed values above the norm for all the critical compounds apart from Pb (Table 2). Regarding the organic matter (OM) content (Table 2), all the soils showed relatively high values, with the highest values being measured in MN3 (11.97) and MN4.

3.2 Leachate analysis

Leachates obtained from "Landfill 17" soils reached remarkably low concentrations, as it is represented in Supplementary Table S2. Despite this, MN1 soils presented the highest values for Cd, Ni, and Pb of $7.4{\cdot}10^{-3}$, $5.69{\cdot}10^{-2}$, and $4.2{\cdot}10^{-3}$ mg·kg^{-1}, respectively. For Cr, the maximum value was recorded in MN8 soils ($1.19{\cdot}10^{-1}$ mg·kg^{-1}).

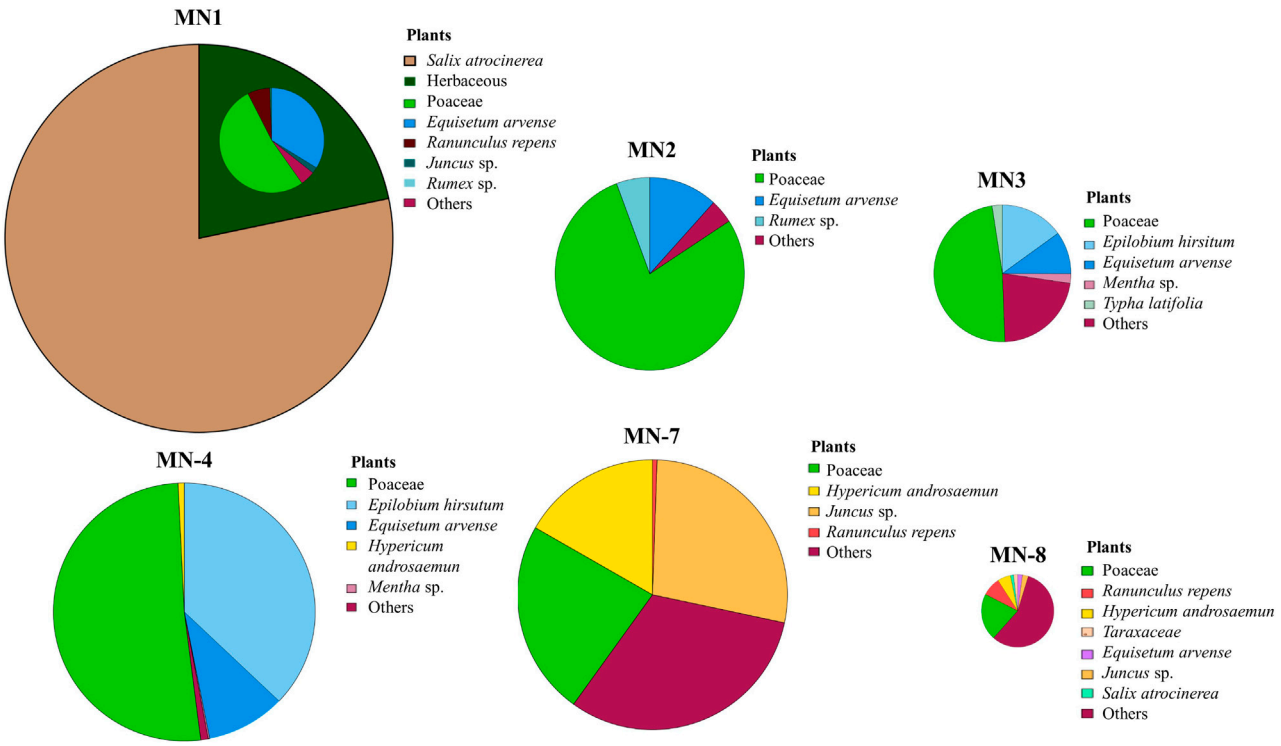

FIGURE 1
Plant diversity expressed as percentage considering total biomass as 100%. Biomass of each soil is represented with the size of the graph which is normalized with these values.

On the opposite end, MN7 soils (farthest location from the WWTP) showed the lowest concentrations of Cd, Cr, Ni, and Pb of $8{\cdot}10^{-4}$, $5.4{\cdot}10^{-3}$, $6.8{\cdot}10^{-3}$, and $9{\cdot}10^{-4}$ mg·kg^{-1}, respectively.

3.3 Biological indicators

Of the microbial parameters (Supplementary Figures S4–S7), basal respiration, Shannon diversity index, and NUS did not show significant differences between treatments. However, significantly higher values in MN3 (0.58) were observed for AWCD than were for MN1 (0.51), MN2 (0.50), and MN8 (0.50). Likewise, basal microbial respiration reached the maximum in MN4 soils (3.23 mg C·kg^{-1}·h^{-1}) and the minimum in MN2 (2.44 mg C·kg^{-1}·h^{-1}). For the Shannon index, similar values were recorded in all the sampling points with estimations approximately 3.93 (MN3) and 3.60 (MN7). Following a similar trend, NUS also achieved the highest value in MN3 soils (19.33) and the lowest in MN7 (15.30).

Plant biomass showed significant differences in MN1 and MN7 compared to MN8 soils, which having the highest plant diversities displayed the lowest biomass values (Figure 1). Statistical differences were also seen between MN3 and MN1 with a higher biomass value recorded in MN1. MN1 showed the highest biomass and low diversity due to the dominating presence of *Salix atrocinerea* (Figure 1). Although no significant differences were obtained for plant diversity (Shannon index), Poaceae family individuals emerged as the most abundant in terms of diversity, apart from MN7 and MN8 sampling points. *Epilobium hirsutum* was the second most abundant, growing at MN2, MN3, and MN4. Overall, the highest diversity values were recorded at MN8, MN7, and MN3 sites, while MN2 and MN1 exhibited the lowest plant diversity levels.

3.4 Metal extraction in plants

Metal extraction, represented in Supplementary Table S8, showed remarkably higher rates of Cd in MN1 (sites subjected to the dominating presence of *Salix atrocinerea*), exhibiting 10-fold higher extraction values than the rest of the sites, whose values ranged from 2.59 g·ha^{-1} (MN8) to 12.28 g·ha^{-1} (MN7). Ni extracted concentrations by the vegetation reached the maximum in the MN1 site (17.91 g·ha^{-1}), while the lowest contents were measured in MN3 and MN8 sites. Contrariwise, the Cr MN1 site presented the lowest concentrations and the highest in MN3 and MN8, where the intragroup variability for this pollutant exceeded 100% of the mean value, masking differences with the other sites.

3.5 Ecotoxicological bioassay with plants

C. sativus pre-germinated seeds did not show statistical differences in root elongation when exposed to "Landfill 17" soils for 72 h, as can be seen in Supplementary Figure S9. Despite a similar growth being described in all the samples with values ranging from 62% to 83%, exposure to MN3 soils determined a slightly

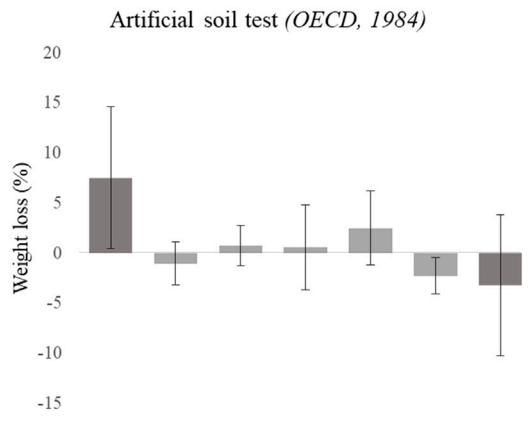

FIGURE 2
Weight loss (% respect initial weight) of *Eisenia fetida* earthworms exposed for 14 days to "Landfill 17" soils moistened up to 40% of the WHC of each soil. Error bar represents standard deviation. Different letters represent significant differences studied through one-way ANOVA (p-value < 0.05).

higher (not significant) growth rate for *C. sativus* roots. On the contrary, a lower growth tendency was exhibited by pre-germinated seeds on being exposed to MN1 soils for 72 h.

3.6 Bioassays with earthworms

After 72 h of exposure to the leachate-moistened filter paper, the recorded mortalities were all below 10%, and no significant weight losses were recorded. Nevertheless, earthworm weight loss in this test showed lower values in MN3 (12.68%) than in MN1, MN4, and MN8, thus these soils displayed the highest weight losses for dermal exposure, reaching 20.40%, 20.65%, and 20.57%, respectively.

After 14 days of exposure to co-polluted soils from "Landfill 17," earthworm mortality was lower than 10%. The weight loss recorded variability within MN1, MN2, MN3, MN4, and MN8 soils trespassed above a 100% of the mean value, thus no significant differences were recorded. Moreover, as is represented in Figure 2, earthworms gained weight with respect to their initial weight with some of the treatments. This happened notably when exposed to MN8 soils, where the lowest weight loss value was achieved (−11.22%). On the contrary, earthworms exposed to the control (OECD soils) displayed the highest weight loss value, losing 17.93% of their initial value.

3.7 Earthworm chemical analysis

In earthworms exposed to landfill soils for 14 days, Cd was the most accumulated metal in tissues for all the treatments compared with the control, exhibiting the highest values for MN1, MN2, and MN8 at 17.27, 16.73, and 11.54 mg·kg^{-1}, respectively (Table 3). The highest Cr, Ni, and Pb accumulations were measured in MN8. Contrariwise, Pb was the pollutant with the lowest accumulation values, with quantifications from 0.56 (control) to 5.39 mg·kg^{-1} (MN8).

3.8 Calcein AM

After 14 days of exposure, calcein signal was measured on coelomocytes extruded from earthworms, as represented in Supplementary Figure S10, which presented significantly lower values in MN8 (79.26% respect to the control) as against MN3, MN4, and MN7 where the signal displayed the highest levels of 127.3%, 126.66%, and 122.00%, respectively.

3.9 Biochemical marker

The GST activity (Figure 3A) did not significantly differ from the control at all the points. However, earthworms exposed to MN1 soils showed significantly higher enzyme activity values (reaching an average value of 131.18% with respect to the control) than MN2 and MN8 soils that showed enzyme activities of approximately 52.80% and 49.92%, respectively.

The CbE activity (Figure 3B) in earthworms belonging to the control, MN1, and MN2 soils showed a trend of increase in relation to the other groups; however, there were no significant differences ($p > 0.05$). The mean for MN1 and MN2 was 88.06% and 106.47%, respectively, while the values for MN3, MN4, and MN7 varied from 54.26% to 56.00%. However, earthworms exposed to MN8 soils showed light CbE activity inhibition with an average value of 72.06%.

For CAT activity (Figure 3.C), the control showed significantly higher activity than MN2 and MN4 soils, presenting the highest inhibition levels with an average value of 63.82% and 63.26%, respectively. The highest production was also recorded in MN1 soils, with an average value of 113.20% with respect to the control and an important variability within the replicates. However, no significant differences were noted.

The AChE activity (Figure 3D) was significantly decreased in the MN4 group (55.65%) when compared to the control and MN1, with 100% and 126.75%, respectively. For the other groups, there was also a decrease in the activity compared to the control, although differences were not significant.

Protein carbonyl (Figure 3E) increased in all exposure groups compared to the control; however, no significant differences were recorded. Furthermore, for MDA (Figure 3F), the levels at points MN2 (142.53%), MN3 (114.40%), and MN4 (109.28%) were higher than those of the control (100%), MN1 (80.30%), and MN8 (78.38%), but there were no significant differences between the groups. It has to be taken into account that the remarkable variability between replicates exhibited in MDA for most of the treatments, which included the control group, exceeded 50% of the mean value.

3.10 Integrative biomarker response (IBR/n)

The responses of five biomarkers (AChE, GST, CAL, PB, and BR) are represented in six axes start site in Supplementary Figure S11. The general distribution of the integrative response index displays the most severe affectation in MN8 impated (2.91) explained by GST and CAL, even though AChE was the less responsive biomarker in these soils. Contrariwise, AChE showed the highest signal at MN4, where basal respiration was shown to be

TABLE 3 Concentrations (mg·kg^{-1}) of cadmium, chromium, nickel, and lead in *Eisenia fetida* tissue after 14 days of exposure to "Landfill 17" soils measured through ICP-MS.

	Control	MN1	MN2	MN3	MN4	MN7	MN8
Cd (mg kg^{-1})	2.14 ± 0.25	17.27 ± 2.40	16.73 ± 3.83	9.97 ± 1.80	7.56 ± 0.28	9.39 ± 0.76	11.54 ± 3.30
Cr (mg kg^{-1})	0.56 ± 0.16	6.28 ± 3.87	5.53 ± 3.92	8.71 ± 0.99	2.48 ± 0.43	5.71 ± 3.69	41.10 ± 15.16
Ni (mg kg^{-1})	0.71 ± 0.06	4.22 ± 1.45	3.62 ± 1.85	3.78 ± 0.28	2.15 ± 0.30	4.00 ± 1.56	16.33 ± 5.04
Pb (mg kg^{-1})	0.56 ± 0.14	2.18 ± 1.08	2.16 ± 1.61	3.67 ± 0.47	0.95 ± 0.28	2.36 ± 1.22	5.39 ± 2.28

Concentration values are represented as mean ± standard deviation.

the most sensitive parameter, but GST and CAL could not explain the affectation of these soils. Although in MN1, AChE and basal respiration were the two most sensitive parameters, while the CAL signal did not explain the impact on this point.

In addition, MN3 and MN7 were more influenced by basal respiration, and MN3 is also explained by GST, CAL, and AChE signals. As MN7 showed the lowest affectation according to the IBR/n index (1.26), the remaining biomarkers did not seem to be related with the affectation in this soil. Despite MN2 also exhibiting a low affectation value (1.37), basal respiration turned out as the most sensitive parameter, supported by weight loss and GST signal; AChE is slightly related with the degree of impact in this soil.

As it is represented in Figure 4, the general overview of this index denotes the worst ecosystem health status in the MN8 soils, followed by MN1. On the contrary, following the index, the healthiest soils are the ones from MN2.

4 Discussion

After 1.5 years of complementary remediation strategy, the concentrations of Cd, Cr, Ni, Pb, benzo(a)pyrene, and dieldrin were found reduced in all the points, except in MN3. In this point, metal concentrations increased maybe due to the diffuse character of the contamination and the high agronomical alterations suffered during the intensive research assay carried out by Urionabarrenetxea et al. (2021). Soils from MN8 (non-treated) exhibited values for Cr, Cd, Ni, and B(a)P above the legal thresholds in the Basque Country.

In fact, metals were removed between 20% and 32%, while B(a)P exhibited elimination yields approximately 50% (Supplementary Material). For dieldrin, the final concentration could not be obtained because they were under the LOD, although they were below the reference value. The abovementioned reductions were probably influenced by plant growth that improves rhizosphere interactions by releasing root exudates. These interactions help to create a suitable environment for microbial development, increasing rhizodegradation and microbial degradation processes (Reilley et al., 1996; Epelde et al., 2009; Stefanowicz et al., 2012; Nui et al., 2021; Gómez-Sagasti et al., 2021). Different authors (Park et al., 2011; Niu et al., 2021) have already reported that plants can influence metal uptake and/or immobilization through different interactions in the rhizosphere. However, plant growth was not the unique factor to be taken into consideration regarding pollutants toxicity. It is essential to consider bioavailability affected by soil physicochemical properties, such as OM content, cation exchange capacity, granulometry, or pH, due to their strong influence on pollutants adsorption and availability to biological organisms (Berthelot et al., 2009; Lacalle et al., 2018). In agreement with other studies (Gondek and Kopec, 2006; Gondek et al., 2014; Lacalle et al., 2018; Urionabarrenetxea et al., 2021, 2022), metals are strongly absorbed by soil OM content through the formation of strong metal-OM ligands. The aged character of contamination from "Landfill 17," where active sludges were poured 30 years ago, leads to highly persistent OM-metal bounds, making the pollution remarkably recalcitrant (Lacalle et al., 2018; Urionabarrenetxea et al., 2021). This is directly linked to low metal concentrations (mostly ppb order) present in the leachates, suggesting that soil physicochemical properties, along with the influence of rhizosphere interactions, hindered the migration of contaminants to the aqueous matrix. This hypothesis is reinforced by the fact that if the pollution is mobile, it would have already been washed and transported through the fluvial system.

Following the same pattern, a low migration of the compounds was observed (Supplementary Table S3), with Pb being less mobilized with a migration between 0.014% and 0.055%. This could be related to the predominance of non-soluble species that could be strongly attached to the soil, thereby affecting the removal efficiency. Otherwise, Cr also had low migration to the lixiviates. Gondek and Kopec (2006), Lacalle et al. (2020), and Urionabarrenetxea et al. (2021) reported that this metal is strongly correlated with OM levels, suggesting the potential formation of metal-OM ligands. However, MN1 showed the highest Cd mobilization (1.25%), probably due to the notorious presence of *Salix* sp., whose organic acid and peptides in root exudates release metals from soil colloids due to changes in pH (Greger, 2005).

Once the soil quality improvement was assessed, the soil health status was diagnosed by using measurements at different levels of biological complexity and applying the following three different methodological approaches: evaluating soil microbiological communities, regarding the effects upon soil flora, and studying the impacts upon soil fauna (i.e., earthworms).

Microorganisms (especially bacteria and fungi) form most of the soil biomass and diversity, performing a key role in different soil processes and participating in the majority of the soil ecosystem services. This makes microbial parameters good descriptors of the ecosystem health status (Garbisu et al., 2007; Gómez-Sagasti et al., 2012). In fact, AWCD, NUS, and the Shannon index are frequently used to assess microbial communities' functional richness. Thus, AWCD differences in MN3 may be related to the alterations linked with the intensive experimental procedure carried out by Urionabarrenetxea et al. (2021). However, NUS and the Shannon

10.3389/fenvs.2024.1370820

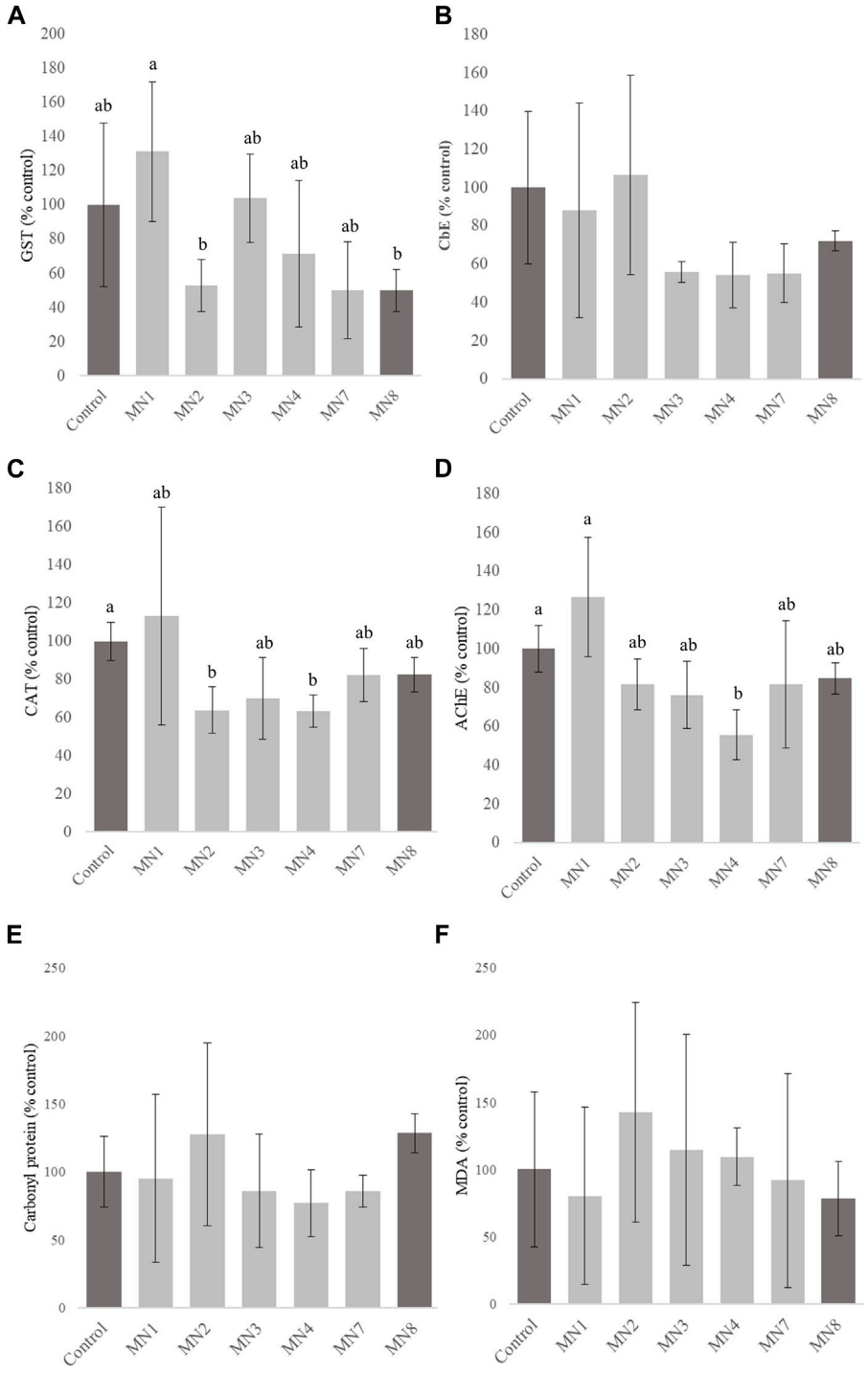

FIGURE 3
Glutathione S-transferase (GST) **(A)**, carboxylesterase (CbE) **(B)**, catalase (CAT) **(C)**, acetylcholinesterase (AChE) **(D)**, carbonyl protein **(E)**, and malondialdehyde (MDA) **(F)** activities measured in *Eisenia fetida* after 14 days of exposure to "Landfill 17" soils. Error bar represents standard deviation. Different letters indicate significant differences analyzed through Tukey and Dunn's tests (p-value < 0.05). A lack of letters indicates the absence of statistical differences among groups.

index did not present significant differences. Furthermore, basal respiration did not present significant differences among groups, so it can be stated that conditions for microbiota are similar (or similarly affected) among the sites, mainly because the microbial parameters are carried out in the native bacterial communities of the sites and all the treated sites had the same bioaugmentation treatment. These native microbial communities must be highly adapted to soil conditions of the site, unlike non-native plants and worms used in bioassays.

Regarding ecological amelioration and restoration of contaminated soils, plant growth and diversity are frequently used as indicators of soil health status (Gómez-Sagasti et al.,

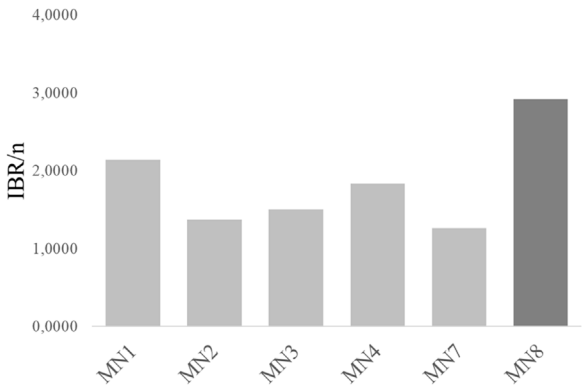

FIGURE 4
Integrative biomarker response (IBR/n) of the "Landfill 17" soils.

2021). In fact, the scarce but diverse native flora found in MN8 soils (non-treated) could suggest a competition between species for resources. Moreover, the existing pollution together with high flood probability due to the proximity to the estuary could also be related with the scarce biomass generated. On the other hand, the highest production and a less diverse native vegetation were present in MN1, dominated by *Salix atrocinerea*, a species tolerant to a variety of conditions such as flooding and disturbed soils. The high biomass of this species can explain the high phytoextraction at the site MN1 and could greatly contribute to remove metals and organic pollutants in this site. It must be mentioned that a high percentage of *Epilobium hirsutum* was observed in MN4 soils. It was reported by Biurrun et al. (2008) that this species together with *Mentha longifolia* shaped the hygronitrophilous communities in the Basque Country. These communities are commonly linked with degraded environments settled over alluvial deposits as is the case of MN4, which is at the closest point to the WWTP and the most altered by inert material or human activity.

As could be expected, soils subjected to complementary treatment exerted a positive effect on plant production. Although alfalfa was planted at the site, in the long term, it was progressively displaced by the colonization of native vegetation, better adapted to the periodic flooding conditions of the site. In fact, we find greater plant biodiversity and observe that most of the final biomass was due to native vegetation contributing to the improvement of soil health. Regarding metal accumulation in plant tissues, low values for metals were recorded in all the sites, maybe due to the already mentioned low metal bioavailability. However, the non-treated MN8 soils showed the lowest accumulation values, especially for Cd. On the contrary, MN1 showed the highest accumulation values, which is positively correlated with the presence of *S. atrocinerea.* This fast-growing species has a very high biomass, and it has been reported to be a high metal accumulator (Landberg and Greger, 1996; Unterbrunner et al., 2007), although different variations can be found between species (Greger, 2005). In accordance with the obtained results, Moreno-Jimenez et al. (2009) had reported high extraction of Cd by *Salix atrocinerea*. This, together with its tolerance to several edaphoclimatic factors make this species an excellent candidate for remediation soils such as those in this study with mixed contamination and periodic flooding.

Phytotoxicity of treated "Landfill 17" soils was carried out with the root elongation test. Despite root elongation being considered the most sensitive endpoint, as its inhibition indicates the first evident effect of metal toxicity (Ali et al., 2004; Visioli et al., 2014), no significant differences in root elongation were observed among the groups. Thus, it can be suggested that "Landfill 17" soils did not exert any phytotoxic effects upon *C. sativus* seedlings. These may be explained by the low concentrations observed in the leachates and phytoextracted fraction, which could suggest that pollutants' migration and/or the available fraction was very low.

Efroymson et al. (1997) developed, for terrestrial plants, a toxicological benchmark for contaminants with a potential concern effect, where the established thresholds were 4 mg $Cd{\cdot}kg^{-1}$, 1 mg $Cr{\cdot}kg^{-1}$, 50 mg $Pb{\cdot}kg^{-1}$, and 30 mg $Ni{\cdot}kg^{-1}$. The concentrations estimated in this work are found to be far from the abovementioned values. Furthermore, Aparicio et al. (2019) obtained for Cr, in *Lactuca sativa*—also a dicotyledonous species, an EC_{50} value of 90 $mg{\cdot}kg^{-1}$, while An et al. (2004) reported in *C. sativus* EC_{50} values for Cd and Pb of approximately 102 and 403 $mg{\cdot}kg^{-1}$, respectively, which are also very far from those measured in this study.

In order to evaluate the impacts upon soil fauna, different standard assays were carried out with *Eisenia fetida* earthworms. The chosen approach was to assess the different uptake pathways in order to elucidate the origin of potential toxicities. Pollutant uptake in earthworms occurs through two different pathways: via the dermis incorporating them from the aqueous matrix and via the digestive tract, by soil ingestion (Rodriguez-Campos et al., 2014). To assess the potential toxicity of the soil water fraction, an OECD filter paper test (OECD-207, 1984) was carried out. Nevertheless, the lack of significant differences between the groups and the observed low weight losses suggested the absence of toxicity via the dermis, just as Urionabarrenetxea et al., observed in 2021. This is something expected, taking into consideration the low metal values observed in the leachates and the LC_{50} values observed in the bibliographical review. For instance, Boyd et al. (2001) reported in *Caenorhadbitis elegans*, LC_{50} in Tifton soils of 18 mg $Cd{\cdot}kg^{-1}$, 34 mg $Ni{\cdot}kg^{-1}$, and 43 mg $Pb{\cdot}kg^{-1}$, while Aparicio et al. (2019) reported a value of 30 $mg{\cdot}kg^{-1}$ for Cr.

The assessment of the exposure through dermal contact and the digestive tract was carried out following OECD artificial soil testing guidelines (1984), where neither significant mortality nor weight loss was recorded. Indeed, in some groups, the earthworms gained biomass, while the control group showed the highest weight loss. This is directly related with the high OM contents of the "Landfill 17" soils, which was the destination of sewage sludge discharges for decades (Urionabarrenetxea et al., 2022). In this sense, different authors have reported a positive correlation between soil ingestion and OM content in *E. fetida*, improving their nutritional status and reducing potential biomass loss when facing pollutant exposure (Irizar et al., 2014a, 2015b; Lacalle et al., 2020; Urionabarrenetxea et al., 2021). However, and as previously discussed, soil organic matter affects metal bioavailability and toxicity by forming different organometallic ligands, and consequently, metal accumulation in earthworm tissues increases due to the incorporation of polluted soil colloids (Irizar et al., 2015b). The metal accumulation tendency found in this study presents a positive correlation with the biomass recorded. Thereby, MN8 is the group showing the lowest biomass loss (in fact, weight was gained) but the highest metal accumulation rates.

The assessment of earthworm coelomocytes has an important role in the study of immunological responses, providing valuable information about the early response to pollutants (Plytycz et al., 2010; Kwak et al., 2014; García Velasco et al., 2019). In this study, coelomocyte viability and cytotoxicity were assessed by using the calcein-AM assay. After 14 days of exposure to soils from "Landfill 17," MN8 soils (non-treated) showed a significant decrease in calcein signal, suggesting strong cell damage and cytotoxicity. Similarly, Irizar et al. (2015a) and Plytycz and Morgan (2011a) have reported changes in coelomocyte viability (cytotoxicity) when exposed to Cr. At the same time, MN1 and MN2 exhibited a slight decrease in calcein retention, suggesting that Cd presence in these sites could induce affectation upon immune system and cell integrity (Irizar et al., 2015a; Aparicio et al., 2019). However, the lower retention present in the control (OECD soil) may be related to different soil conditions when compared with "Landfill 17" soils. Furthermore, slight alterations in retention ability could also be influenced by soil pH conditions and coelomocyte subpopulation variations: amoebocytes can phagocyte death eleocytes (Irizar, 2015a), which are more sensitive to metal pollution (Plytycz et al., 2009; Plytycz et al., 2010; Plytycz et al., 2011b; Irizar et al., 2015a).

Alterations in the activity of the enzymes could occur due to the different contaminants present in "Landfill 17" soils. The significant increase in GST activity observed in earthworms exposed to MN1 soils indicates an activation of the detoxification mechanism, allowing the organism to overcome, totally or partially, the stress caused by exposure to xenobiotics (Liu et al., 2015). Similar results were observed in *Eisenia fetida* when exposed to Cd (Liang et al., 2022). Moreover, the decrease in CAT activity in MN2 and MN4 may suggest a greater accumulation of H_2O_2 and potential formation of ROS (Lisbôa et al., 2021). However, under the conditions studied, there was no occurrence of oxidative stress due to the absence of alterations on protein carbonyl and MDA levels in all groups. This may be related to the increase in and/or unchanged activity of the GST and CbE enzymes, which can exert a protective effect and prevent the occurrence of oxidative damage, also an alleviation of lipid peroxidation (Wheelock et al., 2008; Hellou et al., 2012).

To evaluate neurotoxicity, the activity of the AChE enzyme was determined. This enzyme acts in the transmission of nerve impulses and has the function of hydrolyzing the neurotransmitter acetylcholine (Tiwari et al., 2016). The decrease in AChE in earthworms may result in less locomotion capacity, which also compromises feeding and reproduction, leading to death (Gambi et al., 2007; Wang et al., 2015). Thus, the decrease in AChE activity observed in MN4 may have occurred due to exposure to a mixture of metals such as dieldrin and B(a)P present at this location. The activity of this enzyme may decrease depending on the type of contaminant and the species of earthworm. In fact, a decrease in AChE was observed in *Eisenia andrei* when exposed to Pb, in *E. fetida* when exposed to soils contaminated with Cr, Ni, and Pb (Zheng et al., 2013), in *Eisenia fetida* when exposed to Ni, Zn, Cd, Cu and Hg (Frasco et al., 2005; Zheng et al., 2013), in *E. fetida* when exposed to a mixture of Cd and B(a)P (Zhang et al., 2019), and in *E. fetida* when exposed to insecticide imidacloprid (Wang et al., 2015).

For the IBR/n index, the recommendations of Asensio et al. (2013) about using multiple organisms to achieve an accurate approximation of the whole ecosystem status were followed. Thus, the integrative biomarker response index was developed with five of the most representative measured biological parameters and biomarkers from each organism to integrate responses at different levels of biological complexity (molecular > enzyme activity > cellular > community) and represent, from a holistic point of view, the ecosystem status based on soil–microorganism–plant–earthworm interactions. Hence, according to the IBR/n index developed by Aparicio et al. (2021) for microbiota, basal respiration (BR) was considered to represent microbial communities' activity. The most representative parameter considered to represent the vegetation was plant biomass, which exhibited significant differences between treatments. For earthworms, different representative biomarkers (biochemical and cellular) exhibiting significant differences were considered: at the cellular level—CAL and at biochemical level—AChE and GST.

The signals at the lower biological levels (GST and CAL) were more responsive against stress related with pollution, just as basal respiration gives a global response more based on stress provoked by environmental conditions. High affectation of the ecosystem status was readily evidenced in non-treated MN8, while in MN4, a remarkable stress over microbial communities and high neurotoxic effects upon fauna could be observed. Meanwhile, the best ecosystem health was recorded in MN7, the furthest point from the WWTP.

5 Conclusion

After the application of the complementary remediation strategy for 1.5 years in a soil with mixed contamination, the concentrations of the critical compounds [Cd, Cr, Ni, Pb, benzo(a)pyrene, and dieldrin] were reduced in most of the "Landfill 17" sampled points, where a high sequestration of the pollutants was present due to several factors such as OM content, aged contamination, the presence of plants, or even the enhancement of rhizosphere interactions.

Microbiological parameters did not indicate differences between non-treated (MN8) and treated sites due to the adaptation of native microbial communities to the soil conditions of the sites. However, the treated sites presented a notable colonization of native vegetation and increased plant biomass. In our case, the spontaneous native vegetation helped in the recovery of the soil and ecosystem health. However, it should be taken into account that due to their limitations soils can make difficult the growth of other cultivars in sites. The bioassays did not present phytotoxicity upon *C. sativus* or toxicity upon *E. fetida* earthworms. Nevertheless, in the sites subjected to the complementary remediation strategy, earthworms could alleviate toxicity through detoxifying and immune systems. Additionally, the IBR indexes helped integrate multiple organisms' information in a helpful and comprehensive way for scientists, regulators, and other stakeholders. Therefore, the combination of bioremediation technologies (micro-, phyto-, and vermiremediation) followed by a complementary strategy has been proven to be an accurate approach to improve soil functionality, quality, and health under natural conditions.

Data availability statement

The original contributions presented in the study are included in the article/Supplementary Material; further inquiries can be directed to the corresponding author.

Ethics statement

The manuscript presents research on animals that do not require ethical approval for their study. As the animals are not included in Annex I of the Royal Decree 53/2013, assessment and follow-up by the Ethics and Teaching Commission (CEID) was not required.

Author contributions

AP-V: Data curation, formal analysis, investigation, methodology, manuscript writing—original draft, review, and editing. EU: Data curation, formal analysis, investigation, methodology, project administration, supervision, validation, manuscript writing—original draft, review, and editing. UA: Data curation, investigation, methodology, project administration, supervision, manuscript writing—original draft, review, and editing. CR: Data curation, investigation, manuscript writing—original draft, review, and editing. MG-S: Investigation, methodology, supervision, manuscript writing—original draft, review, and editing. NG-V: Investigation, methodology, manuscript writing—original draft, review, and editing. BZ: Investigation, methodology, supervision, manuscript writing—original draft, review, and editing. MA: Investigation, methodology, supervision, manuscript writing—original draft, review, and editing. LE: Methodology, project administration, resources, supervision, manuscript writing—original draft, review, and editing. CG: Funding acquisition, methodology, project administration, resources, supervision, manuscript writing—original draft, review, and editing. JB: Funding acquisition, methodology, project administration, resources, supervision, manuscript writing—original draft, review, and editing. MS: Funding acquisition, methodology, project administration, resources, supervision, manuscript writing—original draft, review, and editing.

Funding

The authors declare financial support was received for the research, authorship, and/or publication of this article. This study was supported by the Phy2SUDOE (SOE4/P5/E1021) project funded by the Interreg Sudoe Program through the European Regional Development Fund (ERDF), PRADA project (PID2019110055RB-C21 and PID 2019-110055RB-C22) from MINECO, and the Consolidated Research Grant of the Basque Government (GV IT-1648-22).

Conflict of interest

The authors declare that the research was conducted in the absence of any commercial or financial relationships that could be construed as a potential conflict of interest.

Publisher's note

All claims expressed in this article are solely those of the authors and do not necessarily represent those of their affiliated organizations, or those of the publisher, editors, and reviewers. Any product that may be evaluated in this article, or claim that may be made by its manufacturer, is not guaranteed or endorsed by the publisher.

Supplementary material

The Supplementary Material for this article can be found online at: https://www.frontiersin.org/articles/10.3389/fenvs.2024.1370820/full#supplementary-material

References

Aebi, H. (1984). Catalase *in vitro*. *Methods Enzym.* 105, 121–126. doi:10.1016/S0076-6879(84)05016-3

Ali, N. A., Ater, M., Sunahara, G. I., and Robidoux, P. Y. (2004). Phytotoxicity and bioaccumulation of copper and chromium using barley (*Hordeum vulgare* L.) in spiked artificial and natural forest soils. *Ecotoxicol. Environ. Saf.* 57 (3), 363–374. doi:10.1016/S0147-6513(03)00074-5

Almeida, E. A., Bainy, A. C. D., Dafre, A. L., Gomes, O. F., Medeiros, M. H. G., and Di Mascio, P. (2005). Oxidative stress in digestive gland and gill of the brown mussel (*Perna perna)* exposed to air and re-submersed. *J. Exp. Mar. Biol. Ecol.* 318, 21–30. doi:10.1016/j.jembe.2004.12.007

An, Y.-J., Kim, Y.-M., Kwon, T.-I., and Jeong, S.-W. (2004). Combined effect of copper, cadmium, and lead upon *Cucumis sativus* growth and bioaccumulation. *Sci. Total Environ.* 326, 85–93. doi:10.1016/j.scitotenv.2004.01.002

Antoci, A., Galeotti, M., and Sordi, S. (2018). Environmental pollution as engine of industrialization. *Commun. Nonlinear Sci. Numer. Simul.* 58, 262–273. doi:10.1016/j.cnsns.2017.06.016

Aparicio, J. D., Garcia-Velasco, N., Urionabarrenetxea, E., Soto, M., Álvarez, A., and Polti, M. A. (2019). Evaluation of the effectiveness of a bioremediation process in experimental soils polluted with chromium and lindane. *Ecotoxicol. Environ. Saf.* 181, 255–263. doi:10.1016/j.ecoenv.2019.06.019

Aparicio, J. D., Lacalle, R. G., Artetxe, U., Urionabarrenetxea, E., Becerril, J. M., Polti, M. A., et al. (2021). Successful remediation of soils with mixed contamination of chromium and lindane: integration of biological and physico-chemical strategies. *Environ. Res.* 194, 110666. doi:10.1016/j.envres.2020.110666

Asensio, V., Rodríguez-Ruiz, A., Garmendia, L., Andre, J., Kille, P., Morgan, A. J., et al. (2013). Towards an integrative soil health assessment strategy: a three tier (integrative biomarker response) approach with *Eisenia fetida* applied to soils subjected to chronic metal pollution. *Sci. Total Environ.* 442, 344–365. doi:10.1016/j.scitotenv.2012.09.048

Basque Country (2023). Inventory of soils with potentially contaminating activities or facilities. Available at: https://www.geo.euskadi.eus/geobisorea.

Basque Government (2012). Plan de Suelos Contaminados del País Vasco (2007-2012). Available at: http://www.ingurumena.ejgv.euskadi.eus/r49orokorra/es/contenidos/plan/suelos_contaminados/es_plan/adjuntos/plan_suelos_contaminados.pdf.

Beliaeff, B., and Burgeot, T. (2002). Integrated biomarker response: a useful tool for ecological risk assessment. *Environ. Toxicol. Chem.* 21 (6), 1316–1322. doi:10.1002/etc.5620210629

Berthelot, Y., Trottier, B., and Robidoux, P. (2009). Assessment of soil quality using bioaccessibility-based models and a biomarker index. *Environ. Int.* 35 (1), 83–90. doi:10.1016/j.envint.2008.07.008

Biurrun, I., García-Mijangos, I., Crespo, M. B., and Fernández-González, F. (2008). Los herbazales higronitrófilos de *Epilobium hirsutum* y *Mentha longifolia* en los cursos fluviales de la Península Ibérica. *Lazaroa* 29, 69–86.

BOE núm. 25. Sect. I. Disposiciones generales. 3507-3521. Boletin Oficial del Estado, Ministerio de Medio Ambiente (2002). Available at: https://www.boe.es/eli/es/rd/2001/12/27/1481

Boyd, W. A., Stringer, V. A., and Williams, P. L. (2001). Metal LC50s of a soil nematode compared to published earthworm data. *Environ. Toxicol. Risk Assess. Sci. Policy, Stand. Implic. Environ. Decis.* 10, 223–235. doi:10.1520/STP10257S

Bradford, M. M. (1976). A rapid and sensitive method for the quantitation of microgram quantities of protein utilizing the principle of protein-dye binding. *Elsevier BV* 72, 248–254. doi:10.1006/abio.1976.9999

Broeg, K., and Lehtonen, K. K. (2006). Indices for the assessment of environmental pollution of the Baltic Sea coasts: integrated assessment of a multi-biomarker approach. *Mar. Pollut. Bull.* 53 (8–9), 508–522. doi:10.1016/j.marpolbul.2006.02.004

Cajaraville, M. P., Marigómez, I., and Angulo, E. (1993). Correlation between cellular and organismic responses to oil-induced environmental stress in mussels. *Sci. Tot. Environ.* 134, 1353–1371. doi:10.1016/S0048-9697(05)80142-1

Efroymson, R. A., Will, M. E., Ii, G. W. S., and Wooten, A. C., 1997. Toxicological benchmarks for screening contaminants of potential concern for effects on terrestrial plants. doi:10.2172/10107985

Ellman, G. L., Courtney, K. D., Andres, V., and Featherstone, R. M. (1961). A new and rapid colorimetric determination of acetylcholinesterase activity. *Biochem. Pharmacol.* 7 (2), 88–95. doi:10.1016/0006-2952(61)90145-9

Epelde, L., Becerril, J. M., Hernández-Allica, J., Barrutia, O., and Garbisu, C. (2008). Functional diversity as indicator of the recovery of soil health derived from *Thlaspi caerulescens* growth and metal phytoextraction. *Appl. Soil Ecol.* 39 (3), 299–310. doi:10.1016/j.apsoil.2008.01.005

Epelde, L., Mijangos, I., Becerril, J. M., and Garbisu, C. (2009). Soil microbial community as bioindicator of the recovery of soil functioning derived from metal phytoextraction with sorghum. *Soil Biol. Biochem.* 41 (9), 1788–1794. doi:10.1016/j.soilbio.2008.04.001

Franco, H. A., Silva, M. E. R. V. D., Silveira, M. F. D., Marques, M. R. D. C., and Thode Filho, S. (2017). Impact of landfill leachate on the germination of Cucumber (*Cucumis sativus*). *Rev. Eletrônica Em Gestão, Educ. Tecnol. Ambient.* 21, 32. doi:10.5902/2236117029719

Frasco, M. F., Fournier, D., Carvalho, F., and Guilhermino, L. (2005). Do metals inhibit acetylcholinesterase (AChE)? Implementation of assay conditions for the use of AChE activity as a biomarker of metal toxicity. *Biomarkers* 10 (5), 360–375. doi:10.1080/13547500500264660

Gambi, N., Pasteris, A., and Fabbri, E. (2007). Acetylcholinesterase activity in the earthworm *Eisenia andrei* at different conditions of carbaryl exposure. *Comp. Biochem. Physiology Part C Toxicol. Pharmacol.* 145 (4), 678–685. doi:10.1016/j.cbpc.2007.03.002

Garbisu, C., Becerril, J. M., Epelde, L., and Alkorta, I. (2007). *Bioindicadores de la calidad del suelo: herramienta metodológica para la evaluación de la eficacia de un proceso fitorremediador*.

Garcia-Velasco, N., Irizar, A., Urionabarrenetxea, E., Scott-Fordsmand, J. J., and Soto, M. (2019). Selection of an optimal culture medium and the most responsive viability assay to assess AgNPs toxicity with primary cultures of *Eisenia fetida* coelomocytes. *Ecotoxicol. Environ. Saf.* 183, 109545. doi:10.1016/j.ecoenv.2019.109545

Gómez-Sagasti, M. T., Alkorta, I., Becerril, J. M., Epelde, L., Anza, M., and Garbisu, C. (2012). Microbial monitoring of the recovery of soil quality during heavy metal phytoremediation. *Water, Air, & Soil Pollut.* 223 (6), 3249–3262. doi:10.1007/s11270-012-1106-8

Gómez-Sagasti, M. T., Garbisu, C., Urra, J., Míguez, F., Artetxe, U., Hernández, A., et al. (2021). Mycorrhizal-assisted phytoremediation and intercropping strategies improved the health of contaminated soil in a peri-urban area. *Front. Plant Sci.* 12, 693044. doi:10.3389/fpls.2021.693044

Gondek, K., Baran, A., and Kopec, M. (2014). The effect of low-temperature transformation of mixtures of sewage sludge and plant materials on content, leachability and toxicity of heavy metals. *Chemos* 117, 33–39. doi:10.1016/j.chemosphere.2014.05.032

Gondek, K., and Kopec, M. (2006). Heavy metal binding by organic substance in sewage sludge of various origin. *EJPAU Environ. Dev.* 9 (3). Available at: http://www.ejpau.media.pl/volume9/issue3/art-01.html.

Greger, M. (2005). *Biogechemistry of trace metals in the rhizosphere*. Germany: Elsevier.

Hakanson, L. (1980). An ecological risk index for aquatic pollution control. A sedimentological approach. *Water Res.* 14 (8), 975–1001. doi:10.1016/0043-1354(80)90143-8

Hellou, J., Ross, N. W., and Moon, T. W. (2012). Glutathione, glutathione S-transferase, and glutathione conjugates, complementary markers of oxidative stress in aquatic biota. *Environ. Sci. Pollut. Res.* 19 (6), 2007–2023. doi:10.1007/s11356-012-0909-x

Htwe, T., Chotikarn, P., Duangpan, S., Onthong, J., Buapet, J., and Sinutok, S. (2022). Integrated biomarker responses of rice associated with grain yield in copper-contaminated soil. *Environ. Sci. Pollut. Res.* 29, 8947–8956. doi:10.1007/s11356-021-16314-y

Irizar, A., Duarte, D., Guilhermino, L., Marigómez, I., and Soto, M. (2014a). Optimization of NRU assay in primary cultures of *Eisenia fetida* for metal toxicity assessment. *Ecotoxicology* 23 (7), 1326–1335. doi:10.1007/s10646-014-1275-x

Irizar, A., Izagirre, U., Diaz De Cerio, O., Marigómez, I., and Soto, M. (2014b). Zonation in the digestive tract of *Eisenia fetida*: implications in biomarker measurements for toxicity assessment. *Comp. Biochem. Physiology Part C Toxicol. Pharmacol.* 160, 42–53. doi:10.1016/j.cbpc.2013.11.006

Irizar, A., Rivas, C., García-Velasco, N., De Cerio, F. G., Etxebarria, J., Marigómez, I., et al. (2015a). Establishment of toxicity thresholds in subpopulations of coelomocytes (amoebocytes vs. eleocytes) of *Eisenia fetida* exposed *in vitro* to a variety of metals: implications for biomarker measurements. *Ecotoxicology* 24 (5), 1004–1013. doi:10.1007/s10646-015-1441-9

Irizar, A., Rodríguez, M. P., Izquierdo, A., Cancio, I., Marigómez, I., and Soto, M. (2015b). Effects of soil organic matter content on cadmium toxicity in *Eisenia fetida*: implications for the use of biomarkers and standard toxicity tests. *Archives Environ. Contam. Toxicol.* 68 (1), 181–192. doi:10.1007/s00244-014-0060-4

ISO 16072 (2002). *Soil quality - laboratory methods for determination of microbial soil respiration*. Geneva: International Organization for Standardization ISO.

Jan, A. T., Ali, A., and Rizwanul Haq, Q. M. (2015). "Phytoremediation," in *Soil remediation and plants* (Germany: Elsevier), 63–84. doi:10.1016/B978-0-12-799937-1.00003-6

Keen, J. H., Habig, W. H., and Jakoby, W. B. (1976). Mechanism for the several activities of the glutathione S-transferases. *J. Biol. Chem.* 251 (20), 6183–6188. doi:10.1016/S0021-9258(20)81842-0

Kwak, J. I., Kim, S. W., and An, Y.-J. (2014). A new and sensitive method for measuring *in vivo* and *in vitro* cytotoxicity in earthworm coelomocytes by flow cytometry. *Environ. Res.* 134, 118–126. doi:10.1016/j.envres.2014.07.014

Lacalle, R. G., Aparicio, J. D., Artetxe, U., Urionabarrenetxea, E., Polti, M. A., Soto, M., et al. (2020). Gentle remediation options for soil with mixed chromium (VI) and lindane pollution: biostimulation, bioaugmentation, phytoremediation and vermiremediation. *Heliyon* 6 (8), e04550. doi:10.1016/j.heliyon.2020.e04550

Lacalle, R. G., Gómez-Sagasti, M. T., Artetxe, U., Garbisu, C., and Becerril, J. M. (2018). *Brassica napus* has a key role in the recovery of the health of soils contaminated with metals and diesel by rhizoremediation. *Sci. Total Environ.* 618, 347–356. doi:10.1016/j.scitotenv.2017.10.334

Landberg, T., and Greger, M. (1996). Differences in uptake and tolerance to heavy metals in Salix from unpolluted and polluted areas. *Appl. Geochem.* 11, 175–180. doi:10.1016/0883-2927(95)00082-8

Liang, X., Zhou, D., Wang, J., Li, Y., Liu, Y., and Ning, Y. (2022). Evaluation of the toxicity effects of microplastics and cadmium on earthworms. *Sci. Total Environ.* 836, 155747. doi:10.1016/j.scitotenv.2022.155747

Lisbôa, R. D. M., Storck, T. R., Silveira, A. D. O., Wolff, D., Tiecher, T. L., Brunetto, G., et al. (2021). Ecotoxicological responses of *Eisenia andrei* exposed in field-contaminated soils by sanitary sewage. *Ecotoxicol. Environ. Saf.* 214, 112049. doi:10.1016/j.ecoenv.2021.112049

Liu, K., Chen, L., Zhang, W., Lin, K., and Zhao, L. (2015). EPR detection of hydroxyl radical generation and oxidative perturbations in lead-exposed earthworms (*Eisenia fetida*) in the presence of decabromodiphenyl ether. *Ecotoxicology* 24 (2), 301–308. doi:10.1007/s10646-014-1378-4

Marigómez, I., Garmendia, L., Soto, M., Orbea, A., Izagirre, U., and Cajaraville, M. P. (2013). Marine ecosystem health status assessment through integrative biomarker indices: a comparative study after the Prestige oil spill "Mussel Watch.". *Ecotoxicology* 22 (3), 486–505. doi:10.1007/s10646-013-1042-4

Meshalkin, V. P., Kozlovskiy, R. A., Kozlovskiy, M. R., Ibatov, Y. A., Voronov, M. S., Kozlovskiy, I. A., et al. (2023). Experimental and mathematical analysis of the kinetics of the low-waste process of butyl lactate synthesis. *Energies* 16 (4), 1746. doi:10.3390/en16041746

Míguez, F., Gómez-Sagasti, M. T., Hernández, A., Artetxe, U., Blanco, F., Castañeda, J. H., et al. (2020). *In situ* phytomanagement with *Brassica napus* and bio-stabilised municipal solid wastes is a suitable strategy for redevelopment of vacant urban land. *Urban For. Urban Green.* 47, 126550. doi:10.1016/j.ufug.2019.126550

Moreno-Jiménez, E., Peñalosa, J. M., Manzano, R., Carpena-Ruiz, R. O., Gamarra, R., and Esteban, E. (2009). Heavy metals distribution in soils surrounding an abandoned mine in NW Madrid (Spain) and their transference to wild flora. *J. Hazard. Mater.* 162 (2–3), 854–859. doi:10.1016/j.jhazmat.2008.05.109

Morillo, E., and Villaverde, J. (2017). Advanced technologies for the remediation of pesticide-contaminated soils. *Sci. Total Environ.* 586, 576–597. doi:10.1016/j.scitotenv.2017.02.020

Niu, H., Wu, H., Chen, K., Sun, J., Cao, M., and Luo, J. (2021). Effects of decapitated and root-pruned Sedum alfredii on the characterization of dissolved organic matter and enzymatic activity in rhizosphere soil during Cd phytoremediation. *J. Hazard. Mater.* 417, 125977. doi:10.1016/j.jhazmat.2021.125977

OECD (1984). Terrestrial plant: growth test OECD. Guideline for chemicals, No., 208. Organization for economic cooperation and development, Paris on the crossroads of remediation. *Soil Rem. Plant*, 63–84.

Pankhurst, C. E., Doube, B. M., and Gupta, V. V. S. R. (1997). in *Biological indicators of soil health: synthesis. En biological indicators of soil health*. Editors C. E. Pankhurst, B. M. Doube, and V. V. S. R. Gupta (New York, USA: CAB International), 419–435.

Park, J. H., Lamb, D., Paneerselvam, P., Choppala, G., Bolan, N., and Chung, J. W. (2011). Role of organic amendments on enhanced bioremediation of heavy metal(loid) contaminated soils. *J. Hazard. Mater.* 185, 549–574. doi:10.1016/j.jhazmat.2010.09.082

Parvez, S., and Raisuddin, S. (2005). Protein carbonyls: novel biomarkers of exposure to oxidative stress-inducing pesticides in freshwater fish *Channa punctata* (Bloch). *Environ. Toxicol. Pharmacol.* 20 (1), 112–117. doi:10.1016/j.etap.2004.11.002

Pirincciogluo, A. G., Gökalp, D., Pirincciogluo, M., Kizil, G., and Kizil, M. (2010). Malondialdehyde (MDA) and protein carbonyl (PCO) levels as biomarkers of oxidative stress in subjects with familial hypercholesterolemia. *Clin. Biochem.* 43 (15), 1220–1224. doi:10.1016/j.clinbiochem.2010.07.022

Plytycz, B., Kielbasa, E., Grebosz, A., Duchnowski, M., and Morgan, A. J. (2010). Riboflavin mobilization from eleocyte stores in the earthworm *Dendrodrilus rubidus* inhabiting aerially contaminated Ni smelter soil. *Chemosphere* 81 (2), 199–205. doi:10.1016/j.chemosphere.2010.06.056

Plytycz, B., Klimek, M., Homa, J., Mazur, A. I., Kruk, J., and Morgan, A. J. (2011b). Species-specific sensitivity of earthworm coelomocytes to dermal metal (Cd, Cu, Ni, Pb, Zn) exposures: methodological approach. *Pedobiologia* 54, S203–S210. doi:10.1016/j.pedobi.2011.06.002

Plytycz, B., Lis-Molenda, U., Cygal, M., Kielbasa, E., Grebosz, A., Duchnowski, M., et al. (2009). Riboflavin content of coelomocytes in earthworm (*Dendrodrilus rubidus*) field populations as a molecular biomarker of soil metal pollution. *Environ. Pollut.* 157 (11), 3042–3050. doi:10.1016/j.envpol.2009.05.046

Plytycz, B., and Morgan, A. J. (2011a). Riboflavin storage in earthworm chloragocytes/eleocytes in an eco-immunology perspective. *Int. Sci. J.* 8, 199–209.

Reilley, K. A., Schwab, A. P., and Banks, M. K. (1996). Dissipation of polycyclic aromatic hydrocarbons in the rhizosphere. *Dissipation Polycycl. Aromatic Hydrocarbons Rhizosphere* 25, 212–219. doi:10.2134/jeq1996.00472425002500020002x

Rodriguez-Campos, J., Dendooven, L., Alvarez-Bernal, D., and Contreras-Ramos, S. M. (2014). Potential of earthworms to accelerate removal of organic contaminants from soil: a review. *Appl. Soil Ecol.* 79, 10–25. doi:10.1016/j.apsoil.2014.02.010

Schindelin, J., Arganda-Carreras, I., Frise, E., Kaynig, V., Longair, M., Pietzsch, T., et al. (2012). Fiji: an open-source platform for biological-image analysis. *Nat. Methods* 9 (7), 676–682. doi:10.1038/nmeth.2019

Stefanowicz, A. M., Kapusta, P., Szarek-Łukaszewska, G., Grodzińska, K., Niklińska, M., and Vogt, R. D. (2012). Soil fertility and plant diversity enhance microbial performance in metal-polluted soils. *Sci. Total Environ.* 439, 211–219. doi:10.1016/j.scitotenv.2012.09.030

Tiwari, R. K., Singh, S., Pandey, R. S., and Sharma, B. (2016). Enzymes of earthworm as indicators of pesticide pollution in soil. *Adv. Enzyme Res.* 04, 113–124. doi:10.4236/aer.2016.44011

Unterbrunner, R., Puschenreiter, M., Sommer, P., Wieshammer, G., Tlustoõs, P., Zupan, M., et al. (2007). Heavy metal accumulation in trees growing on contaminated sites in Central Europe. *Environ. Pollut.* 148, 107–114. doi:10.1016/j.envpol.2006.10.035

Urionabarrenetxea, E., Garcia-Velasco, N., Anza, M., Artetxe, U., Lacalle, R., Garbisu, C., et al. (2021). Application of *in situ* bioremediation strategies in soils amended with sewage sludges. *Sci. Total Environ.* 766, 144099. doi:10.1016/j.scitotenv.2020.144099

Urionabarrenetxea, E., Garcia-Velasco, N., Zaldibar, B., and Soto, M. (2022). Impacts of sewage sludges deposition on agricultural soils: effects upon model soil organisms. *Comp. Biochem. Physiology Part C Toxicol. Pharmacol.* 255, 109276. doi:10.1016/j.cbpc.2022.109276

US- EPA (1982). *Seed germination/root elongation toxicity tests EC12*. Office of Toxic Substances, Washington, DC: US Environmental Protection Agency.

US-EPA Method 3051A (2007). *Microwave assisted acid digestion of sediments, sludges, soils and oils*. third ed. Washington, DC: US Environmental Protection Agency.

Vasylkiv, O.Yu., Kubrak, O. I., Storey, K. B., and Lushchak, V. I. (2010). Cytotoxicity of chromium ions may be connected with induction of oxidative stress. *Chemosphere* 80 (9), 1044–1049. doi:10.1016/j.chemosphere.2010.05.023

Visioli, G., Conti, F. D., Gardi, C., and Menta, C. (2014). Germination and root elongation bioassays in six different plant species for testing Ni contamination in soil. *Bull. Environ. Contam. Toxicol.* 92 (4), 490–496. doi:10.1007/s00128-013-1166-5

Wang, K., Huang, Y., Li, X., and Chen, M. (2018). Functional analysis of a carboxylesterase gene associated with isoprocarb and cyhalothrin resistance in *Rhopalosiphum padi*(L.). *Front. Physiology* 9, 992. doi:10.3389/fphys.2018.00992

Wang, K., Qi, S., Mu, X., Chai, T., Yang, Y., Wang, D., et al. (2015). Evaluation of the toxicity, AChE activity and DNA damage caused by imidacloprid on earthworms, *Eisenia fetida*. *Bull. Environ. Contam. Toxicol.* 95 (4), 475–480. doi:10.1007/s00128-015-1629-y

Wheelock, C. E., Phillips, B. M., Anderson, B. S., Miller, J. L., Miller, M. J., and Hammock, B. D. (2008). Applications of carboxylesterase activity in environmental monitoring and toxicity identification evaluations (TIEs). *Rev. Environ. Contam. Toxicol.* 195, 117–178. doi:10.1007/978-0-387-77030-7_5

Zhang, L., Zhou, L., Han, L., Zhao, C., Norton, J. M., Li, H., et al. (2019). Benzo(a)pyrene inhibits the accumulation and toxicity of cadmium in subcellular fractions of *Eisenia fetida*. *Chemosphere* 219, 740–747. doi:10.1016/j.chemosphere.2018.12.083

Zheng, K., Liu, Z., Li, Y., Cui, Y., and Li, M. (2013). Toxicological responses of earthworm (*Eisenia fetida)* exposed to metal-contaminated soils. *Environ. Sci. Pollut. Res.* 20 (12), 8382–8390. doi:10.1007/s11356-013-1689-7

frontiers | Frontiers in Environmental Science

TYPE Original Research
PUBLISHED 16 May 2024
DOI 10.3389/fenvs.2024.1403989

OPEN ACCESS

EDITED BY
Qi Liao,
School of Metallurgy and Environment, Central South University, China

REVIEWED BY
Hao Li,
Kunming University of Science and Technology, China
Peng Wang,
Chengdu University of Technology, China

*CORRESPONDENCE
Jian Long,
longjiancsuft@yeah.net

†These authors have contributed equally to this work and share first authorship

RECEIVED 20 March 2024
ACCEPTED 30 April 2024
PUBLISHED 16 May 2024

CITATION
Fan H, Tang S, Long J, He R, Xiao Z, Hou H and Peng P (2024), Effects of exogenous chloride ions on the migration and transformation of Cd in a soil-rice system.
Front. Environ. Sci. 12:1403989.
doi: 10.3389/fenvs.2024.1403989

Effects of exogenous chloride ions on the migration and transformation of Cd in a soil-rice system

Haijin Fan[1,2†], Shengshuang Tang[1,2†], Jian Long[1,2*], Rujing He[1,2], Ziman Xiao[1,2], Hongbo Hou[1,2] and Peiqin Peng[1,2]

[1]College of Life and Environmental Science, Central South University of Forestry and Technology, Changsha, China, [2]Yuelu Shan Laboratory, Changsha, China

Soil cadmium (Cd) contamination has emerged as a significant global environmental concern, posing numerous risks to individual organisms and entire ecosystems. Concurrently, the global increase in pesticide usage has elevated the influx of chloride ions (Cl^-) into the soil. Given Cl^-'s robust ability to coordinate and complex with various heavy metal ions, understanding its influence on the migration and transformation of Cd in soil-rice systems is essential for the rational application of pesticides and the effective mitigation of soil heavy metal pollution. In this paper, we explained the effect of Cl^- on the environmental behavior of Cd in the soil-rice system in terms of growth traits, Cd uptake and accumulation by rice, and Cd solid-solution phase interface behavior through pot experiments and sand culture experiments. The results showed that Cd concentrations in all parts of the rice treated with $CaCl_2$ during the filling period were lower than those in the $Ca(NO_3)_2$-treated group, with Cd accumulation diminishing as Cl^- concentration increased. This suggests that the filling period is critical for Cd uptake and accumulation in rice. Unlike the accompanying anion NO_3^-, exogenous Cl^- reduced Cd concentrations in the soil solution but increased them in rice. Notably, when the Cd/Cl ratio ranged from 0.625 to 2.5, Cl^- formed predominantly $CdCl^+$-complexes with free Cd^{2+} in the soil solution, enhancing the mobilization of Cd bound to soil particles and its subsequent absorption by rice. This study aims to assess Cl^-'s effect on Cd migration and transformation in soil-rice systems, providing insights for safe rice production on Cd-contaminated soils and rational use of chlorine-containing pesticides.

KEYWORDS

agrochemicals, chloride, rice, Cd accumulation, complex

1 Introduction

Cadmium (Cd) represents a significant biotoxic heavy metal and the primary contaminant in agricultural soils across China (Fu et al., 2021). Beyond natural sources, human activities constitute the primary contributors to soil Cd pollution. The extensive application of cadmium and cadmium-bearing minerals in agriculture and industry facilitates the entry of this heavy metal into agricultural soils through various pathways (Wang et al., 2019; Hussain et al., 2020). Cadmium, a non-essential metal, enters the human body primarily through the soil-food-human transfer chain (Feng et al., 2020). Compared

to other heavy metals, cadmium exhibits higher mobility in soils, facilitating its absorption, transfer, and accumulation by animals, plants, and microorganisms in significant quantities. This accumulation impairs the biological functions of soil organisms and poses severe health risks to humans (Xu et al., 2020). Additionally, cadmium disrupts nutrient uptake and accumulation in plants, hinders photosynthesis, and induces oxidative stress and genetic damage, consequently retarding plant growth. Exposure to cadmium inhibits the growth of various plant parts, such as leaves, stems, and roots. For instance, 6 mg kg^{-1} of cadmium exposure significantly reduces the root and stem length, area, and number of rice seedlings (Song et al., 2015). Given these impacts, cadmium contamination has attracted extensive global attention in recent years.

The extensive use of agricultural chemicals has significantly contributed to the surge in annual rice production in China (Li et al., 2015; Deng et al., 2020; Huang et al., 2020). This widespread application of inorganic fertilizers introduces a diverse array of ions into the soil solution, facilitating various reactions such as precipitation, dissolution, adsorption, and desorption (Zhang et al., 2018a; Sun et al., 2019). Conversely, research indicates that the addition of other divalent cations, like manganese, zinc, or silicon, to the growth solution can reduce Cd uptake and translocation from roots to shoots in several plant species (Sterckeman et al., 2015; Ge et al., 2016). However, studies in agrochemistry have predominantly concentrated on the effects of cations on the soil environment, often overlooking the roles of the accompanying anions.

Chloride (Cl^-) is a predominant anion in soils, originating from multiple sources. Soluble salts such as NaCl, $MgCl_2$, and $CaCl_2$, resulting from the weathering of parent material, along with Cl^--containing agricultural chemicals, represent major sources of chloride in soils (Christoph-Martin, 2019). Since 2012, Chinese agriculture has utilized approximately 11 million tons of ammonium chloride annually, a figure that continues to rise each year (Lu et al., 2019a). The consistent introduction of Cl^- into the soil is significant; its strong leaching properties not only reduce the content of exchangeable Ca^{2+} and Mg^{2+} ions but also reduce the soil's cation exchange capacity (CEC). Additionally, the negative charge of Cl^- disrupts the soil solution's neutrality, leading to reduced adsorption of other anions like SO_4^{2-} and NO_3^- by soil particles (Zhang et al., 2016; León-Romero et al., 2017). Chloride's limited adsorption onto soil colloids and its robust complexing capability allow it to form stable complexes with metal cations, thereby influencing the adsorption of cations by the soil (Yuan et al., 2017; Zheng et al., 2022).

Numerous studies have examined the environmental chemical behaviors of Cl^- in soil, particularly its interactions with heavy metal ions such as Cd^{2+}, Pb^{2+}, and Zn^{2+}. These ions can form soluble metal-Cl complexes with chloride, thereby increasing the dissolution of heavy metals into the soil solution. Elevated ionic strength in the soil solution has been shown to facilitate a greater release of Cd compared to other metals (Acosta et al., 2011; Zhai et al., 2018; Li et al., 2019a). Specifically, Zhang et al. (2018a) demonstrated that Cl^- forms highly soluble Cd-chloro complexes ($CdCl_n^{2-n}$) with Cd^{2+}, enhancing Cd's bioavailability in the soil, which leads to increased Cd absorption by *C. rossii*. Contrarily, some researchers argue differently. Ishtiyaq et al. (2023) observed that Cl^- could enhance A. halimus's resistance to Cd toxicity by reducing heavy metal uptake and boosting the synthesis of osmoprotective compounds, a finding echoed by (Filipović et al., 2018).

Rice (*Oryza sativa* L.), a crop cultivated since ancient times and a principal staple in China, exhibits an average consumption rate of 219 g/capita/day—nearly 50% higher than the global average of 148 g/capita/day (Hu et al., 2016; Lu et al., 2019b). Notably, Hunan Province, a major rice-producing region, also ranks among the provinces most severely contaminated with Cd. Results indicate that the Yangtze River basin, especially Hunan, required more attention due to the elevated Cd concentrations in soil-rice ecosystems (Zou et al., 2021). This study aims to investigate the quantitative relationship between Cl^- and Cd interactions. To our knowledge, the effects of Cl^- on the interface behavior of Cd in the soil-water medium and its migration in rice remain unexplored. Thus, we analyzed the morphology of Cd in soil, the fluctuations in Cd concentrations in the soil solution, and the Cd levels in rice at various growth stages under different Cl^- concentrations during a rice pot experiment. The soil solution was collected via field capacity-derived extraction, and the Cd concentration in the soil liquid phase was measured under ambient conditions to explore Cl^-'s influence on Cd transformation in the soil liquid phase. Our findings clarify the impact of Cl^- on Cd bioavailability within the soil-rice system and unveil the underlying mechanisms, providing insights for the rational use of agricultural chemicals in farmland management and heavy metal pollution prevention.

2 Materials and methods

2.1 Sand culture experiment

The sand culture experiment provides a controlled environment to precisely investigate the impact of chloride ions on cadmium morphology. In this experiment, the high Cd accumulation variety, Huang Huazhan (HH), was first sterilized using a 30% (v/v) hydrogen peroxide (H_2O_2) solution for 1 h and subsequently immersed in deionized water. The seeds were then germinated in the dark at a constant temperature of 28°C ± 0.5°C for 48 h.

Following germination, seeds were cleaned and wound, and 250 g of quartz sand was placed in each black nonporous plastic pot. A solution of $Cd(NO_3)_2$ was added to achieve a concentration of 5 mg kg^{-1}. The substrate was saturated with 1/2 Kimura B nutrient solution (Chen and Xiong, 2021). To establish a chloride concentration gradient, $CaCl_2$ was added at 0, 2, 4, 6, and 8 mmol kg^{-1} levels. Similarly, to mitigate the effects of Ca^{2+}, a matching gradient of $Ca(NO_3)_2$ was used as a control.

Five treatments were established: control (SCK), $CaCl_2$ (ST1–ST4 without Cd), $Ca(NO_3)_2$ (SCK1–SCK4 without Cd), $CaCl_2$ with Cd (ST1–ST4), and $Ca(NO_3)_2$ with Cd (SCK1–SCK4). Each treatment was replicated three times, totaling 54 potted plants. Seeds with uniform germination rates were selected and placed in the prepared plastic pots, which were refreshed with 1/2 Kimura B nutrient solution every 3 days. The pots were maintained in incubators set at 30°C and 25°C with 75% relative

TABLE 1 Basic physicochemical properties of the test soil.

Soil type	OM ($g \cdot kg^{-1}$)	pH	CEC ($cmol \cdot kg^{-1}$)	Total Cd ($mg \cdot kg^{-1}$)	DTPA-Cd ($mg \cdot kg^{-1}$)	Clay content (%)	Cl^-(mg kg^{-1})
Purple clayey soil	17.24	7.7	38.86	0.19	0.039	35.21	16.84

OM, organic matter; CEC, cation exchange capacity; clay content (≤0.0002 mm).

humidity, a light intensity of 150 umol m^{-2} s^{-1}, and a 16/8 h day/night cycle.

2.2 Pot experiment

The experimental soil was collected from the upper cultivating layer (0–20 cm) of a typical purple paddy field in Xiangtan County (27°32′47.26″N, 112°41′1.87″E), Xiangtan City, Hunan Province. Visible debris such as stone particles and root fragments were removed using wooden blocks. The soil was then air-dried, ground, and sieved through a 10-mesh screen to ensure uniformity for subsequent experiments. The basic physical and chemical properties of the soil are detailed in Table 1.

The study utilized the conventional double-cropping rice cultivar, Xiang wanxian13 (WX13), grown in cylindrical plastic pots (200 mm diameter × 200 mm depth). The rice seedlings, sourced from a rice base in Ningxiang County (28°21′N, 112°38′E), Hunan Province, underwent a cadmium analysis before transplantation, which indicated negligible Cd content.

This experiment was carried out during the rice growing season from July 15 to 20 October 2023, in a greenhouse located at the Rice Quality and Safety Control Hunan Engineering Laboratory, Central South University of Forestry Science and Technology. The laboratory is situated in a region characterized by a subtropical monsoon climate, with four distinct seasons and abundant rainfall. The average annual temperature, sunshine duration, and precipitation are 17.2°C, 1529.3 $h \cdot a^{-1}$, and 1361.6 mm, respectively.

After grinding and sieving, 1.5 kg of the test soil was placed into each cylindrical plastic pot. $Cd(NO_3)_2$ solution was added to achieve a Cd concentration of 5 $mg \cdot kg^{-1}$ soil. The mixture was then aged for 30 days to stabilize. Following the aging period, base fertilizers N (0.15 $g \cdot kg^{-1}$), P_2O_5 (0.1 $g \cdot kg^{-}$), and K_2O (0.15 $g \cdot kg^{-1}$) were applied. During the rice growth stage, additional fertilizations of 1/2 and 1/4 base fertilizer doses of urea were administered.

A gradient of $CaCl_2$ concentrations (0, 2, 4, 6, and 8 $mmol \cdot kg^{-1}$ Cl^-, designated as CK, T1, T2, T3, and T4, respectively) was employed. The same concentration gradient of $Ca(NO_3)_2$ served as a control (CK1, CK2, CK3, and CK4, respectively). Given that $Ca(NO_3)_2$ contains binary anions, using it as a control helps mitigate the potential interference of Ca^{2+} in the experimental results. Each treatment was replicated three times to ensure the reliability of the results. NO_3^- from the $Ca(NO_3)_2$ treatment introduced excess elemental N, potentially impacting rice growth; thus, urea was added to balance the nitrogen content in each pot.

For consistent growth conditions, two healthy rice seedlings were transplanted into each pot of aging soil. The water management strategy involved maintaining flooded conditions throughout the reproductive period. The experimental design included four growth stages of rice (tillering, heading, filling, and maturity), with each stage divided into blocks. Each block received treatments across the five Cl^- levels plus the $Ca(NO_3)_2$ control, totaling 108 pots.

2.3 Sample collection

Destructive sampling methods were employed in both experiments, meaning the samples collected were not used in subsequent tests. Samples from the rice plants, soil, and soil solution were collected at four critical growth stages: tillering, heading, filling, and maturity. The soil samples were air-dried in a cool area, finely ground, and sieved through 10-mesh and 100-mesh nylon sieves before being stored in sealed plastic bags for analysis.

Rice samples were thoroughly rinsed with tap water followed by ultrapure water. The roots, stems, leaves, and brown rice grains were then separated and initially dried at 105°C for 30 min, followed by a final drying at 70°C until a constant weight was achieved. The dried samples were then ground to pass through a 60-mesh sieve using a grinder and stored for subsequent analysis.

Soil solution samples were collected using the field capacity-derived soil solution extraction (SSE) technique as described by Chen et al. (2019a). For this method, 450 g of fresh soil was placed into a centrifuge tube and centrifuged at 8000 $r \cdot min^{-1}$ for 10 min.

2.4 Sample determination and quality control

Soil pH values were measured using a glass electrode (PHS-3C, Leici, China) in a 1:2.5 soil-to-water suspension ratio (Kargas et al., 2020). Soil organic matter (OM) was quantified calorimetrically through oxidation with potassium dichromate (Wu et al., 2017), while the CEC was assessed using the ammonium acetate method followed by distillation in a Kjeldahl bottle (Zhang et al., 2020a). The concentration of Cd extractable with 0.005 $mol \cdot L^{-1}$ DTPA (soil-DTPA solution ratio, 1:2) was determined using inductively coupled plasma–optical emission spectroscopy (ICAP 6000, Thermo Elemental). Additionally, the Cd concentration in the soil solution was measured with graphite furnace atomic absorption spectroscopy (Hitachi Z5000).

Soil samples were digested using a mixture of HCl-HNO_3-$HClO_4$ (7.5:2.5:3, v:v:v) for total Cd analysis (Gaudino et al., 2007), and plant powder was digested in a mixture of HNO_3-$HClO_4$ (8:2, v:v) for the same purpose (Yang et al., 2019a). The chemical forms of Cd in soils were characterized using the modified European Community Bureau of Reference (BCR) sequential extraction procedure (Bakircioglu et al., 2011). Cd concentrations

in all soil fractions and rice plants were determined using flame atomic absorption spectrometry and graphite furnace atomic absorption spectrometry (AAS: iCE-3500, Thermo Fisher Scientific, Waltham, MA, United States). The content of Cl in rice plants was quantified by silver nitrate titration.

To ensure the reliability and accuracy of the data, each sample was measured three times during the assessment of soil and plant Cd concentrations. Additionally, a quality control protocol was implemented using the national standard soil sample GBW(E)-070009 and the Chinese plant sample GSB-23. The relative standard deviation (RSD) for these measurements was maintained below 5%.

2.5 Statistical methods

The data were statistically evaluated using an F-test to determine overall significance, supplemented by Duncan's new multiple range test (MRT) for differentiating between treatment means at a significance level of $p < 0.05$. Analysis was conducted using Excel 2013, SPSS 22.0, and Origin 9.0 (OriginLab and IBM, USA). The accumulated cadmium (Cd) in plant tissue, expressed as mg·plant^{-1}, was computed by multiplying the dry weight of the tissue (g·plant^{-1}) by the Cd concentration in each tissue (mg·kg^{-1}).

2.6 Calculation of the complex components in soil solution

(1) The ionic strength in soil solution was calculated with the following Eq. 1:

$$I = 0.0013EC \quad (1)$$

where I is ionic strength (mol·kg^{-1}), and EC is the electrical conductivity measured in the soil solution (μs·cm^{-1}).

(2) The activity coefficient was calculated using the modified Debye-Huckel equation and equation below (2):

$$\lg r_i = -Az^2\sqrt{I} \quad (2)$$

where r is the ratio of an ion's activity to its concentration in a solution, A is a parameter associated with the absolute of the solvent (when the solvent is water, at 25°C, A = 0.509 (mol·kg^{-1})$^{-1/2}$), and z is the valence.

(3) Because the concentration of organic ligands in the soil solution was minimal, and the propensity of Cd to form organic ligands was inferior to that of other heavy metals, the influence of organic ligands was not accounted for in this study. The interaction between Cd^{2+} and Cl^- in forming complexes was characterized using their conditional formation constants as reported by Griffin and Jurinak (1973):

$$[CdCl^+] = 10^{1.98} \cdot r_2 \cdot [Cl^-][Cd^{2+}] \quad (3)$$

$$\left[CdCl_2^0\right] = 10^{2.60} \cdot r_1^2 \cdot r_2 \cdot [Cl^-]^2[Cd^{2+}] \quad (4)$$

where r_1 and r_2 are the activity coefficients of Cl^- and Cd^{2+} respectively, and [Cl^-] and [Cd^{2+}] represent the concentrations of free Cl^- and Cd^{2+} ions (mol·L^{-1}), respectively.

3 Results

3.1 Effect of Cl^- on rice biomass

The influence of Cl^- on rice biomass was investigated by recording the fresh weight and plant height at various growth stages (Figure 1). In the sand culture experiment, there were significant differences in plant height among the treatments (Figure 1B). Without Cd, the plant height in treatments ST1 to ST4 was 11.19%–17.16% higher than in the SCK group. Conversely, with Cd present, plant height decreased by 15.45%–43.64%.

In the pot experiment, the fresh weight of rice consistently increased with the exogenous addition of Cl^-, with significant variations noted among the treatments throughout the rice's growth period. Specifically, the fresh weight in the T1–T4 treatments rose by 1.6%–25.5% compared to the control group (CK), and by 4.4%–60.2% relative to the $Ca(NO_3)_2$-treated groups (CK1–CK4), with the most substantial increases observed during the heading stage. This suggests that Cl^- can enhance rice growth within certain concentration limits (Figure 1C). Additionally, no significant differences in plant height were found between the T1–T4 treatments, the control group (CK), and the $Ca(NO_3)_2$-treated groups during any growth stage, with peak plant heights achieved during the heading stage (Figure 1D).

3.2 Cd concentrations in different parts of rice at different growth stages

Figure 2 illustrates the distribution of Cd concentrations in different parts of rice at various growth stages. In the sand culture experiment, Cd content was markedly higher in the roots compared to the shoots. Furthermore, the addition of Cl^- led to a gradual increase in the Cd content in these components (Figure 2A).

In the pot experiment, during the tillering stage, the differences in Cd concentrations across different parts of the rice were minimal among the treatments. Specifically, root Cd concentrations ranged from 2.12 to 2.24 mg·kg^{-1}, averaging 2.19 mg·kg^{-1}. Stem Cd concentrations were between 0.43 and 0.46 mg·kg^{-1}, with an average of 0.45 mg·kg^{-1}, and leaf Cd concentrations varied from 0.17 to 0.26 mg·kg^{-1}, with an average of 0.22 mg·kg^{-1} (Figure 2B). During the heading and filling stages, Cd concentrations in each part of the T1–T4 treated rice were consistently lower than those in the $Ca(NO_3)_2$ treatment groups (CK1–CK4), showing reductions ranging from 3.45% to 32.17%, 1.52%–26.17%, 0.43%–25.67%, and 1.14%–32.03%, respectively (Figures 2C,D). These stages were identified as critical periods during which Cl^- notably influenced Cd uptake in rice. At the maturity stage, the Cd content in each part of T1–T4 treated rice exceeded that in the corresponding parts of the control group, with increases spanning 5.31%–42.56%, 2.74%–23.04%, 1.27%–32.73%, and 2.48%–31.68%, respectively (Figure 2E).

10.3389/fenvs.2024.1403989

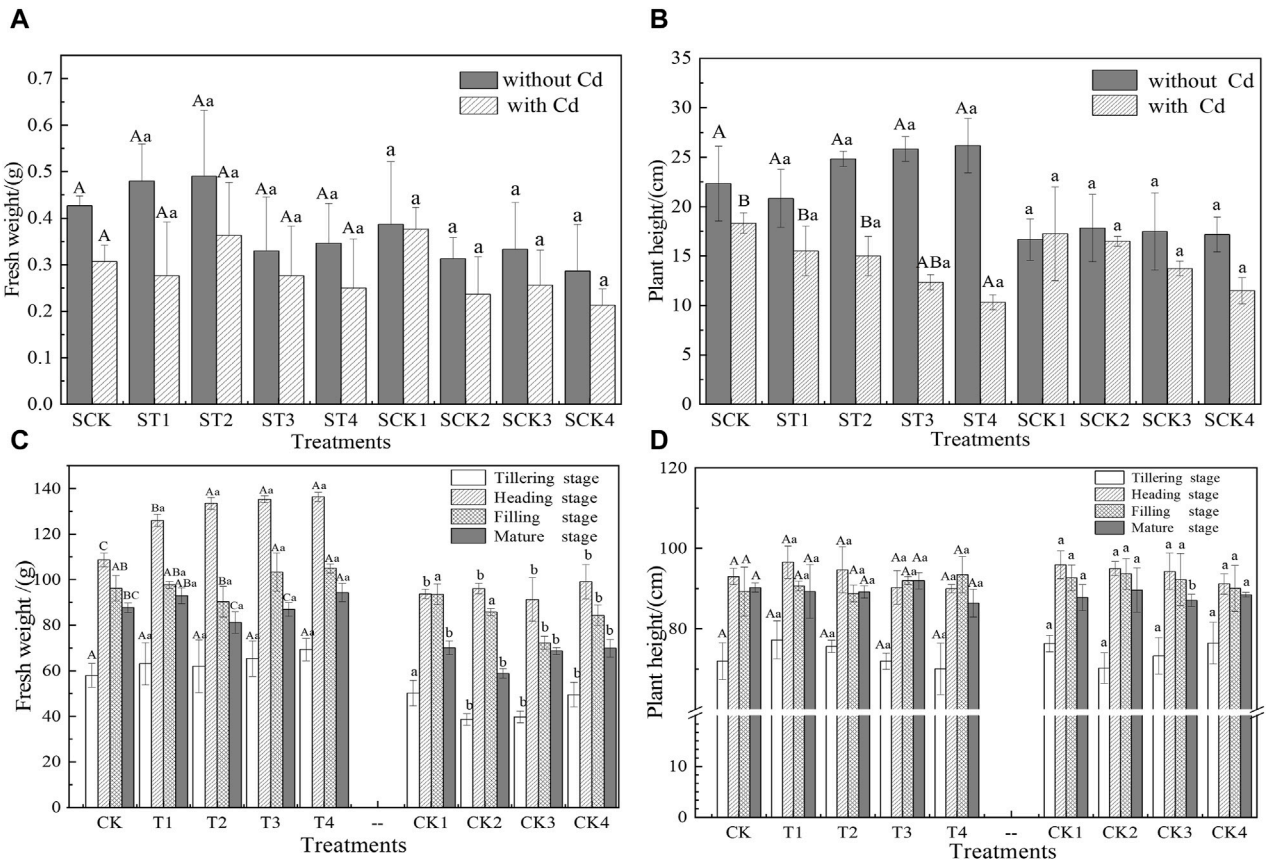

FIGURE 1
Effects of Cl^- on the growth of rice. **(A,B)** and **(C,D)** are the results of sand culture and rice pot experiments, respectively. Different capital letters indicate that there was a significant difference between the effects of different Cl^- additions on rice in the same stage ($p < 0.05$). Different lowercase letters indicate that there was a significant difference between the effects of Cl^- on rice after offsetting the effect of Ca^{2+} in the same period ($p < 0.05$).

3.3 Cd accumulation in rice plants under different treatments

The study quantified total plant Cd accumulation by measuring the Cd concentration and dry weight of various parts of the rice (roots, stems, leaves, husks, and brown rice). Figure 3 presents the effects of Cl^- on Cd accumulation at different growth stages. As depicted in Figure 3, Cd accumulation predominantly occurred during the maturity stage. During the tillering stage, the addition of Cl^- resulted in varying trends of Cd accumulation. Relative to the CK, there was a decrease in Cd accumulation of 4.02% and 4.51% in the T1 and T2 treatments, respectively, while an increase of 7.34% and 2.96% was observed in the T3 and T4 treatments, respectively. In the subsequent heading and filling stages, unlike the tillering stage, increased Cl^- addition led to a general decrease in Cd accumulation, with the most pronounced decrease occurring during the filling stage. This suggests that the filling stage is particularly critical in influencing Cd accumulation in rice. Compared to the CK treatment group, the Cd accumulation in the T1–T4 treatments decreased by 5.87%–31.24%. In the maturity stage, only the T4 treatment exhibited higher Cd accumulation than the control (CK), showing an increase of 7.71%. Conversely, in the other treatments, Cd accumulation decreased by 6.44%–12.02%, which may be due to the varying concentrations of Cl^-. Throughout the four growth stages, Cd accumulation in each treatment (T1–T4) was consistently higher than in the $Ca(NO_3)_2$ treatment groups (CK1–CK4), indicating that compared to NO_3^-, Cl^- has a more substantial effect on Cd uptake by rice.

3.4 Changes in the Cd concentration in soil solution at different growth stages

Figure 4 illustrates the Cd concentrations measured using the field capacity-SSE method across different rice growth stages. There were significant differences in the Cd concentration of the soil solution between the initial growth periods (tillering and heading stages) and the later stages (filling and maturity stages) across all treatments. In both the CK and the T1–T4 treatments, the Cd concentration determined by SSE remained consistent throughout the growth period, ranging from 0.1170 to 0.3973 $\mu g \cdot L^{-1}$. During the maturity stage, the SSE-Cd concentration in the T1–T4 treatments was 0.116–0.672 times higher than that in the CK treatment. Throughout the rice's growth, the SSE-Cd concentration in the T1–T4 treatments varied from 0.068 to 2.994 times lower than in the CK1–CK4 treatments.

To clarify the interaction between chloride Cl^- and Cd in the soil, Eqs 1–4 were used to calculate the concentrations of each component in the complexes ($CdCl_n^{2-n}$). These calculations aid in

10.3389/fenvs.2024.1403989

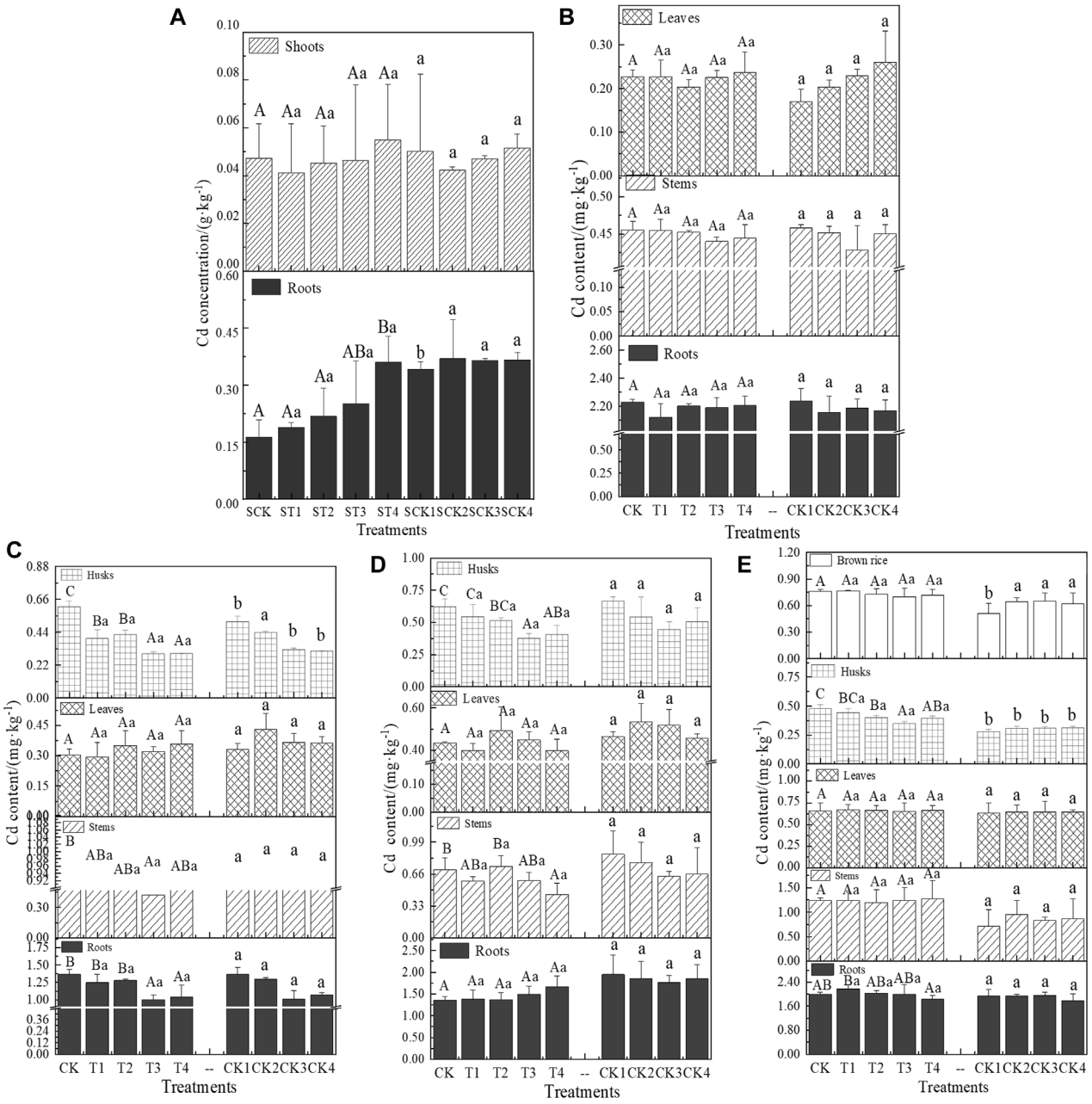

FIGURE 2
Cadmium concentrations in various parts of rice at different growth stages. **(A)** is the sand culture experiment. **(B–E)** are the tillering, heading, filling, and maturity stages of rice growth, respectively. Different capital letters indicate that there was a significant difference between the effects of different Cl^- additions on the same part of the rice in the same stage ($p < 0.05$). Different lowercase letters indicate that there was a significant difference between the effects of Cl^- on rice after offsetting the effect of Ca^{2+} in the same period ($p < 0.05$).

analyzing the impact of Cl^- on the bioavailability of Cd, with the results detailed in Table 2. Generally, Cl^- can form complexes such as $CdCl^+$, $CdCl_2^0$, $CdCl_3^-$, and $CdCl_4^{2-}$ with Cd. However, due to the relatively low concentrations of $CdCl_3^-$ and $CdCl_4^{2-}$ ($<1 \times 10^{-9}$ *M*), these complexes were not considered significant in this study. As shown in Table 2, when the Cd/Cl ratio (m:n) in the soil-water medium ranges from 0.625 to 2.5, an increase in Cl^- added also increased the concentrations of $CdCl^+$ and $CdCl_2^0$ in all treatments, with the concentration of $CdCl^+$ being significantly higher than that of $CdCl_2^0$. The findings indicate that under these conditions, the predominant complexes formed by Cl^- and Cd^{2+} in the soil solution were mainly $CdCl^+$.

3.5 Effects of Cl^- on the chemical form of soil Cd

Figure 5 illustrates the distribution of different chemical forms of Cd in the soil, both with and without Cl^- additions, across various growth stages of rice. Predominantly, the soil Cd was found in the

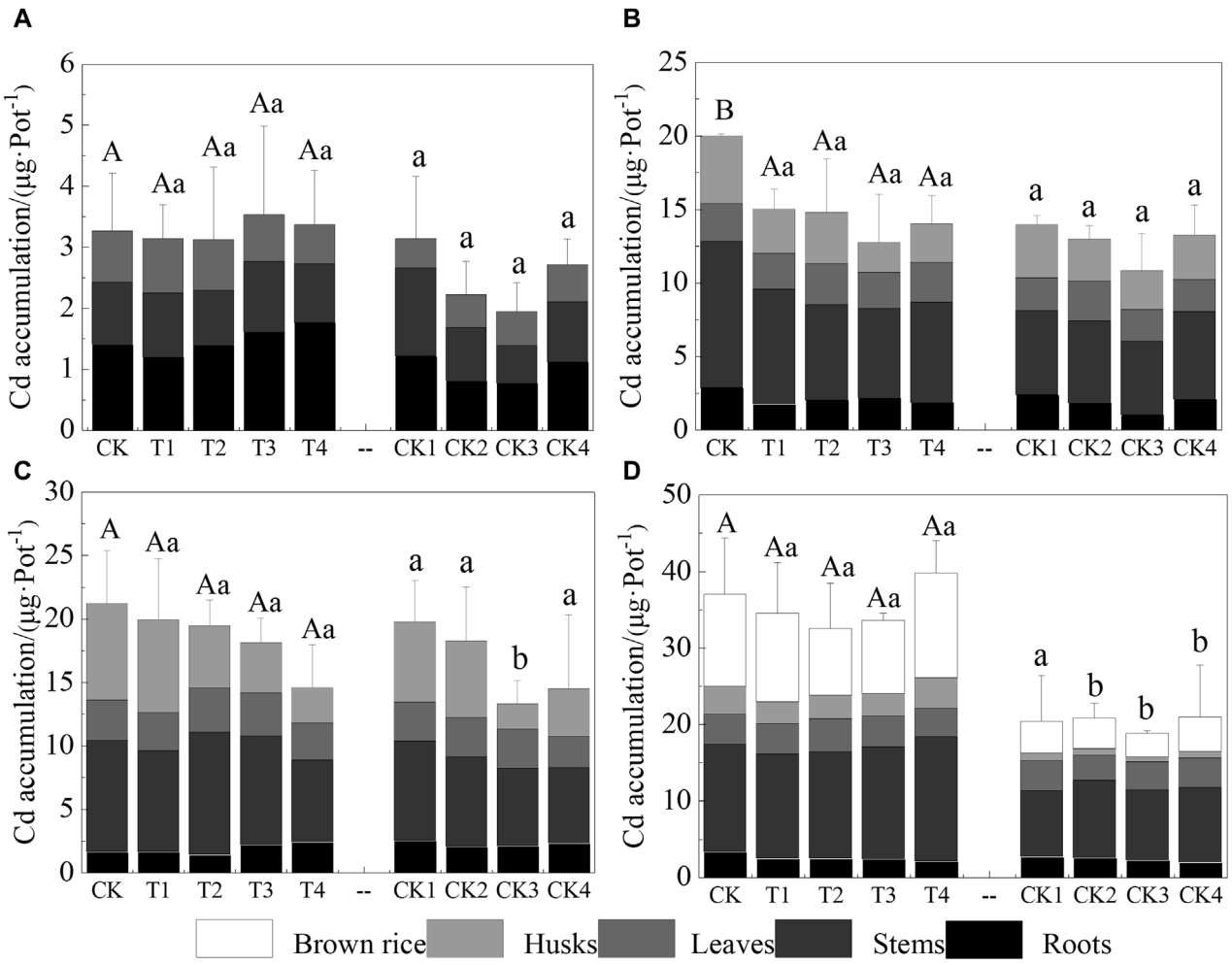

FIGURE 3
Cadmium accumulation in rice at different growth stages. **(A–D)** are the tillering, heading, filling, and maturity stages of rice growth, respectively. Different capital letters indicate that there was a significant difference between the effects of different Cl^- additions on the Cd accumulation of rice in the same stage ($p < 0.05$). Different lowercase letters indicate that there was a significant difference between the effects of Cl^- on the Cd accumulation of rice after offsetting the effect of Ca^{2+} in the same period ($p < 0.05$).

acid-soluble fraction (E1), which accounted for approximately 50%–80% of the total Cd. Relative to the CK, the inclusion of Cl^- in treatments T1–T4 significantly enhanced the E1 form of Cd throughout the entire growth period of the rice, showing increases ranging from 4.27% to 16.90%, 1.62%–15.68%, 0.90%–3.99%, to 2.66%–13.47%, respectively. Conversely, the trend observed in the residual fraction (E4) of Cd varied across the different growth periods. During the filling stage, the E4 form of Cd saw an increase of 2.14%–9.83% compared to CK. However, during the other growth periods, there were decreases in E4, specifically 6.07%–19.54%, 2.97%–12.67%, and 6.86%–21.97%, respectively. Over the whole growth period, the addition of Cl^- appeared to have minimal impact on the organic fraction (E3) of Cd.

4 Discussion

The data illustrated in Figure 1 demonstrate that with the increase in Cl^- addition compared to the CK, the fresh weight of rice saw an increase ranging from 1.6% to 25.5%. Similarly, in the sand culture experiment without Cd treatment, an evident upward trend in plant height was observed when compared to the SCK group. Conversely, with the addition of Cd, there was a progressive decrease in plant height as Cl^- levels increased. This trend can be attributed to chlorine's role as an essential micronutrient that supports and enhances plant photosynthesis, regulates osmotic pressure within cells, and maintains cellular charge balance (Geilfus, 2018). Consequently, these functions promote rice growth. However, when Cl^- and Cd^{2+} coexist in the soil, Cl-complexes ($CdCl_n^{2-n}$) form, reducing the surface charge on plant cells and thus facilitating the transfer and diffusion of Cd within the plant (Hussain et al., 2022). Additionally, during the early stages of rice growth, where protein synthesis is predominant, Cd can bind to proteins containing sulfhydryl groups, disrupting their function and intensifying its toxic effects, particularly during the seedling stage (Cai et al., 2020). As the rice matures, its resistance to Cd toxicity increases, leading to varied responses to Cd toxicity at different growth stages (Li et al., 2020).

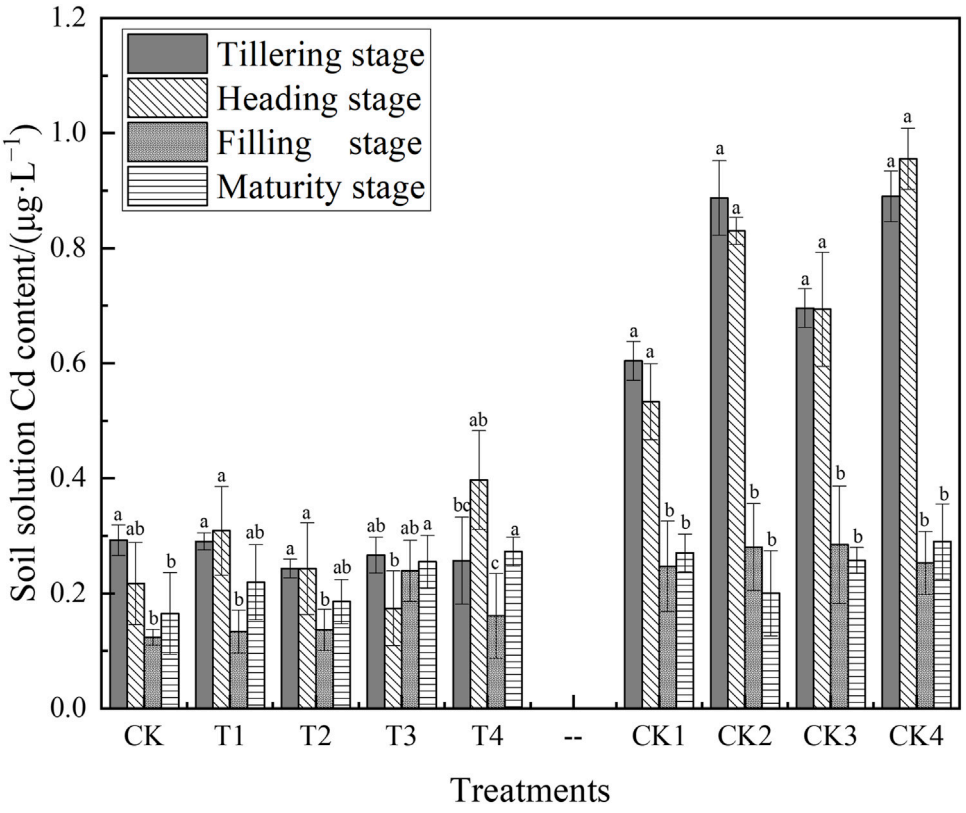

FIGURE 4
Cadmium concentrations in soil solution across different growth stages of rice. Different lowercase letters indicate significant differences in the same treatment between the different growth stages ($p < 0.05$).

TABLE 2 The concentration of different kinds of $CdCl_n^{2-n}$ in the soil solution at different growth stages of rice (10^{-9} *M*). Because the $CdCl_3^-$ and $CdCl_4^{2-}$ concentrations were relatively small (<1 × 10^{-9} *M*), they were not considered in this study.

Treatment	Tillering stage		Heading stage		Filling stage		Mature stage	
	$[CdCl^+]$	$[CdCl_2^0]$	$[CdCl^+]$	$[CdCl_2^0]$	$[CdCl^+]$	$[CdCl_2^0]$	$[CdCl^+]$	$[CdCl_2^0]$
CK	-	-	-	-	-	-	-	-
T1	341.2	0.558	341.7	0.559	345.3	0.568	324.2	0.517
T2	628.8	1.974	621.8	1.941	611.6	1.894	627.1	1.966
T3	891.9	4.084	901.6	4.151	869.0	3.928	890.7	4.076
T4	1159.1	6.987	1157.8	6.975	1173.9	7.121	1212.5	7.475

The concentration of different kinds of $CdCl_n^{2-n}$ in the soil solution at different growth stages of rice (10^{-9} *M*). Because the $CdCl_3^-$ and $CdCl_4^{2-}$ concentrations were relatively low (<1 × 10^{-9} *M*), they were not considered in this study.

It is widely recognized that the uptake of Cd by rice varies across different growth stages (Rodda et al., 2011; Li et al., 2017; Chen et al., 2019b). During the early vegetative growth stages, rice exhibits rapid biomass accumulation, necessitating substantial nutrient uptake. Concurrently, bioavailable Cd from the soil is absorbed by the roots along with these nutrients, predominantly accumulating in the roots (Zare et al., 2018; Yang et al., 2019b; Rehman et al., 2019). Additionally, $CdCl_n^{2-n}$ complexes can directly enter the roots and/or dissociate at the root surface, subsequently entering cells as Cd^{2+} (Filipović et al., 2018). This mechanism is supported by the observed higher Cd concentration in rice roots at the tillering stage compared to other stages (Figure 2B). Results from the sand culture experiment indicate that increasing Cl^- levels correspond with increased Cd accumulation in the roots, without significant changes in shoot Cd content (Figure 2A). This suggests that Cl^- enhances Cd uptake in rice roots.

However, the transport of Cd from roots to shoots may be regulated by physiological mechanisms that limit Cd translocation when shoot concentrations reach a certain threshold, thereby preventing excessive accumulation in aerial parts of the plant (Zhang et al., 2018b; Zhou et al., 2020). Studies have highlighted the role of the natural resistance-associated

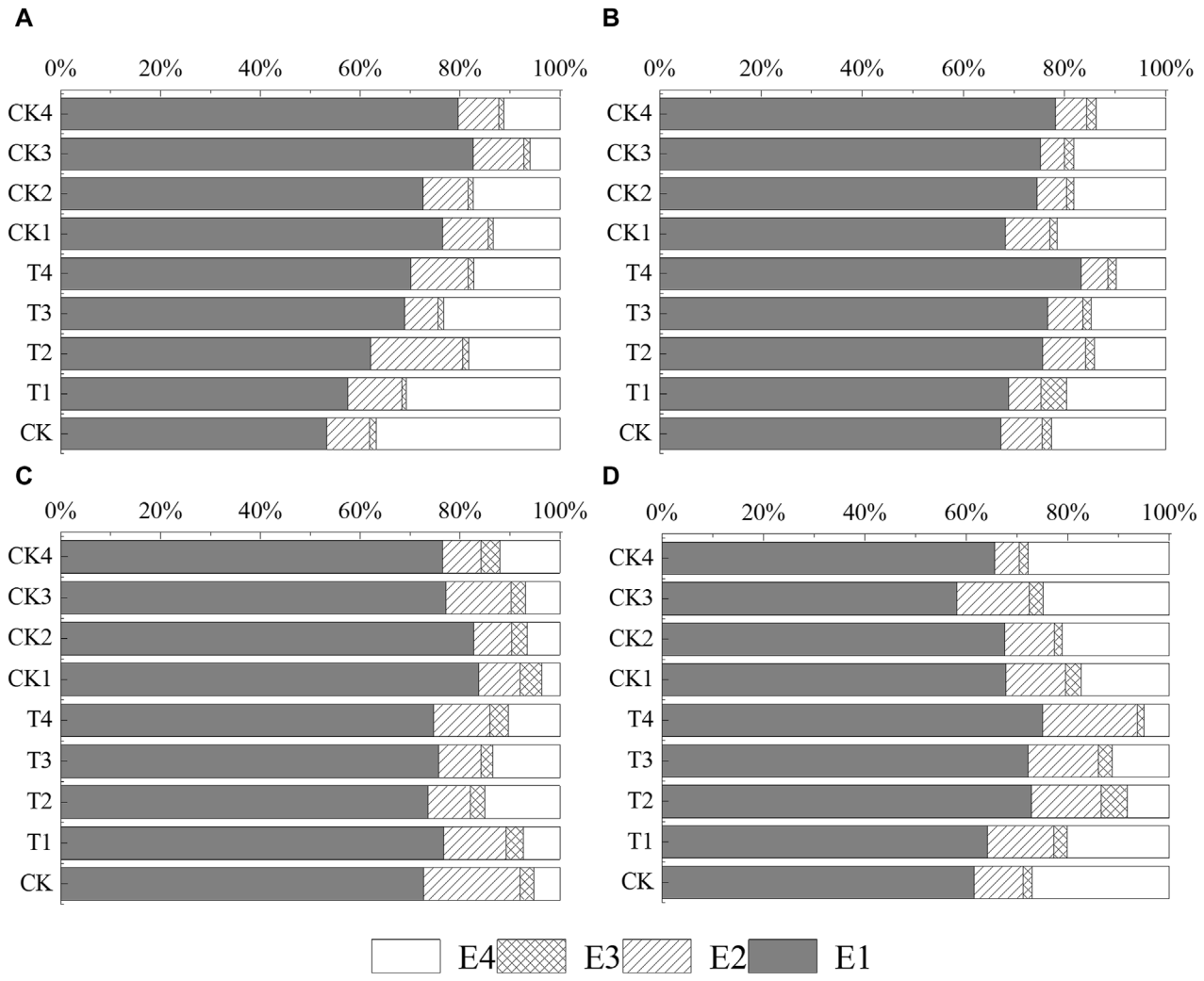

FIGURE 5
The average percentage soil Cd content obtained by the BCR method in different growth stages of rice. **(A–D)** are the tillering stage, heading stage, filling stage, and maturity stage, respectively. The terms E1, E2, E3, and E4 refer to the acid-soluble fraction (E1), iron and manganese oxide fraction (E2), organic fraction (E3), and residual fraction (E4).

macrophage protein (NRAMP) family in mediating the transport of divalent metal cations including Fe, Mn, Cd, and Zn (Yuan et al., 2019). Among these, OsNRAMP5, located in rice root cells, is crucial in the uptake and transport of Mn^{2+}, Cd^{2+}, and Fe^{2+} from roots to shoots, accounting for nearly 90% of Cd uptake (Ishimaru et al., 2012; Huang et al., 2021). OsNRAMP5 functions as an efflux transporter, moving Cd from ectodermal and endodermal cells into the xylem for transfer to the shoots (Hao et al., 2018).

Cd uptake by rice involves its absorption by the OsNRAMP5 transporter in root cells, after which the absorbed Cd is partly sequestered in vesicles, while the remainder is released into the xylem for transfer to the shoots (Skuza et al., 2022). A significant finding by Tang et al. (2017) showed that rice mutants lacking the OsNRAMP5 gene exhibited substantially lower Cd levels in both roots and shoots compared to wild-type plants. This suggests a regulatory mechanism where, upon reaching a specific concentration of Cd in the shoots, the plant suppresses OsNRAMP5 expression, thereby inhibiting further Cd transport from the roots to the shoots.

During the heading and filling stages, the Cd concentrations in rice treated with T1–T4 were notably lower than those in the $Ca(NO_3)_2$ treatment group (CK1–CK4). This difference is attributed to the stronger coordination ability of Cl^- compared to NO_3^-, which enables Cl^- to form more stable complexes with Cd^{2+} (general formula $CdCl_n^{2-n}$) (Li et al., 2024). The specific composition of these complexes varies depending on the relative concentrations of Cd and Cl^-.

The influence of soil type on Cd absorption by rice is well-documented, with significant variations in Cd uptake across different soil conditions (Yu et al., 2016; He et al., 2017). A key study by Ye et al. (2014) across 19 representative paddy soils in China employed aggregated boosted tree analysis to assess how various soil properties contribute to Cd bioaccumulation in rice grains. Their findings highlighted soil pH and organic carbon content as key determinants of Cd uptake. In soils such as purple

mud, the predominant clay minerals—montmorillonite and illite—exhibited a 2:1 layer structure enriched with variable cations such as iron, magnesium, and alkali metals, which can undergo isomorphous substitution. This substitution often facilitates the exchange of these cations for others of similar size but lower charge (Moldoveanu and Papangelakis, 2013; Kumari and Mohan, 2021).

From the analyses using the Debye-Hückel limit equation (Eqs 1–4), it was deduced that the predominant complexes formed between chloride Cl^- and Cd^{2+} in the soil solution are mainly $CdCl^+$ (Table 2). This suggests that $CdCl^+$ is more readily adsorbed onto soil particles through ion exchange, thereby reducing the concentration of free Cd^{2+} in the soil solution (Figure 4). Consequently, Cl^- diminishes the mobility of Cd in the soil. Despite this, our study noted a significant increase in Cd accumulation in rice plants treated with Cl^- (Figure 3), indicating an enhanced uptake of some $CdCl^+$ by plant roots. This finding confirms reports that the formation of $CdCl_n^{2-n}$ complexes in soil solution increases Cd uptake, probably by direct uptake of the $CdCl_n^{2-n}$ complexes by plants (Cheng et al., 2018).

Furthermore, plants exhibit a dynamic and reversible adjustment mechanism to environmental stresses, including ion toxicity. When Cl^- is externally supplied, it helps establish an osmotic balance between the cytoplasm and the external environment, alleviating stress by neutralizing cations such as Ca^{2+} and Cd^{2+} in the soil solution (Guo et al., 2018). Hence, the presence of free Cd^{2+} in the soil solution alone does not fully account for the bioavailability of Cd. This necessitates an in-depth analysis based on its chemical form, particularly in the presence of multiple competing anions, to better understand the bioactive forms of Cd under varied agricultural conditions.

Cl^- plays a multifaceted role in the soil solution dynamics and the variety of chlorine-based complexes, directly influencing the formation of various chlorine-based complexes. Soil layered alumino-silicate minerals and organic colloids, which are predominantly negatively charged (Doi et al., 2019), exhibit relatively low adsorption strength for $CdCl^+$ and $CdCl_2$ compared to Cd^{2+}. Furthermore, negatively charged complexes such as $CdCl_3^-$ and $CdCl_4^{2-}$ may even induce negative adsorption, potentially leading to the desorption of previously adsorbed cadmium from the soil matrix (Cheng et al., 2017).

In the solid phase of the soil, Cl^- can destabilize various chemosynthetic states of Cd through competitive interactions with other ligands. Zheng et al. (2023) demonstrated that the intervention of Cl^- could result in the redistribution of organically bound Cd to the soil solution as Cd^{2+}. The interaction of Cl^- with layered clay minerals provides further insight into these complex dynamics. The strong negative charge on the surface of clay minerals tends to repel Cl^-, while the weak positive charge present on the edges of these minerals can adsorb Cl^-. This absorption of Cl^- at the edges of clay minerals influences the specialized adsorption processes of Cd^{2+} on the surface of clay oxides (García et al., 2021). The strong coordination ability of Cl^- significantly impacts the behavior of Cd in the soil environment, affecting its availability for uptake by plants.

Figure 3 demonstrates that Cd accumulation in rice at maturity was significantly greater compared to other growth stages. Differing concentrations of exogenously added Cl^- influenced Cd accumulation in rice, as depicted in Figure 3D. Consistent with our findings, Zhang et al. (2020b) reported that Cd concentration and accumulation in S. glauca shoots were significantly increased by the addition of exogenous Cl-compared to the control. Similarly, Li et al. (2019b) observed that low Cl^- concentrations (0.1–2.0 $g{\cdot}kg^{-1}$) did not significantly affect DTPA-extracted Cd levels in soil, whereas higher concentrations (5.0 $g{\cdot}kg^{-1}$) increased these levels by 24.79%. DTPA-extracted Cd is commonly utilized to assess Cd bioavailability. Our findings suggest that the addition of Cl^- to soil enhances Cd absorption and accumulation in rice. At various growth stages, Cl^- significantly increased acid-extractable Cd while reducing residual Cd, with the exception of the filling stage, as illustrated in Figure 5. This effect can be attributed to several mechanisms: 1) High concentrations of Cl^- facilitate the release of exchangeable, organically bound, and carbonate-bound Cd in the soil; 2) Cl^- promotes the secretion of organic acids from rice roots, thereby enhancing the desorption of residual Cd and increasing Cd solubility in the rice rhizosphere (Zeng et al., 2017); and/or 3) Dissolved organic matter (DOM) is one of the most active soil components influencing Cd migration, transformation, bioavailability, and toxicity in soils (Zhang et al., 2022). The organic ligands in DOM can also be complexed with Cd to form soluble organic metal complexes; thus, improving the migration of Cd in the soil (Chen et al., 2021).

5 Conclusion

The purpose of this study was to explore the impact of exogenous Cl^- addition on Cd migration across various growth stages of rice within a soil-rice system. Based on the experimental findings, we drew the following conclusions:

(1) Rice sand culture experiments revealed that exogenous Cl^- addition within a specific concentration range could enhance the fresh weight and plant height of rice. However, in the presence of Cd, chloride ions facilitated the uptake of Cd by rice roots, resulting in significantly higher Cd levels in the roots compared to the shoots. This increased concentration of Cd in the roots increased its toxic effects on rice, leading to reductions in both fresh weight and plant height.
(2) Pot experiments demonstrated that exogenous chloride ion addition significantly reduced Cd content and accumulation in all parts of rice compared to the $Ca(NO_3)_2$ treatment group during both the tassel and filling stages. The reduction was most pronounced at the filling stage, suggesting that this is a critical period for chloride ions to influence Cd accumulation in rice.
(3) Exogenous chloride ions increase the concentration of acid-extractable Cd and $CdCl^+$ in the soil. When the Cd/Cl ratio in the soil-water medium ranged from 0.625 to 2.5, Cl^- in the soil formed a complex with free Cd^{2+} in the solution, resulting in a $CdCl^+$-based complex. This complex enhanced the adsorption of Cd by soil particles and promoted the uptake of $CdCl^+$ by rice roots, thereby increasing the Cd concentration in rice.

In conclusion, in the studied concentration range, Cl^- could complex with free Cd^{2+} to form $CdCl^+$ in the soil solution, which might then be absorbed by rice plants. This complexation process

could reduce the mobility of cadmium in the soil, thereby potentially enhancing its uptake and accumulation in rice. For effective field management, it is crucial to consider the level of Cl^- input to ensure both the mass production and safe utilization of rice in systems with moderate to light cadmium contamination. Additionally, this study not only guides the evaluation of soil environmental quality but also serves as a reference for the rational application of chemical fertilizers.

Data availability statement

The raw data supporting the conclusion of this article will be made available by the authors, without undue reservation.

Author contributions

HF: Writing–original draft, Data curation, Formal Analysis, Visualization. ST: Data curation, Formal Analysis, Writing–original draft. JL: Funding acquisition, Supervision, Validation, Writing–review and editing. RH: Data curation, Writing–review and editing. ZX: Data curation, Writing–review and editing. HH: Supervision, Writing–review and editing. PP: Supervision, Writing–review and editing.

Funding

The author(s) declare that financial support was received for the research, authorship, and/or publication of this article. This research was funded by the National Natural Science Foundation of China (42107444), the Reuter Foundation of Education Bureau of Hunan Province, China (21B0245), and the National Key Research and Development Program of China (2022YFD1700104).

Conflict of interest

The authors declare that the research was conducted in the absence of any commercial or financial relationships that could be construed as a potential conflict of interest.

The handling editor QL declared a shared affiliation with the authors at the time of review.

Publisher's note

References

Acosta, J. A., Jansen, B., Kalbitz, K., Faz, A., and Martínez-Martínez, S. (2011). Salinity increases mobility of heavy metals in soils. *Chemosphere* 85 (8), 1318–1324. doi:10.1016/j.chemosphere.2011.07.046

Bakircioglu, D., Kurtulus, Y. B., and Ibar, H. (2011). Investigation of trace elements in agricultural soils by BCR sequential extraction method and its transfer to wheat plants. *Environ. Monit. Assess.* 175 (1), 303–314. doi:10.1007/s10661-010-1513-5

Cai, Y., Zhang, S., Cai, K., Huang, F., Pan, B., and Wang, W. (2020). Cd accumulation, biomass and yield of rice are varied with silicon application at different growth phases under high concentration cadmium-contaminated soil. *Chemosphere* 242, 125128. doi:10.1016/j.chemosphere.2019.125128

Chen, G., and Xiong, S. (2021). OsHIPP24 is a copper metallochaperone which affects rice growth. *Plant Biol.* 64, 145–153. doi:10.1007/s12374-020-09287-x

Chen, H. R., Yang, Y., Ye, Y. F., Tao, L., Fu, X., Liu, B., et al. (2019). Differences in cadmium accumulation between indica and japonica rice cultivars in the reproductive stage. *Ecotoxicol. Environ. Saf.* 186, 109795. doi:10.1016/j.ecoenv.2019.109795

Chen, M. S., Ding, S. M., Li, C., Tang, Y., Fan, X., Xu, H., et al. (2021). High cadmium pollution from sediments in a eutrophic lake caused by dissolved organic matter complexation and reduction of manganese oxide. *Water Res.* 190, 116711. doi:10.1016/j.watres.2020.116711

Chen, Q., Peng, P. Q., Long, J., Li, X. Y., Ding, X., Hou, H. B., et al. (2019). Cadmium phytoavailability evaluation in rice-soil system using a field capacity-derived soil solution extraction: an entire growth period study in subtropical China. *Soil Tillage Res.* 194, 104315. doi:10.1016/j.still.2019.104315

Cheng, F., Guo, S., Li, G., Wang, S., Li, F., and Wu, B. (2017). The loss of mobile ions and the aggregation of soil colloid: results of the electrokinetic effect and the cause of process termination. *Electrochem. Acta* 258, 1016–1024. doi:10.1016/j.electacta.2017.11.153

Cheng, M. M., Wang, A. A., Liu, Z. Q., Gendall, A. R., Rochfort, S., and Tang, C. (2018). Sodium chloride decreases cadmium accumulation and changes the response of metabolites to cadmium stress in the halophyte *Carpobrotus rossii*. *Ann. Bot.* 122, 373–385. doi:10.1093/aob/mcy077

Christoph-Martin, G. (2019). Chloride in soil: from nutrient to soil pollutant. *Environ. Exp. Bot.* 157, 299–309. doi:10.1016/j.envexpbot.2018.10.035

Deng, X., Chen, Y., Yang, Y., Yuan, X., Zeng, H., Zeng, Q., et al. (2020). Cadmium accumulation in rice (Oryza sativa L.) alleviated by basal alkaline fertilizers followed by topdressing of manganese fertilizer. *Environ. Pollut.* 262, 114289. doi:10.1016/j.envpol.2020.114289

Doi, A., Ejtemaei, M., and Nguyen, A. V. (2019). Effects of ion specificity on the surface electrical properties of kaolinite and montmorillonite. *Miner. Eng.* 143, 105929. doi:10.1016/j.mineng.2019.105929

Feng, J., Shen, R. F., and Shao, J. F. (2020). Transport of cadmium from soil to grain in cereal crops: a review. *Pedosphere* 31 (1), 3–10. doi:10.1016/S1002-0160(20)60015-7

Filipović, L., Romić, M., Romić, D., Filipović, V., and Ondrašek, G. (2018). Organic matter and salinity modify cadmium soil (phyto) availability. *Ecotoxicol. Environ. Saf.* 147, 824–831. doi:10.1016/j.ecoenv.2017.09.041

Fu, Y. H., Li, F. M., Guo, S. H., and Zhao, M. (2021). Cadmium concentration and its typical input and output fluxes in agricultural soil downstream of a heavy metal sewage irrigation area. *J. Hazard. Mater.* 412, 125203. doi:10.1016/j.jhazmat.2021.125203

García, K. I., Quezada, G. R., Arumí, J. L., Urrutia, R., and Toledo, P. G. (2021). Adsorption of phosphate ions on the basal and edge surfaces of kaolinite in low salt aqueous solutions using molecular dynamics simulations. *J. Phys. Chem. C* 125 (38), 21179–21190. doi:10.1021/acs.jpcc.1c05995

Gaudino, S., Galas, C., Belli, M., Barbizzi, S., de Zorzi, P., Jaćimović, R., et al. (2007). The role of different soil sample digestion methods on trace elements analysis: a comparison of ICP-MS and INAA measurement results. *Accreditation Qual. Assur.* 12 (2), 84–93. doi:10.1007/s00769-006-0238-1

Ge, L. Q., Cang, L., Liu, H., and Zhou, D. M. (2016). Effects of warming on uptake and translocation of cadmium (Cd) and copper (Cu) in a contaminated soil-rice system under Free Air Temperature Increase (FATI). *Chemosphere* 155, 1–8. doi:10.1016/j.chemosphere.2016.04.032

Geilfus, C. M. (2018). Review on the significance of chlorine for crop yield and quality. *Plant Sci.* 270, 114–122. doi:10.1016/j.plantsci.2018.02.014

Griffin, B. A., and Jurinak, J. J. (1973). Estimation of activity coefficients from the electrical conductivity of natural aquatic systems and soil extracts. *Soil Sci.* 116 (1), 26–30. doi:10.1097/00010694-197307000-00005

Guo, S. H., Hu, N., Li, Q. S., Yang, P., Wang, L. L., Xu, Z. M., et al. (2018). Response of edible amaranth cultivar to salt stress led to Cd mobilization in rhizosphere soil: a metabolomic analysis. *Environ. Pollut.* 241, 422–431. doi:10.1016/j.envpol.2018.05.018

Hao, X. G., Zeng, M., Wang, J., Zeng, Z., Dai, J., Xie, Z., et al. (2018). A node-expressed transporter OsCCX2 is involved in grain cadmium accumulation of rice. *Front. Plant Sci.* 9 (9), 476. doi:10.3389/fpls.2018.00476

He, H., Tam, N. F. Y., Yao, A., Qiu, R., Li, W. C., and Ye, Z. (2017). Growth and Cd uptake by rice (Oryza sativa) in acidic and Cd-contaminated paddy soils amended with steel slag. *Chemosphere* 189, 247–254. doi:10.1016/j.chemosphere.2017.09.069

Hu, Y., Cheng, H., and Tao, S. (2016). The challenges and solutions for cadmium-contaminated rice in China: a critical review. *Environ. Int.* 92, 515–532. doi:10.1016/j.envint.2016.04.042

Huang, F., Zhou, H., Gu, J. F., Liu, C., Yang, W., Liao, B., et al. (2020). Differences in absorption of cadmium and lead among fourteen sweet potato cultivars and health risk assessment. *Ecotoxicol. Environ. Saf.* 203, 111012. doi:10.1016/j.ecoenv.2020.111012

Huang, W. X., Zhang, D. M., Cao, Y. Q., Dang, B. J., Jia, W., Xu, Z. C., et al. (2021). Differential cadmium translocation and accumulation between Nicotiana tabacum L. and Nicotiana rustica L.by transcriptome combined with chemical form analyses. *Ecotoxicol. Environ. Saf.* 208, 111412. doi:10.1016/j.ecoenv.2020.111412

Hussain, B., Ma, Y., Li, J., Gao, J., Ullah, A., and Tahir, N. (2022). Cadmium in rice is affected by fertilizer-borne chloride and sulfate anions: long-term field versus pot experiments. *Processes* 10 (7), 1253. doi:10.3390/pr10071253

Hussain, B., Umer, M. J., Li, J., Ma, Y., Abbas, Y., Ashraf, M. N., et al. (2020). Strategies for reducing cadmium accumulation in rice grains. *J. Clean. Prod.* 286, 125557. doi:10.1016/j.jclepro.2020.125557

Ishimaru, Y., Takahashi, R., Bashir, K., Shimo, H., Senoura, T., Sugimoto, K., et al. (2012). Characterizing the role of riceNRAMP5 in manganese, iron and cadmium transport. *Sci. Rep.* 2, 286. doi:10.1038/srep00286

Ishtiyaq, S., Kumar, H., D'Souza, R. J., Varun, M., Favas, P. J. C., and Paul, M. S. (2023). Physiological responses and adaptations of the halophyte Atriplex halimus to soil contaminated with Cd, Ni, and NaCl. *Soil Syst.* 7 (2), 46. doi:10.3390/soilsystems7020046

Kargas, G., Londra, P., and Sgoubopoulou, A. (2020). Comparison of soil EC values from methods based on 1:1 and 1:5 soil to water ratios and ECe from saturated paste extract based method. *Water* 12 (4), 1010. doi:10.3390/w12041010

Kumari, N., and Mohan, C. (2021). "Basics of clay minerals and their characteristic properties," in *Clay and clay minerals* (Brazil: IntechOpen). doi:10.5772/intechopen.97672

León-Romero, M. A., Soto-Ríos, P. C., Fujibayashi, M., and Nishimura, O. (2017). Impact of NaCl solution pretreatment on plant growth and the uptake of multi-heavy metal by the model plant *Arabidopsis thaliana*. *Water, Air, & Soil Pollut.* 228 (2), 64. doi:10.1007/s11270-017-3241-8

Li, H., Li, Z., Khaliq, M. A., Xie, T., Chen, Y., and Wang, G. (2019). Chlorine weaken the immobilization of Cd in soil-rice systems by biochar. *Chemosphere* 235, 1172–1179. doi:10.1016/j.chemosphere.2019.06.203

Li, H., Luo, N., Li, Y. W., Cai, Q. Y., Mo, C. H., Wong, M. H., et al. (2017). Cadmium in rice: transport mechanisms, influencing factors, and minimizing measures. *Environ. Pollut.* 224, 622–630. doi:10.1016/j.envpol.2017.01.087

Li, J., Hashimoto, Y., Riya, S., Terada, A., Hou, H., Shibagaki, Y., et al. (2019). Removal and immobilization of heavy metals in contaminated soils by chlorination and thermal treatment on an industrial-scale. *Chem. Eng. J.* 359, 385–392. doi:10.1016/j.cej.2018.11.158

Li, S. X., Huang, L. C., Jia, B. J., Feng, X., Cao, Y., Chen, Y., et al. (2024). Effect and mechanism of inorganic anions on the adsorption of Cd2+ on two-dimensional copper-based metal–organic framework. *Inorg. Chem. Commun.* 159, 111819. doi:10.1016/j.inoche.2023.111819

Li, X., Peng, P., Long, J., Dong, X., Jiang, K., and Hou, H. (2020). Plant-induced insoluble Cd mobilization and Cd redistribution among different rice cultivars. *J. Clean. Prod.* 256, 120494. doi:10.1016/j.jclepro.2020.120494

Li, Z., Liu, Z., Anderson, W., Yang, P., Wu, W., Tang, H., et al. (2015). Chinese rice production area adaptations to climate changes, 1949–2010. *Environ. Sci. Technol.* 49 (4), 2032–2037. doi:10.1021/es505624x

Lu, J., Bai, Z., Velthof, G. L., Wu, Z., Chadwick, D., and Ma, L. (2019). Accumulation and leaching of nitrate in soils in wheat-maize production in China. *Agric. Water Manag.* 212, 407–415. doi:10.1016/j.agwat.2018.08.039

Lu, Q., Xu, Z., Xu, X., Liu, L., Liang, L., Chen, Z., et al. (2019). Cadmium contamination in a soil-rice system and the associated health risk: an addressing concern caused by barium mining. *Ecotoxicol. Environ. Saf.* 183, 109590. doi:10.1016/j.ecoenv.2019.109590

Moldoveanu, G. A., and Papangelakis, V. G. (2013). Recovery of rare earth elements adsorbed on clay minerals: II. Leaching with ammonium sulfate. *Hydrometallurgy* 131, 158–166. doi:10.1016/j.hydromet.2012.10.011

Rehman, M. Z., Rizwan, M., Rauf, A., Ayub, M. A., Ali, S., Qayyum, M. F., et al. (2019). Split application of silicon in cadmium (Cd) spiked alkaline soil plays a vital role in decreasing Cd accumulation in rice (Oryza sativa L.) grains. *Chemosphere* 226, 454–462. doi:10.1016/j.chemosphere.2019.03.182

Rodda, M. S., Li, G., and Reid, R. J. (2011). The timing of grain Cd accumulation in rice plants: the relative importance of remobilisation within the plant and root Cd uptake post-flowering. *Plant Soil* 347 (1-2), 105–114. doi:10.1007/s11104-011-0829-4

Skuza, L., Izabela, S. K., Filip, E., and Bożek, I. (2022). Natural molecular mechanisms of plant hyperaccumulation and hypertolerance towards heavy metals. *Int. J. Mol. Sci.* 23 (16), 9335. doi:10.3390/ijms23169335

Song, W. E., Chen, S. B., Liu, J. F., Chen, L., Song, N., Li, N., et al. (2015). Variation of Cd concentration in various rice cultivars and derivation of cadmium toxicity thresholds for paddy soil by species-sensitivity distribution. *J. Integr. Agric.* 14 (09), 1845–1854. doi:10.1016/s2095-3119(14)60926-6

Sterckeman, T., Goderniaux, M., Sirguey, C., Cornu, J. Y., and Nguyen, C. (2015). Do roots or shoots control cadmium accumulation in the hyperaccumulator Noccaea caerulescens? *Plant Soil* 392 (1-2), 87–99. doi:10.1007/s11104-015-2449-x

Sun, Y., Qiu, T., Gao, M., Shi, M., Zhang, H., and Wang, X. (2019). Inorganic and organic fertilizers application enhanced antibiotic resistome in greenhouse soils growing vegetables. *Ecotoxicol. Environ. Saf.* 179, 24–30. doi:10.1016/j.ecoenv.2019.04.039

Tang, L., Mao, B. G., Li, Y. K., Lv, Q., Zhang, L., Chen, C., et al. (2017). Knockout of OsNramp5 using the CRISPR/Cas9 system produces low Cd-accumulating indica rice without compromising yield. *Sci. Rep.* 7, 14438. doi:10.1038/s41598-017-14832-9

Wang, P., Chen, H., Kopittke, P. M., and Zhao, F. J. (2019). Cadmium contamination in agricultural soils of China and the impact on food safety. *Environ. Pollut.* 249, 1038–1048. doi:10.1016/j.envpol.2019.03.063

Wu, W., Wu, J., Liu, X., Chen, X., Wu, Y., and Yu, S. (2017). Inorganic phosphorus fertilizer ameliorates maize growth by reducing metal uptake, improving soil enzyme activity and microbial community structure. *Ecotoxicol. Environ. Saf.* 143, 322–329. doi:10.1016/j.ecoenv.2017.05.039

Xu, J. H., Wang, M., and Zhang, R. (2020). Advances in the biotoxicity of soil cadmium pollution. *J. Ecotoxicol.* 15 (05), 82–91. doi:10.7524/AJE.1673-5897.20200424002

Yang, X., Lin, R., Zhang, W., Xu, Y., Wei, X., Zhuo, C., et al. (2019). Comparison of Cd subcellular distribution and Cd detoxification between low/high Cd-accumulative rice cultivars and sea rice. *Ecotoxicol. Environ. Saf.* 185, 109698. doi:10.1016/j.ecoenv.2019.109698

Yang, Y., Ge, Y., Tu, P., Zeng, H., Zhou, X., Zou, D., et al. (2019). Phytoextraction of Cd from a contaminated soil by tobacco and safe use of its metal-enriched biomass. *J. Hazard. Mater.* 363, 385–393. doi:10.1016/j.jhazmat.2018.09.093

Ye, X., Li, H., Ma, Y., Wu, L., and Sun, B. (2014). The bioaccumulation of Cd in rice grains in paddy soils as affected and predicted by soil properties. *J. soils sediments* 14 (8), 1407–1416. doi:10.1007/s11368-014-0901-9

Yu, H. Y., Liu, C., Zhu, J., Li, F., Deng, D. M., Wang, Q., et al. (2016). Cadmium availability in rice paddy fields from a mining area: the effects of soil properties highlighting iron fractions and pH value. *Environ. Pollut.* 209, 38–45. doi:10.1016/j.envpol.2015.11.021

Yuan, D., Huang, L., and Zeng, L. (2017). Acute toxicity of mercury chloride (Hgcl2) and cadmium chloride (Cdcl2) on the behavior of freshwater fish, Percocypris Pingi. *Int. J. Aquac.* 3 (3), 066–070. doi:10.17352/2455-8400.000031

Yuan, X., Ma, H., and Ma, Y. F. (2019). Research progress on cadmium accumulation-related gene family in rice. *Anhui Agric. Sci.* 47 (16), 1–4+17. doi:10.3969/j.issn.0517-6611.2019.16.001

Zare, A. A., Khoshgoftarmanesh, A. H., Malakouti, M. J., Bahrami, H., and Chaney, R. (2018). Root uptake and shoot accumulation of cadmium by lettuce at various Cd: Zn ratios in nutrient solution. *Ecotoxicol. Environ. Saf.* 148, 441–446. doi:10.1016/j.ecoenv.2017.10.045

Zeng, G., Wan, J., Huang, D., Hu, L., Huang, C., Cheng, M., et al. (2017). Precipitation, adsorption and rhizosphere effect: the mechanisms for phosphate-induced Pb immobilization in soils-a review. *J. Hazard. Mater.* 339, 354–367. doi:10.1016/j.jhazmat.2017.05.038

Zhai, X., Li, Z., Huang, B., Luo, N., Huang, M., Zhang, Q., et al. (2018). Remediation of multiple heavy metal-contaminated soil through the combination of soil washing and *in situ* immobilization. *Sci. Total Environ.* 635, 92–99. doi:10.1016/j.scitotenv.2018.04.119

Zhang, B. L., Ouyang, Y. N., Xu, J. Y., and Liu, K. (2018). Cadmium remobilization from shoot to grain is related to pH of vascular bundle in rice. *Ecotoxicol. Environ. Saf.* 147, 913–918. doi:10.1016/j.ecoenv.2017.09.064

Zhang, C., Sale, P. W. G., and Tang, C. (2016). Cadmium uptake by *Carpobrotus rossii* (Haw.) Schwantes under different saline conditions. *Environ. Sci. Pollut. Res.* 23 (13), 13480–13488. doi:10.1007/s11356-016-6508-5

Zhang, J. Y., Zhou, H., Gu, J. F., Huang, F., Yang, W. J., Wang, S. L., et al. (2020). Effects of nano-Fe3O4-modified biochar on iron plaque formation and Cd accumulation in rice (Oryza sativa L.). *Environ. Pollut.* 260, 113970. doi:10.1016/j.envpol.2020.113970

Zhang, S. L., Ni, X. L., Arif, M., Yuan, Z., and Li, L. (2020). Salinity influences Cd accumulation and distribution characteristics in two contrasting halophytes, Suaeda glauca and Limonium aureum. *Ecotoxicol. Environ. Saf.* 191, 110230. doi:10.1016/j.ecoenv.2020.110230

Zhang, X. Q., Li, Y., Ye, J., Chen, Z., Ren, D., and Zhang, S. (2022). The spectral characteristics and cadmium complexation of soil dissolved organic matter in a wide range of forest lands. *Environ. Pollut.* 299, 118834. doi:10.1016/j.envpol.2022.118834

Zhang, Y., Yin, C., Cao, S., Cheng, L., Wu, G., and Guo, J. (2018). Heavy metal accumulation and health risk assessment in soil-wheat system under different nitrogen levels. *Sci. Total Environ.* 622, 1499–1508. doi:10.1016/j.scitotenv.2017.09.317

Zheng, X., Zhao, M., Oba, B. T., and Ding, H. (2023). Effects of organo-mineral complexes on Cd migration and transformation: from pot practice to adsorption mechanism. *Int. J. Environ. Sci. Technol.* 20, 579–586. doi:10.1007/s13762-022-04012-2

Zheng, X. J., Li, Q., Peng, H., Zhang, J. X., Chen, W. J., Zhou, B. C., et al. (2022). Remediation of heavy metal-contaminated soils with soil washing: a review. *Sustainability* 14 (20), 13058. doi:10.3390/su142013058

Zhou, Y. M., Long, S. S., Li, B. Y., Huang, Y. Y., Li, Y. J., Yu, J. Y., et al. (2020). Enrichment of cadmium in rice (Oryza sativa L.) grown under different exogenous pollution sources. *Environ. Sci. Pollut. Res.* 27 (35), 44249–44256. doi:10.1007/s11356-020-10282-5

Zou, M., Zhou, S., Zhou, Y., Jia, Z., Guo, T., and Wang, J. (2021). Cadmium pollution of soil-rice ecosystems in rice cultivation dominated regions in China: a review. *Environ. Pollut.* 280, 116965. doi:10.1016/j.envpol.2021.116965

frontiers | Frontiers in Environmental Science

TYPE Original Research
PUBLISHED 16 May 2024
DOI 10.3389/fenvs.2024.1347330

OPEN ACCESS

EDITED BY
Qi Liao,
Central South University, China

REVIEWED BY
Arup Giri,
Baba Mastnath University, India
Mariusz Gusiatin,
University of Warmia and Mazury in Olsztyn, Poland

*CORRESPONDENCE
Jianmin Wang,
wangjia@mst.edu
John Yang,
yangj@lincolnu.edu

RECEIVED 30 November 2023
ACCEPTED 08 April 2024
PUBLISHED 16 May 2024

CITATION
Farrow EM, Wang J, Shi H, Yang J, Hua B and Deng B (2024), Selected trace element uptake by rice grain as affected by soil arsenic, water management and cultivar -a field investigation. *Front. Environ. Sci.* 12:1347330. doi: 10.3389/fenvs.2024.1347330

Selected trace element uptake by rice grain as affected by soil arsenic, water management and cultivar -a field investigation

Eric M. Farrow[1], Jianmin Wang[1]*, Honglan Shi[2], John Yang[3]*, Bin Hua[3] and Baolin Deng[4]

[1]Department of Civil, Architectural and Environmental Engineering, Missouri University of Science and Technology, Rolla, MO, United States, [2]Department of Chemistry, Missouri University of Science and Technology, Rolla, MO, United States, [3]Department of Agriculture and Environmental Sciences and Cooperative Research, Lincoln University of Missouri, Jefferson City, MO, United States, [4]Department of Civil and Environmental Engineering, University of Missouri, Columbia, MO, United States

Accumulation of arsenic (As) in rice grain was reported in many regions of the world, including the United States, which has been a threat to human health. This field research investigated the grain As accumulation and its relationship with the uptake of selenium (Se), molybdenum (Mo), and cadmium (Cd) in soils with and without monosodium methanearsonate (MSMA) amended, as effects of selected rice cultivars and water management. Results indicated that MSMA increased the accumulation of As and Se but decreased Mo for all six cultivars under four irrigation management. MSMA also increased grain-Cd in some cultivars. In no MSMA-amended soil (Native soil), intermittent flooding decreased grain-As by 66%, grain-Se by 21%, and grain-Mo by 63%, but increased grain-Cd by 64% in Zhe 733, a straighthead resistant cultivar, while in MSMA-amended soil, intermittent flooding decreased grain-As by 63% and grain-Mo by 44% but increased grain-Se by 68% and grain-Cd by three times. For all other five cultivars, intermittent flooding generally decreased grain-As and grain-Mo but increased grain-Se and grain-Cd. Zhe 733 cultivar resulted in the lowest grain concentrations of all trace elements in all water treatments. A negative grain As-Se correlation and a positive grain As-Mo correlation were significant but not the As-Cd correlation. This research showed that the uptake of As, Se, Mo, and Cd by rice grain occurred as a complex function of multiple variables, including cultivar type and soil chemistry. As a result, accumulation of As and other trace elements in rice grain may be controlled by selecting appropriate cultivars and adopting appropriate water management practices.

KEYWORDS

rice cultivar, arsenic, trace elements, accumulation, water management

Introduction

Inorganic arsenic (As) has been determined to be a human carcinogen by the United States Environmental Protection Agency (U.S. EPA) (ATSDR, 2007). The contamination of As in rice grain, though primarily composed of less toxic organic As, has also been recognized as carcinogenic (Florea et al., 2005; Williams et al., 2005). Increased As in rice grain could be caused by elevated As levels in soils of traditional cotton growing regions in the south central U.S. (Loebenstein, 1994), because of a century of

arsenical herbicide, pesticide, and defoliant applications such as monosodium methanearsonate (MSMA) (ATSDR, 2007). Average total grain-As concentrations of rice grown in the south-central U.S. region was 0.27 μg A g-1 with approximately inorganic As of 0.11 μg g-1 (Williams et al., 2007; Batres-Marquez et al., 2009), which has an oral reference dose of 0.3 μg kg body weight (bw)$^{-1}$ day^{-1} for chronic oral exposures (EPA and U. S., 2019). Although the total As in rice is primarily in an organic form, arsenic in subsequent rice food products, such as toddler formula, cereal bars, rice syrup, and energy shots, is primarily in the inorganic form (Meacher et al., 2002; Liang et al., 2010; Jackson et al., 2012; Yüksel et al., 2023). Therefore, the daily consumption of these majorly unregulated rice and rice products could exceed the equivalent of the USEPA's and World Health Organization's (WHO) drinking water standard of 10 μg L-1 (EPA, 2001; WHO, 2008), making it imperative that the agricultural practices directly responsible for total As in foods be further studied.

Environmental factors impacting As uptake by rice plants may include soil As content, irrigation management, and genotypes of rice cultivars. Elevated soil As has been found to correspond to higher grain As content (Xie and Huang, 1998; Heikens, 2006; Topaldemir et al., 2023). Straighthead disease is common in rice crops grown with elevated soil-As conditions, where panicle sterility and significant yield loss have been observed (Yan et al., 2005). Grain-As is exacerbated further, where flooded conditions create a reducing environment that can lead to increasing As uptake (Masscheleyn et al., 1991; Xie and Huang, 1998; Somenahally et al., 2011). Plant As uptake also varies among the genotypes of cultivars (Jian et al., 2008; Norton et al., 2009). Thus, cultivar selection could also be useful to reduce grain-As (Pillai et al., 2010).

In addition to As, the accumulation of other trace elements, such as selenium (Se), molybdenum (Mo), and cadmium (Cd) in rice grain could also be of concern. Se is an essential element to human health, and lack of Se could cause cardiovascular disease and cancer (Navarro-Alarcon and Cabrera-Vique, 2008). However, excess Se may also negatively impact human health. USEPA regulates Se in drinking water with a maximum contaminant level (MCL) of 50 μg L-1 (EPA and U. S., 2009) and an oral reference dose of 5 μg kg bw^{-1} day^{-1} (EPA and U. S., 2019). By understanding Se transport mechanisms, rice Se concentrations could be regulated, as necessary, to minimize Se biofortification practices and provide optimal dosage for human consumption (Zhu et al., 2009; Premarathna et al., 2012). Mikkelsen et al. (Mikkelsen et al., 1989) showed that flooded condition could reduce Se uptake, while Premarathna et al. (Premarathna et al., 2012) indicated that irrigation management may impact total grain Se in the order: field capacity > submerged > submerged/drained.

Mo is also an essential trace element for humans, but also has a negative effect at high exposure, which is listed on the USEPA's drinking water Contaminant Candidate List 3 (CCL3) (EPA and U. S., 2009). The USEPA oral reference dose is 5 μg Mo kg bw^{-1} day^{-1} (EPA and U. S., 2019). Mo has been found to regulate calcium (Ca), magnesium (Mg) and copper (Cu) metabolisms in humans, where the greatest risk of Mo toxicity occurs in humans with Cu deficiencies (Antoine et al., 2012). Dunn and Dunn (Dunn and Dunn, 2012) discovered that increasing yield of rice grain (i.e., decreasing in total grain-As) resulted in a decrease in grain-Mo, suggesting a positive As-Mo correlation. Mo toxicity may be a factor for crops grown in poorly drained soils, where the tolerance varied with cultivar (Rout and Das, 2002).

In recent years, the accumulation of Cd in rice has been reported in many areas, especially China (Liu et al., 2003; Arao et al., 2009). Unlike As, Se, and Mo, which are mostly in anionic form, Cd is a cation form. The Cd bioaccumulation in rice may be greater than some other essential elements (Liu et al., 2003). Further, Cheng et al. (Cheng et al., 2006) showed a positive As-Cd correlation in rice roots and straw. Negative health impacts are known for Cd, including kidney dysfunction (Jakubowski et al., 2002). The USEPA oral reference dose is 1 μg Cd kg bw^{-1} day^{-1} (EPA and U. S., 2019). The Joint Food and Agriculture Organization/World Health Organization Expert Committee (JECFA) has set the Cd provisional tolerable weekly intake (PTWI) at 7 μg kg bw^{-1} wk^{-1} (FAO/WHO, 2003).

Previously, most studies on the uptake of trace elements by rice focused on individual elements. In this research, it was hypothesized that the uptake of multiple elements of concern is correlated. The objectives of this research were to provide an understanding of i) the impact of soil chemistry, such as MSMA amendment and water management (intermittent flooding vs continuous flooding), on total grain concentrations of selected trace elements of six cultivars, and ii) correlations among trace elements of concern in rice grain. The findings from this research would help rice growers adopt appropriate management practices that control the uptake of As and selected trace elements by rice grain.

Materials and methods

Field experiment

The field study was conducted at the USDA-ARS Dale Bumpers National Rice Research Center near Stuttgart, Arkansas in 2009. The soil on the site is a Dewitt silt-loam soil (fine, smectitic, thermic Typic Albaqualf). The experiment was arranged in a split-split plot design with four replications per treatment, in which MSMA-amended soils were main plots and water management as sub-plots. The main plots included MSMA-amended and no MSMA treatments. The MSMA-amended plots were established since 1980s for the straighthead resistance study (Yan et al., 2005), where MSMA was sprayed and incorporated into soil at a rate of 6.7 kg MSMA ha-1 prior to planting, as described by Yan et al. (Yan et al., 2005). The Native plot was located nearby where no MSMA was applied. Topsoil (0–20 cm) were collected from both MSMA-amended and Native plots before rice planting for soil characterization (Hua et al., 2011). Each main plot was divided into four completely randomized sub-plots for water treatments. The water treatment included four water management practices: one intermittent flooding and three continuous flooding. Intermittent flooding conditions were maintained by initially flooding the soil, and then allowing soil to dry until small, surface cracks were evident. At this point, the plots were irrigated up to 10 cm water depth with a nearby reservoir water (pH ~7.0, <2 μg A L-1). Continuous floodings were conditions under which plots were drained at 10, 20, or 35 days after the heading date (50% panicle emergence from flag leaf). Each sub-plot contained six-row (1.8 m by 1.5 m) blocks in a completely randomized arrangement with four replications per

cultivar (Pillai et al., 2010). Six rice cultivars were selected in this study: Cocodrie, Rondo and Wells from the south-central U.S.; Zhe 733 and GP-2 from China; and Spalcik from Russian Federation (Yan et al., 2008; Yan and McClung, 2010). These six cultivars included early, mid- and late-maturity and varied with the resistance or tolerance for As-induced straighthead disease (resistant, moderate, and susceptible) (Yan et al., 2008; Yan and McClung, 2010). This field study concurred with development of the practical solution to minimize grain-As accumulation in field conditions and primarily focused on Zhe 733 cultivar, since it has been identified as an As tolerant cultivar and widely studied for As-induced straighthead disease (Yan et al., 2005; Yan et al., 2008) and grain-As uptake (Yan et al., 2005; Pillai et al., 2010; Hua et al., 2011).

At maturity, rice grains from each plot were harvested, dried at 65°C to approximately 12% of moisture content, and stored at room temperature for digestion and then chemical analysis. Prior to digestion, grain samples were de-hulled using a ceramic mortar and pestle and oven dried at 65°C for 48 h and stored in a desiccator. 127.

Chemical analysis

A Multiwave 3,000 microwave digester (Anton Paar, Austria) was used for grain and soil sample digestion. In particular, EPA Method 3,052 was followed to digest rice grain samples, and slightly modified EPA Method 3051A was used to digest soil samples for the determination of the total concentrations of trace elements. For rice grain digestion, 0.5 g rice grain was placed in the acid cleaned Rotor 48 (MF50) digestion vessels and added with 8.0 mL optima grade nitric acid (HNO3) and 0.3 mL trace metal hydrogen peroxide (H2O2) (Fisher Scientific Co., Boston, U.S.). The digestion program consisted of a 10-min ramp to 100°C with a 10-min hold, followed by a 10-min ramp to 140°C, with a 15-min hold, then a 10-min ramp to 170°C, with a 10-min hold before cooling down.

For soil digestion, 0.5 g soil samples were placed in acid cleaned Rotor 8 (XF100) digestion vessels and digested with 9.0 mL trace metal grade HNO3 and 3.0 mL trace metal grade hydrochloric acid (HCl). The digestion program consisted of a 10-min ramp to 1100 W, with a 20-min hold before cooling down. All digested samples were allowed to cool down to <50°C before venting. Digested samples were rinsed from digestion vessels to acid-cleaned 50 mL conical tubes, and then diluted to 20 mL using Millipore water (18.2 MΩ-cm).

Standard reference materials (NIST, Gaithersburg, MD) for rice grain (SRM1568a) and soil (SRM2711a Montana II) were included in respective digestions for quality assurance and quality control (QA/QC). Additional digestion QA/QC included one sample blank, one sample duplicate, and one sample spike per 10 samples for rice and soil digestion. Spike concentrations were analyzed at an estimated two times of average sample concentrations.

Total As, Se, Mo, and Cd concentrations in digested grain samples and extractable Se, Mo, and Cd concentration in soil samples were determined using inductively coupled mass spectrometry (ICP-MS) (PerkinElmer Elan DRC-e, MDS Sciex, Concord, Ontario, Canada). Extractable As from soil was determined using graphite furnace atomic adsorption spectroscopy (GFAA) (PerkinElmer AAnalystTM 600, Shelton, CT, United States). Digested grain and soil samples were diluted using 10% and 5% HNO3 prior to chemical analysis, respectively. Sample method detection limits (MDLs) for all tested elements were determined for GFAA and ICP-MS, according to EPA Method 200.9 and 200.8, respectively. Estimated soil MDLs for As, Se, Mo, and Cd were 0.10, 0.08, 0.02, and 0.02 mg kg-1, respectively, while rice grain MDLs for As, Se, Mo, and Cd were 0.004, 0.031, 0.003, and 0.003 mg kg-1, respectively. Sample concentrations greater than 2–3 times MDL were required. QA/QC was validated if the following criteria were met: (a) relative difference of a duplicate sample less than 20%; (b) spike recovery between 85% and 115%; and (c) the accuracy of a calibration standard within 10% per 10 samples analyzed.

Statistical analysis

The analysis of variance (ANOVA) procedure that was appropriate for the split-split-plot design was accrued out using SAS 9.2 to estimate the impact of experimental variables on trace element uptake. The experimental variables (factors) were soil-As (Soil), irrigation management (Water), and rice cultivar (Cultivar), with Soil as the main-plot factor, Water as the sub-plot factor and Cultivar as the sub-sub-plot factor. ANOVA allows interaction terms representing the combined impact of different factors on element uptake to be tested, whereby a significant interaction term signifies that the impact of the changing levels of one factor is influenced by the level of the other factor(s). Least square means with Tukey's adjustment were used to contrast means of specific Soil-Water combinations. Tukey's means adjustment allowed experiment-wise error to be kept at the selected rate, $\alpha = 0.05$ (Montgomery, 2009). Pearson's partial correlations between grain-As and grain-Se, grain-Mo, and grain-Cd were also estimated.

Results and discussion

Soil characterization

Characterization and major physiochemical properties of two soils, Native and MSMA-amended soils, were presented in Hua et al. (Hua et al., 2011) and Yan et al. (Yan et al., 2008). The average As content in Native soil was 5.9 ± 0.25 mg kg^{-1} while MSMA-amended soil 19.5 ± 0.36 mg kg^{-1}. Furthermore, Native soil contained 0.230 ± 0.004 mg Se kg^{-1}, 0.38 ± 0.04 mg Mo kg^{-1}, and 0.060 ± 0.003 mg Cd kg^{-1} Cd, while MSMA-amended soil contained 0.53 ± 0.09 mg Se kg^{-1}, 0.63 ± 0.24 mg Mo kg^{-1}, and 0.060 ± 0.006 mg Cd kg^{-1}.

Effect of soil As level

For each type of soil, total concentrations of the four trace elements analyzed were found not significantly different among three continuous flooding treatments (drain at 10, 20, and 35 days after heading), but MSMA amendment resulted in significantly higher grain-As and lower grain-Mo, as indicated in Table 1. Thus, the average value of three continuous flooding treatments

TABLE 1 Total grain trace element concentrations for rice grown under three continuous flooding conditions (drained 10, 20, and 35 days after heading, respectively).

Soil	Days	As	Se (b)	Mo	Cd
		mg kg^{-1} (b)			
Native	10	0.291a*	0.373	1.173c	0.021d
	20	0.341a	0.337b	1.243c	0.014d
	35	0.365a	0.319b	1.150c	0.012d
MSMA-amended	10	0.981a	0.396b	0.581c	0.029d
	20	1.141a	0.445b	0.625c	0.019de
	35	1.360a	0.488b	0.556c	0.016e

*Values followed by the same letter (a, b, c, d, e, and de) are not significantly different ($p > 0.05$).

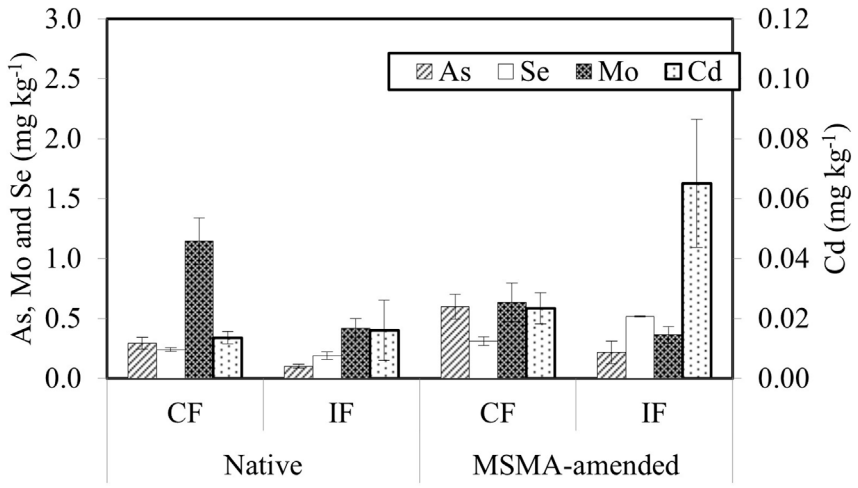

FIGURE 1
Average grain trace element concentrations of Zhe 733 grown in two soil treatments and two water managements.

was used when compared with that from the intermittent flooding treatment.

Elevated grain-As concentrations were reported in low-As soils under both continuous and intermittent flooding conditions, and the presence of trace MSMA quantities could strongly affect grain-As (Pillai, 2009). Yan et al. (Yan et al., 2005) showed increased grain-As and reduced grain yield due to MSMA-induced straighthead susceptibility under continuous flooding conditions.

The effect of soil-As on average grain concentrations of As, Se, Mo, and Cd under continuous and intermittent flooding for the As-tolerant Zhe 733 was presented in Figure 1. Data can be compared with current global As standards of the United Kingdom Food Statutory General Limit (1.0 mg kg-1 fresh weight in food) (Kingdom et al., 1959). Currently, there is no food standards established for As, Se, Mo, and Cd in United States. Zhe 733 cultivar grown under continuous flooding and MSMA-amendments significantly increased grain-As from 0.30 to 0.60 mg kg-1 (103%), grain-Se from 0.24 to 0.31 mg kg-1 (30%), grain-Cd from 0.014 to 0.016 mg kg-1 (18%), and decreased grain-Mo from 1.15 to 0.64 mg kg-1 (45%) (Figure 1). Under intermittent flooding, MSMA-amendments increased As from 0.10 to 0.22 mg kg-1 (115%), Se from 0.19 to 0.52 mg kg-1 (175%), Cd from 0.023 to 0.065 mg kg-1 (183%), and decreased Mo from 0.42 to 0.36 mg kg-1 (−13%). Thus, MSMA amendment resulted in the same trend on trace element concentrations in both irrigation managements, with a greater impact by intermittent flooding. The highest grain-As levels from MSMA-amended and continuous flooding were considerably less than the United Kingdom Food Statutory General Limit (Kingdom et al., 1959). However, rice consumption at the average U.S. consumer diet of ≥61.2 g rice grain day-1 (Batres-Marquez et al., 2009) and the average Asian-American diet of 400 g rice grain day-1 (Navarro-Alarcon and Cabrera-Vique, 2008) may result in an ingestion of approximately 0.52 and 3.4 μg A kg^{-1} day^{-1}, respectively, which is substantially greater than the regulated intake amount of 0.29 μg A kg^{-1} day^{-1} through drinking water (EPA, 2001). The highest grain- Cd levels of 0.065 mg kg^{-1} were found in MSMA-amended intermittent flooding conditions. Consuming such rice grain for the average U.S. consumer and the Asian-American may intake 0.4 and 2.6 μg kg^{-1} wk^{-1}, which is less than the JEFCA Cd standard (FAO/WHO, 2003). Furthermore, increased soil-As level

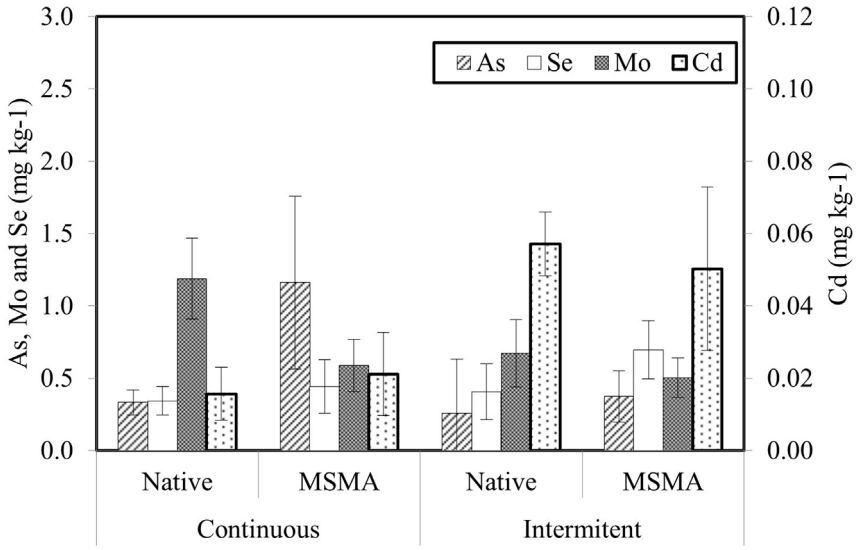

FIGURE 2
Average grain trace element concentrations of five cultivars grown in two soil treatments and two water managements.

not only increased grain-As, but also impacted the uptake of Se, Mo, and Cd, especially under intermittent flooding conditions.

A general trend of soil-As on average grain trace element concentrations of other five cultivars under continuous and intermittent flooding was illustrated in Figure 2. For the five cultivars under continuous flooding, MSMA amendment increased As from 0.33 to 1.16 mg kg-1 (252%), Se from 0.34 to 0.44 mg kg-1 (29%), Cd from 0.016 to 0.021 mg kg-1 (31%), and decreased Mo from 1.19 to 0.59 mg kg-1 (50%). Under intermittent flooding, MSMA amendment increased grain-As from 0.26 to 0.38 mg kg-1 (46%), Se from 0.41 to 0.70 mg kg-1 (71%), decreased Mo from 0.67 to 0.50 mg kg-1 (25%) and Cd from 0.057 to 0.050 mg kg-1 (12%). Overall, increasing soil-As increased levels of grain-As and grain-Se, but decreased grain-Mo level for both irrigation management practices. However, MSMA amendment slightly increased grain-Cd under continuous flooding but slightly decreased grain-Cd under intermittent flooding.

Zhe 733 cultivar had been widely used as a resistant check cultivar for As-induced straighthead disease studies (Yan et al., 2005; Yan et al., 2008; Pillai, 2009; Pillai et al., 2010; Hua et al., 2011; Somenahally et al., 2011). Comparing with five other cultivars, Zhe 733 had much less grain-As concentrations in all of the irrigation-MSMA treatments: 9% less in Native-continuous, 48% less in MSMA-continuous, 62% less in Native-intermittent, and 42% less in MSMA-intermittent (Figures 1, 2). Data suggested that straighthead resistance be associated with less As uptake.

Effect of water management

Also shown in Figure 1, in compared with the continuous flooding, Zhe 733 cultivar in Native soil under intermittent flooding significantly decreased grain-As from 0.30 to 0.10 mg kg-1 (66%), grain-Se from 0.24 to 0.19 mg kg-1 (21%), grain-Mo from 1.15 to 0.42 mg kg-1 (63%) and increased grain-Cd from 0.014 to 0.023 mg kg-1 (64%). The other five cultivars grown in same soil under intermittent flooding slightly decreased grain-As from 0.33 to 0.26 mg kg-1, slightly increased grain-Se from 0.34 to 0.41 mg kg-1, significantly decreased grain-Mo from 1.19 to 0.67 mg kg-1, and significantly increased grain-Cd from 0.016 to 0.057 mg kg-1 (Figure 2).

Soil redox potential had a large impact on the fate and transport of As, due to the presence of insoluble FeIII (hydr)oxides and, consequently, the formation of AsV-FeIII complexes in aerobic systems (Charlet et al., 2011; Wang et al., 2011). Soil redox measurements in intermittent and continuous flooding plots (339 ± 84 vs 160 ± 52 mV) supports the above analysis because intermittent flooding condition provided a more oxidized condition facilitating the formation of AsV-FeIII complexes, decreasing As solubility and subsequent plant uptake (Masscheleyn et al., 1991). In addition, under more oxidized conditions, As is likely in the less mobile AsV form (Cullen and Reimer, 1989).

For Zhe 733, intermittent flooding also significantly decreased grain-Se. However, the overall trend of the other five cultivars indicated a slight increase in grain-Se under intermittent flooding, confirming the results from Mikkelsen et al. (Mikkelsen et al., 1989). This further suggested that the Se uptake mechanism by rice was more of a function of cultivar. Therefore, cultivar selection based on minimizing grain-As may also have implications on other elements. Similar to grain-As, overall grain-Mo significantly decreased as a result of intermittent flooding. The primary uptake mechanism for Mo and As under aerobic conditions occurs via the phosphate pathway (Balistrieri et al., 1994). Thus, it is evident that the oxidized soil environment would regulate and reduce Mo bioavailability by the formation of immobile iron (hydr) oxide complexes, resulting in lower mobility and thus plant uptake (Moore and Patrick, 1991). Overall grain-Cd concentrations significantly increased under the intermittent flooding. Due to

TABLE 2 Effects of cultivar on total grain trace element concentration of As, Se, Mo, and Cd under soil As and water management interactions.

	Native soil		MSMA-amended soil	
	Continuous	Intermittent	Continuous	Intermittent
As	Spalcik ↑	Zhe 733 ↓	-	-
		Spalcik ↑		
Se	Zhe 733 ↓	-	-	-
	GP-2 ↑			
Mo	Rondo ↓	Zhe 733 ↓	Spalcik ↓	-
	Wells ↑	Spalcik ↑		
Cd	GP-2 ↑	-	GP-2 ↑	-

the oxidized conditions associated with intermittent flooding, insoluble CdS may have converted to the more soluble $CdSO_4$, resulting in a greater Cd availability for rice uptake (Ito and Iimura, 1976).

The significant impact of cultivars on the soil As and water management interaction in both Native and MSMA-amended soils was presented in Table 2. In compared to other cultivars, Zhe 733 grown in Native soil under intermittent flooding had the most significant decrease in grain-As. Among the six cultivars in Native soil under both continuous and intermittent flooding, cultivar selection had at least one significant impact on the uptake of selected elements. Results from this research could provide evidence that cultivar selection alone would significantly affect grain trace element concentration, varying with irrigation management practice.

Data in Figure 1 also showed the effect of water management on grain concentrations of As, Se, Mo, and Cd for Zhe 733 under MSMA-amended soil. In MSMA-amended soil and compared to continuous flooding, intermittent flooding significantly decreased grain-As from 0.60 to 0.22 mg kg-1 (63%) and grain-Mo from 0.64 to 0.36 mg kg-1 (44%), and significantly increased grain-Se from 0.31 to 0.52 mg kg-1 (68%) and grain-Cd from 0.016 to 0.065 mg kg-1 (3.1 times). Therefore, water management resulted in a similar effect on As, Mo, and Cd uptake in both Native and MSMA-amended soil, however, the effect on grain-Se was the opposite. For other five cultivars in MSMA-amended soil and compared to continuous flooding, intermittent flooding significantly decreased grain-As from 1.16 to 0.38 mg kg-1 and grain-Mo from 0.59 to 0.50 mg kg-1, and significantly increased grain-Se from 0.44 to 0.70 mg kg-1 and grain-Cd from 0.021 to 0.050 mg kg-1 (Figure 2). As compared to Native soil, intermittent flooding resulted in a greater decrease in grain-As for MSMA-amended soil. The grain-As concentrations determined in MSMA-amended soil were slightly different from those reported (Williams et al., 2007; Pillai et al., 2010), which was likely due to the cultivar variation used in this study.

The increase in grain-Se as a result of intermittent flooding in MSMA-amended soil in the current research confirms Mikkelsen et al. (Mikkelsen et al., 1989) and constant with Native soil results. Se is most prevalent in the mobile selenate form under aerobic conditions, therefore causing the increase in grain-Se in intermittent flooding (Mikkelsen et al., 1989). The increase in grain-Cd as a result of intermittent flooding discovered in the current research in MSMA-amended soil is consistent with Arao et al. (Arao et al., 2009). This increase in Cd concentrations of rice grain due to aerobic treatments makes it difficult to simultaneously decrease human exposure to both As and Cd elements based on irrigation management.

Among the six cultivars in MSMA-amended soil under continuous or intermittent flooding, cultivar selection had a significant impact on grain-Mo and grain-Cd (Table 2). Compared to other cultivars, GP-2 had the most significant increase in grain-Cd under continuous flooding and MSMA-amended soil, validating that cultivar can significantly alter grain element accumulation varying with water management. This is most likely due to cultivar specific uptake mechanisms. Though the cultivar impact on grain-As, Se, Mo, and Cd in MSMA-amended soil under intermittent flooding was determined to be negligible, Zhe 733 cultivar minimized grain-As in MSMA-amended soil, consistent with findings by Hua et al. (Hua et al., 2011). Overall, this result verified previous findings that cultivar selection is a useful practice to control trace element uptake in rice grain (Jian et al., 2008; Zhang et al., 2008; Norton et al., 2009).

Correlations among trace elements

Correlations among trace elements in all six cultivars grown from both Native and MSMA-amended soils were developed. The impacts of grain As uptake on Se, Mo, and Cd concentrations for Zhe 733 cultivar were presented Figure 3. Grain-As and grain-Se showed a positive correlation in Native soil, but a negative relationship in MSMA-amended soil. The correlation between grain-As and grain-Mo was positive in both soils. However, grain-As was negatively corelated with grain-Cd in both soils. Measurements contradicted the findings by Cheng et al. (Cheng et al., 2006) who reported a positive As-Cd correlation in rice root and straw.

The correlations of grain-As with Se, Mo, and Cd for other five cultivars indicated an overall negative trend between grain-As and grain-Se, but with a weak correlation. Similar to Zhe 733 cultivar, a strong positive grain As-Mo trends were found for Cocodrie, Rondo,

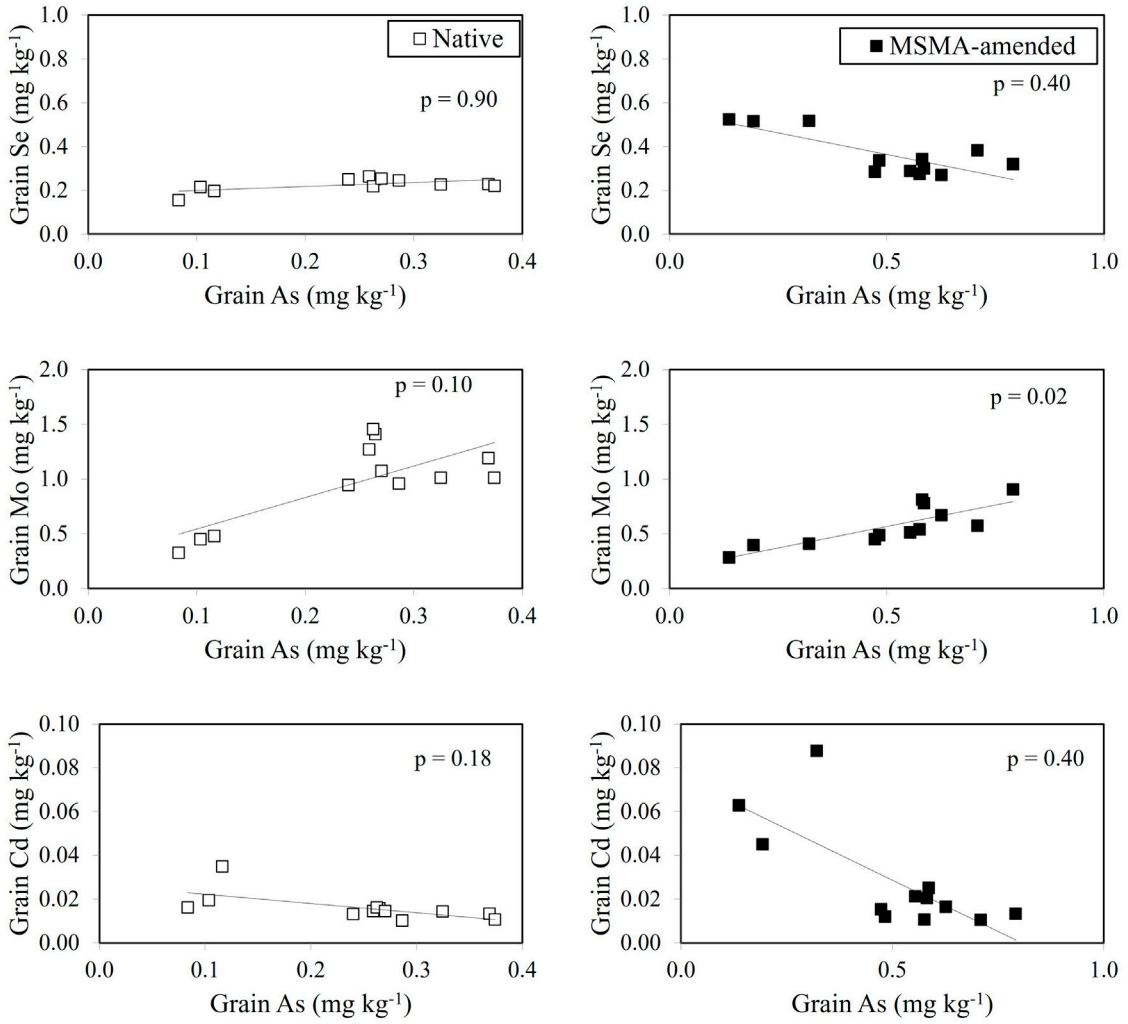

FIGURE 3
Trace element correlations for Zhe 733 cultivar in both Native (left) and MSMA-amended soils (right).

and Wells cultivars. Dunn and Dunn (Dunn and Dunn, 2012) discovered that plant Mo was negatively correlated with the straighthead score, suggesting that grain Mo decreased with increasing the straighthead score and total grain-As, which contradicted to the overall positive grain As-Mo trend found in this study. A negative grain As-Mo correlation was also reported by Norton et al. (Norton et al., 2012). Strong neutral As-Cd trends were discovered for Cocodrie, Spalcik, Zhe 733 cultivars grown in MSMA-amended soil, and GP-2 in Native soil.

Analysis of variance

ANOVA was performed on all cultivars to determine the significance of main effects and the corresponding interactions. The significant levels of main effects and interactions were shown in Table 3. The soil × water interaction for Zhe 733 was significant for Mo only, indicating that the impact of soil-As on grain-Mo was influenced by water management. Soil-As level significantly affected As and Se content in grain, confirming the increase in grain-As and grain- Se in MSMA-amended soil as compared to that in Native soil. For all six cultivars, the interaction of cultivar × soil × water was significant for grain-As and Se, and the interaction of cultivar × soil was significant for grain-Mo. Further analysis by Tukey's means adjustment indicated that the occurrence of multiple significant interactions for As, Se, Mo, and Cd uptake by the six cultivars was a complex function rather than a function of a single element.

This field study demonstrated that the uptake of trace elements by rice was strongly impacted by soil chemistry, such as element contents or availability and redox conditions in soil. In addition, the correlations among grain trace elements revealed that these elements interacted with each other during the uptake process. Therefore, the uptake of an element could also be indirectly impacted by another element. The cultivar selection was also important for controlling the accumulation of trace elements. Conclusions based on single element uptake may not be appropriate for another element, even though they are in the same group. This research provided evidence that rice grain accumulation of trace elements may be selectively controlled by management practices during rice cultivation.

TABLE 3 Analysis of variance of grain trace element concentration for six cultivars studied.

	Element (Pr > F)†					
	DF	F_C†	As	Se	Mo	Cd
	Zhe 733					
Soil	1	4.49	0.01**	0.01**	<0.001***	0.59
Water	3	3.25	0.09	0.59	<0.001***	0.73
Soil x Water	3	3.25	0.69	0.19	0.04*	0.9
Cocodrie, GP-2, Rondo, Spalcik, Wells, Zhe 733						
Cultivar	5	2.31	<0.001***	<0.001***	<0.001***	0.3557
Cultivar x Soil	5	2.31	<0.001***	<0.001***	0.0149*	0.5216
Cultivar x Water	15	1.77	0.0377*	0.0377	0.7994	0.2005
Cultivar x Soil x Water	15	1.49	<0.001***	<0.001***	0.8591	0.7908

MS, experiment-wise = 0.051, 0.014, 0.023, and 0.003 for As, Se, Mo, and Cd, respectively. *, **, *** indicate significance at $p < 0.05$, 0.01, and 0.001. †$\alpha = 0.05$ 354.

Conclusion

The impact of MSMA amendment and irrigation management on the accumulation of As, Se, Mo, and Cd in rice grains was assessed using six different rice cultivars. The findings demonstrated that the addition of MSMA might lead to elevated levels of As, Se, and Cd in the grain, while simultaneously reducing the amount of Mo accumulation. Intermittent flooding resulted in a reduction in grain-As and grain-Mo, while dramatically increasing grain-Se and grain-Cd. The Zhe 733 cultivar, which is resistant to straighthead disease, exhibited lower grain-As compared to other five cultivars across all treatments. A negative correlation between grain-Se and As concentrations was found in the MSMA amended soil. Additionally, a positive correlation between grain-As and Mo was found in the same soil. The accumulation of selected elements in grains was significantly influenced by soil chemistry and the specific rice cultivar. By selecting the straighthead-resistant Zhe 733 cultivar and implementing intermittent flooding, it is possible to greatly decrease the levels of As, Se, and Mo in the grain and help mitigate the health risks associated with the As buildup in the grain.

Data availability statement

The raw data supporting the conclusion of this article will be made available by the authors, without undue reservation.

Author contributions

EF: Formal Analysis, Investigation, Data curation, Writing–original draft. JW: Conceptualization, Funding acquisition, Investigation, Project administration, Supervision, Writing–original draft. HS: Methodology, Writing–review and editing. JY: Conceptualization, Funding acquisition, Investigation, Project administration, Resources, Supervision, Validation, Writing–review and editing. BH: Investigation, Writing–review and editing. BD: Writing–review and editing.

Funding

The author(s) declare financial support was received for the research, authorship, and/or publication of this article. This study was supported by USDA-NIFA. This research was funded by the USDA-NIFA (Award No. 2008-38814-04727) to Missouri University of Science and Technology (Missouri S&T) through Lincoln University of Missouri. The authors gratefully acknowledge supports from Dr. Wengui Yan and Ms. Tiffany Sookaserm at USDA Dale Bumpers National Rice Research Center in Stuttgart, Arkansas, for sample collection and preparation, and Ms. Brandi Clark and Dr. Joel Burket at Missouri S&T for assistance with analytical method development and facility support, respectively.

Conflict of interest

The authors declare that the research was conducted in the absence of any commercial or financial relationships that could be construed as a potential conflict of interest.

Publisher's note

References

Antoine, J. M. R., Hoo Fung, L. A., Grant, C. N., Dennis, H. T., and Lalor, G. C. (2012). Dietary intake of minerals and trace elements in rice on the Jamaican market. *J. Food Compos. Analysis* 26 (1-2), 111–121. doi:10.1016/j.jfca.2012.01.003

Arao, T., Kawasaki, A., Baba, K., Mori, S., and Matsumoto, S. (2009). Effects of water management on cadmium and arsenic accumulation and dimethylarsinic acid concentrations in Japanese rice. *Environ. Sci. Technol.* 43 (24), 9361–9367. doi:10.1021/es9022738

ATSDR (2007). "Toxicological profile for arsenic," in *Usdhhs* (Atlanta, Georgia: Public Health Service Agency for Toxic Substances and Disease Registry).

Balistrieri, L. S., Murray, J. W., and Paul, B. (1994). The geochemical cycling of trace elements in a biogenic meromictic lake. *Geochimica Cosmochimica Acta* 58 (19), 3993–4008. doi:10.1016/0016-7037(94)90262-3

Batres-Marquez, S. P., Jensen, H. H., and Upton, J. (2009). Rice consumption in the United States: recent evidence from food consumption surveys. *J. Am. Dietetic Assoc.* 109 (10), 1719–1727. doi:10.1016/j.jada.2009.07.010

Charlet, L., Morin, G., Rose, J., Wang, Y., Auffan, M., Burnol, A., et al. (2011). Reactivity at (nano)particle-water interfaces, redox processes, and arsenic transport in the environment. *Comptes Rendus Geosci.* 343 (2-3), 123–139. doi:10.1016/j.crte.2010.11.005

Cheng, W. D., Zhang, G. P., Yao, H. G., Wu, W., and Xu, M. (2006). Genotypic and environmental variation in cadmium, chromium, arsenic, nickel, and lead concentrations in rice grains. *J. Zhejiang Univ. Sci. B* 7 (7), 565–571. doi:10.1631/jzus.2006.b0565

Cullen, W. R., and Reimer, K. J. (1989). Arsenic speciation in the environment. *Chem. Rev.* 89 (4), 713–764. doi:10.1021/cr00094a002

Dunn, B. W., and Dunn, T. S. (2012). Influence of soil type on severity of straighthead in rice. *Commun. Soil Sci. Plant Analysis* 43 (12), 1705–1719. doi:10.1080/00103624.2012.681742

EPA (2001). National primary drinking water regulations; arsenic and clarifications to compliance and new source contaminants monitoring. Available at: https://www.federalregister.gov/documents/2001/01/22/01-1668/national-primary-drinking-water-regulations-arsenic-and-clarifications-to-compliance-and-new-source.

EPA, U. S. (2009). Drinking water contaminant candidate list 3. Available at: https://www.federalregister.gov/documents/2009/10/08/E9-24287/drinking-water-contaminant-candidate-list-3-final.

EPA, U. S. (2019). Integrated risk information system. Available at: http://www.epa.gov/IRIS/.

FAO/WHO (2003) *Joint FAO/WHO Expert committee on food additives*. Rome, Italy: FAO/WHO.

Florea, A.-M., Yamoah, E. N., and Dopp, E. (2005). Intracellular calcium disturbances induced by arsenic and its methylated derivatives in relation to genomic damage and apoptosis induction. *Environ. Health Perspect.* 113 (6), 659–664. doi:10.1289/ehp.7634

Heikens, A. (2006). "Arsenic contamination of irrigation water, soil and crops in Bangladesh: risk implications for sustainable agriculture and food safety in Asia," in *Food and agriculture organization of the united nations*, 46.

Hua, B., Yan, W., Wang, J., Deng, B., and Yang, J. (2011). Arsenic accumulation in rice grains: effects of cultivars and water management practices. *Environ. Eng. Sci.* 28 (8), 591–596. doi:10.1089/ees.2010.0481

Ito, H., and Iimura, K. (1976). The absorption and translocation of cadmium in rice plants and its influence on their growth, in comparison with zinc: studies on heavy metal pollution of soils (Part 1). *Bull. Hokuriku Natl. Agriculuture Exp. Stn.* 19, 71–139.

Jackson, B. P., Taylor, V. F., Karagas, M. R., Punshon, T., and Cottingham, K. L. (2012). Arsenic, organic foods, and Brown rice syrup. *Environ. Health Perspect.* 120 (5), 623–626. doi:10.1289/ehp.1104619

Jakubowski, M., Trzcinka-Ochocka, M., Hałatek, T., Raźniewska, G., and Szymczak, W. (2002). Integrated indexes of occupational exposure as predictors of kidney dysfunction. *Int. J. Occup. Med. Environ. Health* 15 (4), 393–399.

Jian, F. M., Yamaji, N., Mitani, N., Xu, X. Y., Su, Y. H., McGrath, S. P., et al. (2008). Transporters of arsenite in rice and their role in arsenic accumulation in rice grain. *Proc. Natl. Acad. Sci. U. S. A.* 105 (29), 9931–9935. doi:10.1073/pnas.0802361105

Kingdom, U. (1959). "Arsenic in food regulations," in *831, the minister of agriculture, F. A. F.* Editor T. M. o. Health (London: Her Majesty's Stationary Office).

Liang, F., Li, Y., Zhang, G., Tan, M., Lin, J., Liu, W., et al. (2010). Total and speciated arsenic levels in rice from China. *Food Addit. Contam. - Part A Chem. Analysis, Control, Expo. Risk Assess.* 27 (6), 810–816. doi:10.1080/19440041003636661

Liu, J., Li, K., Xu, J., Liang, J., Lu, X., Yang, J., et al. (2003). Interaction of Cd and five mineral nutrients for uptake and accumulation in different rice cultivars and genotypes. *Field Crops Res.* 83 (3), 271–281. doi:10.1016/s0378-4290(03)00077-7

Loebenstein, J. R. (1994). The materials flow of arsenic in the United States. *Bureau Mines Inf. Circular* 9382.

Masscheleyn, P. H., Delaune, R. D., and Patrick Jr, W. H. (1991). Effect of redox potential and pH on arsenic speciation and solubility in a contaminated soil. *Environ. Sci. Technol.* 25 (8), 1414–1419. doi:10.1021/es00020a008

Meacher, D. M., Menzel, D. B., Dillencourt, M. D., Bic, L. F., Schoof, R. A., Yost, L. J., et al. (2002). Estimation of multimedia inorganic arsenic intake in the U.S. population. *Hum. Ecol. Risk Assess.* 8 (7), 1697–1721. doi:10.1080/20028091057565

Mikkelsen, R. L., Mikkelsen, D. S., and Abshahi, A. (1989). Effects of soil flooding on selenium transformations and accumulation by rice. *Soil Sci. Soc. Am. J.* 53 (1), 122–127. doi:10.2136/sssaj1989.03615995005300010023x

Montgomery, D. C. (2009) *Design and analysis of experiments*. Hoboken, New Jersey, United States: John Wiley and Sons.

Moore, P. A., Jr., and Patrick, Jr. W. H. (1991). Aluminium, boron and molybdenum availability and uptake by rice in acid sulfate soils. *Plant Soil* 136, 171–181. doi:10.1007/bf02150048

Navarro-Alarcon, M., and Cabrera-Vique, C. (2008). Selenium in food and the human body: a review. *Sci. Total Environ.* 400 (1-3), 115–141. doi:10.1016/j.scitotenv.2008.06.024

Norton, G. J., Duan, G., Dasgupta, T., Islam, M. R., Lei, M., Zhu, Y., et al. (2009). Environmental and genetic control of arsenic accumulation and speciation in rice grain: comparing a range of common cultivars grown in contaminated sites across Bangladesh, China, and India. *Environ. Sci. Technol.* 43 (21), 8381–8386. doi:10.1021/es901844q

Norton, G. J., Duan, G. L., Lei, M., Zhu, Y. G., Meharg, A. A., and Price, A. H. (2012). Identification of quantitative trait loci for rice grain element composition on an arsenic impacted soil: influence of flowering time on genetic loci. *Ann. Appl. Biol.* 161 (1), 46–56. doi:10.1111/j.1744-7348.2012.00549.x

Pillai, T. R. (2009) *Variability of grain arsenic concentration and speciation in rice (Oryza sative)*. College Station, TX: Texas A&M University.

Pillai, T. R., Yan, W., Agrama, H. A., James, W. D., Ibrahim, A. M. H., McClung, A. M., et al. (2010). Total grain-arsenic and arsenic-species concentrations in diverse rice cultivars under flooded conditions. *Crop Sci.* 50 (5), 2065–2075. doi:10.2135/cropsci2009.10.0568

Premarathna, L., McLaughlin, M. J., Kirby, J. K., Hettiarachchi, G. M., Stacey, S., and Chittleborough, D. J. (2012). Selenate-enriched urea granules are a highly effective fertilizer for selenium biofortification of paddy rice grain. *J. Agric. Food Chem.* 60 (23), 6037–6044. doi:10.1021/jf3005788

Rout, G. R., and Das, P. (2002). Rapid hydroponic screening for molybdenum tolerance in rice through morphological and biochemical analysis. *Rostl. Vyroba* 48 (11), 505–512. doi:10.17221/4404-pse

Somenahally, A. C., Hollister, E. B., Yan, W., Gentry, T. J., and Loeppert, R. H. (2011). Water management impacts on arsenic speciation and iron-reducing bacteria in contrasting rice-rhizosphere compartments. *Environ. Sci. Technol.* 45 (19), 8328–8335. doi:10.1021/es2012403

Topaldemir, H., Tas, B., Yüksel, B., and Ustaoglu, F. (2023). Potentially hazardous elements in sediments and Ceratophyllum demersum: an ecotoxicological risk assessment in Miliç Wetland, Samsun, Türkiye. *Environ. Sci. Pollut. Res.* 30, 26397–26416. doi:10.1007/s11356-022-23937-2

Wang, Y., Morin, G., Ona-Nguema, G., Juillot, F., Calas, G., and Brown, G. E. (2011). Distinctive arsenic(V) trapping modes by magnetite nanoparticles induced by different sorption processes. *Environ. Sci. Technol.* 45 (17), 7258–7266. doi:10.1021/es200299f

WHO (2008). "Guidelines for drinking-water quality," in *Incorporating the first and second addenda* (Geneva: World Health Organization).

Williams, P. N., Price, A. H., Raab, A., Hossain, S. A., Feldmann, J., and Meharg, A. A. (2005). Variation in arsenic speciation and concentration in paddy rice related to dietary exposure. *Environ. Sci. Technol.* 39 (15), 5531–5540. doi:10.1021/es0502324

Williams, P. N., Raab, A., Feldmann, J., and Meharg, A. A. (2007). Market basket survey shows elevated levels of as in South Central U.S. processed rice compared to California: consequences for human dietary exposure. *Environ. Sci. Technol.* 406 (7), 2178–2183. doi:10.1021/es061489k

Xie, Z. M., and Huang, C. Y. (1998). Control of arsenic toxicity in rice plants grown on an arsenic-polluted paddy soil. *Commun. Soil Sci. Plant Analysis* 29 (15-16), 2471–2477. doi:10.1080/00103629809370125

Yan, W., Agrama, H. A., Slaton, N. A., and Gibbons, J. W. (2008). Soil and plant minerals associated with rice straighthead disorder induced by arsenic. *Agron. J.* 100 (6), 1655–1661. doi:10.2134/agronj2008.0108

Yan, W., Dilday, R. H., Tai, T. H., Gibbons, J. W., McNew, R. W., and Rutger, J. N. (2005). Differential response of rice germplasm to straighthead induced by arsenic. *Crop Sci.* 45 (4), 1223–1228. doi:10.2135/cropsci2004.0348

Yan, W., and McClung, A. M. (2010). 'Rondo', a long-grain *indica* rice with resistances to multiple diseases. *J. Plant Registrations* 4 (2), 131–136. doi:10.3198/jpr2009.07.0404crc

Yüksel, B., Ustaoğlu, F., Yazman, M. M., Şeker, M. E., and Öncü, T. (2023). Exposure to potentially toxic elements through ingestion of canned non-alcoholic drinks sold in Istanbul, Türkiye: a health risk assessment study. *Food Compos. Analysis* 121, 105361. doi:10.1016/j.jfca.2023.105361

Zhang, J., Zhu, Y. G., Cheng, W. D., Qian, Q., and Duan, G. L. (2008). Mapping quantitative trait loci associated with arsenic accumulation in rice (Oryza sativa). *New Phytol.* 177 (2), 350–355. doi:10.1111/j.1469-8137.2007.02267.x

Zhu, Y. G., Pilon-Smits, E. A. H., Zhao, F. J., Williams, P. N., and Meharg, A. A. (2009). Selenium in higher plants: understanding mechanisms for biofortification and phytoremediation. *Trends Plant Sci.* 14 (8), 436–442. doi:10.1016/j.tplants.2009.06.006

frontiers | Frontiers in Environmental Science

TYPE Original Research
PUBLISHED 17 June 2024
DOI 10.3389/fenvs.2024.1393609

OPEN ACCESS

EDITED BY
Weichun Yang,
Central South University, China

REVIEWED BY
Ying-heng Fei,
Guangzhou University, China
Qi Wang,
Zhejiang Gongshang University, China

*CORRESPONDENCE
Jiyan Shi,
shijiyan@zju.edu.cn

RECEIVED 29 February 2024
ACCEPTED 09 May 2024
PUBLISHED 17 June 2024

CITATION
Pan S, Tong J, Luo Y, Pang J, Zhang H, Wang J and Shi J (2024), Synergy of carboxymethyl cellulose stabilized nanoscale zero-valent iron and *Penicillium oxalicum* SL2 to remediate Cr(VI) contaminated site soil.
Front. Environ. Sci. 12:1393609.
doi: 10.3389/fenvs.2024.1393609

Synergy of carboxymethyl cellulose stabilized nanoscale zero-valent iron and *Penicillium oxalicum* SL2 to remediate Cr(VI) contaminated site soil

Siyi Pan, Jianhao Tong, Yating Luo, Jingli Pang, Haonan Zhang, Jing Wang and Jiyan Shi*

Department of Environmental Engineering, College of Environmental and Resource Science, Zhejiang University, Hangzhou, China

Nano zero-valent iron (nZVI) acting as a high-cost disposable material in soil Cr(VI) remediation faces significant challenges due to its easily oxidizable nature and biological toxicity. In addressing this issue, the present study undertook the synthesis of a series of modified nZVI and combined the selected material with Cr(VI)-resistant filamentous fungus *Penicillium oxalicum* SL2 for real-site chromium pollution remediation. Adsorption experiments demonstrated that the inclusion of carboxymethyl cellulose (CMC) significantly enhanced the adsorption capacity of nZVI for Cr(VI) by 19.3% (from 73.25 to 87.4 mg/L), surpassing both biochar (37.42 mg/L) and bentonite modified nZVI (48.03 mg/L). Characterization results validated the successful synthesis of the nano composite material. Besides, oxidative stress analysis explained the unique detoxification effects of CMC on SL2, acting as a free radical scavenger and isolating layer. In real-sites soil remediation experiments, a low dosage (0.4% w/w) of nZVI/CMC@SL2 (CMC modified nZVI combined with SL2) exhibited an impressive reduction of over 99.5% in TCLP-Cr(VI) and completely transformed 18% of unstable Cr to stable forms. Notably, nZVI/CMC demonstrated its capability to facilitate SL2 colonization in highly contaminated soil and modulate the microbial community structure, enriching chromium-removing microorganisms. In summary, the synergistic system of nZVI/CMC@SL2 merges as a cost-effective and efficient approach for Cr(VI) reduction, providing meaningful insights for its application in the remediating contaminated site soils.

KEYWORDS

nZVI stabilization, carboxymethyl cellulose, Cr(VI) reduction, soil microcommunity, *Penicillium oxalicum* SL2

1 Introduction

The extensive use of chromium in industrial processes, such as electroplating, chromate production, and leather tanning (Ma et al., 2024), due to its excellent corrosion resistance and metallic luster, has resulted in its widespread release into the soil. China's 2014 nationwide soil pollution survey revealed a 1.1% excess of Cr pollution beyond national standards, with particularly severe cases in industrial zones. Recognized as a class "A" carcinogen by the United States Environmental Protection Agency (EPA) (Chen et al.,

2020) hexavalent chromium poses severe health risks through long-term exposure and food chain transmission which will cause great harm to human health and cause various diseases (Fu et al., 2023). Therefore, the urgent remediation of Cr(VI) contaminated site soil is imperative.

The main remediation method involves reducing Cr(VI) to Cr(III) (Du et al., 2023; Wang et al., 2024). Recently, because of its high reactivity and reduction capability, nano zero-valent iron (nZVI) has gained widespread use in research focusing on the remediation of Cr(VI) contaminated soil (Yang et al., 2021). However, its application potential is greatly hindered by challenges such as aggregation (Phenrat et al., 2007) and biotoxicity (Auffan et al., 2008; Ye et al., 2021). To address these issues, numerous studies have been conducted based on the surface modification of nZVI such as biochar (Su et al., 2016), chitosan (Liu et al., 2010), hydrophobic stabilizers such as carboxymethyl cellulose (CMC) (Raychoudhury et al., 2012), poly acrylic acid (Laumann et al., 2014) or starch (Wang et al., 2014). These materials can impede the gathering and oxidation of nZVI (Ambika et al., 2016), mitigate its biotoxicity (Chen et al., 2012) and enhance particle mobility in the soil (Chekli et al., 2016). However, the application dosages of these materials were often relatively high (Supplementary Table S1), leading to elevated remediation costs and potential alterations to the original physicochemical properties of the soil. Therefore, the identification of a low-dosage, efficient, and environmentally friendly remediation strategy is of paramount importance.

Beyond chemical remediation approaches, microbial remediation, regarded as an environmentally sustainable and economically feasible method for soil contamination control is extensively researched. Certain bacteria, including QY-1, extremely thermophilic bacterium *(Caldicellulosiruptor saccharolyticus)*, *Shewanella oneidensis* MR-1 as well as sulfate-reducing bacteria (SRB) and iron reducing bacteria (IRB) (Peng et al., 2015; Bai et al., 2018; Hou et al., 2020; Ma et al., 2021; Lin et al., 2022) exhibited ability of Cr(VI) reduction. Bacteria can mitigate the toxicity of heavy metals through various mechanisms such as enzymatic detoxification and intracellular isolation (Bruins et al., 2000), *etc.* There are also studies that amalgamate bacteria with nZVI to address chromium contamination (Tan et al., 2020). Nevertheless, their tolerance to Cr(VI) are relatively lower, such as *Arthrobacter* sp., *Bacillus* sp. and *Streptomyces* sp. (Megharaj et al., 2003; Elangovan et al., 2006; Morales et al., 2007) (Minimum Inhibitory Concentration range, MIC, range from 80 to 500 mg/L), the survival and remediation capabilities in actual highly contaminated site soil remain ambiguous. Contaminated site soil, characterized by diverse and elevated heavy metal concentrations (Wu et al., 2018; Sun et al., 2022) and limited organic matter, imposes constraints on microbial growth, underscoring the critical importance of identifying suitable microorganisms.

Fungi, despite demonstrating high tolerance to heavy metals and thriving in low-nutrient environments (Chen et al., 2020), have received comparatively less attention in remediation studies. *Penicillium oxalicum* SL2, a filamentous fungus with high resistance to Cr(VI) (MIC greater than 1,000 mg/L Cr(VI)), was isolated in our antecedent study (Long et al., 2018), it could grow rapidly and completely remove 96.1 mg/L Cr(VI) in electroplating wastewater after inoculation for 96 h. Strain SL2 produced acidic metabolites such as LMWOAs playing important role in the mobilization of chromium and improving bioleaching (Long et al., 2023). Its mechanisms for heavy metal pollution abatement encompass the production of small organic acids, extracellular absorption, bioprecipitation, and transmembrane transport (Tong et al., 2023). Moreover, SL2 exhibited marked iron precipitate and Fe(II) regeneration capabilities, rendering its amalgamation with nZVI a promising avenue for remediation.

To the best of our knowledge, there is currently no study on the combination of nZVI/CMC and anti-chromium fungus SL2 for the remediation of high Cr(VI) polluted sites soil (Cr(VI) ranging from 348 to 1,305 mg/kg) (Li et al., 2023). Moreover, previous studies often simulated pollution with lower Cr(VI) concentrations (Supplementary Table S1), significantly differing from the complex conditions found in real contaminated soils. Hence, the overall objective of this study was to demonstrate the effect and practicability of the integrate remediation of Cr(VI) polluted site soil by using the stabilized nZVI with SL2. Consequently, this study is specifically structured as follows: (1) synthesize various stabilized nZVI composites and determine their efficacy in removing Cr(VI) in liquid; (2) investigate the biocompatibility of stabilized nZVI with SL2 for Cr(VI) removal from aqueous solutions and determinate the optimal combination; (3) explore the detoxification effect and immobilization of Cr(VI) in soil by the developed composite system consisting of nZVI/CMC and microorganism and elucidating their potential mechanisms; (4) evaluate the impact of these materials on soil microecology. This study aims to provide a scientific basis and technological support for the practical application of nZVI/CMC@SL2 in the remediation of Cr(VI) contaminated site soil.

2 Materials and methods

2.1 Preparation of stabilized nZVI

The sample was prepared by sieving pine powder through a 100-mesh, washed with deionized water to remove impurities, and subsequently dried. Under the protection of nitrogen gas, it underwent thermal decomposition at a heating rate of 10°C/min until reaching 600°C for a duration of 2 h, resulting in the sample referred to as C. A solution containing 5.40 g $FeCl_3{\cdot}H_2O$ dissolved in 100 mL oxygen-free water with 30% anhydrous ethanol was prepared. Different loading materials and concentrations of nano zero-valent iron (nZVI) were synthesized by adding 1% carboxymethyl cellulose (CMC), varying quantities of biochar or bentonite. The solute mixture was thoroughly mixed by shaking at room temperature and at a speed of 150 r/min for 24 h. Subsequently, under a nitrogen atmosphere, sodium borohydride ($NaBH_4$) weighing 3.04 g was slowly added dropwise into the above mixture to form nZVI stabilized by CMC, biochar or bentonite (Supplementary Text S1 and Figure S1), named as nZVI/CMC, nZVI/C, nZVI/B, respectively.

2.2 Adsorption experiments and material characterization

To assess the removal efficiency of stabilized nZVI for Cr(VI) in aqueous solution, a concentration of 2 g/L of the aforementioned material was added to a solution containing Cr(VI) with an initial concentration of 200 mg/L. The reaction was conducted in a reactor operating at a rotation speed of 150 rpm and a temperature of 25°C for a duration of 72 h. Supernatant was regularly collected and

filtered through a 0.22 μm filter. The concentration of Cr(VI) in the filtrate was determined by employing the diphenyl-carbohydrazide spectrophotometric method. Subsequently, several stable materials with the best effect were selected to establish isothermal adsorption experiments with initial concentration gradients of 10, 20, 50, 100, 200, 400, and 800 mg/L for Cr(VI). Various kinetic models, including the pseudo-first-order model, pseudo-second-order model, Avrami model and intraparticle diffusion model were employed to fit the adsorption process of Cr(VI), along with adsorption isotherm models such as Langmuir, Freundlich and Sips models.

The microstructure of synthesized materials above was imaged by scanning electron microscopy (SEM, Zeiss Sigma500). Also, the products were analyzed by X-ray diffraction (XRD, D8 Advance, Bruker, U.S.A) and data were collected the 2θ range from 10 to 90°. The functional groups on the surface of the materials were characterized by Fourier Transform Infrared Spectroscopy (FTIR, Thermo Scientific Nicolet iS20). In addition, the species of Cr and Fe on the surface of reaction products were analyzed by X-ray photoelectron spectroscopy (XPS, Escalab 250Xi, UK).

2.3 Metabolic activity of SL2 suffering from nZVIs and Cr(VI)

To assess the oxidative stress response of SL2 to stable nZVI, 1% spore SL2 suspension (10^7 CFU/mL) and 1 g/L different materials (nZVI/B was not measured because of the poor growth of SL2) were introduced into Cr(VI) solution. The mixture was incubated in a shaker at 30°C and 150 rpm for 2 days. After centrifugation, the collected bacterial slurry was analyzed for intracellular ATP, reactive oxygen species (ROS), and glutathione (GSH) levels (Supplementary Text S2) as indicators of the oxidative stress reaction.

2.4 Remediation of site soil by nZVI/CMC@SL2

2.4.1 Soil preparation and experimental design

Cr(VI) polluted soil samples were collected from a chromium slag dump site in Inner Mongolia (NM), and an electroplating contamination site in Zhangjiakou, Hebei Province (soil sample with higher and lower Cr(VI) pollution was named ZH and ZL respectively), China. After removing larger impurities, the soil was sieved through a 10-mesh screen, thoroughly mixed, and air-dried, referred to as NM, ZH and ZL, respectively. Soil heavy metal concentration and physicochemical characteristics were shown in Supplementary Tables S2, S3. Candidate nZVI/CMC, exhibiting optimal performance, was chosen for soil remediation. 20 g contaminated soil was treated with a 0.4% (w/w) nZVI/CMC addition, 10^7 CFU/g soil of SL2, and deionized water to maintain a 25% moisture level, 25°C. Five treatments were set for each soil sample, carried out in triplicate: (1) Control Check; (2) sterile potato dextrose liquid medium (1:4; PDL:H_2O; v/v); (3) PDL + SL2; (4) nZVI/CMC; (5) PDL + nZVI/CMC@SL2. The soil and additives were thoroughly mixed. Samples were collected on days 0, 3, 7, 15, and 30 (Supplementary Figure S2).

2.4.2 Chemical stability of Cr in the soil after remediation

Analysis of five different chromium species in soil was performed using the Tessier sequential extraction method. The extraction solution was filtered through a 0.45 μm membrane and analyzed using an atomic absorption spectrometer. Additionally, total Cr(VI) in the soil was measured using an alkaline extraction method, leachable Cr(VI) using the TCLP extraction method and Fe(II) concentrations was determined using colorimetric method with 1,10-o-phenanthroline. Detailed extraction and measurement methods can be found in the Supplementary Text S3.

2.4.3 Soil microecology analysis

Fresh soil samples were collected from each pot to evaluate the soil microecology—SL2 microbial counts (Supplementary Text S4) and microbial community.

Soil genomic DNA was extracted using E.Z.N.A. Soil DNA Kit (Omega Bio-tek, Inc., United States) following the manual. Concentration and quality of the genomic DNA were checked by NanoDrop 2000 spectrophotometer (Thermo Scientific Inc., United States). The fungal ITS region and the bacterial 16S rRNA genes were amplified using the primer sets ITS1F/ITS2R and 338F/806R (Yao et al., 2017; Tang et al., 2018) respectively by PCR system (Applied Biosystems, Inc., United States). The amplicons were sequenced through the Illumina's Miseq PE300 platform (Illumina, Inc., United States). Qualified sequences were clustered into operational taxonomic units (OTUs) at a similarity threshold of 97% use Uparse (Edgar, 2013) algorithm of Vsearch (v2.7.1) software. Refer to Supplementary Text S5 for detailed analytical methods.

3 Results and discussion

3.1 Adsorption performance of different stabilized nZVI

3.1.1 Adsorption kinetics

In order to examine the correlation between contact time and the rate of reduction of Cr(VI) by different materials, kinetics investigations were performed with results presented in Figure 1. It could be noticed that Cr(VI) uptake increased within the initial 240 min, which might be attribute to the plentiful adsorption sites provided by the loading material and the reduction reaction of nZVI to Cr(VI). Nonetheless, with the gradual occupation of adsorption sites by Cr(VI), the rate of pollutant adsorption increased at a slower pace, reaching equilibrium after 500 min.

To quantitatively evaluate the kinetic process on Cr(VI) uptake by stabilized nZVI, four acknowledged models involving pseudo-first/second-order, Avrami fractional-order as well as intra-particle diffusion models were chosen to analyze the data (Dai et al., 2019; Qu et al., 2021; Qu et al., 2022), the formulas were shown below (Eqs 1-4):

$$q_t = q_e\left(1 - e^{-k_1 t}\right) \quad (1)$$

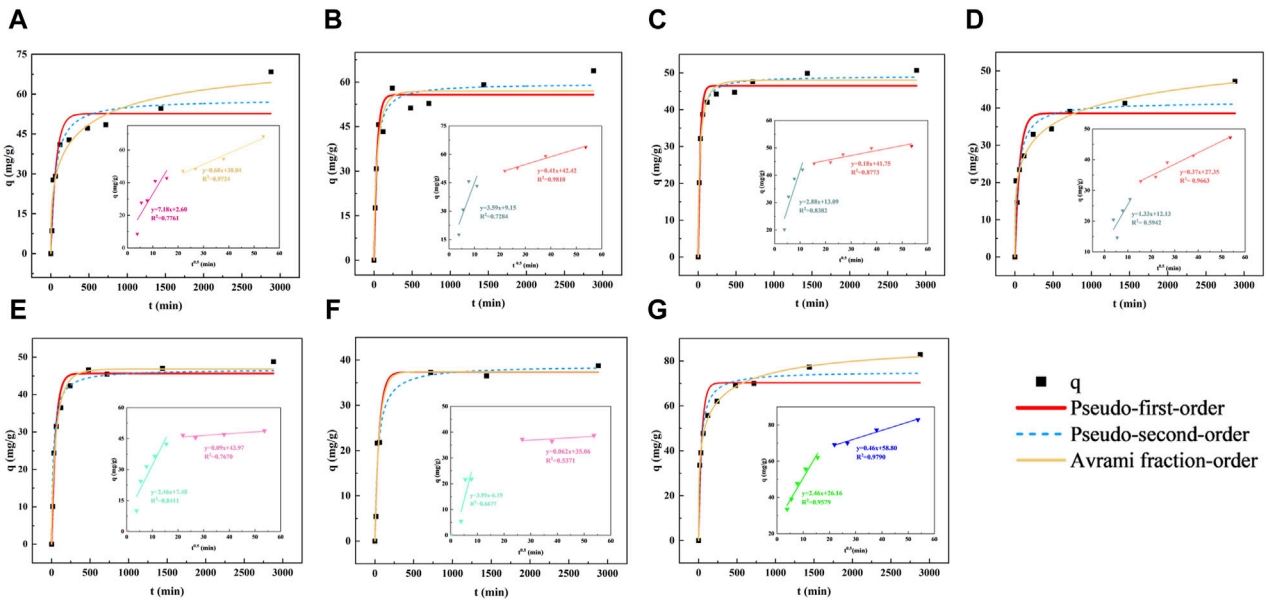

FIGURE 1
Kinetic fitting results of pseudo first-order, second-order and Avrami fractional models for Cr(VI) uptake onto stabilized nZVI (inset: intraparticle diffusion model).**(A)** nZVI; **(B–D)** nZVI/B with ratio of 1:2, 1:1, 2:1; **(E, F)** nZVI/C with ratio of 1:1, 1:2; **(G)** nZVI/CMC, T = 25°C, [Cr(VI)] = 200 mg/L, [Material dosage] = 2 g/L.

TABLE 1 Kinetic model parameters for the uptake of Cr(VI) onto stabilized nZVI.

Material	Pseudo-first-order model				Pseudo-second-order model			Avrami fractional-order model					
	q_e (mg/g)	k_1 (min^{-1})	R^2	SD	q_e (mg/g)	k_2 (g mg^{-1} min^{-1})	R^2	SD	q_e (mg/g)	k_3 (min^{-1})	n	R^2	SD
nZVI	52.65	0.0146	0.8822	3.50	58.07	0.0003	0.9297	3.47	73.25	0.0025	0.3771	0.9452	21.29
nZVI/C(1:1)	45.65	0.0192	0.9755	1.25	46.75	0.0008	0.9290	0.05	46.81	0.0166	0.7340	0.9842	1.27
nZVI/C(2:1)	37.36	0.0182	0.9599	1.98	38.77	0.0006	0.9622	2.12	37.42	0.0175	0.9116	0.9605	2.20
nZVI/B(1:1)	55.72	0.0249	0.9432	2.20	59.51	0.0005	0.9596	2.24	56.99	0.0220	0.7242	0.9505	2.57
nZVI/B(1:2)	46.51	0.0358	0.9730	1.14	49.13	0.0011	0.9904	0.80	48.03	0.0318	0.5992	0.9826	1.24
nZVI/B(2:1)	38.60	0.0162	0.8281	2.81	41.67	0.0005	0.9033	2.59	61.38	0.0012	0.2865	0.9733	25.70
nZVI/CMC	70.28	0.0244	0.8949	3.66	75.30	0.0004	0.9615	2.67	87.42	0.0076	0.3284	0.9981	3.02

$$q_t = \frac{q_e^2 k_2 t}{1 + q_e k_2 t} \quad (2)$$

$$q_t = q_e\left[1 - e^{-(k_3 t)^n}\right] \quad (3)$$

$$q_t = k_4 t^{1/2} + n \quad (4)$$

in which, q_t (mg/g) express the quantity of Cr(VI) taken up at time t; q_e (mg/g) represents the uptake of Cr(VI) adsorbed at equilibrium; kinetic constants associating with different models are k_1, k_2, k_3 and k_4. The n (mg/g) is the intercept of intraparticle diffusion model. Values of n give information about the thickness of the boundary layer, the larger intercept the greater is the boundary layer effect (Zhu et al., 2010).

Standard deviation (SD) and coefficient (R^2) were used to evaluate the suitability of each model, that was, data with lower SD and higher R^2 indicated superior applicability of the kinetic model. Detail fitting parameters were provided in Table 1. As shown, Avrami fractional-order model showed the highest R^2 value (0.9981) among these models, demonstrated to present the best appropriateness for depicting the uptake performance for Cr(VI), revealing that there were multiple kinetics during the binding processes of Cr(VI) onto nZVI/CMC (Qu et al., 2022). In addition, the R^2 (0.9615) of the pseudo-second-order is also higher than that of the pseudo-first-order model (0.8949), indicating that the rate-limiting step during the reaction was chemical adsorption involving electron exchange between adsorbent and adsorbate, rather than physical diffusion (Lyu et al., 2017). According to the intra-particle diffusion model consequences (insets of Figure 1G), two stages were involved in Cr(VI) uptake nZVI/CMC, intraparticle diffusion and external

surface binding. Besides, both of the fitting curves deviated from the base point (n = 26.16), which suggested that the intraparticle diffusion was not the rate-controlling step in Cr(VI) uptake process, but the boundary layer diffusion controlled the adsorption to some degree.

3.1.2 Adsorption isotherms

In order to investigate the effect of Cr(VI) concentration gradient on the adsorption capacity of stabilized nZVI, the interaction between them was quantitatively described using isothermal adsorption.

Three famous isotherm models including Langmuir, Freundlich and Sips models were then applied for fitting the uptake results (Eqs 5-7), which are expressed as:

$$q_e = \frac{q_{max} K_L C_e}{1 + K_L C_e} \tag{5}$$

$$q_e = K_F C_e^{1/n_F} \tag{6}$$

$$q_e = \frac{q_s (K_s C_e)^{m_s}}{1 + (K_s C_e)^{m_s}} \tag{7}$$

in which, the maximum adsorbing quantity of Cr(VI) represented by q_{max} (mg/g); K_L, K_F and n_F respectively involve the Langmuir coefficient, Freundlich coefficient and Freundlich intensity parameters; K_S and m_S are the identical Sips heterogeneity divisors.

In the Langmuir model, adsorption is considered to occur on homogeneous surface. Freundlich is an empirical model for heterogeneous systems. Sips model is a combination of Langmuir and Freundlich (Deng et al., 2020) capable of modeling both homogeneous and heterogeneous binding surfaces (Zhang et al., 2019). The results (Supplementary Figure S3; Supplementary Table S4) showed that the Sips model had the best fitting results (R^2 = 0.9302), which suggested that adsorption of Cr(VI) was a non-ideal sorption on heterogeneous (Tang et al., 2016).

In summary, the introduction of CMC significantly enhanced the removal efficiency of Cr(VI) by nZVI, for its maximum adsorption capacity of 87.42 mg/g, surpassing the performance of biochar and bentonite. Moreover, the process involved multiple kinetic mechanisms, with boundary layer diffusion identified as the primary rate-limiting step.

3.2 Characterizations of stabilized nZVI

The morphology and size of the newly prepared stabilized nZVI were characterized by scanning electron microscopy (SEM). As depicted in Figure 2A, individual particles of nZVI appeared irregularly spherical and had a diameter of approximately 50 nm. After stabilization, the nZVI was uniformly dispersed on the surface of the carriers. The CMC stabilized nZVI exhibited a reticular dendritic structure and smaller particle size, due to the significant influence of high-concentration CMC solution on the nucleation of nZVI. Throughout the nanoscale particle growth process, CMC molecules adhere to the particle surface, impeding further growth through electrostatic repulsion and steric hindrance (He and Zhao, 2007). This preservation of smaller particle sizes for nZVI results in higher reactivity in reactions. In the EDS maps, each material exhibited elevated levels of Fe element, along with characteristic elements of the loaded material, such as C, Si and Al, indicating successful loading of iron onto the material. It is noteworthy that the iron element content on the surface of nZVI/CMC (89.4%) is significantly higher than that of biochar (53.28%) and bentonite (20.21%). This characteristic enables better preservation of the nZVI properties and facilitates the reactivity towards Cr(VI) reduction. To elucidate the stabilization mechanisms and gain further insight into the various functional groups of the nanoparticles, XRD, FTIR and XPS measurements were carried out on stabilized nanoparticles. From XRD pattern, a distinctive peak corresponding to Fe (0) is observed at 2θ = 45° (Bian et al., 2021; Zhou et al., 2022). The broad peak signified the body-centered cubic (bcc) Fe (0) crystal lattice plane (110) (Lin et al., 2010) with a relatively poor crystallinity (Gong et al., 2017), providing further evidence of the presence of iron in the material in the form of zero-valent iron. The types of surface functional groups on the nanoparticles were qualitatively analyzed using FTIR spectroscopy, the characteristic broad peaks near 3,400 cm^{-1} related to the stretching vibration of -OH (Xu et al., 2020; Ji et al., 2022) were observed in all materials, potentially associated with iron hydroxides (Bian et al., 2021). Additionally, bands corresponding to C=O were identified in the range of 1,610–1,660 cm^{-1}, those acidic O-containing functional groups were reported to have a great effect on absorption and reduction of Cr(VI) (Wang K. et al., 2020). Particularly, nZVI/CMC revealed a carboxyl group (-COO) at 1,420 cm^{-1}, suggesting its role as one of the binding sites for Fe. To identify the carboxylate-metal complexation mechanism, the separation of the symmetric and asymmetric stretches [Δν = Δ(asym) − Δ(sym)] of the carboxylate group was calculated (Deng et al., 2021). In the present work, Δν was determined to be 189 cm^{-1} (1,615–1,426 cm^{-1}), proved that bidentate bridging was the primary mechanism for binding CMC molecules to Fe nanoparticles, same as the previous research (He et al., 2007; Lin et al., 2010). Simultaneously, polydentate ligands were commonly reported to possess stronger chelating affinities compared to monodentate ligands (Su and Puls, 2004), this structural characteristic enhanced the stability of nZVI/CMC, underlining the increased robustness conferred by the multidentate coordination in this complex. It is noteworthy that oxygen-containing functional groups in the materials, such as C=O, -OH and -COO may concurrently contribute electrons, thereby facilitating the reduction of Cr(VI) (Zhao et al., 2022). The implication is that the O functional groups may play a crucial role as electron transfer stations in the Cr-Fe reaction.

Further, XPS was performed for CMC-nZVI before and after Cr(VI) uptake (Figure 3). The XPS spectra before the reaction confirmed the presence of zero-valent iron in the material by a characteristic peak of Fe2p with a binding energy of 706.23 eV (Ren et al., 2018), accounting for 30.21%. Another portion of Fe, likely oxidized upon exposure to air during transportation and storage, formed Fe(II), constituting 69.79% (Yamashita and Hayes, 2008). After reaction, the peaks corresponding to Fe (0) and Fe(II) disappeared, and a characteristic satellite peak of Fe(III) emerged (Liu et al., 2020), indicating the complete oxidation of iron in the material to trivalent state. Additionally, the results of the Cr elemental partition spectra revealed that the Cr in the reaction

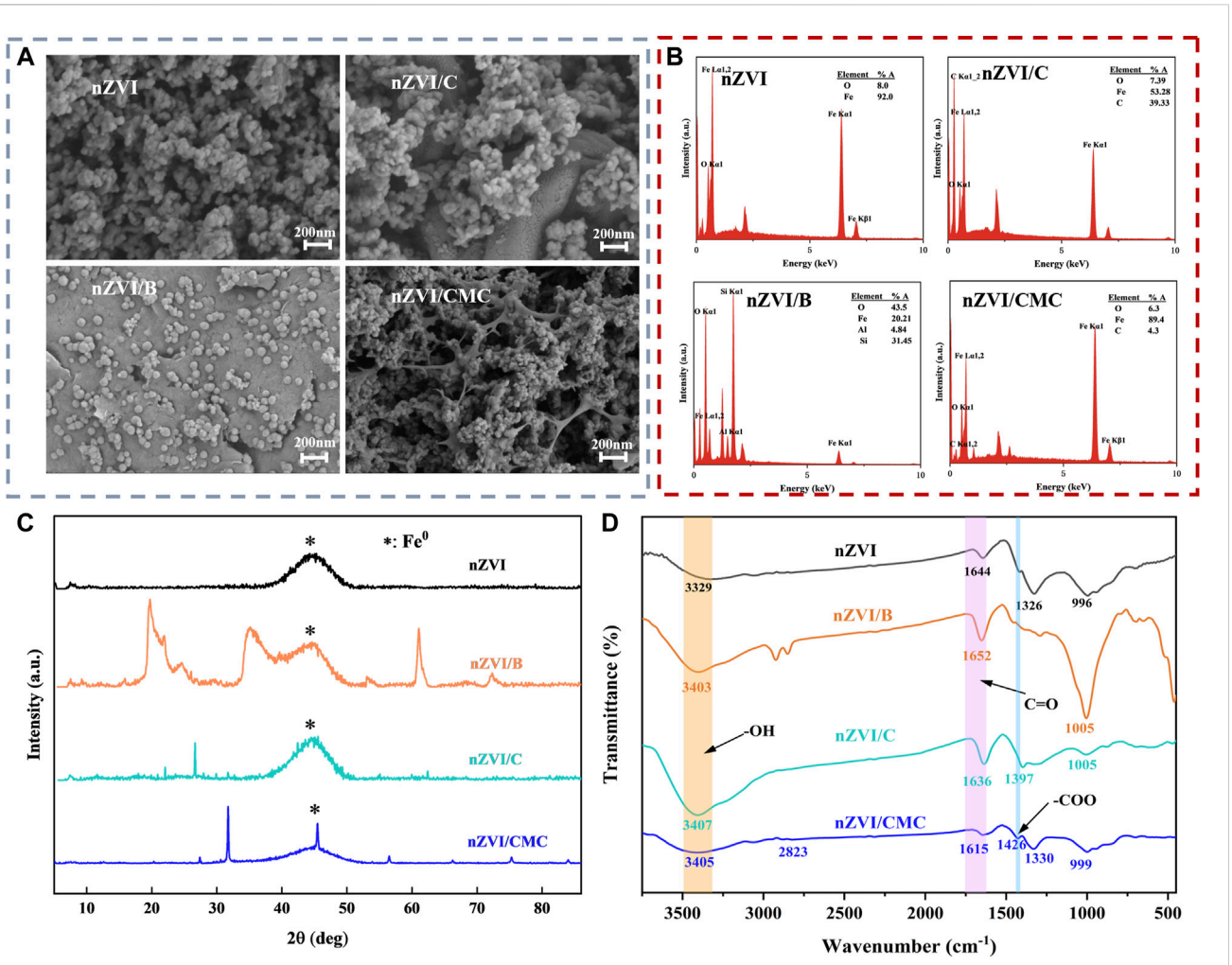

FIGURE 2
SEM **(A)**, EDS **(B)**, XRD **(C)**, FTIR **(D)** patterns of stabilized nZVI.

product existed mainly in the valence state of Cr(III), including chromium oxides and hydroxides. Therefore, both Fe (0) and Fe(II) in the material directly serve as electron donors for the reduction of Cr(VI) to Cr(III). Subsequently, these Cr(III) species co-precipitate with Fe^{3+}, forming $Cr_nFe_{1-n}(OH)_3$ (Pan et al., 2016; Ye et al., 2021). Moreover, upon contact with water, zero-valent iron generated H*, which was confirmed to be the predominant reactive species for Cr(VI) reduction (Qian et al., 2014). Besides, the abundant -OH and -C=O groups on CMC play a crucial role as electron donors for the reduction of Cr(VI) (Rajapaksha et al., 2018; Xu et al., 2019). In conclusion, the analysis confirmed that the removal of Cr(VI) by nZVI/CMC involved both adsorption and reduction processes, consistent with previous study (Fang et al., 2011).

In summary, the potential electrostatic repulsion and spatial hindrance capabilities of CMC contributed to maintaining the small size of nZVI particles, preventing its easy aggregation. Additionally, the combination of nZVI with CMC was achieved through a more stable bidentate bridging mechanism. Furthermore, it revealed that both Fe (0) and Fe(II) contributed to the reduction of Cr(VI), and the presence of oxygen-containing acidic functional groups suggested the potential for electron donation in the reduction of Cr(VI).

3.3 Mechanistic implications about CMC detoxifying

Through the assessment of intracellular ATP, GSH, and ROS concentrations, we compared the toxicity of nZVI with different stabilization methods on SL2. ATP, which is known to play a crucial role in cellular metabolism, and its concentration reflects the cellular activity (Tsitonaki et al., 2010; Wu et al., 2013). In the experimental group where only SL2 was added, the intracellular ATP content was highest, while the ATP levels significantly decreased in the groups with added materials, indicating a certain toxicity of the materials to SL2, affecting its metabolism. In comparison, the ATP content in the nZVI/CMC experimental group (0.5981 μmol/g) was higher than that in the nZVI (0.1655 μmol/g) and nZVI/C (0.2532 μmol/g) groups, suggesting that the encapsulation of CMC reduced the toxicity of nZVI to SL2.

nZVI exhibits considerable oxidative power in oxygen-containing water (Cheng et al., 2016). It can be oxidated to generate Fe(II) and H_2O_2 (Kim et al., 2011), followed by Fenton reaction to produce highly toxic ROS, such as ·OH and $\cdot O_2^-$ (Keenan and Sedlak, 2008; Xu et al., 2022). The reaction equations are as follows (Eqs 8-11):

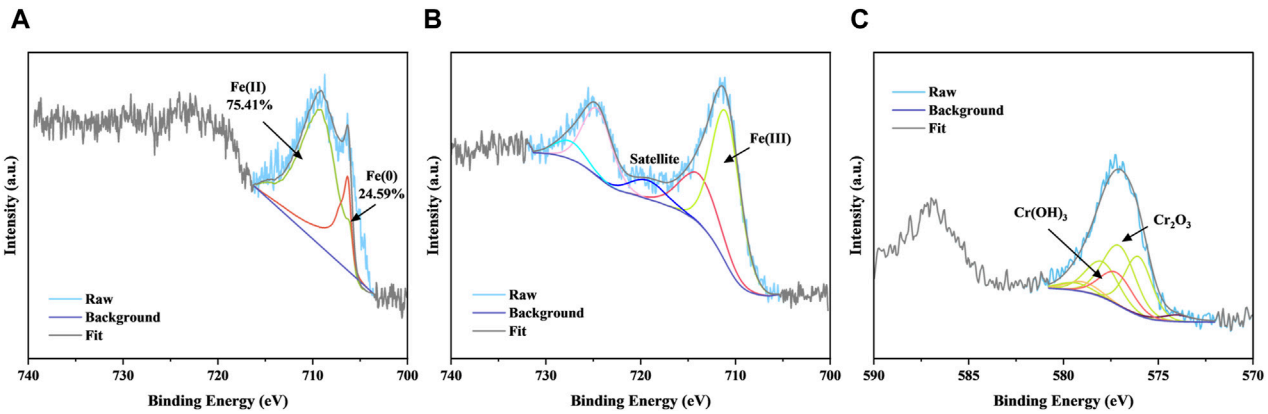

FIGURE 3
XPS spectra of Fe 2p **(A)** for fresh nZVI/CMC, Fe 2p **(B)** and Cr 2p **(C)** for product after Cr(VI) reduction. [Cr(VI)] = 200 mg/L, [nZVI/CMC] = 2 g/L, shanked at 150rpm for 24 h at 25°C.

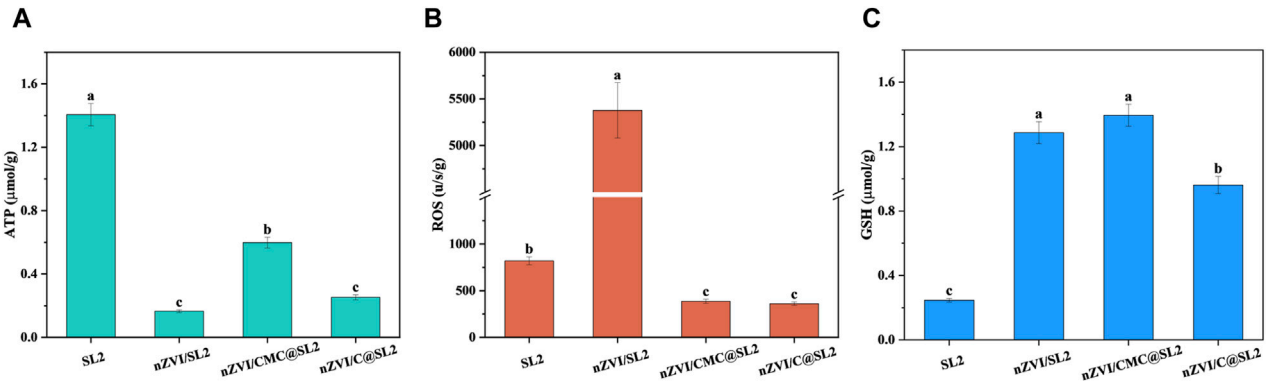

FIGURE 4
Intracellular levels of **(A)** ATP, **(B)** ROS, **(C)** GSH contents in SL2. Experimental conditions: [SL2] = 10^5 CFU/mL, [Cr(VI)] = 128 mg/L, [stabilized nZVI] = 1 g/L, 2 days.

$$Fe^0 + O_2 + 2H^+ \rightarrow Fe(II) + H_2O_2 \quad (8)$$

$$Fe^0 + H_2O_2 + 2H^+ \rightarrow Fe(II) + 2H_2O \quad (9)$$

$$Fe(II) + H_2O_2 \rightarrow Fe(III) + \cdot OH + 2OH^- \quad (10)$$

$$Fe(II) + O_2 \rightarrow Fe(III) + \cdot O_2^- \quad (11)$$

Typically, ROS produced at low frequencies are easily neutralized by antioxidant defenses (Nel et al., 2006). However, excessive ROS can overwhelm cellular antioxidant defenses, causing membrane damage (Xia et al., 2020), DNA fragmentation (Xia et al., 2019), and even cellular inactivation (Nel, 2005). Therefore, cellular oxidative stress responses were further investigated by assessing intracellular levels of ROS and GSH to elucidate the molecular mechanisms. As depicted in the Figure 4, the ROS content in the nZVI-treated group exhibited a dramatic increase (5376 u/s/g), surpassing that of other groups (819, 387 and 361 u/s/g respectively). This elevation suggested a potential dual effect: an increase in endogenous ROS production within the cells and a possible disruption of cell structures (Liu et al., 2011; Mao et al., 2019) allowing enhanced penetration of exogenous ROS (Li et al., 2022), leading to a substantial concentration surge. Simultaneously, the ROS content in the nZVI/CMC and nZVI/C remained comparatively lower, indicating a certain degree of mitigation of cellular oxidative stress reactions. From the perspective of GSH content, CMC-stabilized nZVI generated a significant amount of antioxidant enzymes to shield itself from external oxidation, thereby maintaining lower ROS levels. Although the nZVI-treated group also exhibited elevated GSH levels, it proved insufficient to eliminate the excessive intracellular ROS, resulting in an imbalance in the cellular redox state and compromising the cell's self-protective capacity.

Taken together, the results presented herein indicate a significant enhancement in surface reactivity after CMC-coating, accompanied by a concurrent reduction in the nanomaterial's toxicity towards SL2. This aligns with findings from previous studies conducted on *Escherichia coli* (Zhou et al., 2014). We hypothesize that the detoxifying effect of this CMC-coating can be attributed to three key factors: Firstly, its role as a scavenger of free radicals, leading to the substantial elimination of ·OH radicals (·OH + CMC → H_2O+ CMC*) (Joo and Zhao, 2008); Secondly, its ability to prevent direct contact between SL2 and nZVI particles (Dong et al., 2016), thereby mitigating oxidative stress reactions in

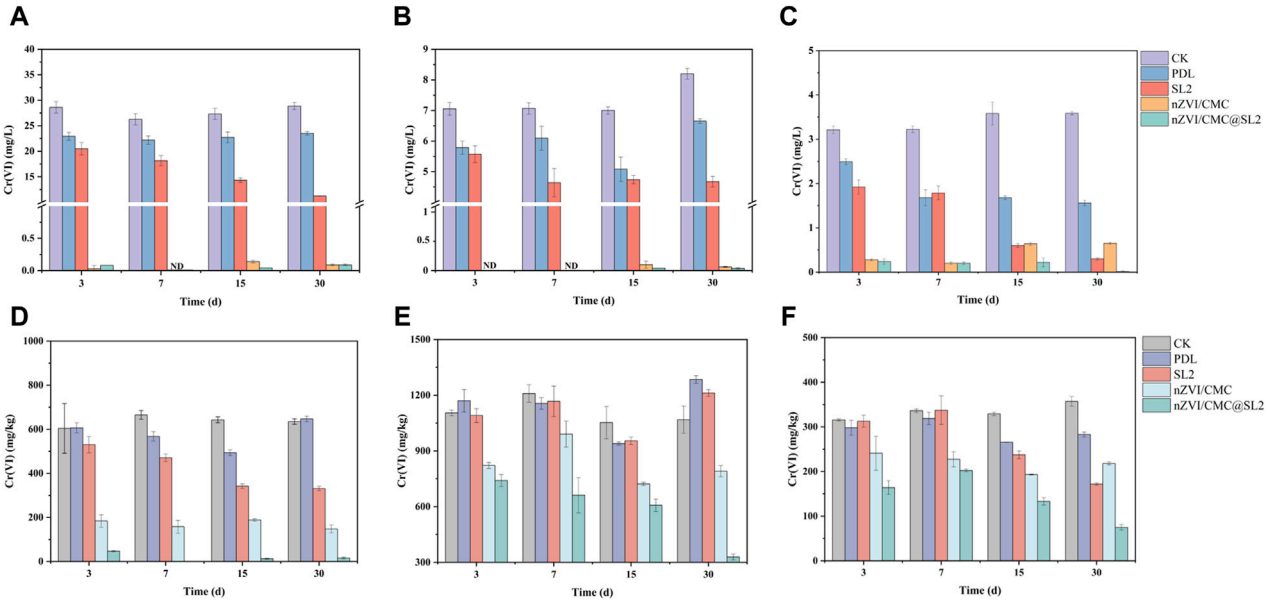

FIGURE 5
The TCLP **(A–C)** and total Cr(VI) **(D–F)** concentrations in different soils after diverse treatments, NM **(A, D)**, ZH **(B, E)**, ZL **(C, F)**.

cells and ensuring their viability; Thirdly, CMC can provide an organic carbon source for the growth of SL2 (Wang ZY. et al., 2020).

3.4 Soil remediation

In order to investigate the application potential of nZVI/CMC@SL2 in reducing Cr(VI) in soil, we conducted remediation experiments using soils from different types of contaminated sites. The TCLP method was employed to assess the leaching risk of Cr, and the changes in the total Cr(VI) content in the soil were also measured. As shown in Figure 5, after a 3-day remediation period, a significant reduction in TCLP-Cr(VI) was observed in soils amended with 0.4% nZVI/CMC. For NM, ZH, and ZL soils, the Cr(VI) concentration decreased from 28.6, 7.05, and 3.21 mg/L to less than 0.5 mg/L. However, a slight rebound was observed after 15 days, potentially attributed to the oxidation of ferrous species (Wang et al., 2023), leading to a loss of remediation capacity. Notably, the rebound was less pronounced in the presence of nZVI/CMC@SL2, indicating that the addition of SL2 could inhibit the oxidation of Cr(III). Furthermore, after 30-days remediation, the Fe(II) concentration in the nZVI/CMC@SL2 treatment group was significantly higher than in the group that only received nZVI/CMC (Figure 6). This observation indicated that SL2 could effectively facilitate the reduction of Fe(III) to Fe(II), thereby sustaining the reduction of Cr(VI). According to previous studies, oxalic acid was the most abundant LMWOA produced by strain SL2, and the affinity of oxalic acid with Cr(VI) leads to the expansion of Cr(VI) coordination from tetrahedron to hexahedron, which was preferable for hexahedral species of Cr(III). Oxalic acid was used as a substitute electron donor for Cr(VI) reduction through intramolecular electron transfer reaction, which significantly improved the Cr(VI) removal efficiency (Jiang et al., 2017). Furthermore, nZVI promoted oxalic acid secretion by SL2, and its generated iron ions could accelerate the reduction of Cr(VI) by oxalic acid (Hug et al., 1997). Studies have detected the formation of compounds containing Fe(II), Cr(V), and oxalate salts ($HCrFeC_4O_9$)(Luo et al., 2023), providing crucial evidence for the involvement of Fe(II)/Fe(III) cycling in organic acid reduction of Cr(VI). In the case of the reaction group with only SL2 added, the removal efficiency for Cr(VI) increased with prolonged incubation time within the 30-day period, suggesting that SL2 successfully colonized and persisted in the soil, continuously fixing Cr(VI) through biological processes, in accordance with SL2 biomass change (Supplementary Figure S4). For all nZVI/CMC@SL2 composite systems, the treatment groups achieved a removal efficiency of over 99.5% for TCLP-Cr(VI) after 30 days, and the TCLP-Cr(VI) was lower than the level IV standard of groundwater quality criterion in China (0.1 mg/L, GB/T 14848–2017). In addition, the total Cr(VI) in the NM soil decreased from over 600 mg/kg to 16 mg/kg, which was below the regulatory limit for Class I construction land specified in GB36600-2018 (30 mg/kg). In heavily contaminated soil (ZH, Figure 5E) with elevated concentrations of Cr(VI), the growth of SL2 was suboptimal due to the toxic effects of Cr(VI), therefore basically did not demonstrate any removal effectiveness against Cr(VI). However, with the addition of nZVI/CMC, the pollutant concentration was reduced to a level conducive to growth. This combination successfully decreased the total Cr(VI) content from around 1,200 mg/kg to approximately 300 mg/kg within a 30-day period.

This study evaluated sequential extraction procedures for identifying the relative availability of soil-bound heavy metal by partitioning the particulate trace metals into five fractions. The five species have been defined as exchangeable (F1), bound to carbonates (F2), Fe-Mn oxides-bound (F3), organic matter-bound (F4) and residual (F5). Figure 7 showed the transformation in chromium

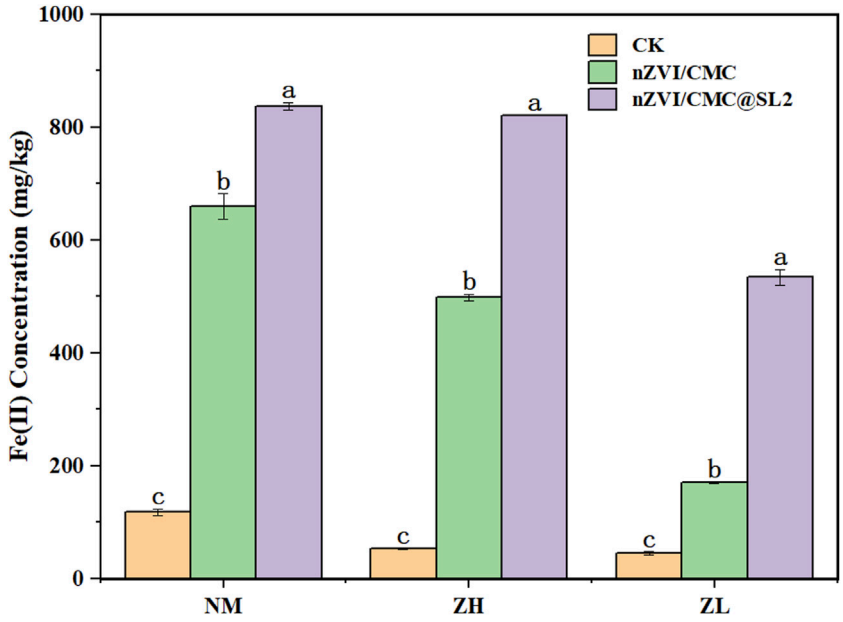

FIGURE 6
Fe(II) concentration in soil after 30-days remediation.

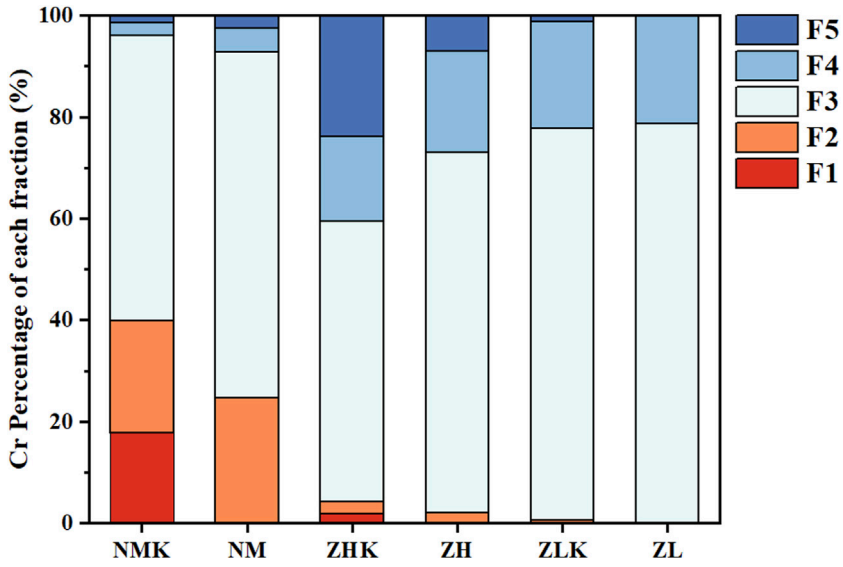

FIGURE 7
Soil Cr speciation after 30-days remediation with 0.4% nZVI/CMC@SL2. (Cr species: F1: exchangeable (EX); F2: carbonate bound (CB); F3: Fe-Mn oxide bound (OX); F4: organic matter bound (OM); F5: residual (RS); NMK and NM represented the control check and nZVI/CMC@SL2 treatment of NM soil, ZHK and ZH, ZLK and ZL were the same).

components in different treatment group which aligned with the earlier leaching results. After a 30-day treatment period, the exchangeable Cr content in all soils significantly decreased, undergoing transformation into Fe-Mn oxide-bound and the organic-bound forms. According to previous investigations, the elevated Fe-Mn oxides-bound fraction might be largely attributed to the precipitation of $Cr(OH)_3$ or Cr(III)/Fe(III) oxides/hydroxides ($Cr_nFe_{1-n}OOH$ and Cr_nFe_{1-n} $(OH)_3$) during the CMC-nZVI remediation (Manning et al., 2007). Specifically, 17.82% of exchangeable chromium in the NM soil was completely transformed into other more stable forms of Cr. According to Supplementary Figure S5, after 7 days of treatment, noticeable changes in pH were observed in the experimental groups. The group with the addition of nZVI/CMC exhibited the highest pH increase, rising from 8.70, 8.55, and 8.45 to 8.93, 8.72, and 8.70, respectively. This phenomenon may be attributed to the

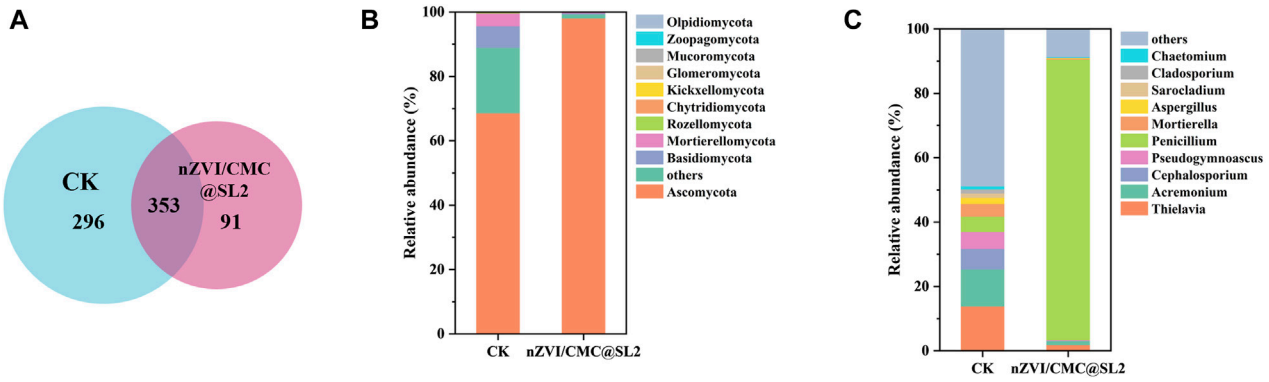

FIGURE 8
Venn diagram **(A)** based on OTU and microbial community structures (fungi) at the phylum **(B)** and genus **(C)** level of different treatments after 30-days.

alkaline nature of the material and the reduction of Cr(VI) acting in concert. In the experimental group with the addition of SL2, the pH initially showed a decline followed by an upward trend, gradually stabilizing. This suggested that SL2 proliferated extensively in the early stages, producing acidic substances, and later reached a stable state. Due to the natural buffering capacity of the complex soil system, the fluctuation range of pH during the remediation process remained relatively small.

In short, the results indicated the excellent stabilization and environmental adaptability of the nZVI/CMC@SL2 composite remediation system towards chromium. It promoted the conversion of more easily available Cr (EX and CB) to the less available (OX and OM) and thus reduce the toxic effect of Cr. Furthermore, SL2 possessed the ability to regenerate Fe(II), facilitating the sustained reduction of Cr(VI).

3.5 Microecology analysis

After 30 days of treatment, the quantity of SL2 in the nZVI/CMC@SL2 treatment group gradually stabilized and maintained at a high level (4.23×10^4 CFU/mL, Supplementary Figure S4). Microbial community analysis of the ZL soil revealed an average of 81,938 quality sequences and 740 OUTs generated from the ITS1 gene. The fungal community's similarities and differences were analyzed based on OTUs using a Venn diagram (Figure 8A). There were 353 shared OTUs, constituting 47.7% of the total observed OTUs (740), with 296 and 91 unique OUTs in the CK and treatment groups, respectively. This indicates that different treatments cultivated distinct microbial populations. Comparing with the CK, the treatment group exhibited a slight reduction in OUT levels, suggesting that this composite system could influence the fungal abundance in the soil. In terms of alpha diversity, both fungi and bacteria were significantly affected (Supplementary Table S6). In the CK group, the three most abundant fungi were *Ascomycota* (68.66%), *Basidiomycota* (6.65%), and *Mortierellomycota* (4.03%). In the experimental group, the relative abundance of *Ascomycota* surged to 98.09%. As SL2 belongs to *Ascomycota*, its relative abundance increased from 4.75% to 87.18% at genus level, further confirming the successful colonization of SL2 in the soil and its competition with indigenous microorganisms to become the dominant strain (Figure 8). Looking at the bacterial community (Supplementary Figure S6), there was a significant increase in the relative abundance of *Proteobacteria* and *Firmicutes*, rising from 38.70% to 10.68%–55.84% and 35.47%, respectively. Meanwhile, *Actinobacteria* decreased substantially (38.66%–7.35%). *Proteobacteria* was often found as a dominant species in chromium-contaminated soil (Desai et al., 2009), with *Bacillus* within this phylum known to possess Cr(VI) reductase activity, capable of resisting and reducing high concentrations of Cr(VI) (Elangovan et al., 2006; Desai et al., 2008). *Firmicutes* harbored various heavy metal resistance genes, exhibiting stronger adaptability to heavy metal-polluted environments. Also, they are reported typically to be Fe(III)-reducing bacteria (FeRB)(Jin et al., 2023), thus regenerating Fe(II) and reduce Cr(VI).

In conclusion, the nZVI/CMC@SL2 composite system enabled the successful colonization of SL2 in soils highly contaminated with Cr(VI). It demonstrates the ability to enrich chromium-tolerant and chromium-removing microorganisms, thereby promoting the reduction of Cr(VI).

4 Conclusion

In this study, nano zero-valent iron (nZVI) stabilized in different ways were successfully prepared and compared. Specifically, nZVI/CMC not only efficiently removed Cr(VI) but also exhibited a detoxification effect on SL2. The heightened reactivity towards Cr(VI) can be attributed to the smaller size of the nano particles and the abundant oxygen-containing acidic groups in CMC. The detoxification effect may result from its identity as a free radical scavenger and the direct isolation achieved through CMC-coating. Furthermore, this combination of nZVI/CMC and SL2 for the stabilization of Cr(VI) in actual contaminated site soil was successfully applied, and through multiple perspectives such as leaching risk, chemical speciation changes, and soil microecology, we revealed the composite system's application potential in soil remediation. In conclusion, the chemical-fungal composite system of nZVI/CMC@SL2 explored in this study offers a novel approach for the remediation of highly contaminated Cr(VI) site soil. However, the

mechanism by which SL2 reduces Fe(III) and the long-term stability of the nZVI/CMC@SL2 composite system remain unclear. It is recommended to delve deeper into the reduction mechanism in future research and conduct studies at field scales and real heavy metal-contaminated sites for a more comprehensive understanding.

Data availability statement

The datasets presented in this study can be found in online repositories. The names of the repository/repositories and accession number(s) can be found below: https://www.ncbi.nlm.nih.gov/bioproject/, accession number PRJNA1117622.

Author contributions

SP: Writing–review and editing, Writing–original draft, Visualization, Methodology, Investigation, Formal Analysis, Data curation, Conceptualization. JT: Writing–review and editing, Supervision, Methodology, Investigation, Formal Analysis. YL: Writing–review and editing, Methodology, Investigation, Formal Analysis. JP: Writing–review and editing, Supervision, Software. HZ: Writing–review and editing, Visualization, Resources. JW: Writing–review and editing, Visualization, Data curation. JS: Writing–review and editing, Supervision, Project administration, Funding acquisition.

Funding

The author(s) declare that financial support was received for the research, authorship, and/or publication of this article. This research was supported by the National Natural Science Foundation of China (42277004) and the National Key Research and Development Program of China (2022YFC3702104).

Acknowledgments

The authors thank the editors and reviewers for their valuable comments to improve this article.

Conflict of interest

The authors declare that the research was conducted in the absence of any commercial or financial relationships that could be construed as a potential conflict of interest.

Publisher's note

All claims expressed in this article are solely those of the authors and do not necessarily represent those of their affiliated organizations, or those of the publisher, the editors and the reviewers. Any product that may be evaluated in this article, or claim that may be made by its manufacturer, is not guaranteed or endorsed by the publisher.

Supplementary material

The Supplementary Material for this article can be found online at: https://www.frontiersin.org/articles/10.3389/fenvs.2024.1393609/full#supplementary-material

References

Ambika, S., Nambi, I. M., and Senthilnathan, J. (2016). Low temperature synthesis of highly stable and reusable CMC-Fe^{2+}(-nZVI) catalyst for the elimination of organic pollutants. *Chem. Eng. J.* 289, 544–553. doi:10.1016/j.cej.2015.12.063

Auffan, M., Achouak, W., Rose, J., Roncato, M., Chanéac, C., Waite, D. T., et al. (2008). Relation between the redox state of iron-based nanoparticles and their cytotoxicity toward *Escherichia coli*. *Environ. Sci. Technol.* 42 (17), 6730–6735. doi:10.1021/es800086f

Bai, Y., Lu, Y., Shen, N., Lau, T., and Zeng, R. J. (2018). Investigation of Cr(VI) reduction potential and mechanism by Caldicellulosiruptor saccharolyticus under glucose fermentation condition. *J. Hazard Mater* 344, 585–592. doi:10.1016/j.jhazmat.2017.10.059

Bian, H., Wan, J., Muhammad, T., Wang, G., Sang, L., Jiang, L., et al. (2021). Computational study and optimization experiment of nZVI modified by anionic and cationic polymer for Cr(VI) stabilization in soil: kinetics and response surface methodology (RSM). *Environ. Pollut.* 276, 116745. doi:10.1016/j.envpol.2021.116745

Bruins, M. R., Kapil, S., and Oehme, F. W. (2000). Microbial resistance to metals in the environment. *Ecotox Environ. Safe* 45 (3), 198–207. doi:10.1006/eesa.1999.1860

Chekli, L., Brunetti, G., Marzouk, E. R., Maoz-Shen, A., Smith, E., Naidu, R., et al. (2016). Evaluating the mobility of polymer-stabilised zero-valent iron nanoparticles and their potential to co-transport contaminants in intact soil cores. *Environ. Pollut.* 216, 636–645. doi:10.1016/j.envpol.2016.06.025

Chen, P., Tan, S., and Wu, W. (2012). Stabilization or oxidation of nanoscale zerovalent Iron at environmentally relevant exposure changes bioavailability and toxicity in medaka fish. *Environ. Sci. Technol.* 46 (15), 8431–8439. doi:10.1021/es3006783

Chen, X., Li, X., Xu, D., Yang, W., and Bai, S. (2020). Application of nanoscale zero-valent iron in hexavalent chromium-contaminated soil: a review. *A Rev.* 9 (1), 736–750. doi:10.1515/ntrev-2020-0059

Cheng, R., Li, G., Shi, L., Xue, X., Kang, M., and Zheng, X. (2016). The mechanism for bacteriophage f2 removal by nanoscale zero-valent iron. *Water Res.* 105, 429–435. doi:10.1016/j.watres.2016.09.025

Dai, Y., Zhang, K., Meng, X., Li, J., Guan, X., Sun, Q., et al. (2019). New use for spent coffee ground as an adsorbent for tetracycline removal in water. *Chemosphere* 215, 163–172. doi:10.1016/j.chemosphere.2018.09.150

Deng, J., Li, X., Wei, X., Liu, Y., Liang, J., Shao, Y., et al. (2020). Different adsorption behaviors and mechanisms of a novel amino-functionalized hydrothermal biochar for hexavalent chromium and pentavalent antimony. *Bioresour. Technol.* 310, 123438. doi:10.1016/j.biortech.2020.123438

Deng, N., Li, Z., Zuo, X., Chen, J., Shakiba, S., Louie, S. M., et al. (2021). Coprecipitation of Fe/Cr hydroxides with organics: roles of organic properties in composition and stability of the coprecipitates. *Environ. Sci. Technol.* 55 (8), 4638–4647. doi:10.1021/acs.est.0c04712

Desai, C., Jain, K., and Madamwar, D. (2008). Evaluation of *in vitro* Cr(VI) reduction potential in cytosolic extracts of three indigenous *Bacillus* sp. isolated from Cr(VI) polluted industrial landfill. *Bioresour. Technol.* 99 (14), 6059–6069. doi:10.1016/j.biortech.2007.12.046

Desai, C., Parikh, R. Y., Vaishnav, T., Shouche, Y. S., and Madamwar, D. (2009). Tracking the influence of long-term chromium pollution on soil bacterial community structures by comparative analyses of 16S rRNA gene phylotypes. *Res. Microbiol.* 160 (1), 1–9. doi:10.1016/j.resmic.2008.10.003

Dong, H., Xie, Y., Zeng, G., Tang, L., Liang, J., He, Q., et al. (2016). The dual effects of carboxymethyl cellulose on the colloidal stability and toxicity of nanoscale zero-valent iron. *Chemosphere* 144, 1682–1689. doi:10.1016/j.chemosphere.2015.10.066

Du, H., Li, N., Yang, L., Li, Q., Yang, G., and Wang, Q. (2023). Plasmonic Ag modified Ag_3VO_4/AgPMo S-scheme heterojunction photocatalyst for boosted Cr(VI) reduction

under visible light: performance and mechanism. *Sep. Purif. Technol.* 304, 122204. doi:10.1016/j.seppur.2022.122204

Edgar, R. C. (2013). UPARSE: highly accurate OTU sequences from microbial amplicon reads. *Nat. Methods* 10 (10), 996–998. doi:10.1038/nmeth.2604

Elangovan, R., Abhipsa, S., Rohit, B., Ligy, P., and Chandraraj, K. (2006). Reduction of Cr(VI) by a *Bacillus* sp. *Biotechnol. Lett.* 28 (4), 247–252. doi:10.1007/s10529-005-5526-z

Fang, Z., Qiu, X., Huang, R., Qiu, X., and Li, M. (2011). Removal of chromium in electroplating wastewater by nanoscale zero-valent metal with synergistic effect of reduction and immobilization. *Desalination* 280 (1), 224–231. doi:10.1016/j.desal.2011.07.011

Fu, Y., Xu, Y., Mao, Y., Tan, M., He, Q., Mao, H., et al. (2023). Multi-functional Ag/Ag_3PO_4/AgPMo with S-scheme heterojunction for boosted photocatalytic performance. *Sep. Purif. Technol.* 317, 123922. doi:10.1016/j.seppur.2023.123922

Gong, Y., Gai, L., Tang, J., Fu, J., Wang, Q., and Zeng, E. Y. (2017). Reduction of Cr(VI) in simulated groundwater by FeS-coated iron magnetic nanoparticles. *Sci. Total Environ.* 595, 743–751. doi:10.1016/j.scitotenv.2017.03.282

He, F., and Zhao, D. (2007). Manipulating the size and dispersibility of zerovalent iron nanoparticles by use of carboxymethyl cellulose stabilizers. *Environ. Sci. Technol.* 41 (17), 6216–6221. doi:10.1021/es0705543

He, F., Zhao, D., Liu, J., and Roberts, C. B. (2007). Stabilization of Fe–Pd nanoparticles with sodium carboxymethyl cellulose for enhanced transport and dechlorination of trichloroethylene in soil and groundwater. *Ind. Eng. Chem. Res.* 46 (1), 29–34. doi:10.1021/ie0610896

Hou, S., Wu, B., Luo, Y., Li, Y., Ma, H., Peng, D., et al. (2020). Impacts of a novel strain QY-1 allied with chromium immobilizing materials on chromium availability and soil biochemical properties. *J. Hazard Mater* 382, 121093. doi:10.1016/j.jhazmat.2019.121093

Hug, S. J., Laubscher, H., and James, B. R. (1997). Iron(III) catalyzed photochemical reduction of chromium(VI) by oxalate and citrate in aqueous solutions. *Environ. Sci. Technol.* 31 (1), 160–170. doi:10.1021/es960253l

Ji, X., Wan, J., Wang, X., Peng, C., Wang, G., Liang, W., et al. (2022). Mixed bacteria-loaded biochar for the immobilization of arsenic, lead, and cadmium in a polluted soil system: effects and mechanisms. *Sci. Total Environ.* 811, 152112. doi:10.1016/j.scitotenv.2021.152112

Jiang, B., Xin, S., Gao, L., Luo, S., Xue, J., and Wu, M. (2017). Dramatically enhanced aerobic Cr(VI) reduction with scrap zero-valent aluminum induced by oxalate. *Chem. Eng. J.* 308, 588–596. doi:10.1016/j.cej.2016.09.098

Jin, Y., Wang, Y., Li, X., Luo, T., Ma, Y., Wang, B., et al. (2023). Remediation and its biological responses to Cd(II)-Cr(VI)-Pb(II) multi-contaminated soil by supported nano zero-valent iron composites. *Sci. Total Environ.* 867, 161344. doi:10.1016/j.scitotenv.2022.161344

Joo, S. H., and Zhao, D. (2008). Destruction of lindane and atrazine using stabilized iron nanoparticles under aerobic and anaerobic conditions: effects of catalyst and stabilizer. *Chemosphere* 70 (3), 418–425. doi:10.1016/j.chemosphere.2007.06.070

Keenan, C. R., and Sedlak, D. L. (2008). Factors affecting the yield of oxidants from the reaction of nanoparticulate zero-valent iron and oxygen. *Environ. Sci. Technol.* 42 (4), 1262–1267. doi:10.1021/es7025664

Kim, J. Y., Lee, C., Love, D. C., Sedlak, D. L., Yoon, J., and Nelson, K. L. (2011). Inactivation of MS2 coliphage by ferrous ion and zero-valent iron nanoparticles. *Environ. Sci. Technol.* 45 (16), 6978–6984. doi:10.1021/es201345y

Laumann, S., Micić, V., and Hofmann, T. (2014). Mobility enhancement of nanoscale zero-valent iron in carbonate porous media through co-injection of polyelectrolytes. *Water Res.* 50, 70–79. doi:10.1016/j.watres.2013.11.040

Li, L., Dong, H., Lu, Y., Zhang, H., Li, Y., Xiao, J., et al. (2022). In-depth exploration of toxicity mechanism of nanoscale zero-valent iron and its aging products toward *Escherichia coli* under aerobic and anaerobic conditions. *Environ. Pollut.* 313, 120118. doi:10.1016/j.envpol.2022.120118

Li, Y., Pan, S., Wang, L., Jia, F., Lu, F., and Shi, J. (2023). Soil chromium accumulation in Industrial regions across China: pollution and health risk assessment, spatial pattern, and temporal trend (2002-2021). *Toxics* 11, 363. doi:10.3390/toxics11040363

Lin, W., Chen, C., Ou, J., Sheu, Y., Hou, D., and Kao, C. (2022). Bioremediation of hexavalent-chromium contaminated groundwater: microcosm, column, and microbial diversity studies. *Chemosphere* 295, 133877. doi:10.1016/j.chemosphere.2022.133877

Lin, Y., Tseng, H., Wey, M., and Lin, M. (2010). Characteristics of two types of stabilized nano zero-valent iron and transport in porous media. *Sci. Total Environ.* 408 (10), 2260–2267. doi:10.1016/j.scitotenv.2010.01.039

Liu, K., Li, F., Cui, J., Yang, S., and Fang, L. (2020). Simultaneous removal of Cd(II) and As(III) by graphene-like biochar-supported zero-valent iron from irrigation waters under aerobic conditions: synergistic effects and mechanisms. *J. Hazard Mater* 395, 122623. doi:10.1016/j.jhazmat.2020.122623

Liu, S., Zeng, T. H., Hofmann, M., Burcombe, E., Wei, J., Jiang, R., et al. (2011). Antibacterial activity of graphite, graphite oxide, graphene oxide, and reduced graphene oxide: membrane and oxidative stress. *Acs Nano* 5 (9), 6971–6980. doi:10.1021/nn202451x

Liu, T., Zhao, L., Sun, D., and Tan, X. (2010). Entrapment of nanoscale zero-valent iron in chitosan beads for hexavalent chromium removal from wastewater. *J. Hazard Mater* 184 (1), 724–730. doi:10.1016/j.jhazmat.2010.08.099

Long, B., Liao, L., Jia, F., Luo, Y., He, J., Zhang, W., et al. (2023). Oxalic acid enhances bioremediation of Cr(VI) contaminated soil using *Penicillium oxalicum* SL2. *Chemosphere* 311, 136973. doi:10.1016/j.chemosphere.2022.136973

Long, B., Ye, B., Liu, Q., Zhang, S., Ye, J., Zou, L., et al. (2018). Characterization of *Penicillium oxalicum* SL2 isolated from indoor air and its application to the removal of hexavalent chromium. *Plos One* 13 (1), e0191484. doi:10.1371/journal.pone.0191484

Luo, Y., Pang, J., Peng, C., Ye, J., Long, B., Tong, J., et al. (2023). Cr(VI) reduction and Fe(II) regeneration by *Penicillium oxalicum* SL2-enhanced nanoscale zero-valent iron. *Environ. Sci. Technol.* 57 (30), 11313–11324. doi:10.1021/acs.est.3c01390

Lyu, H., Tang, J., Huang, Y., Gai, L., Zeng, E. Y., Liber, K., et al. (2017). Removal of hexavalent chromium from aqueous solutions by a novel biochar supported nanoscale iron sulfide composite. *Chem. Eng. J.* 322, 516–524. doi:10.1016/j.cej.2017.04.058

Ma, L., Du, Y., Chen, S., Zhang, F., Zhan, W., Du, D., et al. (2021). Nanoscale zero-valent iron coupling with Shewanella oneidensis MR-1 for enhanced reduction/removal of aqueous Cr(VI). *Sep. Purif. Technol.* 277, 119488. doi:10.1016/j.seppur.2021.119488

Ma, X., Du, H., Tan, M., Qian, J., Deng, M., Hao, D., et al. (2024). Photocatalytic fuel cell with cathodic P-$BiVO_4$/CQDs and anodic WO_3 for efficient Cr(VI) reduction and stable electricity generation. *Sep. Purif. Technol.* 339, 126644. doi:10.1016/j.seppur.2024.126644

Manning, B. A., Kiser, J. R., Kwon, H., and Kanel, S. R. (2007). Spectroscopic investigation of Cr(III)- and Cr(VI)-treated nanoscale zerovalent iron. *Environ. Sci. Technol.* 41 (2), 586–592. doi:10.1021/es061721m

Mao, C., Xiang, Y., Liu, X., Zheng, Y., Yeung, K. W. K., Cui, Z., et al. (2019). Local photothermal/photodynamic synergistic therapy by disrupting bacterial membrane to accelerate reactive oxygen species permeation and protein leakage. *Acs Appl. Mater Inter* 11 (19), 17902–17914. doi:10.1021/acsami.9b05787

Megharaj, M., Avudainayagam, S., and Naidu, R. (2003). Toxicity of hexavalent chromium and its reduction by bacteria isolated from soil contaminated with tannery waste. *Curr. Microbiol.* 47 (1), 51–54. doi:10.1007/s00284-002-3889-0

Morales, D. K., Ocampo, W., and Zambrano, M. M. (2007). Efficient removal of hexavalent chromium by a tolerant *Streptomyces* sp. affected by the toxic effect of metal exposure. *J. Appl. Microbiol.* 103 (6), 2704–2712. doi:10.1111/j.1365-2672.2007.03510.x

Nel, A. (2005). Air pollution-related illness: effects of particles. *Science* 308 (5723), 804–806. doi:10.1126/science.1108752

Nel, A., Xia, T., Mädler, L., and Li, N. (2006). Toxic potential of materials at the nanolevel. *Science* 311 (5761), 622–627. doi:10.1126/science.1114397

Pan, C., Troyer, L. D., Catalano, J. G., and Giammar, D. E. (2016). Dynamics of chromium(VI) removal from drinking water by iron electrocoagulation. *Environ. Sci. Technol.* 50 (24), 13502–13510. doi:10.1021/acs.est.6b03637

Peng, L., Liu, Y., Gao, S., Dai, X., and Ni, B. (2015). Assessing chromate reduction by dissimilatory iron reducing bacteria using mathematical modeling. *Chemosphere* 139, 334–339. doi:10.1016/j.chemosphere.2015.06.090

Phenrat, T., Saleh, N., Sirk, K., Tilton, R. D., and Lowry, G. V. (2007). Aggregation and sedimentation of aqueous nanoscale zerovalent iron dispersions. *Environ. Sci. Technol.* 41 (1), 284–290. doi:10.1021/es061349a

Qian, A., Liao, P., Yuan, S., and Luo, M. (2014). Efficient reduction of Cr(VI) in groundwater by a hybrid electro-Pd process. *Water Res.* 48, 326–334. doi:10.1016/j.watres.2013.09.043

Qu, J., Wang, Y., Tian, X., Jiang, Z., Deng, F., Tao, Y., et al. (2021). KOH-activated porous biochar with high specific surface area for adsorptive removal of chromium (VI) and naphthalene from water: affecting factors, mechanisms and reusability exploration. *J. Hazard Mater* 401, 123292. doi:10.1016/j.jhazmat.2020.123292

Qu, J., Wei, S., Liu, Y., Zhang, X., Jiang, Z., Tao, Y., et al. (2022). Effective lead passivation in soil by bone char/CMC-stabilized FeS composite loading with phosphate-solubilizing bacteria. *J. Hazard Mater* 423, 127043. doi:10.1016/j.jhazmat.2021.127043

Rajapaksha, A. U., Alam, M. S., Chen, N., Alessi, D. S., Igalavithana, A. D., Tsang, D. C. W., et al. (2018). Removal of hexavalent chromium in aqueous solutions using biochar: chemical and spectroscopic investigations. *Sci. Total Environ.* 625, 1567–1573. doi:10.1016/j.scitotenv.2017.12.195

Raychoudhury, T., Tufenkji, N., and Ghoshal, S. (2012). Aggregation and deposition kinetics of carboxymethyl cellulose-modified zero-valent iron nanoparticles in porous media. *Water Res.* 46 (6), 1735–1744. doi:10.1016/j.watres.2011.12.045

Ren, L., Dong, J., Chi, Z., and Huang, H. (2018). Reduced graphene oxide-nano zero value iron (rGO-nZVI) micro-electrolysis accelerating Cr(VI) removal in aquifer. *J. Environ. Sci-China* 73, 96–106. doi:10.1016/j.jes.2018.01.018

Su, C., and Puls, R. W. (2004). Nitrate reduction by zerovalent iron: effects of formate, oxalate, citrate, chloride, sulfate, borate, and phosphate. *Environ. Sci. Technol.* 38 (9), 2715–2720. doi:10.1021/es034650p

Su, H., Fang, Z., Tsang, P. E., Zheng, L., Cheng, W., Fang, J., et al. (2016). Remediation of hexavalent chromium contaminated soil by biochar-supported zero-valent iron nanoparticles. *J. Hazard Mater* 318, 533–540. doi:10.1016/j.jhazmat.2016.07.039

Sun, J., Luo, Y., Ye, J., Li, C., and Shi, J. (2022). Chromium distribution, leachability and speciation in a chrome plating site. *Processes* 10, 142. doi:10.3390/pr10010142

Tan, H., Wang, C., Li, H., Peng, D., Zeng, C., and Xu, H. (2020). Remediation of hexavalent chromium contaminated soil by nano-FeS coated humic acid complex in combination with Cr-resistant microflora. *Chemosphere* 242, 125251. doi:10.1016/j.chemosphere.2019.125251

Tang, J., Huang, Y., Gong, Y., Lyu, H., Wang, Q., and Ma, J. (2016). Preparation of a novel graphene oxide/Fe-Mn composite and its application for aqueous Hg(II) removal. *J. Hazard Mater* 316, 151–158. doi:10.1016/j.jhazmat.2016.05.028

Tang, X., Liu, B., Deng, Q., Zhang, R., Li, X., and Xu, H. (2018). Strengthening detoxication impacts of Coprinus comatus on nickel and fluoranthene co-contaminated soil by bacterial inoculation. *J. Environ. Manage* 206, 633–641. doi:10.1016/j.jenvman.2017.11.009

Tong, J., Ye, B., Jiang, X., Wu, H., Xu, Q., Luo, Y., et al. (2023). Synergy among extracellular adsorption, bio-precipitation and transmembrane transport of *Penicillium oxalicum* SL2 enhanced Pb stabilization. *J. Hazard Mater* 454, 131537. doi:10.1016/j.jhazmat.2023.131537

Tsitonaki, A., Petri, B., Crimi, M., Mosbek, H., Siegrist, R., and Bjerg, P. (2010). *In situ* chemical oxidation of contaminated soil and groundwater using persulfate: a review. *Crit. Rev. Env. Sci. Tec.* 40 (1), 55–91. doi:10.1080/10643380802039303

Wang, K., Sun, Y., Tang, J., He, J., and Sun, H. (2020a). Aqueous Cr(VI) removal by a novel ball milled Fe0-biochar composite: role of biochar electron transfer capacity under high pyrolysis temperature. *Chemosphere* 241, 125044. doi:10.1016/j.chemosphere.2019.125044

Wang, L., Luo, Y., Pang, J., Li, Y., Wu, H., Jiang, X., et al. (2023). Fe-biochar for simultaneous stabilization of chromium and arsenic in soil: rational design and long-term performance. *Sci. Total Environ.* 862, 160843. doi:10.1016/j.scitotenv.2022.160843

Wang, Q., Ma, W., Qian, J., Li, N., Zhang, C., Deng, M., et al. (2024). S-scheme towards interfacial charge transfer between POMs and MOFs for efficient visible-light photocatalytic Cr (VI) reduction. *Environ. Pollut.* 347, 123707. doi:10.1016/j.envpol.2024.123707

Wang, Y., Fang, Z., Kang, Y., and Tsang, E. P. (2014). Immobilization and phytotoxicity of chromium in contaminated soil remediated by CMC-stabilized nZVI. *J. Hazard Mater* 275, 230–237. doi:10.1016/j.jhazmat.2014.04.056

Wang, Z. Y., Wang, R. X., Zhou, J. S., Cheng, J. F., and Li, Y. H. (2020b). An assessment of the genomics, comparative genomics and cellulose degradation potential of Mucilaginibacter polytrichastri strain RG4-7. *Bioresour. Technol.* 297, 122389. doi:10.1016/j.biortech.2019.122389

Wu, D., Shen, Y., Ding, A., Mahmood, Q., Liu, S., and Tu, Q. (2013). Effects of nanoscale zero-valent iron particles on biological nitrogen and phosphorus removal and microorganisms in activated sludge. *J. Hazard Mater* 262, 649–655. doi:10.1016/j.jhazmat.2013.09.038

Wu, W., Wu, P., Yang, F., Sun, D., Zhang, D., and Zhou, Y. (2018). Assessment of heavy metal pollution and human health risks in urban soils around an electronics manufacturing facility. *Sci. Total Environ.* 630, 53–61. doi:10.1016/j.scitotenv.2018.02.183

Xia, D., Liu, H., Xu, B., Wang, Y., Liao, Y., Huang, Y., et al. (2019). Single Ag atom engineered 3D-MnO_2 porous hollow microspheres for rapid photothermocatalytic inactivation of *E. coli* under solar light. *Appl. Catal. B Environ.* 245, 177–189. doi:10.1016/j.apcatb.2018.12.056

Xia, D., Tang, Z., Wang, Y., Yin, R., He, H., Xie, X., et al. (2020). Piezo-catalytic persulfate activation system for water advanced disinfection: process efficiency and inactivation mechanisms. *Chem. Eng. J.* 400, 125894. doi:10.1016/j.cej.2020.125894

Xu, X., Huang, H., Zhang, Y., Xu, Z., and Cao, X. (2019). Biochar as both electron donor and electron shuttle for the reduction transformation of Cr(VI) during its sorption. *Environ. Pollut.* 244, 423–430. doi:10.1016/j.envpol.2018.10.068

Xu, Z., Wan, Z., Sun, Y., Gao, B., Hou, D., Cao, X., et al. (2022). Electroactive Fe-biochar for redox-related remediation of arsenic and chromium: distinct redox nature with varying iron/carbon speciation. *J. Hazard Mater* 430, 128479. doi:10.1016/j.jhazmat.2022.128479

Xu, Z., Xu, X., Tsang, D. C. W., Yang, F., Zhao, L., Qiu, H., et al. (2020). Participation of soil active components in the reduction of Cr(VI) by biochar: differing effects of iron mineral alone and its combination with organic acid. *J. Hazard Mater* 384, 121455. doi:10.1016/j.jhazmat.2019.121455

Yamashita, T., and Hayes, P. (2008). Analysis of XPS spectra of Fe^{2+} and Fe^{3+} ions in oxide materials. *Appl. Surf. Sci.* 254 (8), 2441–2449. doi:10.1016/j.apsusc.2007.09.063

Yang, Z., Zhang, X., Jiang, Z., Li, Q., Huang, P., Zheng, C., et al. (2021). Reductive materials for remediation of hexavalent chromium contaminated soil – a review. *Sci. Total Environ.* 773, 145654. doi:10.1016/j.scitotenv.2021.145654

Yao, Q., Liu, J., Yu, Z., Li, Y., Jin, J., Liu, X., et al. (2017). Three years of biochar amendment alters soil physiochemical properties and fungal community composition in a black soil of northeast China. *Soil Biol. Biochem.* 110, 56–67. doi:10.1016/j.soilbio.2017.03.005

Ye, J., Luo, Y., Sun, J., and Shi, J. (2021). Nanoscale zero-valent iron modified by bentonite with enhanced Cr(VI) removal efficiency, improved mobility, and reduced toxicity. *Nanomaterials* 11, 2580. doi:10.3390/nano11102580

Zhang, S., Lyu, H., Tang, J., Song, B., Zhen, M., and Liu, X. (2019). A novel biochar supported CMC stabilized nano zero-valent iron composite for hexavalent chromium removal from water. *Chemosphere* 217, 686–694. doi:10.1016/j.chemosphere.2018.11.040

Zhao, N., Tan, X., Xiong, J., Chen, N., Gao, J., Wang, R., et al. (2022). Quantitative analysis on the redox conversion mechanism of Cr(VI) and As(III) by iron carbide based biochar composites. *Chem. Eng. J.* 446, 137417. doi:10.1016/j.cej.2022.137417

Zhou, H., Ma, M., Zhao, Y., Baig, S. A., Hu, S., Ye, M., et al. (2022). Integrated green complexing agent and biochar modified nano zero-valent iron for hexavalent chromium removal: a characterisation and performance study. *Sci. Total Environ.* 834, 155080. doi:10.1016/j.scitotenv.2022.155080

Zhou, L., Thanh, T. L., Gong, J., Kim, J., Kim, E., and Chang, Y. (2014). Carboxymethyl cellulose coating decreases toxicity and oxidizing capacity of nanoscale zerovalent iron. *Chemosphere* 104, 155–161. doi:10.1016/j.chemosphere.2013.10.085

Zhu, H., Jiang, R., Xiao, L., and Li, W. (2010). A novel magnetically separable γ-Fe_2O_3/crosslinked chitosan adsorbent: preparation, characterization and adsorption application for removal of hazardous azo dye. *J. Hazard Mater* 179 (1), 251–257. doi:10.1016/j.jhazmat.2010.02.087

frontiers | Frontiers in Environmental Science

TYPE Original Research
PUBLISHED 06 September 2024
DOI 10.3389/fenvs.2024.1380867

OPEN ACCESS

EDITED BY
Mariusz Gusiatin,
University of Warmia and Mazury in Olsztyn, Poland

REVIEWED BY
Marko Černe,
Institute of Agriculture and Tourism, Croatia
Dafeng Hui,
Tennessee State University, United States

*CORRESPONDENCE
Adnan Mustafa,
adnanmustafa780@gmail.com
Muhammad Naveed,
Muhammad.naveed@uaf.edu.pk

RECEIVED 02 February 2024
ACCEPTED 03 July 2024
PUBLISHED 06 September 2024

CITATION
Naveed M, Fatima M, Naseem Z, Ahmad Z, Gaafar A-RZ, Shabbir M, Farooq QuA, Hodhod MS, Khan MI, Shahid D and Mustafa A (2024), Improving the growth of pea plant by biochar–polyacrylamide association to cope with heavy metal stress under sewage water application in a greenhouse.
Front. Environ. Sci. 12:1380867.
doi: 10.3389/fenvs.2024.1380867

Improving the growth of pea plant by biochar–polyacrylamide association to cope with heavy metal stress under sewage water application in a greenhouse

Muhammad Naveed[1]*, Maryum Fatima[1], Zainab Naseem[1], Zulfiqar Ahmad[1], Abdel-Rhman Z Gaafar[2], Mubashra Shabbir[3], Qurrat ul Ain Farooq[4,5], Mohamed S. Hodhod[6], Muhammad Imran Khan[1], Dua Shahid[7] and Adnan Mustafa[7]*

[1]Institute of Soil and Environmental Sciences, University of Agriculture, Faisalabad, Pakistan, [2]Department of Botany and Microbiology, College of Science, King Saud University, Riyadh, Saudi Arabia, [3]Livestock and Dairy Development Department, Government of Punjab, Lahore, Pakistan, [4]Phytophthora Science and Management, Harry Buttler Institute, Murdoch University, Murdoch, WA, Australia, [5]Department of Horticulture, Faculty of Agricultural Sciences, University of the Punjab, Lahore, Punjab, Pakistan, [6]Faculty of Biotechnology, October University for Modern Sciences & Arts, Giza, Egypt, [7]Guangdong Provincial Key Laboratory of Applied Botany, South China Botanical Garden, Chinese Academy of Sciences, Guangzhou, China

Sewage water is extensively used for irrigation, serving as a valuable resource for plant growth to enhance agricultural productivity. However, this practice also results in a significant accumulation of heavy metals in the soil, posing potential environmental and health risks. A study was designed to evaluate the combined effect of amendments on heavy metal immobilization in soil and improved growth and yield in pea plants. For this, the soil for each treatment was mixed with biochar (BC) (1% *w/w*), polyacrylamide (PAM) (0.5% *w/w*), and also applied in combination. Pea plants were irrigated with tap water (TW), sewage water (SW), and tap + sewage water (TW + SW). A factorial design was applied to analyze data statistically. The combined application of the biochar and polymer showed a positive response by significantly enhancing the plant growth parameters (39%–84%), physiological attributes (67%–69%), and reducing Cd (56%) and Cr (65%) concentration in soil applied with SW and TW + SW. Moreover, treatment with a combined application of BC and PAM significantly reduced Cd concentrations by 43% in roots, 50% in shoots, and 91% in grains. Similarly, Cr concentrations were reduced by 51% in roots, 51% in shoots, and 94% in grains compared to the control. Overall, the study results indicate reduced bioaccumulation and health risks associated with potentially toxic elements (PTEs), supporting the application of the polymer and biochar for irrigating pea plants with TW + SW. Leveraging the combined benefits of polymer and biochar amendments appears to be an effective strategy to remediate PTE-contaminated soil, thereby increasing plant growth and yield.

KEYWORDS

polymer, biochar, pea plant, phytoremediation, potentially toxic elements

Introduction

Extensive urbanization and industrialization have caused a six-fold increase in the demand for unpolluted water (Nzediegwu et al., 2019), resulting in a global scarcity of potable water. Anthropogenic activities have degraded freshwater quality worldwide by introducing industrial and agricultural contaminants (Mohan et al., 2014). This issue is particularly severe in countries like Pakistan, an agricultural state in a semi-arid region with limited freshwater resources. As a large volume of potable water is consumed for irrigation of agricultural lands (FAO. AQUASTAT, 2016; UNESCO, 2016), farmers are dependent on the consumption of sewage water as an alternative to freshwater.

The use of wastewater for irrigation has been proposed and encouraged by many researchers to tackle the problem of freshwater scarcity (Rusan et al., 2007; Dhiman et al., 2020). However, in developing countries, the release of untreated wastewater into freshwater resources is a common practice, causing the contamination of arable land when irrigated with untreated wastewater (Qadir et al., 2010). Wastewater comprises nutrients; surfactants; potentially toxic elements (PTEs) like cadmium (Cd), chromium (Cr), nickel (Ni), and lead (Pb) (Khan et al., 2008); and organic pollutants (Khalid et al., 2018). Therefore, the increased wastewater generation caused by extensive urbanization and industrialization demands the safe disposal of wastewater.

PTEs are considered environmentally toxic pollutants and substances that pose health risks, and their accumulation in animals and humans has been aggravated by anthropogenic activities (Sabir et al., 2022a). In developing countries like Pakistan, due to lack of awareness and resources, poor management of industrial waste contributes to the spread of PTEs in the environment. This accumulation of PTEs in the soil system is a matter of concern for growing industries in developing countries. The wastewater contains trace metals from domestic, commercial, surface runoff, and industrial origins (Fuerhacker et al., 2010), and their presence in the soil induces toxicity by ionic imbalance, leading to declined growth in plants.

Chromium toxicity in plants resulted in reduced germination, growth, and disturbed photosynthesis, nutrient and water uptake, and enzymatic activity. This triggers the production of reactive oxygen species (ROS) to oxidize biomolecules causing plant death (Ekere et al., 2020). High toxicity, persistent nature, increased bioavailability in open environments, and resulting bioaccumulation and biomagnification are the important factors causing health risks in plants, animals, and humans (Naveed et al., 2021). Various approaches (Jiang et al., 2022) such as chemical methods (Allegre et al., 2004), bioremediation (Naseem et al., 2023), physical treatment (Abbas et al., 2015), and phytoremediation (Naveed et al., 2021) have been reported for remediation of PTE-contaminated soils (Jan et al., 2021). However, adsorption by biochar (BC) and polymers is the most economical, practical, efficient, effective, and eco-friendly approach among all the available techniques for immobilization of PTEs.

Super adsorbent polymers, sometimes called hydrogels, are highly hydrophilic networks of loosely crosslinked polymer chains that can absorb and retain up to hundreds of times their weight of water or aqueous solutions (Dhiman et al., 2020) and slow water release, which could improve the growth of the plant in water stress conditions (Beckett and Augarde, 2013), supply the cation, and decrease the availability of some toxic elements. Superabsorbent polymers (SAPs), also identified as soil polymers or macromolecular polymers, are proficient in repeatedly absorbing, retaining, and releasing extremely large amounts of water, relative to their own weight. SAPs can absorb more than a thousand times their original weight in water, and they can retain liquids even under pressure (Liu et al., 2009). These polymers are applied in agriculture to improve the soil's physical properties like water- and nutrient-holding potential and promote crop growth in arid and semi-arid areas. Recently, the most commoditized polymers are mainly polypropylic acid (PAA) or polyacrylamide (PAM) (Islam et al., 2011; Li et al., 2022).

Acrylamide is a white, colorless, chemical compound that is soluble in water, ethanol, ether, and chloroform and is produced synthetically. The large surface area and presence of various functional groups make usage of polymers ideal in various fields like agriculture, horticulture, biomedicine, bioengineering, food storage, and treatment of wastewater (Li et al., 2022). Modified-polyacrylamide hydrogels are used commercially for the purification of wastewater and metal extraction (Dhiman et al., 2015). Due to their hydrophilic nature and carboxylic functional groups, polymers can tightly bind to PTE, thereby minimizing the uptake of heavy metals by plants (Huttermann et al., 2009). Synthesized polymers have been used extensively with adsorbents for heavy metal removal since the surface properties of the adsorbents can be modified by enhancing available functional groups to improve their adsorption ability for pollutants (Wang et al., 2015). One way to decrease PTE availability to plants is by increasing binding sites for PTEs in soil through amendment application.

Biochar is the end product of pyrolysis, carbonization, and gasification of plant and animal-based materials (ASABE, 2011) and contains a high surface area, numerous pores, various oxygen-containing functional groups, and high cation exchange capacity with alkaline pH (Lehmann, 2007; Al-Wabel et al., 2017). BC application may improve crop yield by cultivating polluted land. A more recent study (Nie et al., 2018) showed that sugarcane bagasse-derived BC significantly reduced Cd, Cu, and Pb uptake by Pak Choi (*Brassica chinensis* L.) plants grown in wastewater-polluted soil, significantly increasing the yield. A pot experiment study with tobacco stem-derived BC showed that the application of BC led to immobilization of Cr, Cu, and Pb in soil (Zhang et al., 2019). Additionally, BC can serve as a low-cost adsorbent for heavy metal removal in wastewater treatment plants (Inyang et al., 2016).

Generally, soils are good accumulators of PTEs, and application of BC in the topsoil leads to further immobilization of PTE. Due to its diverse surface characteristics, BC is known to be effective in the adsorption of PTE (Lehmann, 2007). Modification of BC with foreign materials such as silica, zeolites, polymers, and nutrient enrichment improves its physiochemical properties and ameliorates its efficiency and environmental influence (Ok et al., 2015; Rafique et al., 2022). The use of BC amendments along with synthetic (acrylamide, polyurethane, polyvinyl, and resins) and natural polymer derivatives of algal polysaccharides has shown a promising influence on the immobilization of chromium in soil (de-Bashan and Bashan, 2010).

Considering the interaction of wastewater irrigation, soil PTE, and polymers and BC, it is suggested that employing cost-effective

techniques, such as incorporating polymers and BC into the soil, could be safe for using sewage water in arable soils In previous studies, the use of BC with other organic amendments like compost has been reported (Coelho et al., 2018; Naveed et al., 2021). Polymers along with BC induce a large number of binding sites to hold cationic contaminants and sequester carbon from the environment (Ekebafe et al., 2012). Polymers also help reduce BC pH and improve its performance in alkaline soils as well.

The simultaneous use of polymers and BC emerges as an effective approach to enhance the growth and yield of plants facing heavy metal stress. Application of polymers in soil will increase immobilization of PTE and improve soil properties like water- and nutrient-holding capacity, which would be beneficial for plant growth. The use of BC will help in increased immobilization of PTE in soil, providing essential nutrients. Moreover, the combined application of BC and polymer has not been reported previously. Therefore, we hypothesized that the co-application of BC and polymer could be a better strategy to mitigate risks of PTEs, while enhancing soil properties like water-holding capacity, nutrient availability and organic matter, and improving the growth, physiology, and yield of plants. The objectives of this experiment were to evaluate the impact of polymer–BC and their combined application on growth, physiology, water relations, yield of pea plants grown under different levels of sewage water along with the phytoremediation potential, and associated health risks of pea plants grown with sewage water containing Cd and Cr PTE.

Materials and methods

Pot experiment

The research area is located in Faisalabad, Punjab, Pakistan, at latitude (31.41°) and longitude (73.07°). Soil samples were collected from the research area of the Institute of Soil and Environmental Sciences, University of Agriculture, Faisalabad. The soil was sand clay loam with 7.85 pH, 1.29 dS m^{-1} EC, 13.2 cmolc kg^{-1} CEC, 0.55% organic matter, 0.54% total nitrogen, 4.09 mg kg^{-1} available phosphorus, and 126 mg kg^{-1} extractable potassium. The cadmium and chromium concentrations were not detected in the field soils. The soil samples were air-dried and sieved (2.0 mm) to make it homogenized, and a total of 36 pots were filled with soil. Sewage water from the sewage canal Saeed Abad near the University of Agriculture Faisalabad, Pakistan, was collected. The experiment was conducted following completely randomized design (CRD) with factorial settings and three replications.

The sewage water was analyzed for determination of PTE Cd and Cr, and their concentrations were found above the safe limit (World Health Organization, 2011). BC derived from sugarcane bagasse was prepared in a laboratory muffle furnace (at the pyrolysis temperature of 300 °C with a retention time of 60 min), previously reported to enhance metal tolerance and pea plant health (Naveed et al., 2020). The polyacrylamide (anionic) was acquired from Yixing Bluwat Chemicals Co., Ltd, Jiangsu, China. BC (1% *w/w*), polyacrylamide (0.5% *w/w*), and their combined application were used in pots filled with 8 kg of soil. Pots were irrigated with tap water (TW), sewage water (SW), and tap + sewage water (TW + SW). Sewage water was used without any dilution, whereas TW + SW contained 50% tap water and 50% sewage water. Seeds of pea cultivar "Meteor Faisalabad" were collected from the vegetable lab of the Institute of Horticultural Sciences, University of Agriculture, Faisalabad. Five seeds per pot were sown, and after germination, three plants were maintained during the crop growth. After 100 days, at maturity, the plants were harvested and analyzed for various growth parameters. Data regarding different growth and yield parameters during growth and after harvesting were collected.

Measurement of growth parameters

Plant growth parameters were measured at different time intervals. At maturity, the plant height was measured with a measuring tape. After harvesting, the plant's fresh aboveground and root biomass were weighted, and the average values were calculated. Roots and shoots were sun-dried for 3 days and then put in an oven at 60 °C for 24 h to calculate root and shoot dry weight (Naveed et al., 2020).

Measurement of physiological parameters

The Soil Plant Analysis Development (SPAD) index was estimated using a portable chlorophyll meter (SPAD-502-m Minolta, Osaka, Japan). For osmotic potential, a leaf was kept in the refrigerator for 48 h, then ground, and sap measurement was calculated by the potential meter. To estimate relative water contents, leaves were dipped in distilled water for 24 h and blotted carefully with tissue paper, the turgid weight was calculated, leaves were put in the oven for 24 h, and their dry weight was calculated. Relative water content was calculated by using this formula by Barrs and Watherley (1968):

$$RWC\ (\%) = Fresh\,wt - Dry\,wt/Turgid\,wt - Dry\,wt \times 100.$$

For electrolyte leakage, fresh leaves were dipped in 50 mL distilled water. The EC meter was dipped in that flask, and EC1 was calculated; after that, these flasks were put into a shaker for approximately 3 h, and EC2 was calculated; after that, these flasks were put into the autoclave for 4 h, and EC3 was calculated. Electrolyte leakage was calculated by using the below formula by Yang et al. (1996):

$$Electrolyte\ leakage\ (\%) = (EC2 - EC1)/EC3 \times 100.$$

Yield analyses

Yield-related parameters were calculated after harvesting. Pods' fresh weight was calculated on a digital electronic balance. After taking pods' fresh weight, pods were kept in shade and sun-dried for 3 days and then oven-dried at 60 °C for 24 h. Then, their weight was calculated on a digital electronic balance. The number of pods was calculated for each treatment, and the number of peas per pod of each treatment was also recorded.

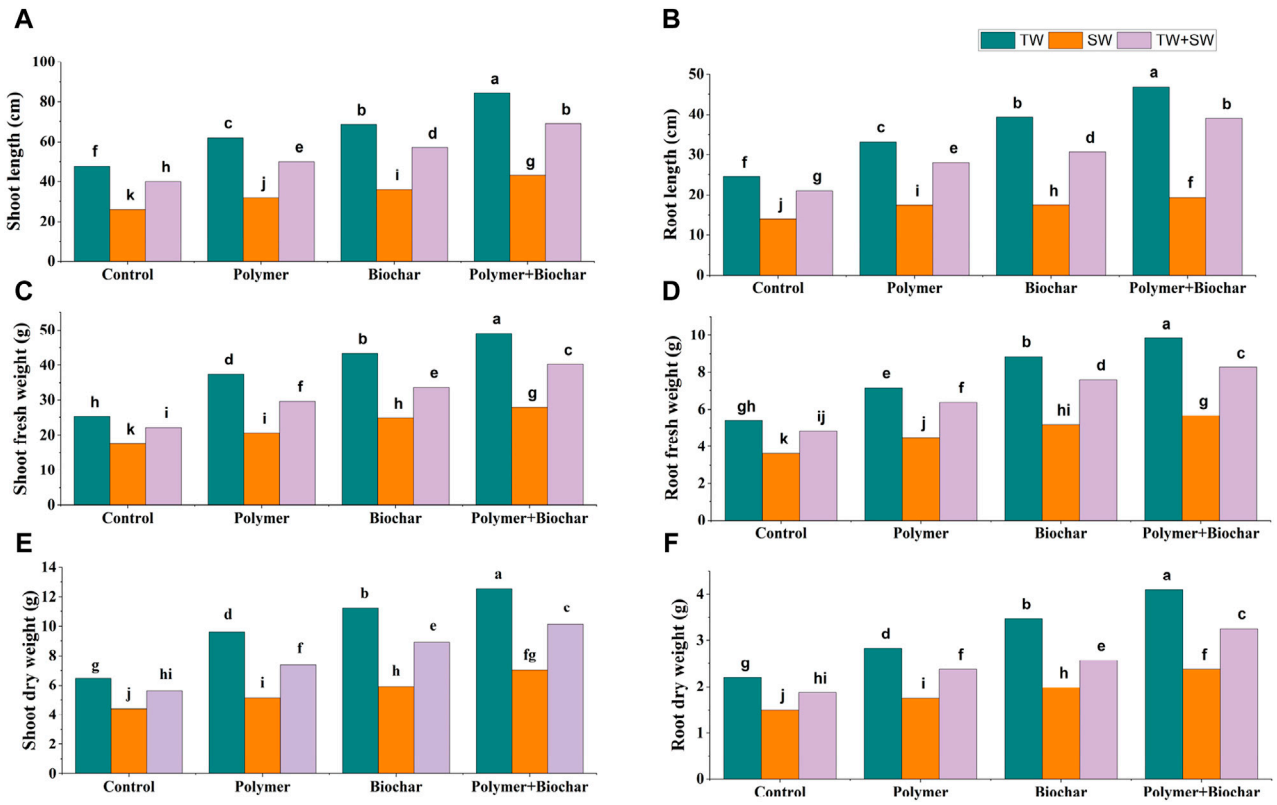

FIGURE 1
Synergistic use of biochar and polymer on shoot length **(A)**, root length **(B)**, shoot fresh weight **(C)**, root fresh weight **(D)**, shoot dry weight **(E)**, and root dry weight **(F)** of Pisum sativum upon application of sewage water. Here, TW, SW, TW + SW represents tap water, sewage water and tap water + sewage water, respectively. The values are presented as mean (n = 3). The values sharing the same letter(s) in bars are statistically non-significant with each other at $p< 0.05$.

Chemical analyses

The plant samples were digested as described by Wolf (1982). The dried samples of root/shoot and grain were ground into powder by using a rotary mill. Approximately 0.5 g sample was taken in a 100-mL Pyrex digestion flask, 5 mL of nitric and perchloric acid at a ratio of 2:1 was added into the samples, and these samples were put in a fume hood overnight.

Flasks were put on the hot plate and heated up to 350 centigrade until the sample appeared pale white. Samples were removed from the hot plate and cooled. Then, 50 mL distilled water was added in the samples and filtered and stored in plastic bottles that were further used for the determination of PTE. Toxic metal concentrations, i.e., chromium (Cr) and cadmium (Cd), in the prepared samples were determined by using an atomic absorption spectrophotometer (Hitachi Polarized Zeeman AAS, Z-8200, Japan).

Phytoremediation potential of plants

The enrichment factor (EF) is calculated (Lorestani et al., 2011) as follows:

$$\text{Enrichment factor (EF)} = \frac{\text{Potentially toxic elements (PTE) in the grain (mg kg} - 1\text{ DW)}}{\text{Potentially toxic elements (PTE) in soil (mg kg} - 1\text{ DW)}}.$$

The bioaccumulation coefficient (BAC) of pea plants was calculated (Rizova, 2020) as follows:

$$\text{Bioaccumulation coefficient (BAC)} = \frac{\text{Potentially toxic elements (PTE) in the shoot (mg kg} - 1\text{ DW)}}{\text{Potentially toxic elements (PTE) in soil (mg kg} - 1\text{ DW)}}.$$

Health risk assessment parameter

The daily intake of metal (DIM) for Cd and Cr was calculated by using the following equation:

$$\text{DIM} = \frac{\text{M} \times \text{I}}{B.Wt},$$

where M is the concentration of Cd and Cr in plants (mg kg^{-1}), I is the daily intake of vegetables, and W is the average body weight (B.Wt). The average adult B.Wt was considered 60 kg, while the

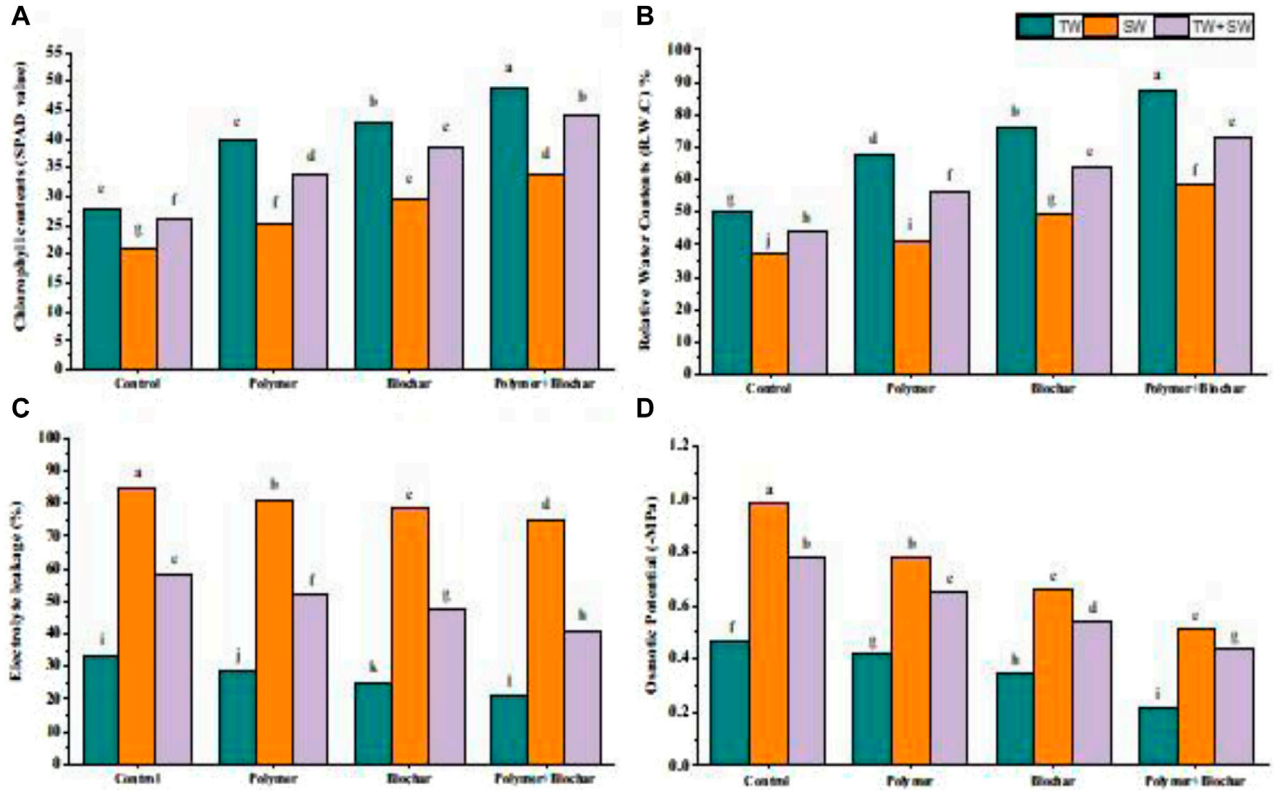

FIGURE 2
Synergistic use of biochar and polymer on chlorophyll contents **(A)**, relative water contents **(B)**, electrolyte leakage **(C)**, and osmotic potential **(D)** of *Pisum sativum* upon application of sewage water. Here, TW, SW, and TW + SW represent tap water, sewage water, and tap water + sewage water, respectively. The values are presented as mean (n = 3). The values sharing the same letter(s) in bars are statistically non-significant with each other at $p< 0.05$.

average daily vegetable intake for adults was considered 0.345 kg^{-1} $person^{-1}$ (Latif et al., 2018).

The hazard quotient (HQ) (Hazard quotient) for Cd and Cr caused by the consumption of contaminated vegetables was calculated using the following equation:

$$HQ = \frac{DIM}{RFD}.$$

The oral reference dose (RFD) for Cd is 0.5 (Yahaya et al., 2020) and for Cr is 1.5 (Adebayo et al., 2020).

Lifetime cancer risk (LTCR) through Cd- and Cr-contaminated grain ingestion was calculated using the following formula:

$$LTCR = DIM \times CSF.$$

where CSF represents the oral cancer slope factor for metal. For this study, Cd and Cr have a CSF of 0.38 and 0.5, respectively (U.S. Department of Energy's Oak Ridge Operations Office ORO, 2011).

Statistical analysis

The statistical design applied for data analysis was 2-factor factorial (Package doebioresearch), and the software used for analysis was RStudio (4.3.1). Data obtained were analyzed through analysis of variance to estimate the differences among the mean (n = 3) values by comparing the means of each treatment by LSD at a 5% probability level using computer-based software, Rstudio (RStudio Team, 2021). The Pearson correlation analysis of different parameters of the pea plant was performed with Origin Pro software, while principal components analysis (PCA) was performed in RStudio, and for the construction of the PCA plot, the packages used were ggplot2, factoextra, and factoMiner (RStudio Team, 2021). The ANOVA (analysis of variance) for parameters studied is provided as (Supplementary Tables S1–S6).

Results

Growth analyses of pea plants

The highest increase of 76% in shoot length (Figure 1A), 91% in root length (Figure 1B), 95% in shoot fresh weight (Figure 1C), 83% in root fresh weight (Figure 1D), 94% in shoot dry weight (Figure 1E), and 86% in root dry weight (Figure 1F) was observed in plants applied with TW when polymer and BC was used in combination. Application of TW + SW showed an increase of 73% in shoot length and an 86% increase in root length when both polymer and BC were applied, while the least impact of SW was observed in the combined application of polymer and biochar by showing an increase of 65% and 38% in shoot length and root length as compared to the control, respectively.

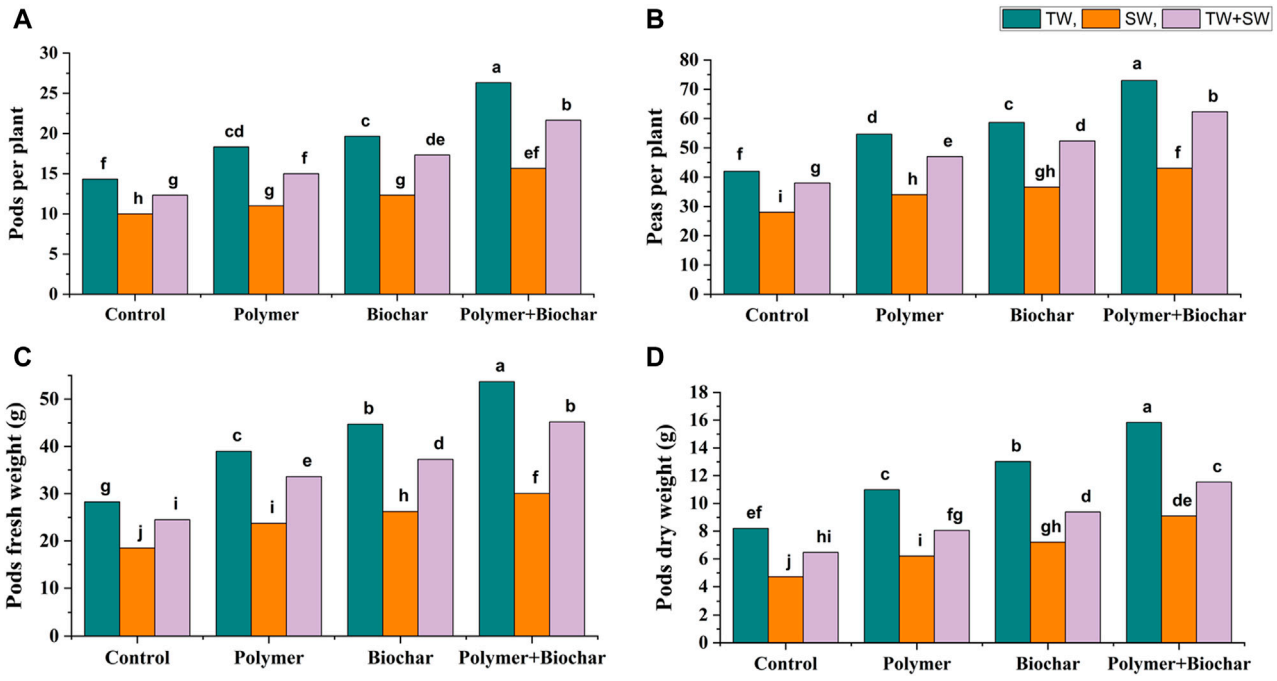

FIGURE 3
Synergistic use of biochar and polymer on pea pods per plant **(A)**, peas per plant **(B)**, pod fresh weight **(C)**, and pod dry weight **(D)** of *Pisum sativum* upon application of sewage water. Here, TW, SW, and TW + SW represent tap water, sewage water, and tap water + sewage water, respectively. The values are presented as mean (n = 3). The values sharing the same letter(s) in bars are statistically non-significant with each other at $p < 0.05$.

Physiological analyses

The combined effect of polymer and BC showed a maximum increase in chlorophyll contents by 75%, 62%, and 69% in treatments receiving TW, SW, and TW + SW, respectively (Figure 2A) and a maximum RWC of 75%, 58%, and 69% in treatments receiving TW, SW, and TW + SW, respectively (Figure 2B), in contrast to control. A maximum decline of 38% in EL (Figure 2C) and 53% in osmotic potential (Figure 2D) was found in plants when applied with polymer and BC in combination under irrigation of TW as compared to the control. However, irrigation with TW + SW also showed much reduced EL (30%) and osmotic potential (44%) in pea plants when polymer and BC were used in combination.

Yield analyses

A maximum yield was exhibited by the application of TW when a combination of polymer and BC was used for irrigation of pea plants. Data showed an increase of 84% in pea pods per plant (Figure 3A), 74% in pea per plant (Figure 3B), 90% in pods' fresh weight (Figure 3C), and 93% in pods' dry weight (Figure 3D) as compared to control, when TW was used with combined application of polymer and BC.

Chemical analyses

The data revealed that application of polymer and BC caused increased immobilization of Cd metal in soil by 56% in TW + SW-treated plants (Figure 4A), in contrast to the control. The plants irrigated with TW + SW showed a maximum decline of 43% in roots (Figure 4B), 49% in shoots (Figure 4C), and 91% in grain (Figure 4D), as compared to control when supplemented with both polymer and BC. Similarly, the application of TW + SW resulted in declined enrichment factor (0.013) and bioaccumulation coefficient (0.19), as illustrated in Figures 4E, F, respectively.

Supplementation of polymer and BC showed increased immobilization of Cr (Figure 5A) by 65% in soil, whereas reduced metal uptake of 51% in roots (Figure 5B), 51% in shoots (Figure 5C), and 94% in grains (Figure 5D), as compared to the control, was found in pea plants irrigated with TW + SW. Irrigation with TW + SW in pea plants receiving a combined dose of polymer and BC showed a decline in the Cr enrichment factor of 0.006 (Figure 5E) and Cr bioaccumulation coefficient of 0.14 (Figure 5F).

The data obtained from the phytoremediation-related parameters like enrichment factor and bioaccumulation coefficient for Cd (Figures 4E, F) and for Cr (Figures 5E, F) presented that all the plants treated with the combined use of polymer and BC showed significantly reduced accumulation of metals in plants irrigated with sewage water alone as well as mixing of sewage water with tap water. The health risk assessment parameters in pea plants irrigated with sewage water showed minimum values 0.000241 for DIM, 0.000482 for HQ, and 0.000635 for LCR for Cd metal (Table 1) and for Cr (Table 2) showed least value 0.000104 for DIM, 6.95E-05 for HQ, and 0.000209 for LCR, when polymer and BC were used in combination.

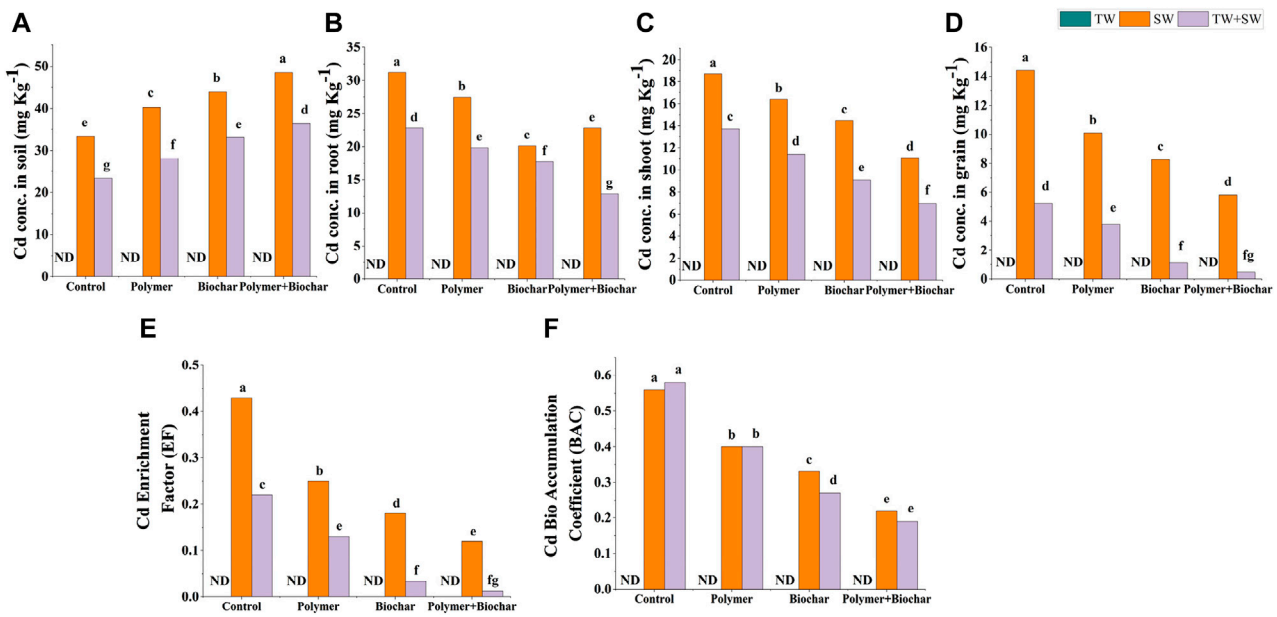

FIGURE 4
Synergistic use of biochar and polymer on Cd concentration (mg kg^{-1}) in soil **(A)**, root **(B)**, shoot **(C)**, grain **(D)**, EF **(E)**, and BAC **(F)** of *Pisum sativum* upon application of sewage water. Here, TW, SW, and TW + SW represent tap water, sewage water, and tap water + sewage water, respectively. The values are presented as mean (n = 3). The values sharing the same letter(s) in bars are statistically non-significant with each other at $p < 0.05$.

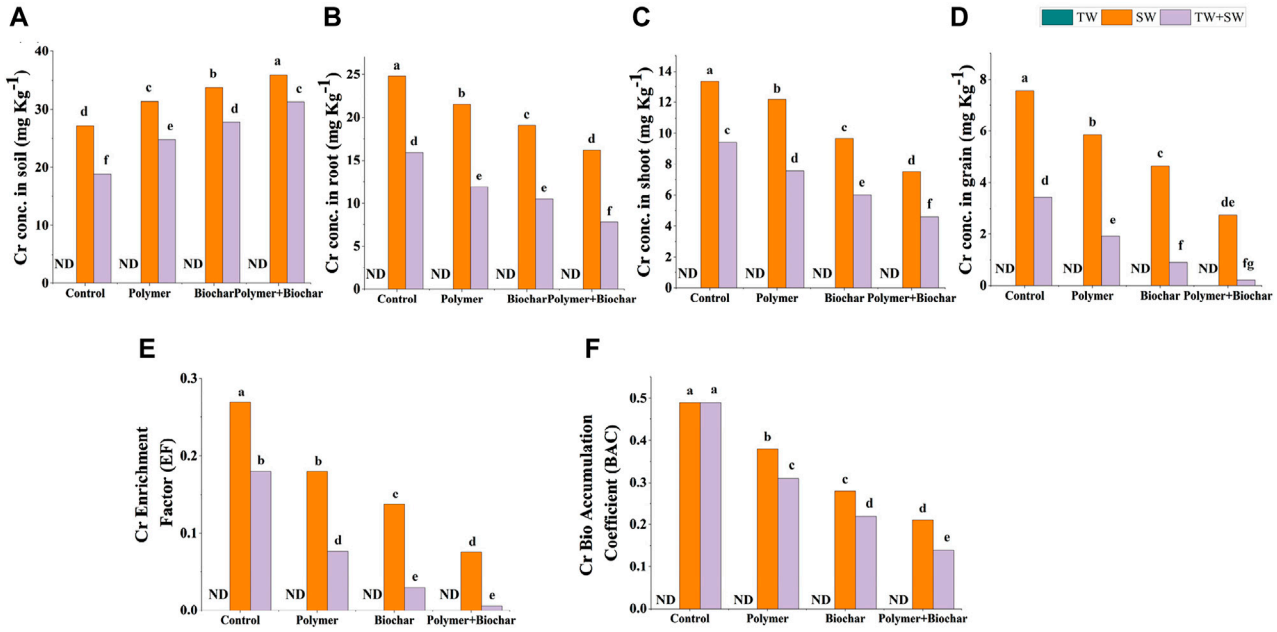

FIGURE 5
Synergistic use of biochar and polymer on Cr concentration (mg kg^{-1}) in soil **(A)**, root **(B)**, shoot **(C)**, grain **(D)**, EF **(E)**, and BAC **(F)** of *Pisum sativum* upon application of sewage water. Here, TW, SW, and TW + SW represent tap water, sewage water, and tap water + sewage water, respectively. The values are presented as mean (n = 3). The values sharing the same letter(s) in bars are statistically non-significant with each other at $p < 0.05$.

TABLE 1 Values of average daily intake of metal (DIM; mg kg^{-1} day^{-1}), hazard quotient (HQ), and lifetime cancer risk (LCR) for cadmium (Cd) concentration in the grain of pea plants (coarse and fine) grown in sewage wastewater.

Treatment		DIM	HQ	LCR
Tap water	Control	ND	ND	ND
	Polymer	ND	ND	ND
	Biochar	ND	ND	ND
	Polymer + biochar	ND	ND	ND
Sewage water	Control	0.007054	0.014109	0.018564
	Polymer	0.00494	0.009879	0.012999
	Biochar	0.004044	0.008087	0.010641
	Polymer + biochar	0.002846	0.005692	0.00749
Tap + sewage water	Control	0.002572	0.005145	0.00677
	Polymer	0.001861	0.003721	0.004896
	Biochar	0.000556	0.001111	0.001462
	Polymer + biochar	0.000241	0.000482	0.000635

Here, ND represents not detected. The values are mean of three replications.

TABLE 2 Values of average daily intake of metal (DIM; mg kg^{-1} day^{-1}), hazard quotient (HQ), and lifetime cancer risk (LCR) for chromium (Cr) concentration in grain of pea plants (coarse and fine) grown in sewage wastewater.

Treatment		DIM	HQ	LCR
Tap water	Control	ND	ND	ND
	Polymer	ND	ND	ND
	Biochar	ND	ND	ND
	Polymer + biochar	ND	ND	ND
Sewage water	Control	0.003695	0.002463	0.00739
	Polymer	0.002864	0.001909	0.005727
	Biochar	0.002272	0.001515	0.004545
	Polymer + biochar	0.001343	0.000895	0.002685
Tap + Sewage water	Control	0.001678	0.001119	0.003356
	Polymer	0.000935	0.000623	0.00187
	Biochar	0.000446	0.000298	0.000893
	Polymer + Biochar	0.000104	6.95E-05	0.000209

Here, ND represents not detected. The values are mean of three replications.

Correlation and principal component analysis (PCA) of pea plants under various treatments

The Pearson correlation analysis of pea plants under the application of different treatments showed a positive correlation among different parameters of growth, yield, and physiological activities, as shown in Figure 6. There is a strong correlation (1) among parameters like SL (shoot length), RL (root length), SFWT (shoot fresh weight), RFWT (root fresh weight), SDWT (shoot dry weight), RDWT (root dry weight), P-pp (pods per plant), NP-pp (number of peas per plants), P-FWT (pea fresh weight), P-DWT (pea dry weight), T. Chl. (total chlorophyll), and RWC (relative water contents) under application of different treatments, whereas EL (electrolyte leakage) and O.P (osmotic potential), S-Cd (Cd in soil), S-Cr (Cr in soil), R-Cd (Cd in root), Sh-Cd (Cd in shoot), G-Cd (Cd in grain), R-Cr (Cr in root), Sh-Cr (Cr in shoot), and G-Cr (Cr in grains) showed a negative correlation with growth, yield, and physiological parameters.

The PCA of treatments and parameters has been displayed in Figure 7. The growth, yield, and physiological parameters like SL (shoot length), RL (root length), SFWT (shoot fresh weight), RFWT (root fresh weight), SDWT (shoot dry weight), RDWT (root dry weight), P-pp (pods per plant), NP-pp (number of peas per plants), P-FWT (pea fresh weight), P-DWT (pea dry weight), T. Chl. (total chlorophyll), and RWC (relative water contents) are strongly correlated with each other. However, EL (electrolyte leakage) and O.P (osmotic potential) are negatively correlated with growth, yield, and physiological parameters of pea plants. The heavy metal analysis showed that parameters of S-Cd (Cd in soil) and S-Cr (Cr in soil) are very strongly correlated with each other and negatively correlated with growth, yield, and physiological parameters of pea plants under different treatments. The parameters like R-Cd (Cd in root), Sh-Cd (Cd in the shoot), G-Cd (Cd in grain), R-Cr (Cr in root), Sh-Cr (Cr in the shoot), and G-Cr (Cr in grains) are also negatively correlated with growth, yield, and physiological parameters.

Discussion

Contamination of soil with potentially toxic elements has been responsible for an indisputable impact on the plants inhabiting polluted soil. However, the impact of toxicity caused by these pollutants on plants amended with BC and polymer in metal-contaminated soils remains unclear and is, therefore, the subject of the present research.

The soil without amendments and irrigated with different levels of sewage water showed reduced shoot and root length, shoot fresh and dry weight, and root fresh and dry weight in pea plants (Figure 1) due to the presence of heavy metals like cadmium (Cd) and chromium (Cr). Various researchers reported reduced growth parameters under PTE stress (Gill and Tuteja, 2010; Maqbool et al., 2018; Naveed et al., 2021; Sabir et al., 2022a). Cr toxicity inhibits cell division and elongation in plant root cells (Adrees et al., 2015), thus reducing the root surface area for enhanced water and nutrient uptake from the soil (Medda and Mondal, 2017; Ahmad et al., 2020) and ultimately growth and biomass production. Our findings are supporting by those of studies by Jun et al. (2009) and Naveed et al. (2021) that Cr-contaminated soil reduced shoot length, root growth, and biomass production in cereals, vegetables, and forages.

The structural and functional properties of BC and polymers are well known to stimulate the growth of plants under metal stress. The high cation exchange capacity, water-holding capacity, and gradual release of nutrients by the polymer and BC facilitated increased growth in pea plants. Results showed that the application of polymer and BC significantly ($p< 0.05$) improved the growth attributes of pea plants (Figure 1) in both sewage water- and tap + sewage water-contaminated soils. The polymer has a large surface area with various functional properties like high nutrient and water-holding

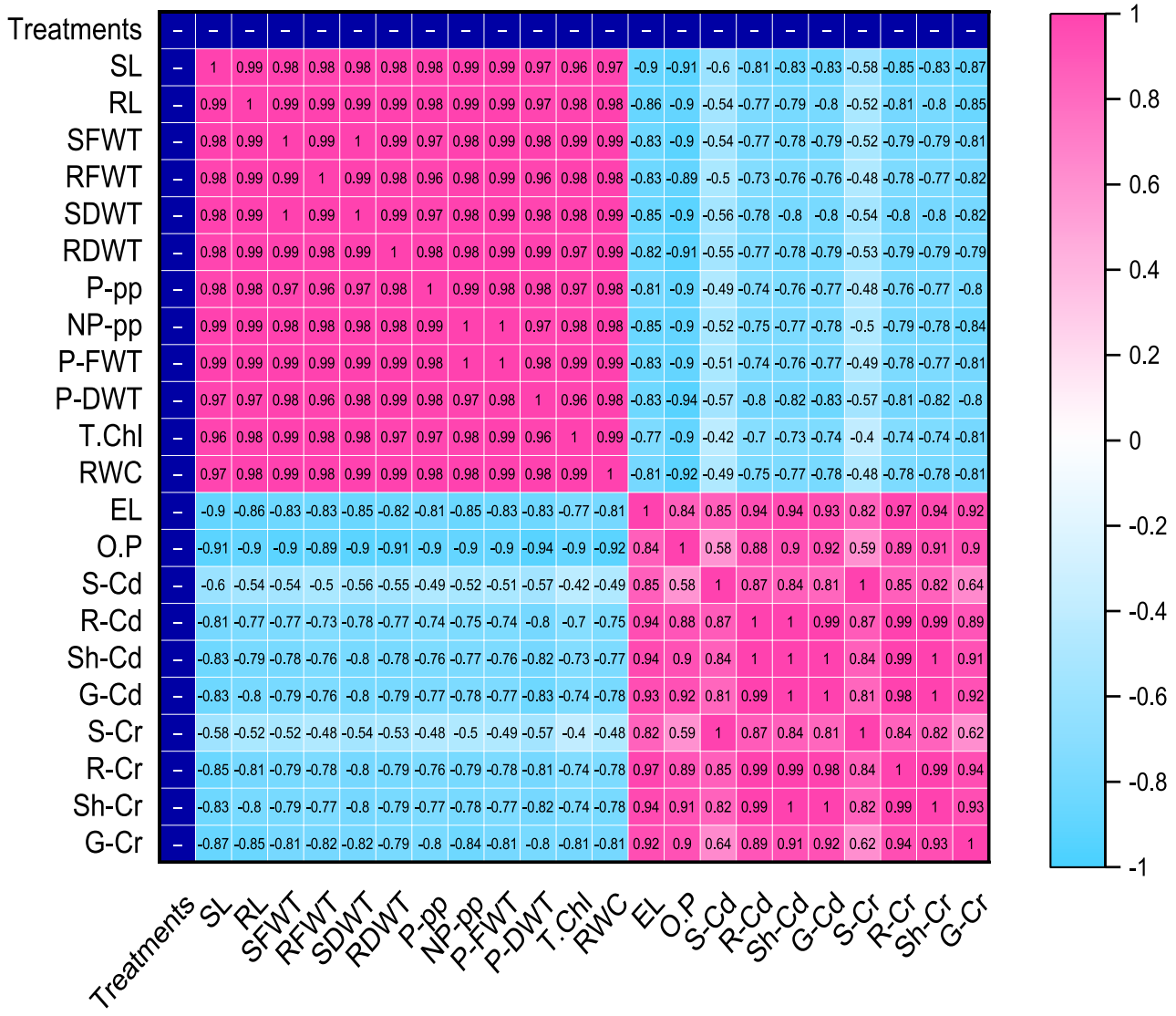

FIGURE 6
Pearson correlation analysis of pea plant growth, yield, physiology, and heavy metal concentration under application of different treatments. Here, SL (shoot length), RL (root length), SFWT (shoot fresh weight), RFWT (root fresh weight), SDWT (shoot dry weight), RDWT (root dry weight), P-pp (pods per plant), NP-pp (number of peas per plants), P-FWT (pea fresh weight), P-DWT (pea dry weight), T. Chl. (total chlorophyll), RWC (relative water contents), EL (electrolyte leakage), O.P (osmotic potential), S-Cd (Cd in soil), R-Cd (Cd in root), Sh-Cd (Cd in shoot), G-Cd (Cd in grain), S-Cr (Cr in soil), R-Cr (Cr in root), Sh-Cr (Cr in shoot), and G-Cr (Cr in grains) are the parameters analyzed.

capacity with slow release. These characteristics help in the provision of nutrients and water upon need (Zhang et al., 2013). BC is a porous material produced from the pyrolysis of biomass and hence restores the macro and micronutrients in BC. Rafique et al. (2020) reported that polymer-treated BC increased the growth of plants under Cr toxicity. Our finding of increased biomass and length of pea plants with the application of polymer and BC under sewage water irrigation aligns with those of the previous studies (Wang and Xu, 2013; Rafique et al., 2021). Therefore, the combined application of polymer and BC showed significant growth of peas under irrigation with tap and sewage-contaminated water.

The application of metal-contaminated sewage water reduced physiological attributes such as chlorophyll contents and relative water contents, while increasing electrolyte leakage and osmotic potential (Figure 2). The reduced physiological attributes could be due to continuous irrigation using low water quality, which may lead to an accumulation of PTE in soil and plants (El-Hassanin et al., 2020), which disrupts plant physiology due to production of ROS that oxidizes biomolecules under heavy metal stress (Sabir et al., 2022b) and threatens soil biology, like plant growth promoting bacteria, soil enzymes, organic matter contents, and nutrients and water contents in soil (Ahmad et al., 2013; Cheng et al., 2020). These factors have a great impact on various plant physiological activities. Previous studies also confirm this finding (Ali et al., 2018; Saffan et al., 2022).

The presence of nutrients and organic matter in sewage water improved physical and chemical properties along with the increased nutrient status of soil, therefore triggering improved physiological activities of pea plants when polymer and BC were used. The immobilized PTE by polymer and BC showed enhanced chlorophyll contents and relative water contents, with reduced electrolyte leakage and

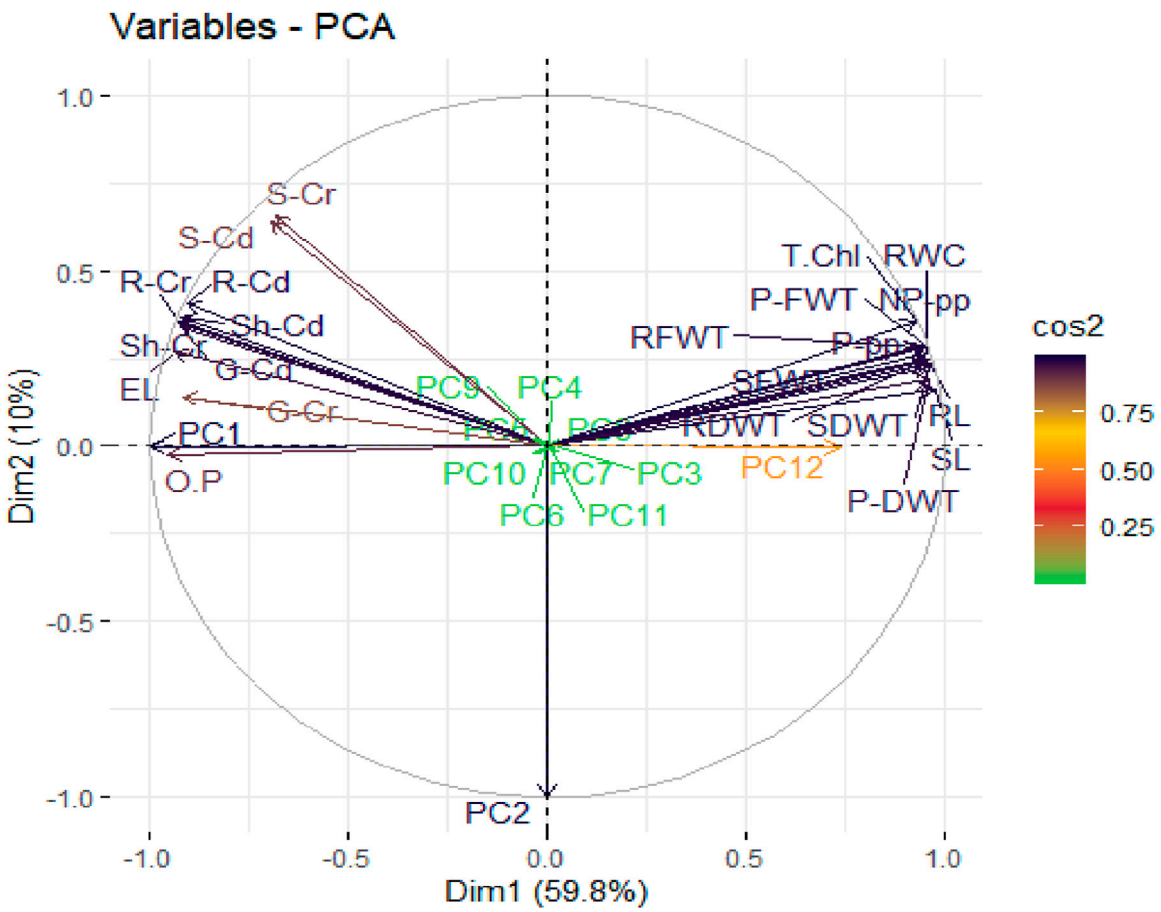

FIGURE 7
Principal component analysis (PCA) of plant growth, yield, and physiological properties as well as concentration of heavy metals in soil and plants. Biplot showing scores in the first two principal components (PC1 and PC2) for the maximum presentation of data components correlated with treatments and parameters like SL (shoot length), RL (root length), SFWT (shoot fresh weight), RFWT (root fresh weight), SDWT (shoot dry weight), RDWT (root dry weight), T. Chl. (total chlorophyll), RWC (relative water contents), P-pp (pods per plant), NP-pp (number of peas per plants), P-FWT (pea fresh weight), EL (electrolyte leakage), O.P (osmotic potential), S-Cd (Cd in soil), R-Cd (Cd in root), Sh-Cd (Cd in shoot), G-Cd (Cd in grain), S-Cr (Cr in soil), R-Cr (Cr in root), Sh-Cr (Cr in shoot), and G-Cr (Cr in grains).

osmotic potential in pea plants under sewage water irrigation. This finding is aligned with previous findings (Arshad et al., 2017; Waheed et al., 2019) that wastewater irrigation significantly augmented organic matter contents, which comprises numerous types of organic compounds and inducing fertility of soil with immobilized PTE, thus inducing a positive response on overall plant physiology (Figure 7). Thus, with notable nutrients and organic matter content, the usage of sewage water is encouraged by researchers (Akbar et al., 2021; Naseem et al., 2022).

The use of sewage water for irrigation of pea plants reduces the yield of pea plants (Figure 3). The presence of PTE and salts among various pollutants significantly affects the development of pea pods and pea grains when sewage water was applied. The pollutants in sewage water reduced the nutrient uptake, which caused an imbalanced uptake of nutrients. This could lead to poor development of plant tissues, and hence yield was compromised. However, with the application of BC and polymer, pea plants showed increased yield when sewage water was applied with tap water (Figure 3). A significant increase in yield was observed with the combined use of polymer and BC when tap water was mixed with sewage water for irrigation. Functional groups like hydroxyl and carboxylic functional groups facilitate metal binding (Mehmood et al., 2021; Murtaza et al., 2021).

Moreover, the high surface area of both BC and polymers provides more adsorption sites for heavy metal binding, whereas increased adsorption of PTE by polymer due to electrostatic interactions (Inyang et al., 2010; Nigussie et al., 2012) resulted in reduced metal content in soil. BC and polymer ensured the uptake of nutrients in plants essential for the proper functioning of plants, which resulted in improved development of pea plants and hence enhanced the yield of pea plants (Jun et al., 2009). Application of BC affected soil properties like pH, cation exchange capacity (CEC), soil organic matter, and nutrient availability and ultimately increased soil fertility and plant growth (Agegnehu et al., 2015).

Reduced Cr and Cd uptake in root, shoot, and grains of pea plants was found with application of amendment polymer and BC when sewage water was applied for irrigation. These amendments helped in the mitigation of the toxicity of sewage water and hence immobilized the metals Cr (Figure 4) and Cd (Figure 5). The presence of oxygenated and hydrogenated functional groups on the BC surface might have formed complexation with CrVI and reduced its availability (Beesley et al., 2014; Niamat et al., 2019). Moreover, it is reported that Cr VI is converted to Cr III by BC, hence reducing the toxicity (Shahid et al., 2017; Wang et al., 2019).

It was found that BC immobilized soil Cr, thus reducing its bioavailability, which is consistent with the findings of Islam et al. (2021). Moreover, lower plant availability of CrVI, as affected by applied BC, could be due to the presence of more active and binding sites on the BC's surface, which strengthens its ability in fixing PTE (Ekebafe et al., 2012; Wang et al., 2015). Moreover, BC can reduce PTE bioavailability by influencing soil pH, water contents, adsorption, and changing HM redox state (Ditta et al., 2016; Rizwan et al., 2016; Cheng et al., 2020).

Polymers have remedial potential due to the presence of ionic functional groups, which help in their bonding with PTE (Dhiman et al., 2015). Polymers have significant potential to adsorb water in comparison to other conventional adsorbents. Acrylamide base polymer showed effective remediation (>75%) of PTE cadmium, cobalt, copper, and nickel from water (Moreno-Sader et al., 2019). The presence of highly dense metal chelating groups in some polymers made them perfect for the immobilization of PTE in soil, and hence reducing their bioavailability. The reduced uptake of Cd and Cr in pea plants in our study is supported by these findings. Moreover, all treatments receiving SW alone as well as TW + SW showed values of EF and BAC less than 1, for both Cd (Figures 4E, F) and Cr (Figures 5E, F) in pea plants. The health risk assessment parameters of DIM, HQ, and LCR for Cd (Table 1) and for Cr (Table 2) showed that consumption of pea plants irrigated with TW + SW in the presence of polymers and BC is safe.

Conclusion

We found that the application of sewage water negatively influenced growth, physiological parameters, and yield of the pea plant. Combined application of BC and polymer significantly alleviated PTE (i.e., Cd and Cr) stress and enhanced the growth and yield of pea plants. The combined impact of BC and polymer enhanced the immobilization of PTEs like Cd and Cr in soil, which ultimately resulted in reduced bioaccumulation of PTE in pea plants irrigated with sewage water. Moreover, the usage of same amendments significantly reduced the health risks associated with the consumption of pea plants under Cd and Cr stress, as indicated by the lowest values of DIM, HQ, and LCR, when sewage water was used for irrigation. In conclusion, the application of PAM-BC association could serve as an effective approach in mitigating the toxicity of PTE in pea plants irrigated with TW + SW by immobilization of PTE and their associated health risks. Application of BC and PAM could be used as a potential approach to remediate sewage water toxicity and improve growth and yield of plants. The impact of BC and PAM, both as individual and combined application, on soil quality should be studied at the molecular level. More studies should be conducted to find the optimized dose rate to promote soil microbial activity, plant growth, and immobilization of PTE with use of tap water + sewage water for irrigation.

Data availability statement

The original contributions presented in the study are included in the article/Supplementary Material; further inquiries can be directed to the corresponding author.

Author contributions

MN: conceptualization, data curation, formal analysis, software, and writing–original draft. MF: data curation, investigation, and writing–original draft. ZN: data curation, methodology, software, and writing–review and editing. ZA: conceptualization, formal analysis, supervision, and writing–review and editing. A-RZG: software and writing–review and editing. MS: data curation, investigation, and writing–review and editing. QF: formal analysis, software, and writing–review and editing. MH: software and writing–review and editing. MK: investigation, methodology, software, and writing–review and editing. DS: methodology, software, and writing–review and editing. AM: conceptualization, supervision, and writing–review and editing.

Funding

The author(s) declare that financial support was received for the research, authorship, and/or publication of this article. This study was supported by the Researchers Supporting Project number (RSPD2024R686), King Saud University, Riyadh, Saudi Arabia.

Acknowledgments

The authors would like to extend their sincere appreciation to the Researchers Supporting Project number (RSPD2024R686), King Saud University, Riyadh, Saudi Arabia. The authors also extend their appreciation to Higher Education Islamabad (NRPU6443), Pakistan.

Conflict of interest

The authors declare that the research was conducted in the absence of any commercial or financial relationships that could be construed as a potential conflict of interest.

Publisher's note

Supplementary material

The Supplementary Material for this article can be found online at: https://www.frontiersin.org/articles/10.3389/fenvs.2024.1380867/full#supplementary-material

References

Abbas, W., Bokhari, T. H., Bhatti, I. A., Iqbal, M., Usman, M., Bukhari, H. I., et al. (2015). Impact of UV/TiO2/H2O2 on degradation of disperse red F3BS. *Asian J. Chem.* 27, 282–286. doi:10.14233/ajchem.2015.17553

Adebayo, R. K., Hassan, U. F., Adamu, H. M., Hassan, H. F., Baba, H., and Ajiya, D. A. (2020). Levels of heavy metals and their health risk assessment from wastewater irrigated spinach in railway quarters, Bauchi, Bauchi state, Nigeria. *Int. J. Adv. Chem. Res.* 2, 12–17. doi:10.33545/26646781.2020.v2.i2a.22

Adrees, M., Ali, S., Iqbal, M., Bharwana, S. A., Siddiqi, Z., Farid, M., et al. (2015). Mannitol alleviates chromium toxicity in wheat plants in relation to growth, yield, stimulation of anti-oxidative enzymes, oxidative stress and Cr uptake in sand and soil media. *Ecotoxicol. Environ. Saf.* 122, 1–8. doi:10.1016/j.ecoenv.2015.07.003

Agegnehu, G., Bass, A. M., Nelson, P. N., Muirhead, B., Wright, G., and Bird, M. I. (2015). Biochar and biochar-compost as soil amendments: effects on peanut yield, soil properties and greenhouse gas emissions in tropical North Queensland, Australia. *Austr. Agric. Ecosyst. Environ.* 213, 72–85. doi:10.1016/j.agee.2015.07.027

Ahmad, I., Tahir, M., Daraz, U., Ditta, A., Hussain, M. B., and Khan, Z. U. H. (2020). *Responses and tolerance of cereal crops to metals and metalloids toxicity in Agronomic Crops*. Editor H. Mirza (Singapore: Springer), 235–264.

Ahmad, M., Rajapaksha, A. U., Lim, J. E., Zhang, M., Bolan, N., Mohan, D., et al. (2013). Biochar as a sorbent for contaminant management in soil and water: a review. *Chemosphere* 99, 19–33. doi:10.1016/j.chemosphere.2013.10.071

Akbar, S., Ali, Z., Hussain, S., Mohammad, A., Riaz, Y., Shakeel, A., et al. (2021). Metal accumulation potential, human health risks, and yield attributes of hundred bread wheat genotypes on irrigation with municipal and remediated wastewater. *Environ. Sci. Pollut. Res.* 28, 35023–35037. doi:10.1007/s11356-021-13085-4

Ali, S., Rizwan, M., Bano, R., Bharwana, S. A., Ur Rehman, M. Z., Hussain, M. B., et al. (2018). Effects of biochar on growth, photosynthesis, and chromium (Cr) uptake in Brassica rapa L. under Cr stress. *Arab. J. Geosci.* 11, 1–9. doi:10.1007/s12517-018-3861-3

Allegre, C., Maisseu, M., Charbit, F., and Moulin, P. (2004). Coagulation–flocculation–decantation of dye house effluents: concentrated effluents. *J. Hazard. Mater.* 16, 57–64. doi:10.1016/j.jhazmat.2004.07.005

Al-Wabel, M. I., Usman, A. R. A., Al-Farraj, A. S., Ok, Y. S., Abduljabbar, A., Al-Faraj, A. I., et al. (2017). Date palm waste biochars alter a soil respiration, microbial biomass carbon, and heavy metal mobility in contaminated mined soil. *Environ. Geochem. Health* 41, 1705–1722. doi:10.1007/s10653-017-9955-0

Arshad, M., Khan, A. H. A., Hussain, I., Anees, M., Iqbal, M., Soja, M. G., et al. (2017). The reduction of chromium (VI) phytotoxicity and phytoavailability to wheat (*Triticum aestivum* L.) using biochar and bacteria. *Appl. Soil Ecol.* 114, 90–98. doi:10.1016/j.apsoil.2017.02.021

ASABE (2011). *S593.1: terminology and definitions for biomass production, harvesting and collection, storage, processing, conversion, and utilization*. St. Joseph, MI: ASABE.

Barrs, H. D., and Watherley, P. E. (1968). A re-examination of the relative turgidity technique for estimating water deficit in leaves. *Aust. J. Biol. Sci.* 15, 413–428.

Beckett, C. T. S., and Augarde, C. E. (2013). Prediction of soil water retention properties using pore-size distribution and porosity. *Can. Geotech. J.* 50, 435–450. doi:10.1139/cgj-2012-0320

Beesley, L., Inneh, O. S., Norton, G. J., Moreno-Jimenez, E., Pardo, T., Clemente, R., et al. (2014). Assessing the influence of compost and biochar amendments on the mobility and toxicity of metals and arsenic in a naturally contaminated mine soil. *Environ. Pollut.* 186, 195–202. doi:10.1016/j.envpol.2013.11.026

Cheng, S., Chen, T., Xu, W., Huang, J., Jiang, S., and Yan, B. (2020). Application research of biochar for the remediation of soil heavy metals contamination: a review. *Molecules* 25, 3167. doi:10.3390/molecules25143167

Coelho, M. A., Fusconi, R., Pinheiro, L., Ramos, I. C., and Ferreira, A. S. (2018). The combination of compost or biochar with urea and NBPT can improve nitrogen-use efficiency in maize. *An. Braz. Acad. Sci.* 90, 1695–1703. doi:10.1590/0001-3765201820170416

de-Bashan, L. E., and Bashan, Y. (2010). Immobilized microalgae for removing pollutants: review of practical aspects. *Bioresour. Technol.* 101, 1611–1627. doi:10.1016/j.biortech.2009.09.043

Dhiman, J., Prasher, S., Mannan, A., ElSayed, E., and Nzediegwu, C. (2015) "Use of super absorbent polymers (hydrogels) to promote safe use of wastewater in agriculture," in *Proc. 22nd Canadian hydrotechnical conf. On water for sustainable development: coping with climate and environmental changes*. Montreal, QC, Canada: Canadian Society of Civil Engineers.

Dhiman, J., Prasher, S. O., ElSayed, E., Patel, R., Nzediegwu, C., and Mawof, A. (2020). Use of polyacrylamide superabsorbent polymers and plantain peel biochar to reduce heavy metal mobility and uptake by wastewater-irrigated potato plants. *Amer. Soc. Agri. Biol. Engin.* 63 (1), 11–28. doi:10.13031/trans.13195

Ditta, A., and Khalid, A. (2016). "Bio-organo-phos: a sustainable approach for managing phosphorus deficiency in agricultural soils," in *Organic Fertilizers - from Basic Concepts to Applied Outcomes*. Editors M. Larramendy and S. Soloneski (Croatia: In Tech), 109–136. doi:10.5772/62473

Ekebafe, L. O., Ogbeifun, D. E., and Okieimen, F. E. (2012). Effect of cassava starch hydrogel on the water requirement of maize (*Zea may*) seedlings and selected properties of sandy loam soil. *Int. J. Basic. Appl. Sci.* 1, 132–139.

Ekere, N. R., Ugbor, M. C. J., Ihedioha, J. N., Ukwueze, N. N., and Abugu, H. O. (2020). Ecological and potential health risk assessment of heavy metals in soils and food crops grown in abandoned urban open waste dump site. *J. Environ. Health Sci. Eng.* 18, 711–721. doi:10.1007/s40201-020-00497-6

El-Hassanin, A. S., Samak, M. R., Abdel-Rahman, G. N., Abu-Sree, Y. H., and Saleh, E. M. (2020). Risk assessment of human exposure to lead and cadmium in maize grains cultivated in soils irrigated either with low-quality water or freshwater. *Toxicol. Rep.* 7, 10–15. doi:10.1016/j.toxrep.2019.11.018

FAO. AQUASTAT (2016). *FAO's information system on water and agriculture*. Rome, Italy: United Nations FAO. Available at: https://www.fao.org/nr/water/aquastat/water_use/index.stm#maps.

Fuerhacker, M., and Haile, T. M. (2010). "Treatment and reuse of sludge," in *Waste water treatment and reuse in the mediterranean region*. Editors D. Barceló and M. Petrovic (Berlin Heidelberg: Springer-Verlag), 63–92.

Gill, S. S., and Tuteja, N. (2010). Reactive oxygen species and antioxidant machinery in abiotic stress tolerance in crop plants. *Plant Physiol. Biochem.* 48, 909–930. doi:10.1016/j.plaphy.2010.08.016

Huttermann, A., Orikiriza, L. J., and Agaba, H. (2009). Application of superabsorbent polymers for improving the ecological chemistry of degraded or polluted lands. *Clean. - Soil Air Water* 37 (7), 517–526. doi:10.1002/clen.200900048

Inyang, M., Gao, B., Pullammanappallil, P., Ding, W., and Zimmerman, A. R. (2010). Biochar from anaerobically digested sugarcane bagasse. *Bioresour. Technol.* 101, 8868–8872. doi:10.1016/j.biortech.2010.06.088

Inyang, M. I., Gao, B., Yao, Y., Xue, Y., Zimmerman, A., Mosa, A., et al. (2016). A review of biochar as a low-cost adsorbent for aqueous heavy metal removal. *Crit. Rev. Environ. Sci. Tech.* 46 (4), 406–433. doi:10.1080/10643389.2015.1096880

Islam, M. R., Hu, Y. G., Mao, S. S., Mao, J. Z., Eneji, A. E., and Xue, X. Z. (2011). Effectiveness of a water-saving super-absorbent polymer in soil water conservation for corn (Zea Mays L.) based on eco-physiological parameters. *J. Sci. Food Agri.* 91 (11), 1998–2005. doi:10.1002/jsfa.4408

Islam, S. N., Rahman, M. L., Tareq, M. Z., Mostofa, B., Karim, M. M., Sultana, A., et al. (2021). Nutrient combination with biochar: improving yield and quality of jute seed. *Malays. J. Sustain. Agric.* 5, 43–50. doi:10.26480/mjsa.01.2021.43.50

Jan, A. U., Hadi, F., Shah, A., Ditta, A., Nawaz, M. A., and Tariq, A. (2021). Plant growth regulators, and EDTA improve phytoremediation potential and antioxidant response of Dysphania ambrosioides (L.) Mosyakin & Clemants in a Cd-spiked soil. *Environ. Sci. Pollut. Res.* 28, 43417–43430. doi:10.1007/s11356-021-13772-2

Jiang, Y., Wen, H., Zhang, Q., Yuan, L., and Liu, L. (2022). Source apportionment and health risk assessment of potentially toxic elements in soil from mining areas in northwestern China. *Environ. Geochem. Health* 44, 1551–1566. doi:10.1007/s10653-021-00907-0

Jun, R., Ling, T., and Guanghua, Z. (2009). Effects of chromium on seed germination, root elongation and coleoptile growth in six pulses. *Int. J. Environ. Sci. Technol.* 6, 571–578. doi:10.1007/bf03326097

Khalid, S., Shahid, M., Natasha., Bibi, I., Sarwar, T., Shah, A. H., et al. (2018). A review of environmental contamination and health risk assessment of wastewater use for crop irrigation with a focus on low and high-income countries. *Int. J. Environ. Res. Public Health.* 15 (5), 895. doi:10.3390/ijerph15050895

Khan, S., Cao, Q., Zheng, Y. M., Huang, Y. Z., and Zhu, Y. G. (2008). Health risks of heavy metals in contaminated soils and food crops irrigated with wastewater in Beijing, China. *Environ. Pollut.* 152 (3), 686–692. doi:10.1016/j.envpol.2007.06.056

Latif, A., Bilal, M., Asghar, W., Azeem, M., Ahmad, M. I., Abbas, A., et al. (2018). Heavy metal accumulation in vegetables and assessment of their potential health risk. *J. Environ. Ana. Chem.* 5, 234. doi:10.4172/2380-2391.1000234

Lehmann, J. (2007). Bio-energy in the black. *Front. Ecol. Environ.* 5, 381–387. doi:10.1890/1540-9295(2007)5[381:bitb]2.0.co;2

Li, R., Hou, X., Li, P., and Wang, X. (2022). Multifunctional superabsorbent polymer under residue incorporation increased maize productivity through improving sandy soil properties. *Advan. Polym. Technol.* 2022, 1–12. doi:10.1155/2022/6554918

Liu, Z. X., Miao, Y. G., Wang, Z. Y., and Yin, G. H. (2009). Synthesis and characterization of a novel super-absorbent based on chemical modified pulverized wheat straw and acryl.

Lorestani, B., Cheraghi, M., and Yousefi, N. (2011). Accumulation of Pb, Fe, Mn, Cu and Zn in plants and choice of hyperaccumulator plant in the industrial town of Vian, Iran. *Arch. Biol. Sci.* 63, 739–745. doi:10.2298/abs1103739l

Maqbool, A., Ali, S., Rizwan, M., Ishaque, W., Rasool, N., Ur Rehman, M. Z., et al. (2018). Management of tannery wastewater for improving growth attributes and reducing chromium uptake in spinach through citric acid application. *Environ. Sci. Pollut. Res.* 25, 10848–10856. doi:10.1007/s11356-018-1352-4

Medda, S., and Mondal, N. K. (2017). Chromium toxicity and ultrastructural deformation of Cicer arietinum with special reference of root elongation and coleoptile growth. *Ann. Agrar. Sci.* 15, 396–401. doi:10.1016/j.aasci.2017.05.022

Mehmood, S., Wang, X., Ahmed, W., Imtiaz, M., Ditta, A., Rizwan, M., et al. (2021). Removal mechanisms of slag against potentially toxic elements in soil and plants for sustainable agriculture development: a critical review. *Sustainability* 13, 5255. doi:10.3390/su13095255

Mohan, D., Sarswat, A., Ok, Y. S., and Pittman, C. U. (2014). Organic and inorganic contaminants removal from water with biochar, a renewable, low cost, and sustainable adsorbent: a critical review. *Bioresour. Tech.* 160, 191–202. doi:10.1016/j.biortech.2014.01.120

Moreno-Sader, K., García-Padilla, A., Realpe, A., Acevedo-Morantes, M., and Soares, J. B. P. (2019). Removal of heavy metal water pollutants (Co^{2+} and Ni^{2+}) using polyacrylamide/sodium montmorillonite (PAM/Na-MMT) nanocomposites. *ACS Omega* 4, 10834–10844. doi:10.1021/acsomega.9b00981

Murtaza, G., Ditta, A., Ullah, N., Usman, M., and Ahmed, Z. (2021). Biochar for the management of nutrient impoverished and metal contaminated soils: preparation, applications, and prospects. *J. Soil Sci. Plant Nutr.* 21, 2191–2213. doi:10.1007/s42729-021-00514-z

Naseem, Z., Naveed, M., Asghar, H. N., and Hameed, M. (2022). Metal resistant *Enterobacter cloacae* ZA14 enhanced seedling vigor and metal tolerance through improved growth, physiology and antioxidants in tomato (*Solanum lycopersicum*) irrigated with textile effluents. *Sustainability* 14, 13619. doi:10.3390/su142013619

Naseem, Z., Naveed, M., Imran, M., Saqlain, M., Asif, M., Bashir, M., et al. (2023). Elucidating the potential of dye-degrading *Enterobacter cloacae* ZA14 for cultivation of solanum lycopersicum plants with textile effluents. *Water* 15, 3163. doi:10.3390/w15173163

Naveed, M., Mustafa, A., Majeed, S., Naseem, Z., Saeed, Q., Khan, A., et al. (2020). Enhancing cadmium tolerance and pea plant health through *Enterobacter* sp. MN17 inoculation together with biochar and gravel sand. *Plants* 9, 530. doi:10.3390/plants9040530

Naveed, M., Tanvir, B., Xiukang, W., Brtnicky, M., Ditta, A., Kucerik, J., et al. (2021). Co-composted biochar enhances growth, physiological, and phytostabilization efficiency of *Brassica napus* and reduces associated health risks under chromium stress. *Front. Plant Sci.* 12, 775785. doi:10.3389/fpls.2021.775785

Niamat, B., Naveed, M., Ahmad, Z., Yaseen, M., Ditta, A., Mustafa, A., et al. (2019). Calcium-enriched animal manure alleviates the adverse effects of salt stress on growth, physiology and nutrients homeostasis of *Zea mays* L. *Plants* 8, 480. doi:10.3390/plants8110480

Nie, C., Yang, X., Niazi, N. K., Xu, X., Wen, Y., Rinklebe, J., et al. (2018). Impact of sugarcane bagasse-derived biochar on heavy metal availability and microbial activity: a field study. *Chemosphere* 200, 274–282. doi:10.1016/j.chemosphere.2018.02.134

Nigussie, A., Kissi, E., Misganaw, M., and Ambaw, G. (2012). Effect of biochar application on soil properties and nutrient uptake of lettuces (*Lactuca sativa*) grown in chromium polluted soils. Am-Eurasian. *J. Sustain. Agric.* 12, 369–376.

Nzediegwu, C., Prasher, S., Elsayed, E., Dhiman, J., Mawof, A., and Patel, R. (2019). Effect of biochar on heavy metal accumulation in potatoes from wastewater irrigation. *J. Environ. Manag.* 232, 153–164. doi:10.1016/j.jenvman.2018.11.013

Ok, Y. S., Chang, S. X., Gao, B., and Chung, H. J. (2015). SMART biochar technology—a shifting paradigm towards advanced materials and healthcare research. *Environ. Technol. Innov.* 4, 206–209. doi:10.1016/j.eti.2015.08.003

Qadir, M., Wichelns, D., Raschid-Sally, L., McCornick, P. G., Drechsel, P., Bahri, A., et al. (2010). The challenges of wastewater irrigation in developing countries. *Agric. Water. Mgmt.* 97 (4), 561–568. doi:10.1016/j.agwat.2008.11.004

Rafique, M. I., Ahmad, M., Al-Wabel, M. I., Ahmad, J., and Al-Farraj, A. S. (2022). Mitigating the toxic effects of chromium on wheat (*Triticum aestivum* L.) seed germination and seedling growth by using biochar and polymer-modified biochar in contaminated soil. *Sustainability.* 14, 16093. doi:10.3390/su142316093

Rafique, M. I., Usman, A. R., Ahmad, M., and Al-Wabel, M. I. (2021). Immobilization and mitigation of chromium toxicity in aqueous solutions and tannery waste-contaminated soil using biochar and polymer-modified biochar. *Chemosphere.* 266, 129198. doi:10.1016/j.chemosphere.2020.129198

Rafique, M. I., Usman, A. R., Ahmad, M., Sallam, A., and Al-Wabel, M. I. (2020). *In situ* immobilization of Cr and its availability to maize plants in tannery waste contaminated soil: effects of biochar feedstock and pyrolysis temperature. *J. Soils. Sediments.* 20, 330–339. doi:10.1007/s11368-019-02399-z

Rizova, V. A. (2020). Assessment of phytoremediation potential of indigenous plants growing around the solid waste open dumpsite. *Environ. Eng. Res.* 24, 234.

Rizwan, M., Ali, S., Qayyum, M. F., Ibrahim, M., Zia-ur-Rehman, M., Abbas, T., et al. (2016). Mechanisms of biochar-mediated alleviation of toxicity of trace elements in plants: a critical review. *Environ. Sci. Pollut. Res.* 23, 2230–2248. doi:10.1007/s11356-015-5697-7

RStudio Team (2021). *RStudio: integrated development environment for R; RStudio*. Boston, MA, USA: PBC. Available at: https://www.rstudio.com/(accessed on May 20, 2023).

Rusan, M. J. M., Hinnawi, S., and Rousan, L. (2007). Long-term effect of wastewater irrigation of forage crops on soil and plant quality parameters. *Desalination* 215 (1), 143–152. doi:10.1016/j.desal.2006.10.032

Sabir, M., Baltrenait-Gedien, E., Ditta, A., Ullah, H., Kanwal, A., Ullah, S., et al. (2022a). Bioaccumulation of heavy metals in a soil–plant system from an open dumpsite and the associated health risks through multiple routes. *Sustainability* 14, 13223. doi:10.3390/su142013223

Sabir, M., Naseem, Z., Ahmad, W., Usman, M., Nadeem, F., Saifullah, , et al. (2022b). Alleviation of adverse effects of nickel on growth and concentration of copper and manganese in wheat through foliar application of ascorbic acid. *Int. J. Phytoremed.* 24, 695–703. doi:10.1080/15226514.2021.1962801

Saffan, M. M., Koriem, M. A., El-Henawy, A., El-Mahdy, S., El-Ramady, H., Elbehiry, F., et al. (2022). Sustainable production of tomato plants (*Solanum lycopersicum* L.) under low-quality irrigation water as affected by bio-nanofertilizers of selenium and copper. *Sustainability* 14, 3236. doi:10.3390/su14063236

Shahid, M., Shamshad, S., Rafiq, M., Khalid, S., Bibi, I., Niazi, N. K., et al. (2017). Chromium speciation, bioavailability, uptake, toxicity and detoxification in soil-plant system: a review. *Chemosphere* 178, 513–533. doi:10.1016/j.chemosphere.2017.03.074

UNESCO (2016). *Water security*. Paris, France: United Nations Educational, Scientific, and Cultural Organization. Available at: https://www.unesco.org/new/en/naturalsciences/environment/water.

U.S. Department of Energy's Oak Ridge Operations Office (2011). *The risk assessment information system (RAI)*. Washington, D.C.: USDOE.

Waheed, H., Ilyas, N., Iqbal Raja, N., Mahmood, T., and Ali, Z. (2019). Heavy metal phyto-accumulation in leafy vegetables irrigated with municipal wastewater and human health risk repercussions. *Int. J. Phytoremediation* 21, 170–179. doi:10.1080/15226514.2018.1540547

Wang, G., and Xu, Z. (2013). The effects of biochar on germination and growth of wheat in different saline-alkali soil. *Asian Agric. Res.* 5, 116.

Wang, K., Qiu, G., Cao, H., and Jin, R. (2015). Removal of chromium (VI) from aqueous solutions using Fe3O4 magnetic polymer microspheres functionalized with amino groups. *Materials* 8, 8378–8391. doi:10.3390/ma8125461

Wang, X., Fan, J., Xing, Y., Xu, G., Wang, H., Deng, J., et al. (2019). The effects of mulch and nitrogen fertilizer on the soil environment of crop plants. *Adv. Agron.* 153, 121–173. doi:10.1016/bs.agron.2018.08.003

World Health Organization (2011). *Guidelines for drinking water quality*. 4th edition. Geneva, Switzerland.

Wolf, B. (1982). A comprehensive system of leaf analyses and its use for diagnosing crop nutrient status. *Comm. Soil Sci. Plant Anal.* 13, 1035–1059. doi:10.1080/00103628209367332

Yahaya, T. O., Oladele, E. O., Fatodu, I. A., Abdulazeez, A., and Yeldu, Y. I. (2020). The concentration and health risk assessment of heavy metals and microorganisms in the groundwater of Lagos, Southwest Nigeria. *J. Adv. Environ. Health Res.* 8, 234–242.

Yang, G., Rhodes, D., and Joly, R. J. (1996). Effect of high temperature on membrane stability and chlorophyll fluorescence in glycinebetaine-containing maize lines. *Aust. J. Plant Physiol.* 23, 431–443.

Zhang, J., Zhang, J., Wang, M., Wu, S., Wang, H., Niazi, N. K., et al. (2019). Effect of tobacco stem-derived biochar on soil metal immobilization and the cultivation of tobacco plant. *J. Soils Sediments* 19 (5), 2313–2321. doi:10.1007/s11368-018-02226-x

Zhang, R., Geng, G. J., and Bai, G. S. (2013). Effects of application rate of super absorbent polymers on soil moisture and Solanum lycopersicum growth. *Sci. Soil Water Conserv.* 11, 108–113.

Frontiers in Environmental Science

Explores the anthropogenic impact on our natural world

An innovative journal that advances knowledge of the natural world and its intersections with human society. It supports the formulation of policies that lead to a more inhabitable and sustainable world.

Discover the latest Research Topics

See more →

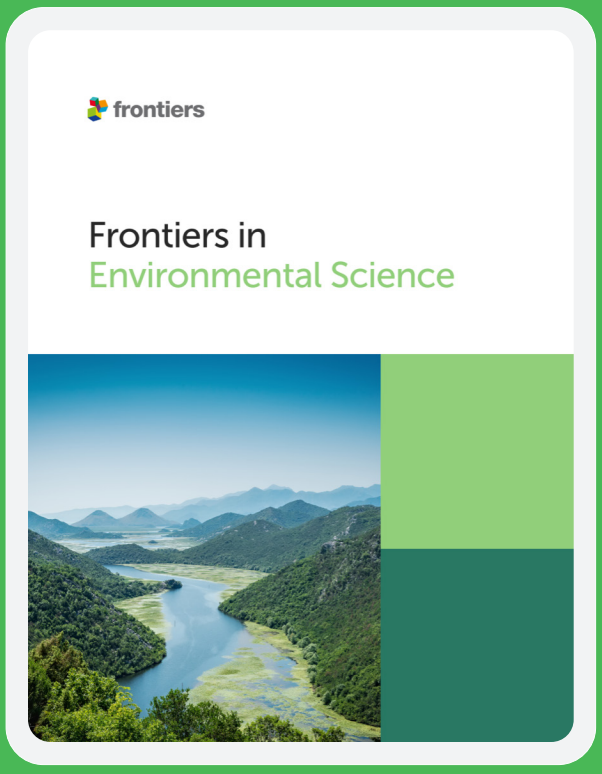

Frontiers

Avenue du Tribunal-Fédéral 34
1005 Lausanne, Switzerland
frontiersin.org

Contact us

+41 (0)21 510 17 00
frontiersin.org/about/contact